REMOVAL OF PHARMACEUTICALS IN WASTEWATER COMBINING DIFFERENT TREATMENT TECHNOLOGIES: SUSPECT SCREENING IDENTIFICATION AND RISK ASSESSMENT OF TRANSFORMATION PRODUCTS

Adrián Jaén Gil

Doctoral Thesis

Removal of pharmaceuticals in wastewater combining different treatment technologies: Suspect screening identification and risk assessment of transformation products

Adrián Jaén Gil

2021

Doctoral program in Water Science and Technology

Supervisors: Dra. Sara Rodríguez Mozaz and Prof. Damià Barceló Cullerès

Academic tutor: Dra. Manuela Hidalgo Muñoz

Thesis submitted in fulfillment of the requirements for the degree of Doctor from the University of Girona.

Girona, March 2021

Dra. Sara Rodríguez Mozaz, supervisor at the Catalan Institute for Water Research; Dr. Damià Barceló Cullerès, supervisor at the Institute of Environmental Assessment and Water Research and the Catalan Institute for Water Research; and Dra. Manuela Hidalgo Muñoz, academic tutor at the University of Girona.

DECLARE:

That the doctoral thesis entitled "**Removal of pharmaceuticals in wastewater combining different treatment technologies: Suspect screening identification and risk assessment of transformation products**" presented by **Adrián Jaén Gil** has been completed under our supervision and fulfills the requirements for its submission to obtain the doctoral degree from the University of Girona with international mention.

For all intents and purposes, I hereby sign this document.

Dra. Sara Rodríguez Mozaz
(Supervisor)

Prof. Damià Barceló Cullerès
(Supervisor)

Dra. Manuela Hidalgo Muñoz
(Academic tutor)

Mr. Adrián Jaén Gil
(Ph.D. candidate)

Agradecimientos

Me gustaría agradecer a mis directores de tesis, la Dra. Sara Rodríguez Mozaz y el Dr. Damià Barceló Cullerès, por brindarme la oportunidad de realizar esta tesis doctoral en el Instituto Catalán de Investigación del Agua. Ha sido una experiencia inolvidable y llena de emociones donde no sólo he podido crecer como científico sino también como persona. Agradecer al Dr. Carlos Escudero Oñate y a la Dra. Laura Ferrando Climent por acogerme durante mi estancia internacional en Noruega y permitirme descubrir una nueva forma de vida en este país. Agradecer a la Dra. Imma Ferrer y el Dr. Michael Thurman que hicieron posible mi estancia internacional en Colorado y recorrerme los lugares más magníficos del mundo. Agradecer a todos los compañeros de ICRA, a todos los colaboradores de la Universidad Autónoma de Barcelona y del Instituto Químico de Sarrià. Finalmente agradecer a toda mi familia y amigos que han sido de gran ayuda a lo largo de este camino.

I would like to thank my thesis supervisors, Dr. Sara Rodríguez Mozaz and Dr. Damià Barceló Cullerès, for giving me the opportunity to do this doctoral thesis at the Catalan Institute for Water Research. It has been an unforgettable and emotional experience where I have not only been able to grow as a scientist but also as a person. I would like to thank Dr. Carlos Escudero Oñate and Dr. Laura Ferrando Climent for hosting me during my international stay in Norway and allowing me to discover a new way of life in this country. Thank you to Dr. Imma Ferrer and Dr. Michael Thurman who made possible my international stay in Colorado and to visit the most magnificent places in the world. Thank all ICRA colleagues, all co-authors from the Autonomous University of Barcelona, and the Chemical Institute of Sarrià. Finally, I would like to thank all my family and friends who have been of great help along this path.

Jeg vil takke avhandlingens veiledere, Dr. Sara Rodríguez Mozaz og Dr. Damià Barceló Cullerès, for at de ga meg muligheten til å gjøre denne doktorgradsavhandlingen ved Katalansk Institutt for Vannforskning. Det har vært en uforglemmelig og emosjonell opplevelse der jeg ikke bare har vært i stand til å vokse som forsker, men også som person. Jeg vil takke Dr. Carlos Escudero Oñate og Dr. Laura Ferrando Climent for at de var verter for meg under mitt internasjonale opphold i Norge og tillot meg å oppdage en ny livsstil i dette landet. Takk til Dr. Imma Ferrer og Dr. Michael Thurman som muliggjorde mitt internasjonale opphold i Colorado og for å besøke de mest fantastiske stedene i verden. Takk alle ICRA-kolleger, alle samarbeidspartnere fra det Autonome Universitetet i Barcelona og Kjemisk Institutt Sarrià. Til slutt vil jeg takke familien min og alle venner som har vært til stor hjelp på denne veien.

Funding

This work was funded by the Spanish State Research Agency of the Spanish Ministry of Science, Innovation and Universities AEI-MICIU and the Fondo Europeo de Desarrollo Regional under the National Program for Research Aimed at the Challenges of Society through the project H2PHARMA (CTM 2013-48548-C2). We acknowledge the FI pre-doctoral grant 2019FI_B2_00202 from the Agency for Management of University and Research Grants (AGAUR) and co-financed by the European Social Fund. We acknowledge the mobility support provided by the European Cooperation in Science and Technology, Cost Action (CA17133) "Implementing nature-based solutions for creating a resourceful circular city".

Table of contents

List of publications

This doctoral thesis is a compendium of research articles. The publications presented as chapters of this thesis are listed below:

i. A. Jaén-Gil, F. Castellet-Rovira, M. Llorca, M. Villagrasa, M. Sarrà, S. Rodríguez-Mozaz, D. Barceló (2019). Fungal treatment of metoprolol and its recalcitrant metabolite metoprolol acid in hospital wastewater: Biotransformation, sorption and ecotoxicological impact. *Water Research,* 152: 171 - 180. DOI: 10.1016/j.watres.2018.12.054. (Impact factor: 9.130, Q1).

ii. A. Jaén-Gil, A. Hom-Diaz, M. Llorca, T. Vicent, P. Blánquez, D. Barceló, S. Rodríguez-Mozaz (2018). An automated on-line turbulent flow liquid-chromatography technology coupled to a high resolution mass spectrometer LTQ-Orbitrap for suspect screening of antibiotic transformation products during microalgae wastewater treatment. *Journal of Chromatography A*, 1568: 57 - 68. DOI: 10.1016/j.chroma.2018.06.027. (Impact factor: 3.813, Q1).

iii. A. Jaén-Gil, G. Buttiglieri, A. Benito, R. Gonzalez-Olmos, D. Barceló, S. Rodríguez-Mozaz (2019). Metoprolol and metoprolol acid degradation in UV/H_2O_2 treated wastewaters: An integrated screening approach for the identification of hazardous transformation products. *Journal of Hazardous Materials*, 380: 120851. DOI: 10.1016/j.jhazmat.2019.120851. (Impact factor: 9.038, Q1).

iv. A. Jaén-Gil, M.J. Farré, A. Sànchez-Melsió, A. Serra-Compte, D. Barceló, S. Rodríguez-Mozaz (2020). Effect-based identification of hazardous antibiotic transformation products after water chlorination. *Environmental Science & Technology*, 54 (14): 9062–9073. DOI: 10.1021/acs.est.0c00944. (Impact factor: 7.864, Q1).

v. A. Jaén-Gil, G. Buttiglieri, A. Benito, J.A. Mir-Tutusaus, R. Gonzalez-Olmos, G. Caminal, D. Barceló, M. Sarrà, S. Rodriguez-Mozaz (2021). Combining biological processes with UV/H_2O_2 for metoprolol and metoprolol acid removal in hospital wastewater. *Chemical Engineering Journal*, 404: 126482 DOI: 10.1016/j.cej.2020.126482. (Impact factor: 10.652, Q1).

List of acronyms

AOPs	Advanced oxidation processes
AZI	Azithromycin
BOD	Biological oxygen demand
CAS	Conventional activated sludge
CFC	Ciprofloxacin
CID	Collision-induced dissociation
COD	Chemical oxygen demand
CTM	Clarithromycin
DBPs	Disinfection by-products
DDA	Data-dependent acquisition
DIA	Data-independent acquisition
EC_{50}	50% effective concentration
ECDs	Endocrine disrupting compounds
ECs	Emerging contaminants
EDA	Effect-directed analysis
EPA	Environmental Protection Agency
ERY	Erythromycin
FBB	Fluidized bed bioreactor
FG	Fungi treatment
FISh	Fragment ion search
FWHM	Full width at half maximum
HCD	Higher-energy collisional dissociation
HESI	Heated electrospray ionization
HRMS	High-resolution mass spectrometry
HRT	Hydraulic retention times
HWW	Hospital wastewater
IF	Identification factor
IWW	Industrial wastewater
LC_{50}	50% lethal concentration
LC-HRMS	Liquid chromatography coupled to high-resolution mass spectrometry
LC–MS/MS	Liquid chromatography coupled to tandem mass spectrometry
m/z	Mass-to-charge ratio

MBR	Membrane bioreactor
MRM	Multiple reaction monitoring
MS	Mass spectrometry
MTP	Metoprolol
MTPA	Metoprolol acid
NFC	Norfloxacin
O-DMTP	O-desmethylmetoprolol
OFC	Ofloxacin
PBR	Photobioreactor
PCA	Principal component analysis
PhACs	Pharmaceutical active compounds
PMA	Pipemidic acid
QSAR	Quantitative structure-activity relationship
RDB	Ring and double bond equivalents
S/N	Signal-to-noise ratio
SPE	Solid phase extraction
SPY	Sulfapyridine
SRT	Sludge retention times
TDS	Total dissolved solids
TFC	Turbo flow column
TMP	Trimethoprim
TPs	Transformation products
TSS	Total suspended solids
TU	Toxic units
UWW	Urban wastewater
WRF	White-rot fungus
WWTPs	Wastewater treatment plants
α-HMTP	α-hydroxymetoprolol

List of figures

List of tables

Summary

The low efficiency of conventional wastewater treatment plants to achieve the complete removal of micropollutants present, including pharmaceuticals, has motivated the development of alternative water technologies to improve their efficiency, sustainability, and operational costs. However, even when the complete elimination of these emerging contaminants is attained, these substances can be transformed into new and unknown intermediates which might be even more persistent and toxic than their parent compounds. Up to now, most of the monitoring studies have focused on the removal of pharmaceuticals during wastewater treatments. However, less attention has been paid to the identification of the transformation products generated, their potential environmental effects and their removal. The main inconvenience for their consideration relies on the lack of advanced analytical methods and commercial analytical standards for confirmation of their presence in treated samples. The use of advanced analytical instrumentation based on high-resolution mass spectrometry has allowed to cope with this issue providing a simultaneous detection of thousands of substances in a single sample analysis. In this doctoral thesis, the development of advanced suspect screening methodologies has been applied for automatic identification of a wide proportion of the transformation products generated in treated effluents along biological and physical and/or chemical treatments. Additionally, *in silico* methods and *in vitro* bioassays based on quantitative structure-activity relationships models, statistical tools and effect-directed analyses were integrated to evaluate the potential environmental effects of transformation products in treated effluents. Finally, these methodologies were applied for monitoring the removal efficiency of pharmaceuticals and their hazardous transformation products in combined treatment technologies. This doctoral thesis demonstrates that target analysis does not provide complete information to draw conclusions about the most efficient water treatment to be applied. The use of advanced suspect screening methodologies for identification of the intermediates generated is highly required. Moreover, this work evidences the high importance of considering their environmental effects of the intermediates generated since some of them may still remain in treated effluents. In conclusion, multidisciplinary research combining analytical chemistry (target and suspect screening analysis), environmental risk assessment and chemical engineering is needed to properly evaluate the best treatment technology to be used.

Resumen

La baja eficiencia de las plantas de tratamiento de aguas residuales convencionales para lograr la completa eliminación de microcontaminantes, incluidos los fármacos, ha motivado el desarrollo de tecnologías alternativas de agua para mejorar su eficiencia, sostenibilidad y costos operativos. Sin embargo, incluso cuando la eliminación de estos contaminantes emergentes es completa, estas sustancias pueden transformarse en intermediarios nuevos y desconocidos que podrían ser incluso más persistentes y tóxicos que sus compuestos parentales. Hasta el momento, la mayoría de los estudios de seguimiento se han centrado en la eliminación de fármacos durante los tratamientos de aguas residuales, sin embargo, se ha prestado menos atención a la identificación de los productos de transformación generados, sus posibles efectos ambientales y su eliminación. El principal inconveniente para su consideración se basa en la falta de métodos analíticos avanzados y estándares de referencia para confirmar su presencia en las muestras tratadas. El uso de instrumentación analítica avanzada basada en espectrometría de masas de alta resolución ha permitido hacer frente a este problema proporcionando una detección simultánea de miles de sustancias en un único análisis. En esta tesis doctoral se ha aplicado el desarrollo de metodologías avanzadas de detección de sospechosos para la identificación automática de una amplia proporción de productos de transformación generados en los efluentes tratados a lo largo de tratamientos biológicos y físicos y/o químicos. Además, se han integrado métodos *in silico* y bioensayos *in vitro* basados en modelos cuantitativos entre estructura-actividad, herramientas estadísticas y análisis de efectos dirigidos para evaluar sus posibles efectos ambientales en efluentes tratados. Finalmente, estas metodologías se han aplicado para monitorear la eficiencia de eliminación de productos farmacéuticos y sus peligrosos productos de transformación en tecnologías de tratamientos combinados. Esta tesis doctoral demuestra que el análisis de compuestos conocidos no proporciona una información completa para extraer conclusiones sobre el tratamiento de agua más eficiente a aplicar. El uso de metodologías avanzadas de análisis de sospechosos para la evaluación de los intermedios generados es necesario. Además, este trabajo demuestra la gran importancia de considerar los efectos ambientales de los productos de transformación generados, ya que algunos de ellos todavía pueden permanecer en los efluentes tratados. En conclusión, la investigación multidisciplinaria combinando química analítica, evaluación de riesgos e ingeniería química es necesaria para evaluar el mejor tratamiento a usar.

Resum

La baixa eficiència de les plantes de tractament d'aigües residuals convencionals per a aconseguir la completa eliminació de microcontaminants presents, incloent els fàrmacs, ha motivat el desenvolupament de tecnologies alternatives d'aigua per a millorar la seva eficiència, sostenibilitat i costos operatius. No obstant, fins i tot quan l'eliminació d'aquests contaminants emergents és completa, aquestes substàncies poden transformar-se en intermediaris nous i desconeguts que podrien ser fins i tot més persistents i tòxics que els seus compostos parentals. Fins al moment, la majoria dels estudis de seguiment s'han centrat en l'eliminació de productes farmacèutics durant els tractaments d'aigües residuals, tanmateix, s'ha donat menys atenció a la identificació dels productes de transformació generats, els seus possibles efectes ambientals i la seva eliminació. El principal inconvenient per a la seva consideració es basa en la falta de mètodes analítics avançats i estàndards de referència per a confirmar la seva presència en les mostres tractades. L'ús d'instrumentació analítica avançada basada en espectrometria de masses d'alta resolució ha permès fer front a aquest problema proporcionant una detecció simultània de milers de substàncies en una única anàlisi. En aquesta tesi doctoral s'ha aplicat el desenvolupament de metodologies avançades de detecció de sospitosos per a la identificació automàtica d'una àmplia proporció de productes de transformació generats en els efluents tractats al llarg de tractaments biològics i físics i/o químics. A més, s'han integrat mètodes *in silico* i bioassaigs *in vitro* basats en models quantitatius d'estructura-activitat, eines estadístiques i anàlisis d'efectes dirigits per a avaluar els seus possibles efectes ambientals en efluents tractats. Finalment, aquestes metodologies s'han aplicat per a monitorar l'eficiència d'eliminació de productes farmacèutics i els seus perillosos productes de transformació en tecnologies de tractaments combinats. Aquesta tesi doctoral demostra que l'anàlisi de compostos coneguts no proporciona una informació completa per a extreure conclusions sobre el tractament d'aigua més eficient a aplicar. L'ús de metodologies avançades d'anàlisis de sospitosos per a l'avaluació dels intermediaris generats és necessari. A més, aquest treball posa de manifest la gran importància de considerar els efectes ambientals dels productes intermedis generats, ja que alguns d'ells encara poden romandre en efluents tractats. En conclusió, la recerca multidisciplinària combinant química analítica, avaluació de riscos mediambientals i enginyeria química és necessària per a avaluar el millor tecnologia de tractament a utilitzar.

Chapter 1

General introduction

1.1 Pharmaceuticals in the aquatic environment

The occurrence of contaminants in the aquatic environment has gained special attention from the scientific community in the last two decades. The so-called *emerging contaminants* (ECs) refer to those non-regulated anthropogenic or natural substances not commonly found in the environment that may have potential adverse effects on wildlife and human health [1]. They consist in a great variety of pollutants such as pharmaceutically active compounds (PhACs), personal care products, endocrine disrupting compounds (ECDs), illicit drugs and other chemicals such as some pesticides, flame retardants and surfactants. Among the different families of micropollutants, PhACs have played an important role in the rapid development of therapeutic treatments and the improvement of life quality of society [2–4]. Up to now, more than 3000 chemicals have been prescribed in the European Union and their production exceeds hundreds of tons per year [5,6]. The overuse and misuse of these substances after the medical prescription has promoted their entrance into sewage systems through urban wastewater (UWW) and hospital wastewater (HWW) discharges, not only as unchanged chemicals but also as transformed human metabolites [7–9]. Likewise, other human activities are sources of pharmaceutical contamination into the aquatic environment (Figure 1.1). Among them, the most relevant ones are the discharges from pharmaceutical manufacturing through industrial wastewater (IWW) as well as landfill, agriculture and livestock activities [10,11].

Conventional activated sludge (CAS), which involves the biological degradation of organic pollutants, is usually applied as a secondary treatment in conventional wastewater treatment plants (WWTPs). One of the main advantages of this treatment is the ability to fulfill the regulatory quality standards for wastewater treatment (Directive 91/271/EEC) at optimal operating and maintenance costs in terms of chemical oxygen demand (COD), biological oxygen demand (BOD), nitrogen, phosphorus and total suspended solids (TSS) [12]. However, these conventional wastewater treatments are not specifically designed for the removal of PhACs, and low removal rates are attained [13]. While the presence of PhACs is mentioned as a key element for risk assessment, no threshold concentrations have been defined yet [14]. Thus, PhACs can pass through wastewater treatment processes as unchanged molecules or transformed substances into the receiving aquatic environment [15,16]. As a result, PhACs

have been commonly detected in natural ecosystems at relatively low concentration levels in surface water [17–19], marine water [20], groundwater [21] and drinking water [22] ranging from few ng L^{-1} to a hundred µg L^{-1}. Their occurrence in the different environmental compartments has been related to negative effects such as short-term and long-term toxicity, endocrine-disrupting effects and antibiotic resistance of microorganisms even at low concentration levels [23–26]. While the Water Framework Directive (2013/39/EC) has listed a list of 45 priority compounds in surface waters including heavy metals, pesticides and industrial pollutants [27], PhACs are still classified as non-regulated compounds. Nevertheless, few of them are considered in the *3rd Watch List* (Decision 2020/1161) as priority substances to be monitored for which the information available might indicate potential concerns for the aquatic environment, including the following substances: ciprofloxacin, amoxicillin, sulfamethoxazole, trimethoprim, and the psychiatric drugs venlafaxine and o-desmethylvenlafaxine (a venlafaxine major human metabolite) [28].

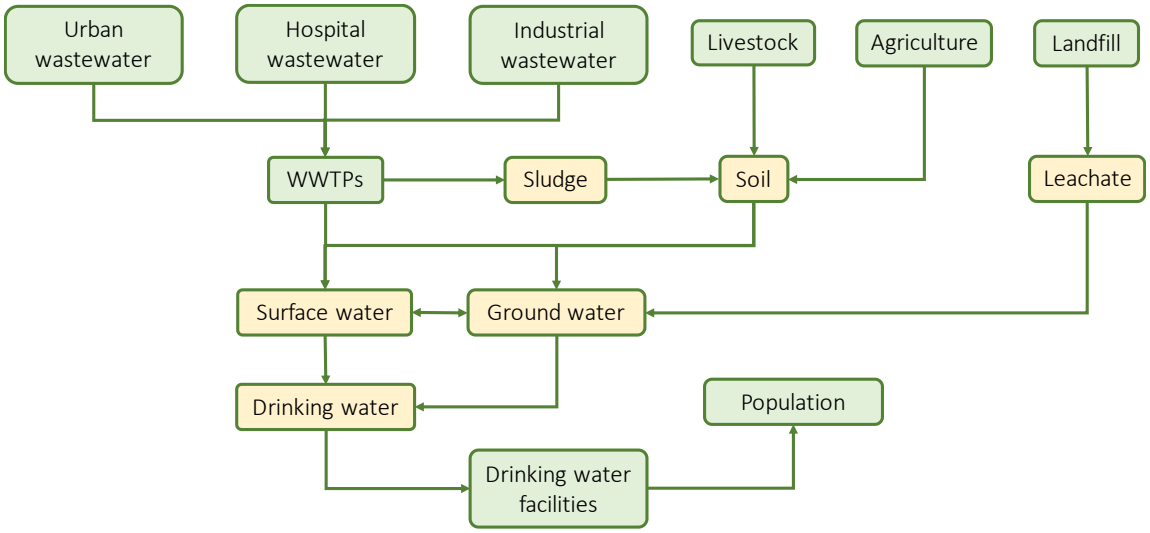

Figure 1.1: Representative sources and input routes of PhACs in the environment (adapted from Yin, L. et al. (2017)). Human activities are highlighted in green color whereas environment compartments are highlighted in yellow.

1.2 Degradation of PhACs in wastewater treatments

The low efficiency of conventional WWTPs for the removal of PhACs in wastewater has fostered the implementation of alternative secondary or/and tertiary wastewater treatments to attain complete removal of these substances prior to effluent discharge [29–35]. Biological

treatments are usually classified as eco-friendly water treatments involving low operational costs and low energy consumption and include membrane bioreactors (MBRs), fungal treatments, microalgae-based systems and artificial wetlands, among others. Otherwise, the application of physical and/or chemical treatments is considered a valuable solution for the elimination of the biorecalcitrant pollutants not eliminated in biological treatments. These last technologies include advanced oxidation processes (AOPs, such as UV/O_3, O_3/H_2O_2, UV/H_2O_2 and photo-Fenton reactions including UV/H_2O_2/Fe^{2+} and Fe^{3+}), chlorination, filtration and adsorption technologies.

1.2.1 Biological treatments

Membrane bioreactors (MBRs) are the most popular biological treatment for the elimination of organic pollutants usually implemented in WWTPs as an alternative to CAS treatment [36]. The key mechanisms that control their elimination are biodegradation and biosorption through the combination of activated sludge and membrane filtration [37,38]. Although many studies have applied MBR technology for the removal of PhACs [36,39,40], these treatments do not always provide enhanced removal efficiencies than those attained in conventional CAS treatments [41,42]. Only the combination of MBR with reverse osmosis or nanofiltration has been reported to be highly efficient, achieving a complete removal efficiency in treated effluents for some PhACs [41,43].

Fungal treatments are classified as a promising treatment strategy for bioremediation of organic contaminants mainly due to the potent fungal enzymatic system, able to degrade lignin [44,45]. Lignin is a heterogeneous biopolymer very resistant to degradation due to the presence of a great number of aromatic rings and a particular branched chemical structure [46]. In order to reach lignin decomposition, fungi species have an intracellular but also excrete an extracellular enzymatic system which includes laccase, manganese peroxidase and lignin peroxidase enzymes [47–49]. The ability of extracellular enzymes for the removal of PhACs has been widely reported, especially for white-rot fungus species (WRF) [50–52]. In particular, *Trametes versicolor* has shown the best enzyme production capacity as well as the highest enzyme activity (above the 75%), while the production of laccase has been reported to be stimulated by the presence of organic contaminants such as PhACs [53,54].

Microalgae-based treatments have recently gained scientific attention as they are solar-power driven, eco-friendly, and sustainable reclamation strategies. One of the main benefits of these technologies is their photosynthetic ability to capture CO_2 and grow in a different class of domestic and industrial wastewaters [55]. Microalgae can successfully assimilate inorganic nitrogen and phosphorus for growth, but also eliminate heavy metals and organic pollutants while producing valuable biomass [56]. Among the intracellular enzymes reported in microalgae, the most studied ones are those included in the superfamily named cytochrome P450 (also present in fungal species) involving Phase I chemical reactions such as oxidation, reduction and hydrolysis [57–59]. However, further biological transformations through Phase II conjugations can also be performed by transferase enzymes such as glutathione S-transferases, among others [60,61]. For instance, the reported removal of antibiotics such as sulfonamides by *Scenedesmus obliquus* [62], and the removal of cefradine and amoxicillin by *Microcystis aeruginosa* and *Chlorella pyrenoidosa* [63] have provided evidence of microalgae-based technologies as potential wastewater treatment alternatives.

Artificial wetlands have also been reported as biological treatments with low energy requirements for their application and attaining similar removal rates of PhACs comparing to conventional WWTPs [64]. The main drawback relies on the land requirements and the high hydraulic time investment for their implementation. Therefore, their application in urban areas has been widely questioned.

1.2.2 Physical and/or chemical treatments

Advanced oxidation processes (AOPs) are designed to remove organic matter and pathogens in wastewater by chemical oxidation using highly reactive and non-selective radicals capable to degrade a wide range of low biodegradable pollutants [65–70]. Ozonation is an eco-friendly treatment technology able to oxidize a broad variety of organic pollutants attaining an oxidation potential of 2.07 V by direct reaction [65]. In particular, ozone is an electrophilic molecule able to react with high electronic density sites such as unsaturated bonds and aromatic rings [29]. This molecule may interact under catalyst conditions with water (an indirect mechanism) and lead to the generation of hydroxyl radicals, with stronger oxidation capability between 2.80 V (pH 0) and 1.95 V (pH 14) [65]. As an alternative, UV/H_2O_2 technology is based on the direct generation of hydroxyl radicals with stronger oxidation potential than

those values obtained by direct ozonation. Both technologies are classified as the most studied systems in wastewater attaining very high removal rates for selected PhACs [70–72]. On the other hand, Fenton-based technologies are based on the addition of ferrous salt and hydrogen peroxide (Fe^{2+} and H_2O_2) reactants to generate hydroxyl radicals in wastewater [73–76]. Fenton oxidation involves several disadvantages such as the limitation to operational acidic conditions and the large quantity of iron-sludge generated usually difficult to be treated [77]. Photocatalytic oxidation has been extensively studied for the degradation of organic pollutants using semi-conductor materials (e.g. TiO_2, ZnS, WO_3 and SnO_2) with the generation of superoxide radicals (• O_2^-) or hydroxyl radicals (• OH) [77,78]. Despite the great advantages of these techniques, AOPs are defined by their relatively high operating costs (comparing to biological processes) treating complex water matrices, since larger energy and chemical reagents demand are required to attain total compound removal in treated effluents [79–81].

Chlorination is a chemical treatment especially important for conventional water reuse activities (besides drinking-water treatment) such as irrigation, food and beverage processing, oil well treatment, algae control and wastewater treatment, among others [82,83]. Due to its low cost, good disinfection and oxidation capacity, chlorination using Cl_2 has been widely applied as a final water treatment to sustain residual chlorine in the network distribution system and preserve public health from the presence of pathogens [84]. In addition, chlorination has also been proved to be able to eliminate PhACs in drinking water treatment [85–89], as well as in wastewater treatment [90,91]. Despite this, chlorine can induce the generation of halogenated pollutant intermediates and disinfection by-products (DBPs) which may also have potentially deleterious effects on the aquatic environment and human health [92].

Filtration is a physical treatment based on membranes able to separate chemical substances such as ions and other impurities from wastewater [93]. As in the case of other physical treatments such as ultrafiltration and reverse osmosis, these technologies have been widely applied for the elimination of PhACs, however, the great majority of micropollutants are not degraded and remain in the concentrated waste, which requires further treatment as a hazardous waste [93].

Adsorption on activated carbon is the process of binding and removing organic pollutants from an aqueous solution through the use of activated carbon as an adsorbent. This technology is effective for the adsorption of PhACs but attained low removal efficiencies for the most polar compounds present in solution [94,95]. On the other hand, this technology requires a continuous regeneration of the activated carbon increasing the total costs of the whole treatment.

1.3 Transformation mechanisms in WWTPs

Due to the low efficiency of WWTPs to attain complete degradation of PhACs in treated effluents, the removal mechanisms involved in this conventional treatment have been largely studied [96,97]. The main mechanisms involved are biodegradation, photo-degradation, sorption, volatilization and hydrolysis. These mechanisms can take place during the different stages of wastewater treatment, which generally consist of a primary, a secondary treatment, and optionally, a tertiary treatment [98,99].

Biodegradation is based on the action of microorganisms for the breakdown of complex chemicals into less hazardous pollutants using them as electron donators to produce energy [99]. The organic compounds are metabolized through intracellular and extracellular enzymes secreted by the microorganisms. The removal of PhACs through biological mechanisms depends on the concentration of pollutants but also on the environmental conditions (such as the quantity of light for growing microorganisms, temperature, oxygen and CO_2 conditions), wastewater characteristics (such as pH total dissolved solids (TDS), turbidity, COD, alkalinity and dissolved oxygen, among others) and treatment optimization conditions (such as sludge retention times (SRT) and hydraulic retention times (HRT)) [37]. Due to the large complexity of these biological systems, much information regarding the degradation of PhACs is missing, and thus, attaining reproducible results for the biodegradation of these pollutants becomes a very challenging task.

Photo-degradation of PhACs can also be carried out by induction of photolysis reactions either by direct or indirect mechanisms after exposure to sunlight or artificial light [72,100–104]. Direct photolysis is related to the absorption of light by the organic pollutant and further chemical transformation by the influence of the type of radiation and the efficiency of photon

emission (wavelength and quantum yield) [105]. Indirect photolysis refers to the degradation of pollutants under light radiation through the oxidant species (e.g. hydroxyl radicals) generated by photoactive dissolved organic matter and natural photosensitizers in solution (e.g. nitrate and humic acids) [106]. However, the efficiency of these mechanisms in conventional wastewater treatment for PhACs removal is low due to the irregular light exposure of pollutants in full-scale treatment systems and the presence of suspended solids blocking the entrance of solar radiation [107].

Sorption is considered the second key mechanism controlling the removal of organic pollutants in conventional wastewater systems based on CAS [108]. This elimination mechanism is also essential in water treatments based on e.g. activated carbon, biochar and other carbonaceous sorbents [109,110]. Sorption depends on the physicochemical properties of involved chemicals and the nature of sludge biomass. In general, pollutants can be removed by sorption depending on the degree of partitioning between sludge and aqueous phases as well as the characteristics of the sorbent agent in adsorption based wastewater treatment [111]. The term sorption comprises absorption and/or adsorption mechanisms [112,113]. Absorption takes place when the organic pollutants are transported from the aqueous phase into the lipophilic cell membrane of biomass; while adsorption is performed when organic pollutants are retained onto the surface of biomass cells [114].

Volatilization consists of the transfer of a compound from the aqueous phase to the atmosphere on the basis of its Henry's law constant [115,116]. This mechanism is carried out under certain environmental conditions of vapor pressure, water solubility and transfer velocity, which is in part dependent on the chemical properties of pollutants including their molecular mass and their atomic diffusion volume [115]. Considering the standard airflow rates applied in conventional CAS treatments (5– 15 m^3 air m^{-3} wastewater [117]) and the reported Henry coefficient of PhACs, losses due to stripping can be considered completely negligible [118].

Hydrolysis is related to the breakdown reaction of chemicals in presence of water molecules in solution [119]. The rate of this transformation mechanism may vary depending on the pH and temperature of effluents [119]. In this sense, increasing pH and temperature in solution leads to an increase in the hydrolysis rate of pollutant transformation [119].

1.4 Study of the TPs generated in wastewater treatments

Even when the elimination of PhACs is completely attained during wastewater treatment, they can be transformed into new and unknown degradation intermediates which might be even more persistent and toxic than their parent compounds [120–122]. While most of the studies have focused on the removal of PhACs after wastewater treatment, less attention has been paid to the identification of the transformation products (TPs) generated [99,120,123,124]. The main drawback of their study is the lack of commercial reference standards for their confirmation and quantification in treated effluents [125]. Hence, advanced analytical instrumentation comprising reliable structural identification is highly required.

1.4.1 Analytical instrumentation

Liquid chromatography coupled to tandem mass spectrometry (LC-MS/MS) has been widely applied for the detection of PhACs in complex aqueous matrices providing high selectivity and sensitivity data. This instrumentation combines the comprehensive separation of the compounds present in samples through the interaction of the analytes in a polar/non-polar stationary phase (in a liquid chromatography system), and further detection of ionized molecules for compound identification and quantification (in a tandem mass spectrometer system) [126,127]. While conventional tandem mass spectrometers (such as triple quadrupole and hybrid triple quadrupole-linear ion trap) exhibit excellent performance for quantitative analysis of known compounds, the main drawback relies on the low mass resolution, which prevents the accurate identification of unknown compounds unless a standard is available for identity confirmation.

In this context, high-resolution mass spectrometry (HRMS) is considered the most promising instrumentation, even when reference standards are not available for confirmation [126]. Their high mass resolving power allows the simultaneous detection of thousands of substances in a single sample analysis based on the reliable measurement of their accurate masses in complex matrices. In addition, the high sensitivity, selectivity and acquisition rates make these instruments a valuable tool for qualitative and quantitative analysis [127–131]. Among HRMS spectrometers, Orbitrap instruments are based on the orbital motion of the ions around an inner electrode that converts the measured frequency into a mass-to-charge (m/z) values using

Fourier Transform. The main advantage of the analyzer is the detection of ionized organic compounds at very high-resolution power up to > 500,000 full-width at half maximum (FWHM) at *m/z* 200, and providing mass accuracy ≤ 5 ppm in collected data spectra [132]. This instrumentation performs full-scan mode analysis of a sample and allows to develop different strategies for the identification of compounds such as TPs in the absence of their corresponding chemical standards. However, the main drawback is the low scan acquisition rate at an increasing mass resolution power (Figure 1.2), which can compromise its capability for reliable compound quantification by reducing the number of points per chromatographic peak in MS full-scan data collected [130,133]. In this doctoral thesis, a LTQ-OrbitrapVelos™ (ThermoFisher Scientific) was used with a maximum resolution capability of 100,000 FWHM at *m/z* 400. Depending on the type of chemicals to be detected in samples (known and/or unknown compounds), different analytical approaches can be developed [126,134–138].

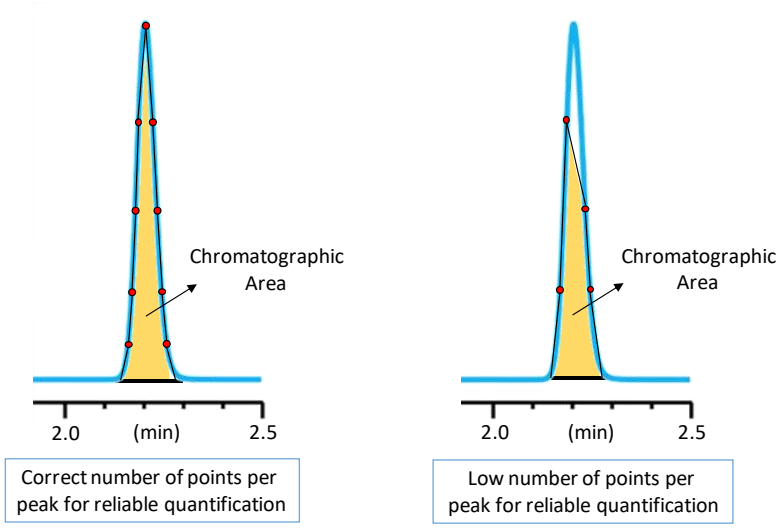

Figure 1.2: Number of acquired points needed to properly perform compound quantification.

1.4.2 Identification strategies

Target analysis has been applied for the characterization of known compounds mainly using multiple reaction monitoring strategies (MRM), also known as selected reaction monitoring (SRM), and analytical reference standards for confirmation purposes [139]. The MRM acquisition mode is a highly specific and sensitive approach to quantify the presence of several compounds in complex environmental matrices in a single sample analysis when reference standards are available for confirmation. This approach consists of the selection of several

target precursor ions in a first stage, and the detection of their selected product ions for quantification in a secondary stage after precursor ion fragmentation [127]. Only compounds that meet the user-defined criteria (the known molecular masses of specific parent ion and their fragment ions) are isolated within the mass spectrometer. Ignoring all other ions present in samples that flow into the mass spectrometer, the analysis increases in sensitivity whilst maintaining high accuracy on detection. Examples of applications for this identification strategy have been widely reported for a large quantity of emerging substances (up to 82 substances in a single analysis) including analgesics/anti-inflammatories [140,141], psychiatric drugs [140,141], β-blocking agents [140,142,143] and antibiotics [140,141,144–147], and their known TPs [140,142,148,149], among others.

Although target analysis has been the analytical methodology of choice in environmental analysis in the last two decades, concerns about the large presence of unknown compounds in samples began to gain a great relevance among researchers [139,150]. One of the main drawbacks of the identification of these unknown pollutants was the absence of analytical reference standards for confirmation purposes [150]. In this context, non-target screening methodologies were developed for the detection of hundreds or even thousands of unknown compounds when prior information of the chemicals was not available for their detection [138]. This strategy is based on the combination of full-scan mass spectrometric detection in HRMS (of precursor ions and, if required, all their product ions) combined with non-limited ion extraction of all substances detected and recorded in raw data. Examples of applications for this identification strategy have been widely reported for the characterization of organic matter in environmental samples using multivariate analysis and exploring the changes in fingerprints [151–154] and for the identification of TPs [148,155–157]. However, this non-selective methodology presents several important drawbacks since untargeted measurements always provide an overwhelming amount of data to be processed, and thus, its application as a routine analysis is not feasible [127]. In addition, although the number of ion masses detected in data collected increases from target analysis to non-target screening analysis, the confidence on compound identification decreases since confirmation and elucidation of all features detected is not possible in a rationale time-period (Figure 1.3).

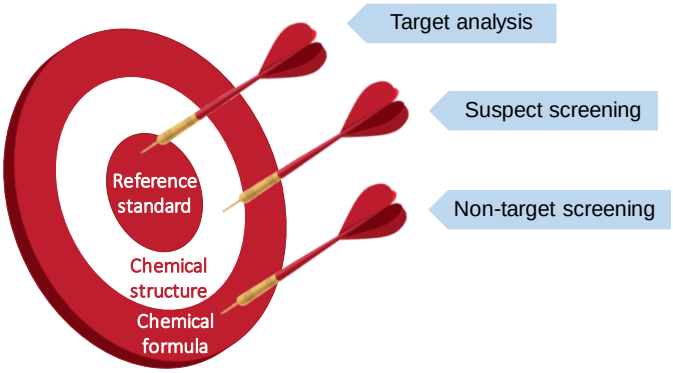

Figure 1.3: Target, suspect and non-target methodologies for compound identification.

Among the so-called non-target methodologies, **suspect screening** analysis has been recently developed as an intermediate approach for the identification of suspected chemicals when analytical reference standards are not available for confirmation *a priori* [127]. This strategy is based on the combination of full-scan acquisition in HRMS (with the fragmentation of selected ions for MS/MS structural elucidation) combined with non-limited ion extraction of all substances detected in raw data. This strategy can alleviate data processing step by identification of suspected TPs by comparison with databases [136,158,159], in-house libraries [160], literature information [160] and *in silico* predictions tools [161–163]. Nonetheless, tentative information of the suspected compounds to be detected in samples is always required.

Different suspect screening methodologies can be applied for the detection and identification of the intermediates generated during conventional and alternative wastewater treatment processes such as biological [164–171] and physical and/or chemical [172–181] treatments. However, manual data processing and compound elucidation still represent a tedious and time-consuming task. The development of automated suspect screening methodologies using computational tools can provide a more rapid and user-friendly identification of the TPs generated, attaining reliable confidence in their identification, and accounting for a greater proportion of the chemical present in mixture samples (in comparison to target analysis). Despite this, even with the best non-target screening approaches, those compounds poorly ionized or not properly retained in the chromatographic column may remain outside the spotlight [127]. In this doctoral thesis, all the analysis performed for the identification of TPs of known contaminants were carried out using different suspect screening methodologies and approaches.

1.5 Automated suspect screening methodologies for the identification of TPs

Automated suspect screening methodologies comprise three consecutive steps: i) analysis and data acquisition, ii) data reduction and prioritization, and iii) compound identification using on-line databases/in-house libraries, literature information, *in silico* prediction tools and reference standards if available (Figure 1.4).

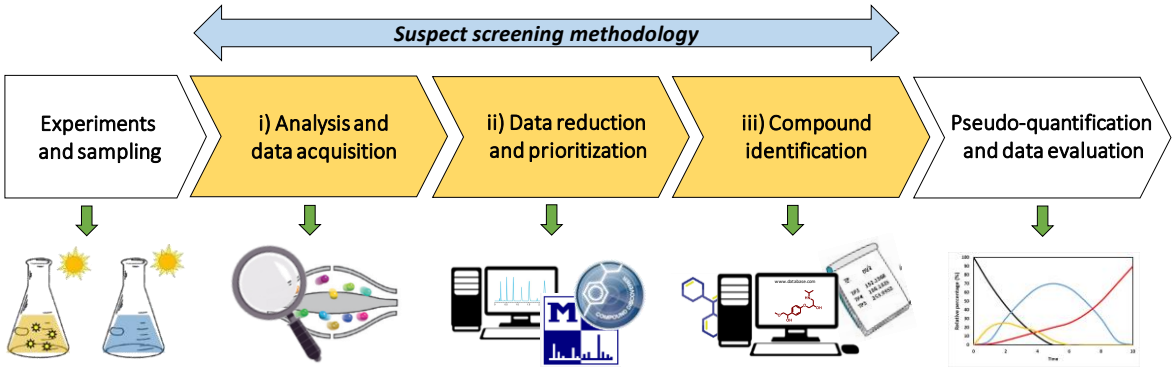

Figure 1.4: Analytical steps comprised in suspect screening methodologies: i) analysis and data acquisition, ii) data reduction and prioritization, and iii) compound identification.

1.5.1 Analysis and data acquisition

The analysis of the TPs generated in wastewater treatment experiments using suspect screening methodologies is usually performed using data-dependent acquisition (DDA) mode [182,183] in the HRMS device. Initially, the mass spectrometer selects the ionized compounds of interest in a first stage of the tandem mass spectrometry (using narrow isolation widths of 2 *m/z* or less) for ion fragmentation. Then, the precursor ions selected are analyzed in the second stage of tandem mass spectrometry. The main advantage of this acquisition mode is the low interferences present in fragmentation full-scans, which ensure more easy and reliable compound identification in comparison to data-independent acquisition (DIA) mode (where a wider isolation width, or no isolation width at all, is selected for compound fragmentation) [184]. To facilitate the structural elucidation of the TPs identified, the DDA mode was applied in this doctoral thesis using three different approaches (Figure 1.5).

List-dependent acquisition can be classified as a pre-acquisition screening strategy, which requires a priority list of precursor ions to be selected for fragmentation. If these parent masses from the included list are detected in data scans (within a specified mass tolerance), they will

be further fragmented starting from the most intense ion to the least intense (this process is performed every cycle time) [185]. One of the main benefits of this strategy is related to its application to real wastewater samples since the ions coming from the matrix interfering substances are not fragmented, and thus, the presence of false suspected compounds to be further investigated is extensively reduced. However, this strategy is mainly applied when prior information of the intermediates to be found in samples is available. This information can be generated from *in silico* software tools or using the information collected from previous experiments reported in the literature, which can be used to automatically generate the accurate mass inclusion list. Most of the mass spectrometry instrument suppliers offer software packages to build specific compound prediction such as MetaboLynx (Waters), Compound Discoverer (Thermo Fisher Scientific), Metabolite Pilot (AB Sciex), MassHunter (Agilent Technologies), MetaboliteTools (Bruker), MetID Solution (Shimadzu), and among others [186,187].

Intensity-dependent acquisition allows to apply a post-acquisition screening strategy, where precursor ions in data scans are selected to be fragmented without previous knowledge of suspected intermediates to be detected in samples (no list of suspected ions is required). When the ions exceed a specified intensity threshold set by the user, these precursor ions are selected for fragmentation starting from the most intense ion to the least intense (this process is performed every cycle time) [185]. Even though this acquisition strategy is useful to identify unknown TPs in samples, its applicability is restricted by the low concentration of some hazardous intermediates and interferences from complex matrices: when the matrix effects are more intense than the suspected intermediates to be investigated, their selection for fragmentation is not promoted. Otherwise, this tool relies on the hypothesis that the selected ions are the most prevalent compounds to be fragmented at a given retention time when those present at low concentration levels are also important to be investigated. To increase the applicability of intensity-dependent mode to real samples, a dynamic mass exclusion can be enabled to avoid continuous re-fragmentation of most intense ions along a selected retention time period, and thus, allow fragmentation of co-eluted ions. In particular, ion masses already fragmented more than "*n*" times can be rejected for fragmentation during a selected chromatographic time period [188,189].

Isotopic-dependent acquisition allows to apply a post-acquisition screening strategy, where the ionized compounds containing characteristic isotope patterns (due to the presence of halogenated groups in their molecular structures) are selected to be fragmented. When the ions meet a specified mass difference and an intensity ratio from their isotopic patterns, these precursor ions are selected for fragmentation starting from the most intense ion to the least intense (this process is performed every cycle time) [185]. For instance, a molecule with a chlorine atom in its chemical structure shows a distinct isotopic pattern with a mass difference of 1.99705 Da and an intensity ratio of about 3:1 during total ion scan from the parent compound to the isotope ^{37}Cl. On the contrary, a molecule containing a bromine atom on its structure shows a wider mass difference of 1.99795 Da and an isotopic ratio of about 1:1. Applying isotopic pattern thresholds for ion selection can be effective for the rapid fragmentation of the halogenated compounds of interest in treated samples [185]. However, it is well known that non-halogenated intermediates can also be generated from halogenated molecules during water treatments which should also be considered for treatment evaluation. Thus, the main limitation of this strategy is the restricted range of ions selected for fragmentation and only those with a specific isotopic pattern previously defined by the user.

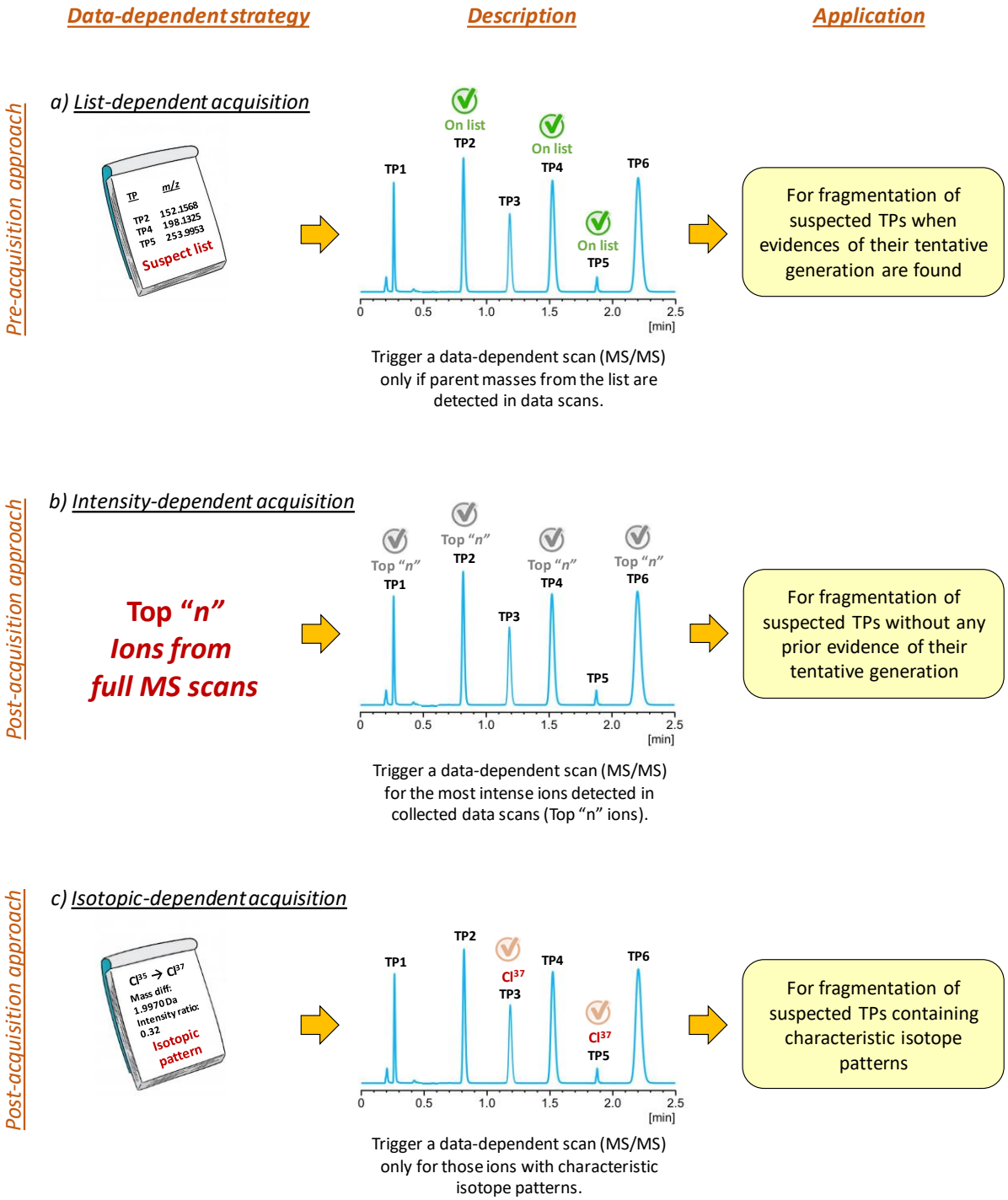

Figure 1.5: Data-dependent strategies for triggering MS/MS fragmentation of tentative intermediates in LTQ-OrbitrapVelos: a) List-dependent acquisition, b) Intensity-dependent acquisition and c) Isotopic-dependent acquisition.

1.5.2 Data reduction and compound prioritization

The number of compounds detected from the samples analyzed can range from a few hundred features to several thousand in real wastewater samples, especially when samples are screened using a post-acquisition approach (Figure 1.5). In order to eliminate false-positive and facilitate further compound identification in post-acquisition suspect screening approaches, data reduction is always required to avoid tedious and time-consuming procedures. Different commercial and open-source software programs are available to optimize data processing workflows. Among them, MZmine was first introduced in 2005 as open-source software that facilitates the implementation of data analysis workflows [190,191]. The development of this software was motivated by the need for flexible and modular platforms with great emphasis on the application of flexible, extendable, and user-friendly tools to support the data processing of LC-HRMS collected data. Up to now, more automatized tools have been developed such as XCMS [192], MZmine 2 [193], and Compound Discoverer [159] containing more advanced modules as well as compound identification tools and statistical data analysis. In this context, the application of automatic software data processing may represent a useful tool for the rapid screening of a wide range of suspect compounds reducing the time invested in data treatment. In addition, it increases the development of methodologies for routine analysis attaining reliable structural information. In this doctoral thesis, Compound Discoverer software (ThermoFisher Scientific) was used to apply modular-based suspect screening data processing workflows for the detection and structural elucidation of suspected compounds. This software allows us to perform simple, flexible and customizable data processing workflows without requiring extended knowledge on computational data scripts and ensures confident detection of TPs in complex samples. The most common modules applied for detection and prioritization of features are described in Table 1.1, which are combined to create customized data processing workflows: select the spectrum, align retention times, generate expected features, detect unknown features, detect expected features, fragment ion search (FISh) scoring, detect unknown features, predict molecular formulas, mark background features, and group detected features. These modules are based on the application of exact mass and retention time tolerances as well as intensity thresholds and signal-to-noise (S/N) ratios for the elimination of false-positives interfering in compound identification.

Table 1.1: Common data filtering modules used in Compound Discoverer for data reduction and compound prioritization.

Module (or node)	Application
Input files	Inclusion of experimental data files collected from LC-MS/MS analysis for data filtering. This module is always applied as the first step in any data processing workflow.
Spectrum selector	Filters the MS scans in each input file by retention time range, ionization polarity, mass range and total intensity threshold. This module is applied to eliminate non-essential information from files and facilitate sample data processing. This module is always applied as a second step in any data processing workflow.
Align retention times	Chromatographically aligns non-reference samples against a reference sample using user-specified mass tolerance windows and a maximum time shift. This module is applied to avoid variances in retention times generated on the samples analyzed along a sample sequence. This module is always applied as a third step in any data processing workflow and can be connected to "detect expected features" and "detect unknown features".
Generate expected features	Generates a list of tentative intermediates after applying computational chemical transformations to the molecular structure of the parent compound (initially defined by the user). This module should always be connected to the "detect expected features" module.
Detect expected features	Detection of suspect features by matching the generated list of expected features with the experimental data collected, based on the user-specified exact mass and retention time tolerances. In addition, the identification of isotopes and adducts is also carried out. This module can be connected to the "Fragment ion search (FISh) scoring" module.
Fragment ion search (FISh) scoring	Generates a list of tentative fragmentation ions from the expected features detected and searches them in experimental MS/MS data files within a user-specified mass tolerance and intensity threshold. This module allows us to generate a FISh scoring percentage indicating the matched fragments regarding the total fragments detected in MS/MS scans.
Detect unknown features	Unknown features present in samples above a selected threshold are reported based on the user-specified exact mass and retention time tolerances. In addition, the identification of isotopes and adducts is also carried out. This module can be connected to the "predict molecular formulas" module.
Predict molecular formulas	Predict molecular formulas from detected features on basis of the exact mass tolerances of detected features in samples.
Mark background features	Extract unknown features detected in blanks from the experimental data collected based on user-defined signal-to-noise ratios. This module can be applied to any data processing workflow.
Group detected features	This module is applied to report a list of the different features detected along the sample sequence containing different exact masses and retention times. This module helps to group the repeated ions reported when the same compounds are detected in several samples along the sequence. This module can be applied to any processing workflow.

1.5.3 Compound identification

After sample filtering and prioritization of candidates, tentative compound identification is based on a comparison of detected features with selected compounds extracted from literature sources, computational prediction (*in silico*) tools and in-house/on-line databases [160]. The reliability of identification using these information sources is presented in Figure 1.6, adapted from the previous study by Schymanski et al. (2014) who assigned levels of confidence to compound identification [134].

Literature comparison includes tentative identification of suspected compounds and ion fragments by comparison of accurate masses with those of compounds reported in the literature. In the case of molecules containing heteroatoms, the identification of isotope patterns can help with the identification of suspected chemical formulas [194]. This strategy is considered as a low confidence strategy since the fragmentation of the tentative TPs identified is not always provided in literature and identification relies solely on the match in the accurate mass. In addition, the possibility to detect structural isomeric compounds from those reported in the literature is also high (false positives). Thus, further identification strategies to improve reliability on compound identification are always required in suspect screening methodologies.

In silico compound prediction of tentative intermediates and elucidation of fragmentation mass spectra has become of great importance to tentatively assign molecular structures to the intermediates generated. In this context, elucidation of intermediates can be performed by using prediction tools such as PathPred, UM-PPS, CATABOL, Compound Discoverer, and Mass Frontier software [159,195]. While PathPred, UM-PPS, and CATABOL are web-servers focused on the prediction of enzyme-catalyzed transformation intermediates through biotransformation, Mass Frontier allows to elucidate fragmentation spectra collected from data files only [196,197]. In Compound Discoverer, both *in silico* prediction (of TP structures and MS/MS fragmentation) can be performed in a single workflow allowing more rapid and user-friendly methodologies. The information collected using *in silico* compound prediction can be included in in-house libraries to alleviate the lack of literature information and to be used in future experiments [120,198–200].

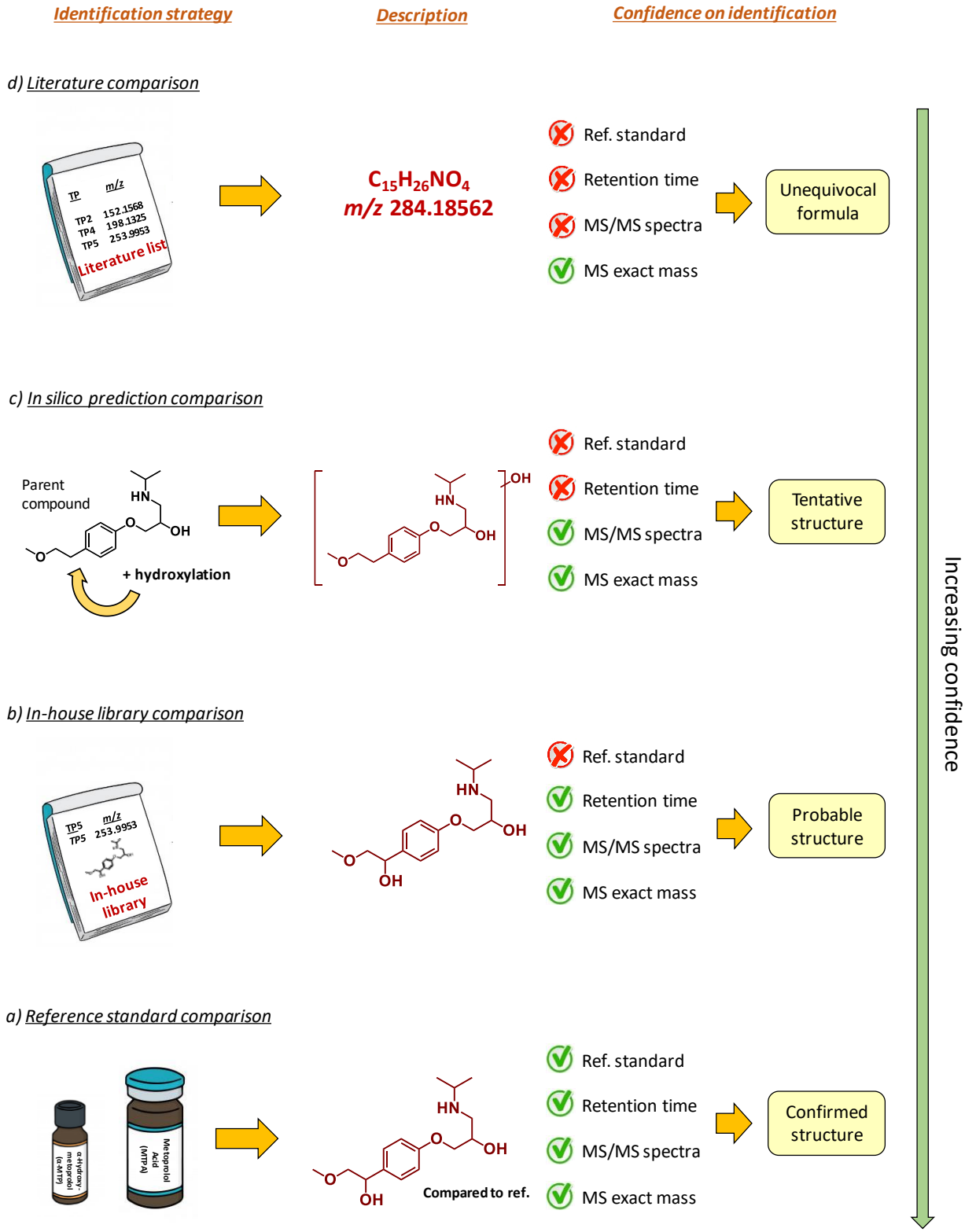

Figure 1.6: Identification strategies for reliable confirmation of the identification of detected TPs by comparison with: a) literature, b) *in silico* prediction tools, c) in-house libraries, and d) analytical reference standards (adapted from previous studies by Schymanski et al. (2014)).

In-house library comparison for compound identification can improve reliability on identification by comparison of acute and exact masses, MS/MS spectra and tentative retention times (when applying the same chromatographic gradient in sample analysis). Since on-line databases do not always provide information on tentative TPs when reference standards are not available for confirmation, the compilation of the information collected from previous experiments provides additional reliability on TP identification. Despite this, their final confirmation by comparison with reference standards is always required for their unequivocal identification [201].

Reference standard comparison is classified as the most reliable strategy for compound confirmation [138]. However, it is well known that most of the TPs generated in wastewater treatment are still unknown. Therefore, this confirmation strategy may represent a very low percentage compared to the total number of TPs generated. This strategy is used as a final confirmation for those TPs tentatively identified by means of the strategies mentioned above.

1.6 Integrated suspect methodologies for the identification of hazardous TPs

The suspected intermediates generated from the incomplete degradation of pollutants in treated effluents are of significant concern since they can retain part of the biological activity of their parent compounds and, on occasion, be also more persistent and toxic [80]. The application of *in vitro* and *in vivo* bioassays (in alive organisms such as *Vibrio fischeri* or *Salmonella*) have been widely applied to understand the relationship between the presence of TPs in complex mixtures with the effects measured in those samples [202]. For instance, some bioassays have been applied to tentatively identify the environmental effects of TPs after biological processes [142,203], and physico-chemical treatments [174,204,205]. However, only in a few cases, it was possible to clearly attribute the bioactivity measured in samples to the presence of an specific intermediate identified (key-hazard intermediate) [206,207]. The application of automated suspect screening methodologies combined with bioanalytical approaches can overcome this challenge. The main drawback relies on the lack of reference standards for confirmation of the individual hazardous effects of TPs. Despite this, different integrated strategies have been suggested based on quantitative structure-activity relationship (QSARs) models, bioassays with statistical approaches, and effect-directed analysis (EDA).

1.6.1 Quantitative structure-activity relationship models

The quantitative structure-activity relationship models (QSARs) allow us to estimate the hazardous effects of unknown TPs by the correlation of their molecular structures with their potential biological effects estimated *in silico* [208]. For the development of these computational models, the effects of a large number of known substances (previously measured using *in vitro* and *in vivo* bioassays) are computationally assessed to elucidate potential relationships between their molecular structures and their measured activity [209]. In combination with suspect screening identification approaches, QSARs can represent a useful tool for estimating the biological activity and toxicological effects of the intermediate generated, even when no reference standards are available for confirmation [150]. Many different QSAR models have already been developed for the identification of the hazardous intermediates present in wastewater treated samples [209–215]. The EPI Suite and the Toxicity Estimation Software Tool (T.E.S.T.) models, both developed by the Environmental Protection Agency (EPA), are the most applied ones [209–213]. However, many other computational models have been developed to evaluate the impact of TPs in environmental samples such as Toxtree [214], CAESAR [214] and CASE Ultra [215] models and considering not only acute toxicity but also other the following endpoints: mutagenicity, carcinogenicity, developmental toxicity and biodegradability, among others.

1.6.2 Combination of bioassays with statistical approaches

The application of statistical approaches, such as principal component analysis (PCA), has been also suggested for the identification of hazardous TPs in water treatment processes. This statistical approach allows us to computational correlate the toxicity found in treated effluents (using *in vitro* or *in vivo* bioassays) with the relative presence of each intermediate during wastewater treatment processes. This strategy has been applied in a few cases attaining high confidence in effect identification [156,216]. For its applicability, the relative areas of identified TPs (area of the peaks detected in chromatogram divided by the area of the chromatographic peak of the parent compound at the initial time) and the effects measured at each sampling point are loaded and treated statistically [156]. In comparison to QSAR models, the performance of *in vitro* and *in vivo* bioassays of treated samples allows the estimation of key-

toxicants based on experimental measurements rather than predictions based on tentative computational models.

1.6.3 Effect-directed analysis

Effect-directed analysis (EDA) can be classified as a promising and more reliable approach for hazard identification when reference standards are not available for confirmation. This methodology is based on the combination of suspect screening methodologies, bioanalytical tools (*in vitro* and *in vivo* bioassays) and preparative liquid chromatography instruments for the elucidation of the hazardous effects of TPs in bioactive samples [217–226]. When potential effects are measured in collected samples, their complexity is gradually reduced using fractionation liquid chromatography to further discard those fractions attaining low or absence of bioactivity [218]. In most cases, several fractionation steps are required until the isolated toxic fractions are ready for toxicant identification [218]. Final analysis of fractions using suspect screening approaches and bioassays are required to confirm the potential key-toxicants identified [222]. In comparison to QSAR models and PCA estimations, higher reliability on hazard identification is attained since experimental bioassays are performed with the isolated intermediates identified. Despite the more than 4000 publications about EDA [218], this approach has been mainly reported using reference standards and/or databases for final confirmation. Indeed, only in a few cases, it has been possible to clearly attribute bioactivity or ecotoxicity to a generated intermediate using EDA and suspect screening approaches [206,207]. This is due to that EDA approaches require advanced analytical instrumentation, complex analysis procedures, high sample volume and the optimization of high-resolution chemical screening methods, which lead to a costly and laborious effort for the identification of few intermediates of concern [227].

1.7 Monitoring of PhACs and their TPs in combined treatments

The presence of a large quantity of TPs with potential hazardous effects on the aquatic environment has promoted the development of advanced wastewater treatments to attain the highest elimination of pollutants in treated effluents. However, it is already known that biological treatments show low capability for the removal of non-biodegradable substances present in wastewater [228]. A suggested solution for their elimination is the application of

advanced technologies such as UV/H_2O_2 [229]. However, chemical oxidation to achieve complete mineralization is sometimes expensive and its applicability is very restricted [228]. In addition, the hazardous intermediates generated during this treatment should be eliminated previous to wastewater discharge [230–232]. In this context, some researchers have evaluated the application of combined biological and physico-chemical treatments to attain an extended removal of PhACs [233–239]. However, most of these studies only assess the removal of the parent compound to evaluate the efficiency of wastewater treatments, but no attention has been paid to the generation and elimination of those intermediates generated. The development of automated suspect screening methodologies can represent a useful tool for the rapid monitoring of the removal of the TPs generated and their parent compounds during advanced and combined water treatments. Up to now, the suspect screening methodologies developed are far from their application in laboratories as routine analysis, and thus, many advances in this field are still required.

Chapter 2

Objectives

The main goal of this doctoral thesis is the development of suspect screening methodologies for the rapid identification of the TPs generated from PhACs in biological and physical and/or chemical water treatments. These methodologies were applied for the elucidation of their chemical structures, their hazardous environmental effects, and evaluate their formation/removal in combined treatment studies. The secondary objectives are thus the following:

i. To rapidly identify the TPs generated from PhACs in biological and physical and/or chemical water treatments when analytical reference standards are not available for confirmation.

ii. To study the elimination and transformation of PhACs pollutants, i.e. biotransformation, photo-transformation, hydrolysis, and sorption occurring in biological water treatments (fungi and microalgae).

iii. To study the removal and transformation of PhACs pollutants, i.e. photo-transformation and hydrolysis mechanisms occurring in physical and/or chemical water treatments (UV/H_2O_2 and chlorination).

iv. To evaluate the hazardous effects of the TPs generated in physical and/or chemical water treatments using the combination of automated suspect screening methodologies with *in vitro* bioassays and *in silico* methods (including QSARs, PCA and EDA approaches).

v. To monitor the removal of the hazardous TPs identified in treated effluents by the combination of biological (fungi and CAS) with physico-chemical (UV/H_2O_2) treatments.

Chapter 3

Automated suspect screening methodologies for the identification of pharmaceutical TPs in biological treatments

Jaén-Gil et al., 2019. Water Research, 152: 171 – 180

Jaén-Gil el al., 2018. Journal of Chromatography A, 1568: 57 – 68

Water Research 152 (2019) 171–180

Contents lists available at ScienceDirect

Water Research

journal homepage: www.elsevier.com/locate/watres

Fungal treatment of metoprolol and its recalcitrant metabolite metoprolol acid in hospital wastewater: Biotransformation, sorption and ecotoxicological impact

Adrián Jaén-Gil [a], Francesc Castellet-Rovira [b], Marta Llorca [c], Marta Villagrasa [a], Montserrat Sarrà [b], Sara Rodríguez-Mozaz [a, *], Damià Barceló [a, c]

[a] Catalan Institute for Water Research (ICRA), H_2O Building, Scientific and Technological Park of the University of Girona, Emili Grahit 101, E-17003, Girona, Spain
[b] Chemical, Biological and Environmental Engineering Department, Universitat Autònoma de Barcelona (UAB), E-08193, Bellaterra, Spain
[c] Water and Soil Quality Research Group, Department of Environmental Chemistry, (IDAEA-CSIC), Jordi Girona 18-26, E-08034, Barcelona, Spain

ARTICLE INFO

Article history:
Received 1 August 2018
Received in revised form
21 December 2018
Accepted 22 December 2018
Available online 10 January 2019

Keywords:
Metoprolol
Metoprolol acid
Fungal water treatment
Fungal biomass
Suspect screening
Transformation products

ABSTRACT

Hospital wastewater (HWW) effluents represent an important source of contaminants such as pharmaceutical compounds and their human metabolites. To better evaluate dedicated treatment of hospital effluents for pollutant mitigation, not only the parent compounds should be considered but also the intermediates generated during treatment. The metabolite metoprolol acid (MTPA) has been found in urban wastewaters at higher concentration than its parent compound metoprolol (MTP), being more recalcitrant to biodegradation. The aim of this study was to investigate degradation, transformation and sorption of the β-blocker MTP, and its recalcitrant metabolite MTPA, during water treatment based on the fungi *Ganoderma lucidum*, *Trametes versicolor* and *Pleurotus ostreatus*. Fourteen intermediates were identified in MTP biotransformation while five of them also attributed to MTPA biodegradation and two to MTPA only. Their identification allowed their correlation in separate biotransformation pathways suggested. The highest degradation rate of metoprolol (up to 51%) and metoprolol acid (almost 77%) was found after 15-days treatment with *Ganoderma lucidum,* with an increase in toxicity up to 29% and 4%, respectively. This fungus was further selected for treating real HWW in a batch fluidized bed bioreactor (FBB). Treated wastewater and fungal biomass samples were used to evaluate the distribution of the target compounds and the intermediates identified between solid and liquid phases. While similar elimination capabilities were observed for the removal of metoprolol, and even higher for its persistent metabolite metoprolol acid, the extent on compound transformation diminished considerably compared with the study treating purified water: a high level of the persistent α-HMTP and TP240 were still present in effluent samples (15% and 6%, respectively), being both TPs present at high proportion (up to 28%) in fungal biomass. This is the first time that pharmaceutical TPs have been investigated in the fungal biomass.

1. Introduction

In recent years, the presence of pharmaceuticals (PhACs) in the environment has been recognized as one of the most concerning environmental issues (Verlicchi et al., 2012). Every day, large quantities of wastewaters containing a broad variety of chemicals coming from domestic and industrial uses are discharged into sewage system. Hospital wastewater (HWW) in particular, have been recognized as important source of PhACs, where they can be found at several μg/L (Carraro et al., 2016; Verlicchi et al., 2015, 2010). Since there is not a specific directive or guideline in Europe for treating HWW before its disposal (Rodriguez-Mozaz et al., 2018), these effluents are usually released into municipal sewer system without applying any previous water pretreatment. Their contribution at municipal wastewater treatment plants (WWTPs)

* Corresponding author. Catalan Institute for Water Research (ICRA), Scientific and Technologic Park of the University of Girona, Emili Grahit 101, E-17003, Girona, Spain.
E-mail address: srodriguez@icra.cat (S. Rodríguez-Mozaz).

https://doi.org/10.1016/j.watres.2018.12.054
0043-1354/

range approximately from 0.2% to 2% of total wastewater volume (Carraro et al., 2016). Considering that conventional WWTPs are not designed to completely eliminate these emerging contaminants (Ratola et al., 2012), they can pass through and find their way into the environment. Therefore, the use of alternative on-site wastewater treatments prior to sewer discharge has been highly recommended (Verlicchi et al., 2015), where a decrease of up to 90% on total pharmaceutical load can be achieved (Pauwels and Verstraete, 2006).

Among the different wastewater treatments, activated sludge is currently considered the treatment of choice (Bletsou et al., 2015). However, alternative treatments based on fungi have been reported to be effective in the removal of micropollutants, thanks to its unspecific ligninolytic systems and intracellular enzymatic complexes (Asgher et al., 2008). *Ganoderma lucidum*, *Trametes versicolor* and *Pleurotus ostreatus* (part of the Basidiomycota division and the Agaricomycetes class) have been successfully applied for the elimination of certain pharmaceuticals (Cruz-Morató et al., 2014; Llorca et al., 2018; Marco-Urrea et al., 2009; Palli et al., 2017) with the overall load elimination of 83% in optimal conditions (Cruz-Morató et al., 2014). Among the extracellular enzymes responsible of pharmaceutical degradation lignin peroxidase, manganese peroxidase and laccase are the most important ones (Asgher et al., 2008). The low specificity of these enzymes make the selected fungi suitable for bioremediation processes. However, while some authors have successfully applied this kind of treatment for pharmaceutical removal (Cruz-Morató et al., 2014; Llorca et al., 2018; Marco-Urrea et al., 2009; Palli et al., 2017), less attention has been paid to the transformation products (TPs) generated, which may sometimes be more persistent or toxic than the parent compound (Escher and Fenner, 2011; Jaén-Gil et al., 2018). Considering that not only PhACs are present in HWW effluents but also their human metabolites, the European Medicines Agency (EMA) has set guidelines on environmental risk assessment indicating that relevant metabolites are those excreted in $\geq$10% of the administered dose (Wharf and Kingdom, 2010). Even so, unknown intermediates from these metabolites can also be generated during wastewater treatment. Therefore, their transformation pathways should also be investigated to better understand pollutant mitigation and properly evaluate wastewater treatment processes.

Among the different PhACs therapeutic families of present in HWWs, β-blockers have been widely detected in such effluents due to the its high consumption for hypertension and cardiovascular diseases (Hughes et al., 2013). Some of them are included into the 20 most commonly encountered pharmaceuticals in European waters (Hughes et al., 2013). For instance, metoprolol (MTP) is largely prescribed in Germany reaching values of almost 100 tons per year (Scheurer et al., 2010) and has been detected in wastewater in the range of 160–2000 ng/L (Maurer et al., 2007; Scheurer et al., 2010), with low elimination rates in conventional WWTPs (usually between 0% and 36%) (Lacey et al., 2012; Rubirola et al., 2014; Scheurer et al., 2010). On the other hand, it is well-known that MTP is mainly eliminated in human body, up to 85% throughout hepatic oxidative metabolism, and transformed into O-desmethylmetoprolol (O-DMTP), α-hydroxymetoprolol (α-HMTP) and metoprolol acid (MTPA) metabolites. Among them, MTPA is the major compound eliminated via renal excretion around 60–65% (Escher et al., 2006; Kern et al., 2010), while the other metabolites can also be present in urine but at much lower concentration (Godbillon and Duval, 1984). This metabolite has been found *ca.* one order of magnitude higher concentrations than MTP in wastewater (Mamo et al., 2018; Rubirola et al., 2014), and its persistence during biological treatment has been reported in some studies (Radjenović et al., 2008; Rubirola et al., 2014), indicating its potential environmental relevance. Although many studies have focused on the elimination of MTP in wastewater effluents (Benner and Ternes, 2009; Cavalcante et al., 2015; Romero et al., 2016a, 2016b; 2015; Šojić et al., 2012; Wilde et al., 2014), only few data was found concerning its elimination during HWW treatment (Wilde et al., 2014), and even less testing its fungal biotransformation by fungal treatments (Ma et al., 2007). Moreover, none of the studies exploring the intermediates generated after MTP degradation has investigated the biotransformation of the main metabolite MTPA (Benner and Ternes, 2009; Cavalcante et al., 2015; Koba et al., 2016; Ma et al., 2007; Romero et al., 2016b, 2016a; 2015; Rubirola et al., 2014; Slegers et al., 2006; Šojić et al., 2012; Tay et al., 2013; Wilde et al., 2014).

In this study, degradation, transformation and sorption of MTP and its main metabolite MTPA were investigated in batch experiments with three fungi (*Ganoderma lucidum*, *Trametes versicolor* and *Pleurotus ostreatus*) by using liquid chromatography coupled to high resolution mass spectrometry (LC-LTQ-Orbitrap-MS/MS) through a suspect screening methodology. Treated wastewater and fungal biomass samples were used to evaluate the presence the target compounds and their TPs in both compartments. To the authors' knowledge, this is the first time that pharmaceutical TPs have been investigated in fungal biomass, as well as the first time that biodegradation and biotransformation of MTPA has been studied in wastewater treatment.

2. Materials and methods

2.1. Chemicals and fungi

Metoprolol tartrate salt (MTP) (Sigma-Aldrich); O-desmethylmetoprolol (O-DMTP), metoprolol acid (MTPA) and α-hydroxymetoprolol (α-HMTP) (Toronto Research Chemicals); and atenolol-d_7 internal standard (CDN isotopes, Quebec, Canada) were purchased at high purity grade (>98%). Ultra-pure water and acetonitrile LiChrosolv grade were supplied by Merck (Darmstadt, Germany). Working standard solutions were prepared in methanol/water (10:90, v/v). Solid phase extraction (SPE) cartridges Oasis HLB (60 mg, 3 mL) were from Waters Corporation (Milford, MA, USA).

Three different species of fungi from different collections were used: *Ganoderma lucidum* (WRF) FP-58537-Sp strain, United States Department of Agriculture, Madison, Wis. Collection; *Trametes versicolor* (WRF) (American Type Culture Collection #42530 strain); and *Pleurotus ostreatus* was isolated from a fruiting body collected from rotting wood, identified through molecular analysis (Palli et al., 2017). *G. lucidum* and *T. versicolor* were subcultured on 2% malt extract agar petri plates while *P. ostreatus* was maintained on malt extract agar (MEA) plates (ATCC medium 325).

Pellet immobilization was achieved for all the fungi following the same procedure described previously (Blánquez et al., 2004). The pellets obtained by this process were washed with sterile deionized water and kept (if needed) in a 0.8% NaCl solution at 4 °C.

2.2. Fungal degradation experiments

Experiments for MTP and MTPA elimination were performed in 250 mL Erlenmeyer flasks for 15 days with *G. lucidum, T. versicolor* and *P. ostreatus* fungi. For each fungus, experiments were carried out in triplicate by spiking selected compounds individually at a concentration of 2.5 mg/L in 100 mL of a defined medium, which consists of 8 g/L of glucose, 3.3 g/L of ammonium tartrate, 1.168 g/L of 2,2-dimethylsuccinate buffer, and 1 and 10 mL of a micronutrient and macronutrient solution from Kirk medium (Kirk et al., 1978). The pH was adjusted to 4.5 before sterilization at 121 °C for 30 min. Flasks were inoculated with pellets equivalent to 3.5 ± 0.8 g/L dry cell weight (DCW). To better assess the different biotransformation

regarding the parent compounds selected (MTP and MTPA), the experimental procedure was performed for each compound separately. Additionally, abiotic control (same conditions described above but without biomass), live control (same conditions but without spiking compounds) and killed control experiments (same conditions but with heat-killed biomass) were also performed in triplicate and used to evaluate other potential physicochemical processes affecting pharmaceutical transformation and sorption. All experiments were performed under natural light conditions and temperature maintained at 25 °C. Samples were collected along 15 days and further centrifuged in glass vials to separate fungus from water phase. Then, 100 μL of internal standard were added to achieve a final concentration of 100 μg/L. Finally, samples were directly injected into the LC-LTQ-Orbitrap-MS/MS system (see the following section 2.4.).

2.3. Fluidized bed bioreactor experiments

Biodegradation, biotransformation and sorption of target pollutants and their TPs were investigated along 7 days in a non-sterilized 0.5 L air-pulsed fluidized bed bioreactor (FBB) treating HWW. The HWW was collected directly from the sewer manifold of Sant Joan de Déu Hospital (Barcelona, Catalonia) and pretreated with coagulation-floculation, which involved the addition of coagulant HyflocAC50 at 43 mg/L during 2 min at 200 rpm and flocculant HimolocDR3000 at 4.8 mg/L for 15 min at 20 rpm (Derypol, Barcelona, Catalonia). Wastewater characteristics were: pH range of 7.8–8.7; chemical oxygen demand (COD) of 633–1012 mg/L O_2; $N{-}NH_4^+$ of 9.9–36 mg/L and total suspended solids (TSS) of 193–284 mg/L. Finally, the pH of wastewater was adjusted to 4.5. Concerning bioreactor operation, the FBB experiments were inoculated in duplicate with *G. lucidum* mycelial pellets equivalent to 2.5 ± 0.8 g/L dry cell weight. Electrovalve was set to supply 1 s of air pulse every 2 s and the aeration rate was 0.8 L/min. Glucose and ammonium chloride were supplied at 7.5 C/N molar ratio from concentrated stock solutions in fed-batch operation mode at consumption rate (0.8 g $C_6H_{12}O_6$ g DCW^{-1} and 0.19 g NH_4Cl g DCW^{-1}). In an attempt to reproduce more realistic conditions, MTP and MTPA were spiked simultaneously at a concentration level of 2.0 ± 0.5 μg/L each. Samples were taken at time 0 and 7 days of operation and further centrifuged in glass vials to separate fungus from water phase. To avoid possible experimental changes during the experiments, *G. lucidum* biomass samples were taken at final experimental time of 7 days only. Then, HWW samples were treated following an SPE methodology described elsewhere (Gros et al., 2012). On the other hand, fungal biomass samples were treated following the solid extraction methodology reported previously (Lucas et al., 2018). Detailed sample preparation procedures are presented in Supplementary Material, S1. Both, water and fungal extracts were reconstituted in 100 μL of methanol/water (10:90, v/v) containing internal standard to a final concentration of 100 μg/L in vial for further injection into LC-LTQ-Orbitrap-MS/MS (see the following section 2.4.)

2.4. Instrumental analysis

Samples collected from flasks experiments and FBB extracts (from wastewater and fungal biomass) were analyzed in a liquid-chromatography system coupled to a hybrid linear ion trap (LTQ)-Orbitrap mass spectrometer. Detection of MTP and MTPA as well as their tentative TPs was performed via a suspect screening methodology using a ready-made list of accurate masses selected from literature, included prior to sample analysis for MS/MS fragmentation (Table S1). Data was acquired in data-dependent acquisition mode (DDA) using collision-induced dissociation (CID) and higher-energy collisional dissociation (HCD) fragmentation energies. For those compounds where reference standards were available (MTP, MTPA, O-DMTP and α-HMTP), verification was performed by comparison with retention times and MS/MS ion fragmentation patterns. When reference standards were not commercially available, confirmation was performed via structural elucidation of MS/MS fragmentation patterns using Mass Frontier 7.0 software (Thermo Scientific). More detailed information of sample analysis is presented in Supplementary Material, S2. After identification, peak area measurement of MTP, MTPA and TPs was performed using the equations presented in Section 2.5. Additionally, accurate quantification of MTP and MTPA in water and biomass of HWW experiments was also performed (see Table S2 for analytical quality parameters).

2.5. Data processing

2.5.1. Elimination of MTP and MTPA in fungal flask experiments

The removal efficiency of MTP and MTPA for the three fungus selected were evaluated along the performed flasks experiments. The contribution of abiotic processes to elimination was calculated using Eq. (1), where A_0 is the area at initial time and A_x^{ac} is the area measured at a particular sampling time in the abiotic control experiments:

$$\textit{Abiotic degradation}\ (\%) = \frac{A_0 - A_x^{ac}}{A_0} \tag{1}$$

Elimination by sorption was calculated using Eq. (2), where A_x^{kc} is the area at the same particular sampling time in killed control experiments:

$$\textit{Sorption}\ (\%) = \frac{A_x^{ac} - A_x^{kc}}{A_0} \tag{2}$$

Finally, biodegradation was calculated using Eq. (3), where A_x^{de} is the area measured in fungal degradation experiments at the certain experimental time:

$$\textit{Biodegradation}\ (\%) = \frac{A_x^{kc} - A_x^{de}}{A_0} \tag{3}$$

2.5.2. Distribution of pollutants in liquid and biomass solid phases in the fluidized bed bioreactors

The distribution of spiked pollutants (MTP and MTPA) in HWW and fungal biomass was calculated using Eq. (4) where A_x^L is the chromatographic area in liquid phase at a specific experimental time, and A_0^L is the area of MTP or MTPA at initial time (all estimated for the total FBB volume of 0.5 L) corrected by the corresponding recovery value in HWW (quality parameters and concentration values are presented in Table S2):

$$\textit{Presence in liquid phase}\ (\%) = \left(\frac{A_x^L}{A_0^L}\right) \tag{4}$$

The presence of MTP and MTPA in solid phase was calculated as it can be seen in Eq. (5), where A_x^S is the corresponding area in the solid phase at a certain experimental time (estimated for the total biomass of 2.5 g/L dry weight), and A_0^L is again the spiked area in liquid phase at initial time (estimated for the total FBB volume of 0.5 L). All areas were also corrected by the recovery values calculated in the corresponding liquid and solid phases (quality parameters and concentration values are presented in Table S2):

$$Presence\ in\ solid\ phase\ (\%) = \left(\frac{A_x^S}{A_0^L}\right) \quad (5)$$

Since reference standards for TPs were not available, a proper quantification was not feasible. However, in order to provide tentative values of the presence of TPs in HWW and fungal biomass, Eq. (4) and Eq. (5) were used considering A_0^L as the sum of MTP and MTPA areas corrected by the mean recovery value of these compounds in liquid (91%) and solid biomass (46%) phases.

2.6. Toxicity evaluation

The ISO 11348-3 protocol (ISO, 1998) for testing bacterial bioluminescence was applied to evaluate acute toxicity of samples along the experiments using the Microtox® Model 500 Toxicity Analyzer (Strategic Diagnostics Inc. Newark, DE, US). For this purpose, all flasks and FBB water samples were centrifuged in glass vials to remove any biomass fragments or suspended solids interfering. Then, the percentage of decay on emitted light was measured when samples were in contact with the bioluminescent bacterium *V. fischeri.* The 50% effective concentration (EC_{50}) was measured after 15 min (expressed in dilution percentage). Changes in toxicity (EC_{50}) at a particular experimental time were calculated in percentage as $(EC_{50(initial)} - EC_{50(x)})/EC_{50(initial)}$ adapted from Font et al. (2003).

3. Results and discussion

3.1. Elimination processes of MTP and MTPA in fungal flasks experiments

Elimination processes such as biodegradation, fungal sorption and other abiotic processes of MTP and its main metabolite MTPA were evaluated in flasks experiments. Fig. 1 summarizes MTP and MTPA presence decay in the different experiments performed as well as the sum of TPs measured for the three-fungal species tested (whose identity is described in Section 3.2). As expected, MTP, MTPA and TPs were not detected in live (non-spiked) control conditions. Abiotic control experiments showed negligible MTP and MTPA elimination which evidences their high chemical stability. In fungal degradation experiments, partial elimination of MTP was achieved reaching removal values as high as 51%, 49% and 17% in water treated with *G. lucidum*, *T. versicolor* and *P. ostreatus* respectively, with high contribution of sorption processes (*ca.* 25 ± 3% of initial compound amount) in all species tested. Only in the experiments with *G. lucidum*, biodegradation is pointed out as the main removal mechanism reaching values up to 28% (Table 1), whereas it was lower in the experiments performed with *T. versicolor* (21%) and not existing in the case of *P. ostreatus*. In any case, overall elimination achieved for MTP by fungi (between 17% and 51%) was lower than that obtained in former activated sludge flasks experiments where MTP was spiked at similar concentration (1 mg/L) and biomass (3 gTSS/L), and where total MTP elimination was achieved after 96 h (Rubirola et al., 2014). Nevertheless, despite from the removal of target pollutants, the generation and elimination of their corresponding TPs should also be considered to properly assess the efficiency of fungal treatment (intermediates are further discussed in Section 3.2). To this respect, higher generation of TPs was observed for those experiments exhibiting higher MTP biodegradation rates (Fig. 1). In general, the highest generation of TPs was observed after 7 days of treatment and maintained until the end of the experiments. This fact indicates that, even though MTP was eliminated during the experiments, the elimination of the TPs generated was not accomplished in the same manner.

MTPA was more extensively removed than MTP yielding values up to 77%, 54% and 35% in water treated with *G. lucidum*, *T. versicolor* and *P. ostreatus,* respectively (Fig. 1). Nonetheless, results reveal lower contribution to sorption processes compared to those values obtained in MTP experiments; biomass sorption percentages ranged from 0% to 11% (Table 1). These levels should be explained by the different partition coefficients of both compounds. However, the predicted distribution coefficients *logD* values for MTP and MTPA at pH 4.5 were quite similar, indicating their low tendency to be present in solid phase (−1.48 for MTP and −1.27 for MTPA calculated with ChemAxon (ChemAxon Chemicalize Calculator, 2018)) and without a direct correlation (*logD*) with actual sorption of MTP and MTPA in fungal biomass. Biodegradation was thus pinpointed as the main removal mechanism for MTPA with the three fungi tested (Fig. 1). Among them, *G. lucidum* was pointed out as the most effective fungus reaching biodegradation values around 63%, being 11% accounted as sorption contribution to total removal (Table 1). *T. versicolor* and *P. ostreatus* attained lower biodegradation rates of about 48% and 32% percentages, respectively. In accordance to this, *G. lucidum* was also reported as the most efficient fungus for biodegradation of venlafaxine and O-desmethylvenlafaxine (spiked at 5 mg/L) with total removal values up to 70% and 100%, respectively (Llorca et al., 2018). The optimal removal of MTPA with these fungi needs to be highlighted since it was previously reported as a concerning metabolite, given its high persistence in previous batch activated sludge experiments, generated from the biodegradation of MTP spiked at 1 mg/L (Rubirola et al., 2014), and from atenolol spiked at 10 mg/L (Radjenović et al., 2008). As in the case of MTP experiments, the highest concentrations of MTPA TPs were measured when the highest MTPA biodegradation rates were registered; *i.e.* after 9 and 15 days of treatment with all three fungi tested. Actually, high levels of MTP and MTPA intermediates (between 7% and 31% for MTP degradation and from 51% to 100% for MTPA transformation, Fig. 1) were always detected at the end of corresponding experiments, which underlines the inability of fungal treatments for total compound mineralization, and the generation of a large quantity of new chemical structures. Thus, their identification, toxicity as well as the elucidation of their transformation pathways are necessary to evaluate the performance of a particular water treatment.

3.2. Identification and monitoring of suspected TPs in fungal flasks experiments

A suspect screening methodology for the detection of tentative TPs was applied based on the comparison of accurate masses obtained after compound detection with those gathered from literature. Since multiple peaks can be detected for the same exact mass, comparison with retention times (when reference standards are available) and chemical structure elucidation based on the MS/MS data were performed for confirmation purposes (Supplementary Material, S5). A summary of accurate masses, elemental composition and tentative chemical structures of TPs detected are presented in Table S3. In accordance to the European Commission Decision 2002/657/EC, measurements were always within mass error of 5 ppm by means of MS^n analysis. This criterion was considered enough to assign the elemental compositions and chemical structures of both parent and fragment ions. Firstly, fragmentation scans were elucidated by using those data acquired in CID fragmentation energy. However, this approach was considered insufficient to discern among similar TP structures. Therefore, HCD fragmentation energy was necessary to obtain complementary small fragments to finally confirm the tentative chemical structures. Once the structures were elucidated (Table S3), proposed degradation pathways were tentatively suggested and

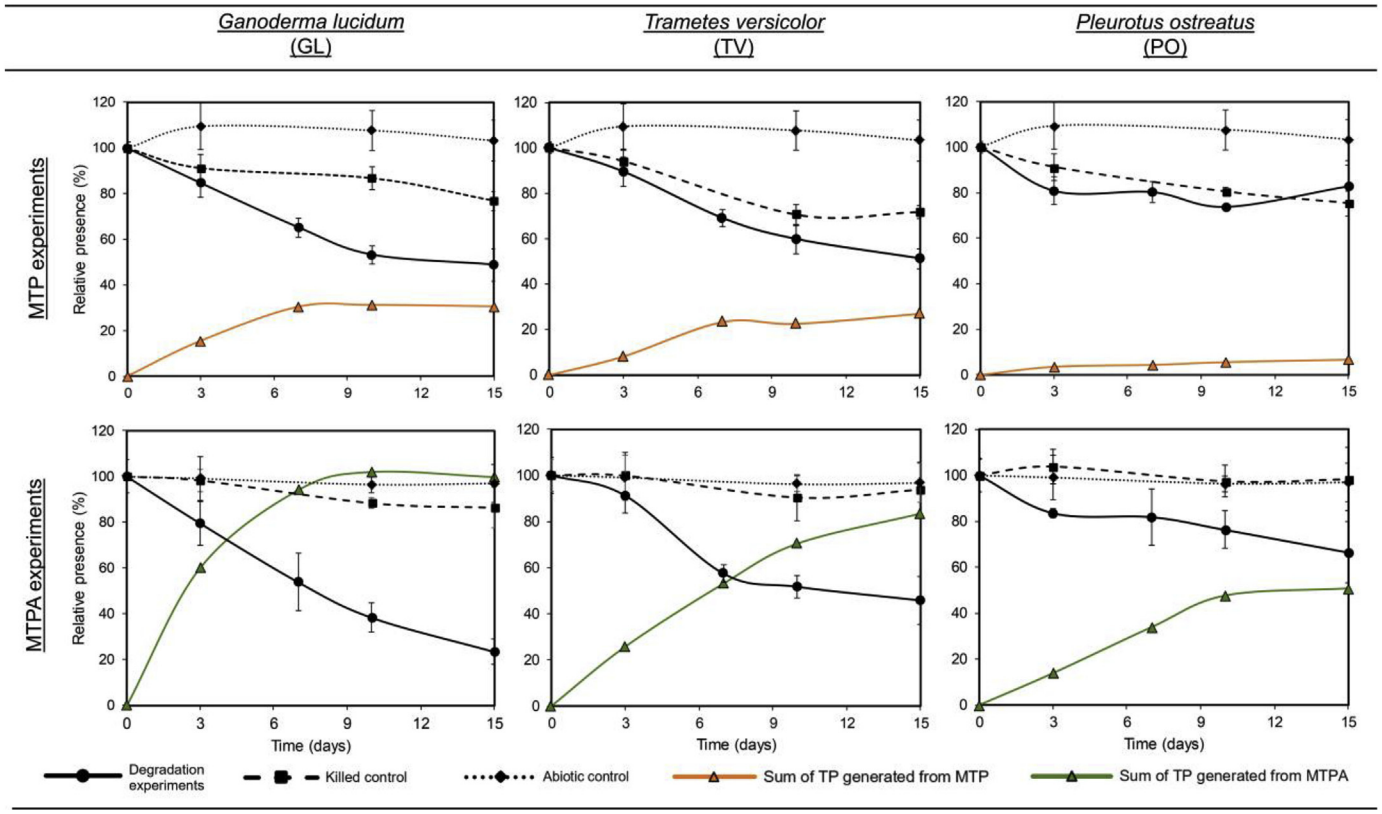

Fig. 1. MTP, MTPA and TP relative presence (A/A_0)-(%) in water samples along the time from abiotic control and fungal conditions, both heat-killed control and fungal degradation experiments with *G. lucidum*, *T. versicolor* and *P. ostreatus*. Colored lines indicate the sum of TPs generated in fungal degradation experiments.

Table 1
Abiotic degradation, sorption and biodegradation percentages of MTP and MTPA along *G. lucidum* (GL), *T. versicolor* (TV) and *P. ostreatus* (PO) experiments along 15 days of treatment. Calculations were performed using Eqs. (1)–(3).

Degradation mechanism	Fungi	MTP				MTPA			
		0d	3d	10d	15d	0d	3d	10d	15d
Abiotic degradation (%)	–	0	0	0	0	0	1	4	3
Sorption (%)	GL	0	9	13	23	0	1	8	11
	TV	0	6	29	28	0	0	6	3
	PO	0	9	20	25	0	0	0	0
Biodegradation (%)	GL	0	6	34	28	0	19	50	63
	TV	0	5	11	21	0	9	39	48
	PO	0	10	6	0	0	20	21	32

presented in Fig. 2. Those compounds with relative abundances higher than 1% were chosen for further consideration.

3.2.1. Metoprolol biotransformation

Fourteen major TPs were tentatively identified along fungi experiments from MTP biodegradation (Fig. 2). Relative TP percentages obtained for the three fungi tested are presented in Fig. 3. Among them, no intermediates were detected in abiotic conditions indicating the absence of any chemical degradation in further MTP elimination. Regarding fungal degradation experiments, the highest number of intermediates was detected after 15 days of treatment, when MTP had already been eliminated in all fungi tested. Among them, TP238, α-HMTP, TP282A, TP284, TP300, TP316 and TP134 were classified as the major compounds detected coming from biotransformation mechanisms such as hydroxylation, oxidation and O-dealkylation (Bletsou et al., 2015). Although these TPs were widely detected in water treated with advanced oxidation processes (AOPs) (Cavalcante et al., 2015; Romero et al., 2016a; Wilde et al., 2014), the presence of the cytochrome P450 in fungi species was also suggested to generate them through enzymatic oxidation (Meunier et al., 2004). Moreover, the enzymes known as lignin peroxidases (LiP) and manganese–dependent peroxidases (MnP), also present in these fungal species, allow to carry out oxidative reactions such as carbon–carbon bond cleavages, demethylations, hydroxylations and benzylic alcohol oxidations (Barr and Aust, 1994).

In this study, the most significant degradation pathway, with generation of O-DMTP, TP240, TP238 and TP254 (Fig. 3), was identified in all fungi experiments, being especially notorious for those experiments with higher MTP biodegradation rates. Among them, TP238 was identified as the most persistent compound generated at 9% in the experiments with *G. lucidum*, and further transformed into TP254 (at 1%) after 15 days of treatment. The formation of TP238 and TP240 were suggested after O-demethylation of MTP and further benzylic hydroxylation through the formation of a radical intermediate (after hydrogen abstraction and stabilized by resonance) of O-DMTP (also a human metabolite), detected at low concentration (up to 1% in *T. versicolor*). The rapid metabolization/biodegradation of O-DMTP in fungal experiments was in agreement with the results obtained in MTP degradation experiments with activated sludge, where the complete elimination of this TP was achieved after 48 h and a maximum concentration observed at 24 h operation (Rubirola et al., 2014). Further TP240 was also classified as a non-recalcitrant compound being detected at < 1%, however, O-DMTP was rapidly transformed into TP238 and TP254 in pure water. This last compound generated from the oxidation of the aldehyde intermediate onto a carboxylic acid (in TP254) could be related to lignin peroxidases (LiP), manganese-

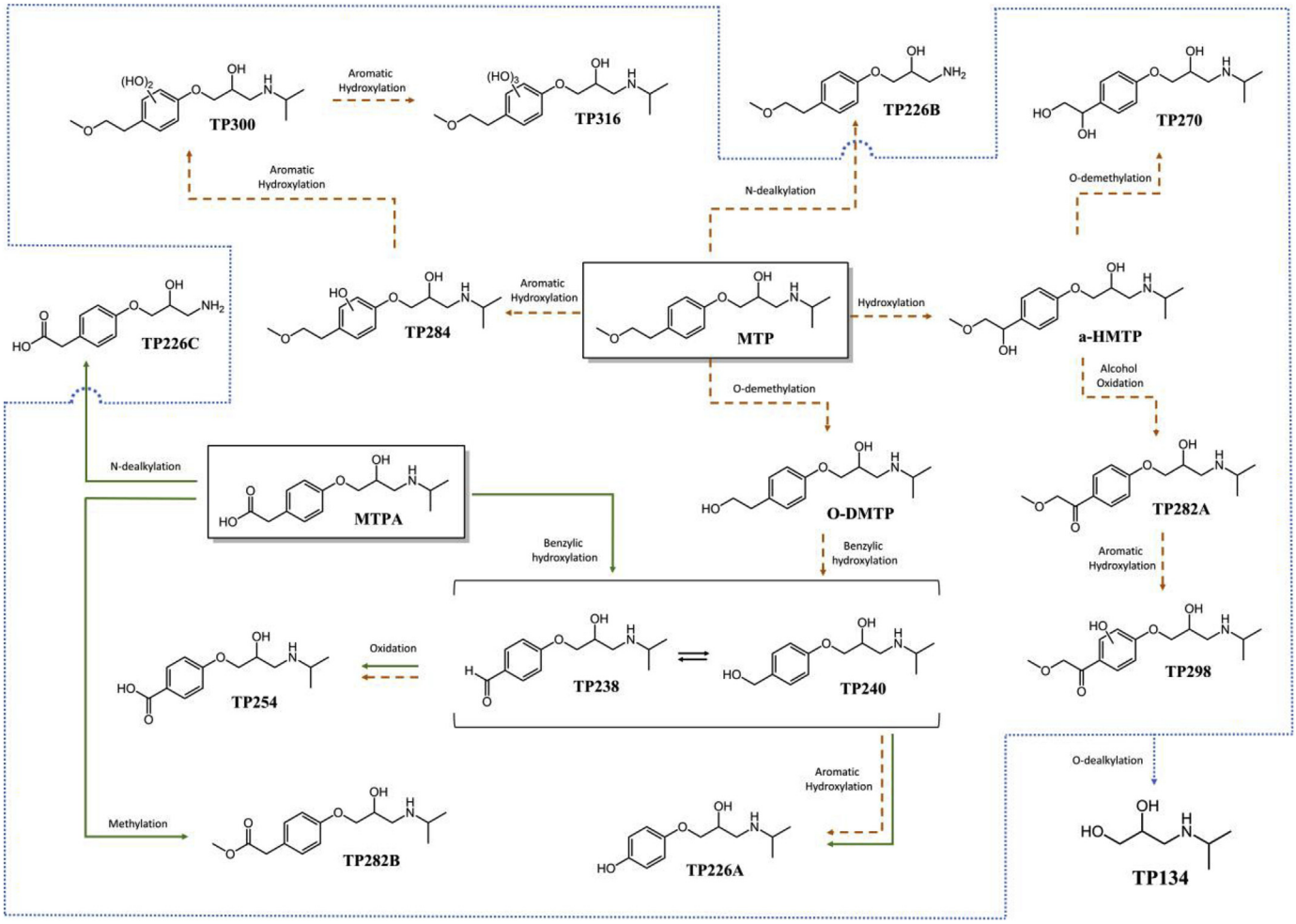

Fig. 2. Transformation pathways suggested of MTP (dotted orange lines) and its main metabolite MTPA (solid green lines) elucidated from *G. lucidum*, *T. versicolor* and *P. ostreatus* fungal degradation experiments. MTP, MTPA and all intermediates identified except TP226B and TP226C may generate TP134. (For interpretation of the references to color in this figure legend, the reader is referred to the Web version of this article.)

dependent peroxidases (MnP) and/or cytochrome P450 enzymes (Barr and Aust, 1994). A secondary degradation pathway was suggested with generation of α-HMTP (another human metabolite generated after pharmaceutical consumption) followed by TP282A and TP298. α-HMTP was found up to 5% in the experiments with *G. lucidum* and *T. versicolor,* where higher MTP biodegradation rates were observed. Further oxidation to TP282A and hydroxylation to TP298 was found with gradually lower occurrence comparing to α-HMTP, which indicates the great persistence of α-HMTP in fungal treatments, as well as in treatments performed with activated sludge (Rubirola et al., 2014). The last degradation pathway was characterized by the multiple oxidations of aromatic ring with formation of the intermediates TP284, TP300 and TP316, especially notorious throughout *T. versicolor* biodegradation. As it can be seen, the TP284 was generated and rapidly transformed to the subsequent TP300. The same profile was identified for this last TP being practically degraded at 15-days treatment to further generate TP316 up to 6%. These compounds could be generated from the unspecific and aromatic peroxygenase (UPO) also secreted by fungi, able to catalyse the hydroxylation of aromatic rings and alkyl chains (Hofrichter et al., 2010). Finally, other TPs worth to mention are TP134, formed from the transformation of those TPs with secondary amine structure (Fig. 2). Since it can be designed as a residual TP, its formation might be considered as an indicator to evaluate the extent of mineralization through O-dealkylation catalysed by cytochrome P450 monooxygenases (Urlacher and Girhard, 2012). In fact, the presence of TP134 increased at the same time as biodegradation values of the parent compound (Table 1). Another remarkable aspect to consider in fungal degradation experiments is that MTPA is not generated from MTP biodegradation whereas in activated sludge experiments was identified as the major TP, with levels up to 40% of initial MTP concentration after 96 h treatment (Rubirola et al., 2014); and when atenolol was spiked at 10 mg/L in 26 days of treatment reaching values up to 60% (Radjenović et al., 2008). Likewise, MTP biotransformation into MTPA metabolite achieved conversion values of 59% in experiments performed with fungus *Cunninghamella blakesleeana* (Ma et al., 2007). Since the presence of TP226C and TP282B were also negligible in MTP fungal experiments, it seems that this transformation pathway does not take place along fungal water treatments with *G. lucidum*, *T. versicolor* and *P. ostreatus*. In fact, the high relative percentages of TP238 compared to the other TPs formed denoted a significant prioritization of its transformation pathway instead of the metabolic pathway that favours the generation of MTPA metabolite. However, the rapid degradation rate of MTPA intermediates prior to sampling at 3 days of treatment cannot be discarded. This difference on metabolite formation depending on the treatment used was also observed in man, dogs and rats where the same MTP

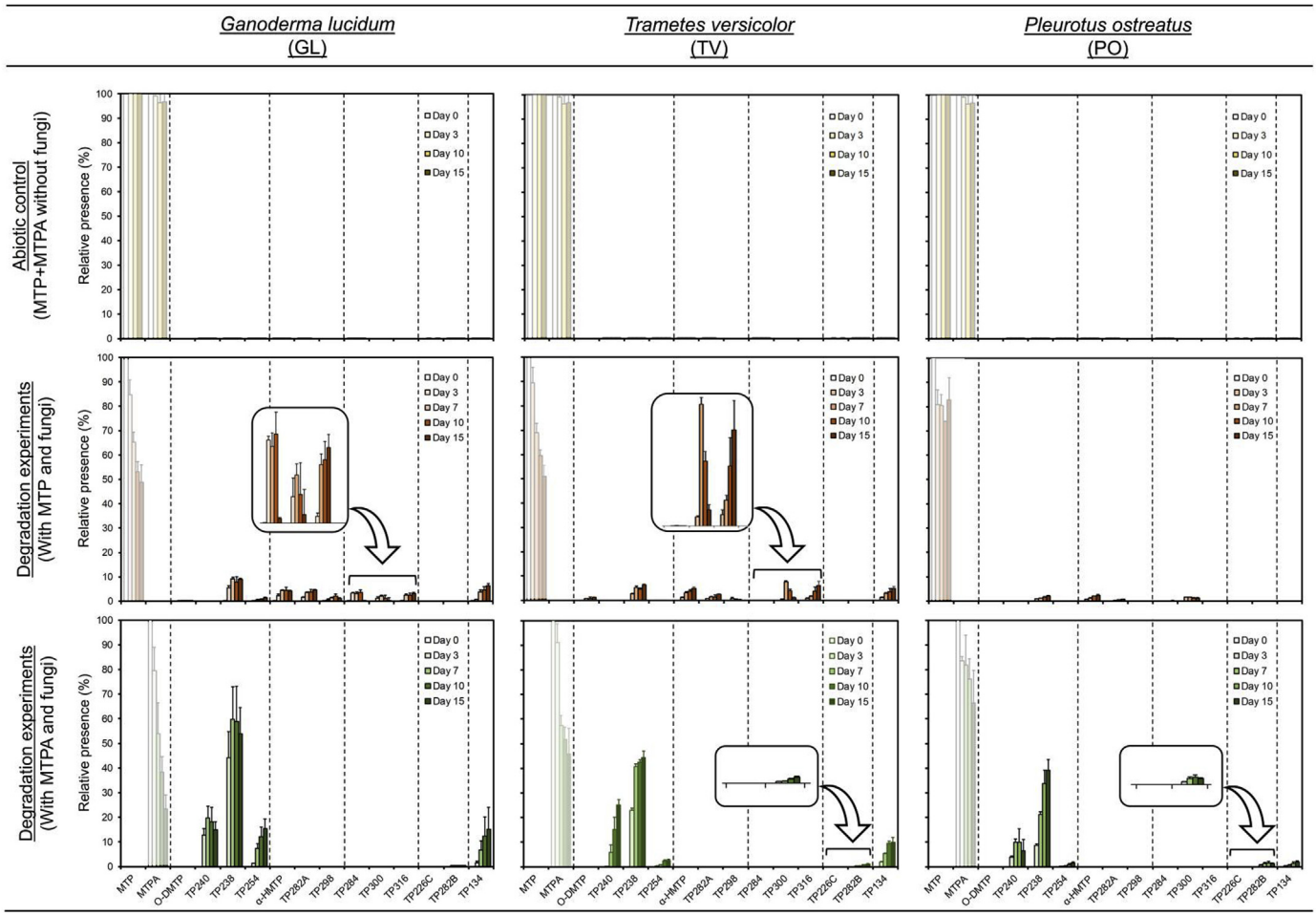

Fig. 3. MTP, MTPA and TP relative presence (A/A_0)-(%) in abiotic control and fungal degradation experiments with *G. lucidum*, *T. versicolor* and *P. ostreatus* along 15 days of treatment. TPs are grouped based on their direct connection in degradation pathways.

metabolites were recovered but in different relative proportions (Borg et al., 1975). Therefore, the presence of such recalcitrant MTPA in biological based treatment technologies was thus depending on the organisms used for water treatment.

3.2.2. Metoprolol acid biotransformation

Seven major TPs were tentatively identified during MTPA biodegradation experiments (Fig. 2). Relative TP percentages obtained for the three fungi tested are presented in Fig. 3. Also in this case, no intermediates were detected in abiotic conditions indicating the absence of factors involved in MTPA transformation. Among them TP238, TP240, TP254 and TP134 were classified as the major compounds detected in fungal degradation experiments. As expected, the highest presence of TPs was found after 15 days of treatment when the maximum concentration of MTPA had already been eliminated. In contrast to MTP biodegradation experiments, only three biodegradation pathways were suggested. However, the presence of O-DMTP was not detected while the generation of TP240 and TP238 were much higher reaching values up to 60%. Their formation might be also related to a benzylic hydroxylation through the formation of the radical intermediate after hydrogen abstraction (Barr and Aust, 1994). Such high levels allowed the further generation of TP254 up to 15% whereas this compound was only detected at 1% in MTP degradation experiments. The higher biodegradation of MTPA and the reduced number of transformation pathways compared to MTP might explain the higher amount of the TPs detected in MTPA experiments. On the other hand, the generation of TP282B and TP226C was only detected when treating MTPA in fungal experiments, but at low concentration levels. This fact indicates that the transformation pathway involving the generation of TP238 was also prioritized when treating MTPA in single experiments, as observed in MTP fungal biodegradation. In this case, the methylation of MTPA to TP282B could be mediated by the methyltransferases enzymes present in fungi (Wessjohann et al., 2013) while N-dealkylation of TP226C could be catalysed by cytochrome P450 monooxygenases (Urlacher and Girhard, 2012). Otherwise, the high levels of TP134 (more than 2.5 times higher than in MTP experiments), previously suggested as an indicator of mineralization, pointing out the more extended progress in the transformation pathway in fungi experiments but still the incomplete elimination of MTPA TPs.

3.3. Toxicity tests in flasks experiments

Toxicity was monitored in water samples to detect potential toxic TPs generated along the fungal flask experiments. A slightly increase on toxicity values along MTP experiments was observed in all fungi tested (29% in *G. lucidum*, 15% in *T. versicolor* and 24% in *P. ostreatus*, Table S4). In the case of MTPA experiments, a slight increase on toxicity at the end of the experiment was also observed (4%, 11% and 29% for *G. lucidum*, *T. versicolor* and *P. ostreatus*, respectively). These results are higher than those reported in batch

experiments using activated sludge at 1 mg/L of MTP and 3 gTSS/L during 72 h, where no significant differences among toxic units were observed (Rubirola et al., 2014). In the later study, the metabolite O-DMTP from MTP elimination was reported to be the most toxic compound detected (EC_{50} of 18 mg/L). However, in the present study, this TP was always below than 1.5% of the MTP and MTPA initial concentration (2.5 mg/L), probably not enough concentration to elicit any toxicity on *V. fischeri*.

3.4. Monitoring of MTP, MTPA and TPs in HWW treated in a FBB bioreactor

HWW was spiked with both MTP and MTPA at 2 μg/L each in order to be able to follow the fate and transformation of both compounds in a fungal fluidized bed bioreactor using *G. lucidum* in realistic conditions (Maurer et al., 2007; Scheurer et al., 2010). This fungus was selected due to the optimal elimination percentages observed for MTP and MTPA in the flask experiments compared to the other fungi tested. Fig. 4 shows the presence of MTP and MTPA as well as the intermediates present in both liquid and solid phases at initial time and after 7 days of treatment. In contrast to the previous batch experiments under sterile conditions, in the bioreactor the fungus was competing against bacteria for nutrients. In addition, the presence of other contaminants (including pharmaceuticals) in the real HWW could affect fungus metabolism and growth. However, *G. lucidum* treatment was successfully implemented with real HWW and the elimination rates of MTP were rather similar: 33% of MTP elimination in the FBB bioreactor compared to the 35% obtained in flask experiments for the same period of time (7 days). Therefore, other factors involved (*e.g.* organic matter, bacteria, pollutant concentration among others) thus seemed not to interfere excessively in MTP elimination. In fact, MTPA removals in bioreactor were even higher than in batch experiments: 64% of MTPA elimination compared to the 46% obtained in flasks experiments. Although this extent on degradation of MTP was less than those values obtained in CAS experiments (Rubirola et al., 2014), the recalcitrant metabolite MTPA observed was successfully eliminated in fungal experiments. Likewise, direct sorption measures into biomass were also similar to those calculated in the previous flasks experiments, up to 13% and 4% for MTP and MTPA, respectively. These values are in accordance with those measured in the previous study reporting the greater sorption capabilities of *G. lucidum* than *T. versicolor* for pharmaceutical elimination in spiked synthetic medium (Lucas et al., 2018). In the present study, and for the first time, not only the target pollutants were investigated in solid phase biomass, but also the sorption of the different intermediates generated along FBB batch experiments.

Eleven out of sixteen intermediates detected in flasks experiments were also found in water and biomass samples from *G. lucidum* FBB experiments (Fig. 4). Most of them (O-DMTP, TP238, TP282A, TP298, TP300, TP316, TP226C, TP282B and TP134) were detected in water at low percentage values (<5%) comparing to those values obtained in flasks experiments, except α-HMTP at 15% from MTP degradation and TP240 at 6% also generated from MTPA elimination. After 7 days of treatment, most of the TP300 was detected in the biomass solid phase (11%) while α-HMTP (28%) and TP240 (25%) were retained in less proportion in comparison to their presence in HWW liquid phase. These high levels may be related to the sorption of these TPs from liquid phase, but also to the transformation of MTP and MTPA occurring directly in the biomass phase. Regarding the transformation pathway, the extent on MTP and MTPA transformation did not go as far as in flask experiments: TP240 and α-HMTP were still present at high level in FBB effluents (at 6% and 15%, respectively), while their further intermediates (TP254, TP282A and TP298; generated up to 15% in flasks experiments after 7 days of treatment, Fig. 3) were not equally detected in the same real effluents. Likewise, the relative presence of the residual TP134 in *G. lucidum* FBB experiments attained a percentage <1%, lower than those obtained in pure water flasks experiments (4% and 7% from MTP and MTPA degradation, respectively). This lower extent on TP transformation might be related to the presence of other contaminants competing on fungal degradation capacity, as well as natural organic matter. Otherwise, a slight increase on toxicity values about 36% (initial EC_{50} of 64% and final EC_{50} of 41%, expressed in dilution percentage) after wastewater treatment was also observed. This might be associated to the transformation products of other contaminants present in HWW.

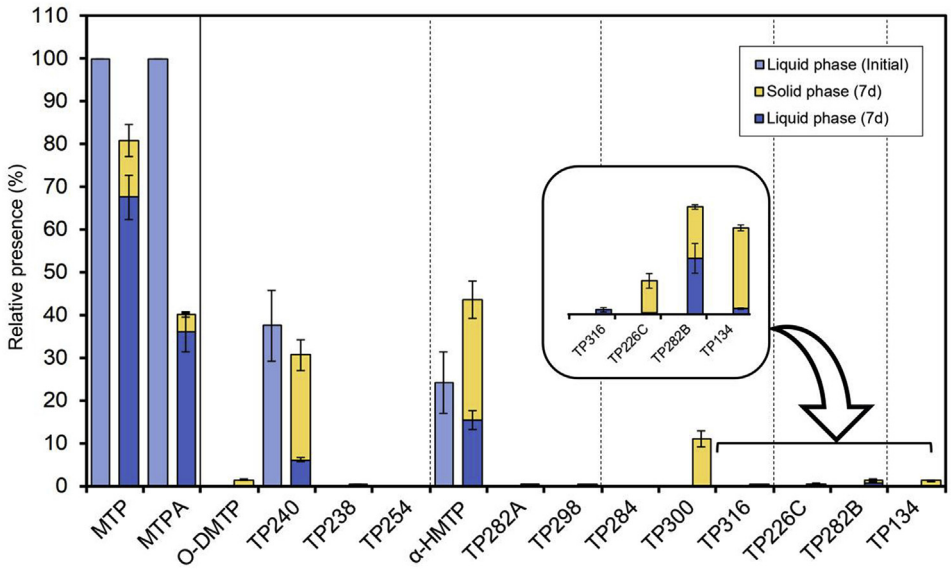

Fig. 4. MTP, MTPA and TP relative presence in water and biomass at 0 and 7 days treating HWW in a FBB bioreactor. Calculations were performed using Eqs. (4) and (5). TPs are grouped based on their direct connection in degradation pathways.

4. Conclusions

Degradation, transformation and sorption capabilities of *Ganoderma lucidum*, *Trametes versicolor* and *Pleurotus ostreatus* fungi were investigated to evaluate the elimination of metoprolol and its recalcitrant metabolite metoprolol acid from water. Fourteen transformation products were detected as generated from MTP biodegradation and within them, five were identified as generated also from MTPA biotransformation. In addition, two TPs were specifically generated from MTPA biodegradation. Results revealed an increase on toxic effects along the fungal treatment of both MTP and MTPA, attributed to the TPs generated from their biodegradation. The maximum efficiency was achieved through *G. lucidum* with removals up to 51% and 77% for MTP and MTPA, respectively (at 15 days of treatment), and therefore, this fungus was further selected for treating HWW in an aerobic fluidized bed bioreactor. Even though degradation rates achieved for MTP were quite similar to those obtained in Erlenmeyer flasks experiments, MTPA removals obtained were even better (64% at 7 days of treatment). However, the extent on compound transformation decreased, with the presence of less transformed and persistent intermediates such as TP240 and α-HMTP, detected and highly eliminated through their generation and/or sorption into solid biomass phase. This is the first time that pharmaceutical TPs have been investigated in the biomass from fungal treatment. A slight increase on toxicity along water treatment was also observed in the experiments with real water, though, in this case, it is not easy to correlate with MTP and MTPA TPs formation, since many other TPs originated form the degradation of other contaminants can also be generated.

Author's contribution

A.J.G., S.R.M., F.C.R., M.L. and M.S. designed the experiment; F.C.R. carried out the fungal bioreactors; A.J.G. performed the sample treatment, chromatographic analysis and data processing; M.V. performed the bioassays; A.J.G. wrote the manuscript; S.R.M and D.B. supervised the writing of the manuscript. All authors reviewed the manuscript and agree on the content.

Acknowledgements

This work was supported funded by the Spanish Ministry of Economy and Competitiveness (CTM2013-48548-C2), partly funded by the European Union through the European Regional Development Fund (ERDF) and supported by the Generalitat de Catalunya (Consolidate Research Group 2017 SGR 14, 2017 SGR 1404 and ICRA-ENV 2017 SGR 1124). The Department of Chemical, Biological and Environmental Engineering of the Universitat Autònoma de Barcelona is a member of the Xarxa de Referència en Biotecnologia de la Generalitat de Catalunya. A. Jaén-Gil acknowledges his PhD scholarship from AGAUR (2018FI_B1_00212), F. Castellet-Rovira acknowledges a predoctoral grant from UAB and S. Rodriguez-Mozaz acknowledges the Ramon y Cajal program (RYC-2014-16707). We would like to thank Sant Joan de Déu Hospital staff for their collaboration during the sampling campaign.

Appendix A. Supplementary data

Supplementary data to this article can be found online at https://doi.org/10.1016/j.watres.2018.12.054.

References

Asgher, M., Bhatti, H.N., Ashraf, M., Legge, R.L., 2008. Recent developments in biodegradation of industrial pollutants by white rot fungi and their enzyme system. Biodegradation 19, 771–783. https://doi.org/10.1007/s10532-008-9185-3.

Barr, D.P., Aust, S.D., 1994. Mechanisms white rot fungi use to degrade pollutants. Environ. Sci. Technol. 28 https://doi.org/10.1021/es00051a002.

Benner, J., Ternes, T.A., 2009. Ozonation of metoprolol: elucidation of oxidation pathways and major oxidation products. Environ. Sci. Technol. 43, 5472–5480. https://doi.org/10.1021/es900280e.

Blánquez, P., Casas, N., Font, X., Gabarrell, X., Sarrà, M., Caminal, G., Vicent, T., 2004. Mechanism of textile metal dye biotransformation by *Trametes versicolor*. Water Res. 38, 2166–2172. https://doi.org/10.1016/j.watres.2004.01.019.

Bletsou, A.A., Jeon, J., Hollender, J., Archontaki, E., Thomaidis, N.S., 2015. Targeted and non-targeted liquid chromatography-mass spectrometric workflows for identification of transformation products of emerging pollutants in the aquatic environment. TrAC Trends Anal. Chem. 66, 32–44. https://doi.org/10.1016/j.trac.2014.11.009.

Borg, K.O., Carlsson, E., Hoffmann, K.-J., Jönsson, T.-E., Thorin, H., Wallin, B., 1975. Metabolism of metoprolol-(3H) in man, the dog and the rat. Acta Pharmacol. Toxicol. (Copenh) 36, 125–135. https://doi.org/10.1111/j.1600-0773.1975.tb03329.x.

Carraro, E., Bonetta, S., Bertino, C., Lorenzi, E., Bonetta, S., Gilli, G., 2016. Hospital effluents management: chemical, physical, microbiological risks and legislation in different countries. J. Environ. Manag. 168, 185–199. https://doi.org/10.1016/j.jenvman.2015.11.021.

Cavalcante, R.P., Dantas, R.F., Wender, H., Bayarri, B., González, O., Giménez, J., Esplugas, S., Machulek, A., 2015. Photocatalytic treatment of metoprolol with B-doped TiO_2: effect of water matrix, toxicological evaluation and identification of intermediates. Appl. Catal. B Environ. 176–177, 173–182. https://doi.org/10.1016/j.apcatb.2015.04.007.

ChemAxon Chemicalize Calculator, 2018 [WWW Document]. https://www.chemaxon.com/ (Accessed 3.20.18).

Cruz-Morató, C., Lucas, D., Llorca, M., Rodriguez-Mozaz, S., Gorga, M., Petrovic, M., Barceló, D., Vicent, T., Sarrà, M., Marco-Urrea, E., 2014. Hospital wastewater treatment by fungal bioreactor: removal efficiency for pharmaceuticals and endocrine disruptor compounds. Sci. Total Environ. 493, 365–376. https://doi.org/10.1016/j.scitotenv.2014.05.117.

Escher, B.I., Bramaz, N., Richter, M., Lienert, J., 2006. Comparative ecotoxicological hazard assessment of beta-blockers and their human metabolites using a mode-of-action-based test battery and a QSAR approach. Environ. Sci. Technol. 40, 7402–7408. https://doi.org/10.1021/es052572v.

Escher, B.I., Fenner, K., 2011. Recent advances in environmental risk assessment of transformation products. Environ. Sci. Technol. 45, 3835–3847. https://doi.org/10.1021/es1030799.

Font, X., Caminal, G., Gabarrell, X., Romero, S., Vicent, M.T., 2003. Black liquor detoxification by laccase of *Trametes versicolor* pellets. J. Chem. Technol. Biotechnol. 78, 548–554. https://doi.org/10.1002/jctb.834.

Godbillon, J., Duval, M., 1984. Determination of two metoprolol metabolites in human urine by high-performance liquid chromatography. J. Chromatogr. B Biomed. Sci. Appl. 309, 198–202.

Gros, M., Rodríguez-Mozaz, S., Barceló, D., 2012. Fast and comprehensive multi-residue analysis of a broad range of human and veterinary pharmaceuticals and some of their metabolites in surface and treated waters by ultra-high-performance liquid chromatography coupled to quadrupole-linear ion trap tandem. J. Chromatogr. A 1248, 104–121. https://doi.org/10.1016/j.chroma.2012.05.084.

Hofrichter, M., Ullrich, R., Pecyna, M.J., Liers, C., Lundell, T., 2010. New and classic families of secreted fungal heme peroxidases. Appl. Microbiol. Biotechnol. 87, 871–897. https://doi.org/10.1007/s00253-010-2633-0.

Hughes, S.R., Kay, P., Brown, L.E., 2013. Global synthesis and critical evaluation of pharmaceutical data sets collected from river systems. Environ. Sci. Technol. 47, 661–677. https://doi.org/10.1021/es3030148.

ISO 11348-3:1998, Determination of the inhibitory effect of water samples on the light emission of *Vibrio fischeri* (Luminescent bacteria test). Int. Organ. Stand. (ISO), 1998.

Jaén-Gil, A., Hom-Diaz, A., Llorca, M., Vicent, T., Blánquez, P., Barceló, D., Rodríguez-Mozaz, S., 2018. An automated on-line turbulent flow liquid-chromatography technology coupled to a high resolution mass spectrometer LTQ-Orbitrap for suspect screening of antibiotic transformation products during microalgae wastewater treatment. J. Chromatogr. A. https://doi.org/10.1016/j.chroma.2018.06.027.

Kern, S., Baumgartner, R., Helbling, D.E., Hollender, J., Singer, H., Loos, M.J., Schwarzenbach, R.P., Fenner, K., 2010. A tiered procedure for assessing the formation of biotransformation products of pharmaceuticals and biocides during activated sludge treatment. J. Environ. Monit. 12, 2100. https://doi.org/10.1039/c0em00238k.

Kirk, T.K., Schultz, E., Connors, W.J., Lorenz, L.F., Zeikus, J.G., 1978. Influence of culture parameters on lignin metabolism by phanerochaete chrysosporium. Arch. Microbiol. 117, 277–285. https://doi.org/10.1007/BF00738547.

Koba, O., Golovko, O., Kodešová, R., Klement, A., Grabic, R., 2016. Transformation of atenolol, metoprolol, and carbamazepine in soils: the identification, quantification, and stability of the transformation products and further implications for the environment. Environ. Pollut. 218, 574–585. https://doi.org/10.1016/j.envpol.2016.07.041.

Lacey, C., Basha, S., Morrissey, A., Tobin, J.M., 2012. Occurrence of pharmaceutical compounds in wastewater process streams in Dublin, Ireland. Environ. Monit. Assess. 184, 1049–1062. https://doi.org/10.1007/s10661-011-2020-z.

Llorca, M., Castellet-Rovira, F., Farré, M.-J., Jaén-Gil, A., Martínez-Alonso, M., Rodríguez-Mozaz, S., Sarrà, M., Barceló, D., 2018. Fungal biodegradation of the NDMA precursors venlafaxine and O-desmethylvenlafaxine in water. Environ. Pollut. https://doi.org/10.1016/j.envpol.2018.12.008.

Lucas, D., Castellet-Rovira, F., Villagrasa, M., Badia-Fabregat, M., Barceló, D., Vicent, T., Caminal, G., Sarrà, M., Rodríguez-Mozaz, S., 2018. The role of sorption processes in the removal of pharmaceuticals by fungal treatment of wastewater. Sci. Total Environ. 610–611, 1147–1153. https://doi.org/10.1016/j.scitotenv.2017.08.118.

Ma, B., Huang, H.H., Chen, X.Y., Sun, Y.M., Lin, L.H., Zhong, D.F., 2007. Biotransformation of metoprolol by the fungus *Cunninghamella blakesleeana*. Acta Pharmacol. Sin. 28, 1067–1074. https://doi.org/10.1111/j.1745-7254.2007.00567.x.

Mamo, J., García-Galán, M.J., Stefani, M., Rodríguez-Mozaz, S., Barceló, D., Monclús, H., Rodriguez-Roda, I., Comas, J., 2018. Fate of pharmaceuticals and their transformation products in integrated membrane systems for wastewater reclamation. Chem. Eng. J. 331, 450–461. https://doi.org/10.1016/j.cej.2017.08.050.

Marco-Urrea, E., Pérez-Trujillo, M., Vicent, T., Caminal, G., 2009. Ability of white-rot fungi to remove selected pharmaceuticals and identification of degradation products of ibuprofen by *Trametes versicolor*. Chemosphere 74, 765–772. https://doi.org/10.1016/j.chemosphere.2008.10.040.

Maurer, M., Escher, B.I., Richle, P., Schaffner, C., Alder, A.C., 2007. Elimination of β-blockers in sewage treatment plants. Water Res. 41, 1614–1622. https://doi.org/10.1016/j.watres.2007.01.004.

Meunier, B., de Visser, S.P., Shaik, S., 2004. Mechanism of oxidation reactions catalyzed by cytochrome P450 enzymes. Chem. Rev. 104, 3947–3980. https://doi.org/10.1021/cr020443g.

Palli, L., Castellet-Rovira, F., Pérez-Trujilloc, M., Caniani, D., Sarrà-Adroguer, M., Gori, R., 2017. Preliminary evaluation of *Pleurotus ostreatus* for the removal of selected pharmaceuticals from hospital wastewater. Biotechnol. Prog. 33, 1529–1537. https://doi.org/10.1002/btpr.2520.

Pauwels, B., Verstraete, W., 2006. The treatment of hospital wastewater: an appraisal. J. Water Health 4, 405–416. https://doi.org/10.2166/wh.2006.025.

Radjenović, J., Pérez, S., Petrović, M., Barceló, D., 2008. Identification and structural characterization of biodegradation products of atenolol and glibenclamide by liquid chromatography coupled to hybrid quadrupole time-of-flight and quadrupole ion trap mass spectrometry. J. Chromatogr. A 1210, 142–153. https://doi.org/10.1016/j.chroma.2008.09.060.

Ratola, N., Cincinelli, A., Alves, A., Katsoyiannis, A., 2012. Occurrence of organic microcontaminants in the wastewater treatment process. Mini Rev. J. Hazard. Mater. 239–240, 1–18. https://doi.org/10.1016/j.jhazmat.2012.05.040.

Rodriguez-Mozaz, S., Lucas, D., Barceló, D., 2018. Full-scale plants for dedicated treatment of hospital effluents. In: Handbook of Environmental Chemistry. Springer, Berlin, Heidelberg, pp. 189–208. https://doi.org/10.1007/698_2017_13.

Romero, V., Acevedo, S., Marco, P., Giménez, J., Esplugas, S., 2016a. Enhancement of Fenton and photo-Fenton processes at initial circumneutral pH for the degradation of the β-blocker metoprolol. Water Res. 88, 449–457. https://doi.org/10.1016/j.watres.2015.10.035.

Romero, V., González, O., Bayarri, B., Marco, P., Giménez, J., Esplugas, S., 2016b. Degradation of metoprolol by photo-Fenton: comparison of different photoreactors performance. Chem. Eng. J. 283, 639–648. https://doi.org/10.1016/j.cej.2015.07.091.

Romero, V., González, O., Bayarri, B., Marco, P., Giménez, J., Esplugas, S., 2015. Performance of different advanced oxidation technologies for the abatement of the beta-blocker metoprolol. Catal. Today 240, 86–92. https://doi.org/10.1016/j.cattod.2014.03.060.

Rubirola, A., Llorca, M., Rodriguez-Mozaz, S., Casas, N., Rodriguez-Roda, I., Barceló, D., Buttiglieri, G., 2014. Characterization of metoprolol biodegradation and its transformation products generated in activated sludge batch experiments and in full scale WWTPs. Water Res. 63, 21–32. https://doi.org/10.1016/j.watres.2014.05.031.

Scheurer, M., Ramil, M., Metcalfe, C.D., Groh, S., Ternes, T.A., 2010. The challenge of analyzing beta-blocker drugs in sludge and wastewater. Anal. Bioanal. Chem. 396, 845–856. https://doi.org/10.1007/s00216-009-3225-7.

Slegers, C., Maquille, A., Deridder, V., Sonveaux, E., Habib Jiwan, J.L., Tilquin, B., 2006. LC-MS analysis in the e-beam and gamma radiolysis of metoprolol tartrate in aqueous solution: structure elucidation and formation mechanism of radiolytic products. Radiat. Phys. Chem. 75, 977–989. https://doi.org/10.1016/j.radphyschem.2006.02.001.

Šojić, D., Despotović, V., Orčić, D., Szabó, E., Arany, E., Armaković, S., Illés, E., Gajda-Schrantz, K., Dombi, A., Alapi, T., Sajben-Nagy, E., Palágyi, A., Vágvölgyi, C., Manczinger, L., Bjelica, L., Abramović, B., 2012. Degradation of thiamethoxam and metoprolol by UV, O_3 and UV/O_3 hybrid processes: kinetics, degradation intermediates and toxicity. J. Hydrol. 472–473, 314–327. https://doi.org/10.1016/j.jhydrol.2012.09.038.

Tay, K.S., Rahman, N.A., Abas, M.R. Bin, 2013. Ozonation of metoprolol in aqueous solution: ozonation by-products and mechanisms of degradation. Environ. Sci. Pollut. Res. 20, 3115–3121. https://doi.org/10.1007/s11356-012-1223-3.

Urlacher, V.B., Girhard, M., 2012. Cytochrome P450 monooxygenases: an update on perspectives for synthetic application. Trends Biotechnol. 30, 26–36. https://doi.org/10.1016/j.tibtech.2011.06.012.

Verlicchi, P., Al Aukidy, M., Zambello, E., 2015. What have we learned from worldwide experiences on the management and treatment of hospital effluent? - an overview and a discussion on perspectives. Sci. Total Environ. 514, 467–491. https://doi.org/10.1016/j.scitotenv.2015.02.020.

Verlicchi, P., Al Aukidy, M., Zambello, E., 2012. Occurrence of pharmaceutical compounds in urban wastewater: removal, mass load and environmental risk after a secondary treatment-A review. Sci. Total Environ. 429, 123–155. https://doi.org/10.1016/j.scitotenv.2012.04.028.

Verlicchi, P., Galletti, A., Petrovic, M., Barceló, D., 2010. Hospital effluents as a source of emerging pollutants: an overview of micropollutants and sustainable treatment options. J. Hydrol. 389, 416–428. https://doi.org/10.1016/j.jhydrol.2010.06.005.

Wessjohann, L.A., Keim, J., Weigel, B., Dippe, M., 2013. Alkylating enzymes. Curr. Opin. Chem. Biol. 17, 229–235. https://doi.org/10.1016/j.cbpa.2013.02.016.

Wharf, C., Kingdom, U., 2010. Questions and Answers on 'Guideline on the Environmental Risk Assessment of Medicinal Products for Human Use' 2010, pp. 1–9.

Wilde, M.L., Montipó, S., Martins, A.F., 2014. Degradation of β-blockers in hospital wastewater by means of ozonation and Fe^{2+}/ozonation. Water Res. 48, 280–295. https://doi.org/10.1016/j.watres.2013.09.039.

Journal of Chromatography A, 1568 (2018) 57–68

Contents lists available at ScienceDirect

Journal of Chromatography A

journal homepage: www.elsevier.com/locate/chroma

An automated on-line turbulent flow liquid-chromatography technology coupled to a high resolution mass spectrometer LTQ-Orbitrap for suspect screening of antibiotic transformation products during microalgae wastewater treatment

Adrián Jaén-Gil[a], Andrea Hom-Diaz[b], Marta Llorca[c], Teresa Vicent[b], Paqui Blánquez[b], Damià Barceló[a,c], Sara Rodríguez-Mozaz[a,*]

[a] Catalan Institute for Water Research (ICRA), H2O Building, Scientific and Technological Park of the University of Girona, Emili Grahit 101, E-17003 Girona, Spain
[b] Chemical, Biological and Environmental Engineering Department, Universitat Autònoma de Barcelona (UAB), E-08193 Bellaterra, Spain
[c] Water and Soil Quality Research Group Department of Environmental Chemistry, (IDAEA-CSIC), Jordi Girona 18-26, E-08034 Barcelona, Spain

ARTICLE INFO

Article history:
Received 26 March 2018
Received in revised form 7 June 2018
Accepted 10 June 2018
Available online 11 June 2018

Keywords:
Automated suspect screening
Transformation products
Transformation mechanisms
Microalgae
Antibiotics
Photobioreactor

ABSTRACT

The evaluation of wastewater treatment capabilities in terms of removal of water pollutants is crucial when assessing water mitigation issues. Not only the monitoring of target pollutants becomes a critical point, but also the transformation products (TPs) generated. Since these TPs are very often unknown compounds, their study in both wastewater and natural environment is currently recognized as a tedious task and challenging research field. In this study, a novel automated suspect screening methodology was developed for a comprehensive assessment of the TPs generated from nine antibiotics during microalgae water treatment. Three macrolides (azithromycin, erythromycin, clarithromycin), three fluoroquinolones (ofloxacin, ciprofloxacin, norfloxacin) and three additional antibiotics (trimethoprim, pipemidic acid, sulfapyridine) were selected as target pollutants. The analysis of samples was carried out by direct injection in an on-line turbulent flow liquid chromatography-high resolution mass spectrometry (TFC-LC-LTQ-Orbitrap-MS/MS) system, followed by automatic data processing for compound identification. The screening methodology allowed the identification of 40 tentative TPs from a list of software predicted intermediates created automatically. Once known and unknown TPs were identified, degradation pathways were suggested considering the different mechanisms involved on their formation (biotic and abiotic). Results reveal microalgae ability for macrolide biotransformation, but not for other antibiotics such as for fluoroquinolones. Finally, the intermediates detected were included into an in-house library and applied to the identification of tentative TPs in real toilet wastewater treated in a microalgae based photobioreactor (PBR). The overall approach allowed a comprehensive overview of the performance of microalgae water treatment in a fast and reliable manner: it represents a useful tool for the rapid screening of wide range of compounds, reducing time invested in data analysis and providing reliable structural identification.

1. Introduction

In the last decade, the overuse and misuse of antibiotics has promoted the incidence of an ever-growing spectrum of known and unknown compounds in urban wastewater effluents [1,2]. The presence of these pollutants in wastewater effluents may lead to potential ecological effects and promote bacterial resistance even at low concentration [3,4]. In fact, antibiotic resistant bacteria have been classified by the World Health Organization (WHO) as one of the three biggest threats to public health in the 21st century [5]. Since conventional wastewater treatment plants (WWTPs) are not designed to eliminate these emerging contaminants [6,7], the study of new and alternative wastewater treatment technologies becomes crucial to attain optimal removal efficiencies and increase the knowledge about their environmental fate [8].

* Corresponding autor at: Catalan Institute for Water Research (ICRA), Scientific and Technologic Park of the University of Girona, Emili Grahit 101, E-17003 Girona, Spain.
E-mail address: srodriguez@icra.cat (S. Rodríguez-Mozaz).

https://doi.org/10.1016/j.chroma.2018.06.027
0021-9673/

Bioremediation technologies have been recognized as potential and alternative systems to provide high-removal rates on treated effluents [9]. Among the existing bioremediation technologies, microalgae-based water treatment has been lately suggested as solar power-driven, ecologically friendly and sustainable reclamation strategies [10,11]. In addition, they exhibit higher tolerance to antibiotics than bacterial species, as they are not target organisms for these compounds [12]. Microalgae has been proven to be also effective for elimination of organic substances [13], which cannot only attributed to biotransformation but also to photodegradation and uptake processes [14]. Despite numerous studies have been focused on pharmaceutical removal in microalgae water treatment [9–11,13–17], few attention has been paid to the study of transformation products generated from the target pollutants [18]. The presence of these unknown compounds can play an important role since they might be more persistent and/or toxic than the parent compound [19]. The main difficulty to overcome their identification lies in the lack of pure analytical standards and fast analytical methods to confirm their presence along water treatment [20]. Hence, new analytical approaches comprising reliable structural identification are of high interest to easily overcome this tedious task. To this regard, high resolution mass spectrometry (HRMS) with electrospray ionization (ESI) is considered the analytical technique most widely used, since it makes possible to detect hundreds of unknown compounds in a single run [21]. Suspect screening methodologies, where tentative compounds are suggested by using libraries or prediction tools [20,22–25], are the most applied analytical strategies for the tentative identification of compounds in samples. Up to now, this approach has been widely used by different authors throughout post-acquisition data processing [1,26]. However, the reported workflows comprise several steps such as chromatographic data processing, data reduction, MS library search and MS/MS spectra elucidation [27]. To greatly facilitate analyte identification, most of the studies rely on online databases. However, manual data compiling is always required and the number of compounds identified are limited to those entities already known [28]. According to this, automated TP identification by using prediction tools may represent an important advance to detect new unknown chemicals [29–31], especially when new and alternative water treatment technologies are evaluated. Additionally, such automated data treatment tools for suspect screening analysis would allow the simultaneous evaluation of several target substances in just one experiment, avoiding the performance of multiple single experiments for each compound. On the other hand, although the application of the on-line turbulent flow chromatography for the identification of TPs in real wastewater treatment matrices is not new [15,32,33], this technology permits an on-line direct clean-up of dirty wastewater samples with less sample manipulation and better performance to detect TPs at low concentration levels [34]. Therefore, the application of this technology together with automatic software data processing may represent a useful tool for the rapid screening of wide range of suspect compounds, not only reducing the time invested in sample analysis but also in data treatment to finally attain reliable structural information.

The main objective of this study was to develop an automated analytical methodology to understand the transformation and fate of nine antibiotic compounds during microalgae water treatment, both at batch scale and in a pilot photobioreactor treating toilet wastewater. The screening methodology was based on the analysis by an on-line turbulent-flow liquid chromatography coupled with high resolution mass spectrometry (TFC-HPLC-MS/MS) methodology together with an advanced software data processing tool.

This study provided valuable information about transformation of selected antibiotics to better evaluate the scope of microalgae as an alternative wastewater treatment. In addition, the study of TPs allowed to understand the abiotic and biotic processes involved in pollutant removal.

2. Materials and methods

2.1. Chemicals and reagents

Azithromycin (AZI), erythromycin (ERY), clarithromycin (CTM), ofloxacin (OFC), ciprofloxacin (CFC), norfloxacin (NFC), sulfapyridine (SPY), trimethoprim (TMP) and pipemidic acid (PMA) were purchased at high purity grade (>95%) from Sigma-Aldrich (Steinheim, Germany). Ultra-pure water, acetonitrile and methanol LiChrosolv grade were supplied from Merck (Darmstadt, Germany). Solid phase extraction (SPE) cartridges Oasis HLB (60 mg, 3 mL) were from Waters Corporation (Milford, MA, USA).

2.2. Microalgal batch experiments

Microalgal batch experiments were performed within 14-day by testing three different experimental conditions for each microalga studied: i) light-biomass (selected microalgae with light irradiation) ii) light-abiotic (irradiation of light without algae) and iii) dark-abiotic (without algae and without light). For microalgal live conditions *Chlamydomonas reinhardtii* (UTEX ID 2243), *Chlorella sorokiniana* (UTEX ID 1663), *Dunaliella tertiolecta* (UTEX ID LB999) and *Pseudokirchneriella subcapitata* (UTEX ID 1648) were selected and grown in their respective synthetic culture mediums: Tris-Acetate-Phosphate (TAP) for *C. reinhardtii* and *C. sorokiniana*, Artificial Sea Water for *D. tertiolecta* and in Bold 3 N for *P. subcapitata*. More detailed information about experimental set-up can be found elsewhere [35]. Light experiments were carried out under continuous fluorescent lamp irradiation (172 ± 18 μmol/(m^2 s) irradiance level), measured by a light meter (LI.189, LI-COR Quantum/Radiometer/Photometer, USA) at a controlled temperature (25 ± 1 °C) and 120 rpm (orbital shaker Kuhner, LS-X, Switzerland). All experiments were carried out in triplicate by spiking the nine antibiotics simultaneously at a final concentration of 100 μg/L each in 250 mL of synthetic medium. 1 mL of samples were collected in amber glass vials at initial time, and after 7 and 14 days of treatment. Samples were freeze-dried and stored at −80 °C until analysis. Reconstitution was performed in 100 μL of methanol-water (5:95) before their injection in the TFC-LC-LTQ-Orbitrap-MS/MS system.

2.3. Microalgal photobioreactor

A microalgal photobioreactor treating the toilet wastewater was used to evaluate the elimination and transformation of the 9 antibiotics selected. The experimental set-up of this experiment has been previously described [36] as well as its microbial characterization [37]. Briefly, urban wastewater was collected from the toilet drainage of the "Chemical, Biological and Environmental Engineering Department" (Universitat Autònoma de Barcelona, Barcelona, Spain) and pumped to an enclosed 1200 L multitubular microalgal photobioreactor (PBR). Three samples from the inlet wastewater and three samples PBR effluent were taken in three non-consecutive days after the theoretical hydraulic steady state of twelve days was reached. To enhance concentration of TPs, 25 mL and 50 mL for influent and effluent respectively were preconcentrate up to 1 mL by using the SPE methodology previously reported [38].

2.4. Analytical methodology and data processing

2.4.1. TFC-LC–MS/MS analysis

Samples were analyzed using an on-line turbulent flow liquid-chromatography system coupled to a high resolution mass

spectrometer (HRMS). For sample purification and separation purposes, the Aria TLX-1 chromatographic system (Thermo Fisher Scientific) was used. The system comprised a PAL auto sampler and two mixing quaternary pumps (eluting and loading pumps). 20 μL of samples were directly injected into the chromatographic system. The clean-up step was performed in a Cyclone (50 × 0.5 mm, 60 μm particle size, 60 Å pore size; Thermo Fisher Scientific, Franklin, MA) and the compounds were separated using a ZORBAX Eclipse XD-C18 (150 × 4.6 mm, 5 μm particle size; Agilent Technologies, Santa Clara, CA, USA). Detailed information about the solvent gradient used can be found in Table S1, and an example of total ion chromatogram (TIC) in Fig. S1. The total chromatographic run time was 18 min.

The LC system was connected to a LTQ-OrbitrapVelos™ (Thermo Fisher Scientific Company; Villebon-France) equipped with a diverter valve and a heated electrospray ionization source (HESI-II). The analysis was performed in positive and negative ionization modes. As no results were found for negative mode experiments, data processing was carried out in positive mode only. Chromatograms and mass spectra were acquired in *Data Dependent Acquisition* (DDA) in two parallel scan events: the first one (1) was acquired in full-scan mode within a mass-to-charge (*m/z*) range of 100–800 m/z at a resolving power of 60,000 FWHM (MS) followed by (2) fragmentation of the most intense ion masses detected (MS/MS) at 30,000 FWHM. These MS/MS experiments were performed applying a dynamic mass exclusion mode to discriminate co-eluted compounds: ions fragmented more than 3 times during 25 s were further ignored for fragmentation during the following 30 s (corresponding to peak plus tailing). Mass spectrometry conditions were set up as follows: spray voltage, 3500 V; capillary temperature, 300 °C; sheath gas pressure, 40 arb; and aux gas flow rate, 20 arb; collision energy, 35 eV CID; isolation width, 2 Da. For some particular TPs, a tougher fragmentation through 55 eV HCD was used for final identification. The entire system was controlled via Aria software, version 1.6, under Xcalibur 2.1 software. For inlet and PBR effluents wastewater samples, the previous analytical methodology was adapted: the in-house library containing the information about all tentative TPs identified in the batch experiments was used as a prescreening list to be used as criterion to trigger MS fragmentation in the second scan event for MS/MS fragmentation and confirmation.

2.4.2. Automated data processing

An automated data processing methodology by using Compound Discoverer 1.0 (Thermo Scientific) connected to Mass Frontier 7.0 software (Thermo Scientific) was applied for the identification of the TPs generated. The overall workflow describing all steps involved in data processing is presented in Fig. 1.

Prior to automatic software data processing, computational data files (chromatograms and mass spectra) were loaded into the software. Target antibiotic structures (9 antibiotics) were pinpointed as parent compounds as well as the potential chemical transformations to be applied to them by software simulation: methylation, oxidation, reduction, hydroxylation, reductive defluorination, oxidative defluorination, decarboxylation, oxidative deamination to alcohol, oxidative deamination to ketone, desaturation, dehydration, hydration, acetylation, carboxylation, piperazinyl dealkylation, sulfation, sulfonamide alkylation and sulfur dioxide reduction. A combination of a maximum number of two dealkylation steps for a maximum of three consecutive chemical transformations were selected. Using all this prior information, a list with predicted TPs was created during the automatic data processing run.

Automatic data processing starts with MS data filtering in the *m/z* range between 100 Da and 800 Da, and by setting a peak intensity threshold at 10 signal-to-noise ratio. To compensate small differences in retention times, chromatographic alignment was performed by using a mass tolerance error of 5 ppm and a maximum retention time shift of 0.5 min. In parallel, the list containing the 9 parent compounds and their predicted TPs was automatically generated including the corresponding exact masses and the software transformation applied. This list was automatically compared with experimental data by using an MS mass tolerance of 5 ppm and a minimum chromatographic peak intensity of 1000 counts. Those parent and predicted compounds successfully matched in samples were included into a list of detected compounds. For confirmation purposes, MS/MS spectra were automatically elucidated by using predicted fragment structures with a mass tolerance of 5 ppm and a signal-to-noise ratio of 10. The percentage value obtained for each detected compound (FISh scoring) indicated the MS/MS reliability on automatic compound identification.

After software data processing, results were filtered by selecting those compounds with FISh values ≥ than 65% [39] with at least two characteristic fragments matched with predicted fragment structures. As a final step to avoid false positives, the predicted TP structures and their elucidated MS/MS spectra were manually reviewed. Both parent and confirmed TPs were included into an in-house library and used for the detection of TPs in microalgal-based photobioreactor samples.

3. Results and discussion

3.1. Software data processing

Four data sets (one for each microalga experimental set) were automatically processed by the software (each set lasting 13 h on the software run). Each data set included the experimental files obtained from light-biomass experiments with a particular microalga, a light-abiotic and a dark-abiotic experiment. Automatic processing reduced the number of chromatographic peaks up to 10% without manual refining. In contrast to other methodologies described, this extent on data reduction was only achieved with a combination of automatic and manual processing [40–42]. 73 suspected compounds out 12,291 predicted were tentatively detected in samples after the automatic data processing, including the 9 parent compounds and 64 TPs. After manual review, the confirmed list was reduced to the 9 parent compounds and 40 TPs: 8 TPs for AZI, 6 for ERY, 2 for CTM, 8 for OFC, 5 for CFC, 5 for NFC, 3 for PMA, 2 for TMP and 1 for SPY. Among them, 19 TPs were reported as direct matches, where TP structures were directly proposed by the software from automatic MS/MS spectra elucidation. On the other hand, 21 TPs were reported as shifted matches, where TP structures proposed required additional transformations to define the final chemical structures. An example of direct and shifted matches is presented in Fig. S2. Automated MS/MS elucidation with annotation of the corresponding tentative fragments contributed to reduce the processing time for TPs identification. This workflow allowed the elucidation of a high number of potential TPs without performing degradation experiments for each of the compounds separately, saving time and laboratory resources. Nonetheless, although this methodology provided a rapid tool for peak filtering with less handling operation, manual work was necessary in a final step to avoid false positives and evaluate findings. The final 40 TPs were registered in an in-house library, which included for each compound, its retention time, elemental composition, fragmentation ions, mass error, ring and double bond equivalents (RDB) and the tentative chemical structure (Table S2). The presence of the 9 parent compounds and their 40 suspect TPs was monitored along the experiments performed, both in batch and in microalgal photobioreactor treating toilet wastewater. Their relative concentrations were calculated and presented in Figs. 2–5.

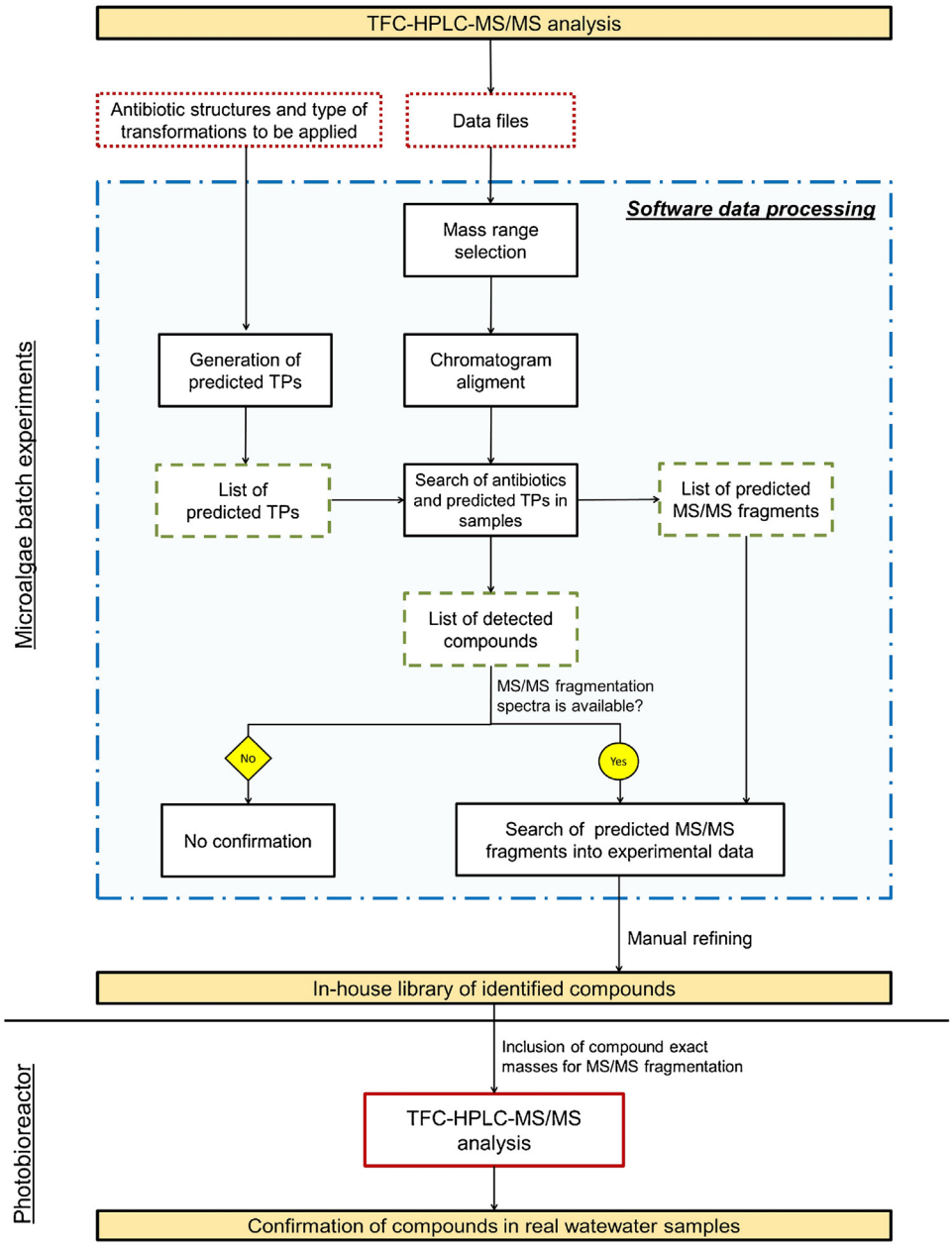

Fig. 1. Analytical workflow.

3.2. Evaluation of antibiotic transformations during microalgae batch experiments

Antibiotic transformation was investigated along microalgae treatment experiments. While the results about removal of parent compounds are discussed in detail elsewhere [35], in this work the results about antibiotic transformations are presented and discussed separately in three different groups: macrolides (azithromycin, erythromycin, clarithromycin), fluoroquinolones (ofloxacin, ciprofloxacin, norfloxacin) and other additional and non-related antibiotics (trimethoprim, pipemidic acid, sulfapyridine). Suggested transformation pathways are presented in Figs. 2a and 4a. Relative percentages (A/A_0)-(%) for each TP (area of the peak detected divided by the area of the chromatographic peak of the parent compound at initial time) at 7 and 14 days of treatment were calculated and summarized in Figs. 2b and 4b. The confirmation and quantification and of the individual TPs would require reference standards, though most of them are not commercially available.

3.2.1. Macrolide transformation

Sixteen major intermediates were tentatively identified coming from macrolide degradation including 8 TPs from azithromycin, 6 TPs from erythromycin and 2 TPs from clarithromycin (Table S2). A shared degradation pathway containing all the TPs detected along the batch experiments are presented in Fig. 2a. Additionally, the relative percentages of those intermediates with values higher than 3% are shown in Fig. 2b for each experimental condition after 7 and 14 days of treatment.

According to dark-abiotic experiments performed in the corresponding TAP, artificial sea water and bold 3 N mediums, macrolide elimination achieved a mean percentage of $22 \pm 16\%$ for AZI, $29 \pm 14\%$ for ERY and $22 \pm 32\%$ for CTM suggesting a direct contribution of abiotic factors on macrolide degradation. Among the

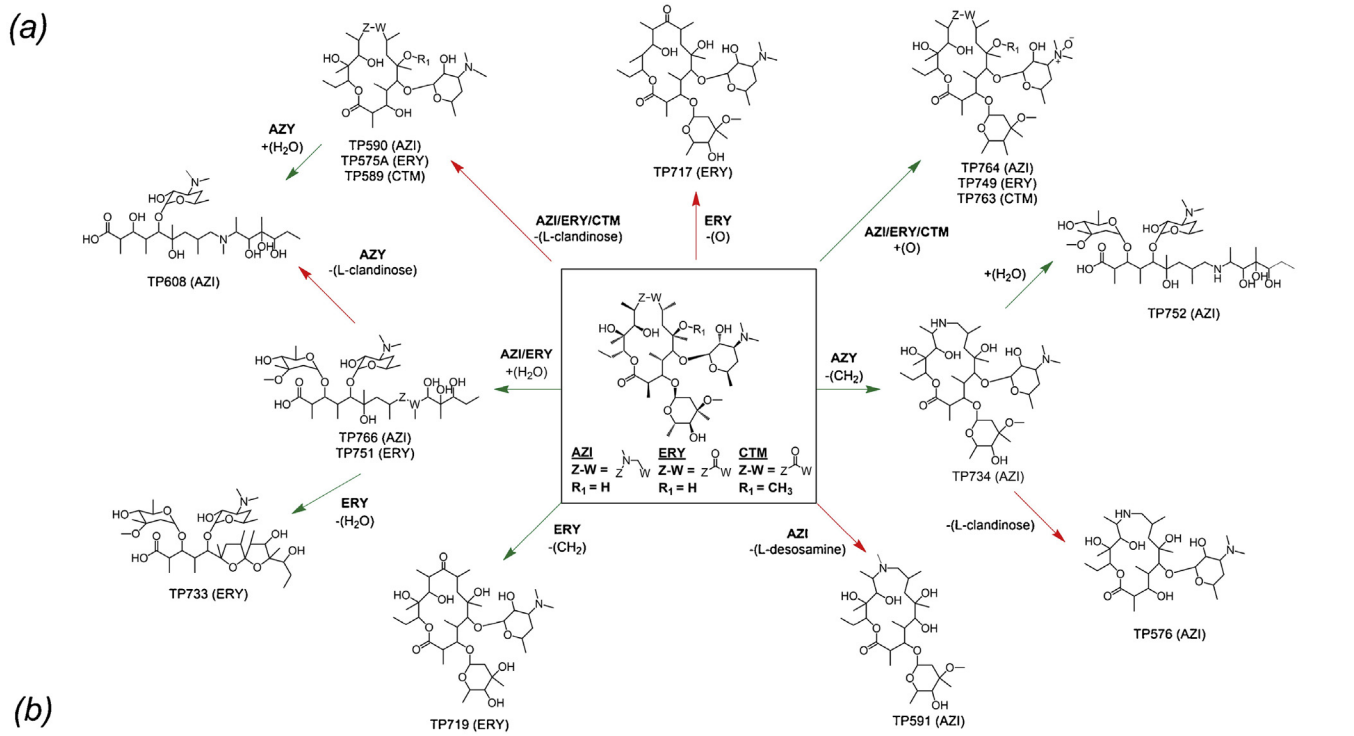

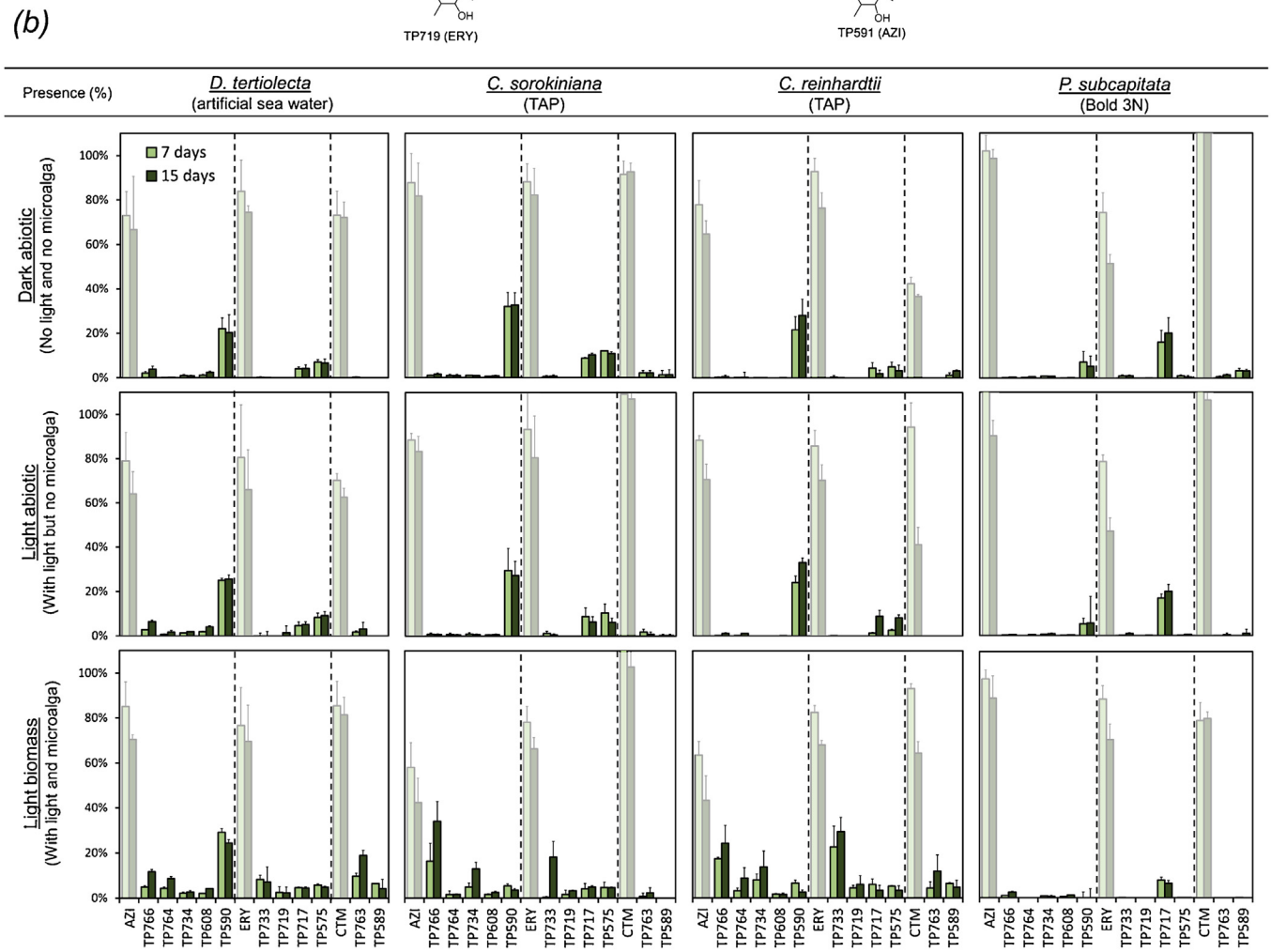

Fig. 2. (a) Tentative degradation pathways proposed for macrolides: green arrows indicate those TPs formed mainly by biotransformation; red arrows indicate those TPs formed mainly by unknown factors. Below (b) relative percentages of TPs at 7 and 15 days for the 4 algae studied in dark-abiotic, light-abiotic and light-biomass experiments. The TPs represented were those with values >3%. (For interpretation of the references to colour in this figure legend, the reader is referred to the web version of this article.)

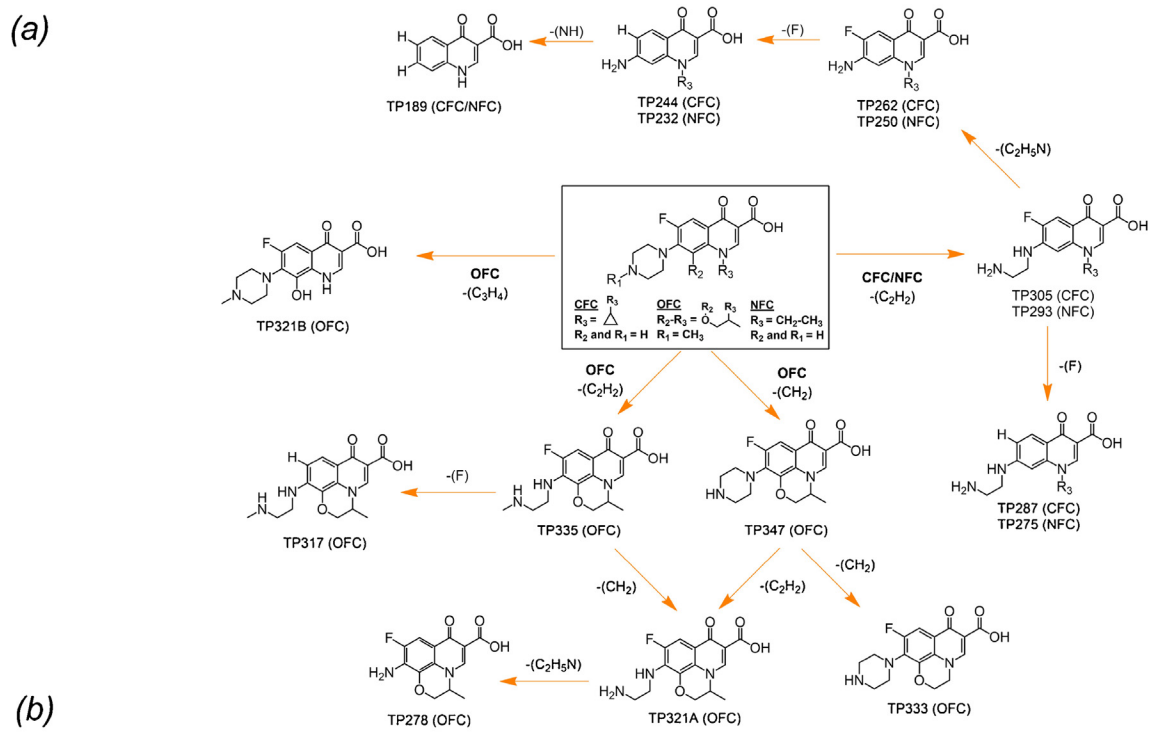

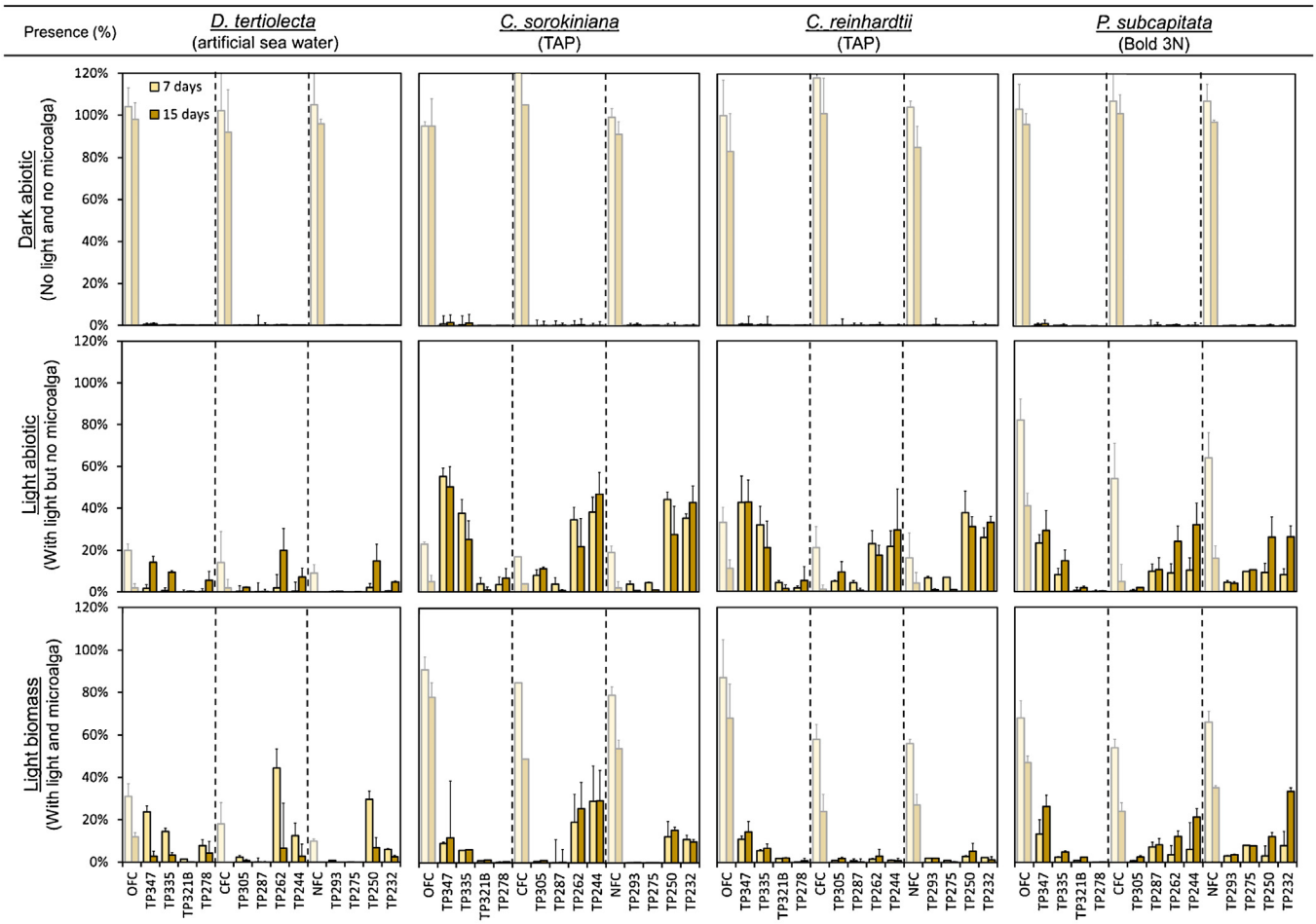

Fig. 3. (a) Tentative degradation pathways proposed for fluoroquinolones: yellow arrows indicate those TPs formed mainly by phototransformation. Below (b) relative percentages of TPs at 7 and 15 days for the 4 algae studied in dark-abiotic, light-abiotic and light-biomass experiments. The TPs represented were those with values >3%. (For interpretation of the references to colour in this figure legend, the reader is referred to the web version of this article.)

(a)

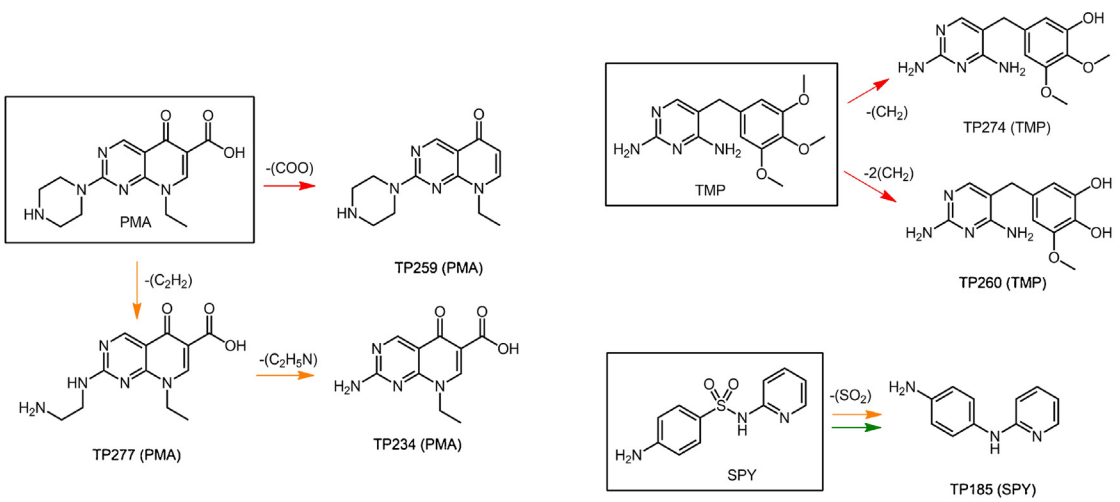

(b)

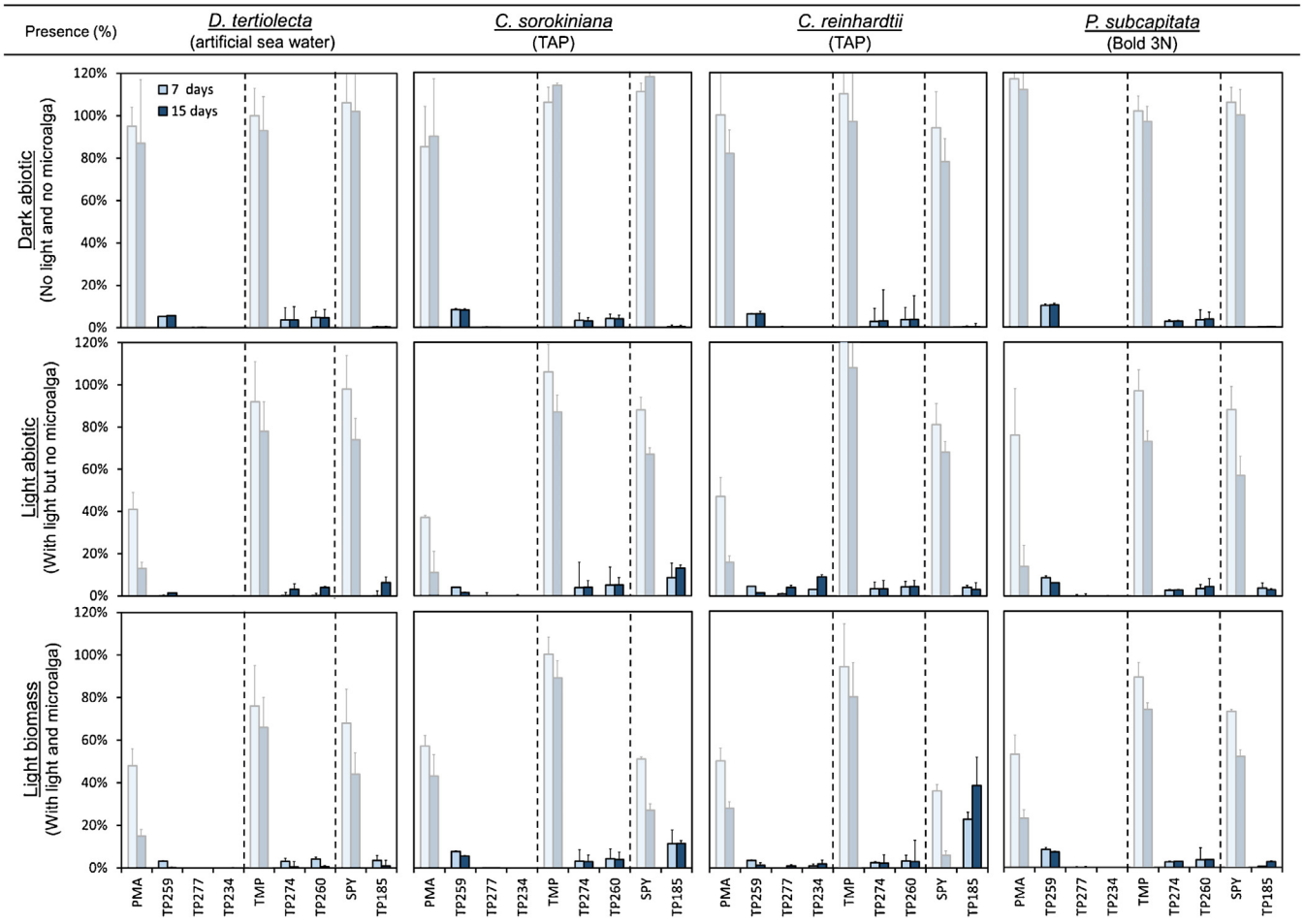

Fig. 4. (a) Tentative degradation pathways proposed for other antibiotics: green arrows indicate those TPs formed mainly by biotransformation; red arrows indicate those TPs formed mainly by unknown factors. Below (b) relative percentages of TPs at 7 and 15 days for the 4 algae studied in dark-abiotic, light-abiotic and light-biomass experiments. The TPs represented were those with values >3%.(For interpretation of the references to colour in this figure legend, the reader is referred to the web version of this article.)

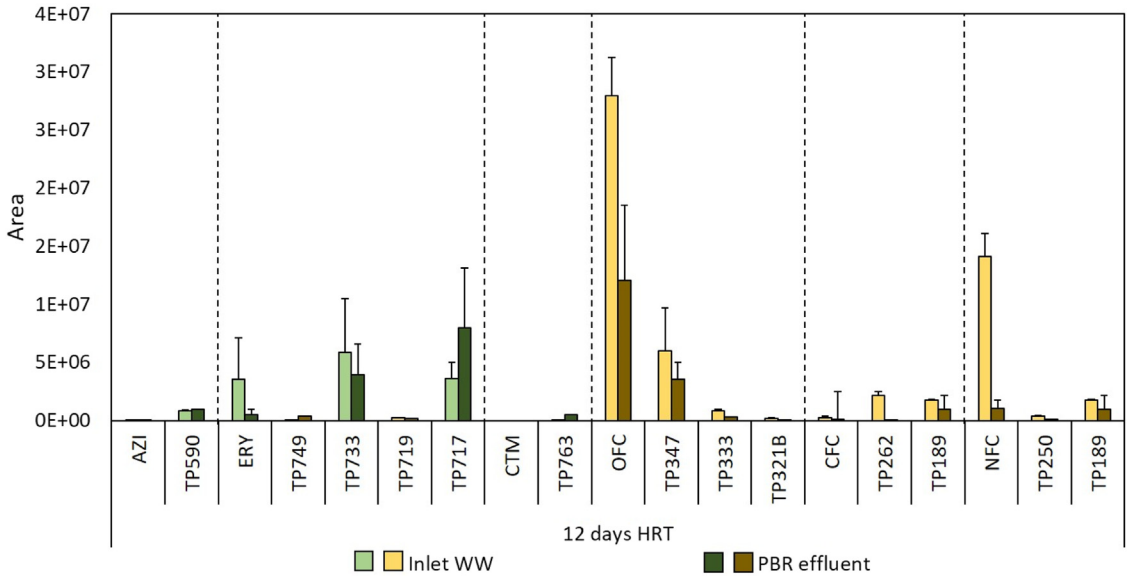

Fig. 5. Area of the transformation products detected in wastewater at the inlet and outlet of photobioreactor (PBR) at 12 days HRT.

intermediates generated, TP590 (up to 33% of the initial AZI), TP575A (up to 12% of initial ERY) and TP589 (up to 6% of initial CTM) were the most common structures identified (Fig. 2b); all formed by O-dealkylation of L-clandinose moiety (Fig. 2b). On the other hand, TP717 (also named erythromycin B) was generated throughout dehydroxylation reaching a ratio formation of about 20% of initial ERY. Their presence was suggested to come from the instability of macrolides in aqueous solution [43,44], confirmed by their presence at initial time at low concentration levels (lower than 3% of initial presence of the corresponding antibiotic; data not shown). In light-abiotic experiments, similar removal rates of parent compounds up to 23 ± 12% for AZI, 34 ± 14% for ERY and 21 ± 33% for CTM were obtained compared to dark-abiotic experiments; as well as similar TP formation profiles. Even though some authors reported the major role of light in the generation of O-dealkyled compounds [45,46], our results cannot confirm a contribution of this factor to such type of transformation in macrolides.

Concerning the experiments performed with the 4 microalgae selected (light-biomass experiments), macrolides treated with *D. tertiolecta* presented similar antibiotic degradation rates (ca. 26 ± 6%) and TP formation profile to the previous abiotic conditions tested. Although some other TPs such as TP766 and TP733 were generated at a low concentration level (up to 12%), TP590 (AZI) was still pointed out as the major intermediate detected. This microalga was thus considered to not contribute extensively on macrolide elimination through biotransformation. Likewise, degradation and TP formation in *P. subcapitata* was much lower than with the other microalgae studied. In this case, average macrolide elimination was around 20 ± 9% and TP formation profile was lower comparing to the abiotic condition tested. On the contrary, *C. reinhardtii* and *C. sorokiniana* showed a decrease on the presence of O-dealkyled intermediates (related to abiotic transformations), along with the generation of new TPs such as TP766 (AZI), TP764 (AZI), TP734 (AZI), TP608 (AZI), TP733 (ERY), TP719 (ERY) and TP763 (CTM). These can be specifically attributed to microalgae biodegradation rather than to abiotic transformations. In fact, for these two microalgae, the elimination of the parent compounds achieved was much higher than with the other microalgae studied, with average removal values 57 ± 1%, 33 ± 1% and 16 ± 28 for azithromycin, erythromycin and clarithromycin respectively.

Among the TPs detected, the opening of the macrocyclic lactone ring by hydrolysis of the lactone ester group can be appointed as the most common structural modification. In the case of erythromycin, hydrolysis was first led by the generation of the intermediate TP751 (ERY) followed by condensation to TP733 (ERY), present at high levels (up to 29%). This mechanism has been widely reported by many authors [47–50] and detected in secondary effluent during soil aquifer treatment [51] and in enzymatic degradation experiments with EreB esterase [32]. In this study, this hydrolysis mechanism was also identified as the major biodegradation pathway in azithromycin biotransformation, with the generation of TP766 (AZI) up to 34% of the initial AZI (Fig. 2). The opening of lactone ring was confirmed by the loss of an instauration grade (RDB) whereas d-desosamine and L-cladinose was maintained (Table S2). Unlike for erythromycin, no further molecular condensation was observed probably due to the presence of a methyl-substituted nitrogen in azithromycin Z-W position, preventing further dehydration step [52]. In the case of clarithromycin, few intermediates were detected, pointing it out as the most recalcitrant macrolide in this study. One of the reasons might be attributed to the presence of a methyl group in R_1 position increasing the steric effects in some TPs to be generated.

In general, the presence of higher amounts of TPs at 14 days than 7 days of treatment in all experimental conditions indicates that, even though macrolides were apparently eliminated to certain extent, they were not mineralized. Nonetheless, they were transformed into new entities that are not necessarily degraded fast enough and could potentially keep some of the activity of the parent compounds. As observed, the use of microalgae for antibiotic biodegradation provided a higher number of intermediates compared to abiotic experiments. Therefore, a careful evaluation of the risk that these transformation products can pose should be performed. It would permit to determine the most beneficial conditions to eliminate macrolide antibiotics.

3.2.2. Fluoroquinolone transformation

Eighteen major intermediates were tentatively identified coming from fluoroquinolone degradation including 8 TPs from ofloxacin, 5 TPs from ciprofloxacin and 5 TPs from norfloxacin (Table S2). A shared degradation pathway containing all the TPs detected along batch experiments are presented in Fig. 3a. Additionally, relative percentages of those intermediates with values higher than 3% are shown in Fig. 3b for each experimental condition at 7 and 14 days of treatment.

According to dark-abiotic experiments, fluoroquinolone abiotic elimination can be considered negligible. These results are in accordance with the lack of intermediates in these dark-abiotic experiments. In contrast, 85 ± 18% for OFC, 97 ± 2% for CFC and 95 ± 7% for NFC were eliminated when light was irradiated in light-abiotic experiments. Several authors have indicated the sensibility of fluoroquinolone to photodegradation, which is pointed out as the most significant transformation mechanism in aquatic systems [53–57]. Amongst the identified TPs via phototransformation (Fig. 3a), ofloxacin demethylation to TP347 (OFC) and ofloxacin desethylation of piperazinyl ring to TP335 (OFC) were described as major intermediates detected up to 55% and 38% respectively of initial parent compounds (Fig. 3b). Ofloxacin was persistent in maintaining piperazinyl ring integrity as first-generation TPs. This might be explained by the further additional stability conferred by a methyl group in position R_1 in ofloxacin structure (Fig. 3a). On the contrary, complete elimination of the piperazinyl ring in ciprofloxacin and norfloxacin to TP262 (CFC) and TP250 (NFC) respectively was occurring more easily. From these last TPs, further reductive defluorination to TP244 (CFC) and TP232 (NFC) as third-generation TPs were identified as the major byproducts generated reaching values about 44% and 47% respectively.

Microalgal live experiments lead to lower removal rates of the parent compounds (and also a lower amount of TPs generated) than those obtained in light-abiotic experiments. In fact, fluoroquinolones were eliminated to an average value of 36 ± 16% for OFC, 68 ± 14% for CFC and 61 ± 14% for NFC in *C. reinhardtii, C. sorokiniana* and *P. subcapitata* experiments. This can be explained by the shielding effect posed by microalgae, partially preventing exposure of pollutants to light. Photodegradation may thus not occur to the same extent than in light-abiotic experiments. The marine microalgae *D. tertiolecta*, was the only one able to achieve fluoroquinolones removal rates as good as those obtained in light-abiotic experiments being almost eliminated at the end of the experiment. In line with it, concentration of TPs generated after 7 days of treatment was quite high, whereas their presence was almost residual at day 14. The better performance of the marine alga *D. tertiolecta* could be explained by the influence of water matrix rather than by the impact of the microalga itself. Actually, the best removal of fluoroquinolones was achieved in the light-abiotic experiments with artificial sea water whereas light-abiotic controls for the freshwater algae *C. reinhardtii, C. sorokiniana* and *P. subcapitata* were performed in less saline media. Matrix composition such as pH, dissolved organic content, chloride ion concentration has actually been reported to have an influence in photodegradation processes [45,54].

3.2.3. Transformation of other antibiotics

Six major intermediates were tentatively identified coming from other antibiotics including 3 TPs from pipemidic acid, 2 TPs from trimethoprim and 1 TP from sulfapyridine (Table S2). Degradation pathways containing all the TPs detected along batch experiments are presented in Fig. 4a. Additionally, relative percentages of those intermediates with values higher than 3% are shown in Fig. 4b for each experimental condition at 7 and 14 days of treatment.

According to dark-abiotic experiments, the abiotic elimination of these 3 compounds can be considered negligible although some residual TPs such as TP259 (PMA), TP274 (TMP) and TP260 (TMP) were generated. These intermediates were also detected in light-abiotic experiments with the same profile, despite of the partial removal of the parent compounds (87 ± 2% for PMA, 14 ± 15% for TMP and 34 ± 7% for SPY) at 14 days of treatment. In general, a more limited number of TPs were detected for these compounds since low mass intermediates might be overlooked by peak interferences at low *m/z* values. Different intermediates were further generated through phototransformation processes (observed in light-abiotic experiments) such as TP259 (PMA), TP277 (PMA), TP234 (PMA) and TP185 (SPY), though at low concentration levels.

Slightly higher removals (73 ± 12% for PMA, 23 ± 10% for TMP and 68 ± 20% for SPY) were achieved after 14 days of treatment with microalgae in light-biomass experiments. However, levels of TPs did not increase in the same proportion except in the case of TP185 (SPY). This TP reached up to 35% of initial SPY concentration in the experiments with *C. reinhardtii* after 14 days of treatment, being SPY removed almost completely at the end of the treatment. Biotransformation would be the main mechanism involved in its generation, although it was already present in abiotic experiments and also reported along UV/H_2O_2 experiments, thought at much lower concentration. Therefore, *C. reinhardtii* was the only microalga able to biotransform sulfapyridine although no mineralization was achieved.

3.2.4. Microalgae for pollutant mitigation

Although monitoring of the antibiotics along the experiment provides information about removal ability of microalgae, a proper evaluation of microalgae performance can only be done by measuring also the TPs generated. These TPs can retain some of the biological activity and even elicit higher toxicity than the parent compound, and therefore their generation might rather introduce additional threats to the environment. Consequently, TP elimination needs to be guaranteed in order to ensure the optimum treatment efficiency. In this study, macrolides were partially eliminated during both abiotic and microalgae live experiments. However, they were transformed into new entities that are not necessarily degraded at the end of the treatment. It is important to remark that different TPs were identified for each biotic and abiotic transformation mechanisms studied. On the other hand, fluoroquinolones were eliminated extensively by photodegradation processes compared to a partial elimination with microalgae live cultures. However, an important amount of TPs was detected in the light-abiotic experiments, which might equally pose a risk for the environment. The characterization of TPs has been pointed out as essential step to understand the effectivity of antibiotic removal treatment. Studies about their toxicity are of outmost importance to finally round up the study treatment assessment.

Concerning removal efficiency of microalgae, *P. subcapitata* was clearly not useful for antibiotic removal since no biotransformation of antibiotics was observed. On the other hand, *C. reinhardtii* and *C. sorokiniana* were especially capable for macrolide biotransformation but not for total compound mineralization. *C. reinhardtii* removed most of the recalcitrant fluoroquinolone TPs (TP244, TP232 and TP347) while they were present at higher concentrations in biotic experiments with *C. sorokiniana*. *D. tertiolecta* experiments showed that abiotic factors lead macrolide transformation with the generation of large amounts of TPs. However, mineralization of fluoroquinolones was achieved to certain extent. Thus, *C. reinhardtii* and *D. tertiolecta* were suggested to be the best microalgae to be used for pollutant removal because of their better antibiotic elimination together with the low TPs formation (in quantity and number). However, none of them were successful to eliminate all type of antibiotics to the same extent.

3.3. Antibiotic transformation products in toilet wastewater treated in a microalgae photobioreactor (PBR)

The in-house library created containing the compounds elucidated in batch experiments (Table S2) was used for comprehensive assessment of the occurrence of antibiotics and their TPs in a microalgae-based photobioreactor treating real toilet wastewater. Fig. 5 shows mean chromatographic areas of the compounds detected for the three samples taken in three non-consecutive days

at inlet wastewater and in PBR effluent. Among target antibiotics selected erythromycin, ofloxacin and norfloxacin were detected at inlet WW and removed 85%, 67% and 95% respectively [36]. Concerning their transformation products, the initial presence of the metabolite TP733 (ERY) at inlet WW was attributed to human metabolization of ERY [58,59]. TP733 was partially eliminated in the photobioreactor, although it can also be generated during the treatment. In fact, PBR was dominated by microalgae from the genus *Chlorella* [37] and TP733 was the major ERY metabolite associated to *Chlorella sorokiniana* in the previous batch experiments (Fig. 2). TP717 (ERY), another erythromycin transformation product, increased its concentration after PRB treatment (aligned with ERY elimination) indicating the apparent transformation of ERY into this compound. This TP was previously described to be generated due to the instability of erythromycin in aqueous solution (Fig. 2 and Section 3.2.1). Other compounds such as TP590 (AZI) and TP763 (CTM) were detected in inlet WW despite the corresponding parent compounds were not present. While the first one was detected from abiotic factors, the latest was generated to come from biotransformation mechanism, also associated to *C. sorokiniana*. Our findings highlight the great importance of monitoring TPs since they can be present even when the parent compound is not or they can be present at higher concentrations than the corresponding parent compound, as it is the case of ERY TPs.

In the case of fluoroquinolones, the major intermediates identified were TP347 (OFC) and TP262 (CFC) and eliminated in PBR treatment up to 44% and 99% respectively. In accordance with microalgae batch experiments, these two TPs were reported as some of the most intense intermediates from ofloxacin and ciprofloxacin generated by phototransformation processes (Fig. 3). Additionally, they were also minimized in presence of *C. sorokiniana*. Finally, most of them were transformed to TP189, a fourth-generation TP of fluoroquinolones, suggesting a greater extent of antibiotic total elimination.

The PBR experiment showed an overall decrease of all intermediates (though not total removal) in theoretical steady state (HRT 12 days) except for TP717, which increases in concentration. Although total compound removal was not achieved, microalgae based PBR wastewater treatment was successfully applied to reduce the concentration of antibiotics and their TPs. The high concentrations of TPs in inlet wastewater demonstrates the great importance of monitoring these compounds. Thus, the development of advanced analytical methodologies based on suspect screening becomes of high interest to properly evaluate water treatment technologies and consider all potentially relevant chemicals present in water.

4. Conclusions

In this study, a novel automated suspect screening methodology using an on-line TFC-LC-LTQ-Orbitrap-MS/MS was developed for the tentative identification of the major TPs of 9 selected antibiotics during microalgae treatment. The positive results indicated that the automated screening tools are a promising approach able to provide reliable information in a fast and efficient manner. By means of the tool developed, the identification of TPs was performed and the corresponding degradation pathways were built taking into account biotic and abiotic factors involved on experimental design. This permitted the evaluation of several microalgae as regards to their efficiency for pollutant removal, allowed to distinguish between removal mechanisms involved, and also to confirm or deny pollutant mineralization.

The set of TPs identified in the batch microalgae experiments was further searched (suspect screening) in the water samples generated during the treatment of toilet wastewater in an algae photobioreactor. Many TPs were present in both raw and treated waters even when the parent compound is not detected, which highlights the relevance of monitoring both parent compounds and their TPs. Further studies are foreseen to investigate how these TPs might introduce deleterious effects in aquatic systems and how this could impact human health.

Acknowledgements

This work was supported by the Spanish Ministry of Economy and Competitiveness (CTM2013-48548-C2), co-financed by the European Union through the European Regional Development Fund (ERDF). This work was partly supported by the Generalitat de Catalunya (Consolidate Research Group 2017 SGR 14, 2017 SGR 1404 and ICRA-ENV 2017 SGR 1124). The Department of Chemical, Biological and Environmental Engineering of the Universitat Autònoma de Barcelona is a member of the Xarxa de Referència en Biotecnologia de la Generalitat de Catalunya. Adrián Jaén-Gil and Andrea Hom-Diaz acknowledge their PhD scholarship from AGAUR (2017FI_B 00778 and 2013FI_B 00302 respectively). Sara Rodriguez-Mozaz acknowledges the Ramon y Cajal program (RYC-2014-16707).

Appendix A. Supplementary data

Supplementary material related to this article can be found, in the online version, at doi:https://doi.org/10.1016/j.chroma.2018.06.027.

References

[1] L. Vergeynst, H. Van Langenhove, P. Joos, K. Demeestere, Suspect screening and target quantification of multi-class pharmaceuticals in surface water based on large-volume injection liquid chromatography and time-of-flight mass spectrometry, Anal. Bioanal. Chem. 406 (2014) 2533–2547, http://dx.doi.org/10.1007/s00216-014-7672-4.
[2] J.Q. Xiong, M.B. Kurade, R.A.I. Abou-Shanab, M.K. Ji, J. Choi, J.O. Kim, B.H. Jeon, Biodegradation of carbamazepine using freshwater microalgae Chlamydomonas mexicana and Scenedesmus obliquus and the determination of its metabolic fate, Bioresour. Technol. 205 (2016) 183–190, http://dx.doi.org/10.1016/j.biortech.2016.01.038.
[3] F. Baquero, J.L. Martínez, R. Cantón, Antibiotics and antibiotic resistance in water environments, Curr. Opin. Biotechnol. 19 (2008) 260–265, http://dx.doi.org/10.1016/j.copbio.2008.05.006.
[4] G.D. Wright, Q&A: antibiotic resistance: where does it come from and what can we do about it? BMC Biol. 8 (2010) 123, http://dx.doi.org/10.1186/1741-7007-8-123.
[5] Y. Chartier, J. Emmanuel, U. Pieper, A. Prüss, P. Rushbrook, R. Stringer, W. Townend, S. Wilburn, R. Zghondi, Safe Management of Wastes from Health-Care Activities, World Heal. Organ., Geneva Switz, 2014.
[6] N. Ratola, A. Cincinelli, A. Alves, A. Katsoyiannis, Occurrence of organic microcontaminants in the wastewater treatment process. A mini review, J. Hazard. Mater. 239–240 (2012) 1–18, http://dx.doi.org/10.1016/j.jhazmat.2012.05.040.
[7] P. Verlicchi, M. Al Aukidy, E. Zambello, Occurrence of pharmaceutical compounds in urban wastewater: removal, mass load and environmental risk after a secondary treatment—a review, Sci. Total Environ. 429 (2012) 123–155, http://dx.doi.org/10.1016/j.scitotenv.2012.04.028.
[8] C. Grandclément, I. Seyssiecq, A. Piram, P. Wong-Wah-Chung, G. Vanot, N. Tiliacos, N. Roche, P. Doumenq, From the conventional biological wastewater treatment to hybrid processes, the evaluation of organic micropollutant removal: a review, Water Res. 111 (2017) 297–317, http://dx.doi.org/10.1016/j.watres.2017.01.005.
[9] V. Matamoros, E. Uggetti, J. García, J.M. Bayona, Assessment of the mechanisms involved in the removal of emerging contaminants by microalgae from wastewater: a laboratory scale study, J. Hazard. Mater. 301 (2016) 197–205, http://dx.doi.org/10.1016/j.jhazmat.2015.08.050.
[10] J. Umamaheswari, S. Shanthakumar, Efficacy of microalgae for industrial wastewater treatment: a review on operating conditions, treatment efficiency and biomass productivity, Rev. Environ. Sci. Biotechnol. 15 (2016) 265–284, http://dx.doi.org/10.1007/s11157-016-9397-7.
[11] J.Q. Xiong, M.B. Kurade, J.R. Kim, H.S. Roh, B.H. Jeon, Ciprofloxacin toxicity and its co-metabolic removal by a freshwater microalga Chlamydomonas mexicana, J. Hazard. Mater. 323 (2017) 212–219, http://dx.doi.org/10.1016/j.jhazmat.2016.04.073.
[12] Y. Liu, Z. Wang, K. Yan, Z. Wang, O.L. Torres, R. Guo, J. Chen, A new disposal method for systematically processing of ceftazidime: the intimate coupling UV/algae-algae treatment, Chem. Eng. J. 314 (2017) 152–159, http://dx.doi.org/10.1016/j.cej.2016.12.110.

[13] Y. Du, S. Zhang, R. Guo, J. Chen, Understanding the algal contribution in combined UV-algae treatment to remove antibiotic cefradine, RSC Adv. 5 (2015) 59953–59959, http://dx.doi.org/10.1039/C5RA10806C.
[14] Z.N. Norvill, A. Shilton, B. Guieysse, Emerging contaminant degradation and removal in algal wastewater treatment ponds: identifying the research gaps, J. Hazard. Mater. 313 (2016) 291–309, http://dx.doi.org/10.1016/j.jhazmat.2016.03.085.
[15] A. Hom-Diaz, M. Llorca, S. Rodríguez-Mozaz, T. Vicent, D. Barceló, P. Blánquez, Microalgae cultivation on wastewater digestate: β-estradiol and 17α-ethynylestradiol degradation and transformation products identification, J. Environ. Manage. 155 (2015) 106–113, http://dx.doi.org/10.1016/j.jenvman.2015.03.003.
[16] F.Q. Peng, G.G. Ying, B. Yang, S. Liu, H.J. Lai, S. Liu, Z.F. Chen, G.J. Zhou, Biotransformation of progesterone and norgestrel by two freshwater microalgae (Scenedesmus obliquus and Chlorella pyrenoidosa): transformation kinetics and products identification, Chemosphere 95 (2014) 581–588, http://dx.doi.org/10.1016/j.chemosphere.2013.10.013.
[17] A.N. Kabra, M.K. Ji, J. Choi, J.R. Kim, S.P. Govindwar, B.H. Jeon, Toxicity of atrazine and its bioaccumulation and biodegradation in a green microalga, Chlamydomonas mexicana, Environ. Sci. Pollut. Res. (2014) 12270–12278, http://dx.doi.org/10.1007/s11356-014-3157-4.
[18] M.A. Stravs, F. Pomati, J. Hollender, Exploring micropollutant biotransformation in three freshwater phytoplankton species, Environ. Sci. Process. Impacts 19 (2017) 822–832, http://dx.doi.org/10.1039/C7EM00100B.
[19] B.I. Escher, K. Fenner, Recent advances in environmental risk assessment of transformation products, Environ. Sci. Technol. 45 (2011) 3835–3847, http://dx.doi.org/10.1021/es1030799.
[20] E.L. Schymanski, H.P. Singer, J. Slobodnik, I.M. Ipolyi, P. Oswald, M. Krauss, T. Schulze, P. Haglund, T. Letzel, S. Grosse, N.S. Thomaidis, A. Bletsou, C. Zwiener, M. Ibáñez, T. Portolés, R. De Boer, M.J. Reid, M. Onghena, U. Kunkel, W. Schulz, A. Guillon, N. Noyon, G. Leroy, P. Bados, S. Bogialli, D. Stipaničev, P. Rostkowski, J. Hollender, Non-target screening with high-resolution mass spectrometry: critical review using a collaborative trial on water analysis, Anal. Bioanal. Chem. 407 (2015) 6237–6255, http://dx.doi.org/10.1007/s00216-015-8681-7.
[21] T. Kosjek, E. Heath, M. Petrović, D. Barceló, Mass spectrometry for identifying pharmaceutical biotransformation products in the environment, TrAC—Trends Anal. Chem. 26 (2007) 1076–1085, http://dx.doi.org/10.1016/j.trac.2007.10.005.
[22] R. Díaz, M. Ibáñez, J.V. Sancho, F. Hernández, Target and non-target screening strategies for organic contaminants, residues and illicit substances in food, environmental and human biological samples by UHPLC-QTOF-MS, Anal. Methods 4 (2012) 196–209, http://dx.doi.org/10.1039/C1AY05385J.
[23] E.L. Schymanski, J. Jeon, R. Gulde, K. Fenner, M. Ruff, H.P. Singer, J. Hollender, Identifying small molecules via high resolution mass spectrometry: communicating confidence, Environ. Sci. Technol. 48 (2014) 2097–2098, http://dx.doi.org/10.1021/es5002105.
[24] E.L. Schymanski, H.P. Singer, P. Longrée, M. Loos, M. Ruff, M.A. Stravs, C. Ripollés Vidal, J. Hollender, Strategies to characterize polar organic contamination in wastewater: exploring the capability of high resolution mass spectrometry, Environ. Sci. Technol. 48 (2014) 1811–1818, http://dx.doi.org/10.1021/es4044374.
[25] D. Task, M. Llorca, S. Rodríguez-mozaz, State-of-the-Art of Screening Methods for the Rapid Identification of Chemicals in Drinking Water ERNCIP Thematic Area Chemical & Biological Risks in the Water Sector, 2013, http://dx.doi.org/10.2788/22645.
[26] C. Hug, N. Ulrich, T. Schulze, W. Brack, M. Krauss, Identification of novel micropollutants in wastewater by a combination of suspect and nontarget screening, Environ. Pollut. 184 (2014) 25–32, http://dx.doi.org/10.1016/j.envpol.2013.07.048.
[27] J. Aceña, S. Stampachiacchiere, S. Pérez, D. Barceló, Advances in liquid chromatography-high-resolution mass spectrometry for quantitative and qualitative environmental analysis, Anal. Bioanal. Chem. 407 (2015) 6289–6299, http://dx.doi.org/10.1007/s00216-015-8852-6.
[28] J. Jimenez-Villarin, A. Serra-Clusellas, C. Martínez, A. Conesa, J. Garcia-Montaño, E. Moyano, Liquid chromatography coupled to tandem and high resolution mass spectrometry for the characterisation of ofloxacin transformation products after titanium dioxide photocatalysis, J. Chromatogr. A 1443 (2016) 201–210, http://dx.doi.org/10.1016/j.chroma.2016.03.063.
[29] L. Chibwe, I.A. Titaley, E. Hoh, S.L.M. Simonich, Integrated framework for identifying toxic transformation products in complex environmental mixtures, Environ. Sci. Technol. Lett. 4 (2017) 32–43, http://dx.doi.org/10.1021/acs.estlett.6b00455.
[30] S. Kern, K. Fenner, H.P. Singer, R.P. Schwarzenbach, J. Hollender, Identification of transformation products of organic contaminants in natural waters by computer-aided prediction and high-resolution mass spectrometry, Environ. Sci. Technol. 43 (2009) 7039–7046, http://dx.doi.org/10.1021/es901979h.
[31] R. Avagyan, M. Åberg, R. Westerholm, Suspect screening of OH-PAHs and non-target screening of other organic compounds in wood smoke particles using HR-orbitrap-MS, Chemosphere 163 (2016) 313–321, http://dx.doi.org/10.1016/j.chemosphere.2016.08.039.
[32] M. Llorca, S. Rodríguez-Mozaz, O. Couillerot, K. Panigoni, J. de Gunzburg, S. Bayer, R. Czaja, D. Barceló, Identification of new transformation products during enzymatic treatment of tetracycline and erythromycin antibiotics at laboratory scale by an on-line turbulent flow liquid-chromatography coupled to a high resolution mass spectrometer LTQ-Orbitrap, Chemosphere 119 (2015) 90–98, http://dx.doi.org/10.1016/j.chemosphere.2014.05.072.
[33] R. López-Serna, M. Petrović, D. Barceló, Direct analysis of pharmaceuticals, their metabolites and transformation products in environmental waters using on-line TurboFlow™ chromatography-liquid chromatography-tandem mass spectrometry, J. Chromatogr. A 1252 (2012) 115–129, http://dx.doi.org/10.1016/j.chroma.2012.06.078.
[34] M. Farré, L. Kantiani, M. Petrovic, S. Pérez, D. Barceló, Achievements and future trends in the analysis of emerging organic contaminants in environmental samples by mass spectrometry and bioanalytical techniques, J. Chromatogr. A 1259 (2012) 86–99, http://dx.doi.org/10.1016/j.chroma.2012.07.024.
[35] A. Hom-Diaz, Degradation of pharmaceutical compounds by microalgae: photobioreactor wastewater treatment, biomass harvesting and methanization, Universitat Autònoma de Barcelona, 2016. http://www.tdx.cat/handle/10803/390962 (accessed June 12, 2018).
[36] A. Hom-Diaz, A. Jaén-Gil, I. Bello-Laserna, S. Rodríguez-Mozaz, T. Vicent, D. Barceló, P. Blánquez, Performance of a microalgal photobioreactor treating toilet wastewater: pharmaceutically active compound removal and biomass harvesting, Sci. Total Environ. 592 (2017) 1–11, http://dx.doi.org/10.1016/j.scitotenv.2017.02.224.
[37] E. Parladé, A. Hom-Diaz, P. Blanquez, M. Martínez-Alonso, T. Vicent, N. Gaju, Effect of cultivation conditions on β-estradiol removal at laboratory and pilot-plant photobioreactor by an algal-bacteria consortium, Water Res. 137 (2018) 86–96, http://dx.doi.org/10.1016/j.watres.2018.02.060.
[38] M. Gros, S. Rodríguez-Mozaz, D. Barceló, Fast and comprehensive multi-residue analysis of a broad range of human and veterinary pharmaceuticals and some of their metabolites in surface and treated waters by ultra-high-performance liquid chromatography coupled to quadrupole-linear ion trap tandem, J. Chromatogr. A 1248 (2012) 104–121, http://dx.doi.org/10.1016/j.chroma.2012.05.084.
[39] A.A. Bletsou, J. Jeon, J. Hollender, E. Archontaki, N.S. Thomaidis, Targeted and non-targeted liquid chromatography-mass spectrometric workflows for identification of transformation products of emerging pollutants in the aquatic environment, TrAC—Trends Anal. Chem. 66 (2015) 32–44, http://dx.doi.org/10.1016/j.trac.2014.11.009.
[40] M. Llorca, D. Lucas, L. Ferrando-Climent, M. Badia-Fabregat, C. Cruz-Morató, D. Barceló, S. Rodríguez-Mozaz, Suspect screening of emerging pollutants and their major transformation products in wastewaters treated with fungi by liquid chromatography coupled to a high resolution mass spectrometry, J. Chromatogr. A 1439 (2016) 124–136, http://dx.doi.org/10.1016/j.chroma.2015.10.077.
[41] M. Solliec, A. Roy-Lachapelle, S. Sauvé, Development of a suspect and non-target screening approach to detect veterinary antibiotic residues in a complex biological matrix using liquid chromatography/high-resolution mass spectrometry, Rapid Commun. Mass Spectrom. 29 (2015) 2361–2373, http://dx.doi.org/10.1002/rcm.7405.
[42] M. del Mar Gómez-Ramos, A. Pérez-Parada, J.F. García-Reyes, A.R. Fernández-Alba, A. Agüera, Use of an accurate-mass database for the systematic identification of transformation products of organic contaminants in wastewater effluents, J. Chromatogr. A 1218 (2011) 8002–8012, http://dx.doi.org/10.1016/j.chroma.2011.09.003.
[43] Y. Nakagawa, S. Itai, T. Yoshida, T. Nagai, Physicochemical properties and stability in the acidic solution of a new macrolide antibiotic, clarithromycin, in comparison with erythromycin, Chem. Pharm. Bull. 40 (1992) 725–728, http://dx.doi.org/10.1248/cpb.40.725.
[44] A. Hassanzadeh, J. Barber, G.A. Morris, P.A. Gorry, Mechanism for the degradation of erythromycin A and erythromycin A 2'-ethyl succinate in acidic aqueous solution, J. Phys. Chem. A 111 (2007) 10098–10104, http://dx.doi.org/10.1021/jp073030y.
[45] S.R. Batchu, V.R. Panditi, K.E. O'Shea, P.R. Gardinali, Photodegradation of antibiotics under simulated solar radiation: implications for their environmental fate, Sci. Total Environ. 470–471 (2014) 299–310, http://dx.doi.org/10.1016/j.scitotenv.2013.09.057.
[46] L. Tong, P. Eichhorn, S. Pérez, Y. Wang, D. Barceló, Photodegradation of azithromycin in various aqueous systems under simulated and natural solar radiation: kinetics and identification of photoproducts, Chemosphere 83 (2011) 340–348, http://dx.doi.org/10.1016/j.chemosphere.2010.12.025.
[47] Y.H. Kim, K. Pak, J.V. Pothuluri, C.E. Cerniglia, Mineralization of erythromycin A in aquaculture sediments, FEMS Microbiol. Lett. 234 (2004) 169–175, http://dx.doi.org/10.1016/j.femsle.2004.03.027.
[48] M. Morar, K. Pengelly, K. Koteva, G.D. Wright, Mechanism and diversity of the erythromycin esterase family of enzymes, Biochemistry 51 (2012) 1740–1751, http://dx.doi.org/10.1021/bi201790u.
[49] P. Barthélémy, D. Autissier, G. Gerbaud, P. Courvalin, Enzymic hydrolysis of erythomycin by a strain of escherichia coli, J. Antibiot. (Tokyo) (1984) 1692–1696, http://dx.doi.org/10.7164/antibiotics.37.1692.
[50] M. Matsuoka, T. Sasaki, Inactivation of macrolides by producers and pathogens, Curr. Drug Targets Infect. Disord. 4 (2004) 217–240, http://dx.doi.org/10.2174/1568005043340696.
[51] L. Wei, K. Qin, N. Zhao, D.R. Noguera, W. Qiu, Q. Zhao, X. Kong, W. Zhang, F.T. Kabutey, Transformation of erythromycin during secondary effluent soil aquifer recharging: removal contribution and degradation path, J. Environ. Sci. (China) 51 (2017) 173–180, http://dx.doi.org/10.1016/j.jes.2016.08.004.
[52] E.F. Fiese, S.H. Steffen, Comparison of the acid stability of azithromycin and erythromycin A, J. Antimicrob. Chemother. 25 (1990) 39–47, http://dx.doi.org/10.1093/jac/25.suppl_A.39.

[53] M. Sturini, A. Speltini, F. Maraschi, L. Pretali, A. Profumo, E. Fasani, A. Albini, R. Migliavacca, E. Nucleo, Photodegradation of fluoroquinolones in surface water and antimicrobial activity of the photoproducts, Water Res. 46 (2012) 5575–5582, http://dx.doi.org/10.1016/j.watres.2012.07.043.
[54] G.E. Linke, J. Chen, W. Xiaoxuan, S. Zhang, X. Qiao, C. Xiyun And, X. Qing, Aquatic photochemistry of fluoroquinolone antibiotics: kinetics, pathways, and multivariate effects of main water constituents, Environ. Sci. Technol. 44 (2010) 2400–2405, http://dx.doi.org/10.1021/es902852v.
[55] I. Michael, E. Hapeshi, J. Aceña, S. Perez, M. Petrović, A. Zapata, D. Barceló, S. Malato, D. Fatta-Kassinos, Light-induced catalytic transformation of ofloxacin by solar Fenton in various water matrices at a pilot plant: mineralization and characterization of major intermediate products, Sci. Total Environ. 461–462 (2013) 39–48, http://dx.doi.org/10.1016/j.scitotenv.2013.04.054.
[56] A.S. Maia, A.R. Ribeiro, C.L. Amorim, J.C. Barreiro, Q.B. Cass, P.M.L. Castro, M.E. Tiritan, Degradation of fluoroquinolone antibiotics and identification of metabolites/transformation products by liquid chromatography-tandem mass spectrometry, J. Chromatogr. A 1333 (2014) 87–98, http://dx.doi.org/10.1016/j.chroma.2014.01.069.
[57] T. Haddad, K. Kümmerer, Characterization of photo-transformation products of the antibiotic drug ciprofloxacin with liquid chromatography-tandem mass spectrometry in combination with accurate mass determination using an LTQ-orbitrap, Chemosphere 115 (2014) 40–46, http://dx.doi.org/10.1016/j.chemosphere.2014.02.013.
[58] S. Alvarez-Elcoro, M.J. Enzler, The macrolides: erythromycin, clarithromycin, and azithromycin, Mayo Clin. Proc. 74 (1999) 613–634, http://dx.doi.org/10.4065/74.6.613.
[59] J.F. Westphal, Macrolide - induced clinically relevant drug interactions with cytochrome P-450A (CYP) 3A4: an update focused on clarithromycin, azithromycin and dirithromycin, Br. J. Clin. Pharmacol. 50 (2000) 285–295, http://dx.doi.org/10.1046/j.1365-2125.2000.00261.x.

Chapter 4

Integrated suspect screening methodologies for the identification of hazardous TPs in physical and/or chemical treatments

Jaén-Gil et al., 2019. Journal of Hazardous Materials, 380: 120851

Jaén-Gil et al., 2020. Environmental Science & Technology, 54 (14): 9062 – 9073

Journal of Hazardous Materials 380 (2019) 120851

Contents lists available at ScienceDirect

Journal of Hazardous Materials

journal homepage: www.elsevier.com/locate/jhazmat

Metoprolol and metoprolol acid degradation in UV/H_2O_2 treated wastewaters: An integrated screening approach for the identification of hazardous transformation products

Adrián Jaén-Gil[a], Gianluigi Buttiglieri[a], Aleix Benito[b], Rafael Gonzalez-Olmos[b], Damià Barceló[a,c], Sara Rodríguez-Mozaz[a,*]

[a] Catalan Institute for Water Research (ICRA), H2O Building, Scientific and Technological Park of the University of Girona, Emili Grahit 101, E-17003, Girona, Spain
[b] IQS School of Engineering, Universitat Ramon Llull, Via Augusta 390, 08017, Barcelona, Spain
[c] Water and Soil Quality Research Group, Department of Environmental Chemistry, (IDAEA-CSIC), Jordi Girona 18-26, E-08034, Barcelona, Spain

GRAPHICAL ABSTRACT

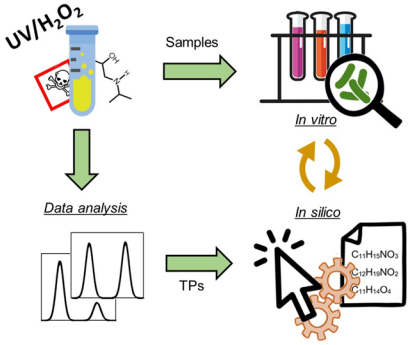

ARTICLE INFO

Editor: G. Li Puma

Keywords:
Metoprolol
Metoprolol acid
Advanced oxidation processes
Suspect screening
Hazard assessment

ABSTRACT

Advancements on analytical strategies to determine the chemicals present in treated wastewater are necessary to clearly link their occurrence with the ecotoxicity of such effluents. This study describes the development of an integrated screening approach to determine the highest number of pharmaceutical transformation products (TPs) in a single run. The identification of TPs was based on the comparison of detected features with literature sources, compound prediction tools, in-house libraries and reference standards using high-resolution mass spectrometry (HRMS). This integrated approach allowed a better estimation (*in silico*) of the ecotoxicological contribution of the individual TPs identified. As a proof of concept, this methodology was applied for identification of the TPs generated from metoprolol and its main human metabolite (metoprolol acid) in pure water, hospital wastewater and industrial wastewater treated by UV/H_2O_2. Twenty-four TPs with potential ecotoxicological implications were identified and their presence was pinpointed as a function of the treated wastewater. An integrated screening approach has been developed using four different screening methodologies in the same run. Additionally, the metabolite MTPA has been considered as a target pollutant in UV/H_2O_2 experiments.

* Corresponding author.
E-mail address: srodriguez@icra.cat (S. Rodríguez-Mozaz).

https://doi.org/10.1016/j.jhazmat.2019.120851
Received 25 January 2019; Received in revised form 25 June 2019; Accepted 29 June 2019
Available online 06 July 2019

1. Introduction

A large number of pharmaceuticals compounds generated from industrial and domestic activities are present in wastewater effluents and released into the natural aquatic environment (Gogoi et al., 2018; Luo et al., 2014; Verlicchi et al., 2012), where they can pose a long-term risk for aquatic organisms and human health (Dévier et al., 2011; Celiz et al., 2009; Hernández et al., 2011). Since conventional wastewater treatment plants (WWTPs) are not designed to eliminate these contaminants completely (Verlicchi et al., 2012), the development of alternative and polishing wastewater treatment processes has become of high interest in order to attain appropriate quality status on treated water. Much time and efforts have been invested to monitor the removal efficiencies of selected pharmaceuticals by means of alternative wastewater treatments (Cruz-Morató et al., 2014; Ferrando-Climent et al., 2015; Hom-Diaz et al., 2017; Arslan et al., 2014; Ooi et al., 2017). In this context, advanced oxidation processes (AOPs) are among the most investigated, and suggested to be included in the wastewater treatment trains (Verlicchi et al., 2015).

Among the pharmaceuticals present in wastewater, metoprolol (MTP) is a highly consumed β-blocker (Dong et al., 2013) detected in wastewater in the range of 160–2000 ng/L (Maurer et al., 2007; Scheurer et al., 2010), with low removal rates in conventional WWTPs (usually between 0 and 36%) (Scheurer et al., 2010; Lacey et al., 2012; Rubirola et al., 2014). After human consumption, 10% of metoprolol is excreted unchanged in urine (Maurer et al., 2007), whereas up to 60–65% of MTP initial dose is excreted as metoprolol acid (MTPA) as well as other metabolites (although at much lower concentration) such as O-desmethylmetorpolol (O-DMTP), α-hydroxymetoprolol (α-HMTP) and deaminated MTP (Escher and Fenner, 2011; Kern et al., 2010; Godbillon and Duval, 1984). According to the guidelines on environmental risk assessment of the European Medicines Agency, MTPA should be considered as a relevant MTP metabolite in monitoring studies being excreted at ≥ 10% of the administered dose (Wharf and Kingdom, 2010). Additionally, MTPA is pointed out to be also a transformation product (TP) of MTP in WWTPs and sometimes more recalcitrant than MTP itself (Rubirola et al., 2014). The generation of this metabolite from atenolol biodegradation in activated sludge (CAS) has also been demonstrated (Radjenović et al., 2008).

Typically, sensitive and selective analytical methods have been developed for monitoring the elimination of target pollutants, driving studies to a limited number of chemicals (Daughton, 2004). The use of this approach becomes incomplete when applying to wastewater effluents, where the formation on unknown chemicals coming from biological and physicochemical transformation processes appears to be extensive (Kern et al., 2010). The presence of TPs are of high concern since they may be more toxic and/or persistent than the parent compounds (Escher and Fenner, 2011). Therefore, the application of advanced analytical instrumentation based on high-resolution mass spectrometry (HRMS) becomes crucial for the detection and identification of unknown TPs in treated wastewater effluents. Different analytical strategies have been successfully applied for the screening of TPs, considering that the analytical reference standards of such TPs are not always available for confirmation (Gago-Ferrero et al. (2015); Moschet et al., 2013; Helbling et al., 2010). Among them, non-target analysis with the selection of the most intense detected peaks represents the simplest applied strategy to prioritize compound identification (Schollée et al., 2015). However, the presence of hundreds of TPs coming from several contaminants within a single sample points out post-acquisition data processing as a tedious, time-consuming and challenging task (Agüera et al., 2013; Chibwe et al., 2017). Suspect screening approaches have partially overcome this challenge, where the information on tentative compounds can be collected from software prediction tools or databases containing a broad number of compounds to be likely detected (Bletsou et al., 2015; Schymanski et al., 2015, 2014a; Krauss et al., 2010). Therefore, the integration of these screening strategies in a single step may allow accounting for a greater proportion of TPs present in samples.

In recent years, hazard-oriented studies have been applied to assess the risk of compound mixtures of TPs using both *in vitro* bioassays and *in silico* studies (Han et al., 2018; Villaverde et al., 2018; Secrétan et al., 2018; Toolaram et al., 2017; Menz et al., 2017). So far, the most common applications for *in silico* modeling are the quantitative structure-activity relationships (QSAR) based methodologies. QSAR allows to estimate the ecotoxicological effects of the selected chemicals by quantitative association of their structural parameters (or physicochemical properties) with their biological activity (Cherkasov et al., 2014). The combination of these bioanalytical and computational tools may represent a holistic approach for a comprehensive assessment of the potential risks in treated wastewater effluents.

The aim of the present study is to develop an integrated screening methodology for comprehensive detection and identification of hazardous TPs in hospital (HWW) and industrial wastewater (IWW). A customized overview of MTP and MTPA transformation in the selected wastewater matrices treated by UV/H_2O_2 photo-oxidation is provided as a proof of concept. The ecotoxicity of the samples was determined by using an *in vitro* bioassay, as well as theoretically estimated using *in silico* QSAR models for all the individual compounds identified. This study highlights the utmost importance to perform an advanced and integrated screening approach for proper identification of hazardous TPs in wastewater effluents.

2. Experimental

2.1. Chemicals and reagents

Metoprolol tartrate salt (MTP) was purchased from Sigma-Aldrich (Barcelona, Spain); metoprolol acid (MTPA), O-desmethylmetoprolol (O-DMTP), and α-hydroxymetoprolol (α-HMTP) were supplied by Toronto Research Chemicals Inc. (North York, Canada) at high purity grade (> 98%). Ultra-pure water, acetonitrile and methanol LiChrosolv grade were supplied by Merck (Darmstad, Germany).

2.2. Experimental set-up

UV/H_2O_2 photo-oxidation experiments were carried out under laboratory conditions at 25 °C using a UV Laboratory Reactor System from UV-Consulting Peschl® with a total working volume of 550 mL, approximately. The UV lamp consisted in a low-pressure mercury vapor lamp 15 W Heraeus Noblelight TNN 15/32 emitting at 254 nm. Preliminary experiments were performed in order to optimize the best AOPs conditions. H_2O_2 consumption was first optimized in pure water fortified at 10 mg/L of MTP and treated with UV, H_2O_2 and UV + H_2O_2 at 25, 100, 250 and 1000 mg/L. The optimized H_2O_2 concentration and the final experimental time (25 mg/L H_2O_2 and 10 min of reaction) were selected to further evaluate the elimination of MTP, MTPA and the generated TPs. Additionally, sodium thiosulfate was added to interrupt oxidation reaction (with stoichiometric excess of 20%). Then, individual degradation experiments at the optimized AOP conditions selected (25 mg/L H_2O_2 and 10 min of reaction) were launched to describe degradation kinetics in pure water of MTP and MTPA (spiked at 2.5 mg/L each).

Afterwards, three sets of experiments were performed in duplicate for the determination of TPs in: (a) pure water fortified with 2.5 mg/L of MTP and MTPA as a reference sample; (b) hospital wastewater (HWW) from the sewer manifold of Sant Joan de Déu Hospital (Barcelona, Catalonia) fortified with 2.0 µg/L of MTP and MTPA to assure the presence of the target pollutants at concentrations commonly detected in wastewater; and (c) industrial wastewater (IWW) from a pharmaceutical industry containing MTP at 33.0 mg/L. The samples were collected in duplicate at initial and final time (10 min) adding 20% in excess of sodium thiosulfate to stop oxidation reaction. Detailed information is presented in Supplementary Material, S1.

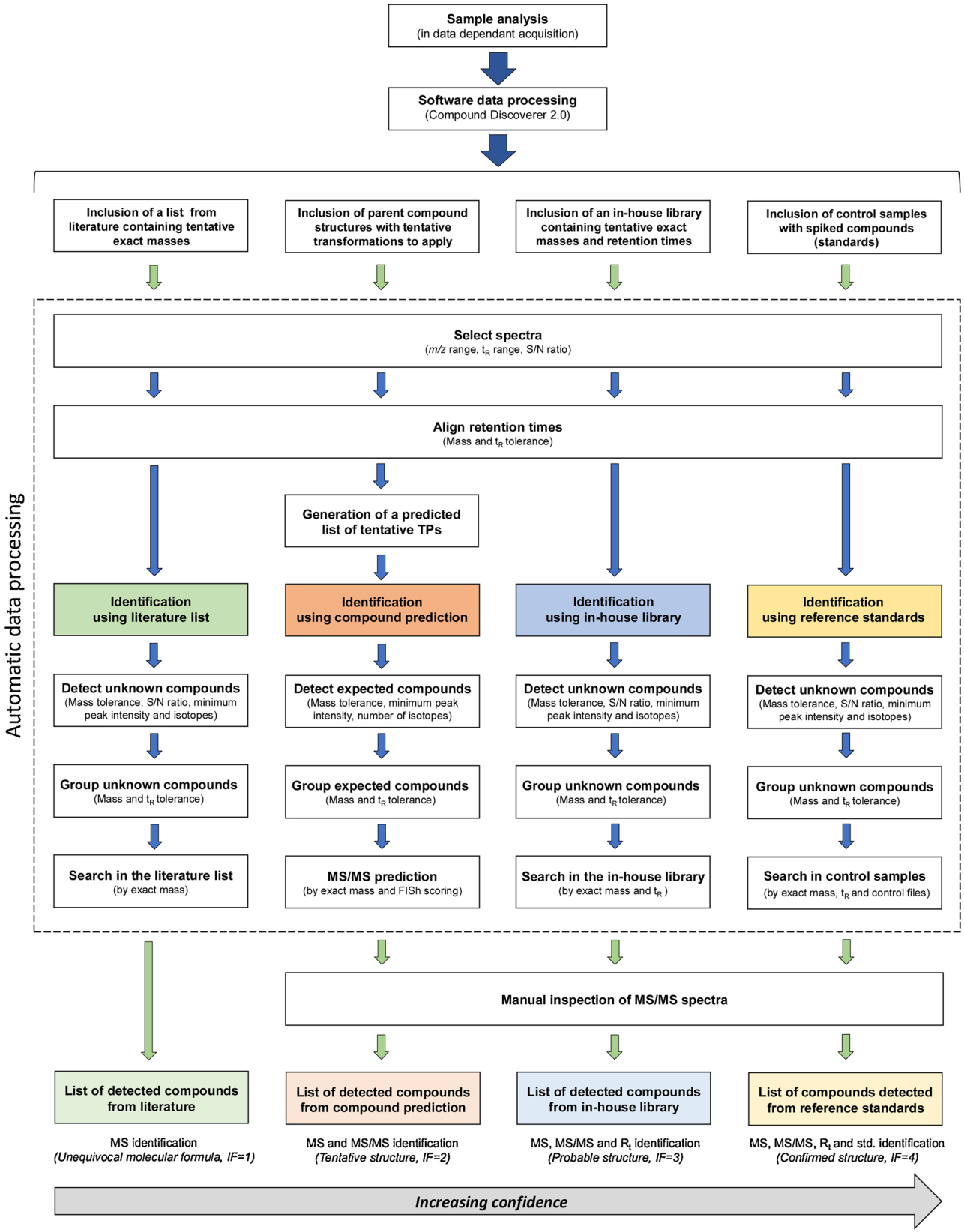

Fig. 1. Screening workflow containing the four different identification strategies used: identification from literature sources, software compound prediction, in-house libraries and analytical reference standards (IF = identification factor).

2.3. Sample analysis and data processing

The samples collected from the three sets of UV/H_2O_2 experiments as well as the reference samples (mix of individual standards available spiked at 2.5 mg/L) were analyzed using a liquid-chromatography system coupled to a (LTQ)-Orbitrap mass spectrometer (Thermo Fisher Scientific Inc., Waltham, MA) as described previously (Jaén-Gil et al., 2019). Detailed information of sample analysis is presented in Supplementary Material, S1.

A comprehensive screening methodology using Compound Discoverer 2.0 connected to Mass Frontier 7.0 software (Thermo Fisher Scientific Inc., Waltham, MA) was applied in a single run to the data collected after MS acquisition from pure water, HWW and IWW samples. The scheme containing the workflow procedure used for data treatment is presented in Fig. 1. Prior to automatic software data processing, input files (chromatograms and mass spectra files) were loaded together with two different lists containing suspected compounds to be present in samples: the 1st list containing compound exact masses from literature sources and the 2nd list (the in-house library) containing compound exact masses and retention times (R_t) obtained from previous experiments (Jaén-Gil et al., 2019). Additionally, MTP and MTPA chemical structures were pinpointed as well as tentative chemical transformations to further create the 3rd list of tentative predicted TPs by the software. Additional information is presented in Table S1.

Automatic data processing starts with MS data filtering between 50 and 400 Da and from 1 to 12 min with a S/N ratio of 3 (Fig. 1, Table S1). To compensate small differences in retention times, chromatographic alignment was performed by using a mass tolerance error of 5 ppm and a maximum retention time shift of 0.3 min. All those masses present in non-spiked pure water (control blank sample) were deducted from all matrix samples, by applying a mass and a retention time tolerance of 5 ppm and of 0.3 min, respectively. Immediately after, data processing was performed in two different steps: a) by detection of unknown compounds (where features above a S/N of 10 with a minimum peak intensity of 10^4 counts were selected) and b) by detection of expected compounds from compound prediction (where more complete MS full scan data was required without being filtered out). Then, the three lists of TPs previously indicated (from literature, in-house library and the one automatically created by the software) were used to identify the TPs generated from MTP and MTPA, jointly with the data acquired from the spiked control samples at a mass tolerance error of 5 ppm. This procedure was performed throughout four identification strategies, in accordance with the clarification scheme previously reported by Schymanski et al. (2014b): (1) the list from the literature (Table S2) was used to identify *unequivocal molecular formulas* (identification factor 1, IF = 1) by comparison of compound exact masses; (2) the list of predicted TPs automatically created from the software (Table S3) was used to identify *tentative structures* (identification factor 2, IF = 2) by comparison of compound exact masses and predicted MS/MS scans; (3) the in-house library (Table S4) was used to identify *probable structures* (identification factor 3, IF = 3) by comparison of reported TP exact masses, experimental retention times and MS/MS ion spectra; (4) *confirmed structures* (identification factor 4, IF = 4) were identified with reference standards through comparison with MS exact masses, retention time and MS/MS ion fragmentation pattern from control files. Since most of the compounds were identified from more than one identification strategy, the maximum confidence attained for each compound was assigned as follows: *unequivocal molecular formulas* (IF = 1) < *tentative structures* (IF = 2) < *probable structures* (IF = 3) < *confirmed structures* (IF = 4).

All information provided by the software was manually checked (to avoid false positives hits) and the compounds with reasonable confidence (IF ≥ 2) were further included into the existing in-house library for the detection of MTP and MTPA TPs in future studies. Then, transformation pathways were suggested and TPs were classified as 1st, 2nd and ≥ 3rd generation regarding the number of chemical transformations applied to the MTP chemical structure (1, 2 or ≥ 3, respectively).

2.4. In silico and in vitro toxicological assessment

Since no reference standards are commercially available for most of the identified TPs, the software EPI Suite™ through ECOSAR™ model was applied to predict the following acute toxicity endpoints (expressed in mg/L) for each compound: 48-h *Daphnia* LC_{50}, 96-h fish LC_{50} and 96-h green algae EC_{50}. Acute Toxicity Estimation (*ATEmix*) was calculated to evaluate the toxicity contribution of all identified chemicals present in each mixture sample, in comparison with the estimated toxicity at the initial time (Eq. (1)) (European Chemicals Agency, 2017). Potential synergistic and antagonistic effects between the compounds are excluded in this equation. C_i denotes the presence of a compound present in a mixture (in %) and ATE_i accounts for the acute toxicity estimated for an ingredient (EC_{50} or LC_{50}).

$$\frac{100}{ATE_{mix}} = \sum_{n} \frac{C_i}{ATE_i} \quad (1)$$

The *in silico* estimations were tentatively correlated with the individual ecotoxicological contribution of the parent compounds (MTP and MTPA) and the TPs identified using *in vitro* bioassays. The ISO 11348-3 protocol presented in Supplementary Material, S1 (ISO 11348-3:1998, 1998) for testing bacterial bioluminescence of wastewater matrices was used to assess toxicity throughout Microtox® Model 500 Toxicity Analyzer (Strategic Diagnostics Inc. Newark, DE, US). The percentage of decay on emitted light was measured when samples were in contact 15 min with the bioluminescent bacterium *V. fischeri* at a final experimental time of 10 min. The presence of sodium thiosulfate in bioassay was tested and had no toxic effect on luminescent bacteria at the added concentration.

Additional parameters were also evaluated in accordance with the individual structural properties of the detected emerging TPs such as bioaccumulation factor, mutagenicity and developmental toxicity using the Toxicity Estimation Software Tool (T.E.S.T.) v. 4.2.1 program (consensus method). Chemical biodegradability, carcinogenicity and toxicological hazards according to the Cramer classification scheme (Cramer et al., 1976) were evaluated using Toxtree (Estimation of Toxic Hazard – A Decision Tree Approach) v. 3.1.0 (Ideaconsult Ltd, Sofia, Bulgaria).

3. Results and discussion

3.1. MTP and MTPA degradation kinetics

The preliminary experiments in fortified pure water (MTP at 10 mg/L) with UV, H_2O_2 and UV + H_2O_2 (at 25, 100, 250 and 1000 mg/L) promoted high removal efficiencies of MTP up to 99% after few minutes in most of the cases (Fig. S1). While H_2O_2 alone had no effect on MTP degradation, UV and UV + H_2O_2 experiments provided increasing MTP degradation rates with increasing H_2O_2 concentration (Fig. S2). Since a very high removal was already achieved at low H_2O_2 dosages, further experiments were performed at 25 mg/L of H_2O_2 and 10 min of reaction. Afterwards, the removal of MTP and MTPA (at an initial concentration of 2.5 mg/L each) was monitored in separated experiments (Fig. S3). The fast removals of MTP and MTPA fitted quite well ($R^2 > 0.98$) pseudo first-order kinetics (Fig. S4) with K_{obs} of 1.95 min^{-1} and 2.39 min^{-1} for MTP and MTPA, respectively. Additional information is provided in Supplementary Material, S3.

Finally, dissimilar results were obtained regarding MTP and MTPA removal for the three matrices tested in TP determination experiments. They were both eliminated almost 100% in pure water (initial concentration 2.5 mg/L each), whereas the elimination rates in hospital wastewater were 71.6 ± 0.8% for MTP and 88.7 ± 1.1% for MTPA

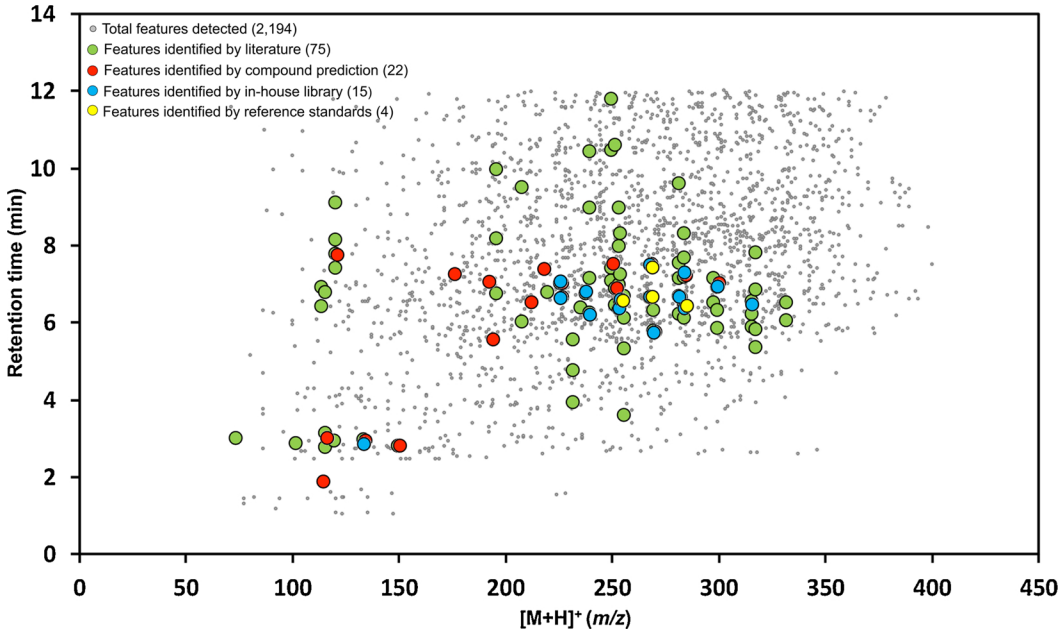

Fig. 2. Total ion features $[M+H]^+$ detected in pure water, HWW and IWW after data filtering grouped by molecular weight and retention time (grey dots). Identified features using the four strategies presented in Fig. 1: literature (green dots), software compound prediction (red dots), in-house libraries (blue dots) and analytical reference standards (yellow dots). (For interpretation of the references to colour in this figure legend, the reader is referred to the web version of this article).

(initial concentration 2.0 µg/L each). In contrast, only 11.1 ± 1.5% of MTP (initial concentration 33.0 mg/L) was eliminated in industrial wastewater. These findings indicate that many other factors are involved (*e.g.* organic matter, bacteria, pollutant concentration and in general matrix effect, among others, Table S5) and seemed to interfere in MTP and MTPA elimination by the AOP technology. Moreover, some recalcitrant by-products might be formed which could not be completely degraded under the selected UV/H_2O_2 conditions. Thus, the elucidation and identification of their transformation pathways as well as the evaluation of their toxicity in the different matrices are required to provide a comprehensive overview of the treatment technology performance.

3.2. Detection and identification of TPs

Characterization of MTP and MTPA transformation through UV/H_2O_2 advanced oxidation processes was performed by applying the methodology described in Section 2.3 in pure water, HWW and IWW matrices. Peak filtering resulted in a total of 2194 features of interest to be further processed through the four identification strategies selected (Fig. 2). After data processing, 85 candidates were finally pinpointed as potential TPs from MTP and MTPA (Table S6), which highlights a dramatic data reduction of 96%.

Among them, 88% (75 features) were detected by automatic comparison with the selected compound exact masses, collected from the literature list in Table S2 (32 exact masses out of 39 compounds were detected at different retention times, Table S6) and their predicted isotopic patterns. Since the molecular formula was the only identification factor that could be considered for each compound (IF = 1), the chance of false positives was especially significant for this suspect screening strategy. For instance, the presence of *m/z* 284.18563 (α-HMTP) was found at five different retention times along the same chromatogram, indicating poor selectivity on peak detection. Among the 75 compounds detected, 92.9% were detected matching two isotopic ions from the predicted pattern, while a 6.7% and a 0.4% were matched with three and four isotopic ions. These TP candidates were classified as *unequivocal molecular formulas* (IF = 1).

Another set of compounds (22 compounds out of the 85 final candidates; 26%) (Fig. 2 and Table S6) was detected based on the comparison of the compound exact masses and fragmentation spectra of the TPs predicted by the software (Table S3) with the data acquired (IF = 2). The total number of predicted candidates automatically generated and included into the prediction list was 357 (264 for MTP and 93 for MTPA, Table S3), meaning that only a small percentage of them was detected in the samples. Even though this strategy provides valuable information to rapidly identify *tentative structures*, manual inspection was always required to avoid false positive hits. Chemical structures were classified as features when the predicted MS/MS spectra included at least 3 characteristic fragments and/or FISh (Fragment Ion Search) coverages ≥ 65% (Jaén-Gil et al., 2018).

The identification using in-house libraries (Table S4) allowed the detection of 15 compounds (18% of the 85 total suspected candidates; Fig. 2 and Table S6), having the same compound exact masses, experimental retention times and product fragmentation patterns as in previous MTP and MTPA degradation studies (Jaén-Gil et al., 2019). For instance, the fragmentation spectra of TP284, previously reported in fungal experiments at R_t of 7.31 min (Jaén-Gil et al., 2019), was also detected in the present study with UV/H_2O_2 treatment at the same retention time. These features summed an additional identification factor (IF = 3) to be classified as *probable structures*.

Finally, 5% (4 compounds) of the 85 candidates were classified as *confirmed structures* after comparison with analytical standards (Fig. 2 and Table S6), being this strategy overly restrictive (IF = 4). Due to the overall limited availability of chemical standards of contaminant TPs, the application of other screening strategies based on literature information, compound prediction and in-house libraries are necessary to attain an enhanced overview of the TPs generated.

The obtained results highlight the increase in the number of features with the decrease of identification factors number. The four compounds confirmed with reference standards were also detected through the other three strategies (in-house library, compound prediction and literature information). The use of the in-house library allowed the detection of 11 additional compounds. However, 4 out of the 15 compounds identified using in-house libraries were not detected using software compound prediction: two of them were not predicted by the software (*e.g. m/z* 238.14376 and *m/z* 240.15940) while the other two were not intense enough to perform MS/MS ion fragmentation (*e.g. m/z* 254.13868 and *m/z* 316.17545). Since no MS/MS confirmation was

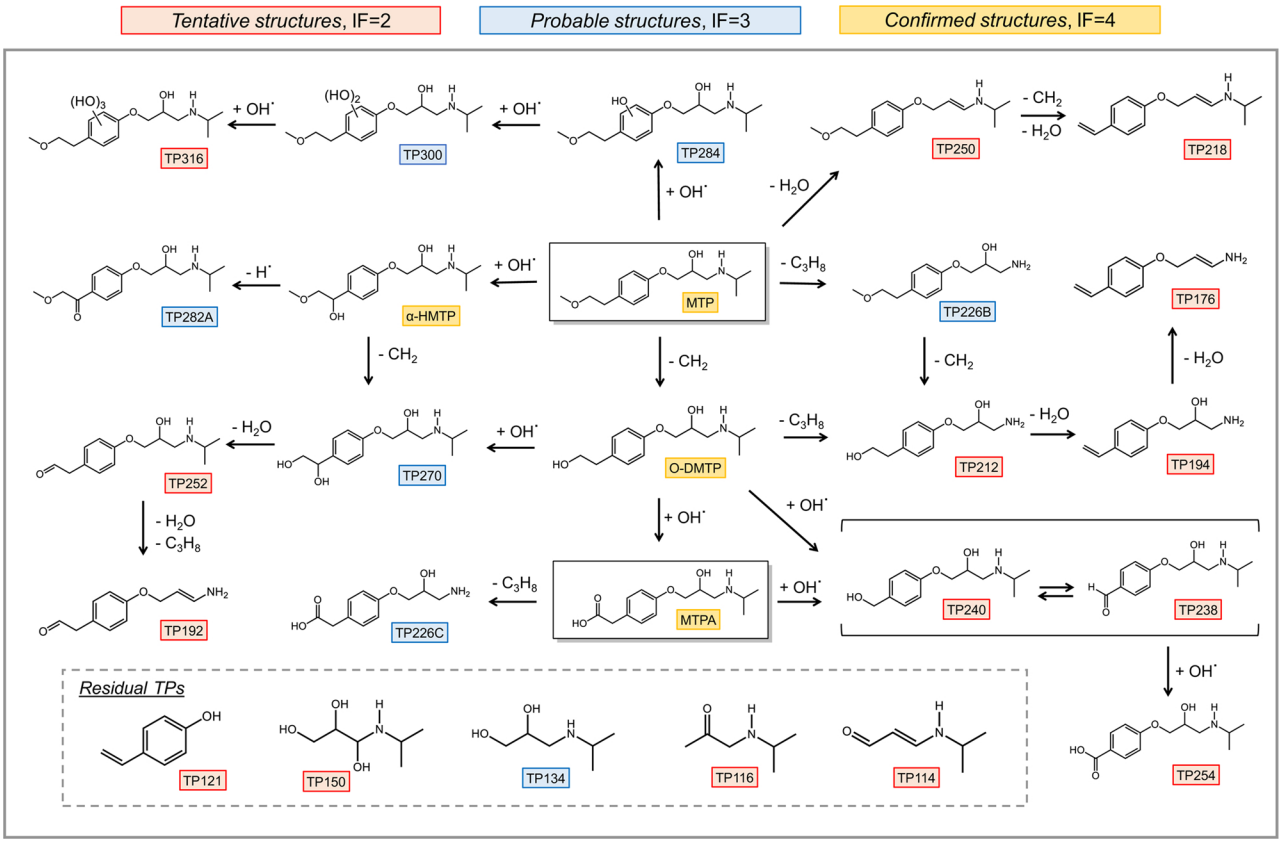

Fig. 3. TPs identified in pure water, HWW and IWW effluents though UV/H_2O_2 treatment: *tentative structures,* IF = 2 (red); *probable structures,* IF = 3 (blue); and *confirmed structures*, IF = 4 (yellow). (For interpretation of the references to colour in this figure legend, the reader is referred to the web version of this article).

possible, these 4 TPs were classified as *tentative structures* through TP exact mass and retention time comparison only (IF = 2). Moreover, 12 out of 37 compounds present in the literature list were not included into the software predicted list either. On the other hand, the use of compound prediction strategy allowed the inclusion of 345 tentative exact masses not present into the ready-made literature list. The obtained results indicate that the combination of different suspect screening strategies is required to account for the highest number of TPs.

After compound identification (Table S7), MTP and MTPA transformation pathways were suggested taking into account the 26 compounds with IF ≥ 2 from the 85 initial candidates (Fig. 3). Finally, the new generated information was included into the in-house database to perform faster and more reliable screening analysis of TPs in future studies. In comparison with other studies previously reported (Jaén-Gil et al., 2018; Llorca et al., 2016; Kaserzon et al., 2017), this methodology limited the presence of false positives at a higher extent, reducing time and efforts invested in data processing.

3.3. MTP and MTPA transformation in wastewater effluents

The removal percentages of MTP and MTPA and the relative abundance of photo-oxidation intermediates were calculated at the final experimental time of 10 min for each of the considered water matrices (Fig. 4). Since no references standards were available for all the intermediates identified (to quantify losses on SPE extraction) and their chemical structure were similar to the parent compound (MTP), the same recovery and matrix effect were considered for all TPs identified in the suggested semi-quantification approach.

The highest removal rates were achieved with MTP and MTPA spiked in pure water (2.5 mg/L) as indicated in Section 3.1. The absence of other interfering contaminants and organic matter led to extremely high elimination rates (≥ 99%). A similar pattern was observed in the elimination of the generated intermediates, with 82% of them classified as ≥ 3rd generation TPs (Fig. 4). These compounds are mainly described as residual TPs (TP114, TP116, TP121, TP134 and TP150) indicating that the treatment process is close to attain total compound mineralization. For instance, TP114 (corresponding to the lowest molecular mass identified in the analyzed samples) was detected at a relative abundance of 72%.

The results of the experiments performed with UV/H_2O_2 treating HWW (spiked with MTP and MTPA at the realistic concentration of 2.0 µg/L) were quite different (Fig. 4): 28% of MTP remained in the samples at the end of the treatment (MTP removal of 72%). Similar removal rates were observed for MTPA (89%). The higher HWW matrix complexity reduced the efficiency of the UV/H_2O_2 treatment in comparison with pure water experiments. There was, in fact, higher relative percentage of 1st and 2nd generation TPs (up to 39% and 53%, respectively) and lower percentages of those ≥ 3rd generation, confirming the delay in terms of global degradation rates. Higher proportion of the recalcitrant intermediates α-HMTP and TP240 were also found in comparison with pure water experiments, attaining percentage of about 39% and 47%, respectively. Among them, the α-HMTP was reported as a persistent TP in activated sludge (Rubirola et al., 2014) while both of them were also detected in fungi experiments (Jaén-Gil et al., 2019).

Finally, the last experiments in IWW were characterized by a high content of organic matter (Table S5) and the extremely high MTP concentration (33.0 mg/L). This source was collected from a pharmaceutical industry producing MTP, whereas no MTPA was detected. The efficiency in terms of MTP elimination was much lower than in previous cases (only 11%). The degradation pathways of MTP were also affected, leading to a large increase in terms of number and presence of 1st generation TPs (64% of the total compounds detected in IWW). This is for example the case of TP300, a 2nd generation TP found in HWW and less present in IWW while TP284, 1st generation TP and intermediate in

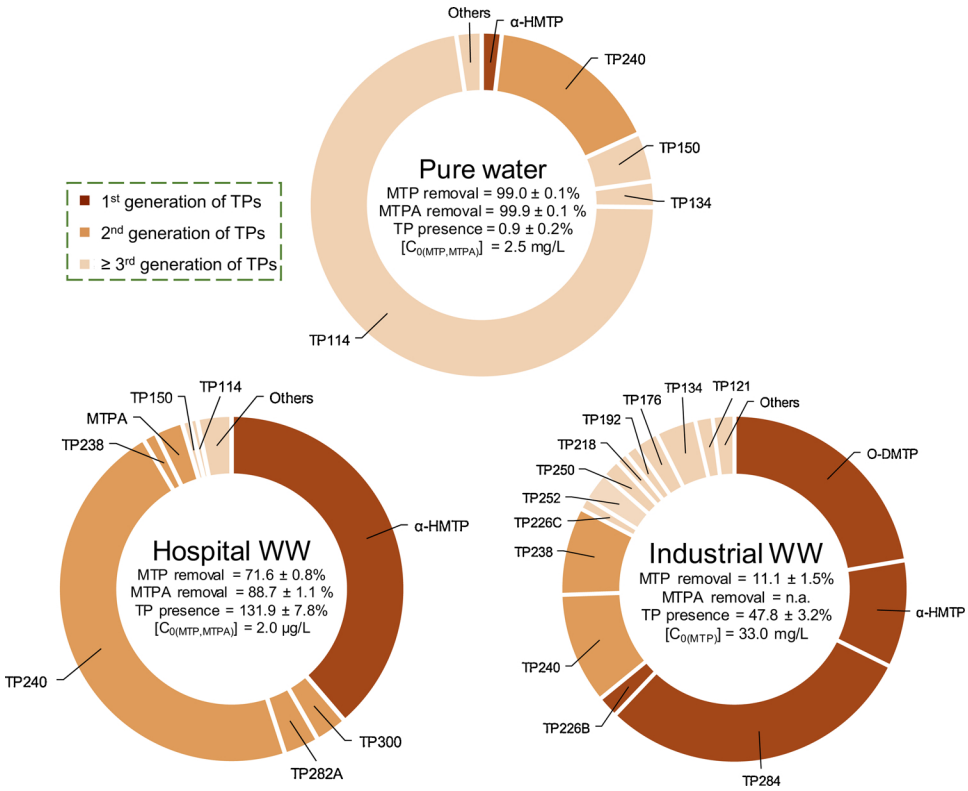

Fig. 4. Presence contribution ($Area^{t}_{TP}/\Sigma Area^{t}_{TPs}$)-(%) of the TPs identified in pure water, HWW and IWW though UV/H_2O_2 treatment at experimental final time of 10 min. TPs are classified as 1st generation (dark brown), 2nd generation (brown), and ≥ 3rd generation (light brown). Initial concentration, MTP and MTPA removal and TP presence as ($\Sigma Area^{t}_{TPs}/\Sigma Area^{0}_{MTP+MTPA}$)-(%) is also included.

the formation of TP300 (Fig. 3), was present at higher concentration in IWW (Fig. 4). Likewise, TP240 (2nd generation TP) was more present in HWW than in IWW whereas O-DMTP, 1st generation TP and intermediate in the formation of TP240 (Fig. 3), was present at higher concentration in IWW (Fig. 4). It is important to mention that O-DMTP has also been reported as a compound of environmental concern (Rubirola et al., 2014). These results emphasize the difficulties in treating this kind of matrices with UV/H_2O_2, as expected, but interestingly shade lights also on TP generation.

As a conclusion, maintaining the same UV/H_2O_2 conditions, different removal profile of MTP and MTPA was observed, as a function of the water matrix and the initial concentration(s) of the parent compound(s). Extremely different scenarios were also observed in terms of presence of the identified intermediates (Fig. 4), also due to the influence of the different organic matter content and other interfering compounds of the water matrix on degradation mechanisms. In contrast with other reported AOP experiments such as Fenton, photo-Fenton, ozonation and Fe^{2+}/ozonation (Romero et al., 2016a, b; Wilde et al., 2014)), it is important to remark that MTPA was highly eliminated by UV/H_2O_2 photo-oxidation not only in pure water but also in such a complex matrix like HWW.

3.4. Ecotoxicological impacts of the generated TPs

The detection and identification of known and unknown intermediates of target compounds provided the possibility to focus on those compounds of potential concern. While the removal of MTP and MTPA decreased from pure water to HWW and IWW experiments (Fig. 5a), the calculated *in silico* acute toxicity, relative to the toxicity estimated at the initial time, increased after AOP treatment up to 35% in IWW (Fig. 5b) and decreased up to 100% and 43% in pure water and HWW, respectively. This fact might be related to the low degradability of MTP in IWW but also to the TPs generated. The presence of some non-residual TPs such as TP176, TP218, TP250 (estimated EC_{50} and LC_{50} lower than MTP for some end-points, Table S8) in IWW might be correlated to the estimated increase in toxicity after UV/H_2O_2 treatment. Actually, an

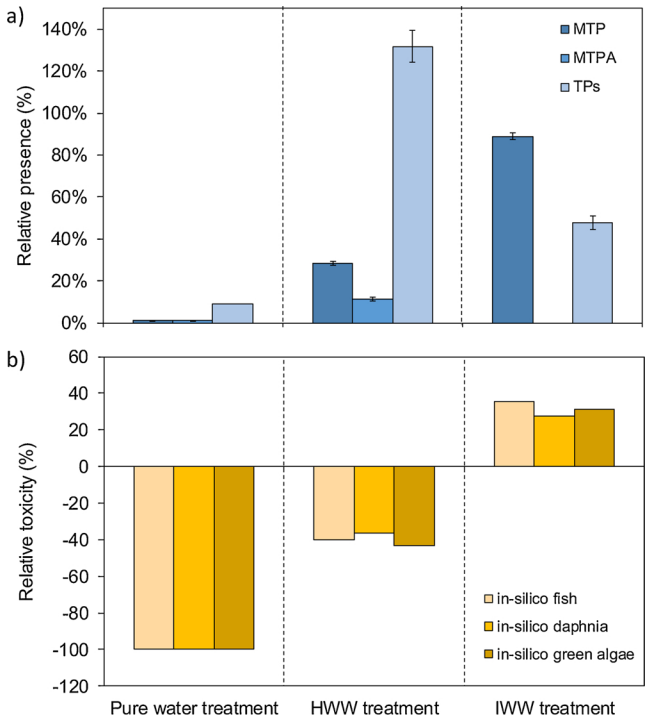

Fig. 5. a) Relative presence of MTP and MTPA in pure water, HWW and IWW after treatment of UV/H_2O_2. TP presence is included as ($\Sigma Area^{t}_{TPs}/\Sigma Area^{0}_{MTP+MTPA}$)-(%). b) Predicted *in silico* fish, *Daphnia* and green algae toxicities of the treated effluents using Eq. (1). Negative values indicate the decrease in toxicity along UV/H_2O_2 treatment.

increase in toxicity in the *V. fischeri* bioassay (*in vitro* toxicity test) was also observed after AOP treatment of real IWW (data not shown). However, it cannot only be attributed to the generation of MTP TPs but also to the generation of intermediates from all the compounds present,

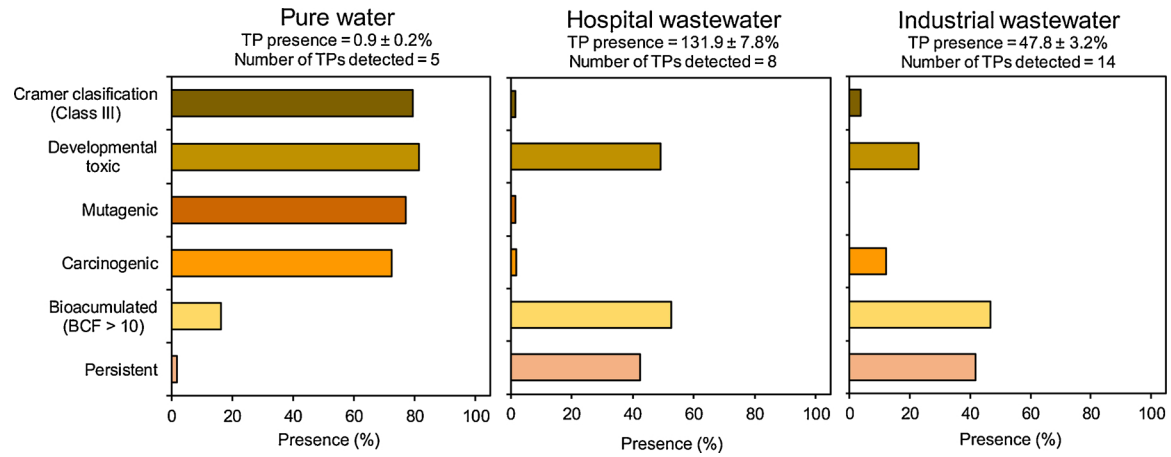

Fig. 6. Presence contribution ($Area^{t}_{TP}/\Sigma Area^{t}_{TPs}$)-(%) of the TPs detected in Fig. 4 grouped as persistent, bioaccumulated, carcinogenic, mutagenic and developmental toxic as well as Cramer hazard classification (Class III). TP presence is included as ($\Sigma Area^{t}_{TPs}/\Sigma Area^{0}_{MTP+MTPA}$)-(%).

apart from MTP. In the case of pure water, no luminescence inhibition in *V. fischeri* bioassays was observed neither before nor after AOP treatment. The absence of measured toxicity in fortified pure water, also at the initial time before the treatment, prevents us to validate the decrease in toxicity observed by the *in silico* estimations (a reduction of almost 100%, Fig. 5b). This decrease in *in silico* toxicity would be explained by the almost total removal of MTP and MTPA and to the relative low presence of detected intermediates (0.9%).

Additionally, the TPs identified in the three treated matrices were qualitatively evaluated in terms of structure-activity to predict if they might be persistent, bioacummulative, carcinogenic, mutagenic or generate adverse effects on the development of the organism (Fig. 6 and Table S9). Although the highest degradation of parent compounds and TPs was achieved treating fortified pure water, the majority of these TPs belong to ≥ 3rd generation TPs, containing α,β-unsaturated aldehydes and carbonyls groups (TP114) as well as aliphatic secondary amines, likely to increase the hazards of treated water (TP114, TP150 and TP134). The identified compounds in treated fortified pure water were less persistent (2%) and bioaccumulative (16%) than in HWW and IWW but more carcinogenic, mutagenic and developmental toxic (up to 81%), being most of them above the Threshold of Toxicological Concern (TTC, Cremer classification class III). This might suggest significant toxicity with appreciable risk to human health. However, it is important to mention that these qualitative analyses do not directly consider the relative presence of TPs (TPs presence in pure water was only 0.9%). Moreover, the parent compound MTP was, in fact, the most bioaccumulative compound present in the samples (Table S9). Total bioaccumulation and persistence of TPs in HWW and IWW resulted similar but the number and concentration of TPs were extremely different among them. Finally, the presence of the carcinogenic TP238 and TP252 (related to aliphatic and aromatic aldehydes in the molecular structures) should be considered of high concern in IWW also because of the high total presence of TPs in this matrix (up to 47.8% of the initial MTP concentration, 33.0 mg/L).

Although treated IWW was the most toxic matrix with persistent transformation products, those found in treated pure water were more degraded (2nd or ≥ 3rd generation) but also more hazardous in terms of mutagenicity and carcinogenicity. The wide differences in the presence and distribution of TPs in the tested treated matrices highlight the importance of performing individual and comprehensive studies to determine all by-products after water and wastewater treatment.

4. Conclusion

An integrated screening approach was applied as a proof of concept for the rapid characterization of metoprolol and metoprolol acid transformation products after UV/H_2O_2 photo-oxidation in spiked pure water, hospital wastewater and industrial wastewater. Among the total features detected, 88% were matched with those extracted from literature sources, 26% from compound prediction tools, 18% from in-house libraries and 5% were confirmed with reference standards. Finally, twenty-six compounds (MTP, MTPA and TPs) were selected for further discussion of their occurrence in the different matrices tested. Depending on the treated water matrix, extremely different scenarios were observed concerning the generation of hazardous TPs (*in silico*): while treated industrial wastewater was the most toxic matrix (containing persistent and less degraded TPs), pure water contained more degraded TPs but also more hazardous in terms of mutagenicity and carcinogenicity (though present at a lower concentration). However, further experiments would be required to better evaluate *in vitro* toxicity effects of TPs, *e.g.* increasing MTP and MTPA concentration and/or considering more appropriate bioassays.

Acknowledgements

This work has been funded by the Spanish Ministry of Economy and Competitiveness (projects CTM 2013 48545-C2-1-R and CTM2017-85385-C2-1-R) and partly supported by the Generalitat de Catalunya (Consolidated Research Groups 2017-SGR-14, 2017-SGR-1404, 2017-SGR-1124, 2017-SGR-1318 and 2017-SGR-1016). S.R.M and R.G.O acknowledge the "Redes de Excelencia 2015" program (CTM2015-71054-REDT). S.R.M and G.B. acknowledge the Ramon y Cajal research fellowships (RYC-2014-16707 and RYC-2014-16754) from the Spanish Ministry of Economy and Competitiveness. A.J.G. acknowledges the predoctoral grant from AGAUR (2018FI_B1_00212). R.G.O thanks to "Obra Social La Caixa" for receiving funding to carry out this research through the Intensification Research Fellowship 2017-URL-IR2Q-023. We would like to thank Sant Joan de Déu Hospital staff for their collaboration during the sampling campaign. We also thank to Thermo Scientific and Marie-Pierre Pavageau for providing us the technical support using Compound Discoverer 2.0 software.

Appendix A. Supplementary data

Supplementary material related to this article can be found, in the online version, at doi:https://doi.org/10.1016/j.jhazmat.2019.120851.

References

Agüera, A., Martínez Bueno, M.J., Fernández-Alba, A.R., 2013. New trends in the analytical determination of emerging contaminants and their transformation products in environmental waters. Environ. Sci. Pollut. Res. 20, 3496–3515. https://doi.org/10.1007/s11356-013-1586-0.

Arslan, A., Veli, S., Bingöl, D., 2014. Use of response surface methodology for pretreatment of hospital wastewater by O_3/UV and O_3/UV/H_2O_2 processes. Sep. Purif. Technol. 132, 561–567. https://doi.org/10.1016/j.seppur.2014.05.036.

Bletsou, A.A., Jeon, J., Hollender, J., Archontaki, E., Thomaidis, N.S., 2015. Targeted and non-targeted liquid chromatography-mass spectrometric workflows for identification of transformation products of emerging pollutants in the aquatic environment. TrAC – Trends Anal. Chem. 66, 32–44. https://doi.org/10.1016/j.trac.2014.11.009.

Celiz, M.D., Tso, J., Aga, D.S., 2009. Pharmaceutical metabolites in the environment: analytical challenges and ecological risks. Environ. Toxicol. Chem. 28, 2473–2484. https://doi.org/10.1897/09-173.1.

Cherkasov, A., Muratov, E.N., Fourches, D., Varnek, A., Baskin, I.I., Cronin, M., Dearden, J., Gramatica, P., Martin, Y.C., Todeschini, R., Consonni, V., Kuz'Min, V.E., Cramer, R., Benigni, R., Yang, C., Rathman, J., Terfloth, L., Gasteiger, J., Richard, A., Tropsha, A., 2014. QSAR modeling: Where have you been? Where are you going to? J. Med. Chem. 57, 4977–5010. https://doi.org/10.1021/jm4004285.

Chibwe, L., Titaley, I.A., Hoh, E., Simonich, S.L.M., 2017. Integrated framework for identifying toxic transformation products in complex environmental mixtures. Environ. Sci. Technol. Lett. 4, 32–43. https://doi.org/10.1021/acs.estlett.6b00455.

Cramer, G.M., Ford, R.A., Hall, R.L., 1976. Estimation of toxic hazard-A decision tree approach. Food Cosmet. Toxicol. 16, 255–276. https://doi.org/10.1016/S0015-6264(76)80522-6.

Cruz-Morató, C., Lucas, D., Llorca, M., Rodriguez-Mozaz, S., Gorga, M., Petrovic, M., Barceló, D., Vicent, T., Sarrà, M., Marco-Urrea, E., 2014. Hospital wastewater treatment by fungal bioreactor: removal efficiency for pharmaceuticals and endocrine disruptor compounds. Sci. Total Environ. 493, 365–376. https://doi.org/10.1016/j.scitotenv.2014.05.117.

Daughton, C.G., 2004. Non-regulated water contaminants: emerging research. Environ. Impact Assess. Rev. 24, 711–732. https://doi.org/10.1016/j.eiar.2004.06.003.

Dévier, M.H., Mazellier, P., Aït-Aïssa, S., Budzinski, H., 2011. New challenges in environmental analytical chemistry: identification of toxic compounds in complex mixtures. Comptes Rendus Chim. 14, 766–779. https://doi.org/10.1016/j.crci.2011.04.006.

Dong, Z., Senn, D.B., Moran, R.E., Shine, J.P., 2013. Prioritizing environmental risk of prescription pharmaceuticals. Regul. Toxicol. Pharmacol. 65, 60–67. https://doi.org/10.1016/j.yrtph.2012.07.003.

Escher, B.I., Fenner, K., 2011. Recent advances in environmental risk assessment of transformation products. Environ. Sci. Technol. 45, 3835–3847. https://doi.org/10.1021/es1030799.

European Chemicals Agency, 2017. Guidance on the Application of the CLP Criteria. https://doi.org/10.2823/124801.

Ferrando-Climent, L., Cruz-Morató, C., Marco-Urrea, E., Vicent, T., Sarrà, M., Rodriguez-Mozaz, S., Barceló, D., 2015. Non conventional biological treatment based on *Trametes versicolor* for the elimination of recalcitrant anticancer drugs in hospital wastewater. Chemosphere 136, 9–19. https://doi.org/10.1016/j.chemosphere.2015.03.051.

Gago-Ferrero, P., Schymanski, E.L., Bletsou, A.A., Aalizadeh, R., Hollender, J., Thomaidis, N.S., 2015. Extended suspect and non-target strategies to characterize emerging polar organic contaminants in raw wastewater with LC-HRMS/MS. Environ. Sci. Technol. 49, 12333–12341. https://doi.org/10.1021/acs.est.5b03454.

Godbillon, J., Duval, M., 1984. Determination of two metoprolol metabolites in human urine by high-performance liquid chromatography. J. Chromatogr. B Biomed. Sci. Appl. 309, 198–202.

Gogoi, A., Mazumder, P., Tyagi, V.K., Tushara Chaminda, G.G., An, A.K., Kumar, M., 2018. Occurrence and fate of emerging contaminants in water environment: a review. Groundw. Sustain. Dev. 6, 169–180. https://doi.org/10.1016/j.gsd.2017.12.009.

Han, Y., Ma, M., Li, N., Hou, R., Huang, C., Oda, Y., Wang, Z., 2018. Chlorination, chloramination and ozonation of carbamazepine enhance cytotoxicity and genotoxicity: multi-endpoint evaluation and identification of its genotoxic transformation products. J. Hazard. Mater. 342, 679–688. https://doi.org/10.1016/j.jhazmat.2017.08.076.

Helbling, D.E., Hollender, J., Kohler, H.P.E., Singer, H., Fenner, K., 2010. High-throughput identification of microbial transformation products of organic micropollutants. Environ. Sci. Technol. 44, 6621–6627. https://doi.org/10.1021/es100970m.

Hernández, F., Ibáñez, M., Gracia-Lor, E., Sancho, J.V., 2011. Retrospective LC-QTOF-MS analysis searching for pharmaceutical metabolites in urban wastewater. J. Sep. Sci. 34, 3517–3526. https://doi.org/10.1002/jssc.201100540.

Hom-Diaz, A., Jaén-Gil, A., Bello-Laserna, I., Rodríguez-Mozaz, S., Vicent, T., Barceló, D., Blánquez, P., 2017. Performance of a microalgal photobioreactor treating toilet wastewater: pharmaceutically active compound removal and biomass harvesting. Sci. Total Environ. 592, 1–11. https://doi.org/10.1016/j.scitotenv.2017.02.224.

ISO 11348-3:1998, 1998. Water Quality – Determination of the Inhibitory Effect of Water Samples on the Light Emission of *Vibrio fischeri* (Luminescent Bacteria Test).

Jaén-Gil, A., Castellet-Rovira, F., Llorca, M., Villagrasa, M., Sarrà, M., Rodríguez-Mozaz, S., Barceló, D., 2019. Fungal treatment of metoprolol and its recalcitrant metabolite metoprolol acid in hospital wastewater: biotransformation, sorption and ecotoxicological impact. Water Res. 152, 171–180. https://doi.org/10.1016/j.watres.2018.12.054.

Jaén-Gil, A., Hom-Diaz, A., Llorca, M., Vicent, T., Blánquez, P., Barceló, D., Rodríguez-Mozaz, S., 2018. An automated on-line turbulent flow liquid-chromatography technology coupled to a high resolution mass spectrometer LTQ-Orbitrap for suspect screening of antibiotic transformation products during microalgae wastewater treatment. J. Chromatogr. A 1568, 57–68. https://doi.org/10.1016/j.chroma.2018.06.027.

Kaserzon, S.L., Heffernan, A.L., Thompson, K., Mueller, J.F., Gomez Ramos, M.J., 2017. Rapid screening and identification of chemical hazards in surface and drinking water using high resolution mass spectrometry and a case-control filter. Chemosphere 182, 656–664. https://doi.org/10.1016/j.chemosphere.2017.05.071.

Kern, S., Baumgartner, R., Helbling, D.E., Hollender, J., Singer, H., Loos, M.J., Schwarzenbach, R.P., Fenner, K., 2010. A tiered procedure for assessing the formation of biotransformation products of pharmaceuticals and biocides during activated sludge treatment. J. Environ. Monit. 12, 2100. https://doi.org/10.1039/c0em00238k.

Krauss, M., Singer, H., Hollender, J., 2010. LC-high resolution MS in environmental analysis: from target screening to the identification of unknowns. Anal. Bioanal. Chem. 397, 943–951. https://doi.org/10.1007/s00216-010-3608-9.

Lacey, C., Basha, S., Morrissey, A., Tobin, J.M., 2012. Occurrence of pharmaceutical compounds in wastewater process streams in Dublin, Ireland. Environ. Monit. Assess. 184, 1049–1062. https://doi.org/10.1007/s10661-011-2020-z.

Llorca, M., Lucas, D., Ferrando-Climent, L., Badia-Fabregat, M., Cruz-Morató, C., Barceló, D., Rodríguez-Mozaz, S., 2016. Suspect screening of emerging pollutants and their major transformation products in wastewaters treated with fungi by liquid chromatography coupled to a high resolution mass spectrometry. J. Chromatogr. A 1439, 124–136. https://doi.org/10.1016/j.chroma.2015.10.077.

Luo, Y., Guo, W., Ngo, H.H., Nghiem, L.D., Hai, F.I., Zhang, J., Liang, S., Wang, X.C., 2014. A review on the occurrence of micropollutants in the aquatic environment and their fate and removal during wastewater treatment. Sci. Total Environ. 473–474, 619–641. https://doi.org/10.1016/j.scitotenv.2013.12.065.

Maurer, M., Escher, B.I., Richle, P., Schaffner, C., Alder, A.C., 2007. Elimination of β-blockers in sewage treatment plants. Water Res. 41, 1614–1622. https://doi.org/10.1016/j.watres.2007.01.004.

Menz, J., Toolaram, A.P., Rastogi, T., Leder, C., Olsson, O., Kümmerer, K., Schneider, M., 2017. Transformation products in the water cycle and the unsolved problem of their proactive assessment: a combined *in vitro/in silico* approach. Environ. Int. 98, 171–180. https://doi.org/10.1016/j.envint.2016.11.003.

Moschet, C., Piazzoli, A., Singer, H., Hollender, J., 2013. Alleviating the reference standard dilemma using a systematic exact mass suspect screening approach with liquid chromatography-high resolution mass spectrometry. Anal. Chem. 85, 10312–10320. https://doi.org/10.1021/ac4021598.

Ooi, G.T.H., Escola Casas, M., Andersen, H.R., Bester, K., 2017. Transformation products of clindamycin in moving bed biofilm reactor (MBBR). Water Res. 113, 139–148. https://doi.org/10.1016/j.watres.2017.01.058.

Radjenović, J., Pérez, S., Petrović, M., Barceló, D., 2008. Identification and structural characterization of biodegradation products of atenolol and glibenclamide by liquid chromatography coupled to hybrid quadrupole time-of-flight and quadrupole ion trap mass spectrometry. J. Chromatogr. A 1210, 142–153. https://doi.org/10.1016/j.chroma.2008.09.060.

Romero, V., Acevedo, S., Marco, P., Giménez, J., Esplugas, S., 2016a. Enhancement of Fenton and photo-Fenton processes at initial circumneutral pH for the degradation of the β-blocker metoprolol. Water Res. 88, 449–457. https://doi.org/10.1016/j.watres.2015.10.035.

Romero, V., González, O., Bayarri, B., Marco, P., Giménez, J., Esplugas, S., 2016b. Degradation of metoprolol by photo-Fenton: comparison of different photoreactors performance. Chem. Eng. J. 283, 639–648. https://doi.org/10.1016/j.cej.2015.07.091.

Rubirola, A., Llorca, M., Rodriguez-Mozaz, S., Casas, N., Rodriguez-Roda, I., Barceló, D., Buttiglieri, G., 2014. Characterization of metoprolol biodegradation and its transformation products generated in activated sludge batch experiments and in full scale WWTPs. Water Res. 63, 21–32. https://doi.org/10.1016/j.watres.2014.05.031.

Scheurer, M., Ramil, M., Metcalfe, C.D., Groh, S., Ternes, T.A., 2010. The challenge of analyzing beta-blocker drugs in sludge and wastewater. Anal. Bioanal. Chem. 396, 845–856. https://doi.org/10.1007/s00216-009-3225-7.

Schollée, J.E., Schymanski, E.L., Avak, S.E., Loos, M., Hollender, J., 2015. Prioritizing unknown transformation products from biologically-treated wastewater using high-resolution mass spectrometry, multivariate statistics, and metabolic logic. Anal. Chem. 87, 12121–12129. https://doi.org/10.1021/acs.analchem.5b02905.

Schymanski, E.L., Singer, H.P., Slobodnik, J., Ipolyi, I.M., Oswald, P., Krauss, M., Schulze, T., Haglund, P., Letzel, T., Grosse, S., Thomaidis, N.S., Bletsou, A., Zwiener, C., Ibáñez, M., Portolés, T., De Boer, R., Reid, M.J., Onghena, M., Kunkel, U., Schulz, W., Guillon, A., Noyon, N., Leroy, G., Bados, P., Bogialli, S., Stipaničev, D., Rostkowski, P., Hollender, J., 2015. Non-target screening with high-resolution mass spectrometry: critical review using a collaborative trial on water analysis. Anal. Bioanal. Chem. 407, 6237–6255. https://doi.org/10.1007/s00216-015-8681-7.

Schymanski, E.L., Singer, H.P., Longrée, P., Loos, M., Ruff, M., Stravs, M.A., Ripollés Vidal, C., Hollender, J., 2014a. Strategies to characterize polar organic contamination in wastewater: exploring the capability of high resolution mass spectrometry. Environ. Sci. Technol. 48, 1811–1818. https://doi.org/10.1021/es4044374.

Schymanski, E.L., Jeon, J., Gulde, R., Fenner, K., Ruff, M., Singer, H.P., Hollender, J., 2014b. Identifying small molecules via high resolution mass spectrometry: communicating confidence. Environ. Sci. Technol. 48, 2097–2098. https://doi.org/10.1021/es5002105.

Secrétan, P.H., Karoui, M., Levi, Y., Sadou-Yayé, H., Tortolano, L., Solgadi, A., Yagoubi, N., Do, B., 2018. Pemetrexed degradation by photocatalytic process: kinetics, identification of transformation products and estimation of toxicity. Sci. Total Environ. 624, 1082–1094. https://doi.org/10.1016/j.scitotenv.2017.12.182.

Toolaram, A.P., Menz, J., Rastogi, T., Leder, C., Kümmerer, K., Schneider, M., 2017. Hazard screening of photo-transformation products from pharmaceuticals: Application to selective β1-blockers atenolol and metoprolol. Sci. Total Environ. 579, 1769–1780. https://doi.org/10.1016/j.scitotenv.2016.10.242.

Verlicchi, P., Al Aukidy, M., Zambello, E., 2012. Occurrence of pharmaceutical compounds in urban wastewater: removal, mass load and environmental risk after a secondary treatment-a review. Sci. Total Environ. 429, 123–155. https://doi.org/10.

1016/j.scitotenv.2012.04.028.
Verlicchi, P., Al Aukidy, M., Zambello, E., 2015. What have we learned from worldwide experiences on the management and treatment of hospital effluent? - An overview and a discussion on perspectives. Sci. Total Environ. 514, 467–491. https://doi.org/10.1016/j.scitotenv.2015.02.020.
Villaverde, J.J., Sevilla-Morán, B., López-Goti, C., Calvo, L., Alonso-Prados, J.L., Sandín-España, P., 2018. Photolysis of clethodim herbicide and a formulation in aquatic environments: fate and ecotoxicity assessment of photoproducts by QSAR models. Sci. Total Environ. 615, 643–651. https://doi.org/10.1016/j.scitotenv.2017.09.300.
Wharf, C., Kingdom, U., 2010. Questions and Answers on 'Guideline on the Environmental Risk Assessment of meDicinal Products for Human Use' 2010. pp. 1–9.
Wilde, M.L., Montipó, S., Martins, A.F., 2014. Degradation of β-blockers in hospital wastewater by means of ozonation and Fe^{2+}/ozonation. Water Res. 48, 280–295. https://doi.org/10.1016/j.watres.2013.09.039.

Environmental Science & Technology

pubs.acs.org/est

Article

Effect-Based Identification of Hazardous Antibiotic Transformation Products after Water Chlorination

Adrián Jaén-Gil,* María-José Farré, Alexandre Sànchez-Melsió, Albert Serra-Compte, Damià Barceló, and Sara Rodríguez-Mozaz*

Cite This: *Environ. Sci. Technol.* 2020, 54, 9062–9073

Read Online

ACCESS | Metrics & More | Article Recommendations | Supporting Information

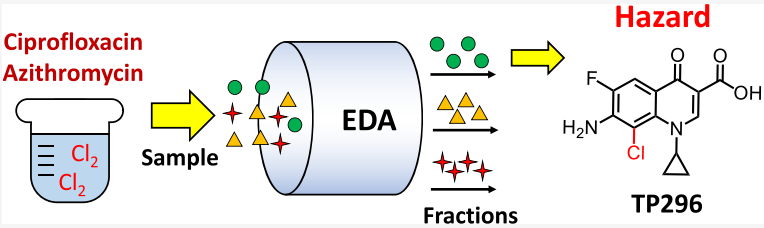

ABSTRACT: Antibiotic transformation products (TPs) generated during water treatment can be considered as an environmental concern, since they can retain part of the bioactivity of the parent compound. Effect-directed analysis (EDA) was applied for the identification of bioactive intermediates of azithromycin (AZI) and ciprofloxacin (CFC) after water chlorination. Fractionation of samples allowed the identification of bioactive intermediates by measuring the antibiotic activity and acute toxicity, combined with an automated suspect screening approach for chemical analysis. While the removal of AZI was in line with the decrease of bioactivity in chlorinated samples, an increase of bioactivity after complete removal of CFC was observed (at >0.5 mgCl_2/L). Principal component analysis (PCA) revealed that some of the CFC intermediates could contribute to the overall toxicity of the chlorinated samples. Fractionation of bioactive samples identified that the chlorinated TP296 (generated from the destruction of the CFC piperazine ring) maintained 41%, 44%, and 30% of the antibiotic activity of the parent compound in chlorinated samples at 2.0, 3.0, and 4.0 mgCl_2/L, respectively. These results indicate the spectrum of antibacterial activity can be altered by controlling the chemical substituents and configuration of the CFC structure with chlorine. On the other hand, the potential presence of volatile DBPs and fractionation losses do not allow for tentative confirmation of the main intermediates contributing to the acute toxic effects measured in chlorinated samples. Our results encourage further development of new and advanced methodologies to study the bioactivity of isolated unknown TPs to understand their hazardous effects in treated effluents.

1. INTRODUCTION

During the past decades, misuse and overuse of antibiotics have contributed to continuous discharges of these contaminants into the aquatic environment.[1] After human consumption, antibiotics are metabolized and excreted into sewage systems as pharmaceutically active forms.[2,3] While their administration clearly provides benefits for human health, the overuse of these substances in animal husbandry may also undergo serious potential risks.[4,5] In this sense, these substances are also widely applied for the treatment, prevention, and prophylaxis in animals.[6] In most cases, conventional wastewater treatment plants (WWTPs) are not specifically designed for antibiotic removal, and these contaminants are released into the receiving aquatic environment.[7,8] The presence of these pollutants in water bodies raises concern since they are associated with hazardous toxic effects and antibiotic resistance.[1,9,10] This is especially important in areas where treated effluents are used for water reuse activities and drinking water production.[11] Due to its low cost, good disinfection, and oxidation capacity, chlorine (Cl_2) has been widely applied as a post-treatment in WWTPs (and/or to maintain a residual chlorine in the distribution system) to protect public health by controlling microbial pathogens.[12] Even so, the presence of chlorine may lead to the formation of halogenated anthropogenic compounds and disinfection by-products (DBPs) which may have potential hazardous effects on the environment and to humans.

Among the antibiotics found in treated wastewater effluents, azithromycin (AZI) represented a breakthrough in the antibiotic era and became one of the best-selling branded antibiotics worldwide in 1980.[13,14] Up to now, AZI was reported in raw urban wastewater up to 1 μg/L.[7] This

Received: February 14, 2020
Revised: June 7, 2020
Accepted: June 26, 2020
Published: June 26, 2020

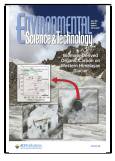

https://dx.doi.org/10.1021/acs.est.0c00944
Environ. Sci. Technol. 2020, 54, 9062–9073

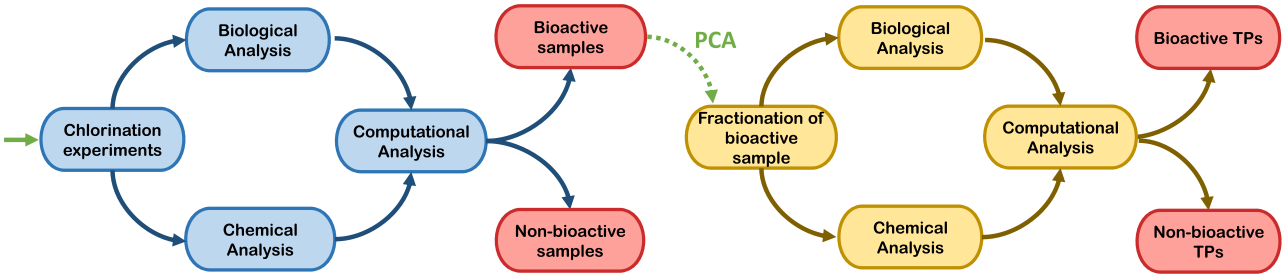

Figure 1. Adapted effect-directed analysis workflow used in this study.

antibiotic is characterized by its bioactivity against Gram-positive bacteria and greatly increases against Gram-negative bacteria to treat some respiratory tract and soft-tissue infections.[13] On the other hand, ciprofloxacin (CFC) has been the center of considerable scientific interest since its discovery in the early 1980s.[15] Up to now, CFC was reported in raw urban wastewater up to 14 μg/L.[7] This pollutant represents one of the most common drugs in the treatment of bacterial infections from urinary tract, upper and low respiratory tract, skin, and bone soft tissue as well as pneumonia with increased potency against Gram-negative bacteria.[16]

Although many efforts have been made to remove these antibiotic drugs from contaminated water, much less attention has been paid to the chlorinated and nonchlorinated intermediates generated after water disinfection. These unknown chemicals might retain part of the bioactivity of the parent compound and entail relevant concerns for the environment and public health even at low concentration levels.[17] In contact with aqueous chlorine, antibiotics may also undergo oxidation/substitution reactions yielding intermediates with higher toxicity than their parent compounds.[18] Since reference standards are not commercially available for most of these unknown transformation products (TPs), the evaluation of their presence and hazardous effects cannot be performed. In this sense, effect-directed analysis (EDA) has overcome this challenge through the identification of bioactive chemicals in complex mixtures applying bioanalysis, separation, and chemical analysis.[19−22] When potential effects are measured in collected samples, their complexity is gradually reduced using fractionation liquid chromatography (LC) to further discard those fractions attaining low or absence of bioactivity.[19] In most of the cases, several fractionation steps are required until the isolated toxic fractions are ready for toxicant identification.[19] Final confirmation to assign their contribution effects is required using analytical approaches for structural identification, effect confirmation of artificial mixtures, and hazard evaluation at different biological organization levels.[23]

For compound identification, many nontarget and suspect screening methodologies have been developed for the identification of these substances by using databases or spectral information.[24−27] Since a broad variety of compounds (up to several thousands of features) can share a given molecular formula, the application of automated suspect screening methodologies by using prediction tools (such as prediction of TP exact masses, MS/MS fragmentation and retention times) may represent an important advance for rapid prioritization of suspected chemicals present in samples.[28,29] Different commercial software and open-source programs are available to optimize LC-MS data processing workflows for detection and prioritization of tentative chemical structures such as XCMS,[30] enviMass,[31] MZmine 2,[32] and Compound Discoverer.[28] Final confirmation of identified structures is performed using, e.g., reference standards and databases. In almost all cases, these EDA approaches have been applied to real polluted waters but not for the assessment of TPs. Only in a few cases, EDA has been applied to study the bioactivity or ecotoxicity to unknown TPs generated in treatment processes when references are not commercially available for confirmation.[33−35]

In this study, an EDA methodology was developed for the identification and elucidation of the bioactive TPs generated after AZI and CFC chlorination experiments. The tentative TPs generated were isolated using a liquid-chromatography system coupled to an automatic sample collector. The elucidation of the generated intermediates was performed using a liquid-chromatography system coupled to high-resolution mass spectrometry with an advanced and automatic suspect screening methodology based on literature information and compound prediction strategies. Antibacterial inhibition (i.e., antibiotic activity) and acute toxicity tests were employed to assess the ecotoxicological implications of the isolated unknown chemicals in chlorinated samples.

2. MATERIALS AND METHODS

2.1. Chemicals and Reagents. Azithromycin (AZI) and ciprofloxacin (CFC) were purchased at high purity grade (>95%) from Sigma-Aldrich (Steinheim, Germany). Ultrapure water, acetonitrile, and methanol LiChrosolv grade were supplied from Merck (Darmstadt, Germany). For antibiotic inhibition tests, *Micrococcus luteus* ATCC 9341 and *Yersinia ruckeri* NCIMB 13282 were used in iso-sensitest agar (Oxid) and 2/3 Plate Count Agar (Difco) medium, respectively. *Vibrio fischeri* bacteria used for Microtox bioassay was purchased from Modern Water (Guildford, United Kingdom). A sodium hypochlorite solution (reagent grade, available chlorine ≥4%, Sigma-Aldrich) was used for the chlorination experiments. For all principal component analysis (PCA) calculations, the R Software version 3.5.3 was used.

2.2. Experimental Setup. Target pollutants (AZI and CFC) were spiked separately at an initial concentration of 2.0 mg/L in ultrapure water (buffered at pH 7.3 with sodium phosphate buffer (10 mM)) for a total working volume of 65 mL in triplicate experiments. Then, a proper volume of chlorine (hypochlorite) was added to achieve the selected initial concentrations of free available chlorine of 0.0, 0.1, 0.5, 1.0, 2.0, 3.0, 4.0, and 6.0 mgCl_2/L. In addition, a control experiment in ultrapure water without spiking the parent compounds was also performed. Batch flasks reactors were sealed avoiding head space and introduced in an incubator at a

https://dx.doi.org/10.1021/acs.est.0c00944
Environ. Sci. Technol. 2020, 54, 9062−9073

constant temperature of 25 °C. All samples were collected after 24 h of treatment, and the free available chlorine of treated water was measured using commercial DPD (*N*,*N*-diethyl-*p*-phenylenediamine) test kits (LCK310, Hach Lange) with a Hach DR2800 spectrophotometer (Düsseldorf, Germany). The final experimental time of 24 h was selected to maximize chlorination byproducts formation while minimizing hydrolysis of the TPs. Experiments containing a concentration higher than 0.05 mgCl_2/L after 24 h were discarded for further analysis (actually only those samples with an initial dose of 6.0 mgCl_2/L were finally discarded).

2.3. Effect-Directed Analysis Approach. An adapted effect-directed analysis (EDA) methodology was applied for the identification of the bioactive intermediates generated after water chlorination (Figure 1).[36] Briefly, samples collected after 24 h of chlorination were biologically (antibiotic activity and acute toxicity) and chemically (chromatographic and mass spectrometry analysis) analyzed. Then, computational assessment was performed for identification of the chemicals present in samples. The bioactivity of each chlorinated sample was plotted together with the presence of each identified intermediate (chromatographic area of the TPs identified divided by the area of the chromatographic peak of the parent compound at initial time) by principal component analysis (PCA). With this information, the suspect hazardous intermediates present in chlorinated samples were tentatively pointed out, and the most representative bioactive sample was selected for fractionation and further isolation of the TPs. Sample fractions were again biologically and chemically analyzed as well as computationally assessed in duplicate to unravel their contribution as hazardous chemicals in chlorinated treated samples.

2.3.1. Biological Analysis. The antibiotic activity and acute toxicity endpoints were selected to evaluate the hazardous effects of the antibiotics selected and TPs in chlorinated samples and fractions. The antibiotic activity was chosen since it is related to the specific mode of action (MoA) of these pollutants. In parallel, the acute toxicity was selected since it is classified as a conventional endpoint measured in the environment.

To evaluate the antibiotic activity,[37] the iso-sensitest agar (Oxid) medium with an addition of 7.5 μg/L of tylosin (adjusted to pH 8.0) and inoculated with *M. luteus* ATCC 9341 bacteria was used for samples collected from AZI experiments. In the case of CFC experiments, 2/3 Plate Count Agar (Difco) 5% of 1 M phosphate buffer with an addition of 8,000 μg/L of cloxacilline (adjusted to pH 6.5) and inoculated with *Y. ruckeri* NCIMB 13282 bacteria was used. In both cases, 35 mL of the inoculated agar was poured into a 120 × 120 mm bioassay plate containing 9 holes per plate. A volume of 250 μL of samples was transferred to individual holes with the addition of 50 μL of 1 M phosphate buffer. Then, sample plates were incubated at 30 °C for 16 h. Antibiotic activity of samples was determined by observing the growth inhibition of the bacterial culture and measuring the diameter of the nonbacterial cell density corresponding to the absence of bacterial growth. All the values were calculated related to the antibiotic activity of the parent compound before chlorination.

Additionally, the ISO 11348-3 protocol for testing bacterial bioluminescence of wastewater matrices was used to assess acute toxicity throughout Microtox Model 500 Toxicity Analyzer (Strategic Diagnostics Inc., Newark, DE, US).[38] Stain of luminescent bacteria *Vibrio fischeri* NRRL B-11177 was prepared from commercially available freeze-dried reagents stored at −20 °C. A volume of 2 mL was required for sample analysis. Then, the percentage of decay on emitted light was measured when samples were in contact 15 min with the bioluminescent bacterium *V. fischeri*. The data expressed as EC_{50} was transformed into toxicity units (TU = 100/EC_{50}),[39] where a higher TU indicates a greater effect.[40]

2.3.2. Chemical Analysis. A liquid chromatography system coupled to a high-resolution mass spectrometer LC-LTQ-Orbitrap-MS/MS was used as described previously.[41] Briefly, 20 μL of samples was injected and separated in a ZORBAX Eclipse XDB-C18 (150 mm × 4.6 mm, 5 μm; Agilent Technologies, Santa Clara, CA). The mobile phases were (A) 10 mM ammonium formate in water at pH 3.0 and (B) acetonitrile. The optimized chromatographic gradient was performed as follows:[41] initial mobile phase composition (95% A) held for 1 min, followed by a decrease in composition A to 5% within 9 min, then to 0% in 3 min, held for 2 min, up to 95% in 1 min, and held for 1 min.

The high-resolution mass spectrometer LTQ-OrbitrapVelos (Thermo Fisher Scientific) was equipped with a heated electrospray ionization source (HESI-II). The analysis was performed in positive and negative ionization modes. As no peaks attributed to TPs were found in negative ion mode chromatograms, further data processing was carried out only with that acquired in positive ion mode. Samples were acquired in full scan data acquisition from m/z 100 to 1,000 range at a resolving power of 60,000 fwhm. For structural elucidation of TPs, MS/MS fragmentation was performed in a data dependent acquisition mode (DDA) at 30,000 fwhm from m/z 100 to 1,000 range, for the three most intense ions from a selected list of 16 exact masses corresponding to potential AZI (Table S1) and 13 exact masses for CFC collected from the literature (Table S2) (preacquisition suspect screening approach). If selected masses were not found, the three most intense ions detected in a full-scan MS spectra were automatically selected for fragmentation. All data were further processed with a postacquisition suspect screening approach (Section 2.3.3). Additionally, isotopic data-dependent (IDD) was performed for the expected isotopic ratios of 0.32 and 0.64 comprising a mass difference of 1.9971 Da. All MS/MS experiments were performed applying a dynamic mass exclusion mode to discriminate coeluted compounds: ions fragmented more than three times during 25 s were further ignored for fragmentation during the following 30 s (corresponding to peak plus tailing). Mass spectrometry conditions were designed as follows: spray voltage, 3.5 kV; source heated at 300 °C; capillary temperature, 350 °C; sheath gas flow, 40 (arbitrary units); and auxiliary gas flow, 20 (arbitrary units).[41] Fragmentation techniques selected were as follows: collision-induced dissociation (CID) at a normalized collision energy of 30 eV (activation Q of 0.250 and an activation time of 30 ms) and higher-energy collisional dissociation (HCD) at a normalized collision energy of 55 eV (activation time of 0.100 ms) with an isolation width of 2 Da. The entire system was controlled via Aria software under Xcalibur 2.1.

2.3.3. Computational Analysis. An advanced postacquisition suspect screening approach for identification of the TPs generated in chlorination experiments and collected in the corresponding fractions was applied using Compound Discoverer 3.0 (Thermo Fisher Scientific Inc., Waltham, MA). The adapted methodology is presented in Figure S1

https://dx.doi.org/10.1021/acs.est.0c00944
Environ. Sci. Technol. 2020, 54, 9062−9073

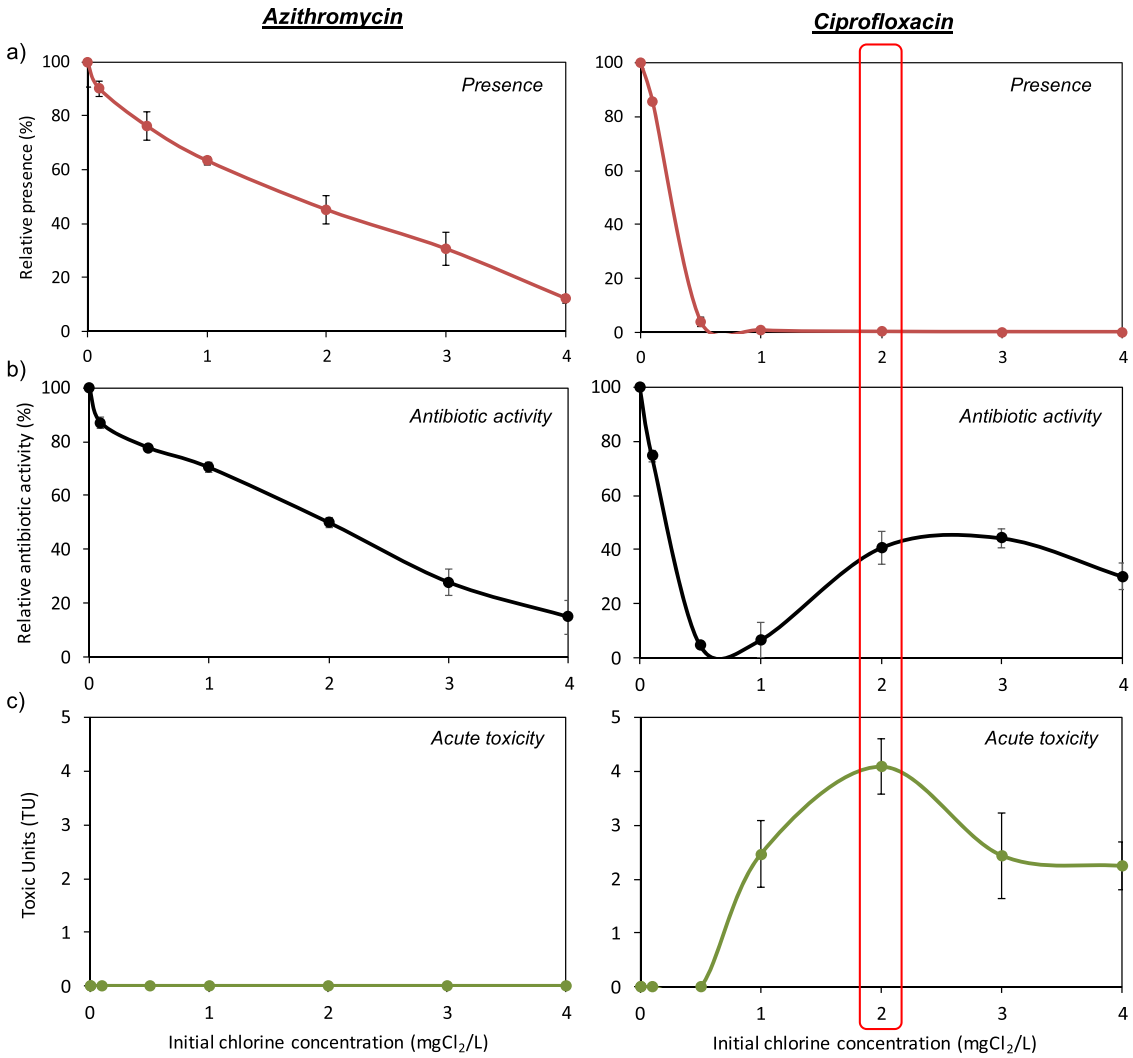

Figure 2. Monitoring of (a) the degradation of spiked antibiotics (azithromycin or ciprofloxacin), (b) antibiotic activity, and (c) acute toxicity after 24 h of treatment in chlorination experiments at different initial chlorine doses. Relative values of the presence and antibiotic activity were calculated with respect to the values measured at the initial time. In the case of acute toxicity, it is calculated in toxic units (TU). The red rectangle indicates the sample selected for further sample fractionation.

and Table S3.[42] Briefly, input files containing the chromatograms and mass spectra files from analyzed samples were loaded separately into the software. In addition, chemical structures of AZI and CFC were also loaded to further create a list of tentative TPs predicted by the software after applying the following chemical reactions to the parent compound structures (a maximum combination of three): dehydration, desaturation, reduction, oxidative deamination to ketone, oxidative deamination to alcohol, chlorination, hydration, oxidation, reductive defluorination, and dealkylation. A number of 1655 and 497 exact masses were predicted from AZI and CFC chemical structures, respectively. Automatic data processing starts with filtering MS data between 100 and 1000 Da and from 1 to 12 min with an S/N ratio of 3. To compensate for small differences in retention times, chromatographic alignment was performed by using a mass tolerance error of ±5 ppm and a maximum retention time shift of 0.3 min. Immediately after, data processing was performed by searching the predicted list of TP exact masses in sample files. Then, the fragments present in collected MS/MS data were automatically matched with the predicted fragments generated using *in silico* fragmentation with a mass tolerance error of ±5 ppm. Those compounds with FISh (Fragment Ion Search) coverages higher than 65% were selected for data evaluation.[42]

2.3.4. Statistical Analysis for the Estimation of Hazardous TPs. Additionally, principal component analysis (PCA) was used to evaluate the correlations between the bioactivity measured (antibiotic activity and acute toxicity, separately) and the TPs identified in chlorinated samples, following the approach previously reported.[43] Relative areas in percentage values (area of the peaks detected in chromatogram divided by the area of the chromatographic peak of CFC before the treatment) were used as input value using the FactoMineR included in the Rcmdr environment (RcmdrPlugin.FactoMineR interface) for automatic data processing. For all calculations, the R Software version 3.5.3 was used.

2.3.5. Sample Fractionation. Taking into account the PCA results of the suspected bioactive intermediates present in

https://dx.doi.org/10.1021/acs.est.0c00944
Environ. Sci. Technol. 2020, 54, 9062−9073

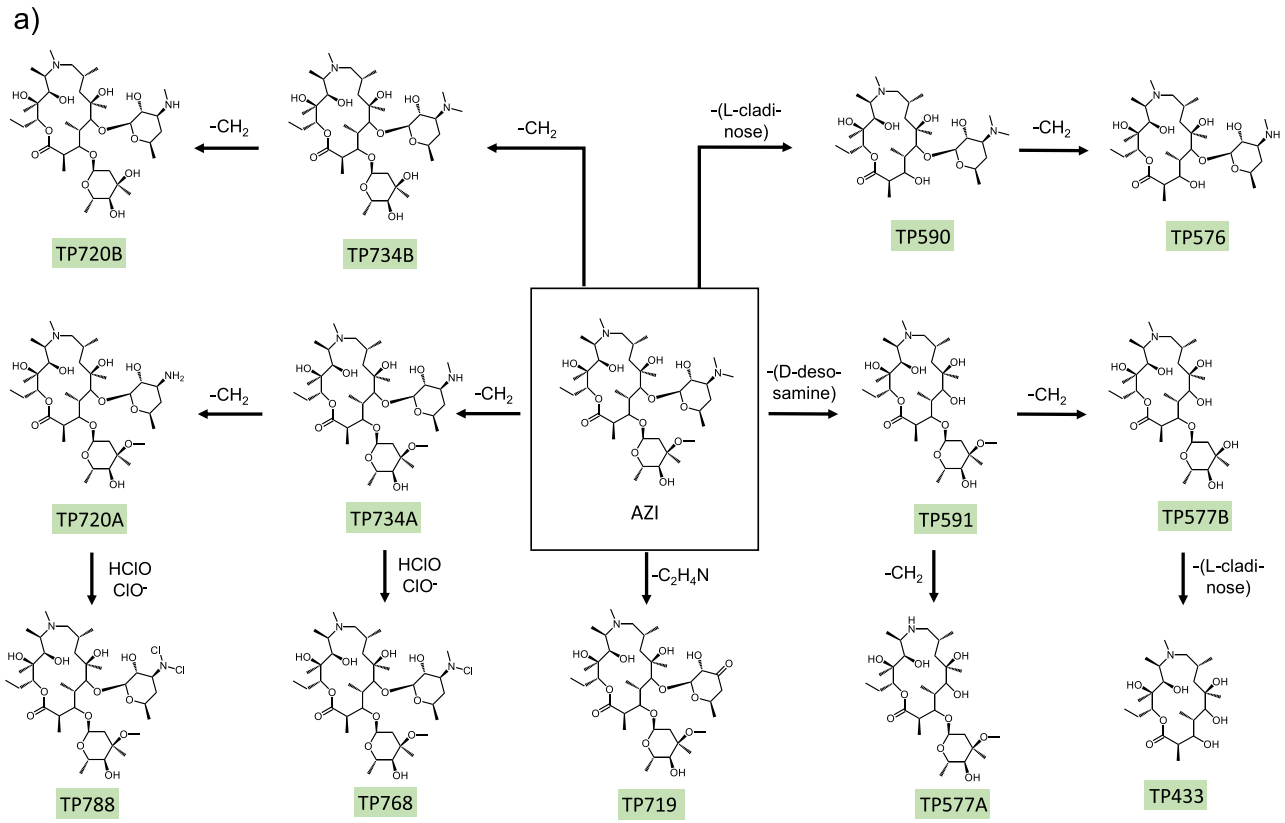

Figure 3. a) Suggested transformation mechanism of azithromycin in chlorination experiments. In green, tentatively identified intermediates detected in this study. b) The relative presence of the most representative intermediates identified after chlorination experiments at different chlorine doses.

chlorinated samples, the most representative bioactive sample containing all the TPs identified was selected for sample fractionation (2 $mgCl_2/L$ vs 2 mg/L of CFC at an initial time). To achieve a proper concentration of the isolated TPs in one fractionation cycle, this experiment was repeated at a higher concentration adding the corresponding proportion of reactants (10 $mgCl_2/L$ vs 10 mg/L CFC at an initial time). This is considered a critical step since a minimal concentration

https://dx.doi.org/10.1021/acs.est.0c00944
Environ. Sci. Technol. 2020, 54, 9062−9073

of the TPs (normally present at low concentration levels) is required to further reach detection limits during LC-MS/MS analysis and the selected bioassays. Then, fractionation was performed by using a preparative HPLC Agilent 1260 Infinity high-pressure liquid-chromatography system coupled to a diode array detector (HPLC-DAD). The fraction collection was automatically carried out in a 1100/1200 fraction collector G1364C using a diverter valve to switch from waste to the collector position. A volume of 100 μL of samples was injected in a ZORBAX Eclipse XDB-C18 column (150 mm × 4.6 mm, 5 μm; Agilent Technologies, Santa Clara, CA) at a flow rate of 1 mL/min and column temperature of 25 °C. Pure mobile phases selected were (A) pure water and (B) acetonitrile to avoid the presence of any residual interference affecting bioassay measurements. The chromatographic gradient was carried out as follows: initial mobile phase composition (90% A) held for 5 min; to 40% in 1 min and held for 7 min; to 30% in 1 min and held for 6 min; to 20% in 1 min and held for 6 min; to 10% in 1 min and held for 6 min; and to 90% in 1 min held for 5 min. Detection was monitored at the maximum absorption wavelength of 271 nm measured in a UV-1800 UV−vis spectrophotometer (Shimadzu Inc., Kyoto, Japan). The total volume collected for each fraction was approximately 2 mL. Since reference standards of TPs are not available to quantify recoveries in solid-phase extraction and pharmaceutical TPs are not usually volatile, fractions were collected in glass collectors, evaporated to dryness with nitrogen, and reconstituted in 0.5 mL of pure water. Reconstitution in pure water was carried out to prevent the presence of organic solvents interfering with bacteria integrity on the bioanalysis of fractions.[44−46] In addition, since pure water was the solvent used in chlorination experiments, a better comparison with the fractions collected is assured. All fractions collected were evaluated using biological (by antibiotic activity and acute toxicity measurement as explained in biological analysis section) and chemical (using the LTQ-Orbitrap for MS/MS compound identification, as explained in the Chemical Analysis section) analyses. Finally, computational assessment (using Compound Discoverer, as presented in the Computational Analysis section) was performed for compound identification.

3. RESULTS AND DISCUSSION

3.1. Biological and Chemical Analyses of Chlorinated Samples. Chemical analyses revealed an AZI removal up to 88% after 24 h of the addition of the highest chlorine dose (4 mgCl_2/L) (Figure 2a). This percentage of elimination is in line with the decrease in the initial antibiotic activity up to 85% (Figure 2b). As observed in other oxidation treatment processes reported in the literature,[47] the decrease of the measured antibiotic activity is due to the elimination of the parent compound as none of the intermediates generated had any relevant contribution to the overall antibiotic activity. In terms of acute toxicity, no effects were observed after any of the chlorination experiments performed (Figure 2c). These results are in accordance with those reported in the literature about oxidation treatment processes, where the absence or reduction of the toxicity of the intermediates generated after AZI degradation was observed.[48,49]

On the other hand, chlorination promoted complete CFC elimination (ca. 100%) after 24 h of treatment adding an initial chlorine dose of 0.5 mgCl_2/L (Figure 2a). These results are in line with the negligible antibiotic activity at 0.5 mgCl_2/L (Figure 2b). The antibiotic activity exceeded 41%, 44%, and 30% of the initial effect of the parent compound in the experiments performed at 2, 3, and 4 mgCl_2/L, respectively (Figure 2b). This fact suggests that some of the CFC intermediates generated might retain part of the antibiotic activity of the parent compound. Controversial data about the antibiotic activity of the intermediates generated during CFC degradation have been reported in the literature. A reduction on antibacterial activity regarding the elimination of CFC was generally observed after photolytic, photocatalytic, electrochemical, and Fe(VI) oxidation.[50−54] In some cases, a negligible antibacterial potency of the TPs generated in those water treatments was reported.[54] On the contrary, the bioactivity of the intermediates generated was sometimes detected after ozonation treatment,[55] in line with the results obtained in this study in chlorination experiments.

Negligible acute toxicity was measured in the absence of chlorine in CFC experiments (Figure 2c). The maximum increase up to 4.1 TU was observed after adding 2 mgCl_2/L (Figure 2c). Also, in this case, controversial data about acute toxicity of the intermediates generated during CFC degradation have been reported in the literature. For instance, a decrease in acute toxicity was observed after sonolysis and UV treatment experiments spiked at 15 mg/L of CFC.[56,57] On the contrary, an increase in acute toxicity of about 18% was observed from the TPs generated after 1 h of CFC chlorination at 10 mol equiv of chlorine dose[58] and up to 26% after radiation-induced experiments at 33 mg/L of CFC.[59]

As shown in this study, the potential intermediates generated during chlorination of AZI did not show any effect in the biological tests applied. The intermediates generated during CFC experiments were pinpointed as concerning TPs since acute toxicity and antibiotic activity were measured after chlorination experiments.

3.2. Computational Analysis of Chlorinated Samples and Elucidation of Transformation Pathways. Thirteen TPs were tentatively identified in AZI chlorinated samples (Table S4), and the transformation pathway and their relative presence are presented in Figure 3. As previously reported, the elimination of the parent compound was mainly led by O-dealkylation of the L-cladinose moiety (TP590) suggested from the instability of macrolides in aqueous solution[42] and confirmed by its presence at the initial time up to 80%. However, the increase of initial chlorine concentration led to its further elimination reaching a presence of 12% in treated samples when 4 mg Cl_2/L was added at the initial time. This intermediate was mainly transformed into TP576 after demethylation of the dimethylamine group in the D-desosamine moiety.[42] As reported previously,[60] both hydrolysis of the D-desosamine moiety and demethylation were also observed directly from the AZI parent compound being transformed into TP591 and TP734A (and found in this study up to 132% and 65% at 4 mgCl_2/L, respectively). It is important to mention that none of the most intense compounds elucidated contain a chlorine substituent in their chemical structures after the experiments were performed. As previously reported,[60] the pseudo-first-order kinetic constants at different pH values showed that the reactivity of AZI with free available chlorine was favored at higher pH within the range of 7.5 and 8.5 (optimal pH value was 8.0). Therefore, the use of a pure water pH at 7.3 may explain the low presence of halogenated TPs after chlorination experiments. As explained previously and in Figure 2, none of these elucidated

https://dx.doi.org/10.1021/acs.est.0c00944
Environ. Sci. Technol. 2020, 54, 9062−9073

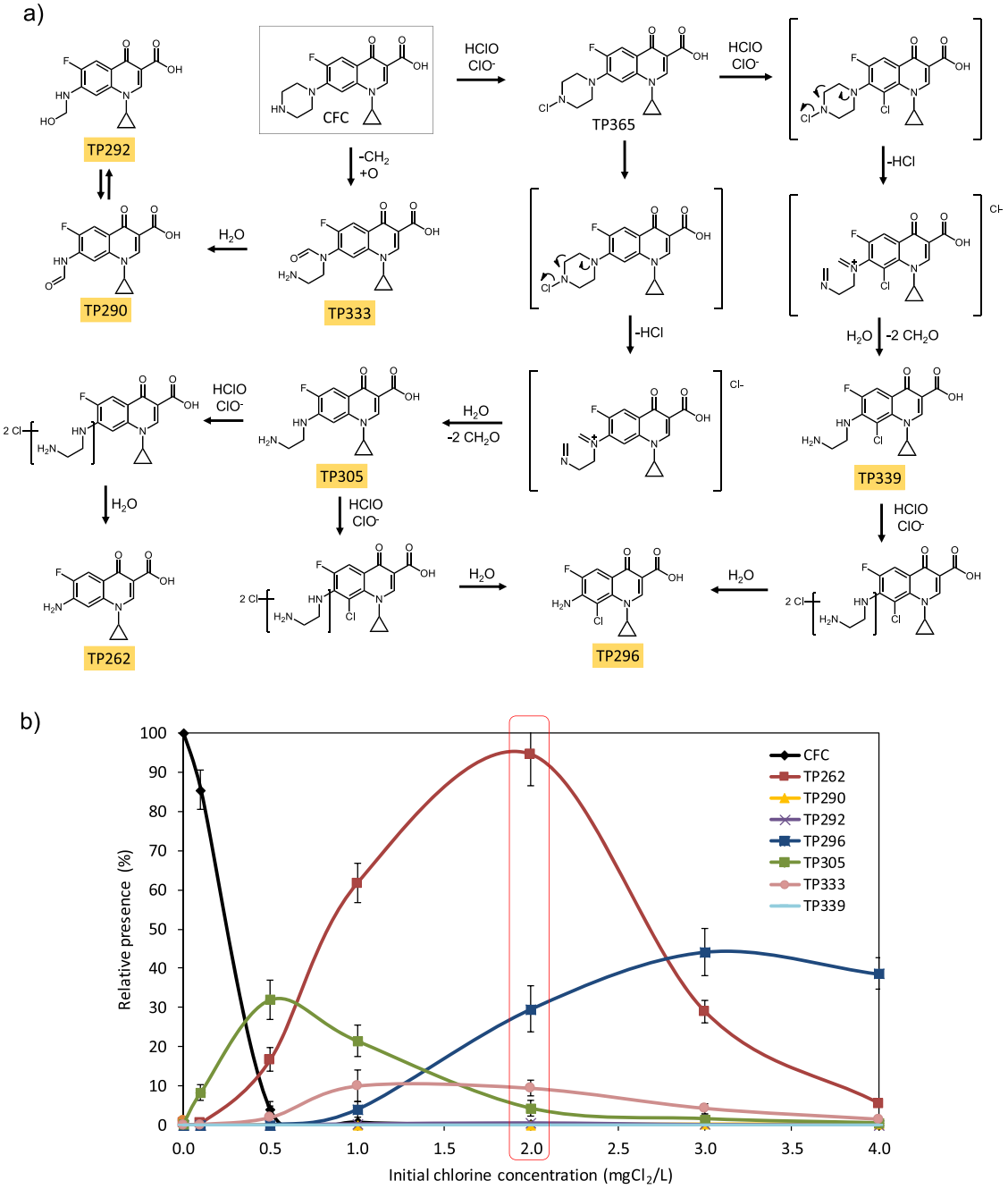

Figure 4. a) Suggested transformation mechanism of ciprofloxacin in chlorination experiments. In yellow, tentatively identified intermediates detected in this study. b) The relative presence of the intermediates identified after chlorination experiments at different chlorine doses. The red rectangle indicates the sample selected for further sample fractionation.

intermediate structures from AZI presented hazardous effects in treated effluents.

Seven TPs were tentatively identified in CFC chlorinated samples (Table S5). The transformation pathway and their relative presence are presented in Figure 4. As previously reported,[61] initial chlorination of the CFC structure induced the destruction of the piperazine ring moiety into TP365 (not detected in this study). The instability of TP365 probably led to the opening of the piperazine ring and rapidly transformed (though imine hydrolysis and the loss of CH_2O) into TP305,[61−63] which was detected in this study at high percentage values (32% relative area to the initial area of CFC) when 0.5 $mgCl_2/L$ of chlorine was added. However, the increase of initial chlorine concentration led to its further elimination reaching low levels (4%) at 2 $mgCl_2/L$ of chlorine dose. In fact, TP305 was most likely transformed by *N*-chlorination and further elimination of the $C_2H_3NCl_2$ moiety generating the compound TP262. In comparison to TP305, TP262 attained the highest concentration when chlorine was added at 2.0 $mgCl_2/L$ at an initial time (up to 95% from the initial presence of CFC). These results are in accordance with the previous data reported in the literature where TP262

https://dx.doi.org/10.1021/acs.est.0c00944
Environ. Sci. Technol. 2020, 54, 9062−9073

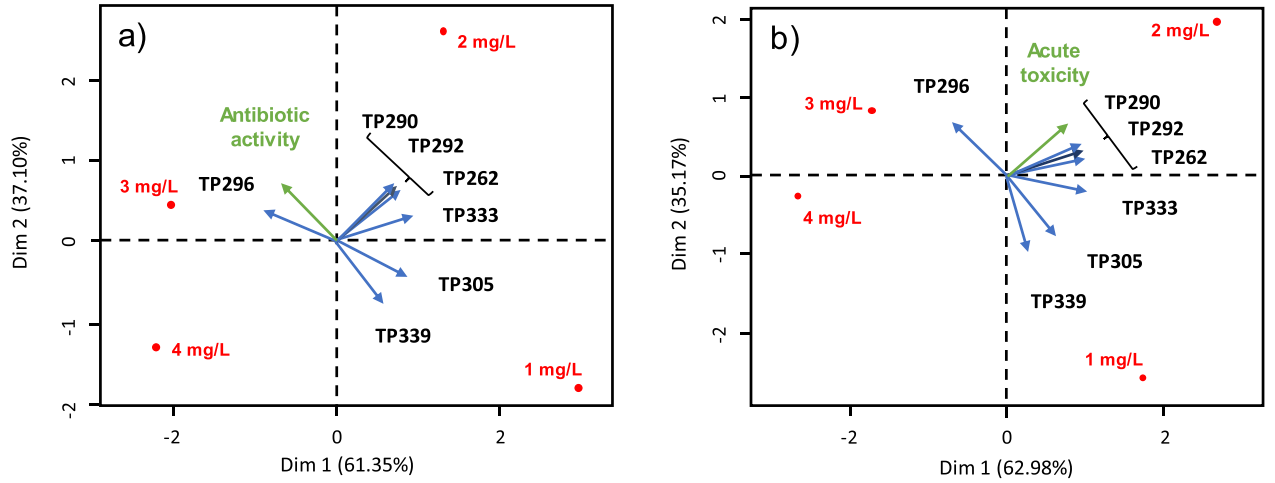

Figure 5. PCA loadings of the presence of the intermediates identified regarding the a) antibiotic activity and b) acute toxicity tested in chlorination samples.

formation was observed from 12.4% (after 2 h of chlorination treatment) to 54.4% (after 50h).[61] Additionally, TP262 was also found as the main intermediate generated in photo-Fenton degradation experiments after 30 min of treatment, 1.5 times-fold higher when compared with the other generated TPs.[51] Finally, the presence of additional intermediates in samples with an excess of chlorine indicates that TP305 may generate further chlorinated compounds in treated samples: the chlorinated TP296 was observed up to 39% when decreasing the presence of TP262 to 5% at an initial chlorine concentration of 4.0 mgCl_2/L. This fact indicated that the highest extent of the transformation pathway was achieved when increasing the chlorine concentration.[62] The most significant concentration of TP296 was detected at 3.0 mgCl_2/L of chlorine up to 44%. Otherwise, other oxidation intermediates (e.g., TP333) were also identified from CFC[61] at a lower concentration than 10% after chlorination experiments (Figure 4). As explained previously and in Figure 2, some of the elucidated intermediate structures for CFC presented hazardous effects in treated effluents.

3.3. Estimation of the Hazardous TPs Generated in CFC Chlorinated Samples. Estimation of the tentative hazardous TPs identified in CFC experiments (in terms of antibiotic activity and acute toxicity) was evaluated using PCA plots (Figure 5), which allowed correlating bioactivity measured with the presence of individual TPs identified in chlorinated samples (Table S6 and Table S7). Since variables were measured on different scales (relative percentages and toxic units), both PCAs were normalized to the specific range of [−1, + 1]. The direct correlation of an intermediate with a given effect estimates its tentative hazardous contribution in chlorinated samples. The first two principal components (PCs) pointed out the TP296 (Figure 5a) as the key intermediate contributing to the increase of 41%, 44%, and 30% in the antibiotic activity in treated samples of the experiments performed at 2, 3, and 4 mgCl_2/L, respectively (Figure 2b). This may be due to the different chemical substituents of this intermediate which may govern antibacterial efficacy and influence the side-effect profile.[64] On the contrary, an inverse correlation was observed for TP339, TP305, and TP333. Otherwise, PCA loadings pointed out a direct correlation between acute toxicity of chlorinated samples and the presence of TP262, TP290, and TP292 (Figure 5b). Since TP262 was found in chlorinated samples at the major relative presence of 95% at 2.0 mgCl_2/L (Figure 4), it might be classified as the key intermediate contributing to the increase of 4.1 TU in the acute toxicity in chlorinated samples (Figure 2c). The contribution of TP290 and TP292 may also exhibit higher toxicity of these intermediates compared to the rest of TPs, and therefore, despite their apparently low relative presence (Figure 4), they may also contribute to the total toxicity of the samples. In addition, the synergic effects of these compounds cannot be discarded. Otherwise, an inverse correlation was observed for TP339 and TP296. These intermediates may result in lower steric resistance and easier penetration into a cell of luminescent bacteria,[65] which subsequently might lead to an increase in toxicity. Additionally, as expected, the electronegative atoms contained in quinolone molecules (such as F, N, and O atoms) may donate electrons to photo-bacterium and thus inhibit the luminance emission.[58]

In both statistical experiments (Figure 5a and Figure 5b), the generation of low molecular mass DBPs, not considered in this study, might have also contributed to the hazardous effects measured in treated samples. In this context, it was previously reported that monochloroacetic acid was the main DBP formed during chlorination of CFC and detected at a concentration around 100 μg/L after 24 h (when CFC was spiked at 16 mg/L adding a chlorine dose of 1 mM).[66] In our conditions selected, the formation of monochloracetic acid was expected to be minimal since CFC was spiked at a much lower concentration of CFC (2 mg/L) and chlorine dose (0.056 mM). Taking into account the PCA results, which tentatively pointed out TP296 and TP262 as hazardous intermediates, fractionation and further chemical and biological analyses, as well as computational assessment, were needed to confirm or rule out the risk of these intermediates in chlorinated samples.

3.4. Confirmation of the Hazardous TPs Generated in Chlorinated Samples. Taking into account the PCA results, the most representative sample containing all the TPs identified was selected for sample fractionation (2 mg Cl_2/L vs 2 mg/L of CFC at an initial time). To achieve a proper concentration of the isolated TPs without launching several sample fractionation cycles, the experiment was repeated at a higher concentration adding the same proportion of reactants

https://dx.doi.org/10.1021/acs.est.0c00944
Environ. Sci. Technol. 2020, 54, 9062−9073

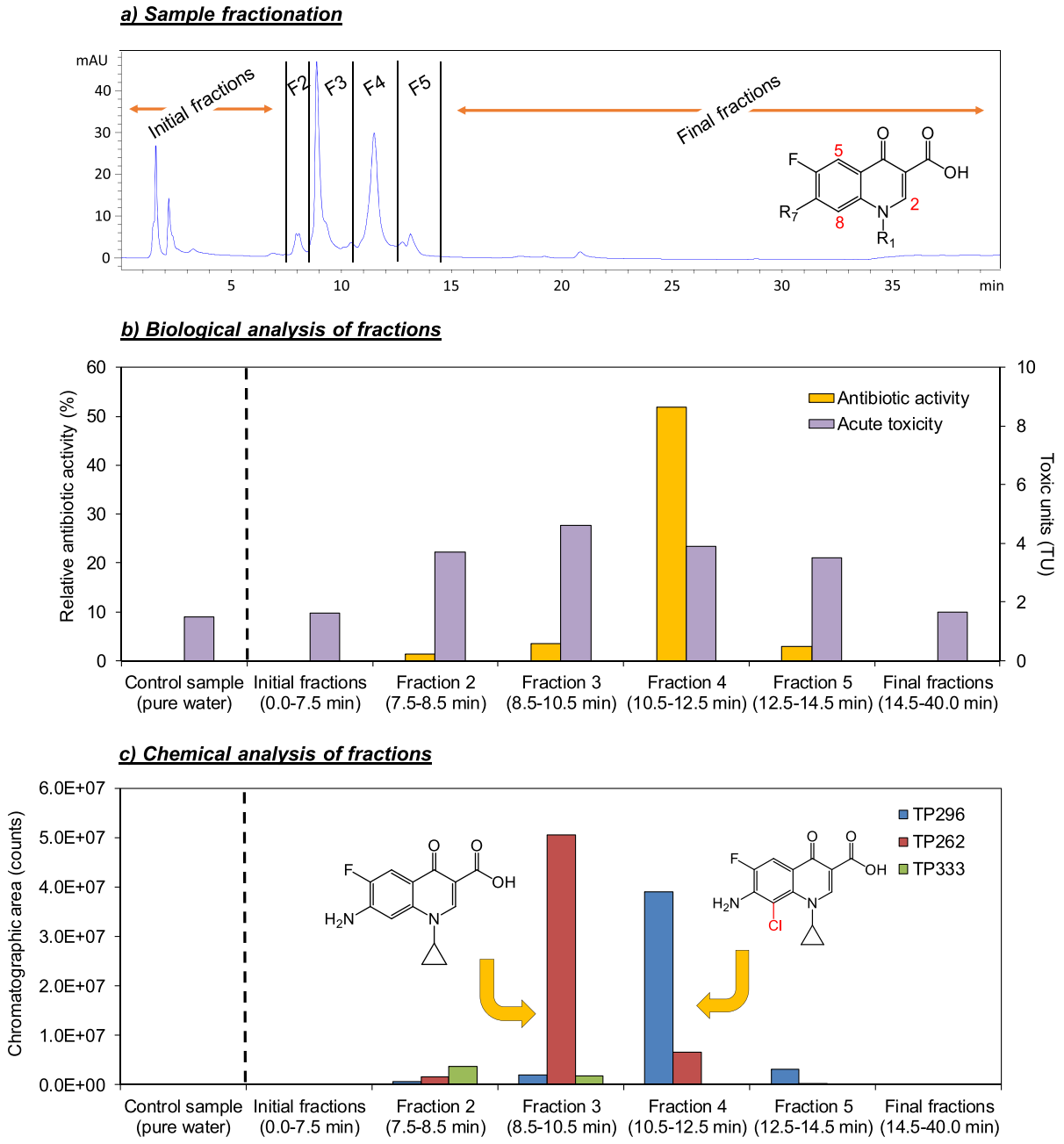

Figure 6. a) Fractionation of the selected bioactive sample (10 mgCl_2/L vs 10 mg/L CFC at the initial time); b) acute toxicity (calculated as EC_{10} and expressed in TU) and relative antibiotic activity of fractions collected and control samples; and c) chemical analysis (chromatographic area) of fractions and control samples.

(10 mgCl_2/L vs 10 mg/L CFC at initial time). After sample fractionation (Figure 6a), measurements on antibiotic activity and acute toxicity indicated no toxic effects (in comparison to control samples) when no chromatographic peaks were detected in the fractions collected (every 2 min approximately) at the beginning and the end of the chromatogram (Figure 6b). Chromatographic and mass spectra data from the LC-MS/MS (Orbitrap Velos) system of fractions showed that TP333 was found in fraction 2 but at low concentration values (Figure 6c). Two intense peaks in fractions 3 and 4 were assigned to TP262 (generated after the elimination of the piperazine ring moiety) and TP296 (a further chlorinated intermediate of the transformation pathway), respectively (Figure 4). Conversely, no compound assignment was possible for fraction 5 (Figure 6c).

Biological analysis showed a relative antibiotic activity of around 1% in fraction 2, 4% in fraction 3, 52% in fraction 4, and 3% in fraction 5 (Figure 6b). The significant presence of TP296 in fraction 4 was in agreement with the 52% of antibiotic activity measured in this fraction. For this intermediate, the fractionation process allowed the recovery of 78% of the chromatographic area from the initial chlorinated sample. Therefore, TP296 (the chlorinated molecule generated from TP305, Figure 4) was tentatively identified to retain the

https://dx.doi.org/10.1021/acs.est.0c00944
Environ. Sci. Technol. 2020, 54, 9062−9073

antibiotic activity of its parent compound CFC in chlorinated samples. Nonetheless, despite 22% of compound losses being observed during fractionation, synergistic and antagonistic effects cannot be discarded. These results are in accordance with the reported literature indicating that the spectrum of antibacterial activity can be altered by controlling the substitution and configuration of position 8 on the CFC structure with C−F, C−Cl, and N substituents (Figure 6a) and expanding the antibacterial spectrum against anaerobes.[15,64,67,68] Additionally, these results confirm the suitability of PCA estimations to identify the most hazardous intermediates generated during water treatment in terms of antibiotic activity (Figure 5).

On the other hand, while chlorinated samples were toxic at an initial concentration of 2 mgCl_2/L (Figure 2c), no acute toxicity was observed in any of the fractions collected exceeding EC_{50} values. In this context, calculations of EC_{10} were performed from the slope of the linear regression of concentration vs % effect and converted in TU values as reported previously[69,70] (Figure S3). In particular, the most abundant intermediate highlighted by chlorination experiments TP262 (Figure 4) was found at the highest acute toxic value of 4.6 TU in fractions collected (Figure 6b and Figure 6c). Yet, the fractionation process allowed the recovery of only 42% of the TP based on the chromatographic areas before and after fractionation. Therefore, partial loss of this TP along sample evaporation and fractionation might also contribute to the reduction of acute toxicity measured in the fractions. It is important to mention that other estimated toxic intermediates (such as TP290 and TP292), present at low concentration levels, were also affected by fractionation losses since they were not detected in fractions collected.

The identification of the most relevant intermediates in terms of antibiotic activity generated from chlorination experiments with CFC was successfully achieved using an EDA approach, which includes fractionation of bioactive samples in combination with biological, chemical, and computational assessment using an automated suspect screening methodology. The TP296 (generated from the destruction of the piperazine ring moiety and its further chlorination) was identified to maintain 41%, 44%, and 30% of the antibiotic activity of the parent compound in chlorinated samples at 2.0, 3.0, and 4.0 mgCl_2/L, respectively (Figure 2) being classified as a potentially concerning intermediate after water chlorination. Therefore, the use of EDA approaches in combination with PCA evaluation represents a potential approach for the identification and confirmation of hazardous TPs in treated samples. Although the complete elimination of antibiotics should eventually be the objective of water treatment processes, the elimination of the potential bioactive TPs generated is also required, even when complete elimination of the parent compound is attained.

■ ASSOCIATED CONTENT

Supporting Information

The Supporting Information is available free of charge at https://pubs.acs.org/doi/10.1021/acs.est.0c00944.

Postacquisition data processing workflow and parameters selected, exact mass list of most common azithromycin and ciprofloxacin TPs found in literature, detected and identified list of AZI and CFC TPs in chlorination experiment, UV spectra of ciprofloxacin intermediates identified, and R-Scripts and acute toxicity measurements of fractions (PDF)

■ AUTHOR INFORMATION

Corresponding Authors

Sara Rodríguez-Mozaz − *Catalan Institute for Water Research (ICRA), 17003 Girona, Spain; Universitat de Girona, Girona, Spain;* orcid.org/0000-0003-2962-8144; Phone: (+34) 972 18 33 80; Email: srodriguez@icra.cat

Adrián Jaén-Gil − *Catalan Institute for Water Research (ICRA), 17003 Girona, Spain; Universitat de Girona, Girona, Spain;* orcid.org/0000-0002-3519-3717; Phone: (+34) 972 18 33 80; Email: ajaen@icra.cat

Authors

María-José Farré − *Catalan Institute for Water Research (ICRA), 17003 Girona, Spain; Universitat de Girona, Girona, Spain;* orcid.org/0000-0002-8971-3722

Alexandre Sànchez-Melsió − *Catalan Institute for Water Research (ICRA), 17003 Girona, Spain; Universitat de Girona, Girona, Spain*

Albert Serra-Compte − *Catalan Institute for Water Research (ICRA), 17003 Girona, Spain; Universitat de Girona, Girona, Spain;* orcid.org/0000-0001-9663-3491

Damià Barceló − *Catalan Institute for Water Research (ICRA), 17003 Girona, Spain; Universitat de Girona, Girona, Spain; Water and Soil Quality Research Group, Department of Environmental Chemistry, IDAEA-CSIC, E-08034 Barcelona, Spain*

Complete contact information is available at: https://pubs.acs.org/10.1021/acs.est.0c00944

Author Contributions

The manuscript was written through the contributions of all authors. All authors have given approval to the final version of the manuscript.

Notes

The authors declare no competing financial interest.

■ ACKNOWLEDGMENTS

This work was funded by the Spanish State Research Agency of the Spanish Ministry of Science, Innovation and Universities AEI-MICIU and the Fondo Europeo de Desarrollo Regional under the National Program for Research Aimed at the Challenges of Society (CTM2017-85335-R). The authors acknowledge the support from the Economy and Knowledge Department of the Catalan Government through the Consolidated Research Group (ICRA-ENV 2017 SGR 1124 and 2017-SGR-1404). ICRA researchers are thankful for funding from the CERCA program. M.J.F. and S.R.M. acknowledge the Ramon y Cajal research fellowships RyC-2015-17108 and RYC-2014-16707 from the Spanish Ministry of Economy and Competitiveness. A.J.G. and A.S.C acknowledge the predoctoral grants 2019FI_B2_00202 and 2018FI_B2_00170 from AGAUR cofinanced by the European Social Fund. The authors would like to thank Wageningen Food Safety Research for their help with the antibiotic inhibition tests.

■ REFERENCES

(1) Rodriguez-Mozaz, S.; Chamorro, S.; Marti, E.; Huerta, B.; Gros, M.; Sànchez-Melsió, A.; Borrego, C. M.; Barceló, D.; Balcázar, J. L.

Occurrence of antibiotics and antibiotic resistance genes in hospital and urban wastewaters and their impact on the receiving river. *Water Res.* **2015**, *69*, 234−242.
(2) Yang, Y.; Ok, Y. S.; Kim, K. H.; Kwon, E. E.; Tsang, Y. F. Occurrences and removal of pharmaceuticals and personal care products (PPCPs) in drinking water and water/sewage treatment plants: A review. *Sci. Total Environ.* **2017**, *596*−*597*, 303−320.
(3) aus der Beek, T.; Weber, F. A.; Bergmann, A.; Hickmann, S.; Ebert, I.; Hein, A.; Küster, A. Pharmaceuticals in the environment-Global occurrences and perspectives. *Environ. Toxicol. Chem.* **2016**, *35* (4), 823−835.
(4) Lees, K.; Fitzsimons, M.; Snape, J.; Tappin, A.; Comber, S. Pharmaceuticals in soils of lower income countries: Physico-chemical fate and risks from wastewater irrigation. *Environ. Int.* **2016**, *94*, 712−723.
(5) Durso, L. M.; Cook, K. L. Impacts of antibiotic use in agriculture: What are the benefits and risks? *Curr. Opin. Microbiol.* **2014**, *19* (1), 37−44.
(6) Wegener, H. C. Antibiotics in animal feed and their role in resistance development. *Curr. Opin. Microbiol.* **2003**, *6* (5), 439−445.
(7) Verlicchi, P.; Al Aukidy, M.; Zambello, E. Occurrence of pharmaceutical compounds in urban wastewater: Removal, mass load and environmental risk after a secondary treatment-A review. *Sci. Total Environ.* **2012**, *429*, 123−155.
(8) Grenni, P.; Ancona, V.; Barra Caracciolo, A. Ecological effects of antibiotics on natural ecosystems: A review. *Microchem. J.* **2018**, *136*, 25−39.
(9) Martinez, J. L. Environmental pollution by antibiotics and by antibiotic resistance determinants. *Environ. Pollut.* **2009**, *157* (11), 2893−2902.
(10) Chartier, Y.; Emmanuel, J.; Pieper, U.; Prüss, A.; Rushbrook, P.; Stringer, R.; Townend, W.; Wilburn, S.; Zghondi, R. *Safe Management of Wastes from Health-Care Activities*; World Heal. Organ.: Geneva, Switzerland, 2014.
(11) Huerta-Fontela, M.; Galceran, M. T.; Ventura, F. Occurrence and removal of pharmaceuticals and hormones through drinking water treatment. *Water Res.* **2011**, *45* (3), 1432−1442.
(12) Diana, M.; Felipe-Sotelo, M.; Bond, T. Disinfection byproducts potentially responsible for the association between chlorinated drinking water and bladder cancer: A review. *Water Res.* **2019**, *162*, 492−504.
(13) Jelić, D.; Antolovic, R. From Erythromycin to Azithromycin and New Potential Ribosome-Binding Antimicrobials. *Antibiotics* **2016**, *5* (3), 29.
(14) Kagkelaris, K. A.; Makri, O. E.; Georgakopoulos, C. D.; Panayiotakopoulos, G. D. An eye for azithromycin: review of the literature. *Ther. Adv. Ophthalmol.* **2018**, *10*, 251584141878362.
(15) Andersson, M. I.; Macgowan, A. P. Development of the quinolones. *J. Antimicrob. Chemother.* **2003**, *51*, 1−11.
(16) Ezelarab, H. A. A.; Abbas, S. H.; Hassan, H. A.; Abuo-Rahma, G. E.-D. A. Recent updates of fluoroquinolones as antibacterial agents. *Arch. Pharm.* **2018**, *351*, 1800141.
(17) Escher, B. I.; Fenner, K. Recent Advances in Environmental Risk Assessment of Transformation Products. *Environ. Sci. Technol.* **2011**, *45* (9), 3835−3847.
(18) Postigo, C.; Richardson, S. D. Transformation of pharmaceuticals during oxidation/disinfection processes in drinking water treatment. *J. Hazard. Mater.* **2014**, *279*, 461−475.
(19) Brack, W.; Ait-Aissa, S.; Burgess, R. M.; Busch, W.; Creusot, N.; Di Paolo, C.; Escher, B. I.; Mark Hewitt, L.; Hilscherova, K.; Hollender, J.; Hollert, H.; Jonker, W.; Kool, J.; Lamoree, M.; Muschket, M.; Neumann, S.; Rostkowski, P.; Ruttkies, C.; Schollee, J.; Schymanski, E. L.; Schulze, T.; Seiler, T. B.; Tindall, A. J.; De Aragão Umbuzeiro, G.; Vrana, B.; Krauss, M. Effect-directed analysis supporting monitoring of aquatic environments - An in-depth overview. *Sci. Total Environ.* **2016**, *544*, 1073−1118.
(20) Brack, W. Effect-directed analysis: a promising tool for the identification of organic toxicants in complex mixtures? *Anal. Bioanal. Chem.* **2003**, *377*, 397−407.
(21) Schymanski, E. L.; Bataineh, M.; Goss, K. U.; Brack, W. Integrated analytical and computer tools for structure elucidation in effect-directed analysis. *TrAC, Trends Anal. Chem.* **2009**, *28* (5), 550−561.
(22) Escher, B. I.; Stapleton, H. M.; Schymanski, E. L. Tracking complex mixtures of chemicals in our changing environment. *Science* **2020**, *367*, 388−392.
(23) Brack, W.; Schmitt-Jansen, M.; MacHala, M.; Brix, R.; Barceló, D.; Schymanski, E.; Streck, G.; Schulze, T. How to confirm identified toxicants in effect-directed analysis. *Anal. Bioanal. Chem.* **2008**, *390* (8), 1959−1973.
(24) Bletsou, A. A.; Jeon, J.; Hollender, J.; Archontaki, E.; Thomaidis, N. S. Targeted and non-targeted liquid chromatography-mass spectrometric workflows for identification of transformation products of emerging pollutants in the aquatic environment. *TrAC, Trends Anal. Chem.* **2015**, *66*, 32−44.
(25) Díaz, R.; Ibáñez, M.; Sancho, J. V.; Hernández, F. Target and non-target screening strategies for organic contaminants, residues and illicit substances in food, environmental and human biological samples by UHPLC-QTOF-MS. *Anal. Methods* **2012**, *4* (1), 196−209.
(26) Li, Z.; Kaserzon, S. L.; Plassmann, M. M.; Sobek, A.; Gómez Ramos, M. J.; Radke, M. A strategic screening approach to identify transformation products of organic micropollutants formed in natural waters. *Environ. Sci. Process. Impacts* **2017**, *19* (4), 488−498.
(27) Schymanski, E. L.; Singer, H. P.; Slobodnik, J.; Ipolyi, I. M.; Oswald, P.; Krauss, M.; Schulze, T.; Haglund, P.; Letzel, T.; Grosse, S.; Thomaidis, N. S.; Bletsou, A.; Zwiener, C.; Ibáñez, M.; Portolés, T.; De Boer, R.; Reid, M. J.; Onghena, M.; Kunkel, U.; Schulz, W.; Guillon, A.; Noyon, N.; Leroy, G.; Bados, P.; Bogialli, S.; Stipaničev, D.; Rostkowski, P.; Hollender, J. Non-target screening with high-resolution mass spectrometry: Critical review using a collaborative trial on water analysis. *Anal. Bioanal. Chem.* **2015**, *407* (21), 6237−6255.
(28) Avagyan, R.; Åberg, M.; Westerholm, R. Suspect screening of OH-PAHs and non-target screening of other organic compounds in wood smoke particles using HR-Orbitrap-MS. *Chemosphere* **2016**, *163*, 313−321.
(29) Gago-Ferrero, P.; Krettek, A.; Fischer, S.; Wiberg, K.; Ahrens, L. Suspect Screening and Regulatory Databases: A Powerful Combination to Identify Emerging Micropollutants. *Environ. Sci. Technol.* **2018**, *52* (12), 6881−6894.
(30) Smith, C. A.; Want, E. J.; O'Maille, G.; Abagyan, R.; Siuzdak, G. XCMS: Processing mass spectrometry data for metabolite profiling using nonlinear peak alignment, matching, and identification. *Anal. Chem.* **2006**, *78* (3), 779−787.
(31) Albergamo, V.; Schollée, J. E.; Schymanski, E. L.; Helmus, R.; Timmer, H.; Hollender, J.; De Voogt, P. Nontarget screening reveals time trends of polar micropollutants in a riverbank filtration system. *Environ. Sci. Technol.* **2019**, *53* (13), 7584−7594.
(32) Pluskal, T.; Castillo, S.; Villar-Briones, A.; Orešič, M. MZmine 2: Modular framework for processing, visualizing, and analyzing mass spectrometry-based molecular profile data. *BMC Bioinf.* **2010**, *11*, 395.
(33) Schulze, T.; Weiss, S.; Schymanski, E.; von der Ohe, P. C.; Schmitt-Jansen, M.; Altenburger, R.; Streck, G.; Brack, W. Identification of a phytotoxic photo-transformation product of diclofenac using effect-directed analysis. *Environ. Pollut.* **2010**, *158* (5), 1461−1466.
(34) Brack, W.; Altenburger, R.; Küster, E.; Meissner, B.; Wenzel, K. D.; Schüürmann, G. Identification of toxic products of anthracene photomodification in simulated sunlight. *Environ. Toxicol. Chem.* **2003**, *22* (10), 2228−2237.
(35) Romanucci, V.; Siciliano, A.; Guida, M.; Libralato, G.; Saviano, L.; Luongo, G.; Previtera, L.; Di Fabio, G.; Zarrelli, A. Disinfection by-products and ecotoxic risk associated with hypochlorite treatment of irbesartan. *Sci. Total Environ.* **2020**, *712*, 135625.
(36) Schymanski, E. L.; Meinert, C.; Meringer, M.; Brack, W. The use of MS classifiers and structure generation to assist in the identification of unknowns in effect-directed analysis. *Anal. Chim. Acta* **2008**, *615* (2), 136−147.

https://dx.doi.org/10.1021/acs.est.0c00944
Environ. Sci. Technol. 2020, 54, 9062−9073

(37) Pikkemaat, M. G.; Van Dijk, S. O.; Schouten, J.; Rapallini, M.; van Egmond, H. J. A new microbial screening method for the detection of antimicrobial residues in slaughter animals: The Nouws antibiotic test (NAT-screening). *Food Control* **2008**, *19* (8), 781−789.
(38) ISO. *ISO 11348-3:1998 - Water quality -- Determination of the inhibitory effect of water samples on the light emission of Vibrio fischeri (Luminescent bacteria test)*; 1998.
(39) Terasaki, M.; Makino, M.; Tatarazako, N. Acute toxicity of parabens and their chlorinated by-products with Daphnia magna and Vibrio fischeri bioassays. *J. Appl. Toxicol.* **2009**, *29* (3), 242−247.
(40) Leusch, F. D. L.; Neale, P. A.; Busetti, F.; Card, M.; Humpage, A.; Orbell, J. D.; Ridgway, H. F.; Stewart, M. B.; van de Merwe, J. P.; Escher, B. I. Transformation of endocrine disrupting chemicals, pharmaceutical and personal care products during drinking water disinfection. *Sci. Total Environ.* **2019**, *657*, 1480−1490.
(41) Jaén-Gil, A.; Castellet-Rovira, F.; Llorca, M.; Villagrasa, M.; Sarrà, M.; Rodríguez-Mozaz, S.; Barceló, D. Fungal treatment of metoprolol and its recalcitrant metabolite metoprolol acid in hospital wastewater: Biotransformation, sorption and ecotoxicological impact. *Water Res.* **2019**, *152*, 171−180.
(42) Jaén-Gil, A.; Hom-Diaz, A.; Llorca, M.; Vicent, T.; Blánquez, P.; Barceló, D.; Rodríguez-Mozaz, S. An automated on-line turbulent flow liquid-chromatography technology coupled to a high resolution mass spectrometer LTQ-Orbitrap for suspect screening of antibiotic transformation products during microalgae wastewater treatment. *J. Chromatogr. A* **2018**, *1568*, 57−68.
(43) Ferrando-Climent, L.; Gonzalez-Olmos, R.; Anfruns, A.; Aymerich, I.; Corominas, L.; Barceló, D.; Rodriguez-Mozaz, S. Elimination study of the chemotherapy drug tamoxifen by different advanced oxidation processes: Transformation products and toxicity assessment. *Chemosphere* **2017**, *168*, 284−292.
(44) Sardessai, Y.; Bhosle, S. Tolerance of bacteria to organic solvents. *Res. Microbiol.* **2002**, *153* (5), 263−268.
(45) Sardessai, Y. N.; Bhosle, S. Industrial potential of organic solvent tolerant bacteria. *Biotechnol. Prog.* **2004**, *20* (3), 655−660.
(46) Reemtsma, T.; Fiehn, O.; Jekel, M. A modified method for the analysis of organics in industrial wastewater as directed by their toxicity to Vibrio fischeri. *Fresenius' J. Anal. Chem.* **1999**, *363* (8), 771−776.
(47) Dodd, M. C.; Kohler, H. P. E.; Von Gunten, U. Oxidation of antibacterial compounds by ozone and hydroxyl radical: Elimination of biological activity during aqueous ozonation processes. *Environ. Sci. Technol.* **2009**, *43* (7), 2498−2504.
(48) Čizmić, M.; Ljubas, D.; Rožman, M.; Ašperger, D.; Ćurković, L.; Babíc, S. Photocatalytic degradation of azithromycin by nano-structured TiO 2 film: Kinetics, degradation products, and toxicity. *Materials* **2019**, *12*, 873.
(49) Radosavljević, K. D.; Lović, J. D.; Mijin, D.; Petrović, S. D.; Jadranin, M. B.; Mladenović, A. R.; Avramov Ivić, M. L. Degradation of azithromycin using Ti/RuO2 anode as catalyst followed by DPV, HPLC-UV and MS analysis. *Chem. Pap.* **2017**, *71* (7), 1217−1224.
(50) Paul, T.; Dodd, M. C.; Strathmann, T. J. Photolytic and photocatalytic decomposition of aqueous ciprofloxacin: Transformation products and residual antibacterial activity. *Water Res.* **2010**, *44* (10), 3121−3132.
(51) Gomes Júnior, O.; Silva, V. M.; Machado, A. E. H.; Sirtori, C.; Lemos, C. R.; Freitas, A. M.; Trovó, A. G. Correlation between pH and molar iron/ligand ratio during ciprofloxacin degradation by photo-Fenton process: Identification of the main transformation products. *J. Environ. Manage.* **2018**, *213*, 20−26.
(52) Zhu, L.; Santiago-Schübel, B.; Xiao, H.; Hollert, H.; Kueppers, S. Electrochemical oxidation of fluoroquinolone antibiotics: Mechanism, residual antibacterial activity and toxicity change. *Water Res.* **2016**, *102*, 52−62.
(53) Ou, H. s.; Ye, J. s.; Ma, S.; Wei, C. h.; Gao, N. y.; He, J. z. Degradation of ciprofloxacin by UV and UV/H2O2 via multiple-wavelength ultraviolet light-emitting diodes: Effectiveness, intermediates and antibacterial activity. *Chem. Eng. J.* **2016**, *289*, 391−401.
(54) Yang, B.; Kookana, R. S.; Williams, M.; Ying, G. G.; Du, J.; Doan, H.; Kumar, A. Oxidation of ciprofloxacin and enrofloxacin by ferrate(VI): Products identification, and toxicity evaluation. *J. Hazard. Mater.* **2016**, *320*, 296−303.
(55) De Witte, B.; Van Langenhove, H.; Demeestere, K.; Saerens, K.; De Wispelaere, P.; Dewulf, J. Ciprofloxacin ozonation in hospital wastewater treatment plant effluent: Effect of pH and H2O2. *Chemosphere* **2010**, *78* (9), 1142−1147.
(56) De Bel, E.; Dewulf, J.; De Witte, B.; Van Langenhove, H.; Janssen, C. Influence of pH on the sonolysis of ciprofloxacin: Biodegradability, ecotoxicity and antibiotic activity of its degradation products. *Chemosphere* **2009**, *77* (2), 291−295.
(57) Yuan, F.; Hu, C.; Hu, X.; Wei, D.; Chen, Y.; Qu, J. Photodegradation and toxicity changes of antibiotics in UV and UV/H2O2 process. *J. Hazard. Mater.* **2011**, *185* (2−3), 1256−1263.
(58) Li, M.; Wei, D.; Du, Y. Acute toxicity evaluation for quinolone antibiotics and their chlorination disinfection processes. *J. Environ. Sci.* **2014**, *26* (9), 1837−1842.
(59) Tegze, A.; Sági, G.; Kovács, K.; Homlok, R.; Tóth, T.; Mohácsi-Farkas, C.; Wojnárovits, L.; Takács, E. Degradation of fluoroquinolone antibiotics during ionizing radiation treatment and assessment of antibacterial activity, toxicity and biodegradability of the products. *Radiat. Phys. Chem.* **2018**, *147* (February), 101−105.
(60) Guo, Q.; Du, Z.; Shao, B. Simulation and experimental study on the mechanism of the chlorination of azithromycin. *J. Hazard. Mater.* **2018**, *359* (July), 31−39.
(61) Wang, H.; Hu, C.; Liu, L.; Xing, X. Interaction of ciprofloxacin chlorination products with bacteria in drinking water distribution systems. *J. Hazard. Mater.* **2017**, *339*, 174−181.
(62) Dodd, M. C.; Shah, A. D.; Von Gunten, U.; Huang, C. H. Interactions of fluoroquinolone antibacterial agents with aqueous chlorine: Reaction kinetics, mechanisms, and transformation pathways. *Environ. Sci. Technol.* **2005**, *39* (18), 7065−7076.
(63) Wang, P.; He, Y. L.; Huang, C. H. Oxidation of fluoroquinolone antibiotics and structurally related amines by chlorine dioxide: Reaction kinetics, product and pathway evaluation. *Water Res.* **2010**, *44* (20), 5989−5998.
(64) Domagala, J. M. Structure-activity and structure-side-effect relationships for the quinolone antibacterials. *J. Antimicrob. Chemother.* **1994**, *33*, 685−706.
(65) Jiao, S.; Zheng, S.; Yin, D.; Wang, L.; Chen, L. Aqueous photolysis of tetracycline and toxicity of photolytic products to luminescent bacteria. *Chemosphere* **2008**, *73* (3), 377−382.
(66) Wang, H.; Shi, W.; Ma, D.; Shang, Y.; Wang, Y.; Gao, B. Formation of DBPs during chlorination of antibiotics and control with permanganate/bisulfite pretreatment. *Chem. Eng. J.* **2020**, *392* (October 2019), 123701.
(67) Sanchez, J. P.; Domagala, J. M.; Hagen, S. E.; Heifetz, C. L.; Hutt, M. P.; Nichols, J. B.; Trehan, A. K. Quinolone Antibacterial Agents. Synthesis and Structure-Activity Relationships of 8-Substituted Quinoline-3-carboxylic Acids and 1,8-Naphthyridine-3-carboxylic Acids. *J. Med. Chem.* **1988**, *31* (5), 983−991.
(68) Higgins, P.; Fluit, A.; Schmitz, F.-J. Fluoroquinolones: Structure and Target Sites. *Curr. Drug Targets* **2003**, *4* (2), 181−190.
(69) Escher, B. I.; Neale, P. A.; Villeneuve, D. L. The advantages of linear concentration−response curves for in vitro bioassays with environmental samples. *Environ. Toxicol. Chem.* **2018**, *37* (9), 2273−2280.
(70) Müller, M. E.; Vikstrom, S.; König, M.; Schlichting, R.; Zarfl, C.; Zwiener, C.; Escher, B. I. Mitochondrial Toxicity of Selected Micropollutants, Their Mixtures, and Surface Water Samples Measured by the Oxygen Consumption Rate in Cells. *Environ. Toxicol. Chem.* **2019**, *38* (5), 1000−1011.

https://dx.doi.org/10.1021/acs.est.0c00944
Environ. Sci. Technol. 2020, 54, 9062−9073

Chapter 5

Monitoring of the removal of PhACs and their hazardous TPs in combined treatments

Jaén-Gil et al., 2021. Chemical Engineering Journal, 404: 126482

Chemical Engineering Journal 404 (2021) 126482

Contents lists available at ScienceDirect

Chemical Engineering Journal

journal homepage: www.elsevier.com/locate/cej

Combining biological processes with UV/H_2O_2 for metoprolol and metoprolol acid removal in hospital wastewater

Adrián Jaén-Gil[a,b], Gianluigi Buttiglieri[a,b], Aleix Benito[c], Josep Anton Mir-Tutusaus[d], Rafael Gonzalez-Olmos[c], Glòria Caminal[e], Damià Barceló[a,b,f], Montserrat Sarrà[d], Sara Rodriguez-Mozaz[a,b,*]

[a] Catalan Institute for Water Research (ICRA), Carrer Emili Grahit 101, 17003 Girona, Spain
[b] Universitat de Girona, Girona, Spain
[c] IQS School of Engineering, Universitat Ramon Llull, Via Augusta 390, 08017 Barcelona, Spain
[d] Departament d'Enginyeria Química Biològica i Ambiental, Escola d'Enginyeria, Universitat Autònoma de Barcelona, 08193 Bellaterra, Barcelona, Spain
[e] Institut de Química Avançada de Catalunya (IQAC-CSIC), C. Jordi Girona 18-26, 08034 Barcelona, Spain
[f] Department of Environmental Chemistry, Institute of Environmental Assessment and Water Research (IDAEA-CSIC), C. Jordi Girona 18-26, 08034 Barcelona, Spain

HIGHLIGHTS

- The transformation of MTP and MTPA was studied in single and combined treatments.
- UV/H_2O_2 single treatments achieved total compound removal in fortified pure water.
- The combination of two treatments was needed to achieve a high removal in HWW.
- UV/H_2O_2 + CAS combination attained the highest removal in fortified HWW.
- The *in vitro* toxicity assays pointed out the presence of some hazardous TPs.

GRAPHICAL ABSTRACT

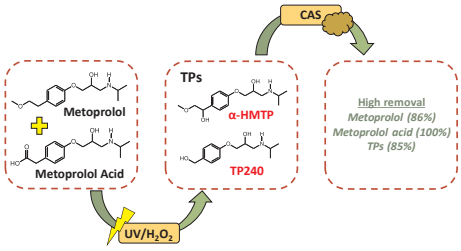

ARTICLE INFO

Keywords:
Metoprolol
Metoprolol acid
Transformation products
Suspect screening
Combined treatments

ABSTRACT

The transformation products (TPs) of water contaminants generated during wastewater treatment can sometimes be equally or even more hazardous than the parent compounds. Therefore, for a comprehensive assessment of removal efficiency of a water treatment technology, it is mandatory to monitor not only the pollutants but also of their TPs. However, this type of evaluation studies is lacking in the case of water combined treatments. In this study, the elimination of metoprolol (MTP), metoprolol acid (MTPA) and the TPs generated was evaluated in pure water and hospital wastewater (HWW) using UV/H_2O_2 before and after fungal (FG) or conventional activated sludge (CAS). The major transformation pathways were suggested in terms of transformation of the parent compounds through bio-transformation and photo-transformation mechanisms. The results reveal an extended removal of MTP, MTPA and TPs after UV/H_2O_2 single experiment treating spiked pure water at 2.5 mg/L, without increasing the treated effluents toxicity. However, combined treatments were required to achieve similar removal percentages in spiked real HWW at 2.0 μg/L: while AOPs combined with FG exhibited lower removal efficiencies with generation of persistent intermediates (such as α-HMTP and TP240), AOPs combined with CAS attained the higher persistent TPs removal. In particular, AOP + CAS was classified as the most effective combination for HWW with the highest removal of the parent compounds (86% for MTP and 100% for MTPA), of the intermediates generated (up to 85%) and with a low presence of toxic TPs (such as O-

* Corresponding author at: Catalan Institute for Water Research (ICRA), Carrer Emili Grahit 101, 17003 Girona, Spain.
E-mail address: srodriguez@icra.cat (S. Rodriguez-Mozaz).

https://doi.org/10.1016/j.cej.2020.126482
Received 19 February 2020; Received in revised form 24 June 2020; Accepted 27 July 2020
Available online 31 July 2020

DMTP). This study demonstrates that comprehensive evaluation of the intermediates generated along water treatment technologies is highly recommended to successfully evaluate their removal efficiencies.

1. Introduction

The occurrence of pharmaceutical active compounds (PhACs) and their metabolites in water bodies has become an imperative concern due to their potential impact on both environment and human health [1–3]. Every day, large quantities of wastewater are discharged into municipal sewer system not only from domestic origin but also from industrial and hospital sources [4]. In particular, hospital wastewater (HWW) has been identified as responsible for introducing high loads of contaminants with potentially toxic effects in aquatic ecosystems [5]. The incomplete elimination of the persistent pollutants in centralized conventional municipal wastewater treatment plants (WWTPs) allows the release of these contaminants into the environment [1,6]. In this sense, dedicated on-site wastewater treatment of HWW has been widely recommended by several authors [5,7]. However, specific directives or guidelines in Europe for the management of hospital effluents are missing and the implementation of full-scale HWW treatment has been introduced only in few cases [5,8]. The use of tailored and dedicated treatment technologies could stir up HWW decentralized treatment.

The use of biological treatments has been widely suggested as a more eco-friendly solution for the removal of organic pollutants from complex wastewater matrices, involving low operational costs and low energy consumption [9–12]. Conventional activated sludge treatments (CAS) cannot always provide satisfactory results in terms of PhACs removal, but they are still the most commonly applied worldwide, and to be considered as a reference to be compared with [13]. Among the different biological based solutions, fungal treatments have been pointed out to provide high removal rates for many PhACs thanks to the generation of unspecific extracellular enzymes able to degrade persistent organic pollutants [14–16]. However, incomplete elimination of non-biodegradable pollutants and bio-recalcitrant intermediates generated in fungal treatments have also been reported [17]. For the remediation of low biodegradable effluents, highly reactive and non-selective advanced oxidation processes (AOPs), such as UV/H_2O_2, have been widely suggested as suitable treatment solutions [18–20]. Despite this, AOPs are characterized by their relatively higher operating costs (compared to biological treatments) [21–23], especially in complex matrices [24]. Therefore, they require larger energy and chemical reagents demand to attain total compound mineralization [13].

Applying AOPs as pre-treatment steps to biological treatments has been suggested to convert the contaminants into more readily biodegradable intermediates and, hence, reducing the total cost of the treatment process [18,25,26]. Among them, solar photo-Fenton, ozonation and UV/H_2O_2 treatments have been applied as tertiary treatments for the remediation of micropollutants present in real municipal WWTP effluents [27,28]. However, the effectivity of combined treatments will always depend on the type of water effluent to be treated [24]. In addition, to properly evaluate the most effective combination for total pollutant mitigation, not only the removal of the parent compounds should be considered but also the presence of the major metabolites and the generated transformation products (TPs) [24,29]. Even though many studies have been focused on the applicability of combined treatments for decontamination of wastewater [13,19,26,30–35], only few of them are related to combined treatment of HWW [36]; and none of them have elucidated tentative transformation pathways of individual PhACs towards a better understanding of the total extent on pollutant removal.

Among the pollutants present in HWW, metoprolol (MTP) has been widely detected in wastewater due to its high consumption for hypertension and cardiovascular diseases [37]. In terms of associated environmental risk, its presence in natural waters has been related to cardiovascular dysfunctions, such as alteration of the heart rate, in aquatic organisms (e.g. *Daphnia magna*) [38]. Likewise, specific effects on scoliosis and growth retardation were reported in zebrafish embryos when exposed to MTP above 12.6 mg/L for 72 h [39]. Up to now, MTP has been pointed out as a compound of high consumption [40], and has been detected in raw wastewater up to 0.2–2.0 μg/L [41,42]. Removals percentage reported for these compounds in conventional WWTPs are usually low, between 0% and 36% [42–44]. After its consumption, the excretion of MTP as metoprolol acid (MTPA), via renal excretion, constitutes up to 60–65% of the initial MTP dose [45–47]. Therefore MTPA, being MTP major human metabolite, is an additional important pollutant to be studied in wastewater treatment [48]. Up to now, there are no regulations limiting discharges of these PhACs in WWTP effluents for those compounds [3]. In 2020, the Council of the European Union adopted a new regulation for efficient water reuse. The substances of emerging concern, including pharmaceutical active compounds, are mentioned in the risk assessment section but without any threshold value yet [49]. Therefore, the evaluation of PhACs presence, effective removal and potential discharge concentrations into the environment are extremely valuable to provide information for forthcoming studies in the field [50]. While some studies reported MTP and MTPA recalcitrance in conventional activated sludge (CAS) [44,51], others demonstrated its biodegradability in fungal (FG) treatment [17]. However, the complete elimination of their TPs has never been reported by any of the studied treatment.

Measuring the unknown intermediates in the evaluation of treatment removal efficiencies is critical due to their potential hazardous effects. Thus, even when complete elimination of the parent compounds is attained, the presence of these TPs should be also considered. To the best of authors' knowledge, this is the first time that four different combinations of treatments (UV/H_2O_2 treatment before/after CAS or FG) were investigated in terms of presence and removal of MTP, MTPA and their TPs in real HWW. The generated intermediates were identified with an automated suspect screening approach which allowed to comprehensively study their presence and transformation pathways along the combined treatments. This study demonstrates that combined treatments are a valuable solution towards a complete removal of MTP, MTPA and their TPs.

2. Methods and materials

2.1. Chemicals and reagents

Metoprolol tartrate salt (MTP) (Sigma-Aldrich), O-desmethylmetoprolol (O-DMTP), metoprolol acid (MTPA) and α-hydroxymetoprolol (α-HMTP) (Toronto Research Chemicals); and atenolol-d^7 internal standard (CDN isotopes, Quebec, Canada) were purchased at high purity grade (> 98%). Standard solutions were prepared on a weight basis in methanol (at a concentration of 1000 mg/L) and stored at −20 °C. Ultra-pure water and acetonitrile LiChrosolv grade were supplied by Merck (Darmstadt, Germany). Working standard solutions containing all pharmaceuticals and labeled internal standard were prepared in methanol/water (10:90, v/v). All FG nutrients used were selected regarding the optimum conditions reported previously [17]. For CAS experiments, organic solution (sodium acetate, propionate and yeast extract), phosphate buffer, trace and inorganic solution were added as described elsewhere [52]. For AOP experiments, the titanium (IV) oxysulfate reagent used was 1.9–2.1% from Sigma-Aldrich. The H_2O_2 reagent was 30% w/v 100 vol stabilized PRS from Panreac [53].

2.2. Experimental set-up

UV/H_2O_2 oxidation processes were combined in parallel with FG and CAS treatments as presented in Fig. 1 (each treatment technology is described in detail below). The experimental scheme was first applied treating pure water fortified with MTP and MTPA at initial concentrations of 2.5 mg/L each. Samples were collected at initial experimental time, prior to perform each individual treatment (to ensure reproducibility of samples between treatments) and after each individual treatment to evaluate treatment efficiency. Samples collected were directly injected into the liquid chromatography system coupled to high-resolution mass spectrometry (LC-HRMS) for monitoring of target compounds and TPs. Subsequently, the same experiments were performed in fortified HWW at initial concentration of 2.0 μg/L (to ensure their presence in real wastewater conditions and allow to properly evaluate their elimination) of MTP and MTPA. Samples preparation and analysis are presented in section 2.3 and 2.4, respectively.

2.2.1. Fungal treatment (FG)

Trametes versicolor (ATCC#42530) was maintained on 2% malt agar slants at 25 °C until use. The mycelial suspension of *T. versicolor* and pellets were obtained as previously described [54,55]. Air-fluidized bed bioreactors were operated as a batch per duplicate for 7 days. Fluidized conditions in the reactors were maintained by using 1 s air pulse every 4 s, resulting in an aeration rate of 0.8 L/min. Nutrients for maintenance, namely, glucose and NH_4Cl, were added with a molar C/N ratio of 7.5 at *T. versicolor* consumption rate to both reactors (1.2 g / (g DCW·d)). Temperature was maintained at 25 °C and pH was controlled at 4.5 by HCl 1 M or NaOH 1 M addition. Samples were collected, filtered through 0.45 μm PVDF filters (Millipore, Barcelona, Spain) and frozen in glass containers for pure water experiments and PET containers for HWW experiments (for safety handling in case of breakage). All these parameters were selected based on the optimum conditions reported previously [17].

2.2.2. Activated sludge treatment (CAS)

Activated sludge batch experiments were performed using a 1 L lab-scale Applikon stirred tank reactor coupled with a proportional-integral-derivative (PID) controller for pH, oxygen and temperature. Bioreactors were operated as a batch for 24 h and each experiment was conducted in duplicate. The activated sludge originated from Celrà WWTP (Catalonia, Spain, 20.000 equivalent inhabitants, 2,100 m^3/d), with a hydraulic retention time (HRT) of 48 h and a sludge retention time (SRT) of 20–22 days. The biomass concentration during the experiments was 3 gTSS/L (0.71 ratio VSS/TSS) and aerobic conditions (> 2.5 mg O_2/L) were achieved with continuous air supply. The pH and temperature were maintained at 7.5 and 25 °C, respectively. Activated sludge after treating pure water or HWW was centrifuged 4 min at 8000 RPM (20 °C), prior to perform AOP post-treatment experiments. Mixed liquor samples were filtered (0.45 μm pore size Millex PVDF) and immediately frozen in glass containers for pure water experiments and PET containers for HWW experiments (for safety handling in case of breakage). All these parameters were selected based on the optimum conditions needed for this treatment [44].

2.2.3. UV/H_2O_2 treatment (AOP)

Photo-oxidation treatment processes were performed in duplicate by using an UV Laboratory Reactor System from UV-Consulting Peschl®, an immersion-type photo-reactor of approximately 550 mL. The UV lamp consisted in a 15 W Heraeus Noblelight TNN 15/32 low-pressure mercury vapor lamp emitting at 254 nm. The photo-reactor was mixed with a magnetic stirrer to assure the homogeneity of the solution. Moreover, the photo-reactor was covered with aluminum foil in order to minimize the loss of UV light and avoid any reflections. Potassium ferrioxalate actinometry [56] was used as in previous work in order to characterize the intensity of the light of the UV lamp, resulting in an irradiance of 0.049 W/cm^2 [53]. The experiments were carried out with 500 mL of wastewater, 15 mg/L of H_2O_2 and a reaction time of 10 min that corresponds to an UV dose or intensity of 29.4 J/cm^2. The H_2O_2 concentration was analyzed by a spectrophotometric method using titanium (IV) oxysulfate as reported previously [57]. A stoichiometric excess of 20% of sodium thiosulfate was added to stop the oxidation reaction in the collected samples [24]. Then, samples were filtered through 0.45 μm PVDF filters at initial and final time for further sample treatment and analysis. Samples were collected and frozen in glass containers for pure water experiments and PET containers for HWW experiments (for safety handling in case of breakage). All these parameters were selected based on the treatment operative conditions applied previously [24].

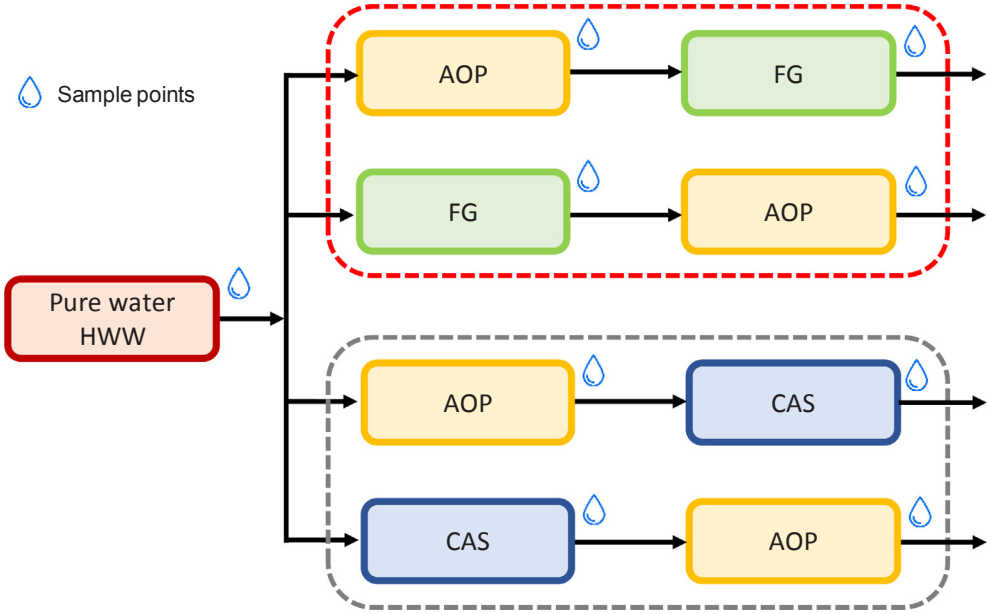

Fig. 1. Scheme of the experimental set-up with UV/H_2O_2 oxidation process (AOP), fungal (FG) and activated sludge (CAS) combined for treating fortified pure water and HWW.

2.3. Hospital wastewater and sample treatment

Hospital wastewater (HWW) was collected directly from the sewer manifold of Sant Joan de Déu Hospital (Barcelona, Catalonia) in the NE of Spain. Fresh samples were collected and pretreated with a coagulation-flocculation process as described previously [58]. The pretreatment used 43 mg/L of coagulant Hyfloc AC50 and 4.8 mg/L of flocculant Himoloc DR3000, both kindly provided by Derypol, S.A. (Barcelona, Spain). Physicochemical conditions of initial HWW were as follows: COD, 210.4 mg/L; TOC, 65.9 mg/L; N-NO_2, 1.6 mg/L; N-NO_3, 5.9 mg/L; P-PO_4, 2.0 mg/L; and N-NH_4, 25.9 mg/L. A volume of 25 mL of raw HWW and 50 mL of treated HWW were pre-concentrated through Solid Phase Extraction in Oasis HLB cartridges (60 mg, 3 mL) (Waters Corp. Mildford, MA, USA) following the methodology previously described elsewhere [59]. The extracts were kept in 1 mL of methanol adding 10 µL of a 1 ng/µL of the isotopically labeled standard. The extracts were further pre-concentrated to facilitate TPs detection though evaporation and reconstitution in 150 µL of methanol:water (10:90, v/v) for LC-LTQ-Orbitrap-MS/MS analysis.

2.4. Instrumental analysis

The detection and identification of the parent compounds and TPs generated in each treatment step were performed with the suspect screening methodology previously described [24]. A liquid chromatography system coupled to a high-resolution mass spectrometer HPLC-LTQ-Orbitrap Velos™ (Thermo Fisher Scientific) was used for the analysis of the samples. The chromatographic separation was performed using a ZORBAX Eclipse XDB-C18 (150 mm × 4.6 mm, 5 µm) for a total run time of 17 min. The instrument was equipped with a heated electrospray ionization source (HESI-II) and analyses were performed in positive and negative mode. As negative mode showed poor ionization efficiencies, data processing was performed for positive mode only. Samples were acquired in Data Dependent Acquisition mode through full scan from 100 to 1000 mass-to-charge (m/z) range at a resolving power of 60.000 FWHM. Selection of the most intense ions (Top 3) for MS/MS full scan fragmentation was performed in a second event and recorded at 30.000 FWHM from 50 to 500 m/z range. MS/MS fragmentation modes were investigated by using collision-induced dissociation at 30 eV CE (Q = 0.250 and an activation time of 30 ms) in an isolation width of 2 Da. The entire system was controlled via Aria software, version 1.6, under Xcalibur 2.1 software.

The data acquired were processed by an integrated suspect screening methodology using Compound Discoverer 3.0 (Thermo Fisher Scientific). The methodology combines comparison with reference standards, in-house databases, compound prediction tools and literature sources for chemical identification. Detailed workflow regarding the analytical suspect screening strategy applied is presented in Fig. S1. In addition, specific parameters selected to ensure reliability on chemical identification and transformation pathways are presented in

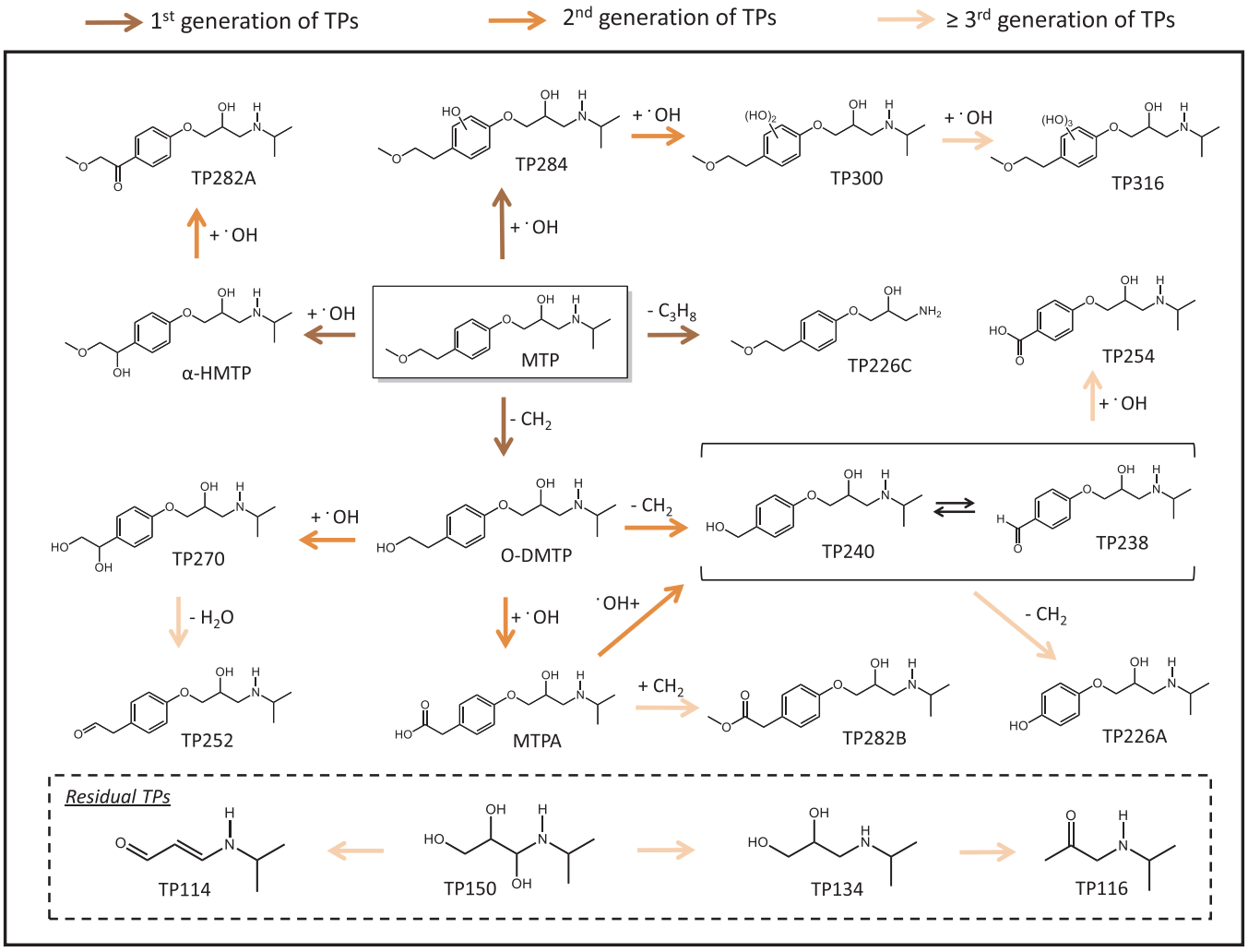

Fig. 2. Suggested transformation pathway of MTP and MTPA in combined treatments treating fortified pure water and HWW. The colored arrows indicate the removal degree in terms of 1st, 2nd and ≥ 3rd generation of TPs from MTP structure.

Table S1. The relative presence (%) of the target pollutants MTP and MTPA was calculated as the area of MTP or MTPA (at a given time), relative to the area of MTP or MTPA before any treatment (at initial time):

$$MTP(A)(\%) = \frac{Area^{x}_{MTP(A)}}{Area^{0}_{MTP(A)}}100 \quad (1)$$

The TPs presence was calculated as the sum of the areas of all the detected TPs generated from MTP and MTPA degradation (at a given time), relative to the sum of the areas of spiked compounds (MTP and MTPA) before any treatment (at initial time):

$$TP_{presence}(\%) = \frac{\sum_{i=1}^{n} Area^{x}_{TPi}}{Area^{0}_{MTP} + Area^{0}_{MTPA}}100 \quad (2)$$

Additionally, the relative distribution of the intermediates generated was calculated (Eq. (3)) as the area of each TP detected relative to the sum of areas of all detected TPs (at a given time). In this specific case, MTPA was considered as a TP since it can be also generated from the degradation of the parent compound MTP (as a 2nd generation TP).

$$TP_{i\ distribution}(\%) = \frac{Area^{x}_{TPi}}{\sum_{i=1}^{n} Area^{x}_{TPi}}100 \quad (3)$$

Finally, statistical comparisons between the effluents generated after the four combinations, tested in pure water and HWW, were performed to compare the generated TPs and their distribution in treated samples. In this context, spearman correlations were calculated through the function "cor" (Package "stats", [60]) and the function "cor.mtest" (Package "corrplot", [61]). Graphics were generated using the function "corrplot" (Package "corrplot", [61]).

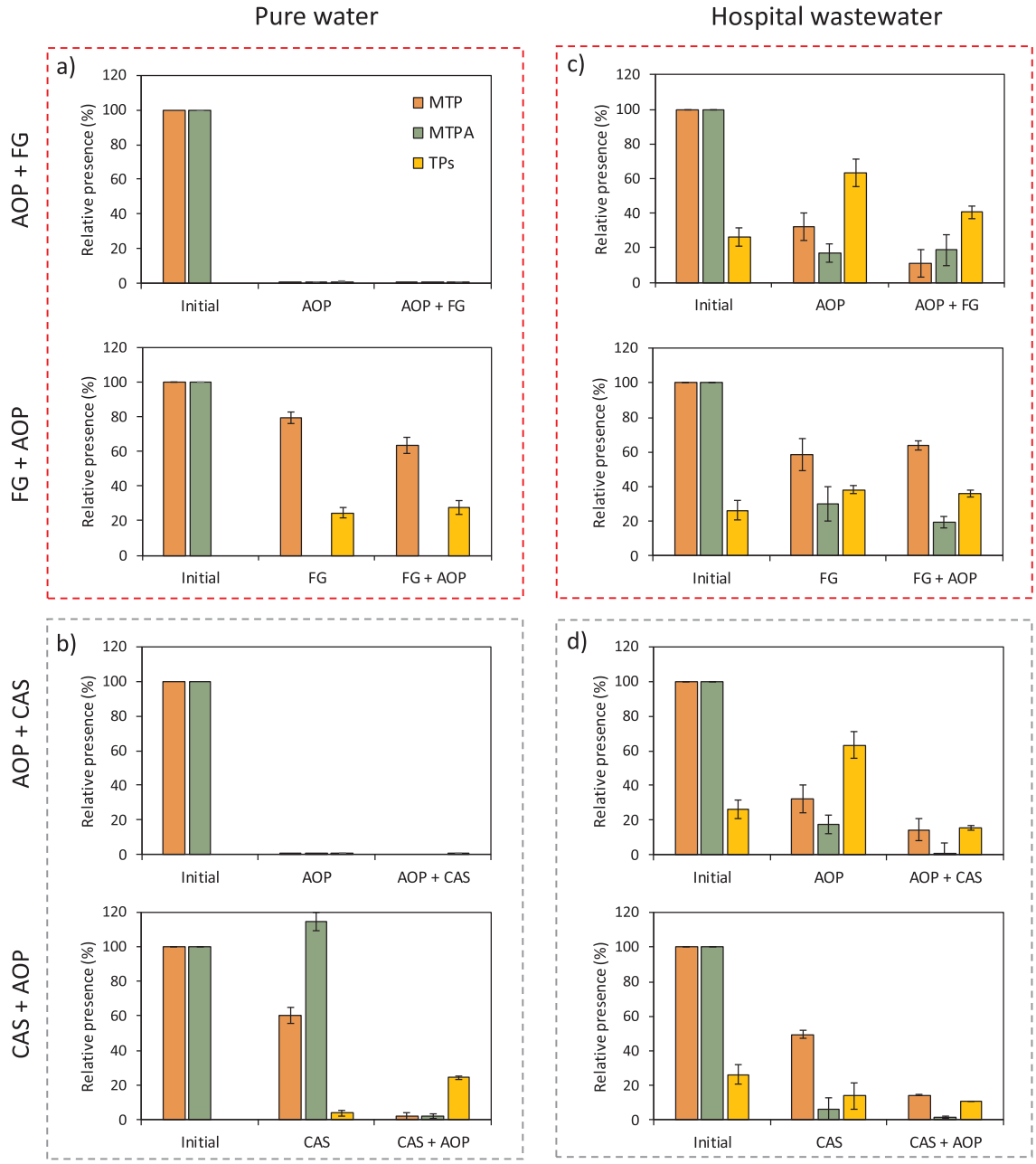

Fig. 3. Relative presence of MTP, MTPA (Eq. (1)) and TPs (Eq. (2)) in combined experiments treating fortified pure water and HWW: a,c) UV/H_2O_2 combined with FG treatment; and b,d) UV/H_2O_2 combined with CAS treatment.

2.5. Toxicological assessment

The ISO 11348–3 protocol [62] for testing bacterial bioluminescence (Microtox® bioassay) was used to measure the toxicity only in spiked pure water experiments where MTP, MTPA and their TPs generated were the only potential toxicants in samples (*in vitro* toxicity). This bioassay was not applied to real HWW samples, since other pharmaceuticals (different from MTP and MTPA) and many other compounds are present and potentially contributing to toxicity signal. All the collected samples in pure water experiments were introduced in glass vials and centrifuged to remove possible interference from biomass fragments or solids in suspension. Then, the decay on emitted light was recorded after 15 min of samples contact with the bacterium *Vibrio fischeri*. The 50% effective concentration (EC_{50}) was expressed in dilution percentage. TU along the combined treatments was calculated as ($TU = 100/EC_{50}$) [63]. The concentration of sodium thiosulfate added after AOP experiments (to stop the oxidation reaction) was tested and had no toxic effect on luminescent bacteria [24].

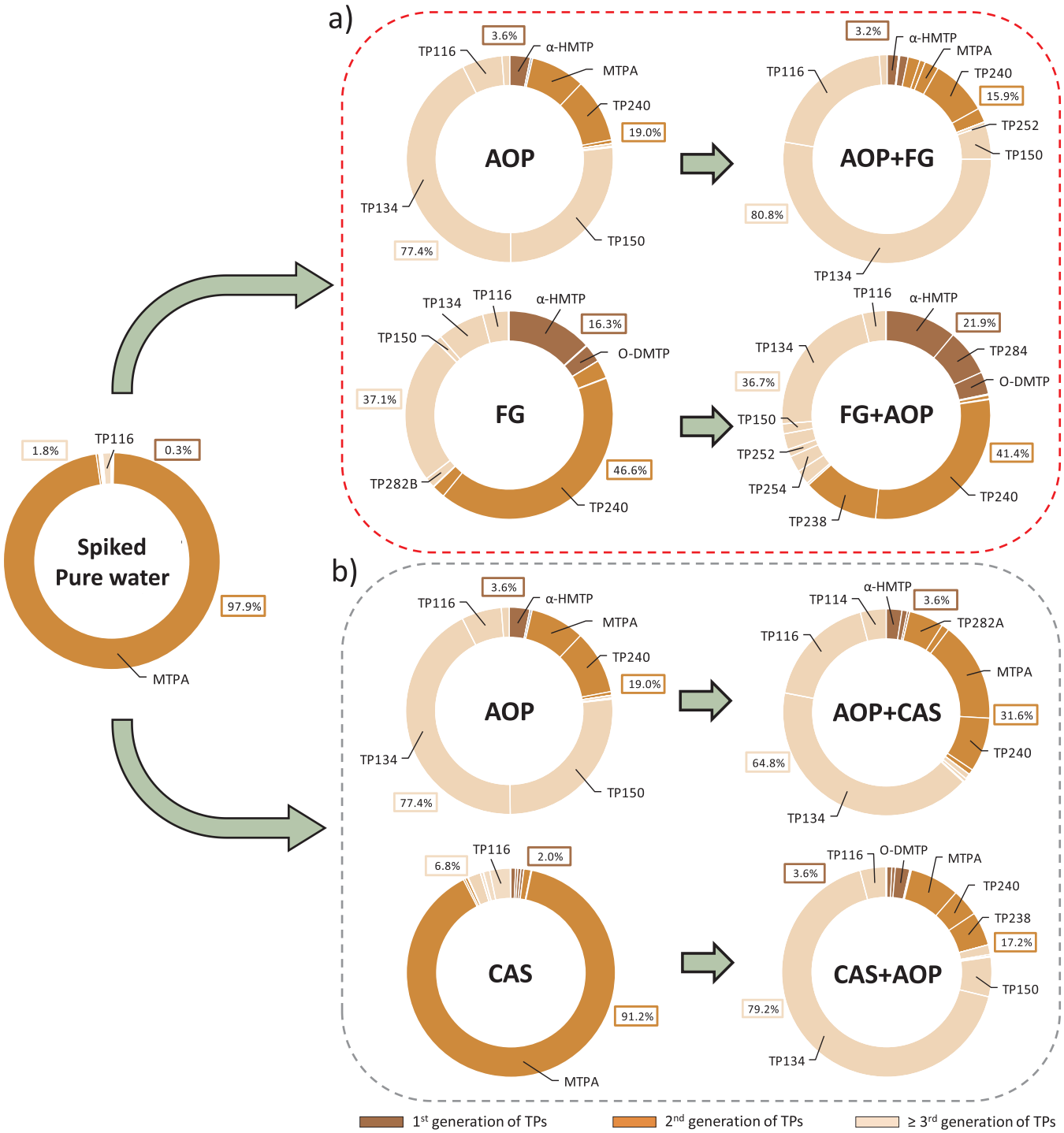

Fig. 4. The circles represent the relative distribution of intermediates in fortified pure water (Eq. (3)), classified regarding their degree on removal (1st, 2nd and ≥ 3rd generation expressed in percentage values, according to Fig. 2) in: a) UV/H_2O_2 combined with FG treatment; b) UV/H_2O_2 combined with CAS treatment.

3. Results and discussion

3.1. Identification of TPs and elucidation of transformation pathways

MTP and MTPA transformation was evaluated for each individual treatment in fortified pure water and HWW. Among the detected compounds, MTP and the human metabolites MTPA, O-DMTP and α-HMTP were confirmed by means of reference standards, retention time, compound exact mass and MS/MS fragmentation spectra. Nineteen intermediates (out of the 29 probable compounds comprised into the in-house database, Table S2), were detected in the samples by comparison of retention time, compound exact mass and MS/MS fragmentation spectra (no reference standard available). No additional TPs were found neither from the list of 356 compounds predicted (Table S3), generated using compound prediction tools of the software Compound Discoverer 3.0. (Table S1), nor from list of 39 compounds collected from literature (Table S4).

The major transformation pathways were suggested from successive hydroxylation, oxidation and O-dealkylation of MTP and MTPA chemical structures (Fig. 2). Among them, the main transformation pathway detected in this study was related to the formation of the intermediates TP238 and TP240 after rapid O-demethylation of MTP structure and benzylic hydroxylation, through the formation of a radical intermediate of O-DMTP in biological treatments [64,65]. These intermediates were also observed in physico-chemical treatments through oxidative reactions involving the attack of highly reactive radicals on the ether side chain of the parent compound [66]. TP238 and TP240 formation was reported not only from the parent compound MTP but also from its main human metabolite MTPA [17]. In this last study, TP238 and TP240 were mainly transformed from MTPA fungal biodegradation into TP254, through the oxidation of the primary alcohol and the aldehyde intermediate onto a carboxylic acid, and detected at high concentration [17]. In the case of CAS, MTP biodegradation resulted in the generation of MTPA, which was the major generated intermediate, and in some cases classified as persistent [44,51]. α-HMTP was both reported as human metabolite, generated after pharmaceutical consumption, and TP in biological treatments [44,51]. α-HMTP is usually persistent, it was detected in influent WWTPs (at 36 ng/L), and consequently it may be classified of important concern [17,44]. Further oxidation of α-HMTP to TP282A was reported at much lower concentration. Alternatively, the binding of the hydroxyl radical in the MTP aromatic ring may lead to the formation of TP284, which is further oxidized to TP300 and TP316 [66]. These TPs were especially relevant in treatments with plausible generation of hydroxyl radicals (e.g. fungi and AOPs, [17,66,67]). It is important to mention that TP284, TP300 and TP316 were generated only from MTP degradation and not from its main metabolite MTPA [17,66,67]. Finally, another worth mentioning intermediate is TP134, generated from the O-dealkylation of the TPs maintaining the secondary amine on their chemical structure. TP134 is a residual TP and it may be considered as an indicator of the removal extent of the generated TPs [17,24].

All detected TPs were classified based on the number of transformations undertaken from the parent compound MTP (1st, 2nd or ≥ 3rd generation of TPs). Only those TPs with relative distributions ≥ 1% were further considered for discussion. Detailed information of TPs distribution percentages is presented in Table S5–S12.

3.2. Combined treatments of fortified pure water

3.2.1. AOP + FG/FG + AOP treatments of fortified pure water

Overall results obtained from the combined experiments in fortified pure water for AOP + FG and FG + AOP treatments are presented in Fig. 3a and Fig. 4a. The combination strategy where biological FG treatment was placed after AOP treatment (AOP + FG) was very effective for the elimination of the parent compounds (Fig. 3a). Almost complete elimination (99.9%) of MTP and MTPA was achieved, although most of the elimination was obtained by AOP alone as a first step (99.6%). In terms of relative presence of all intermediates generated, low values were observed, with a percentage of 0.8% and 0.6% accounted after AOP and AOP + FG, respectively. These results demonstrate the high capability of AOP treatment to achieve high MTP and MTPA removal and almost extended TP removal in pure water matrix. In fact, a high relative distribution percentage of the ≥ 3rd generation TPs (Fig. 4a) was observed after both AOP + FG experiment (80.8%) and AOP single treatment (77.4%). Among them, the most abundant intermediates (TP150, TP134 and TP116) can be classified as residual chemical structures, near to total compound removal (Fig. 2). TP150 was previously classified as a mutagenic compound and TP116 as a persistent compound using *in silico* estimations (due to the aliphatic secondary amines in molecular structure), both likely to increase the hazards on treated water [24]. However, no acute toxicity values were observed using *in vitro* experiments after the treatment(s), probably due to their low TP presence in treated effluents (Fig. 3a).

The combination FG + AOP was much less effective than AOP + FG for MTP removal (from 20.4% with FG alone up to 36.4% with FG + AOP, Fig. 3a) whereas MTPA was completely removed after FG treatment alone. In terms of relative presence of TPs, the percentage value after FG treatment (24.6%) was very similar to the values obtained after FG + AOP (27.6%). Altogether, these values were much higher than in AOP + FG combination (Fig. 3a). Moreover, there were less ≥ 3rd generation intermediates (36.7%) and more 1st and 2nd generation TPs (21.9% and 41.4%, respectively, Fig. 4a). The overall low efficiency of AOP treatment in the configuration FG + AOP might be attributed to the polysaccharide mucus secreted by fungi during fungal treatment, which can affect AOP oxidation afterwards. Considering the generated intermediates, the high contribution of TP240 (41.6%) and its oxidized compound TP254 (23.0%) in FG experiments was previously reported in *Trametes Versicolor* [17]: TP240 was mostly generated from MTPA biotransformation while α-HMTP from MTP only [17]. The slight toxicity measured using *in vitro* experiments, from the initial time (0.0 TU) to FG treated effluents (3.2 TU) and after FG + AOP experiments (4.3 TU), might be explained by the presence of O-DMTP after FG treatment alone (2.8%) and after FG + AOP experiments (3.5%). Actually, O-DMTP was previously described to be 3.6 times more toxic than the parent compound MTP in *vibrio fischeri* bioassays [44]. However, the generation of unknown toxic metabolites from fungi (non-related to MTP and MTPA degradation) cannot be discarded.

3.2.2. AOP + CAS/CAS + AOP treatments of fortified pure water

Overall results obtained from AOP + CAS and CAS + AOP combined experiments in fortified pure water are presented in Fig. 3b and Fig. 4b. AOP + CAS allowed complete elimination of MTP and MTPA (Fig. 3b). In comparison to AOP + FG treatment, this combination slightly reduced the proportion of intermediates in treated effluents from 0.8% after AOP to 0.4% after AOP + CAS treatment. In terms of relative distribution of generated intermediates (Fig. 4b), 2nd generation of TPs increased from 19.0% after AOP to 31.6% after AOP + CAS (15.7% more than in AOP + FG), suggesting the generation of some MTP persistent intermediates after CAS treatment. Indeed, relative MTPA contribution increased 7.1% moving from AOP to AOP + CAS. This is in agreement with some authors indicating the recalcitrant presence of MTPA after CAS experiments along with its generation during MTP degradation, up to 40% of initial MTP concentration (1 mg/L) after 48 h [44,51]. It is important to highlight that the presence of intermediates after AOP + CAS treating fortified pure water treatment was small (0.4%) compared with the spiked parent compounds at 2.5 mg/L, highlights the effectiveness of AOP + CAS combination. Although almost a complete removal of MTP and MTPA and TPs was already achieved by only AOP treatment, CAS as a post-treatment step additionally provided an extended transformation of TP150 into TP116 through the intermediate TP134 (Fig. 2, Fig. 4b), as

also observed after AOP + FG combination (Fig. 4a). As in AOP + FG, no toxic effects were observed after *in vitro* experiments in AOP + CAS effluents.

Considering the last coupling CAS + AOP, MTP and MTPA removal efficiency was high (97.8% and 97.7%, respectively) but not complete (Fig. 3b). In terms of TP presence, the relative amount after CAS + AOP treatment (24.3%) was similar to that after FG + AOP treatment (27.6%), though very different TP distribution was observed (Fig. 4b): the presence of intermediates from ≥ 3rd generation after CAS + AOP treatment was higher (79.2%) than after FG + AOP (36.7%). Those differences between FG + AOP and CAS + AOP might be related to the minor complexity of the matrix after CAS (no mucus generated like it is with FG), allowing a better performance of CAS + AOP. It is also important to highlight how the presence of MTPA even increased after CAS alone, reaching a relative percentage values of 114.4%. MTPA has been described as a major 2nd generation TP in CAS treatment in previous studies [44,51]. However, MTPA was easily removed when coupling CAS + AOP. In addition, no toxic effects were observed after CAS + AOP experiments using the *in vitro* bioassays.

Therefore, UV/H_2O_2 can be considered as the treatment of choice when treating simple matrices, such as fortified pure water. Nevertheless, the implementation of an additional CAS treatment (both before or after AOP treatment) allowed similar extent of pollutant elimination (MTP, MTPA and TPs) without adding any toxic effect in

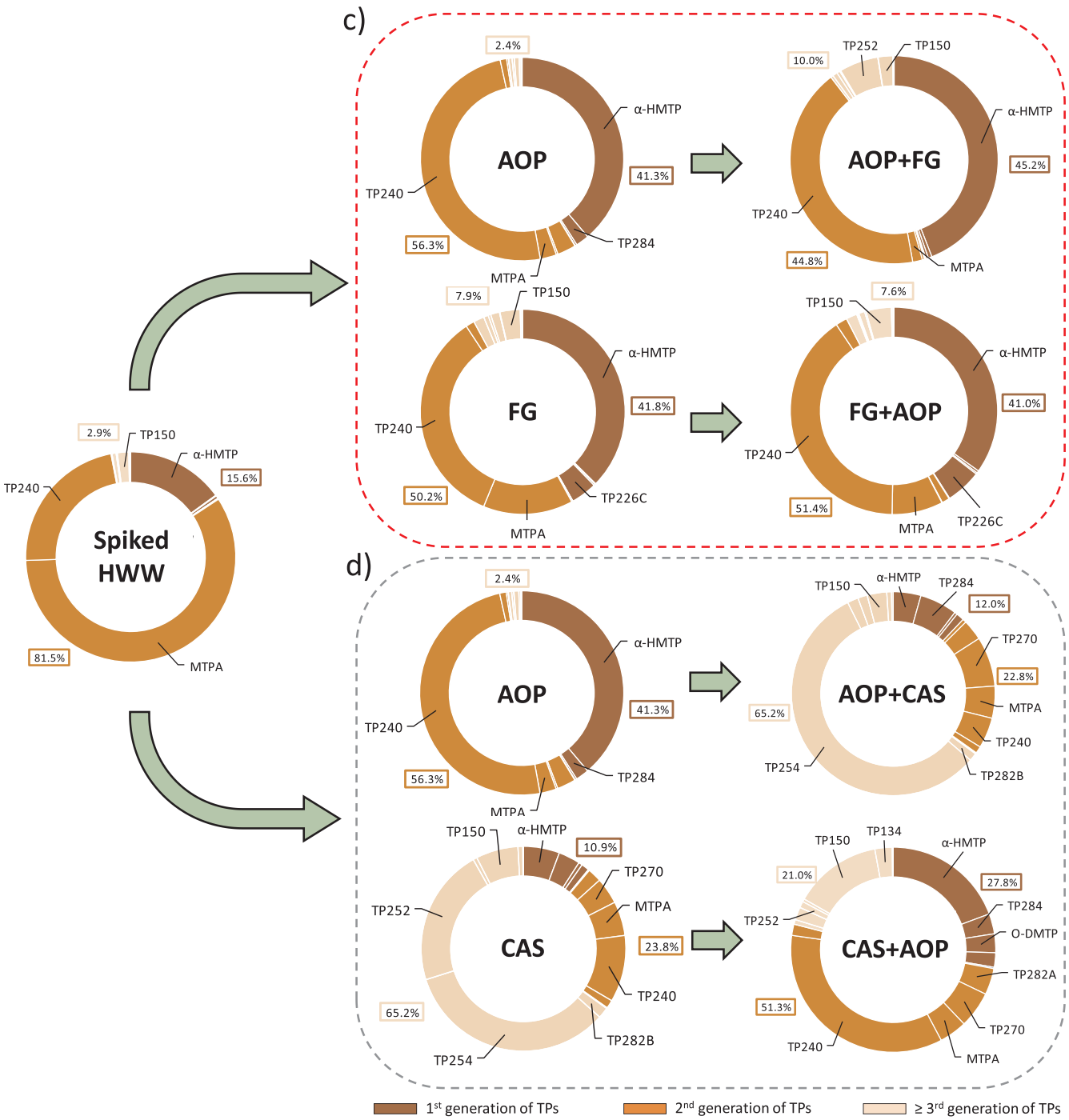

Fig. 5. The circles represent the relative distribution of intermediates in fortified HWW (Eq. (3)), classified regarding their degree on removal (1st, 2nd and ≥ 3rd generation expressed in percentage values, according to Fig. 2) in: c) UV/H_2O_2 combined with FG treatment; d) UV/H_2O_2 combined with CAS treatment.

treated effluents. However, an increase in the *in vitro* toxicity was measured along the FG + AOP experiments due to the tentatively presence of the O-DMTP intermediate. Moreover, the generation of unknown toxic metabolites from fungi (non-related to MTP and MTPA degradation) cannot be discarded.

3.3. Combined treatments of fortified hospital wastewater

The same experimental set-up performed with fortified pure water (Fig. 1) was applied to a real-case scenario to treat real HWW fortified with 2.0 μg/L of MTP and MTPA. Their removal as well as the relative distribution of the generated TPs are presented in Fig. 3c, 3d and Fig. 5. Since these experiments were performed with real HWW, 26.4% TPs were already detected without applying any treatment (α-HMTP and TP240, mainly). Other related pharmaceuticals such as atenolol, present in HWW at an initial concentration of 0.5 μg/L, may also have transformed into MTPA (also named atenolol acid) and generate some of these intermediates after degradation [44,51]. As previously reported, it is important to mention that MTP and MTPA removal efficiency can be altered by many other factors including the presence of organic matter, bacteria and pollutant concentration among others [17,24,44]. Finally, since many more unknown chemicals (different from MTP and MTPA) may contribute to the overall toxicity on treated effluent, *in vitro* measurements were not performed.

3.3.1. AOP + FG/FG + AOP treatments of fortified HWW

Overall results obtained from single and combined treatment experiments in fortified HWW for AOP + FG and FG + AOP are presented in Fig. 3c and Fig. 5c. High removal of MTP and MTPA were observed after AOP alone (67.8% and 82.8%, respectively) though still less effective than in fortified pure water (with removals higher than 99.6% for both MTP and MTPA), due most likely to the matrix complexity. While MTP increased its removal to 88.9% after AOP + FG, this combination did not increase MTPA removal (81.2%). The relative presence of intermediates was higher after AOP (63.2%) than after AOP + FG (40.6%). In comparison with fortified pure water AOP + FG experiments, the contribution of ≥ 3rd generation TPs was lower (10.0%, Fig. 5c) compared with 80.8% observed in pure water (Fig. 4a). These values indicate the low degradation extent of TPs. Among the intermediates detected, TP240 (2nd generation) and α-HMTP (1st generation) were classified as the most persistent compounds, as it was also observed in previous fungal treatment of MTP and MTPA with *Ganoderma lucidum* [17]. These recalcitrant intermediates should be considered of important concern since they were found at a relative distribution of 42.5% and 44.1%, respectively (Fig. 5c). Therefore, further improvements and/or adjustments of the technologies included in this combination may be required to avoid the discharge of these compounds into the environment.

The opposite treatment combination FG + AOP was much less effective for MTP removal (36.1%) than AOP + FG (88.9%). The elimination of MTPA was only slightly lower (80.6%) compared to AOP + FG (81.2%), (Fig. 3c). Moreover, MTPA removal after FG + AOP increased only 10.7% compared to FG alone (69.9%) while no substantial changes were observed on MTP elimination. A similar pattern was observed in terms of relative presence of all generated intermediates (38.2% after FG and 36.2% after FG + AOP). These results demonstrate that FG + AOP was less effective than AOP + FG treating complex matrices. As in AOP + FG treatment, TP240 and α-HMTP were also classified as the most recalcitrant TPs after FG experiments, unable to be eliminated with this combined treatment configuration (Fig. 5c). Altogether, it can be suggested that FG + AOP did not provide any additional advantage compared with AOP + FG.

3.3.2. AOP + CAS/CAS + AOP treatments of fortified HWW

Overall results obtained from the combined experiments in fortified HWW for AOP + CAS and CAS + AOP are presented in Fig. 3d and Fig. 5d. AOP + CAS combination was quite effective in terms of removal of MTP (85.6%) and MTPA (99.5%), as shown in Fig. 3d. The relative percentage of TPs decreased dramatically from 63.2% after AOP treatment to 15.4% after AOP + CAS, much lower than in AOP + FG (40.6%). Moreover, the distribution of ≥ 3rd generation TPs after AOP + CAS treatment increased considerably up to 65.2% compared to those present after AOP alone (2.4%), Fig. 5d. The recalcitrant TP240 and α-HMTP generated after AOP were successfully reduced after CAS post-treatment with the generation of the ≥ 3rd generation intermediate TP254.

In CAS + AOP similar values were obtained in terms of removal of MTP (85.7%) and MTPA (98.5%). In contrast to FG + AOP, this combination lead to a decrease in the relative TP presence: from 13.8% after CAS pre-treatment to 11.0% after CAS + AOP. However, even though TPs presence was slightly lower, their distribution was very different, compared to AOP + CAS: ≥ 3rd generation TPs decreased drastically from CAS (65.2%) to CAS + AOP (21.0%) while 1st and 2nd generation TPs increased up to 27.8% and 51.3%, respectively (Fig. 5d). This was attributed to the formation of the characteristic persistent compounds TP240 and α-HMTP after AOP post-treatment. Otherwise, these persistent compounds were easily eliminated, or not generated extensively, by applying CAS as a post-treatment in AOP + CAS combination (Fig. 5d). This fact confirms that the generation and the elimination of intermediates were dependent also on the chosen sequence of applied treatments. Additionally, and in contrast with CAS treatment of fortified pure water, high reduction of MTPA (93.9%), without any further generation, was observed in CAS treating HWW (Fig. 3d). This can be related to the different matrix conditions, affecting MTP and MTPA degradation pathways. Finally, it is important to remark that the presence of the identified toxic intermediate O-DMTP was observed at a very low concentration < 1%. These results confirm that the elimination of the intermediates generated is directly dependent on the chosen sequence of applied treatments.

3.4. Evaluation of combined treatments and statistical analysis

Different combined treatment strategies were compared in the present study to achieve not only the highest elimination of the parent compounds but also of the generated intermediates. Additionally, the toxicity was evaluated along pure water experiments using *in vitro* measurements.

The experiments performed in fortified pure water demonstrated that the AOP treatment was the most effective treatment, out of the three single treatments tested (AOP, FG and CAS). AOP allowed the complete removal of MTP, MTPA and their intermediates without a toxicity increase. In CAS experiments, MTP was mainly transformed into the recalcitrant metabolite MTPA up to 114.4% whereas MTP was only removed 20.4% in FG experiments. In the latest case, acute toxicity increased from 0.0 TU up to 3.2 TU. The application of an AOP post-treatment was justified in both cases (FG and CAS) in order to reduce the presence of the parent compounds, the intermediates generated and the observed acute toxicity. The CAS + AOP combination, allowed the elimination of the recalcitrant metabolite MTPA up to almost 100% with no toxicity measured in effluents. Spearman correlation (Fig. S2) between AOP + CAS and CAS + AOP combinations, in terms of TP distribution, was classified as moderate (r_s = 0.47). On the other hand, MTP was only eliminated up to 36.4% after FG + AOP and increased *in vitro* toxicity due to the presence of the metabolite O-DMTP up to 4.3 TU. Spearman correlation (Fig. S2) between AOP + FG and FG + AOP combinations, in terms of TP distribution, was classified as non-significant ($p > 0.05$) but similar to CAS + AOP (r_s = 0.65 and 0.52, respectively). In this context, FG + AOP was considered as the least effective combination in terms of removal of MTP, MTPA and generated intermediates in pure water.

The experiments performed with fortified HWW showed that the complete removal of the parent compounds (MTP and MTPA) and their

TPs was not fully accomplished by any of the evaluated single treatments studied. The combined treatments based on CAS and UV/H_2O_2 showed the best efficiency in terms of complete removal. The highest removal degree of target contaminants was observed in AOP + CAS with the largest contribution of ≥ 3rd generation TPs. In CAS + AOP combination, the recalcitrant intermediates α-HMTP and TP240 were generated after the AOP post-treatment from MTP and MTPA removal. These two combinations showed a moderate correlation (r_s = 0.53) among them in terms of TP distribution (Fig. S3). However, non-significant correlation (p > 0.05) was found between the best treatment AOP + CAS and the less efficient combinations AOP + FG and FG + AOP. On the other hand, treated effluents from AOP + FG and FG + AOP showed a strong correlation among them (r_s = 0.68), but quite similar to the combination CAS + AOP (r_s = 0.61 and r_s = 0.62, respectively). As a conclusion, AOP + CAS was significantly the most successful combined treatment in comparison with the other tested combinations. Despite this, a detailed evaluation of the combined technologies would be required (in terms of operating conditions of each of the technologies involved) before scale-up and full-scale application [12,55].

4. Conclusions

A comprehensive overview of MTP and MTPA degradation and transformation was performed in experiments where fortified pure water and real HWW was treated with UV/H_2O_2 combined with FG or CAS biological processes. Major transformation pathways were suggested regarding the transformation of the parent compounds through bio-transformation and photo-transformation mechanisms. This comprehensive study allowed to characterize MTP and MTPA removal/transformation and to identify the most persistent and toxic intermediates. While AOP single treatment was enough to achieve almost total compound removal in spiked pure water experiments, combined treatments were required for hospital wastewater: among the studied combinations, AOP + CAS attained the highest removal rates not only for MTP but also for its recalcitrant metabolite MTPA and the generated intermediates. This study demonstrates that combined treatments may represent a solution when applied to complex wastewater matrices for the extended elimination of the TPs generated. On the other hand, this study demonstrates that target analysis of parent compounds along the water treatment does not provide enough information about the treatment performance. Comprehensive studies of the generated TPs combined with toxicity estimation are highly recommended.

Declaration of Competing Interest

The authors declare that they have no known competing financial interests or personal relationships that could have appeared to influence the work reported in this paper.

Acknowledgements

This work has been funded by the Spanish State Research Agency of the Spanish Ministry of Science, Innovation and Universities and European Fund for Regional Development (CTM 2013-48545-C2-1-R and CTM 2017-85385-C2-1-R). Authors thank Generalitat de Catalunya through Consolidated Research Group (2017-SGR-14, 2017-SGR-1404, ICRA-ENV 2017-SGR-1124, 2017-SGR-1318 and 2017-SGR-1016). ICRA researchers thank funding from CERCA program. S.R.M. and R.G.O. acknowledge the “Redes de Excelencia 2015” program (CTM 2015-71054-REDT). S.R.M. and G.B. acknowledge the Ramon y Cajal research fellowships (RYC-2014-16707 and RYC-2014-16754) from the Spanish State Research Agency of the Spanish Ministry of Science, Innovation and Universities (AEI-MCIU). A.J.G thanks the predoctoral grant from the Agency for Management of University and Research Grants (AGAUR) (2019FI_B2_00202) co-financed by the European Social Fund. R.G.O. thanks to “Obra Social La Caixa” for receiving funding to carry out this research through the Intensification Research Fellowship 2017-URL-IR2Q-023. We would like to thank Sant Joan de Déu Hospital staff for their collaboration during the sampling campaign. We also thank to Thermo Scientific and Marie-Pierre Pavageau for the technical support using Compound Discoverer 3.0 software. This study was supported by the Spanish Ministry of Science and Innovation (IDAEA Excelencia Severo Ochoa CEX2018-000794-S).

Appendix A. Supplementary data

Supplementary data to this article can be found online at https://doi.org/10.1016/j.cej.2020.126482.

References

[1] P. Verlicchi, M. Al Aukidy, E. Zambello, Occurrence of pharmaceutical compounds in urban wastewater: Removal, mass load and environmental risk after a secondary treatment-A review, Sci. Total Environ. 429 (2012) 123–155, https://doi.org/10.1016/j.scitotenv.2012.04.028.
[2] P. Verlicchi, A. Galletti, M. Petrovic, D. Barceló, Hospital effluents as a source of emerging pollutants: An overview of micropollutants and sustainable treatment options, J. Hydrol. 389 (2010) 416–428, https://doi.org/10.1016/j.jhydrol.2010.06.005.
[3] P. Verlicchi, M. Al Aukidy, E. Zambello, What have we learned from worldwide experiences on the management and treatment of hospital effluent? - An overview and a discussion on perspectives, Sci. Total Environ. 514 (2015) 467–491, https://doi.org/10.1016/j.scitotenv.2015.02.020.
[4] L.H.M.L.M. Santos, M. Gros, S. Rodriguez-Mozaz, C. Delerue-Matos, A. Pena, D. Barceló, M.C.B.S.M. Montenegro, Contribution of hospital effluents to the load of pharmaceuticals in urban wastewaters: Identification of ecologically relevant pharmaceuticals, Sci. Total Environ. 461–462 (2013) 302–316, https://doi.org/10.1016/j.scitotenv.2013.04.077.
[5] S. Rodriguez-Mozaz, D. Lucas, D. Barceló, Full-scale plants for dedicated treatment of hospital effluents, in: Handb. Environ. Chem., Springer, Berlin, Heidelberg, 2017: pp. 189–208. doi:10.1007/698_2017_13.
[6] N. Ratola, A. Cincinelli, A. Alves, A. Katsoyiannis, Occurrence of organic microcontaminants in the wastewater treatment process. A mini review, J. Hazard. Mater. 239–240 (2012) 1–18, https://doi.org/10.1016/j.jhazmat.2012.05.040.
[7] B. Pauwels, W. Verstraete, The treatment of hospital wastewater: An appraisal, J. Water Health. 4 (2006) 405–416, https://doi.org/10.2166/wh.2006.025.
[8] E. Carraro, S. Bonetta, C. Bertino, E. Lorenzi, S. Bonetta, G. Gilli, Hospital effluents management: Chemical, physical, microbiological risks and legislation in different countries, J. Environ. Manage. 168 (2016) 185–199, https://doi.org/10.1016/j.jenvman.2015.11.021.
[9] L. Ferrando-Climent, C. Cruz-Morató, E. Marco-Urrea, T. Vicent, M. Sarrà, S. Rodriguez-Mozaz, D. Barceló, Non conventional biological treatment based on *Trametes versicolor* for the elimination of recalcitrant anticancer drugs in hospital wastewater, Chemosphere. 136 (2015) 9–19, https://doi.org/10.1016/j.chemosphere.2015.03.051.
[10] J.A. Mir-Tutusaus, E. Parladé, M. Villagrasa, D. Barceló, S. Rodríguez-Mozaz, M. Martínez-Alonso, N. Gaju, M. Sarrà, G. Caminal, Long-term continuous treatment of non-sterile real hospital wastewater by *Trametes versicolor*, J. Biol. Eng. 13 (2019) 1–13, https://doi.org/10.1186/s13036-019-0179-y.
[11] C.E. Rodríguez-Rodríguez, M. Jesús García-Galán, P. Blánquez, M.S. Díaz-Cruz, D. Barceló, G. Caminal, T. Vicent, Continuous degradation of a mixture of sulfonamides by *Trametes versicolor* and identification of metabolites from sulfapyridine and sulfathiazole, J. Hazard. Mater. 213–214 (2012) 347–354, https://doi.org/10.1016/j.jhazmat.2012.02.008.
[12] J.A. Mir-Tutusaus, R. Baccar, G. Caminal, M. Sarrà, Can white-rot fungi be a real wastewater treatment alternative for organic micropollutants removal? A review, Water Res. 138 (2018) 137–151, https://doi.org/10.1016/j.watres.2018.02.056.
[13] I. Oller, S. Malato, J.A. Sánchez-Pérez, Combination of Advanced Oxidation Processes and biological treatments for wastewater decontamination-A review, Sci. Total Environ. 409 (2011) 4141–4166, https://doi.org/10.1016/j.scitotenv.2010.08.061.
[14] M.B. Asif, F.I. Hai, L. Singh, W.E. Price, L.D. Nghiem, Degradation of Pharmaceuticals and Personal Care Products by White-Rot Fungi—a Critical Review, Curr. Pollut. Reports. 3 (2017) 88–103, https://doi.org/10.1007/s40726-017-0049-5.
[15] M. Asgher, H.N. Bhatti, M. Ashraf, R.L. Legge, Recent developments in biodegradation of industrial pollutants by white rot fungi and their enzyme system, Biodegradation. 19 (2008) 771–783, https://doi.org/10.1007/s10532-008-9185-3.
[16] A.I. Rodarte-Morales, G. Feijoo, M.T. Moreira, J.M. Lema, Degradation of selected pharmaceutical and personal care products (PPCPs) by white-rot fungi, World J. Microbiol. Biotechnol. 27 (2011) 1839–1846, https://doi.org/10.1007/s11274-010-0642-x.
[17] A. Jaén-Gil, F. Castellet-Rovira, M. Llorca, M. Villagrasa, M. Sarrà, S. Rodríguez-Mozaz, D. Barceló, Fungal treatment of metoprolol and its recalcitrant metabolite

metoprolol acid in hospital wastewater: Biotransformation, sorption and ecotoxicological impact, Water Res. 152 (2019) 171–180, https://doi.org/10.1016/j.watres.2018.12.054.
[18] A.C. Vincenzo Naddeo, Wastewater Treatment by Combination of Advanced Oxidation Processes and Conventional Biological Systems, J. Bioremediation Biodegrad. 04 (2013), https://doi.org/10.4172/2155-6199.1000208.
[19] F. Martínez, R. Molina, I. Rodríguez, M.I. Pariente, Y. Segura, J.A. Melero, Techno-economical assessment of coupling Fenton/biological processes for the treatment of a pharmaceutical wastewater, J. Environ. Chem. Eng. 6 (2018) 485–494, https://doi.org/10.1016/j.jece.2017.12.008.
[20] D. Mantzavinos, E. Psillakis, Enhancement of biodegradability of industrial wastewaters by chemical oxidation pre-treatment, J. Chem. Technol. Biotechnol. 79 (2004) 431–454, https://doi.org/10.1002/jctb.1020.
[21] A. Della-Flora, M.L. Wilde, I.D.F. Pinto, É.C. Lima, C. Sirtori, Degradation of the anticancer drug flutamide by solar photo-Fenton treatment at near-neutral pH: Identification of transformation products and in silico (Q)SAR risk assessment, Environ. Res. 183 (2020) 109223, , https://doi.org/10.1016/j.envres.2020.109223.
[22] D. Fatta-Kassinos, M.I. Vasquez, K. Kümmerer, Transformation products of pharmaceuticals in surface waters and wastewater formed during photolysis and advanced oxidation processes - Degradation, elucidation of byproducts and assessment of their biological potency, Chemosphere. 85 (2011) 693–709, https://doi.org/10.1016/j.chemosphere.2011.06.082.
[23] R. Salgado, V.J. Pereira, G. Carvalho, R. Soeiro, V. Gaffney, C. Almeida, V.V. Cardoso, E. Ferreira, M.J. Benoliel, T.A. Ternes, A. Oehmen, M.A.M. Reis, J.P. Noronha, Photodegradation kinetics and transformation products of ketoprofen, diclofenac and atenolol in pure water and treated wastewater, J. Hazard. Mater. 244–245 (2013) 516–527, https://doi.org/10.1016/j.jhazmat.2012.10.039.
[24] A. Jaén-Gil, G. Buttiglieri, A. Benito, R. Gonzalez-Olmos, D. Barceló, S. Rodríguez-Mozaz, Metoprolol and metoprolol acid degradation in UV/H_2O_2 treated wastewaters: An integrated screening approach for the identification of hazardous transformation products, J. Hazard. Mater. (2019) 120851, , https://doi.org/10.1016/j.jhazmat.2019.120851.
[25] D. Mantzavinos, N. Kalogerakis, Treatment of olive mill effluents: Part I. Organic matter degradation by chemical and biological processes - An overview, Environ. Int. 31 (2005) 289–295, https://doi.org/10.1016/j.envint.2004.10.005.
[26] D. Cassano, A. Zapata, G. Brunetti, G. Del Moro, C. Di Iaconi, I. Oller, S. Malato, G. Mascolo, Comparison of several combined/integrated biological-AOPs setups for the treatment of municipal landfill leachate: Minimization of operating costs and effluent toxicity, Chem. Eng. J. 172 (2011) 250–257, https://doi.org/10.1016/j.cej.2011.05.098.
[27] L. Prieto-Rodríguez, I. Oller, N. Klamerth, A. Agüera, E.M. Rodríguez, S. Malato, Application of solar AOPs and ozonation for elimination of micropollutants in municipal wastewater treatment plant effluents, Water Res. 47 (2013) 1521–1528, https://doi.org/10.1016/j.watres.2012.11.002.
[28] A. Monteoliva-García, J. Martín-Pascual, M.M. Muñío, J.M. Poyatos, Removal of carbamazepine, ciprofloxacin and ibuprofen in real urban wastewater by using light-driven advanced oxidation processes, Int. J. Environ. Sci. Technol. (2019), https://doi.org/10.1007/s13762-019-02365-9.
[29] A. Jaén-Gil, A. Hom-Diaz, M. Llorca, T. Vicent, P. Blánquez, D. Barceló, S. Rodríguez-Mozaz, An automated on-line turbulent flow liquid-chromatography technology coupled to a high resolution mass spectrometer LTQ-Orbitrap for suspect screening of antibiotic transformation products during microalgae wastewater treatment, J. Chromatogr. A. 1568 (2018) 57–68, https://doi.org/10.1016/j.chroma.2018.06.027.
[30] C. Sirtori, A. Zapata, I. Oller, W. Gernjak, A. Agüera, S. Malato, Decontamination industrial pharmaceutical wastewater by combining solar photo-Fenton and biological treatment, Water Res. 43 (2009) 661–668, https://doi.org/10.1016/j.watres.2008.11.013.
[31] M.M. Ballesteros Martín, J.A. Sánchez Pérez, F.G. Acién Fernández, J.L. Casas López, A.M. García-Ripoll, A. Arques, I. Oller, S. Malato Rodríguez, Combined photo-Fenton and biological oxidation for pesticide degradation: Effect of photo-treated intermediates on biodegradation kinetics, Chemosphere. 70 (2008) 1476–1483, https://doi.org/10.1016/j.chemosphere.2007.08.027.
[32] I. Oller, S. Malato, J.A. Sánchez-Pérez, M.I. Maldonado, R. Gassó, Detoxification of wastewater containing five common pesticides by solar AOPs-biological coupled system, Catal. Today. 129 (2007) 69–78, https://doi.org/10.1016/j.cattod.2007.06.055.
[33] M. Jiménez-Tototzintle, I. Oller, A. Hernández-Ramírez, S. Malato, M.I. Maldonado, Remediation of agro-food industry effluents by biotreatment combined with supported TiO_2/H_2O_2 solar photocatalysis, Chem. Eng. J. 273 (2015) 205–213, https://doi.org/10.1016/j.cej.2015.03.060.
[34] L. Qi, X. Wang, Q. Xu, Coupling of biological methods with membrane filtration using ozone as pre-treatment for water reuse, Desalination. 270 (2011) 264–268, https://doi.org/10.1016/j.desal.2010.11.054.
[35] Y. Ouarda, B. Tiwari, A. Azaïs, M.A. Vaudreuil, S.D. Ndiaye, P. Drogui, R.D. Tyagi, S. Sauvé, M. Desrosiers, G. Buelna, R. Dubé, Synthetic hospital wastewater treatment by coupling submerged membrane bioreactor and electrochemical advanced oxidation process: Kinetic study and toxicity assessment, Chemosphere. 193 (2018) 160–169, https://doi.org/10.1016/j.chemosphere.2017.11.010.
[36] O. Ganzenko, D. Huguenot, E.D. van Hullebusch, G. Esposito, M.A. Oturan, Electrochemical advanced oxidation and biological processes for wastewater treatment: A review of the combined approaches, Environ. Sci. Pollut. Res. 21 (2014) 8493–8524, https://doi.org/10.1007/s11356-014-2770-6.
[37] S.R. Hughes, P. Kay, L.E. Brown, Global synthesis and critical evaluation of pharmaceutical data sets collected from river systems, Environ. Sci. Technol. 47 (2013) 661–677, https://doi.org/10.1021/es3030148.
[38] A. Villegas-Navarro, E. Rosas-L, J.L. Reyes, The heart of Daphnia magna: Effects of four cardioactive drugs, Comp. Biochem. Physiol. - C Toxicol. Pharmacol. 136 (2003) 127–134, https://doi.org/10.1016/S1532-0456(03)00172-8.
[39] E.J. van den Brandhof, M. Montforts, Fish embryo toxicity of carbamazepine, diclofenac and metoprolol, Ecotoxicol. Environ. Saf. 73 (2010) 1862–1866, https://doi.org/10.1016/j.ecoenv.2010.08.031.
[40] Z. Dong, D.B. Senn, R.E. Moran, J.P. Shine, Prioritizing environmental risk of prescription pharmaceuticals, Regul. Toxicol. Pharmacol. 65 (2013) 60–67, https://doi.org/10.1016/j.yrtph.2012.07.003.
[41] M. Maurer, B.I. Escher, P. Richle, C. Schaffner, A.C. Alder, Elimination of β-blockers in sewage treatment plants, Water Res. 41 (2007) 1614–1622, https://doi.org/10.1016/j.watres.2007.01.004.
[42] M. Scheurer, M. Ramil, C.D. Metcalfe, S. Groh, T.A. Ternes, The challenge of analyzing beta-blocker drugs in sludge and wastewater, Anal. Bioanal. Chem. 396 (2010) 845–856, https://doi.org/10.1007/s00216-009-3225-7.
[43] C. Lacey, S. Basha, A. Morrissey, J.M. Tobin, Occurrence of pharmaceutical compounds in wastewater process streams in Dublin, Ireland, Environ. Monit. Assess. 184 (2012) 1049–1062, https://doi.org/10.1007/s10661-011-2020-z.
[44] A. Rubirola, M. Llorca, S. Rodriguez-Mozaz, N. Casas, I. Rodriguez-Roda, D. Barceló, G. Buttiglieri, Characterization of metoprolol biodegradation and its transformation products generated in activated sludge batch experiments and in full scale WWTPs, Water Res. 63 (2014) 21–32, https://doi.org/10.1016/j.watres.2014.05.031.
[45] B.I. Escher, K. Fenner, Recent Advances in Environmental Risk Assessment of Transformation Products, Environ. Sci. Technol. 45 (2011) 3835–3847, https://doi.org/10.1021/es1030799.
[46] S. Kern, R. Baumgartner, D.E. Helbling, J. Hollender, H. Singer, M.J. Loos, R.P. Schwarzenbach, K. Fenner, A tiered procedure for assessing the formation of biotransformation products of pharmaceuticals and biocides during activated sludge treatment, J. Environ. Monit. 12 (2010) 2100, https://doi.org/10.1039/c0em00238k.
[47] J. Godbillon, M. Duval, Determination of two metoprolol metabolites in human urine by high-performance liquid chromatography, J. Chromatogr., B Biomed. Sci. Appl. 309 (1984) 198–202.
[48] C. Wharf, U. Kingdom, Questions and answers on ' Guideline on the environmental risk assessment of medicinal products for human use ', 2010 (2010) 1–9.
[49] European Comission, REGULATION (EU) 2020/741 OF THE EUROPEAN PARLIAMENT AND OF THE COUNCIL of 25 May 2020 on minimum requirements for water reuse, 2019 (2020) 32–55.
[50] L.F. Angeles, R.A. Mullen, I.J. Huang, C. Wilson, W. Khunjar, H.I. Sirotkin, A.E. McElroy, D.S. Aga, Assessing pharmaceutical removal and reduction in toxicity provided by advanced wastewater treatment systems, Environ. Sci. Water Res. Technol. 6 (2020) 62–77, https://doi.org/10.1039/c9ew00559e.
[51] J. Radjenović, S. Pérez, M. Petrović, D. Barceló, Identification and structural characterization of biodegradation products of atenolol and glibenclamide by liquid chromatography coupled to hybrid quadrupole time-of-flight and quadrupole ion trap mass spectrometry, J. Chromatogr. A. 1210 (2008) 142–153, https://doi.org/10.1016/j.chroma.2008.09.060.
[52] N. Collado, G. Buttiglieri, E. Marti, L. Ferrando-Climent, S. Rodriguez-Mozaz, D. Barceló, J. Comas, I. Rodriguez-Roda, Effects on activated sludge bacterial community exposed to sulfamethoxazole, Chemosphere. 93 (2013) 99–106, https://doi.org/10.1016/j.chemosphere.2013.04.094.
[53] A. Benito, A. Penadés, J.L. Lliberia, R. Gonzalez-Olmos, Degradation pathways of aniline in aqueous solutions during electro-oxidation with BDD electrodes and UV/H_2O_2 treatment, Chemosphere. 166 (2017) 230–237, https://doi.org/10.1016/j.chemosphere.2016.09.105.
[54] P. Blánquez, M. Sarrà, M.T. Vicent, Study of the cellular retention time and the partial biomass renovation in a fungal decolourisation continuous process, Water Res. 40 (2006) 1650–1656, https://doi.org/10.1016/j.watres.2006.02.010.
[55] E. Borràs, P. Blánquez, M. Sarrà, G. Caminal, T. Vicent, Trametes versicolor pellets production: Low-cost medium and scale-up, Biochem. Eng. J. 42 (2008) 61–66, https://doi.org/10.1016/j.bej.2008.05.014.
[56] C.G. Hatchard, C.A. Parker, A New Sensitive Chemical Actinometer. II. Potassium Ferrioxalate as a Standard Chemical Actinometer, Proc. R. Soc. A Math. Phys. Eng. Sci. (1956) 518–536, https://doi.org/10.1098/rspa.1956.0102.
[57] A. Shahbazi, R. Gonzalez-Olmos, F.D. Kopinke, P. Zarabadi-Poor, A. Georgi, Natural and synthetic zeolites in adsorption/oxidation processes to remove surfactant molecules from water, Sep. Purif. Technol. 127 (2014) 1–9, https://doi.org/10.1016/j.seppur.2014.02.021.
[58] J.A. Mir-Tutusaus, M. Sarrà, G. Caminal, Continuous treatment of non-sterile hospital wastewater by *Trametes versicolor*: How to increase fungal viability by means of operational strategies and pretreatments, J. Hazard. Mater. 318 (2016) 561–570, https://doi.org/10.1016/j.jhazmat.2016.07.036.
[59] M. Gros, S. Rodríguez-Mozaz, D. Barceló, Fast and comprehensive multi-residue analysis of a broad range of human and veterinary pharmaceuticals and some of their metabolites in surface and treated waters by ultra-high-performance liquid chromatography coupled to quadrupole-linear ion trap tandem, J. Chromatogr. A. 1248 (2012) 104–121, https://doi.org/10.1016/j.chroma.2012.05.084.
[60] R Core Team, R: A Language and Environment for Statistical Computing, (2020). https://www.r-project.org/.
[61] T. Wei, V. Simko, R package "corrplot": Visualization of a Correlation, Matrix (2017).
[62] ISO, ISO 11348-3:1998 - Water quality – Determination of the inhibitory effect of water samples on the light emission of Vibrio fischeri (Luminescent bacteria test), 1998.
[63] J.B. Carbajo, A.L. Petre, R. Rosal, S. Herrera, P. Letón, E. García-Calvo,

A.R. Fernández-Alba, J.A. Perdigón-Melón, Continuous ozonation treatment of ofloxacin: Transformation products, water matrix effect and aquatic toxicity, J. Hazard. Mater. 292 (2015) 34–43, https://doi.org/10.1016/j.jhazmat.2015.02.075.

[64] W. Engst, R. Landsiedel, H. Hermersdörfer, J. Doehmer, H. Glatt, Benzylic hydroxylation of 1-methylpyrene and 1-ethylpyrene by human and rat cytochromes P450 individually expressed in V79 Chinese hamster cells, Carcinogenesis. 20 (1999) 1777–1785, https://doi.org/10.1093/carcin/20.9.1777.

[65] D.P. Barr, S.D. Aust, Mechanisms white rot fungi use to degrade pollutants, Environ. Sci. Technol. 28 (1994), https://doi.org/10.1021/es00051a002.

[66] V. Romero, O. González, B. Bayarri, P. Marco, J. Giménez, S. Esplugas, Degradation of Metoprolol by photo-Fenton: Comparison of different photoreactors performance, Chem. Eng. J. 283 (2016) 639–648, https://doi.org/10.1016/j.cej.2015.07.091.

[67] V. Romero, S. Acevedo, P. Marco, J. Giménez, S. Esplugas, Enhancement of Fenton and photo-Fenton processes at initial circumneutral pH for the degradation of the β-blocker metoprolol, Water Res. 88 (2016) 449–457, https://doi.org/10.1016/j.watres.2015.10.035.

Chapter 6

General discussion

6.1 Occurrence of PhACs and their TPs in treated effluents

The high excretion of PhACs and metabolites and their presence in wastewater sewage systems promote their occurrence in the natural environment since conventional WWTPs are not designed to attain their complete removal [240]. These substances are mainly transported as unchanged and/or transformed molecules and are widespread in different environmental compartments. In some cases, the TPs generated can be more persistent and toxic than their related parent compound, and thus, they should be monitored in environmental studies [127]. Although the scientific community has been largely focused on the elimination of the parent compounds, less attention has been paid to study the presence and environmental effects of the intermediates generated from PhACs and metabolite degradation during water treatment. Their comprehensive evaluation is limited by the lack of reference standards, and thus tedious and time-consuming analytical approaches are necessary [128]. In this context, the development of high-resolution analytical instrumentation and methodologies to detect the presence of these unknown pollutants are highly required for a better environmental risk assessment [4]. In this doctoral thesis, the development of advanced and user-friendly suspect screening methodologies has overcome this challenge by considering a large proportion of the substances present in samples, while attaining high confidence in their identification. These automated tools also allowed to explore the individual environmental effects of TPs in water effluents and to monitor their removal.

6.2 Automated suspect screening methodologies for the identification of pharmaceutical TPs in biological treatments

The development of suspect screening methodologies is based on the optimization of three different steps: analysis and data acquisition, data reduction and prioritization, and compound identification. These suspect screening methodologies are based on both pre-acquisition and post-acquisition approaches, which allow us to prioritize suspected features present in samples by precursor ion fragmentation and further identification [187]. A summary of the suspect screening methodologies developed during this doctoral thesis is presented in Table 6.1.

Table 6.1: Summary of the automated suspect screening approaches combined with environmental effect tools (QSAR, PCA and EDA) applied in this doctoral thesis (AA, antibiotic activity).

Article	*Treatment*	*Analysis*	*Identification*	*Ecotox. test*	*Pros*	*Cons*
I	MTP and MTPA in fungal treatments	List-DDA	Literature and ref. stand.	Microtox	- Applicable to samples with high matrix effects. - Software data processing tools are not required.	- Requires a time-consuming inclusion list of suspects. - Not suitable for identification of a wide range of TPs. - Non-reported TPs are overlooked for identification.
II	Antibiotics (AZI, ERY, CTM, OFC, CFC, NFC, SPY, TMP and PMA) in microalgae treatments	Intensity-DDA	Software prediction	Not studied	- More automatic suspect screening methodology. - Evaluation of several target substances simultaneously. - Suitable for identification of a wide range of TPs. - Creates new and non-reported information of TPs (These *Pros* also apply to the following studies).	- TPs at low-intensity values can be overlooked. - Ion fragmentation is susceptible to matrix effects. - Requires expensive software data processing tools (These *Cons* also apply to the following studies).
III	MTP and MTPA in UV/H_2O_2 treatments	Intensity-DDA	Combined identification	Microtox + QSAR	- Estimation of a wide range of hazardous TPs. - QSAR models are rapid and economic tools. - *In vitro* or *in vivo* experiments are not always required.	- Questionable reliability on hazard identification. - Synergisms effects between TPs are not considered.
IV	AZI and CFC in chlorination treatments	Intensity-, list-, isotopic-DDA	Combined identification	Microtox/AA + PCA	- Estimation of a wide range of hazardous TPs. - More realistic toxicity estimation than QSAR models. - Synergisms and antagonisms effects are implicit.	- Hazard estimation depends on suspect screening. - *In vitro* or *in vivo* experiments are always required. - Knowledge on statistical tools is required.
				Microtox/AA + EDA	- High reliability for the identification of hazardous TPs.	- Expertise in analytical instrumentation is needed. - Expensive and time-consuming methodology. - Applicable for selective endpoints only.
V	MTP and MTPA in UV/H_2O_2 combined with CAS and FG treatments	Intensity-DDA	Combined identification	Microtox	- Methodology able to be applied for monitoring studies. - Evaluation of several target substances in one analysis. - Suitable for identification of a wide range of TPs.	- Questionable reliability on hazard identification. - Synergisms are not included in hazard estimation.

A pre-acquisition screening (based on the *list-dependent acquisition*) was applied for the tentative identification of TPs generated from a list of suspected candidates collected from literature prior to sample analysis (Article I). This analytical approach allowed us to attain a high selectivity for compound detection and prioritization. While only those compounds in the inclusion list are selected for ion fragmentation, other ions coming from the matrix (not included in the inclusion list) are not prioritized, and thus, false-positives features are avoided for identification. Another advantage of pre-acquisition screening approaches is that software data processing tools are not always required since structure elucidation is sometimes already reported in the literature. Even though this pre-acquisition approach is considered a promising solution when information about tentative TPs is available, it also has some drawbacks. First, the generation of the mass inclusion list for each parent compound is considered a time-consuming task, not applicable for high-throughput identification analyses. Second, this methodology relies on the hypothesis that the selected TPs reported in the literature (or foreseen by prediction tools) are the most important compounds to be found in the samples, while some other unknown intermediates might be overlooked (such as those TPs formed via uncommon biotransformation pathways or after multiple reaction steps). That was observed when applying this strategy to degradation experiments in pure water and HWW fortified with MTP and MTPA acid, where the identified TPs from literature did not properly correlate with the toxicity increase in the treated samples; namely, some unknown relevant TPs might be ignored. In order to consider a greater number of tentative intermediates detected and increase the automation of suspect screening methodologies, the development of post-acquisition approaches (based on *intensity-dependent acquisition*) combined with automated data processing tools were further investigated.

A post-acquisition screening (based on *intensity-dependent acquisition*) was applied for the identification of the most intense intermediates generated using software prediction tools after sample analysis (Article II). This analytical approach provided a less selective and time-consuming strategy since previous knowledge of the tentative TPs to be found in samples was not required for ion fragmentation. In addition, the automatic prediction of tentative TPs allowed considering thousands of features for identification in a single analysis (12,291 predicted TPs from 9 antibiotics). Despite this, some limitations of this methodology were also observed. First, this acquisition mode relies on the hypothesis that the most intense ions

detected in MS full-scan data are the most important ions for identification. Thus, some intermediates present at low concentration values can be overlooked. In addition, the MS/MS fragmentation of ions coming from the sample matrix can lead to the detection of false-positives and involve tedious data filtering procedures after sample analysis. In this context, this analytical approach was recommended for the analysis of samples when the parent compounds are present at high concentration and the matrix effects are low, for instance, in fortified pure water experiments. In order to alleviate the background noise present in samples and also reduce ion suppression, the use of on-line turbulent flow, sample filtration and/or solid-phase extraction was encouraged prior to sample analysis. Moreover, the application of an automatic dynamic mass exclusion in the data acquisition step was also suggested to mitigate continuous re-fragmentation of the most intense ion along the chromatographic peak and allow fragmentation of less intense ions. In comparison to pre-acquisition approaches (where structure elucidation is sometimes already reported in the literature), the structural elucidation of the detected features was highly dependent on available post-acquisition software tools. In addition, the formation of in-house libraries and on-line databases (such as those promoted by NORMAN initiatives [126]) is highly encouraging for the rapid identification of TPs. In this context, although Compound Discoverer software allowed the automatic identification of a broad variety of intermediates using *in silico* MS/MS prediction, the application of combined identification strategies (based on literature, libraries, databases and reference standards when available) is highly recommended.

6.3 Integrated suspect screening methodologies for the identification of hazardous TPs in physical and/or chemical treatments

Integrated suspect screening approaches based on literature, libraries, prediction and reference standards allowed the identification of a great proportion of the intermediates generated in water treatments. This information becomes essential to correlate their relative presence with the hazardous effects measured in treated effluents [221]. In this doctoral thesis, advanced suspect screening methodologies combined with bioanalytical and ecotoxicological tools (such as QSAR models, *in vitro* bioassays with PCA statistical tools and EDA approaches) were investigated to point out those key-toxicants increasing the hazardous effects in physical and/or chemical treatment effluents (Table 6.1). This is considered one of

the most challenging tasks on environmental chemistry since no reference standards are usually available for confirmation of the hazardous effects of TPs.

An integrated suspect screening methodology with QSAR models was applied to evaluate the presence of hazardous chemicals in treated effluents by the quantitative association of their structural parameters with their biological activity (Article III) [208]. This approach is considered a rapid and economic methodology for the estimation of hazardous intermediates since *in vitro* and *in vivo* biological tests are not required. Therefore, they can be easily applied for the high-throughput identification of hazardous TPs in both spiked pure water and real wastewater experiments. However, this methodology presents important drawbacks to be also considered. First, synergism and antagonism effects among the intermediates identified are not considered in QSAR estimations. In most of the cases, their contribution is calculated according to the accepted "concentration addition", where bioactivity of mixture samples is estimated regarding the sum of their relative presence for a given mode of action [241,242]. Since synergy rarely leads to more than a factor of 10 increase in effect and TPs are normally present at low concentration values, this approach has been recently accepted assuming that concentration-effect curves become linear when intermediates are generated [241,243,244]. Nonetheless, the reliability of the identification of hazardous TPs has been widely questioned since the accepted models are specially developed for parent compounds, which do not have to behave in the same manner as the TPs generated. Since reference standards are not available for their confirmation, complementary methodologies are required to increase the reliability of hazard identification.

An integrated suspect screening methodology with PCA statistical tools was applied to correlate the environmental effects measured in treated effluents with the relative presence of each intermediate during wastewater treated processes (Article IV). As previously mentioned in the application of QSAR models, the use of PCA statistical tools are also considered as a cost-effective methodology for the identification of a wide range of hazardous TPs in treated samples [156]. One of the main advantages of PCA is that synergism and antagonism effects between chemical compounds are implicit (since the hazardous effects are directly measured using *in vitro* bioassays from treated effluent containing a mix of the parent compounds and TPs). Thus, higher reliability on hazard identification can be attained. However, this

methodology presents important drawbacks to be also considered. First, this approach is highly dependent on the efficiency of suspect screening methodologies and the total number of TPs identified. In other words, if some intermediates are overlooked during chemical identification, PCA estimations may be wrongly attributed to the identified TPs only. Second, *in vitro* and/or *in vivo* experiments are always required to build the PCA statistical plots, and thus, higher time and economic investments are needed in comparison with QSAR models. Third, knowledge of statistical tools is required to perform the data processing step and the interpretation of results obtained. Despite this, PCA tools can represent a reliable solution for the evaluation of the hazardous effects of TPs when a large quantity of TPs exhibit a given ecotoxicological endpoint: for instance, the acute toxicity, where many TPs present at low concentration levels can contribute to the total toxicity of effluent samples, and their isolation using EDA approaches is also a difficult task. In addition, PCA tools can represent a reliable solution when TPs are difficult to be isolated due to partial losses during sample evaporation and fractionation process leading to a reduction on effect measurement in the fractions.

An integrated suspect screening methodology with an EDA approach was applied to evaluate the generation of hazardous TPs after fractionation of samples and direct measurement of their effects using *in vitro* bioanalytical tools (Article IV) [217–226]. Although this methodology was suggested as the most reliable approach for hazard identification, it presents important drawbacks to be also considered. First, it was classified as a time-consuming approach that requires a battery of different analytical instrumentation as well as multidisciplinary expertise. Second, the evaluation of synergism and antagonism effects among the intermediates identified require additional experiments using different mixes of the fractions collected and further assessing their hazardous effects. Third, the total number of hazardous TPs identified is always lower than in QSAR models and PCA statistical tools due to the complex analytical procedures carried out. Despite this, this strategy represented the most suitable solution for the evaluation of the hazardous effects of TPs when high specific endpoints are investigated: such as antibiotic activity, where only few TPs can contribute to the total toxicity of samples and they are easy to be fractionated.

6.4 Monitoring of the removal of PhACs and their hazardous TPs in combined treatments

In this doctoral thesis, the development of automated suspect screening methodologies using advanced computational tools provided user-friendly approaches to monitor the occurrence of pollutants, even when reference standards are not available for confirmation. However, to properly evaluate the efficiency of the removal in wastewater treatment technologies, not only the parent compounds should be considered but also the TPs generated to ensure safety discharges [228]. A summary of the removal of the parent compounds in fungal, microalgae, UV/H_2O_2, chlorination single treatments, and the combination of UV/H_2O_2 with fungi and CAS treatments are presented in Table 6.2.

Among the technologies studied, none of the single treatments achieved the complete removal of the parent compounds in real wastewater. Among the treatments selected, the removal of MTP and MTPA in UV/H_2O_2 was higher in absence of organic matter (pure water experiments) than in real wastewater samples. However, the UV/H_2O_2 treatment was more effective than fungal treatments for the elimination of the same parent compounds in HWW (at their optimized conditions). Similar results were observed for AZI with higher removal rates after chlorination (up to 88%) than after microalgae treatments (up to 58%). Indeed, all the parent compounds were transformed into a large quantity of hazardous TPs at high relative presence which can pose hazardous effects to the receiving aquatic environment. The results obtained in this doctoral thesis showed the importance of identifying the hazardous TPs generated for the development of wastewater treatment technologies. For instance, the TP238 and TP252 where suggested as carcinogenic compounds from metoprolol and metoprolol acid after UV/H_2O_2 treatments (Article III), while the TP296 retained part of the antibiotic activity of ciprofloxacin after chlorination (Article IV). These results suggest that combined treatment technologies are highly required to attain the complete removal of the hazardous TPs generated, and their parent compounds, prior to wastewater discharge.

Table 6.2: Main results of the treatment technologies applied in this doctoral thesis in their respective optimum conditions.

Article	*Treatment*	*Max. removal in pure water*	*Max. removal in wastewater*	*TPs identified in effluents*	*Main results*
I	MTP and MTPA in fungal treatments (after 15 days, after 7 days in FBB)	MTP (51%) and MTPA (77%) in Erlenmeyer flasks at 2.5 mg/L	MTP (33%) and MTPA (64%) in FBB bioreactor at 2 µg/L in HWW	14 TPs from MTP 7 TPs from MTPA	*Target analysis* allows us to evaluate the percentage of removal of the recalcitrant parent compounds in wastewater. *Suspect screening* allowed us to identify a great variety of transformed TPs in liquid and solid phases.
II	Antibiotics in microalgae treatments (after 14 days, after 12 days in PBR)	AZI (58%), ERY (34%), CTM (36%), OFC (88%), CFC (100%), NFC (100%), PMA (85%), TMP (34%) and SPY (94%) in Erlenmeyer flasks at 100 µg/L	ERY (85%), OFC (67%) and NFC (95%) in a PBR bioreactor (non-spiked in UWW)	16 TPs from macrolides 18 TPs from fluoroquinolones 6 TPs from other antibiotics	*Target analysis* allows detecting a high removal of antibiotics in microalgae experiments. *Suspect screening* confirmed that biodegradation was the mechanism involved in its removal of some antibiotics such as macrolides.
III	MTP and MTPA in UV/H_2O_2 treatments (after 10 min)	MTP (99%) and MTPA (100%) at 2.5 mg/L	MTP (72%) and MTPA (89%) in a UV/H_2O_2 reactor at 2 µg/L in HWW; MTP (11%) in IWW containing 33 mg/L	24 TPs from MTP and MTPA	*Target analysis* reveals that the parent compounds were better eliminated in the absence of organic matter. *Integrated suspect screening* evidenced that the extent of TP removal was also affected by the presence of organic matter providing a different distribution of hazardous TPs in treated effluents.
IV	AZI and CFC in chlorination (after 24h)	AZI (88%) and CFC (100%) in glass flasks at 2 mg/L	Not studied	13 TPs from AZI 7 TPs from CFC	*Target analysis* shows ca. complete elimination of the parent compounds in treated effluents. *Integrated suspect screening* pointed out the most important hazardous TPs in effluents to be also considered for removal evaluation.
V	MTP and MTPA in combined treatments: UV/H_2O_2 (after 10 min) CAS (after 24h) FG (after 7 days)	UV/H_2O_2 + FG at 2.5 mg/L MTP (100%) and MTPA (100%)	UV/H_2O_2 + FG at 2 µg/L MTP (89%) and MTPA (81%)	19 TPs from MTP and MTPA	*Target analysis* allows us to detect the highest removal of the parent compounds in UV/H_2O_2 + CAS and CAS + UV/H_2O_2 combinations. *Suspect screening* allowed to discern between them and identify that the combination UV/H_2O_2 + CAS allowed the highest extent of transformation of TPs.
		FG + UV/H_2O_2 at 2.5 mg/L MTP (36%) and MTPA (100%)	FG + UV/H_2O_2 at 2 µg/L MTP (36%) and MTPA (81%)		
		UV/H_2O_2 + CAS at 2.5 mg/L MTP (100%) and MTPA (100%)	UV/H_2O_2 + CAS at 2 µg/L MTP (86%) and MTPA (100%)		
		CAS + UV/H_2O_2 at 2.5 mg/L MTP (98%) and MTPA (98%)	CAS + UV/H_2O_2 at 2 µg/L MTP (86%) and MTPA (99%)		

In order to attain the greatest extent on parent and intermediate compounds elimination, the combination of UV/H_2O_2 with FG and CAS technologies were evaluated (Article V), using the integrated suspect screening approach previously developed (Article III), for the following combination of treatments: UV/H_2O_2 + FG, FG + UV/H_2O_2, UV/H_2O_2 + CAS and CAS + UV/H_2O_2. Considering the removal of the parent compounds MTP and MTPA in HWW (Table 6.2), a very high and similar elimination was attained for both spiked compounds after UV/H_2O_2 + CAS and CAS + UV/H_2O_2 (higher than 86% and 99% for MTP and MTPA, respectively). Likewise, the total presence of intermediates identified in treated effluents after UV/H_2O_2 + CAS combination was similar (15%) compared to the opposite combination (11%). However, the extent in the transformation of the intermediates generated was different between those combined treatments. For the combination CAS+UV/H_2O_2, the recalcitrant intermediates α-HMTP (1st generation TP) and TP240 (2nd generation TP) were still present in treated effluents, while the 3rd generation of TPs represented 21% of the total intermediates detected. Using the opposite combination UV/H_2O_2 + CAS, all the recalcitrant intermediates identified from the 1st and 2nd generation were practically transformed and increased the presence of 3rd generation TPs, which represented 65% of the total intermediates detected in treated effluents. This last configuration attained the highest transformation of TPs detected in real wastewater at the lowest treatment time (10 min UV/H_2O_2 and 24h CAS). Thus, the combination of UV/H_2O_2 + CAS was classified as the most efficient combination tested for the removal of the parent compounds MTP, MTPA and the TPs generated in HWW. These results evidenced that target analysis does not provide enough information to draw conclusions of the best wastewater treatment to be applied, and the additional application of suspect screening methodologies to routine analysis is highly necessary. Despite this, it was observed that complete removal of TPs was not attained even using the best treatment technology investigated (UV/H_2O_2 + CAS), where a presence of 15% of TPs were still remaining. Since these residual TPs may also be transformed into more hazardous TPs in water bodies, the combination of more advanced treatment processes should be further investigated to attain their total removal prior to wastewater discharge. As a conclusion, multidisciplinary research including analytical chemistry, risk assessment and chemical engineering is needed to properly evaluate the best treatment technology to eliminate all chemicals present in treated effluents.

Chapter 7

General conclusions

i. Comprehensive suspect screening approaches were applied for automated identification of a wide range of intermediates generated from PhACs during water treatment including fungi, microalgae, UV/H_2O_2, chlorination and combined treatments.

ii. The application of automated suspect screening methodologies allowed to elucidate the PhACs transformation pathways through biotransformation, photo-transformation and hydrolysis oxidation occurring during water treatment.

iii. The use of pre-acquisition approaches is suggested when information of the tentative TPs to be found in samples is available and the water matrix is complex. The application of post-acquisition screening is recommended when information about the tentative TPs to be found in samples is not available and the matrix interferences are low.

iv. The continuous generation of new information about unknown TPs and their inclusion into in-house libraries and on-line databases can alleviate data processing workflow while assuring enough confidence in TP identification.

v. Integrated strategies for TP identification (combining literature information, prediction tools, in-house and/or on-line databases, and reference standards) are highly recommended to cover as many potential TPs as possible.

vi. **T**he integration of suspect screening approaches with ecotoxicological tools based in *in silico, in vitro* bioassays and data processing tools (QSAR models, PCA statistics and EDA methodologies) allowed to correlate the presence of TPs with their hazardous effects:

- The QSAR models are the most recommended tools for fast and cost-effective assessment and time investment.
- EDA is the most reliable but time-consuming and expensive approach, recommended in the case of selective endpoints.

- The combination of toxicity test results with statistical analysis (PCA) is recommended for less specific endpoints, and for those TPs difficult to be isolated using EDA approaches.

vii. The application of integrated suspect screening methodologies demonstrates that hazardous intermediates are generated from the parent compounds. In addition, complete removal was not attained along the single treatments selected. Thus, additional water polishing treatments might be required to attain an extended removal of TPs before a safe wastewater discharge.

viii. Target analysis does not provide complete information to draw conclusions about the most efficient water treatment. The use of automated suspect screening methodologies allowed us to select the best water treatment based on the removal of both the parent compounds and the TPs generated. The combination of UV/H_2O_2 + CAS was the most successful treatment among the water treatment chains tested.

ix. The relative presence of the intermediates generated depends on the initial concentration of the parent compounds and the type of water matrix. Thus, suspect screening approaches should always be applied as a routine analysis to evaluate all water treatment conditions.

x. The combination of more advanced treatment processes should be further investigated to attain the complete removal of the TPs detected in effluents prior to wastewater discharge.

xi. Multidisciplinary research including analytical chemistry, environmental risk assessment and chemical engineering is needed to properly evaluate the best treatment technology to eliminate all pollutants present in treated effluents.

Chapter 8

Future perspectives

The study of the intermediates generated from PhACs during wastewater treatment requires a multidisciplinary approach including analytical chemistry, ecotoxicology and chemical engineering. Although many efforts have been carried out in each field individually, further research is necessary to fully understand the behavior of these unknown substances in the aquatic environment. In this context, in line with several of the aspects addressed in the thesis and the conclusions extracted, some future research trends can be foreseen:

I) In terms of analysis of TPs: The DDA mode demonstrated to be a powerful approach to automatize suspect screening methodologies and identify a broad variety of intermediates reducing data processing from months to a few days. However, limitation in the total number of compounds identified in DDA approaches will always be observed since it is based on the fragmentation of the most intense ions only. The development of DIA approaches to generate MS/MS spectra for all the intermediate features in a single sample analysis can provide more information on the total TPs present in samples. As explained in the thesis, one of the main limitations of the latest is related to the broad isolation width (approx. 15-25 Da) used for ion fragmentation (isolation width in DDA approaches is approx. 1 Da) [245]. Thus, less "clearer" MS/MS spectra are provided (with a mixture of ion fragments) and more difficult data processing should be performed for intermediates elucidation. The combination of DIA approaches with on-line databases would be required to alleviate this issue by comparison of data collected with the information collected in those on-line sources. Despite many DIA deconvolution algorithms have been developed in the last few years [246–251], further developments on HRMS instrumentation and software tools would be required for their direct application to real wastewater samples.

II) In terms of compound identification of TPs: the elucidation of the greatest proportion of the chemicals present in real wastewater samples is still one of the main limitations to be solved. The most promising strategy for their direct application to real wastewater samples is the development of on-line databases (or in-house libraries) for reliable identification using standardized chromatographic gradients. However, while most of the on-line libraries are performed for confirmed structures (with analytical reference standards), the generation of their tentative intermediates when reference standards are no available for confirmation is still limited. In this sense, the implementation of databases including TPs between research

institutions and organizations should be promoted as a collective tool for interdisciplinary research. The best example would be the use of initiatives led by NORMAN Suspect List Exchange (NORMAN-SLE), established in 2015 as a central access point for NORMAN members (and others) to find suspect lists relevant for their environmental monitoring question.

III) In terms of the environmental effects of TPs: since most of the TPs presents in samples are still unknown, no legislation exists regarding the maximum residue limits in environmental samples. In this doctoral thesis, the elucidation of potential hazardous intermediates contributing to the total effects measured in treated effluents was attempted using *in silico* and *in vitro* methods through EDA, PCA and QSAR approaches. Although QSAR models were definitely the less reliable approaches to apply, they are considered the most promising strategy for the rapid identification of hazardous TPs in the long-term (due to their low economic investments). As explained before, one of the main limitations of QSAR estimations is the lack of evaluation of synergism and antagonism effects in the treated effluent samples containing the mixture of TPs. Thus, the development of advanced QSAR models, including information from the mixture of target pollutants, would be desirable to increase the reliability of this *in silico* predictions and avoid the more tedious and time-consuming procedures such as EDA approaches. The identification of TPs of concern using QSAR models can be a successful tool to study their effects and put the most hazardous TPs of concern in treated effluents in the spotlight and eventually, to consider them for regulation measures.

IV) In terms of monitoring of TPs: the presence of hazardous TPs in treated effluents has motivated the scientific community to include them in monitoring studies to evaluate the efficiency of wastewater treatments in terms of contaminants removal. To date, most of these under-developed treatments have been performed in batch scales such as Erlenmeyer flasks and bioreactors. In this doctoral thesis, it was demonstrated that the experimental conditions (such as wastewater conditions and treatment parameters) used in wastewater treatments can provide completely different results in terms of TP generation, which should be further explored. Before the application of the investigated treatments at the full-scale level, the use of suspect screening methodologies as monitoring tools should be routinely implemented in all the experimental conditions evaluated. In addition, the application of ecotoxicological tools to evaluate the environmental effects of effluents should be also considered. In this context,

further improvements in analytical workflows are needed for the evaluation and development of more advanced combination of treatment technologies.

Chapter 9

References

[1] J. Wilkinson, P.S. Hooda, J. Barker, S. Barton, J. Swinden, Occurrence, fate and transformation of emerging contaminants in water: An overarching review of the field, Environ. Pollut. 231 (2017) 954–970. doi:10.1016/j.envpol.2017.08.032.

[2] G. Lofrano, G. Libralato, S. Meric, V. Vaiano, O. Sacco, V. Venditto, M. Guida, M. Carotenuto, Occurrence and potential risks of emerging contaminants in water, Elsevier Inc., 2020. doi:10.1016/b978-0-12-818334-2.00001-8.

[3] A. Gogoi, P. Mazumder, V.K. Tyagi, G.G. Tushara Chaminda, A.K. An, M. Kumar, Occurrence and fate of emerging contaminants in water environment: A review, Groundw. Sustain. Dev. 6 (2018) 169–180. doi:10.1016/j.gsd.2017.12.009.

[4] M. de Oliveira, B.E.F. Frihling, J. Velasques, F.J.C.M. Filho, P.S. Cavalheri, L. Migliolo, Pharmaceuticals residues and xenobiotics contaminants: Occurrence, analytical techniques and sustainable alternatives for wastewater treatment, Sci. Total Environ. 705 (2020) 135568. doi:10.1016/j.scitotenv.2019.135568.

[5] V. Calisto, V.I. Esteves, Psychiatric pharmaceuticals in the environment, Chemosphere. 77 (2009) 1257–1274. doi:10.1016/j.chemosphere.2009.09.021.

[6] A.E. Fohner, A. Sparreboom, R.B. Altman, T.E. Klein, PharmGKB summary: Macrolide antibiotic pathway, pharmacokinetics/pharmacodynamics, Pharmacogenet. Genomics. 27 (2017) 164–167. doi:10.1097/FPC.0000000000000270.

[7] P. Verlicchi, M. Al Aukidy, A. Galletti, M. Petrovic, D. Barceló, Hospital effluent: Investigation of the concentrations and distribution of pharmaceuticals and environmental risk assessment, Sci. Total Environ. 430 (2012) 109–118. doi:10.1016/j.scitotenv.2012.04.055.

[8] P. Verlicchi, A. Galletti, M. Petrovic, D. Barceló, Hospital effluents as a source of emerging pollutants: An overview of micropollutants and sustainable treatment options, J. Hydrol. 389 (2010) 416–428. doi:10.1016/j.jhydrol.2010.06.005.

[9] T. aus der Beek, F.A. Weber, A. Bergmann, S. Hickmann, I. Ebert, A. Hein, A. Küster, Pharmaceuticals in the environment-Global occurrences and perspectives, Environ. Toxicol. Chem. 35 (2016) 823–835. doi:10.1002/etc.3339.

[10] K. Lees, M. Fitzsimons, J. Snape, A. Tappin, S. Comber, Pharmaceuticals in soils of lower income countries: Physico-chemical fate and risks from wastewater irrigation, Environ. Int. 94 (2016) 712–723. doi:10.1016/j.envint.2016.06.018.

[11] W.J. Sim, J.W. Lee, E.S. Lee, S.K. Shin, S.R. Hwang, J.E. Oh, Occurrence and distribution of pharmaceuticals in wastewater from households, livestock farms, hospitals and pharmaceutical manufactures, Chemosphere. 82 (2011) 179–186. doi:10.1016/j.chemosphere.2010.10.026.

[12] Council Directive of 21 May 1991 concerning urban waste water treatment (91/271/EEC), Off. J. Eur. Communities. L135 (1991) 40–52.

[13] L.H.M.L.M. Santos, M. Gros, S. Rodriguez-Mozaz, C. Delerue-Matos, A. Pena, D. Barceló, M.C.B.S.M. Montenegro, Contribution of hospital effluents to the load of pharmaceuticals in urban wastewaters: Identification of ecologically relevant pharmaceuticals, Sci. Total Environ. 461–462 (2013) 302–316. doi:10.1016/j.scitotenv.2013.04.077.

[14] Regulation (EU) 2020/741 of the European Parliament and of the Council of 25 May 2020 on minimum requirements for water reuse, Off. J. Eur. Union. L177 (2020) 32–55.

[15] N. Ratola, A. Cincinelli, A. Alves, A. Katsoyiannis, Occurrence of organic microcontaminants in

the wastewater treatment process. A mini review, J. Hazard. Mater. 239–240 (2012) 1–18. doi:10.1016/j.jhazmat.2012.05.040.

[16] P. Verlicchi, M. Al Aukidy, E. Zambello, What have we learned from worldwide experiences on the management and treatment of hospital effluent? - An overview and a discussion on perspectives, Sci. Total Environ. 514 (2015) 467–491. doi:10.1016/j.scitotenv.2015.02.020.

[17] R.P. Deo, Pharmaceuticals in the Surface Water of the USA: A Review, Curr. Environ. Heal. Reports. 1 (2014) 113–122. doi:10.1007/s40572-014-0015-y.

[18] J.W. Kim, H.S. Jang, J.G. Kim, H. Ishibashi, M. Hirano, K. Nasu, N. Ichikawa, Y. Takao, R. Shinohara, K. Arizono, Occurrence of Pharmaceutical and Personal Care Products (PPCPs) in Surface Water from Mankyung River, South Korea, J. Heal. Sci. 55 (2009) 249–258. doi:10.1248/jhs.55.249.

[19] B. Kasprzyk-Hordern, R.M. Dinsdale, A.J. Guwy, The occurrence of pharmaceuticals, personal care products, endocrine disruptors and illicit drugs in surface water in South Wales, UK, Water Res. 42 (2008) 3498–3518. doi:10.1016/j.watres.2008.04.026.

[20] L. Arpin-Pont, M.J. Martínez-Bueno, E. Gomez, H. Fenet, Occurrence of PPCPs in the marine environment: a review, Environ. Sci. Pollut. Res. 23 (2016) 4978–4991. doi:10.1007/s11356-014-3617-x.

[21] C. Postigo, D. Barceló, Synthetic organic compounds and their transformation products in groundwater: Occurrence, fate and mitigation, Sci. Total Environ. 503–504 (2015) 32–47. doi:10.1016/j.scitotenv.2014.06.019.

[22] C. Zwiener, Occurrence and analysis of pharmaceuticals and their transformation products in drinking water treatment, Anal. Bioanal. Chem. 387 (2007) 1159–1162. doi:10.1007/s00216-006-0818-2.

[23] A. Osińska, E. Korzeniewska, M. Harnisz, E. Felis, S. Bajkacz, P. Jachimowicz, S. Niestępski, I. Konopka, Small-scale wastewater treatment plants as a source of the dissemination of antibiotic resistance genes in the aquatic environment, J. Hazard. Mater. 381 (2020) 121221. doi:10.1016/j.jhazmat.2019.121221.

[24] M. Bilal, S. Mehmood, T. Rasheed, H.M.N. Iqbal, Antibiotics traces in the aquatic environment: persistence and adverse environmental impact, Curr. Opin. Environ. Sci. Heal. 13 (2020) 68–74. doi:10.1016/j.coesh.2019.11.005.

[25] P. Kovalakova, L. Cizmas, T.J. Mcdonald, B. Marsalek, M. Feng, V.K. Sharma, Occurrence and toxicity of antibiotics in the aquatic environment: A review, Chemosphere. 251 (2020) 126351. doi:10.1016/j.chemosphere.2020.126351.

[26] B.I. Escher, R. Baumgartner, M. Koller, K. Treyer, J. Lienert, C.S. McArdell, Environmental toxicology and risk assessment of pharmaceuticals from hospital wastewater, Water Res. 45 (2011) 75–92. doi:10.1016/j.watres.2010.08.019.

[27] The European Parlament and the Council of the European Union, Directives of 12 August 2013 amending Directives 2000/60/EC and 2008/105/EC as regards priority substances in the field of water policy, Off. J. Eur. Union. L226 (2013) 1–17.

[28] European Commission, Decision (EU) 2020/1161 of 4 August 2020 establishing a watch list of substances for Union-wide monitoring in the field of water policy pursuant to Directive 2008/105/EC of the European Parliament and of the Council, Off. J. Eur. Union. L257 (2020) 32–35.

[29] J. Gomes, R. Costa, R.M. Quinta-Ferreira, R.C. Martins, Application of ozonation for pharmaceuticals and personal care products removal from water, Sci. Total Environ. 586 (2017) 265–283. doi:10.1016/j.scitotenv.2017.01.216.

[30] L.F. Stadlmair, T. Letzel, J.E. Drewes, J. Grassmann, Enzymes in removal of pharmaceuticals from wastewater: A critical review of challenges, applications and screening methods for their selection, Chemosphere. 205 (2018) 649–661. doi:10.1016/j.chemosphere.2018.04.142.

[31] Y. Li, G. Zhu, W.J. Ng, S.K. Tan, A review on removing pharmaceutical contaminants from wastewater by constructed wetlands: Design, performance and mechanism, Sci. Total Environ. 468–469 (2014) 908–932. doi:10.1016/j.scitotenv.2013.09.018.

[32] I. Sirés, E. Brillas, Remediation of water pollution caused by pharmaceutical residues based on electrochemical separation and degradation technologies: A review, Environ. Int. 40 (2012) 212–229. doi:10.1016/j.envint.2011.07.012.

[33] L. Feng, E.D. van Hullebusch, M.A. Rodrigo, G. Esposito, M.A. Oturan, Removal of residual anti-inflammatory and analgesic pharmaceuticals from aqueous systems by electrochemical advanced oxidation processes. A review, Chem. Eng. J. 228 (2013) 944–964. doi:10.1016/j.cej.2013.05.061.

[34] J. Akhtar, N.A.S. Amin, K. Shahzad, A review on removal of pharmaceuticals from water by adsorption, Desalin. Water Treat. 57 (2016) 12842–12860. doi:10.1080/19443994.2015.1051121.

[35] C. Li, C. Cabassud, C. Guigui, Evaluation of membrane bioreactor on removal of pharmaceutical micropollutants: a review, Desalin. Water Treat. 55 (2015) 845–858. doi:10.1080/19443994.2014.926839.

[36] K. Kimura, H. Hara, Y. Watanabe, Elimination of selected acidic pharmaceuticals from municipal wastewater by an activated sludge system and membrane bioreactors, Environ. Sci. Technol. 41 (2007) 3708–3714. doi:10.1021/es061684z.

[37] M.B. Ahmed, J.L. Zhou, H.H. Ngo, W. Guo, N.S. Thomaidis, J. Xu, Progress in the biological and chemical treatment technologies for emerging contaminant removal from wastewater: A critical review, J. Hazard. Mater. 323 (2017) 274–298. doi:10.1016/j.jhazmat.2016.04.045.

[38] N. Tadkaew, F.I. Hai, J.A. McDonald, S.J. Khan, L.D. Nghiem, Removal of trace organics by MBR treatment: The role of molecular properties, Water Res. 45 (2011) 2439–2451. doi:10.1016/j.watres.2011.01.023.

[39] J. Radjenović, M. Petrović, D. Barceló, Fate and distribution of pharmaceuticals in wastewater and sewage sludge of the conventional activated sludge (CAS) and advanced membrane bioreactor (MBR) treatment, Water Res. 43 (2009) 831–841. doi:10.1016/j.watres.2008.11.043.

[40] M. Clara, B. Strenn, O. Gans, E. Martinez, N. Kreuzinger, H. Kroiss, Removal of selected pharmaceuticals, fragrances and endocrine disrupting compounds in a membrane bioreactor and conventional wastewater treatment plants, Water Res. 39 (2005) 4797–4807. doi:10.1016/j.watres.2005.09.015.

[41] J. Mamo, M.J. García-Galán, M. Stefani, S. Rodríguez-Mozaz, D. Barceló, H. Monclús, I. Rodriguez-Roda, J. Comas, Fate of pharmaceuticals and their transformation products in integrated membrane systems for wastewater reclamation, Chem. Eng. J. 331 (2018) 450–461. doi:10.1016/j.cej.2017.08.050.

[42] M.J. García Galán, M.S. Díaz-Cruz, D. Barceló, Removal of sulfonamide antibiotics upon

conventional activated sludge and advanced membrane bioreactor treatment, Anal. Bioanal. Chem. 404 (2012) 1505–1515. doi:10.1007/s00216-012-6239-5.

[43] D. Dolar, M. Gros, S. Rodriguez-Mozaz, J. Moreno, J. Comas, I. Rodriguez-Roda, D. Barceló, Removal of emerging contaminants from municipal wastewater with an integrated membrane system, MBR-RO, J. Hazard. Mater. 239–240 (2012) 64–69. doi:10.1016/j.jhazmat.2012.03.029.

[44] M. Naghdi, M. Taheran, S.K. Brar, A. Kermanshahi-pour, M. Verma, R.Y. Surampalli, Removal of pharmaceutical compounds in water and wastewater using fungal oxidoreductase enzymes, Environ. Pollut. 234 (2018) 190–213. doi:10.1016/j.envpol.2017.11.060.

[45] S.B. Pointing, Feasibility of bioremediation by white-rot fungi, Appl. Microbiol. Biotechnol. 57 (2001) 20–33. doi:10.1007/s002530100745.

[46] A.O. Falade, L. V. Mabinya, A.I. Okoh, U.U. Nwodo, Ligninolytic enzymes: Versatile biocatalysts for the elimination of endocrine-disrupting chemicals in wastewater, Microbiologyopen. 7 (2018) 1–17. doi:10.1002/mbo3.722.

[47] X. Font, G. Caminal, X. Gabarrell, S. Romero, M.T. Vicent, Black liquor detoxification by laccase of *Trametes versicolor* pellets, J. Chem. Technol. Biotechnol. 78 (2003) 548–554. doi:10.1002/jctb.834.

[48] M. Hofrichter, R. Ullrich, M.J. Pecyna, C. Liers, T. Lundell, New and classic families of secreted fungal heme peroxidases, Appl. Microbiol. Biotechnol. 87 (2010) 871–897. doi:10.1007/s00253-010-2633-0.

[49] E. Noman, A. Al-Gheethi, R.M.S.R. Mohamed, B.A. Talip, Myco-Remediation of Xenobiotic Organic Compounds for a Sustainable Environment: A Critical Review, Top. Curr. Chem. 377 (2019) 1–41. doi:10.1007/s41061-019-0241-8.

[50] M. Badia-Fabregat, D. Lucas, M. Gros, S. Rodríguez-Mozaz, D. Barceló, G. Caminal, T. Vicent, Identification of some factors affecting pharmaceutical active compounds (PhACs) removal in real wastewater. Case study of fungal treatment of reverse osmosis concentrate, J. Hazard. Mater. 283 (2015) 663–671. doi:10.1016/j.jhazmat.2014.10.007.

[51] C. Cruz-Morató, L. Ferrando-Climent, S. Rodriguez-Mozaz, D. Barceló, E. Marco-Urrea, T. Vicent, M. Sarrà, Degradation of pharmaceuticals in non-sterile urban wastewater by *Trametes versicolor* in a fluidized bed bioreactor, Water Res. 47 (2013) 5200–5210. doi:10.1016/j.watres.2013.06.007.

[52] D. Lucas, D. Barceló, S. Rodriguez-Mozaz, Removal of pharmaceuticals from wastewater by fungal treatment and reduction of hazard quotients, Sci. Total Environ. 571 (2016) 909–915. doi:10.1016/j.scitotenv.2016.07.074.

[53] C. Mougin, A. Kollmann, C. Jolivalt, Enhanced production of laccase in the fungus *Trametes versicolor* by the addition of xenobiotics, Biotechnol. Lett. 24 (2002) 139–142. doi:10.1023/A:1013802713266.

[54] V. Valášková, P. Baldrian, Estimation of bound and free fractions of lignocellulose-degrading enzymes of wood-rotting fungi *Pleurotus ostreatus*, *Trametes versicolor* and *Piptoporus betulinus*, Res. Microbiol. 157 (2006) 119–124. doi:10.1016/j.resmic.2005.06.004.

[55] S. Abinandan, S. Shanthakumar, Challenges and opportunities in application of microalgae (*Chlorophyta*) for wastewater treatment: A review, Renew. Sustain. Energy Rev. 52 (2015) 123–132. doi:10.1016/j.rser.2015.07.086.

[56] L.B. Sukla, E. Subudhi, D. Pradhan, The Role of Microalgae in Wastewater Treatment, 1st ed., Springer Nature, 2019. doi:10.1007/978-981-13-1586-2.

[57] S. Pflugmacher, H. Sandermann, Cytochrome P450 monooxygenases for fatty acids and xenobiotics in marine macroalgae, Plant Physiol. 117 (1998) 123–128. doi:10.1104/pp.117.1.123.

[58] N.T. Mthakathi, I.K.R. Kgosiemang, W. Chen, M.E. Mohlatsane, T.J. Mojahi, J.-H. Yu, S.S. Mashele, K. Syed, Cytochrome P450 monooxygenase analysis in free-living and symbiotic microalgae *Coccomyxa sp.* C-169 and *Chlorella sp.* NC64A, Algae. 30 (2015) 233–239. doi:10.4490/algae.2015.30.3.233.

[59] V.B. Urlacher, M. Girhard, Cytochrome P450 monooxygenases: An update on perspectives for synthetic application, Trends Biotechnol. 30 (2012) 26–36. doi:10.1016/j.tibtech.2011.06.012.

[60] P. Xie, C. Chen, C. Zhang, G. Su, N. Ren, S.H. Ho, Revealing the role of adsorption in ciprofloxacin and sulfadiazine elimination routes in microalgae, Water Res. 172 (2020) 115475. doi:10.1016/j.watres.2020.115475.

[61] N. Nakajima, T. Teramoto, F. Kasai, T. Sano, M. Tamaoki, M. Aono, A. Kubo, H. Kamada, Y. Azumi, H. Saji, Glycosylation of bisphenol A by freshwater microalgae, Chemosphere. 69 (2007) 934–941. doi:10.1016/j.chemosphere.2007.05.088.

[62] J.Q. Xiong, S. Govindwar, M.B. Kurade, K.J. Paeng, H.S. Roh, M.A. Khan, B.H. Jeon, Toxicity of sulfamethazine and sulfamethoxazole and their removal by a green microalga, *Scenedesmus obliquus*, Chemosphere. 218 (2019) 551–558. doi:10.1016/j.chemosphere.2018.11.146.

[63] Y. Du, J. Wang, H. Li, S. Mao, D. Wang, Z. Xiang, R. Guo, J. Chen, The dual function of the algal treatment: Antibiotic elimination combined with CO_2 fixation, Chemosphere. 211 (2018) 192–201. doi:10.1016/j.chemosphere.2018.07.163.

[64] D. Zhang, R.M. Gersberg, W.J. Ng, S.K. Tan, Removal of pharmaceuticals and personal care products in aquatic plant-based systems: A review, Environ. Pollut. 184 (2014) 620–639. doi:10.1016/j.envpol.2013.09.009.

[65] Y. Deng, R. Zhao, Advanced Oxidation Processes (AOPs) in Wastewater Treatment, Curr. Pollut. Reports. 1 (2015) 167–176. doi:10.1007/s40726-015-0015-z.

[66] M.A. Oturan, J.J. Aaron, Advanced oxidation processes in water/wastewater treatment: Principles and applications. A review, Crit. Rev. Environ. Sci. Technol. 44 (2014) 2577–2641. doi:10.1080/10643389.2013.829765.

[67] M. Salimi, A. Esrafili, M. Gholami, A. Jonidi Jafari, R. Rezaei Kalantary, M. Farzadkia, M. Kermani, H.R. Sobhi, Contaminants of emerging concern: a review of new approach in AOP technologies, Environ. Monit. Assess. 189 (2017) 414. doi:10.1007/s10661-017-6097-x.

[68] D.B. Miklos, C. Remy, M. Jekel, K.G. Linden, J.E. Drewes, U. Hübner, Evaluation of advanced oxidation processes for water and wastewater treatment – A critical review, Water Res. 139 (2018) 118–131. doi:10.1016/j.watres.2018.03.042.

[69] M. Sillanpää, M.C. Ncibi, A. Matilainen, Advanced oxidation processes for the removal of natural organic matter from drinking water sources: A comprehensive review, J. Environ. Manage. 208 (2018) 56–76. doi:10.1016/j.jenvman.2017.12.009.

[70] D. Kanakaraju, B.D. Glass, M. Oelgemöller, Advanced oxidation process-mediated removal of pharmaceuticals from water: A review, J. Environ. Manage. 219 (2018) 189–207.

doi:10.1016/j.jenvman.2018.04.103.

[71] R. Anjali, S. Shanthakumar, Insights on the current status of occurrence and removal of antibiotics in wastewater by advanced oxidation processes, J. Environ. Manage. 246 (2019) 51–62. doi:10.1016/j.jenvman.2019.05.090.

[72] M. Klavarioti, D. Mantzavinos, D. Kassinos, Removal of residual pharmaceuticals from aqueous systems by advanced oxidation processes, Environ. Int. 35 (2009) 402–417. doi:10.1016/j.envint.2008.07.009.

[73] E. Neyens, J. Baeyens, A review of classic Fenton's peroxidation as an advanced oxidation technique, J. Hazard. Mater. 98 (2003) 33–50. doi:10.1016/S0304-3894(02)00282-0.

[74] H. Monteil, Y. Péchaud, N. Oturan, M.A. Oturan, A review on efficiency and cost effectiveness of electro- and bio-electro-Fenton processes: Application to the treatment of pharmaceutical pollutants in water, Chem. Eng. J. 376 (2019) 119577. doi:10.1016/j.cej.2018.07.179.

[75] M. hui Zhang, H. Dong, L. Zhao, D. xi Wang, D. Meng, A review on Fenton process for organic wastewater treatment based on optimization perspective, Sci. Total Environ. 670 (2019) 110–121. doi:10.1016/j.scitotenv.2019.03.180.

[76] V. Romero, S. Acevedo, P. Marco, J. Giménez, S. Esplugas, Enhancement of Fenton and photo-Fenton processes at initial circumneutral pH for the degradation of the β-blocker metoprolol, Water Res. 88 (2016) 449–457. doi:10.1016/j.watres.2015.10.035.

[77] J. Wang, R. Zhuan, Degradation of antibiotics by advanced oxidation processes: An overview, Sci. Total Environ. 701 (2020) 135023. doi:10.1016/j.scitotenv.2019.135023.

[78] R.P. Cavalcante, R.F. Dantas, H. Wender, B. Bayarri, O. González, J. Giménez, S. Esplugas, A. Machulek, Photocatalytic treatment of metoprolol with B-doped TiO_2: Effect of water matrix, toxicological evaluation and identification of intermediates, Appl. Catal. B Environ. 176–177 (2015) 173–182. doi:10.1016/j.apcatb.2015.04.007.

[79] A. Della-Flora, M.L. Wilde, I.D.F. Pinto, É.C. Lima, C. Sirtori, Degradation of the anticancer drug flutamide by solar photo-Fenton treatment at near-neutral pH: Identification of transformation products and *in silico* (Q)SAR risk assessment, Environ. Res. 183 (2020) 109223. doi:10.1016/j.envres.2020.109223.

[80] D. Fatta-Kassinos, M.I. Vasquez, K. Kümmerer, Transformation products of pharmaceuticals in surface waters and wastewater formed during photolysis and advanced oxidation processes - Degradation, elucidation of byproducts and assessment of their biological potency, Chemosphere. 85 (2011) 693–709. doi:10.1016/j.chemosphere.2011.06.082.

[81] R. Salgado, V.J. Pereira, G. Carvalho, R. Soeiro, V. Gaffney, C. Almeida, V.V. Cardoso, E. Ferreira, M.J. Benoliel, T.A. Ternes, A. Oehmen, M.A.M. Reis, J.P. Noronha, Photodegradation kinetics and transformation products of ketoprofen, diclofenac and atenolol in pure water and treated wastewater, J. Hazard. Mater. 244–245 (2013) 516–527. doi:10.1016/j.jhazmat.2012.10.039.

[82] M. Huerta-Fontela, M.T. Galceran, F. Ventura, Occurrence and removal of pharmaceuticals and hormones through drinking water treatment, Water Res. 45 (2011) 1432–1442. doi:10.1016/j.watres.2010.10.036.

[83] S.B. Jonnalagadda, S. Nadupalli, Chlorine Dioxide for Bleaching, Industrial Applications and Water Treatment, Indian Chem. Eng. 56 (2014) 123–136. doi:10.1080/00194506.2014.881032.

[84] M. Diana, M. Felipe-Sotelo, T. Bond, Disinfection byproducts potentially responsible for the

association between chlorinated drinking water and bladder cancer: A review, Water Res. 162 (2019) 492–504. doi:10.1016/j.watres.2019.07.014.

[85] H. Wang, C. Hu, L. Liu, X. Xing, Interaction of ciprofloxacin chlorination products with bacteria in drinking water distribution systems, J. Hazard. Mater. 339 (2017) 174–181. doi:10.1016/j.jhazmat.2017.06.033.

[86] Y. Yang, J. Shi, Y. Yang, J. Yin, J. Zhang, B. Shao, Transformation of sulfamethazine during the chlorination disinfection process: Transformation, kinetics, and toxicology assessment, J. Environ. Sci. 76 (2019) 48–56. doi:10.1016/j.jes.2018.03.024.

[87] Q. Guo, Z. Du, B. Shao, Simulation and experimental study on the mechanism of the chlorination of azithromycin, J. Hazard. Mater. 359 (2018) 31–39. doi:10.1016/j.jhazmat.2018.07.024.

[88] N.H. El Najjar, M. Deborde, R. Journel, N.K. Vel Leitner, Aqueous chlorination of levofloxacin: Kinetic and mechanistic study, transformation product identification and toxicity, Water Res. 47 (2013) 121–129. doi:10.1016/j.watres.2012.09.035.

[89] M. Li, D. Wei, Y. Du, Acute toxicity evaluation for quinolone antibiotics and their chlorination disinfection processes, J. Environ. Sci. 26 (2014) 1837–1842. doi:10.1016/j.jes.2014.06.023.

[90] G. Hey, A. Ledin, J.L.C. Jansen, H.R. Andersen, Removal of pharmaceuticals in biologically treated wastewater by chlorine dioxide or peracetic acid, Environ. Technol. 33 (2012) 1041–1047. doi:10.1080/09593330.2011.606282.

[91] G. Hey, R. Grabic, A. Ledin, J. la Cour Jansen, H.R. Andersen, Oxidation of pharmaceuticals by chlorine dioxide in biologically treated wastewater, Chem. Eng. J. 185–186 (2012) 236–242. doi:10.1016/j.cej.2012.01.093.

[92] A.D. Nikolaou, S.K. Golfinopoulos, T.D. Lekkas, Formation of organic by-products during chlorination of natural waters, J. Environ. Monit. 4 (2002) 910–916. doi:10.1039/b202965k.

[93] N.K. Arora, Emerging Eco-friendly Green Technologies for Wastewater Treatment, 1st ed., Springer Nature, 2020. doi:10.1007/978-981-15-1390-9.

[94] J. Reungoat, M. Macova, B.I. Escher, S. Carswell, J.F. Mueller, J. Keller, Removal of micropollutants and reduction of biological activity in a full scale reclamation plant using ozonation and activated carbon filtration, Water Res. 44 (2010) 625–637. doi:10.1016/j.watres.2009.09.048.

[95] S.A. Snyder, S. Adham, A.M. Redding, F.S. Cannon, J. DeCarolis, J. Oppenheimer, E.C. Wert, Y. Yoon, Role of membranes and activated carbon in the removal of endocrine disruptors and pharmaceuticals, Desalination. 202 (2007) 156–181. doi:10.1016/j.desal.2005.12.052.

[96] J. Wicker, T. Lorsbach, M. Gütlein, E. Schmid, D. Latino, S. Kramer, K. Fenner, EnviPath - The environmental contaminant biotransformation pathway resource, Nucleic Acids Res. 44 (2016) D502–D508. doi:10.1093/nar/gkv1229.

[97] Z.N. Norvill, A. Shilton, B. Guieysse, Emerging contaminant degradation and removal in algal wastewater treatment ponds: Identifying the research gaps, J. Hazard. Mater. 313 (2016) 291–309. doi:10.1016/j.jhazmat.2016.03.085.

[98] M. Carballa, F. Omil, J.M. Lema, Removal of cosmetic ingredients and pharmaceuticals in sewage primary treatment, Water Res. 39 (2005) 4790–4796. doi:10.1016/j.watres.2005.09.018.

[99] C.F. Couto, L.C. Lange, M.C.S. Amaral, Occurrence, fate and removal of pharmaceutically active compounds (PhACs) in water and wastewater treatment plants—A review, J. Water Process Eng.

32 (2019) 100927. doi:10.1016/j.jwpe.2019.100927.

[100] Z. Zhang, X. Xie, Z. Yu, H. Cheng, Influence of chemical speciation on photochemical transformation of three fluoroquinolones (FQs) in water: Kinetics, mechanism, and toxicity of photolysis products, Water Res. 148 (2019) 19–29. doi:10.1016/j.watres.2018.10.027.

[101] M. Sturini, A. Speltini, F. Maraschi, L. Pretali, A. Profumo, E. Fasani, A. Albini, R. Migliavacca, E. Nucleo, Photodegradation of fluoroquinolones in surface water and antimicrobial activity of the photoproducts, Water Res. 46 (2012) 5575–5582. doi:10.1016/j.watres.2012.07.043.

[102] L. Ge, G. Na, S. Zhang, K. Li, P. Zhang, H. Ren, Z. Yao, New insights into the aquatic photochemistry of fluoroquinolone antibiotics: Direct photodegradation, hydroxyl-radical oxidation, and antibacterial activity changes, Sci. Total Environ. 527–528 (2015) 12–17. doi:10.1016/j.scitotenv.2015.04.099.

[103] A.S. Maia, A.R. Ribeiro, C.L. Amorim, J.C. Barreiro, Q.B. Cass, P.M.L. Castro, M.E. Tiritan, Degradation of fluoroquinolone antibiotics and identification of metabolites/transformation products by liquid chromatography-tandem mass spectrometry, J. Chromatogr. A. 1333 (2014) 87–98. doi:10.1016/j.chroma.2014.01.069.

[104] J.J. López-Peñalver, M. Sánchez-Polo, C. V. Gómez-Pacheco, J. Rivera-Utrilla, Photodegradation of tetracyclines in aqueous solution by using UV and UV/H_2O_2 oxidation processes, J. Chem. Technol. Biotechnol. 85 (2010) 1325–1333. doi:10.1002/jctb.2435.

[105] E.M. Cuerda-Correa, M.F. Alexandre-Franco, C. Fernández-González, Advanced Oxidation Processes for the Removal of Antibiotics from Water. An Overview, Water. 12 (2020) 102. doi:10.3390/w12010102.

[106] A. Nikolaou, S. Meric, D. Fatta, Occurrence patterns of pharmaceuticals in water and wastewater environments, Anal. Bioanal. Chem. 387 (2007) 1225–1234. doi:10.1007/s00216-006-1035-8.

[107] L. Rizzo, C. Manaia, C. Merlin, T. Schwartz, C. Dagot, M.C. Ploy, I. Michael, D. Fatta-Kassinos, Urban wastewater treatment plants as hotspots for antibiotic resistant bacteria and genes spread into the environment: A review, Sci. Total Environ. 447 (2013) 345–360. doi:10.1016/j.scitotenv.2013.01.032.

[108] D. Lucas, F. Castellet-Rovira, M. Villagrasa, M. Badia-Fabregat, D. Barceló, T. Vicent, G. Caminal, M. Sarrà, S. Rodríguez-Mozaz, The role of sorption processes in the removal of pharmaceuticals by fungal treatment of wastewater, Sci. Total Environ. 610–611 (2018) 1147–1153. doi:10.1016/j.scitotenv.2017.08.118.

[109] H. Li, X. Dong, E.B. da Silva, L.M. de Oliveira, Y. Chen, L.Q. Ma, Mechanisms of metal sorption by biochars: Biochar characteristics and modifications, Chemosphere. 178 (2017) 466–478. doi:10.1016/j.chemosphere.2017.03.072.

[110] M. Kah, G. Sigmund, F. Xiao, T. Hofmann, Sorption of ionizable and ionic organic compounds to biochar, activated carbon and other carbonaceous materials, Water Res. 124 (2017) 673–692. doi:10.1016/j.watres.2017.07.070.

[111] K.C. Hyland, E.R.V. Dickenson, J.E. Drewes, C.P. Higgins, Sorption of ionized and neutral emerging trace organic compounds onto activated sludge from different wastewater treatment configurations, Water Res. 46 (2012) 1958–1968. doi:10.1016/j.watres.2012.01.012.

[112] J. Stevens-Garmon, J.E. Drewes, S.J. Khan, J.A. McDonald, E.R.V. Dickenson, Sorption of emerging trace organic compounds onto wastewater sludge solids, Water Res. 45 (2011) 3417–3426. doi:10.1016/j.watres.2011.03.056.

[113] T. Alvarino, S. Suarez, J. Lema, F. Omil, Understanding the sorption and biotransformation of organic micropollutants in innovative biological wastewater treatment technologies, Sci. Total Environ. 615 (2018) 297–306. doi:10.1016/j.scitotenv.2017.09.278.

[114] D. Kaplan, Absorption and Adsorption of Heavy Metals by Microalgae, in: Handb. Microalgal Cult. Appl. Phycol. Biotechnol., 2nd ed., John Wiley & Sons, 2013: pp. 602–611. doi:10.1002/9781118567166.ch32.

[115] Y. Luo, W. Guo, H.H. Ngo, L.D. Nghiem, F.I. Hai, J. Zhang, S. Liang, X.C. Wang, A review on the occurrence of micropollutants in the aquatic environment and their fate and removal during wastewater treatment, Sci. Total Environ. 473–474 (2014) 619–641. doi:10.1016/j.scitotenv.2013.12.065.

[116] L. Gusmaroli, E. Mendoza, M. Petrovic, G. Buttiglieri, How do WWTPs operational parameters affect the removal rates of EU Watch list compounds?, Sci. Total Environ. 714 (2020). doi:10.1016/j.scitotenv.2020.136773.

[117] A. Joss, S. Zabczynski, A. Göbel, B. Hoffmann, D. Löffler, C.S. McArdell, T.A. Ternes, A. Thomsen, H. Siegrist, Biological degradation of pharmaceuticals in municipal wastewater treatment: Proposing a classification scheme, Water Res. 40 (2006) 1686–1696. doi:10.1016/j.watres.2006.02.014.

[118] S. Suárez, M. Carballa, F. Omil, J.M. Lema, How are pharmaceutical and personal care products (PPCPs) removed from urban wastewaters?, Rev. Environ. Sci. Biotechnol. 7 (2008) 125–138. doi:10.1007/s11157-008-9130-2.

[119] E.H. Kerns, L. Di, Chemical stability, in: Compr. Med. Chem. II, 1st ed., Elsevier Ltd, 2006: pp. 453–487. doi:10.1016/b0-08-045044-x/00138-3.

[120] A. Agüera, M.J. Martínez Bueno, A.R. Fernández-Alba, New trends in the analytical determination of emerging contaminants and their transformation products in environmental waters, Environ. Sci. Pollut. Res. 20 (2013) 3496–3515. doi:10.1007/s11356-013-1586-0.

[121] B.I. Escher, K. Fenner, Recent Advances in Environmental Risk Assessment of Transformation Products, Environ. Sci. Technol. 45 (2011) 3835–3847. doi:10.1021/es1030799.

[122] L. Yin, B. Wang, H. Yuan, S. Deng, J. Huang, Y. Wang, G. Yu, Pay special attention to the transformation products of PPCPs in environment, Emerg. Contam. 3 (2017) 69–75. doi:10.1016/j.emcon.2017.04.001.

[123] E.N. Evgenidou, I.K. Konstantinou, D.A. Lambropoulou, Occurrence and removal of transformation products of PPCPs and illicit drugs in wastewaters: A review, Sci. Total Environ. 505 (2015) 905–926. doi:10.1016/j.scitotenv.2014.10.021.

[124] M. la Farré, S. Pérez, L. Kantiani, D. Barceló, Fate and toxicity of emerging pollutants, their metabolites and transformation products in the aquatic environment, Trends Anal. Chem. 27 (2008) 991–1007. doi:10.1016/j.trac.2008.09.010.

[125] A.A. Deeb, S. Stephan, O.J. Schmitz, T.C. Schmidt, Suspect screening of micropollutants and their transformation products in advanced wastewater treatment, Sci. Total Environ. 601–602 (2017) 1247–1253. doi:10.1016/j.scitotenv.2017.05.271.

[126] J. Hollender, E.L. Schymanski, H.P. Singer, P.L. Ferguson, Nontarget Screening with High Resolution Mass Spectrometry in the Environment: Ready to Go?, Environ. Sci. Technol. 51 (2017) 11505–11512. doi:10.1021/acs.est.7b02184.

[127] Y. Picó, D. Barceló, Transformation products of emerging contaminants in the environment and high-resolution mass spectrometry: A new horizon, Anal. Bioanal. Chem. 407 (2015) 6257–6273. doi:10.1007/s00216-015-8739-6.

[128] E.L. Schymanski, H.P. Singer, J. Slobodnik, I.M. Ipolyi, P. Oswald, M. Krauss, T. Schulze, P. Haglund, T. Letzel, S. Grosse, N.S. Thomaidis, A. Bletsou, C. Zwiener, M. Ibáñez, T. Portolés, R. De Boer, M.J. Reid, M. Onghena, U. Kunkel, W. Schulz, A. Guillon, N. Noyon, G. Leroy, P. Bados, S. Bogialli, D. Stipaničev, P. Rostkowski, J. Hollender, Non-target screening with high-resolution mass spectrometry: Critical review using a collaborative trial on water analysis, Anal. Bioanal. Chem. 407 (2015) 6237–6255. doi:10.1007/s00216-015-8681-7.

[129] J. Aceña, S. Stampachiacchiere, S. Pérez, D. Barceló, Advances in liquid chromatography–high-resolution mass spectrometry for quantitative and qualitative environmental analysis, Anal. Bioanal. Chem. 407 (2015) 6289–6299. doi:10.1007/s00216-015-8852-6.

[130] F. Hernández, J. V. Sancho, M. Ibáñez, E. Abad, T. Portolés, L. Mattioli, Current use of high-resolution mass spectrometry in the environmental sciences, Anal. Bioanal. Chem. 403 (2012) 1251–1264. doi:10.1007/s00216-012-5844-7.

[131] M. Zedda, C. Zwiener, Is nontarget screening of emerging contaminants by LC-HRMS successful? A plea for compound libraries and computer tools, Anal. Bioanal. Chem. 403 (2012) 2493–2502. doi:10.1007/s00216-012-5893-y.

[132] F. Fenaille, P. Barbier Saint-Hilaire, K. Rousseau, C. Junot, Data acquisition workflows in liquid chromatography coupled to high resolution mass spectrometry-based metabolomics: Where do we stand?, J. Chromatogr. A. 1526 (2017) 1–12. doi:10.1016/j.chroma.2017.10.043.

[133] R. Bade, N.I. Rousis, L. Bijlsma, E. Gracia-Lor, S. Castiglioni, J. V. Sancho, F. Hernandez, Screening of pharmaceuticals and illicit drugs in wastewater and surface waters of Spain and Italy by high resolution mass spectrometry using UHPLC-QTOF MS and LC-LTQ-Orbitrap MS, Anal. Bioanal. Chem. 407 (2015) 8979–8988. doi:10.1007/s00216-015-9063-x.

[134] E.L. Schymanski, J. Jeon, R. Gulde, K. Fenner, M. Ruff, H.P. Singer, J. Hollender, Identifying small molecules via high resolution mass spectrometry: Communicating confidence, Environ. Sci. Technol. 48 (2014) 2097–2098. doi:10.1021/es5002105.

[135] P. Gago-Ferrero, E.L. Schymanski, A.A. Bletsou, R. Aalizadeh, J. Hollender, N.S. Thomaidis, Extended Suspect and Non-Target Strategies to Characterize Emerging Polar Organic Contaminants in Raw Wastewater with LC-HRMS/MS, Environ. Sci. Technol. 49 (2015) 12333–12341. doi:10.1021/acs.est.5b03454.

[136] P. Gago-Ferrero, A. Krettek, S. Fischer, K. Wiberg, L. Ahrens, Suspect Screening and Regulatory Databases: A Powerful Combination to Identify Emerging Micropollutants, Environ. Sci. Technol. 52 (2018) 6881–6894. doi:10.1021/acs.est.7b06598.

[137] C. Moschet, A. Piazzoli, H. Singer, J. Hollender, Alleviating the reference standard dilemma using a systematic exact mass suspect screening approach with liquid chromatography-high resolution mass spectrometry, Anal. Chem. 85 (2013) 10312–10320. doi:10.1021/ac4021598.

[138] E.L. Schymanski, H.P. Singer, P. Longrée, M. Loos, M. Ruff, M.A. Stravs, C. Ripollés Vidal, J. Hollender, Strategies to characterize polar organic contamination in wastewater: Exploring the capability of high resolution mass spectrometry, Environ. Sci. Technol. 48 (2014) 1811–1818. doi:10.1021/es4044374.

[139] M. Krauss, H. Singer, J. Hollender, LC-high resolution MS in environmental analysis: From target

screening to the identification of unknowns, Anal. Bioanal. Chem. 397 (2010) 943–951. doi:10.1007/s00216-010-3608-9.

[140] M. Gros, S. Rodríguez-Mozaz, D. Barceló, Fast and comprehensive multi-residue analysis of a broad range of human and veterinary pharmaceuticals and some of their metabolites in surface and treated waters by ultra-high-performance liquid chromatography coupled to quadrupole-linear ion trap tandem, J. Chromatogr. A. 1248 (2012) 104–121. doi:10.1016/j.chroma.2012.05.084.

[141] R. Loos, R. Carvalho, D.C. António, S. Comero, G. Locoro, S. Tavazzi, B. Paracchini, M. Ghiani, T. Lettieri, L. Blaha, B. Jarosova, S. Voorspoels, K. Servaes, P. Haglund, J. Fick, R.H. Lindberg, D. Schwesig, B.M. Gawlik, EU-wide monitoring survey on emerging polar organic contaminants in wastewater treatment plant effluents, Water Res. 47 (2013) 6475–6487. doi:10.1016/j.watres.2013.08.024.

[142] A. Rubirola, M. Llorca, S. Rodriguez-Mozaz, N. Casas, I. Rodriguez-Roda, D. Barceló, G. Buttiglieri, Characterization of metoprolol biodegradation and its transformation products generated in activated sludge batch experiments and in full scale WWTPs, Water Res. 63 (2014) 21–32. doi:10.1016/j.watres.2014.05.031.

[143] J. Radjenović, S. Pérez, M. Petrović, D. Barceló, Identification and structural characterization of biodegradation products of atenolol and glibenclamide by liquid chromatography coupled to hybrid quadrupole time-of-flight and quadrupole ion trap mass spectrometry, J. Chromatogr. A. 1210 (2008) 142–153. doi:10.1016/j.chroma.2008.09.060.

[144] M. Gros, S. Rodríguez-Mozaz, D. Barceló, Rapid analysis of multiclass antibiotic residues and some of their metabolites in hospital, urban wastewater and river water by ultra-high-performance liquid chromatography coupled to quadrupole-linear ion trap tandem mass spectrometry, J. Chromatogr. A. 1292 (2013) 173–188. doi:10.1016/j.chroma.2012.12.072.

[145] A. Jia, Y. Wan, Y. Xiao, J. Hu, Occurrence and fate of quinolone and fluoroquinolone antibiotics in a municipal sewage treatment plant, Water Res. 46 (2012) 387–394. doi:10.1016/j.watres.2011.10.055.

[146] E. Zuccato, S. Castiglioni, R. Bagnati, M. Melis, R. Fanelli, Source, occurrence and fate of antibiotics in the Italian aquatic environment, J. Hazard. Mater. 179 (2010) 1042–1048. doi:10.1016/j.jhazmat.2010.03.110.

[147] S. Babić, D. Mutavdžić Pavlović, D. Ašperger, M. Periša, M. Zrnčić, A.J.M. Horvat, M. Kaštelan-Macan, Determination of multi-class pharmaceuticals in wastewater by liquid chromatography-tandem mass spectrometry (LC-MS-MS), Anal. Bioanal. Chem. 398 (2010) 1185–1194. doi:10.1007/s00216-010-4004-1.

[148] L. Ferrando-Climent, N. Collado, G. Buttiglieri, M. Gros, I. Rodriguez-Roda, S. Rodriguez-Mozaz, D. Barceló, Comprehensive study of ibuprofen and its metabolites in activated sludge batch experiments and aquatic environment, Sci. Total Environ. 438 (2012) 404–413. doi:10.1016/j.scitotenv.2012.08.073.

[149] M.J. García-Galán, M. Petrovic, S. Rodríguez-Mozaz, D. Barceló, Multiresidue trace analysis of pharmaceuticals, their human metabolites and transformation products by fully automated on-line solid-phase extraction-liquid chromatography-tandem mass spectrometry, Talanta. 158 (2016) 330–341. doi:10.1016/j.talanta.2016.05.061.

[150] L. Chibwe, I.A. Titaley, E. Hoh, S.L.M. Simonich, Integrated Framework for Identifying Toxic Transformation Products in Complex Environmental Mixtures, Environ. Sci. Technol. Lett. 4

(2017) 32–43. doi:10.1021/acs.estlett.6b00455.

[151] J. Sanchís, A. Jaén-Gil, P. Gago-Ferrero, E. Munthali, M.J. Farré, Characterization of organic matter by HRMS in surface waters: Effects of chlorination on molecular fingerprints and correlation with DBP formation potential, Water Res. 176 (2020) 115743. doi:10.1016/j.watres.2020.115743.

[152] M.J. Farré, A. Jaén-Gil, J. Hawkes, M. Petrovic, N. Catalán, Orbitrap molecular fingerprint of dissolved organic matter in natural waters and its relationship with NDMA formation potential, Sci. Total Environ. 670 (2019) 1019–1027. doi:10.1016/ j.scitotenv.2019.03.280.

[153] Y. Verkh, M. Rozman, M. Petrovic, A non-targeted high-resolution mass spectrometry data analysis of dissolved organic matter in wastewater treatment, Chemosphere. 200 (2018) 397–404. doi:10.1016/j.chemosphere.2018.02.095.

[154] O. Brock, R. Helmus, K. Kalbitz, B. Jansen, Non-target screening of leaf litter-derived dissolved organic matter using liquid chromatography coupled to high-resolution mass spectrometry (LC-QTOF-MS), Eur. J. Soil Sci. 71 (2020) 420–432. doi:10.1111/ejss.12894.

[155] M. Llorca, S. Rodríguez-Mozaz, O. Couillerot, K. Panigoni, J. de Gunzburg, S. Bayer, R. Czaja, D. Barceló, Identification of new transformation products during enzymatic treatment of tetracycline and erythromycin antibiotics at laboratory scale by an on-line turbulent flow liquid-chromatography coupled to a high resolution mass spectrometer LTQ-Orbitrap, Chemosphere. 119 (2015) 90–98. doi:10.1016/j.chemosphere.2014.05.072.

[156] L. Ferrando-Climent, R. Gonzalez-Olmos, A. Anfruns, I. Aymerich, L. Corominas, D. Barceló, S. Rodriguez-Mozaz, Elimination study of the chemotherapy drug tamoxifen by different advanced oxidation processes: Transformation products and toxicity assessment, Chemosphere. 168 (2017) 284–292. doi:10.1016/j.chemosphere.2016.10.057.

[157] M. Llorca, F. Castellet-rovira, M.-J. Farré, A. Jaén-Gil, M. Martínez-Alonso, S. Rodríguez-Mozaz, M. Sarrà, D. Barceló, Fungal biodegradation of the N-nitrosodimethylamine precursors venlafaxine and O-desmethylvenlafaxine in water, Environ. Pollut. 246 (2019) 346–356. doi:10.1016/j.envpol.2018.12.008.

[158] A.M. Brunner, C. Bertelkamp, M.M.L. Dingemans, A. Kolkman, B. Wols, D. Harmsen, W. Siegers, B.J. Martijn, W.A. Oorthuizen, T.L. ter Laak, Integration of target analyses, non-target screening and effect-based monitoring to assess OMP related water quality changes in drinking water treatment, Sci. Total Environ. 705 (2020) 135779. doi:10.1016/j.scitotenv.2019.135779.

[159] R. Avagyan, M. Åberg, R. Westerholm, Suspect screening of OH-PAHs and non-target screening of other organic compounds in wood smoke particles using HR-Orbitrap-MS, Chemosphere. 163 (2016) 313–321. doi:10.1016/j.chemosphere.2016.08.039.

[160] M. Llorca, D. Lucas, L. Ferrando-Climent, M. Badia-Fabregat, C. Cruz-Morató, D. Barceló, S. Rodríguez-Mozaz, Suspect screening of emerging pollutants and their major transformation products in wastewaters treated with fungi by liquid chromatography coupled to a high resolution mass spectrometry, J. Chromatogr. A. 1439 (2016) 124–136. doi:10.1016/j.chroma.2015.10.077.

[161] L.H.M.L.M. Santos, A.L. Maulvault, A. Jaén-Gil, A. Marques, D. Barceló, S. Rodríguez-Mozaz, Insights on the metabolization of the antidepressant venlafaxine by meagre (*Argyrosomus regius*) using a combined target and suspect screening approach, Sci. Total Environ. 737 (2020) 140226. doi:10.1016/j.scitotenv.2020.140226.

[162] A.M. Brunner, D. Vughs, W. Siegers, C. Bertelkamp, R. Hofman-Caris, A. Kolkman, T. ter Laak, Monitoring transformation product formation in the drinking water treatments rapid sand filtration and ozonation, Chemosphere. 214 (2019) 801–811. doi:10.1016/j.chemosphere.2018.09.140.

[163] A. Jaén-Gil, L. Ferrando-Climent, I. Ferrer, E.M. Thurman, S. Rodríguez-Mozaz, D. Barceló, C. Escudero-Oñate, Sustainable microalgae-based technology for biotransformation of benzalkonium chloride in oil and gas produced water: A laboratory-scale study, Sci. Total Environ. 748 (2020) 141526. doi:10.1016/j.scitotenv.2020.141526.

[164] N. Golan-Rozen, B. Seiwert, C. Riemenschneider, T. Reemtsma, B. Chefetz, Y. Hadar, Transformation Pathways of the Recalcitrant Pharmaceutical Compound Carbamazepine by the White-Rot Fungus *Pleurotus ostreatus*: Effects of Growth Conditions, Environ. Sci. Technol. 49 (2015) 12351–12362. doi:10.1021/acs.est.5b02222.

[165] A. Hom-Diaz, M. Llorca, S. Rodríguez-Mozaz, T. Vicent, D. Barceló, P. Blánquez, Microalgae cultivation on wastewater digestate: β-estradiol and 17α-ethynylestradiol degradation and transformation products identification, J. Environ. Manage. 155 (2015) 106–113. doi:10.1016/j.jenvman.2015.03.003.

[166] V.G. Beretsou, A.K. Psoma, P. Gago-Ferrero, R. Aalizadeh, K. Fenner, N.S. Thomaidis, Identification of biotransformation products of citalopram formed in activated sludge, Water Res. 103 (2016) 205–214. doi:10.1016/j.watres.2016.07.029.

[167] M. Llorca, M. Badia-Fabregat, S. Rodríguez-Mozaz, G. Caminal, T. Vicent, D. Barceló, Fungal treatment for the removal of endocrine disrupting compounds from reverse osmosis concentrate: Identification and monitoring of transformation products of benzotriazoles, Chemosphere. 184 (2017) 1054–1070. doi:10.1016/j.chemosphere.2017.06.053.

[168] T. Kosjek, N. Negreira, E. Heath, M. López de Alda, D. Barceló, Aerobic activated sludge transformation of vincristine and identification of the transformation products, Sci. Total Environ. 610–611 (2018) 892–904. doi:10.1016/j.scitotenv.2017.08.061.

[169] S. Terzic, N. Udikovic-kolic, T. Jurina, I. Krizman-Matasic, I. Senta, I. Mihaljevic, J. Loncar, T. Smital, M. Ahel, Biotransformation of macrolide antibiotics using enriched activated sludge culture: Kinetics, transformation routes and ecotoxicological evaluation, J. Hazard. Mater. 349 (2018) 143–152. doi:10.1016/j.jhazmat.2018.01.055.

[170] B. Chefetz, R. Marom, O. Salton, M. Oliferovsky, V. Mordehay, J. Ben-Ari, Y. Hadar, Transformation of lamotrigine by white-rot fungus *Pleurotus ostreatus*, Environ. Pollut. 250 (2019) 546–553. doi:10.1016/j.envpol.2019.04.057.

[171] C. Kiki, A. Rashid, Y. Wang, Y. Li, Q. Zeng, C.P. Yu, Q. Sun, Dissipation of antibiotics by microalgae: Kinetics, identification of transformation products and pathways, J. Hazard. Mater. 387 (2020) 121985. doi:10.1016/j.jhazmat.2019.121985.

[172] A. Jelic, I. Michael, A. Achilleos, E. Hapeshi, D. Lambropoulou, S. Perez, M. Petrovic, D. Fatta-Kassinos, D. Barcelo, Transformation products and reaction pathways of carbamazepine during photocatalytic and sonophotocatalytic treatment, J. Hazard. Mater. 263 (2013) 177–186. doi:10.1016/j.jhazmat.2013.07.068.

[173] D. Šojić, V. Despotović, D. Orčić, E. Szabó, E. Arany, S. Armaković, E. Illés, K. Gajda-Schrantz, A. Dombi, T. Alapi, E. Sajben-Nagy, A. Palágyi, C. Vágvölgyi, L. Manczinger, L. Bjelica, B. Abramović, Degradation of thiamethoxam and metoprolol by UV, O_3 and UV/O_3 hybrid processes: Kinetics, degradation intermediates and toxicity, J. Hydrol. 472–473 (2012) 314–327.

doi:10.1016/j.jhydrol.2012.09.038.

[174] M.J. García-Galán, A. Anfruns, R. Gonzalez-Olmos, S. Rodriguez-Mozaz, J. Comas, Advanced oxidation of the antibiotic sulfapyridine by UV/H_2O_2: Characterization of its transformation products and ecotoxicological implications, Chemosphere. 147 (2016) 451–459. doi:10.1016/j.chemosphere.2015.12.108.

[175] B. Yang, R.S. Kookana, M. Williams, G.G. Ying, J. Du, H. Doan, A. Kumar, Oxidation of ciprofloxacin and enrofloxacin by ferrate(VI): Products identification, and toxicity evaluation, J. Hazard. Mater. 320 (2016) 296–303. doi:10.1016/j.jhazmat.2016.08.040.

[176] I. Carpinteiro, R. Rodil, J.B. Quintana, R. Cela, Reaction of diazepam and related benzodiazepines with chlorine. Kinetics, transformation products and *in-silico* toxicological assessment, Water Res. 120 (2017) 280–289. doi:10.1016/j.watres.2017.04.063.

[177] M. Voigt, M. Jaeger, On the photodegradation of azithromycin, erythromycin and tylosin and their transformation products – A kinetic study, Sustain. Chem. Pharm. 5 (2017) 131–140. doi:10.1016/j.scp.2016.12.001.

[178] A. Gupta, A. Garg, Degradation of ciprofloxacin using Fenton's oxidation: Effect of operating parameters, identification of oxidized by-products and toxicity assessment, Chemosphere. 193 (2018) 1181–1188. doi:10.1016/j.chemosphere.2017.11.046.

[179] Y. Han, M. Ma, N. Li, R. Hou, C. Huang, Y. Oda, Z. Wang, Chlorination, chloramination and ozonation of carbamazepine enhance cytotoxicity and genotoxicity: Multi-endpoint evaluation and identification of its genotoxic transformation products, J. Hazard. Mater. 342 (2018) 679–688. doi:10.1016/j.jhazmat.2017.08.076.

[180] Y. Yang, Y. Cao, J. Jiang, X. Lu, J. Ma, S. Pang, J. Li, Y. Liu, Y. Zhou, C. Guan, Comparative study on degradation of propranolol and formation of oxidation products by UV/H_2O_2 and UV/persulfate (PDS), Water Res. 149 (2019) 543–552. doi:10.1016/j.watres.2018.08.074.

[181] J. Hollman, J.A. Dominic, G. Achari, Degradation of pharmaceutical mixtures in aqueous solutions using UV/peracetic acid process: Kinetics, degradation pathways and comparison with UV/H_2O_2, Chemosphere. 248 (2020) 125911. doi:10.1016/j.chemosphere.2020.125911.

[182] P. Gago-Ferrero, A.A. Bletsou, D.E. Damalas, R. Aalizadeh, N.A. Alygizakis, H.P. Singer, J. Hollender, N.S. Thomaidis, Wide-scope target screening of >2000 emerging contaminants in wastewater samples with UPLC-Q-ToF-HRMS/MS and smart evaluation of its performance through the validation of 195 selected representative analytes, J. Hazard. Mater. 387 (2020) 121712. doi:10.1016/j.jhazmat.2019.121712.

[183] A. Ccanccapa-Cartagena, Y. Pico, X. Ortiz, E.J. Reiner, Suspect, non-target and target screening of emerging pollutants using data independent acquisition: Assessment of a Mediterranean River basin, Sci. Total Environ. 687 (2019) 355–368. doi:10.1016/j.scitotenv.2019.06.057.

[184] J.D. Canterbury, G.E. Merrihew, M.J. MacCoss, D.R. Goodlett, S.A. Shaffer, Comparison of data acquisition strategies on quadrupole ion trap instrumentation for shotgun proteomics, J. Am. Soc. Mass Spectrom. 25 (2014) 2048–2059. doi:10.1007/s13361-014-0981-1.

[185] S. Perez, P. Eichhorn, D. Barcelo, Applications of Time-of-Flight and Orbitrap Mass Spectrometry in Environmental, Food, Doping, and Forensic Analysis, 1st ed., Elsevier B.V., 2016.

[186] T. Cai, C. Wu, Q. Ruan, S. Ma, M. Zhu, High-resolution mass spectrometry-based data acquisition and data-mining technologies for detecting and characterizing drug metabolites and traditional Chinese medicine components, 2nd ed., Elsevier B.V., 2020. doi:10.1016/b978-0-12-820018-

6.00003-x.

[187] S. Ma, S.K. Chowdhury, Data acquisition and data mining techniques for metabolite identification using LC coupled to high-resolution MS, Bioanalysis. 5 (2013) 1285–1297. doi:10.4155/bio.13.103.

[188] C. Vannini, G. Domingo, M. Marsoni, F. De Mattia, M. Labra, S. Castiglioni, M. Bracale, Effects of a complex mixture of therapeutic drugs on unicellular algae *Pseudokirchneriella subcapitata*, Aquat. Toxicol. 101 (2011) 459–465. doi:10.1016/j.aquatox.2010.10.011.

[189] Y. Ji, C. Ferronato, A. Salvador, X. Yang, J.M. Chovelon, Degradation of ciprofloxacin and sulfamethoxazole by ferrous-activated persulfate: Implications for remediation of groundwater contaminated by antibiotics, Sci. Total Environ. 472 (2014) 800–808. doi:10.1016/j.scitotenv.2013.11.008.

[190] M. Katajamaa, J. Miettinen, M. Orešič, MZmine: Toolbox for processing and visualization of mass spectrometry based molecular profile data, Bioinformatics. 22 (2006) 634–636. doi:10.1093/bioinformatics/btk039.

[191] M. Katajamaa, M. Orešič, Processing methods for differential analysis of LC/MS profile data, BMC Bioinformatics. 6 (2005) 179. doi:10.1186/1471-2105-6-179.

[192] C.A. Smith, E.J. Want, G. O'Maille, R. Abagyan, G. Siuzdak, XCMS: Processing mass spectrometry data for metabolite profiling using nonlinear peak alignment, matching, and identification, Anal. Chem. 78 (2006) 779–787. doi:10.1021/ac051437y.

[193] T. Pluskal, S. Castillo, A. Villar-Briones, M. Orešič, MZmine 2: Modular framework for processing, visualizing, and analyzing mass spectrometry-based molecular profile data, BMC Bioinformatics. 11 (2010) 395. doi:10.1186/1471-2105-11-395.

[194] R. Díaz, M. Ibáñez, J. V. Sancho, F. Hernández, Target and non-target screening strategies for organic contaminants, residues and illicit substances in food, environmental and human biological samples by UHPLC-QTOF-MS, Anal. Methods. 4 (2012) 196–209. doi:10.1039/C1AY05385J.

[195] Y. Moriya, D. Shigemizu, M. Hattori, T. Tokimatsu, M. Kotera, S. Goto, M. Kanehisa, PathPred: An enzyme-catalyzed metabolic pathway prediction server, Nucleic Acids Res. 38 (2010) 138–143. doi:10.1093/nar/gkq318.

[196] J. Guo, D. Deng, Y. Wang, H. Yu, W. Shi, Extended suspect screening strategy to identify characteristic toxicants in the discharge of a chemical industrial park based on toxicity to *Daphnia magna*, Sci. Total Environ. 650 (2019) 10–17. doi:10.1016/j.scitotenv.2018.08.215.

[197] J. Jimenez-Villarin, A. Serra-Clusellas, C. Martínez, A. Conesa, J. Garcia-Montaño, E. Moyano, Liquid chromatography coupled to tandem and high resolution mass spectrometry for the characterisation of ofloxacin transformation products after titanium dioxide photocatalysis, J. Chromatogr. A. 1443 (2016) 201–210. doi:10.1016/j.chroma.2016.03.063.

[198] C. Hug, N. Ulrich, T. Schulze, W. Brack, M. Krauss, Identification of novel micropollutants in wastewater by a combination of suspect and nontarget screening, Environ. Pollut. 184 (2014) 25–32. doi:10.1016/j.envpol.2013.07.048.

[199] N.A. Alygizakis, J. Urík, V.G. Beretsou, I. Kampouris, A. Galani, M. Oswaldova, T. Berendonk, P. Oswald, N.S. Thomaidis, J. Slobodnik, B. Vrana, D. Fatta-Kassinos, Evaluation of chemical and biological contaminants of emerging concern in treated wastewater intended for agricultural reuse, Environ. Int. 138 (2020) 105597. doi:10.1016/j.envint.2020.105597.

[200] S.H. López, M.M. Ulaszewska, M.D. Hernando, M.J. Martínez-Bueno, M.J. Gómez, A.R. Fernández-Alba, Post-acquisition data processing for the screening of transformation products of different organic contaminants. Two-year monitoring of river water using LC-ESI-QTOF-MS and GCxGC-EI-TOF-MS, Environ. Sci. Pollut. Res. 21 (2014) 12583–12604. doi:10.1007/s11356-014-3187-y.

[201] S. Kern, K. Fenner, H.P. Singer, R.P. Schwarzenbach, J. Hollender, Identification of transformation products of organic contaminants in natural waters by computer-aided prediction and high-resolution mass spectrometry, Environ. Sci. Technol. 43 (2009) 7039–7046. doi:10.1021/es901979h.

[202] A. Jia, B.I. Escher, F.D.L. Leusch, J.Y.M. Tang, E. Prochazka, B. Dong, E.M. Snyder, S.A. Snyder, *In vitro* bioassays to evaluate complex chemical mixtures in recycled water, Water Res. 80 (2015) 1–11. doi:10.1016/j.watres.2015.05.020.

[203] L. Ferrando-Climent, C. Cruz-Morató, E. Marco-Urrea, T. Vicent, M. Sarrà, S. Rodriguez-Mozaz, D. Barceló, Non conventional biological treatment based on *Trametes versicolor* for the elimination of recalcitrant anticancer drugs in hospital wastewater, Chemosphere. 136 (2015) 9–19. doi:10.1016/j.chemosphere.2015.03.051.

[204] J.B. Carbajo, A.L. Petre, R. Rosal, S. Herrera, P. Letón, E. García-Calvo, A.R. Fernández-Alba, J.A. Perdigón-Melón, Continuous ozonation treatment of ofloxacin: Transformation products, water matrix effect and aquatic toxicity, J. Hazard. Mater. 292 (2015) 34–43. doi:10.1016/j.jhazmat.2015.02.075.

[205] J.J. García-Galán, A. Anfruns, R. Gonzalez-Olmos, S. Rodríguez-Mozaz, J. Comas, UV/H_2O_2 degradation of the antidepressants venlafaxine and O-desmethylvenlafaxine: Elucidation of their transformation pathway and environmental fate, J. Hazard. Mater. 311 (2016) 70–80. doi:10.1016/j.jhazmat.2016.02.070.

[206] T. Schulze, S. Weiss, E. Schymanski, P.C. von der Ohe, M. Schmitt-Jansen, R. Altenburger, G. Streck, W. Brack, Identification of a phytotoxic photo-transformation product of diclofenac using effect-directed analysis, Environ. Pollut. 158 (2010) 1461–1466. doi:10.1016/j.envpol.2009.12.032.

[207] W. Brack, R. Altenburger, E. Küster, B. Meissner, K.D. Wenzel, G. Schüürmann, Identification of toxic products of anthracene photomodification in simulated sunlight, Environ. Toxicol. Chem. 22 (2003) 2228–2237. doi:10.1897/02-450.

[208] A. Cherkasov, E.N. Muratov, D. Fourches, A. Varnek, I.I. Baskin, M. Cronin, J. Dearden, P. Gramatica, Y.C. Martin, R. Todeschini, V. Consonni, V.E. Kuz'Min, R. Cramer, R. Benigni, C. Yang, J. Rathman, L. Terfloth, J. Gasteiger, A. Richard, A. Tropsha, QSAR modeling: Where have you been? Where are you going to?, J. Med. Chem. 57 (2014) 4977–5010. doi:10.1021/jm4004285.

[209] J.J. Villaverde, B. Sevilla-Morán, C. López-Goti, L. Calvo, J.L. Alonso-Prados, P. Sandín-España, Photolysis of clethodim herbicide and a formulation in aquatic environments: Fate and ecotoxicity assessment of photoproducts by QSAR models, Sci. Total Environ. 615 (2018) 643–651. doi:10.1016/j.scitotenv.2017.09.300.

[210] Z. Tousova, J. Froment, P. Oswald, J. Slobodník, K. Hilscherova, K. V. Thomas, K.E. Tollefsen, M. Reid, K. Langford, L. Blaha, Identification of algal growth inhibitors in treated waste water using effect-directed analysis based on non-target screening techniques, J. Hazard. Mater. 358 (2018) 494–502. doi:10.1016/j.jhazmat.2018.05.031.

[211] H. Yang, Y. Li, Y. Chen, G. Ye, X. Sun, Comparison of ciprofloxacin degradation in reclaimed water

by UV/chlorine and UV/persulfate advanced oxidation processes, Water Environ. Res. 91 (2019) 1576–1588. doi:10.1002/wer.1144.

[212] P.H. Secrétan, M. Karoui, Y. Levi, H. Sadou-Yayé, L. Tortolano, A. Solgadi, N. Yagoubi, B. Do, Pemetrexed degradation by photocatalytic process: Kinetics, identification of transformation products and estimation of toxicity, Sci. Total Environ. 624 (2018) 1082–1094. doi:10.1016/j.scitotenv.2017.12.182.

[213] R. Salgado, D. Brito, J.P. Noronha, B. Almeida, M.R. Bronze, A. Oehmen, G. Carvalho, M.T. Barreto Crespo, Metabolite identification of ibuprofen biodegradation by *Patulibacter medicamentivorans* under aerobic conditions, Environ. Technol. 41 (2020) 450–465. doi:10.1080/09593330.2018.1502362.

[214] T. Matsushita, S. Honda, T. Kuriyama, Y. Fujita, T. Kondo, Y. Matsui, N. Shirasaki, H. Takanashi, T. Kameya, Identification of mutagenic transformation products generated during oxidation of 3-methyl-4-nitrophenol solutions by orbitrap tandem mass spectrometry and quantitative structure–activity relationship analyses, Water Res. 129 (2018) 347–356. doi:10.1016/j.watres.2017.11.033.

[215] J. Menz, A.P. Toolaram, T. Rastogi, C. Leder, O. Olsson, K. Kümmerer, M. Schneider, Transformation products in the water cycle and the unsolved problem of their proactive assessment: A combined *in vitro*/*in silico* approach, Environ. Int. 98 (2017) 171–180. doi:10.1016/j.envint.2016.11.003.

[216] M. Čvančarová, M. Moeder, A. Filipová, T. Cajthaml, Biotransformation of fluoroquinolone antibiotics by ligninolytic fungi - Metabolites, enzymes and residual antibacterial activity, Chemosphere. 136 (2014) 311–320. doi:10.1016/j.chemosphere.2014.12.012.

[217] E.L. Schymanski, M. Bataineh, K.U. Goss, W. Brack, Integrated analytical and computer tools for structure elucidation in effect-directed analysis, Trends Anal. Chem. 28 (2009) 550–561. doi:10.1016/j.trac.2009.03.001.

[218] W. Brack, S. Ait-Aissa, R.M. Burgess, W. Busch, N. Creusot, C. Di Paolo, B.I. Escher, L. Mark Hewitt, K. Hilscherova, J. Hollender, H. Hollert, W. Jonker, J. Kool, M. Lamoree, M. Muschket, S. Neumann, P. Rostkowski, C. Ruttkies, J. Schollee, E.L. Schymanski, T. Schulze, T.B. Seiler, A.J. Tindall, G. De Aragão Umbuzeiro, B. Vrana, M. Krauss, Effect-directed analysis supporting monitoring of aquatic environments - An in-depth overview, Sci. Total Environ. 544 (2016) 1073–1118. doi:10.1016/j.scitotenv.2015.11.102.

[219] E. Simon, M.H. Lamoree, T. Hamers, J. de Boer, Challenges in effect-directed analysis with a focus on biological samples, Trends Anal. Chem. 67 (2015) 179–191. doi:10.1016/j.trac.2015.01.006.

[220] N. Bandow, R. Altenburger, U. Lübcke-Von Varel, A. Paschke, G. Streck, W. Brack, Partitioning-based dosing: An approach to include bioavailability in the effect-directed analysis of contaminated sediment samples, Environ. Sci. Technol. 43 (2009) 3891–3896. doi:10.1021/es803453h.

[221] W. Brack, Effect-directed analysis: a promising tool for the identification of organic toxicants in complex mixtures?, Anal. Bioanal. Chem. 377 (2003) 397–407. doi:10.1007/s00216-003-2139-z.

[222] W. Brack, M. Schmitt-Jansen, M. MacHala, R. Brix, D. Barceló, E. Schymanski, G. Streck, T. Schulze, How to confirm identified toxicants in effect-directed analysis, Anal. Bioanal. Chem. 390 (2008) 1959–1973. doi:10.1007/s00216-007-1808-8.

[223] M. Hecker, H. Hollert, Effect-directed analysis (EDA) in aquatic ecotoxicology: state of the art and future challenges, Environ. Sci. Pollut. Res. 16 (2009) 607–613. doi:10.1007/s11356-009-0229-y.

[224] S. Hong, J.P. Giesy, J. Lee, J. Lee, J.S. Khim, Effect-Directed Analysis: Current Status and Future Challenges, Ocean Sci. J. 51 (2016) 413–433. doi:10.1007/s12601-016-0038-4

[225] T. Schulze, S. Weiss, E. Schymanski, P.C. von der Ohe, M. Schmitt-Jansen, R. Altenburger, G. Streck, W. Brack, Identification of a phytotoxic photo-transformation product of diclofenac using effect-directed analysis, Environ. Pollut. 158 (2010) 1461–1466. doi:10.1016/j.envpol.2009.12.032.

[226] E.L. Schymanski, C. Meinert, M. Meringer, W. Brack, The use of MS classifiers and structure generation to assist in the identification of unknowns in effect-directed analysis, Anal. Chim. Acta. 615 (2008) 136–147. doi:10.1016/j.aca.2008.03.060.

[227] Y. Shao, H. Hollert, Z. Tarcai, B. Deutschmann, T.B. Seiler, Integrating bioassays, chemical analysis and *in silico* techniques to identify genotoxicants in surface water, Sci. Total Environ. 650 (2019) 3084–3092. doi:10.1016/j.scitotenv.2018.09.288.

[228] I. Oller, S. Malato, J.A. Sánchez-Pérez, Combination of Advanced Oxidation Processes and biological treatments for wastewater decontamination-A review, Sci. Total Environ. 409 (2011) 4141–4166. doi:10.1016/j.scitotenv.2010.08.061.

[229] F. Martínez, R. Molina, I. Rodríguez, M.I. Pariente, Y. Segura, J.A. Melero, Techno-economical assessment of coupling Fenton/biological processes for the treatment of a pharmaceutical wastewater, J. Environ. Chem. Eng. 6 (2018) 485–494. doi:10.1016/j.jece.2017.12.008.

[230] A.C. Vincenzo Naddeo, Wastewater Treatment by Combination of Advanced Oxidation Processes and Conventional Biological Systems, J. Bioremediation Biodegrad. 4 (2013) 1000208. doi:10.4172/2155-6199.1000208.

[231] O. Ganzenko, D. Huguenot, E.D. van Hullebusch, G. Esposito, M.A. Oturan, Electrochemical advanced oxidation and biological processes for wastewater treatment: A review of the combined approaches, Environ. Sci. Pollut. Res. 21 (2014) 8493–8524. doi:10.1007/s11356-014-2770-6.

[232] L. Qi, X. Wang, Q. Xu, Coupling of biological methods with membrane filtration using ozone as pre-treatment for water reuse, Desalination. 270 (2011) 264–268. doi:10.1016/j.desal.2010.11.054.

[233] I. Bavasso, C. Poggi, E. Petrucci, Enhanced degradation of paracetamol by combining UV with electrogenerated hydrogen peroxide and ozone, J. Water Process Eng. 34 (2020) 101102. doi:10.1016/j.jwpe.2019.101102.

[234] Z. Zhang, H. Chen, J. Wang, Y. Zhang, Degradation of carbamazepine by combined radiation and persulfate oxidation process, Radiat. Phys. Chem. 170 (2020) 108639. doi:10.1016/j.radphyschem.2019.108639.

[235] L.F. Angeles, R.A. Mullen, I.J. Huang, C. Wilson, W. Khunjar, H.I. Sirotkin, A.E. McElroy, D.S. Aga, Assessing pharmaceutical removal and reduction in toxicity provided by advanced wastewater treatment systems, Environ. Sci. Water Res. Technol. 6 (2020) 62–77. doi:10.1039/c9ew00559e.

[236] R. Changotra, H. Rajput, A. Dhir, Treatment of real pharmaceutical wastewater using combined approach of Fenton applications and aerobic biological treatment, J. Photochem. Photobiol. A Chem. 376 (2019) 175–184. doi:10.1016/j.jphotochem.2019.02.029.

[237] Y. Ouarda, B. Tiwari, A. Azaïs, M.A. Vaudreuil, S.D. Ndiaye, P. Drogui, R.D. Tyagi, S. Sauvé, M. Desrosiers, G. Buelna, R. Dubé, Synthetic hospital wastewater treatment by coupling submerged membrane bioreactor and electrochemical advanced oxidation process: Kinetic study and toxicity assessment, Chemosphere. 193 (2018) 160–169. doi:10.1016/j.chemosphere.2017.11.010.

[238] R. Changotra, H. Rajput, J.P. Guin, S.A. Khader, A. Dhir, Techno-economical evaluation of coupling ionizing radiation and biological treatment process for the remediation of real pharmaceutical wastewater, J. Clean. Prod. 242 (2020) 118544. doi:10.1016/j.jclepro.2019.118544.

[239] I. Oller, S. Malato, J.A. Sánchez-Pérez, M.I. Maldonado, R. Gassó, Detoxification of wastewater containing five common pesticides by solar AOPs-biological coupled system, Catal. Today. 129 (2007) 69–78. doi:10.1016/j.cattod.2007.06.055.

[240] N. Collado, S. Rodriguez-Mozaz, M. Gros, A. Rubirola, D. Barceló, J. Comas, I. Rodriguez-Roda, G. Buttiglieri, Pharmaceuticals occurrence in a WWTP with significant industrial contribution and its input into the river system, Environ. Pollut. 185 (2014) 202–212. doi:10.1016/j.envpol.2013.10.040.

[241] B.I. Escher, H.M. Stapleton, E.L. Schymanski, Tracking complex mixtures of chemicals in our changing environment, Science. 367 (2020) 388–392. doi:10.1126/science.aay6636.

[242] A. Kortenkamp, Low dose mixture effects of endocrine disrupters and their implications for regulatory thresholds in chemical risk assessment, Curr. Opin. Pharmacol. 19 (2014) 105–111. doi:10.1016/j.coph.2014.08.006.

[243] N. Cedergreen, Quantifying synergy: A systematic review of mixture toxicity studies within environmental toxicology, PLoS One. 9 (2014) e96580. doi:10.1371/journal.pone.0096580.

[244] A. Boobis, R. Budinsky, S. Collie, K. Crofton, M. Embry, S. Felter, R. Hertzberg, D. Kopp, G. Mihlan, M. Mumtaz, P. Price, K. Solomon, L. Teuschler, R. Yang, R. Zaleski, Critical analysis of literature on low-dose synergy for use in screening chemical mixtures for risk assessment, Crit. Rev. Toxicol. 41 (2011) 369–383. doi:10.3109/10408444.2010.543655.

[245] F. Klont, S. Jahn, C. Grivet, S. König, R. Bonner, G. Hopfgartner, SWATH data independent acquisition mass spectrometry for screening of xenobiotics in biological fluids: Opportunities and challenges for data processing, Talanta. 211 (2020) 120747. doi:10.1016/j.talanta.2020.120747.

[246] M. Bern, G. Finney, M.R. Hoopmann, G. Merrihew, M.J. Toth, M.J. MacCoss, Deconvolution of mixture spectra from ion-trap data-independent-acquisition tandem mass spectrometry, Anal. Chem. 82 (2010) 833–841. doi:10.1021/ac901801b.

[247] R. Peckner, S.A. Myers, A.S.V. Jacome, J.D. Egertson, J.G. Abelin, M.J. MacCoss, S.A. Carr, J.D. Jaffe, Specter: Linear deconvolution for targeted analysis of data-independent acquisition mass spectrometry proteomics, Nat. Methods. 15 (2018) 371–378. doi:10.1038/nmeth.4643.

[248] H. Tsugawa, T. Cajka, T. Kind, Y. Ma, B. Higgins, K. Ikeda, M. Kanazawa, J. Vandergheynst, O. Fiehn, M. Arita, MS-DIAL: Data-independent MS/MS deconvolution for comprehensive metabolome analysis, Nat. Methods. 12 (2015) 523–526. doi:10.1038/nmeth.3393.

[249] Y. Yin, R. Wang, Y. Cai, Z. Wang, Z.J. Zhu, DecoMetDIA: Deconvolution of Multiplexed MS/MS Spectra for Metabolite Identification in SWATH-MS-Based Untargeted Metabolomics, Anal. Chem. 91 (2019) 11897–11904. doi:10.1021/acs.analchem.9b02655.

[250] S. Samanipour, M.J. Reid, K. Bæk, K. V. Thomas, Combining a Deconvolution and a Universal Library Search Algorithm for the Nontarget Analysis of Data-Independent Acquisition Mode Liquid Chromatography-High-Resolution Mass Spectrometry Results, Environ. Sci. Technol. 52 (2018) 4694–4701. doi:10.1021/acs.est.8b00259.

[251] I. Nikolskiy, N.G. Mahieu, Y.J. Chen, R. Tautenhahn, G.J. Patti, An untargeted metabolomic workflow to improve structural characterization of metabolites, Anal. Chem. 85 (2013) 7713–7719. doi:10.1021/ac400751j.

Chapter 10

Supplementary information

SUPPLEMENTARY MATERIAL

Fungal treatment of metoprolol and its recalcitrant metabolite metoprolol acid in hospital wastewater: biotransformation, sorption and ecotoxicological impact

Adrián Jaén-Gil[a], Francesc Castellet-Rovira[b], Marta Llorca[c], Marta Villagrasa[a], Montserrat Sarrà[b], Sara Rodríguez-Mozaz[a*], Damià Barceló[a, c]

[a] *Catalan Institute for Water Research (ICRA), H_2O Building, Scientific and Technological Park of the University of Girona, Emili Grahit 101, E-17003 Girona, Spain*

[b] *Chemical, Biological and Environmental Engineering Department, Universitat Autònoma de Barcelona (UAB), E-08193 Bellaterra, Spain*

[c] *Water and Soil Quality Research Group, Department of Environmental Chemistry, IDAEA-CSIC, Jordi Girona 18-26, E-08034 Barcelona, Spain*

S1. Sample treatment

Hospital wastewater samples from FBB bioreactors were treated following an SPE methodology described elsewhere (Gros et al., 2012). Firstly, samples were filtered through 1 µm glass fiber filters followed by 0.45 µm PVDF membrane filters (Millipore; Billerica, MA, USA). Then, 25 and 50 mL of sample at initial and final time respectively were used adding the appropriate volume of Na_2EDTA. Samples were loaded into the SPE cartridges and conditioned with 5 mL of methanol followed by 5 mL of HPLC grade water. Cartridges were rinsed with 6 mL of HPLC grade water and further dried with air for 5 minutes to remove the remaining water. Finally, elution was carried out using 6 mL of pure methanol. Extracts were reconstituted in 100 µL of methanol/water (10:90, v/v) containing internal standard to a final concentration of 100 µg/L in vial.

Fungal biomass samples from FBB bioreactors were treated following the solid extraction methodology reported previously (Lucas et al., 2018). Firstly, samples were freeze dried and homogenized using a mortar. Then, 4 mL of methanol/Na_2EDTA (50:1.5, v/v) were added to 1 g of biomass and vortexed for 30 s. Samples were sonicated for 3 min and centrifuged at 1500 rpm for 5 min at 5 °C. The supernatant was decanted and the procedure was repeated twice more with 3 mL of methanol/Na_2EDTA each time. The total resulting supernatant was centrifuged at 3200 rpm for 20 min and filtered with PVDF membrane filters. Extracts were evaporated under nitrogen stream using a Reacti-Therm 18,824 system (Thermo Scientific) and reconstituted in 100 µL of methanol/water (10:90, v/v) containing internal standard to a final concentration of 100 µg/L in vial.

S2. Instrumental analysis

Chromatographic separation was carried out by using an Aria TLX-1 chromatographic system (Thermo Fisher Scientific) comprising a PAL auto sampler and two mixing quaternary pumps (eluting pump and loading pump). 20 µL of water sample were injected. The chromatographic separation was performed in a ZORBAX Eclipse XDB-C18 (150 mm × 4.6 mm, 5 µm; Agilent Technologies, Santa Clara, CA). The optimized chromatographic gradient was water with ammonium formate (10 mM, pH 3.0) (A) and acetonitrile (B). Solvent gradient was performed as follows: initial mobile phase composition (95% A) held for 1 min, followed by a decrease in composition A to 5% within 9 min, then to 0% in 3 min, held for 2 min, and finally up to 95% in 1 min and held for 1 min. The total MS run time was 17 min.

The high-resolution mass spectrometer LTQ-OrbitrapVelos™ (Thermo Fisher Scientific) was equipped with a heated electrospray ionization source (HESI-II). Analyses were carried out in positive and negative ionization mode. As no results were observed in negative mode, data collected was processed in positive mode only. Samples were acquired through full scan from *m/z* 100 to 1000 range at a resolving power of 60,000 FWHM. MS/MS full scan fragmentation data was acquired in Data Dependent Acquisition mode (DDA) at 30,000 FWHM from *m/z* 50 to 500 range. The compounds selected for fragmentation were those most intense included in a ready-made ion list of tentative transformation products selected from literature and included prior to analysis (Table S1). The conditions for HESI-II were designed as follows: spray voltage at 3.5 kV, source heater temperature at 300 ˚C, capillary temperature at 350 ˚C, sheath gas flow at 40 and auxiliary gas flow at 20 (arbitrary units). Fragmentation techniques selected were: collision-induced dissociation (CID) at a normalized collision energy of 30 eV (activation Q of 0.250 and an activation time of 30 ms) and higher-energy collisional dissociation (HCD) at a normalized collision energy of 55 eV (activation time of 0.100 ms) in an isolation width of 2 Da. The entire system was controlled via Aria software under Xcalibur 2.1.

S3. Pre-acquisition ion list

Table S1. Pre-acquisition list of tentative transformation products gathered from literature.

Name	Molecular formula $[M+H]^+$	Exact mass $[M+H]^+$	References
MTP	$C_{15}H_{26}NO_3$	268.19072	(Rubirola et al., 2014)
MTPA	$C_{14}H_{22}NO_4$	268.15433	(Rubirola et al., 2014)
TP74	$C_4H_{12}N$	74.09643	(Romero et al., 2016b)
TP102	$C_5H_{12}NO$	102.09134	(Wilde et al., 2014)
TP112	$C_6H_{10}NO$	112.07569	(Wilde et al., 2014)
TP114	$C_6H_{12}NO$	114.09134	(Wilde et al., 2014)
TP116	$C_6H_{14}NO$	116.10699	(Cavalcante et al., 2015; Romero et al., 2016a, 2016b)
TP118	$C_6H_{16}NO$	118.12264	(Romero et al., 2016b, 2015)
TP120	$C_5H_{14}NO_2$	120.10191	(Cavalcante et al., 2015)
TP121	C_8H_9O	121.06479	(Romero et al., 2016b)
TP134	$C_6H_{16}NO_2$	134.11756	(Cavalcante et al., 2015; Romero et al., 2016a, 2016b, 2015; Šojić et al., 2012)
TP150	$C_6H_{16}NO_3$	150.11247	(Cavalcante et al., 2015; Romero et al., 2016a, 2016b)
TP193	$C_{12}H_{17}O_2$	193.12231	(Romero et al., 2016a)
TP196	$C_{11}H_{18}NO_2$	196.13321	(Wilde et al., 2014)
TP208	$C_{12}H_{18}NO_2$	208.13321	(Romero et al., 2016a, 2016b, 2015)
TP216	$C_{10}H_{18}NO_4$	216.12303	(Wilde et al., 2014)
TP220	$C_{13}H_{18}NO_2$	220.13321	(Romero et al., 2016a)
TP226	$C_{11}H_{16}NO_4$	226.10738	(Borkar et al., 2016)
TP226	$C_{12}H_{20}NO_3$	226.14377	(Cavalcante et al., 2015; Ma et al., 2007; Romero et al., 2016a, 2016b; Rubirola et al., 2014; Slegers et al., 2006; Wilde et al., 2014)
TP232	$C_{10}H_{18}NO_5$	232.11795	(Romero et al., 2016a, 2016b)
TP236	$C_{13}H_{18}NO_3$	236.12812	(Wilde et al., 2014)
TP238	$C_{13}H_{20}NO_3$	238.14377	(Cavalcante et al., 2015; Romero et al., 2016a, 2016b, 2015; Slegers et al., 2006; Šojić et al., 2012)
TP240	$C_{13}H_{22}NO_3$	240.15942	(Cavalcante et al., 2015; Romero et al., 2016a, 2016b; Šojić et al., 2012; Wilde et al., 2014)
TP241	$C_{12}H_{17}O_5$	241.10705	(Ma et al., 2007)
TP250	$C_{15}H_{24}NO_2$	250.18016	(Romero et al., 2016a)
TP252	$C_{14}H_{22}NO_3$	252.15942	(Cavalcante et al., 2015; Romero et al., 2016a, 2016b; Šojić et al., 2012)
TP254	$C_{13}H_{20}NO_4$	254.13868	(Cavalcante et al., 2015; Ma et al., 2007; Romero et al., 2016a, 2016b; Rubirola et al., 2014; Slegers et al., 2006; Šojić et al., 2012)
TP254	$C_{14}H_{24}NO_3$	254.17507	(Šojić et al., 2012)
TP256	$C_{13}H_{22}NO_4$	256.15433	(Cavalcante et al., 2015)
TP270	$C_{14}H_{24}NO_4$	270.16998	(Cavalcante et al., 2015; Ma et al., 2007; Romero et al., 2016a, 2016b)
TP282	$C_{15}H_{24}NO_4$	282.16998	(Cavalcante et al., 2015; Romero et al., 2016a, 2016b, 2015; Rubirola et al., 2014; Šojić et al., 2012)
TP284	$C_{15}H_{26}NO_4$	284.18563	(Cavalcante et al., 2015; Ma et al., 2007; Romero et al., 2016a, 2016b, 2015; Rubirola et al., 2014; Slegers et al., 2006; Šojić et al., 2012)
TP298	$C_{15}H_{24}NO_5$	298.16490	(Cavalcante et al., 2015; Romero et al., 2016a, 2016b)
TP300	$C_{15}H_{26}NO_5$	300.18055	(Cavalcante et al., 2015; Romero et al., 2016a; Wilde et al., 2014)
TP316	$C_{15}H_{26}NO_6$	316.17546	(Cavalcante et al., 2015; Romero et al., 2016a)
TP318	$C_{15}H_{28}NO_6$	318.19111	(Cavalcante et al., 2015)
TP332	$C_{15}H_{26}NO_7$	332.17038	(Romero et al., 2016a)

S4. Quality parameters for MTP and MTPA quantification in HWW experiments

Table S2. Concentration of MTP and MTPA in liquid phase (wastewater) and solid phase (dried weight fungus) in HWW experiments. Analytical quality parameters, method detection and quantification limits are presented as MDL and MQL, respectively.

	Concentration				Quality Parameters					
	MTP		MTPA		MTP			MTPA		
	Day 0	Day 7	Day 0	Day 7	MDL	MQL	Recovery	MDL	MQL	Recovery
Liquid phase (µg/L)	1.5 ± 0.4	1.0 ± 0.2	2.5 ± 0.3	0.9 ± 0.1	0.01	0.03	88 ± 6%	0.01	0.04	94 ± 14%
Solid phase (µg/kg)	< MDL	0.2 ± 0.03	< MDL	< MQL	0.01	0.04	54 ± 11%	0.02	0.07	38 ± 9%

S5. MS/MS elucidation of TP structures

For confirmation of TP structures, fragmentation scans were elucidated by using those data acquired in CID fragmentation energy. The fragment *m/z* 74.0600 was characteristic in all those TP structures containing a primary amine generated from the loss of the isopropyl moiety attached to the nitrogen atom in MTP structure (TP266B and TP266C). Otherwise, the fragment *m/z* 116.1070 was characteristic for the rest of TPs containing the *N*-bound isopropyl group. Among them, those compounds with the fragment *m/z* 135.0441 were distinctive for the presence of a carbonyl group attached to the aromatic ring in the ether side chain of the MTP structure (TP238, TP282A and TP298). The addition of a hydroxyl group into the aromatic ring was detected by the addition of an oxygen atom (*m/z* 15.9944) to the fragment *m/z* 135.0441, with generation of the *m/z* 151.0390 in TP298 fragmentation spectra (also identified in TP254 as a carboxylic group). On the other hand, *m/z* 133.0648 was characteristic for those TPs with a hydroxyl group in α or β position from the aromatic ring (TP240, O-DMTP, TP270 and α-HMTP). Likewise, the aromatic hydroxylation generated the presence of *m/z* 149.0597 (+ O) and the *m/z* 165.0546 (+ 2O) in TP284 and TP300 fragmentation spectra, respectively.

Even though most of the structures were successfully elucidated using CID fragmentation energy, HCD fragmentation energy became crucial to obtain characteristic and complementary small fragments to finally confirm some tentative chemical structures. Fig. S1 shows an example of TP confirmation using CID and HCD mass spectra. As it can be seen TP238 and TP254 structures contain an aldehyde and a carboxylic group in the ether side chain of the MTP structure, respectively. However, the fragments obtained applying CID fragmentation energy were not enough to predict the position of the alcohol group into TP254 structure (as a carboxylic group or as an aromatic hydroxylation). Using HCD fragmentation energy, the small fragment *m/z* 107.0492 in both TP238 and TP254 confirmed the absence of the hydroxyl group into the aromatic ring.

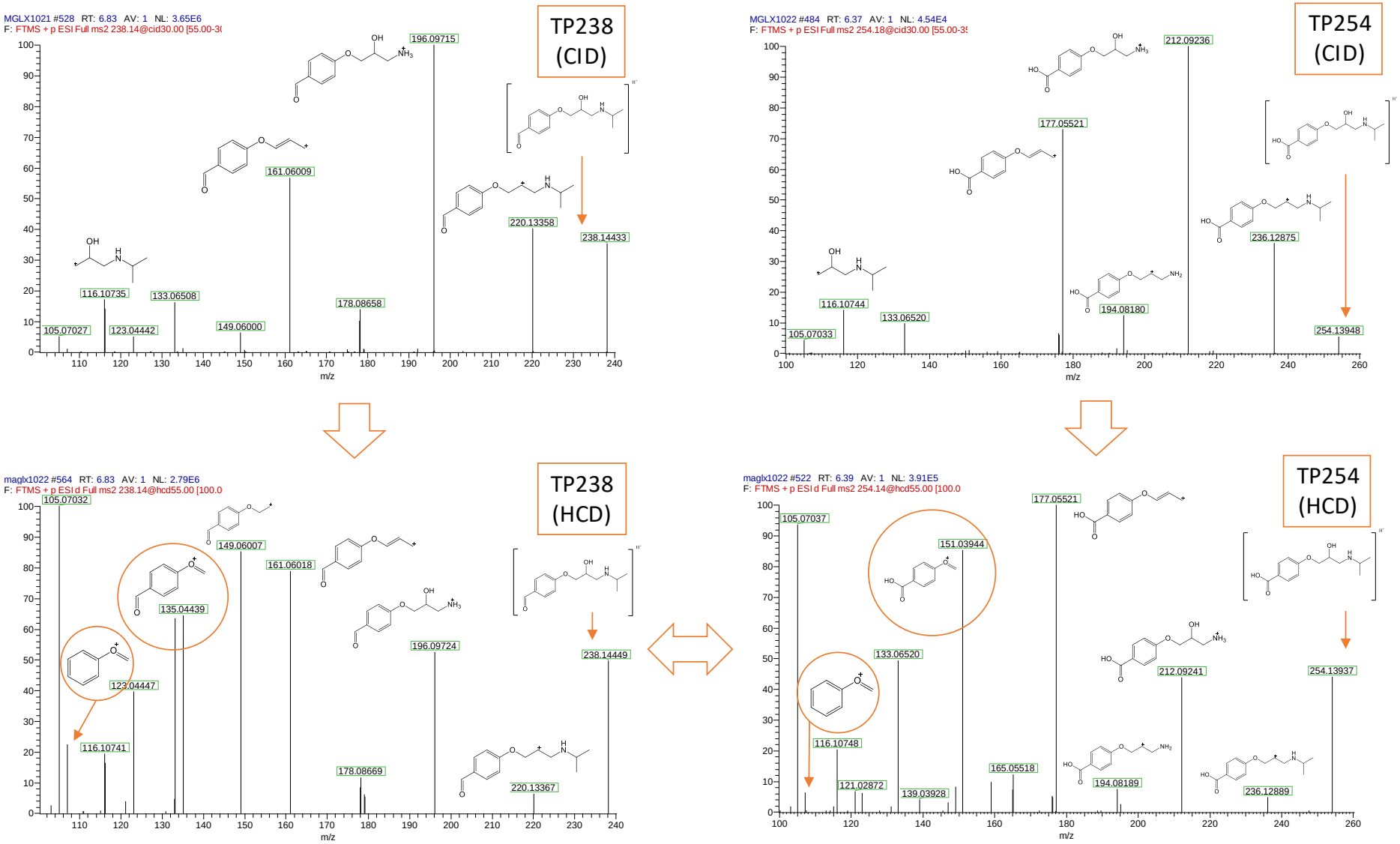

Figure S1. Confirmation of TP structures of TP238 and TP254 by elucidation of product ion scans obtained in CID and HCD fragmentation energies.

S6. Home-made library of detected and identified TPs

Table S3. Home-made library of parent compounds and transformation products suggested in literature and tentatively identified in this work.
* Unexpected transformation products from the suggested exact masses and chemical structures (isomers) gathered from literature.

R_t (min)	Compound	Ion	Molecular formula $[M+H]^+$	Theoretical exact mass $[M+H]^+$	Experiment exact mass $[M+H]^+$	Error mass (ppm)	RDBE	Suggested chemical structure	Ref.
7.64	MTP	$[M+H]^+$	$C_{15}H_{26}NO_3$	268.19070	268.19106	1.34	3.5	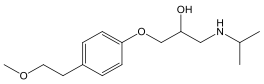	Reference standard
		$[M+H–(H_2O)]^+$	$C_{15}H_{24}NO_2$	250.18016	250.18063	1.87	4.5		
		$[M+H–(C_3H_6)]^+$	$C_{12}H_{20}NO_3$	226.14377	226.14414	1.63	3.5		
		$[M+H–(C_3H_{11}NO)]^+$	$C_{12}H_{15}O_2$	191.10666	191.10689	1.20	5.5		
		$[M+H–(C_7H_{18}NO_2)]^+$	C_8H_9O	121.06479	121.06500	1.73	4.5		
		$[M+H–(C_9H_{12}O_2)]^+$	$C_6H_{14}NO$	116.10699	116.10729	2.58	0.5		
6.68	MTPA	$[M+H]^+$	$C_{14}H_{22}NO_4$	268.15432	268.15534	3.80	4.5	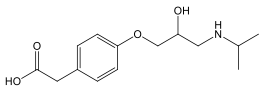	Reference standard
		$[M+H–(H_2O)]^+$	$C_{14}H_{20}NO_3$	250.14377	250.14463	3.43	5.5		
		$[M+H–(C_3H_6)]^+$	$C_{11}H_{16}NO_4$	226.10738	226.10813	3.31	4.5		
		$[M+H–(H_2O)–(C_3H_9N)]^+$	$C_{11}H_{11}O_3$	191.07027	191.07084	2.98	6.5		
		$[M+H–(C_8H_{14}O_3)]^+$	$C_{10}H_9O$	145.06479	145.06527	3.30	6.5		
		$[M+H–(C_8H_8O_3)]^+$	$C_6H_{14}NO$	116.10699	116.10748	4.22	0.5		
2.87	TP134	$[M+H]^+$	$C_6H_{16}NO_2$	134.11754	134.11742	-0.89	-0.5	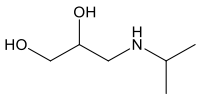	(Cavalcante et al., 2015; Romero et al., 2016a, 2016b, 2015; Šojić et al., 2012)
		$[M+H–(H_2O)]^+$	$C_6H_{14}NO$	116.10699	116.10746	4.04	0.5		
		$[M+H–(C_3H_6)]^+$	$C_3H_{10}NO_2$	92.07061	92.07097	3.91	-0.5		
6.21	TP226 A	$[M+H]^+$	$C_{12}H_{20}NO_3$	226.14376	226.14345	-1.37	3.5	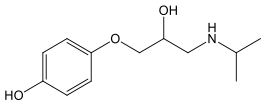	(Collado et al., 2014; Ma et al., 2007; Romero et al., 2016a; Slegers et al., 2006; Wilde et al., 2014)
		$[M+H–(H_2O)]^+$	$C_{12}H_{18}NO_2$	208.13321	208.13408	4.18	4.5		
		$[M+H–(C_3H_6)]^+$	$C_9H_{14}NO_3$	184.09682	184.09763	4.39	3.5		
		$[M+H–(H_2O)–(C_3H_9N)]^+$	$C_9H_9O_2$	149.05971	149.06030	3.95	5.5		
		$[M+H–(C_6H_6O_2)]^+$	$C_6H_{14}NO$	116.10699	116.10757	4.99	0.5		
7.07	TP226 B	$[M+H]^+$	$C_{12}H_{20}NO_3$	226.14376	226.14459	3.67	3.5	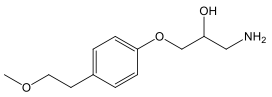	(Ma et al., 2007)
		$[M+H–(H_2O)]^+$	$C_{12}H_{18}NO_2$	208.13321	208.13390	3.31	4.5		
		$[M+H–(H_2O)–(CH_2)]^+$	$C_{11}H_{16}NO_2$	194.11756	194.11819	3.24	4.5		
		$[M+H–(H_2O)–(NH_3)]^+$	$C_{12}H_{15}O_2$	191.10666	191.10698	1.67	5.5		
		$[M+H–(C_4H_{11}O_2)]^+$	C_8H_9O	121.06479	121.06526	3.88	4.5		
		$[M+H–(C_9H_{12}O_2)]^+$	C_3H_8NO	74.06004	74.06012	1.08	0.5		
6.66	TP226 C	$[M+H]^+$	$C_{11}H_{16}NO_4$	226.10738	226.10701	-1.63	4.5	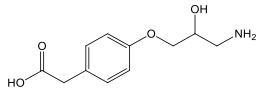	This article*
		$[M+H–(H_2O)]^+$	$C_{11}H_{14}NO_3$	208.09682	208.09669	-0.62	5.5		
		$[M+H–(H_2O)–(NH_3)]^+$	$C_{11}H_{11}O_3$	191.07027	191.07025	-0.10	6.5		
		$[M+H–(CH_7O_3)]^+$	$C_{10}H_9O$	145.06479	145.06467	-0.82	6.5		
		$[M+H–(C_8H_8O_3)]^+$	C_3H_8NO	74.06004	74.06006	0.27	0.5		
6.83	TP238	$[M+H]^+$	$C_{13}H_{20}NO_3$	238.14376	238.14433	2.39	4.5	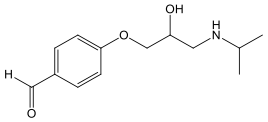	(Cavalcante et al., 2015; Romero et al., 2016a, 2016b, 2015; Slegers et al., 2006; Šojić et al., 2012)
		$[M+H–(H_2O)]^+$	$C_{13}H_{18}NO_2$	220.13321	220.13358	1.68	5.5		
		$[M+H–(C_3H_6)]^+$	$C_{10}H_{14}NO_3$	196.09682	196.09715	1.68	4.5		
		$[M+H–(H_2O)–(C_3H_9N)]^+$	$C_{10}H_9O_2$	161.05971	161.06009	2.35	6.5		
		$[M+H–(C_5H_{13}NO)]^+$ (HCD)	$C_8H_7O_2$	135.04405	135.04441	2.66	5.5		
		$[M+H–(C_7H_6O_2)]^+$	$C_6H_{14}NO$	116.10699	116.10735	3.10	0.5		
6.22	TP240	$[M+H]^+$	$C_{13}H_{22}NO_3$	240.15940	240.15906	-1.41	3.5	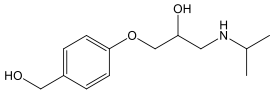	(Cavalcante et al., 2015; Romero et al., 2016a, 2016b; Šojić et al., 2012; Wilde et al., 2014)
		$[M+H–(H_2O)]^+$	$C_{13}H_{20}NO_2$	222.14886	222.14981	4.27	4.5		
		$[M+H–(C_3H_6)]^+$	$C_{10}H_{16}NO_3$	198.11247	198.11319	3.63	3.5		
		$[M+H–(H_2O)–(C_3H_9N)]^+$	$C_{10}H_{11}O_2$	163.07536	163.07599	3.86	5.5		
		$[M+H–(C_4H_{14}NO_2)]^+$	C_9H_9O	133.06479	133.06534	4.13	5.5		
		$[M+H–(C_7H_8O_2)]^+$	$C_6H_{14}NO$	116.10699	116.10755	4.82	0.5		
6.37	TP254	$[M+H]^+$	$C_{13}H_{20}NO_4$	254.13867	254.13955	3.46	3.5	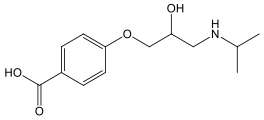	(Koba et al., 2016)
		$[M+H–(H_2O)]^+$	$C_{13}H_{18}NO_3$	236.12812	236.12885	3.09	5.5		
		$[M+H–(C_3H_6)]^+$	$C_{10}H_{14}NO_4$	212.09173	212.09246	3.44	4.5		
		$[M+H–(H_2O)–(C_3H_9N)]^+$	$C_{10}H_9O_3$	177.05462	177.05526	3.61	6.5		
		$[M+H–(C_5H_{13}NO)]^+$ (HCD)	$C_8H_7O_3$	151.03897	151.03952	3.64	5.5		
		$[M+H–(C_7H_6O_3)]^+$	$C_6H_{14}NO$	116.10699	116.10747	4.13	0.5		

6.63	O-DMTP	$[M+H]^+$	$C_{14}H_{24}NO_3$	254.17505	254.17555	1.96	4.5	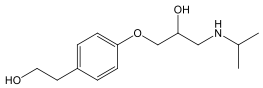	Reference standard
		$[M+H–(H_2O)]^+$	$C_{14}H_{22}NO_2$	236.16451	236.16520	2.92	4.5		
		$[M+H–(C_3H_6)]^+$	$C_{11}H_{18}NO_3$	212.12812	212.12865	2.49	3.5		
		$[M+H–(H_2O)–(C_3H_9N)]^+$	$C_{11}H_{13}O_2$	177.09101	177.09146	2.54	5.5		
		$[M+H–(C_8H_{10}O_2)]^+$	$C_6H_{14}NO$	116.10699	116.10736	3.18	0.5		
5.75	TP270	$[M+H]^+$	$C_{14}H_{24}NO_4$	270.16998	270.17062	2.36	3.5	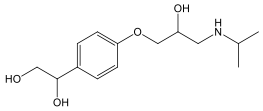	(Ma et al., 2007)
		$[M+H–(H_2O)]^+$	$C_{14}H_{22}NO_3$	252.15942	252.15958	0.63	4.5		
		$[M+H–2(H_2O)]^+$	$C_{14}H_{20}NO_2$	234.14886	234.14890	0.17	5.5		
		$[M+H–(C_3H_6)]^+$	$C_{11}H_{18}NO_4$	228.12303	228.12363	2.63	3.5		
		$[M+H–(C_3H_{10}N)–(H_2O)]^+$	$C_{11}H_{13}O_3$	193.08592	193.08636	2.27	5.5		
		$[M+H–(C_5H_{16}NO_3)]^+$	C_9H_9O	133.06479	133.06516	2.78	5.5		
		$[M+H–(C_8H_{10}NO_3)]^+$	$C_6H_{14}NO$	116.10699	116.10713	1.20	0.5		
6.69	TP282 A	$[M+H]^+$	$C_{15}H_{24}NO_4$	282.16997	282.17083	3.04	4.5	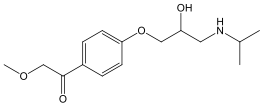	(Rubirola et al., 2014)
		$[M+H–(H_2O)]^+$	$C_{15}H_{22}NO_3$	264.15942	264.16010	2.57	5.5		
		$[M+H–(C_3H_6)]^+$	$C_{12}H_{18}NO_4$	240.12303	240.12373	2.91	4.5		
		$[M+H–(H_2O)–(C_3H_9N)]^+$	$C_{12}H_{13}O_3$	205.08592	205.08648	2.73	6.5		
		$[M+H–(C_2H_5O)–(C_5H_{12}NO)]^+$ (HCD)	$C_8H_7O_2$	135.04405	135.04441	2.66	5.5		
		$[M+H–(C_9H_{10}O_3)]^+$	$C_6H_{14}NO$	116.10699	116.10738	3.35	0.5		
7.48	TP282 B	$[M+H]^+$	$C_{15}H_{24}NO_4$	282.16997	282.17132	4.78	4.5	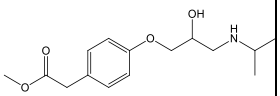	This article*
		$[M+H–(H_2O)]^+$	$C_{15}H_{22}NO_3$	264.15942	264.16019	2.91	5.5		
		$[M+H–(C_3H_6)]^+$	$C_{12}H_{18}NO_4$	240.12303	240.12384	3.37	4.5		
		$[M+H–(H_2O)–(C_3H_9N)]^+$	$C_{12}H_{13}O_3$	205.08592	205.08661	3.36	6.5		
		$[M+H–(C_5H_{16}O_3)]^+$	$C_{10}H_9O$	145.06479	145.06523	3.03	6.5		
		$[M+H–(C_9H_{10}O_3)]^+$	$C_6H_{14}NO$	116.10699	116.10744	3.87	0.5		
6.40	α-HMTP	$[M+H]^+$	$C_{15}H_{26}NO_4$	284.18562	284.18659	3.41	3.5	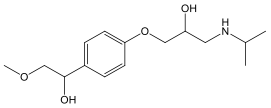	Reference standard
		$[M+H–(H_2O)]^+$	$C_{15}H_{24}NO_3$	266.17507	266.17586	2.96	4.5		
		$[M+H–(H_2O)–(C_3H_5)]^+$	$C_{12}H_{18}NO_3$	224.12812	224.12875	2.81	4.5		
		$[M+H–(H_2O)–(C_3H_9N)]^+$	$C_{12}H_{15}O_3$	207.10157	207.10205	2.31	5.5		
		$[M+H–(CH_5O_2)–(C_5H_{12}NO)]^+$	C_9H_9O	133.06479	133.06514	2.63	5.5		
		$[M+H–(C_9H_{12}O_3)]^+$	$C_6H_{14}NO$	116.10699	116.10744	3.87	0.5		
7.31	TP284	$[M+H]^+$	$C_{15}H_{26}NO_4$	284.18562	284.18530	-1.12	3.5	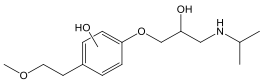	(Cavalcante et al., 2015; Romero et al., 2016a, 2016b, 2015; Slegers et al., 2006; Šojić et al., 2012)
		$[M+H–(H_2O)]^+$	$C_{15}H_{24}NO_3$	266.17507	266.17577	2.62	4.5		
		$[M+H–(CH_4O)]^+$	$C_{14}H_{22}NO_3$	252.15942	252.16009	2.65	4.5		
		$[M+H–(H_2O)–(CH_4O)]^+$	$C_{14}H_{20}NO_2$	234.14886	234.14940	2.30	5.5		
		$[M+H–(CH_5O)–(C_3H_3)]^+$	$C_{11}H_{14}NO_2$	192.10191	192.10233	2.18	5.5		
		$[M+H–(H_2O)–(C_3H_9N)]^+$	$C_{11}H_{11}O_2$	175.07536	175.07580	2.51	6.5		
		$[M+H–(CH_5O)–(C_5H_{12}NO)]^+$ (HCD)	$C_9H_9O_2$	149.05971	149.05998	1.81	5.5		
		$[M+H–(C_9H_{12}O_3)]^+$	$C_6H_{14}NO$	116.10699	116.10735	3.10	0.5		
6.86	TP298	$[M+H]^+$	$C_{15}H_{24}NO_5$	298.16488	298.16470	-0.60	4.5	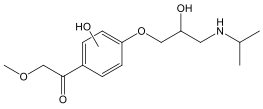	(Cavalcante et al., 2015; Romero et al., 2016a, 2016b)
		$[M+H–(H_2O)]^+$	$C_{15}H_{22}NO_4$	280.15433	280.15537	3.71	5.5		
		$[M+H–(CH_4O)]^+$	$C_{14}H_{20}NO_4$	266.13868	266.13944	2.85	5.5		
		$[M+H–(C_3H_6)–(CH_3O)]^+$	$C_{11}H_{14}NO_4$	224.09173	224.09234	2.72	5.5		
		$[M+H–(C_2H_5O)–(C_5H_{12}NO)]^+$ (HCD)	$C_8H_7O_3$	151.03897	151.03937	2.64	5.5		
		$[M+H–(C_9H_{10}O_4)]^+$	$C_6H_{14}NO$	116.10699	116.10741	3.61	0.5		
6.72	TP300	$[M+H]^+$	$C_{15}H_{26}NO_5$	300.18055	300.18027	-0.93	3.5	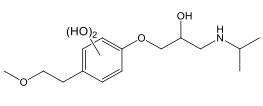	(Cavalcante et al., 2015)
		$[M+H–(H_2O)]^+$	$C_{15}H_{24}NO_4$	282.16998	282.17102	3.68	4.5		
		$[M+H–(CH_4O)]^+$	$C_{14}H_{22}NO_4$	268.15433	268.15536	3.84	4.5		
		$[M+H–(H_2O)–(CH_4O)]^+$	$C_{14}H_{20}NO_3$	250.14377	250.14401	0.95	5.5		
		$[M+H–(CH_5O)–(C_5H_{12}NO)]^+$	$C_9H_9O_3$	165.05462	165.05482	1.21	5.5		
		$[M+H–(C_6H_{18}NO_3)]^+$	$C_9H_9O_2$	149.05971	149.05968	-0.20	5.5		
		$[M+H–(C_{13}H_{12}O_4)]^+$	$C_6H_{14}NO$	116.10699	116.10719	1.72	0.5		
6.50	TP316	$[M+H]^+$	$C_{15}H_{26}NO_6$	316.17545	316.17703	4.99	3.5	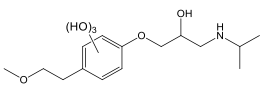	(Cavalcante et al., 2015; Romero et al., 2016a)
		$[M+H–(H_2O)]^+$	$C_{15}H_{24}NO_5$	298.16490	298.16590	3.35	4.5		
		$[M+H–(C_3H_6)]^+$	$C_{12}H_{20}NO_6$	274.12851	274.12985	4.88	3.5		
		$[M+H–(C_3H_8O)]^+$	$C_{12}H_{18}NO_5$	256.11795	256.11917	4.76	4.5		
		$[M+H–(C_6H_{15}NO_2)]^+$	$C_9H_{11}O_4$	183.06519	183.06601	4.47	4.5		
		$[M+H–(C_9H_{12}O_5)]^+$	$C_6H_{14}NO$	116.10699	116.10752	4.56	0.5		

S7. Toxicity test

Table S4. Percentage toxicity values (measured after 15 min of exposure) of samples obtained along fungal treatment of water samples spiked with MTP and MTPA (at 2.5 mg/L each in single experiments). Percentages toxicity expressed as $(EC_{50(initial)} - EC_{50\ (x)})/EC_{50(initial)}$. EC_{50} of MTP was 51.5% and MTPA was 47.8% (expressed in dilution percentage).

	MTP					MTPA				
	0d (%)	3d (%)	7d (%)	10d (%)	15d (%)	0d (%)	3d (%)	7d (%)	10d (%)	15d (%)
G. lucidum	0	11	12	11	29	0	16	18	17	4
T. versicolor	0	28	6	23	15	0	13	8	7	11
P. ostreatus	0	10	11	11	24	0	1	4	14	29

S8. References

Borkar, R.M., Bhandi, M.M., Dubey, A.P., Ganga Reddy, V., Komirishetty, P., Nandekar, P.P., Sangamwar, A.T., Kamal, A., Banerjee, S.K., Srinivas, R., 2016. An evaluation of the CYP2D6 and CYP3A4 inhibition potential of metoprolol metabolites and their contribution to drug–drug and drug–herb interaction by LC-ESI/MS/MS. Biomed. Chromatogr. 30, 1556–1572. doi:10.1002/bmc.3721

Cavalcante, R.P., Dantas, R.F., Wender, H., Bayarri, B., González, O., Giménez, J., Esplugas, S., Machulek, A., 2015. Photocatalytic treatment of metoprolol with B-doped TiO2: Effect of water matrix, toxicological evaluation and identification of intermediates. Appl. Catal. B Environ. 176–177, 173–182. doi:10.1016/j.apcatb.2015.04.007

Collado, N., Rodriguez-Mozaz, S., Gros, M., Rubirola, A., Barceló, D., Comas, J., Rodriguez-Roda, I., Buttiglieri, G., 2014. Pharmaceuticals occurrence in a WWTP with significant industrial contribution and its input into the river system. Environ. Pollut. 185, 202–212. doi:10.1016/j.envpol.2013.10.040

Gros, M., Rodríguez-Mozaz, S., Barceló, D., 2012. Fast and comprehensive multi-residue analysis of a broad range of human and veterinary pharmaceuticals and some of their metabolites in surface and treated waters by ultra-high-performance liquid chromatography coupled to quadrupole-linear ion trap tandem. J. Chromatogr. A 1248, 104–121. doi:10.1016/j.chroma.2012.05.084

Koba, O., Golovko, O., Kodešová, R., Klement, A., Grabic, R., 2016. Transformation of atenolol, metoprolol, and carbamazepine in soils: The identification, quantification, and stability of the transformation products and further implications for the environment. Environ. Pollut. 218, 574–585. doi:10.1016/j.envpol.2016.07.041

Lucas, D., Castellet-Rovira, F., Villagrasa, M., Badia-Fabregat, M., Barceló, D., Vicent, T., Caminal, G., Sarrà, M., Rodríguez-Mozaz, S., 2018. The role of sorption processes in the removal of pharmaceuticals by fungal treatment of wastewater. Sci. Total Environ. 610–611, 1147–1153. doi:10.1016/j.scitotenv.2017.08.118

Ma, B., Huang, H.H., Chen, X.Y., Sun, Y.M., Lin, L.H., Zhong, D.F., 2007. Biotransformation of metoprolol by the fungus Cunninghamella blakesleeana. Acta Pharmacol. Sin. 28, 1067–1074. doi:10.1111/j.1745-7254.2007.00567.x

Romero, V., Acevedo, S., Marco, P., Giménez, J., Esplugas, S., 2016a. Enhancement of Fenton and photo-Fenton processes at initial circumneutral pH for the degradation of the β-blocker metoprolol. Water Res. 88, 449–457. doi:10.1016/j.watres.2015.10.035

Romero, V., González, O., Bayarri, B., Marco, P., Giménez, J., Esplugas, S., 2016b. Degradation of Metoprolol by photo-Fenton: Comparison of different photoreactors performance. Chem. Eng. J. 283, 639–648. doi:10.1016/j.cej.2015.07.091

Romero, V., González, O., Bayarri, B., Marco, P., Giménez, J., Esplugas, S., 2015. Performance of different advanced oxidation technologies for the abatement of the beta-blocker metoprolol. Catal. Today 240, 86–92. doi:10.1016/j.cattod.2014.03.060

Rubirola, A., Llorca, M., Rodriguez-Mozaz, S., Casas, N., Rodriguez-Roda, I., Barceló, D., Buttiglieri, G., 2014. Characterization of metoprolol biodegradation and its transformation products generated in activated sludge batch experiments and in full scale WWTPs. Water Res. 63, 21–32. doi:10.1016/j.watres.2014.05.031

Slegers, C., Maquille, A., Deridder, V., Sonveaux, E., Habib Jiwan, J.L., Tilquin, B., 2006. LC-MS analysis in the e-beam and gamma radiolysis of metoprolol tartrate in aqueous solution: Structure elucidation and formation mechanism of radiolytic products. Radiat. Phys. Chem. 75, 977–989. doi:10.1016/j.radphyschem.2006.02.001

Šojić, D., Despotović, V., Orčić, D., Szabó, E., Arany, E., Armaković, S., Illés, E., Gajda-Schrantz, K., Dombi, A., Alapi, T., Sajben-Nagy, E., Palágyi, A., Vágvölgyi, C., Manczinger, L., Bjelica, L., Abramović, B., 2012. Degradation of thiamethoxam and metoprolol by UV, O3and UV/O3hybrid processes: Kinetics, degradation intermediates and toxicity. J. Hydrol. 472–473, 314–327. doi:10.1016/j.jhydrol.2012.09.038

Wilde, M.L., Montipó, S., Martins, A.F., 2014. Degradation of β-blockers in hospital wastewater by means of ozonation and Fe2+/ozonation. Water Res. 48, 280–295. doi:10.1016/j.watres.2013.09.039

SUPPLEMENTARY MATERIAL

An automated on-line turbulent flow liquid-chromatography technology coupled to a high resolution mass spectrometer LTQ-Orbitrap for suspect screening of antibiotic transformation products during microalgae wastewater treatment

Adrián Jaén-Gil[a], Andrea Hom-Diaz[b], Marta Llorca[c], Teresa Vicent[b], Paqui Blánquez[b], Damià Barceló[a,c], Sara Rodríguez-Mozaz[a*]

[a] *Catalan Institute for Water Research (ICRA), H_2O Building, Scientific and Technological Park of the University of Girona, Emili Grahit 101, E-17003 Girona, Spain*

[b] *Chemical, Biological and Environmental Engineering Department, Universitat Autònoma de Barcelona (UAB), E-08193 Bellaterra, Spain*

[c] *Water and Soil Quality Research Group Department of Environmental Chemistry, (IDAEA-CSIC), Jordi Girona 18-26, E-08034 Barcelona, Spain*

S1. Method development

Table S1
Chromatographic conditions in on-line turbulent flow chromatography system (TFC-LTQ Orbitrap Velos). Acetonitrile (A), acetonitrile:isopropanol:acetone (45:45:10) (B), and water (C) mobile phases were chosen for loading and cleaning TFC column (loading pump), and formic acid 0.1% in methanol (A) and formic acid 0.1% in water (B) mobile phases were selected for analytical separation (eluting pump).

Start time (min)	Time (S)	Loading (TurboFlow) pump							Tee	Eluting (analytical) pump			
		Flow (mL/min)	Gradient	A%	B%	C%	D %	Step		Flow (mL/min)	A%	B%	Step
0.00	15	2.00	Step	-	-	-	100	Loading	Out	0.50	5	95	Conditioning
0.25	30	0.50	Step	-	5	95	-	Transfer	In	0.00	5	95	Loading
0.75	315	0.50	Ramp	-	30	70	-	Separation	In	0.00	30	70	Separation
6.00	480	0.50	Ramp	-	100	-	-	Separation	In	0.00	100	-	Separation
14.00	60	0.50	Step	-	100	-	-	Cleaning	Out	0.50	100	-	Cleaning
15.00	120	0.50	Step	100	-	-	-	Cleaning	Out	0.50	100	-	Cleaning
17.00	60	0.50	Step	-	-	-	100	Run to init. cond.	Out	0.50	5	95	Run to init. cond.

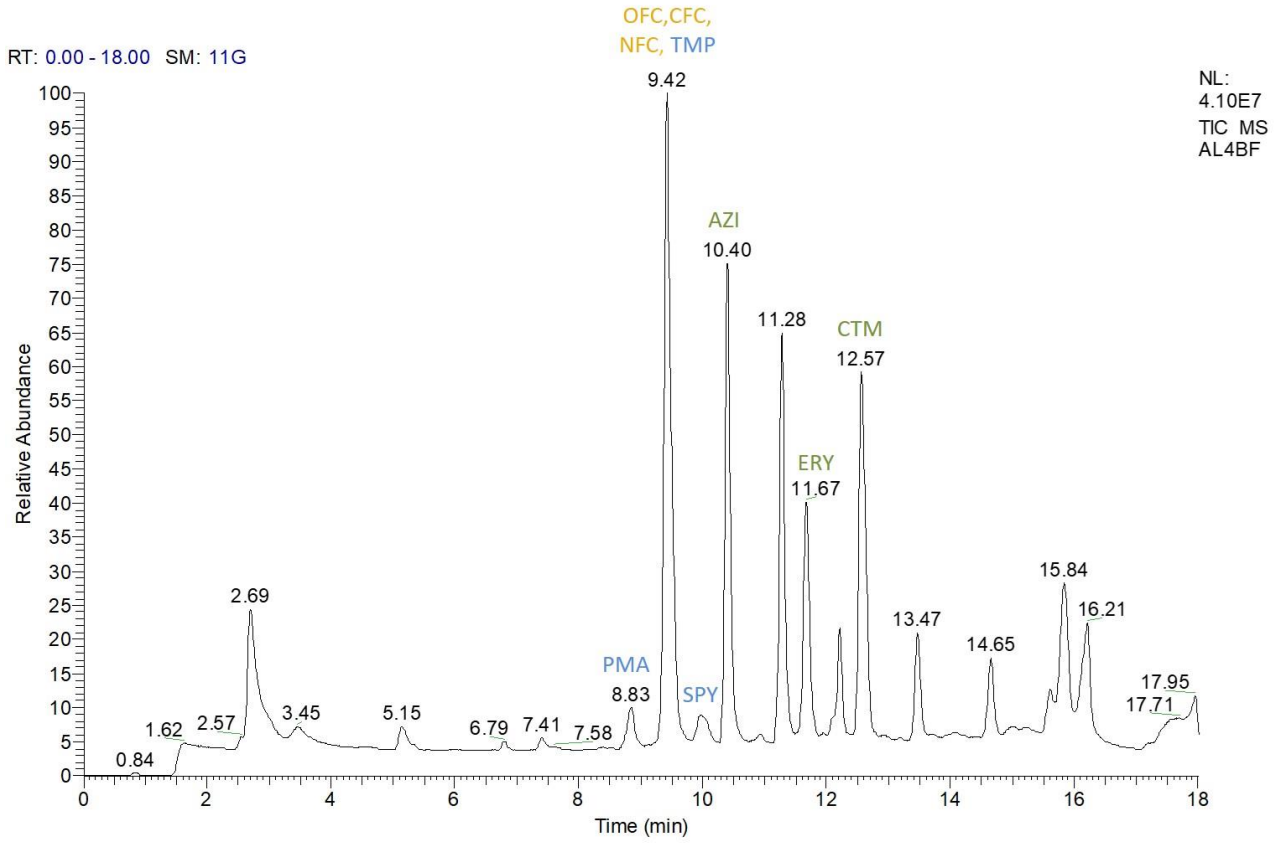

Fig. S1. Example of Total Ion Chromatogram (TIC) using the on-line turbulent flow chromatography system (TFC-LTQ Orbitrap Velos).

S2. Software data processing

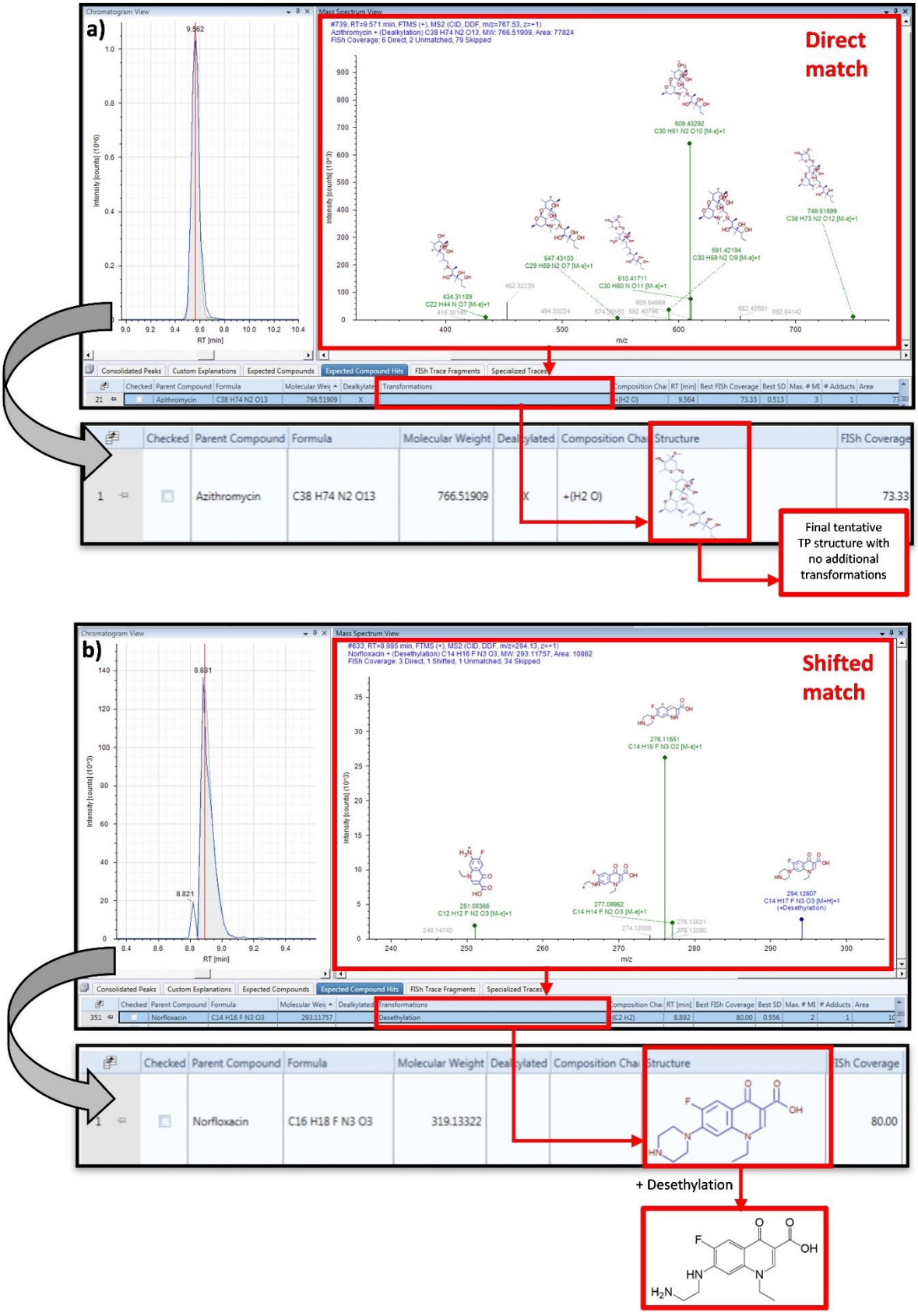

Fig. S2. Example of software data processing results for confirmation: a) Direct match when tentative structures are directly proposed, b) Shifted match when additional transformation are required to a proposed predicted structure.

S3. In-house library

Table S2

In-house library of parent compounds and transformation products identified.

t_R (min)	Name	Ion	Elemental composition	Theoretical m/z	Experimental m/z	Mass error (ppm)	RDB	Type of Confirm.	Suggested chemical structure	Ref.
10.37	**AZI**	$[M+H]^+$ $[M+H–(L\text{-cladinose})]^+$ $[M+H–[O\text{-}(L\text{-cladinose})]]^+$ $[M+H–(d\text{-desosamine})\text{-}(L\text{-cladinose})]^+$	$C_{38}H_{73}N_2O_{12}$ $C_{30}H_{59}N_2O_9$ $C_{30}H_{57}N_2O_8$ $C_{22}H_{44}NO_7$	749.51580 591.42151 573.41094 434.31123	749.51752 591.42334 573.41266 434.31281	2.29 3.09 2.99 3.63	3.5 2.5 3.5 1.5	Direct	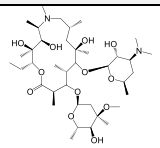	Reference standard
9.47	TP 766 (AZI)	$[M+H]^+$ $[M+H–(d\text{-desosamine})]$ $[M+H–(L\text{-cladinose})]^+$ $[M+H–[(d\text{-desosamine})\text{-}(L\text{-cladinose})]]^+$	$C_{38}H_{75}N_2O_{13}$ $C_{30}H_{60}NO_{11}$ $C_{30}H_{61}N_2O_{10}$ $C_{22}H_{46}NO_8$	767.52637 610.41609 609.43207 452.32179	767.52570 610.41754 609.43317 452.32254	-0.87 2.37 1.80 1.65	2.5 1.5 1.5 0.5	Direct	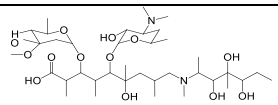	This article
10.82	TP 764 (AZI)	$[M+H]^+$ $[M+H–(C_2H_7NO)]^+$ $[M+H–(L\text{-cladinose})]^+$ $[M+H–(L\text{-cladinose})–(C_2H_7NO)]^+$	$C_{38}H_{73}N_2O_{13}$ $C_{36}H_{66}NO_{12}$ $C_{30}H_{59}N_2O_{10}$ $C_{28}H_{52}NO_9$	765.51072 704.45795 607.41642 546.36366	765.50897 704.45782 607.41626 546.36371	-2.28 -0.18 -0.26 0.09	3.5 4.5 2.5 3.5	Shifted	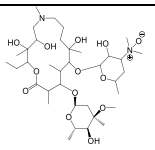	[1,2]
9.38	TP 752 (AZI)	$[M+H]^+$ $[M+H–(d\text{-desosamine})]$	$C_{37}H_{73}N_2O_{13}$ $C_{29}H_{57}NO_{11}$	753.51072 595.39261	753.50879 595.39178	-2.56 -1.39	2.5 2.0	Shifted	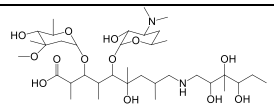	This article
10.34	TP 734 (AZI)	$[M+H]^+$ $[M+H–(L\text{-cladinose})]^+$ $[M+H–[O\text{-}(L\text{-cladinose})]]^+$ $[M+H–(d\text{-desosamine})\text{-}(L\text{-cladinose})]^+$	$C_{37}H_{71}N_2O_{12}$ $C_{29}H_{57}N_2O_9$ $C_{29}H_{55}N_2O_8$ $C_{21}H_{42}NO_7$	735.50015 577.40586 559.39529 420.29558	735.49744 577.40497 559.39447 420.29467	-3.68 -1.54 -1.46 -2.16	3.5 2.5 3.5 1.5	Direct	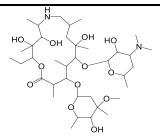	[1]
9.55	TP 608 (AZI)	$[M+H]^+$ $[M+H–(d\text{-desosamine})]^+$	$C_{30}H_{61}N_2O_{10}$ $C_{22}H_{46}NO_8$	609.43207 452.32179	609.43280 452.32303	1.19 2.74	1.5 0.5	Direct	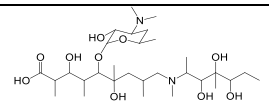	This article
10.57	TP 591 (AZI)	$[M+H]^+$ $[M+H–(L\text{-cladinose})]^+$	$C_{30}H_{58}NO_{10}$ $C_{22}H_{44}NO_7$	592.40552 434.31123	592.40660 434.31128	1.82 0.11	2.5 1.5	Direct	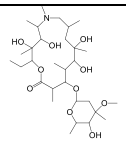	[3]
10.39	TP 590 (AZI)	$[M+H]^+$ $[M+H–H_2O]^+$ $[M+H\text{-}(d\text{-desosamine})]^+$	$C_{30}H_{59}N_2O_9$ $C_{30}H_{57}N_2O_8$ $C_{22}H_{44}NO_7$	591.42151 573.41094 434.31123	591.42261 573.41095 434.31122	1.85 0.01 -0.02	2.5 3.5 1.5	Direct	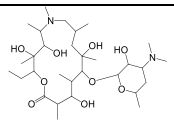	[3]
10.42	TP 576 (AZI)	$[M+H]^+$ $[M+H–H_2O]^+$ $[M+H\text{-}(d\text{-desosamine})]^+$	$C_{29}H_{57}N_2O_9$ $C_{29}H_{55}N_2O_8$ $C_{22}H_{44}NO_7$	577.40586 559.39529 434.31123	577.40576 559.39575 434.31113	-0.17 0.82 -0.23	2.5 3.5 1.5	Shifted	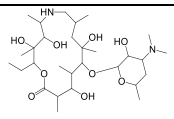	This article
11.69	**ERY**	$[M+H]^+$ $[M+H–H_2O]^+$ $[M+H–(L\text{-cladinose})]^+$ $[M+H–[O\text{-}(L\text{-cladinose})]]^+$	$C_{37}H_{68}NO_{13}$ $C_{37}H_{66}NO_{12}$ $C_{29}H_{54}NO_{10}$ $C_{29}H_{52}NO_9$	734.46852 716.45795 576.37422 558.36366	734.47070 716.46039 576.37628 558.36578	2.97 3.41 3.57 3.80	4.5 5.5 3.5 4.5	Direct	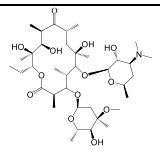	Reference standard
10.52	TP 751 (ERY)	$[M+H]^+$ $[M+H–(L\text{-cladinose})]^+$	$C_{37}H_{70}NO_{14}$ $C_{29}H_{56}NO_{11}$	752.47908 594.38479	752.47925 594.38287	0.23 -3.23	3.5 2.5	Direct	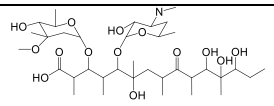	[4,5]

12.13	TP 749 (ERY)	$[M+H]^+$ $[M+H–H_2O]^+$ $[M+H–(L\text{-cladinose})]^+$ $[M+H–(L\text{-cladinose})\text{-}H_2O]^+$	$C_{37}H_{68}NO_{14}$ $C_{37}H_{66}NO_{13}$ $C_{29}H_{54}NO_{11}$ $C_{29}H_{52}NO_{10}$	750.46343 732.45287 592.36914 574.35857	750.46173 732.45276 592.36865 574.35828	-2.26 -0.15 -0.82 -0.50	4.5 5.5 3.5 4.5	Shifted	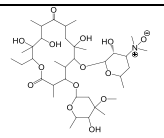	[6]
12.38	TP 733 (ERY)	$[M+H]^+$ $[M+H–(L\text{-cladinose})]^+$	$C_{37}H_{68}NO_{13}$ $C_{29}H_{54}NO_{10}$	734.46852 576.37422	734.46752 576.37382	-1.36 -0.69	4.5 3.5	Shifted	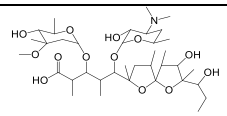	[4,5]
12.00	TP 719 (ERY)	$[M+H]^+$ $[M+H–H_2O]^+$ $[M+H–(L\text{-desmethyl-cladinose})]^+$ $[M+H–[O\text{-}(L\text{-desmethyl-cladinose})]]^+$	$C_{36}H_{66}NO_{13}$ $C_{36}H_{64}NO_{12}$ $C_{29}H_{54}NO_{10}$ $C_{29}H_{52}NO_9$	720.45287 702.44230 576.37422 558.36366	720.45453 702.44360 576.37555 558.36505	2.30 1.85 2.31 2.49	4.5 3.5 4.5 4.5	Direct	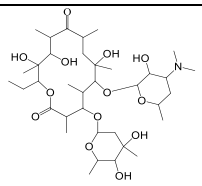	[4]
12.12	TP 717 (ERY)	$[M+H]^+$ $[M+H–(L\text{-cladinose})]^+$ $[M+H–[O\text{-}(L\text{-cladinose})]]^+$	$C_{37}H_{68}NO_{12}$ $C_{29}H_{54}NO_9$ $C_{29}H_{52}NO_8$	718.47360 560.37931 542.36874	718.47351 560.37958 542.36877	-0.13 0.48 0.06	4.5 3.5 4.5	Shifted	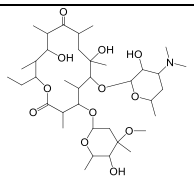	[4]
11.66	TP 575 (ERY)	$[M+H]^+$ $[M+H–H_2O]^+$ $[M+H–2H_2O]^+$ $[M+H–3H_2O]^+$	$C_{29}H_{54}NO_{10}$ $C_{29}H_{52}NO_9$ $C_{29}H_{50}NO_8$ $C_{29}H_{48}NO_7$	576.37422 558.36366 540.35309 522.34253	576.37396 558.36609 540.35388 522.34363	-0.45 4.35 1.46 2.11	3.5 4.5 5.5 6.5	Direct	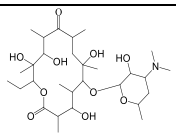	[7]
12.53	**CTM**	$[M+H]^+$ $[M+H–(L\text{-cladinose})]^+$ $[M+H—(L\text{-cladinose})\text{-}(CH_4OH)]^+$	$C_{38}H_{70}NO_{13}$ $C_{30}H_{56}NO_{10}$ $C_{29}H_{52}NO_9$	748.48417 590.38987 558.36366	748.48212 590.38916 558.36285	-2.74 -1.20 -1.45	4.5 3.5 4.5	Direct	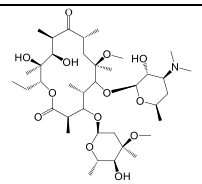	Reference standard
13.04	TP 763 (CTM)	$[M+H]^+$ $[M+H–(L\text{-cladinose})]^+$ $[M+H—[(L\text{-cladinose})\text{-}(CH_4OH)]]^+$	$C_{38}H_{70}NO_{14}$ $C_{30}H_{56}NO_{11}$ $C_{29}H_{52}NO_{10}$	764.47908 606.38479 574.35857	764.48193 606.38776 574.36115	3.73 4.90 4.49	4.5 3.5 4.5	Shifted	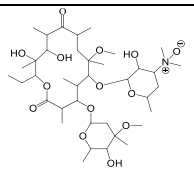	[8]
12.55	TP 589 (CTM)	$[M+H]^+$ $[M+H–CH_4OH]^+$ $[M+H–CH_4OH\text{-}H_2O]^+$ $[M+H–[O\text{-}(L\text{-cladinose})]]^+$	$C_{30}H_{56}NO_{10}$ $C_{29}H_{52}NO_9$ $C_{29}H_{50}NO_8$ $C_{21}H_{33}O_5$	590.38987 558.36366 540.35309 365.23225	590.39136 558.36566 540.35510 365.23373	2.52 3.58 3.72 4.05	3.5 4.5 5.5 5.5	Direct	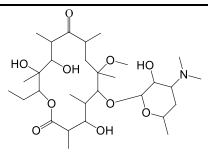	[6]
9.45	**OFC**	$[M+H]^+$ $[M+H\text{-}H_2O]^+$ $[M+H\text{-}CO_2]^+$	$C_{18}H_{21}FN_3O_4$ $C_{18}H_{19}FN_3O_3$ $C_{17}H_{21}FN_3O_2$	362.15106 344.14050 318.16123	362.15048 344.14035 318.16110	-1.60 -0.44 -0.41	9.5 10.5 8.5	Direct	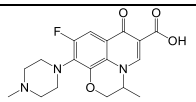	Reference standard
9.29	TP 347 (OFC)	$[M+H]^+$ $[M+H\text{-}H_2O]^+$ $[M+H\text{-}CO_2]^+$ $[M+H\text{-}C_2H_2\text{-}NH_3]^+$	$C_{17}H_{19}FN_3O_4$ $C_{17}H_{17}FN_3O_3$ $C_{16}H_{19}FN_3O_2$ $C_{14}H_{14}FN_2O_2$	348.13541 330.12485 304.14558 261.10338	348.13577 330.12576 304.14651 261.10413	1.03 2.76 3.06 2.87	9.5 10.5 8.5 8.5	Direct	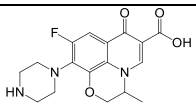	[9]
9.24	TP 335 (OFC)	$[M+H]^+$ $[M+H\text{-}CH_4N]^+$ $[M+H\text{-}C_3H_7N]^+$ $[M+H\text{-}C_3H_7N\text{-}CO_2]^+$	$C_{16}H_{19}FN_3O_4$ $C_{15}H_{14}FN_2O_4$ $C_{13}H_{12}FN_2O_4$ $C_{12}H_{12}FN_2O_2$	336.13541 305.09321 279.07756 235.08773	336.13696 305.09467 279.07892 235.08875	4.61 4.79 4.87 4.34	8.5 9.5 8.5 7.5	Direct	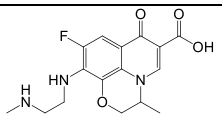	[9]
11.07	TP 333 (OFC)	$[M+H]^+$ $[M+H\text{-}H_2O]^+$ $[M+H\text{-}NH_4]^+$	$C_{16}H_{17}FN_3O_4$ $C_{16}H_{15}FN_3O_3$ $C_{16}H_{13}FN_2O_4$	334.11976 316.10920 316.08539	334.12079 316.11026 316.08658	3.08 3.35 3.76	9.5 10.5 11.0	Direct	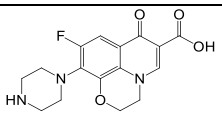	This article

9.03	TP 321A (OFC)	$[M+H]^+$ $[M+H-NH_3]^+$ $[M+H-H_2O]^+$ $[M+H-C_2H_2-NH_3]^+$	$C_{15}H_{17}FN_3O_4$ $C_{15}H_{14}FN_2O_4$ $C_{15}H_{15}FN_3O_3$ $C_{13}H_{12}FN_2O_4$	322.11976 305.09321 304.10920 279.07756	322.11969 305.09406 304.11020 279.07840	-0.22 2.79 3.29 3.01	8.5 9.5 9.5 8.5	Direct	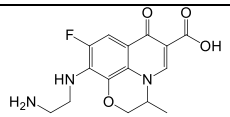	This article
10.91	TP 321B (OFC)	$[M+H]^+$ $[M+H-H_2O]^+$	$C_{15}H_{17}FN_3O_4$ $C_{15}H_{15}FN_3O_3$	322.11976 304.10920	322.11948 304.10901	-0.87 -0.62	8.5 9.5	Direct	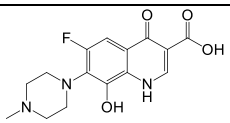	This article
8.22	TP 317 (OFC)	$[M+H]^+$ $[M+H-H_2O]^+$ $[M+H-CO_2]^+$ $[M+H-C_3H_7N]^+$	$C_{16}H_{20}N_3O_4$ $C_{16}H_{18}N_3O_3$ $C_{15}H_{20}N_3O_2$ $C_{13}H_{13}N_2O_4$	318.14483 300.13427 274.15500 261.08698	318.14496 300.13431 274.15506 261.08710	0.41 0.13 0.22 0.46	8.5 9.5 7.5 8.5	Shifted	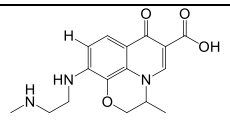	This article
9.11	TP 278 (OFC)	$[M+H]^+$ $[M+H-H_2O]^+$	$C_{13}H_{12}FN_2O_4$ $C_{13}H_{10}FN_2O_3$	279.07756 261.06700	279.07870 261.06808	4.08 4.14	8.5 9.5	Direct	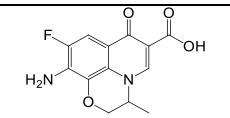	[9]
7.85	TP 189 (NFC)	$[M+H]^+$ $[M+H-H_2O]^+$ $[M+H-H_2O-CO]^+$	$C_{10}H_8NO_3$ $C_{10}H_6NO_2$ C_9H_6NO	190.04987 172.03931 144.04439	190.05061 172.03999 144.04500	3.89 3.95 4.23	7.5 8.5 7.5	Shifted	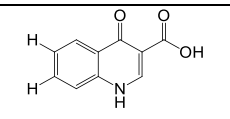	This article
9.50	**CFC**	$[M+H]^+$ $[M+H-H_2O]^+$ $[M+H-CO_2]^+$ $[M+H-H_2O-CO-C_2H_3N]^+$	$C_{17}H_{19}FN_3O_3$ $C_{17}H_{17}FN_3O_2$ $C_{16}H_{19}FN_3O$ $C_{14}H_{14}FN_2O$	332.14050 314.12993 288.15067 245.10847	332.14136 314.13089 288.15149 245.10902	2.59 3.06 2.85 2.24	9.5 10.5 8.5 8.5	Direct	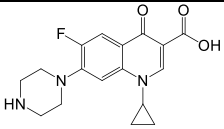	Reference standard
9.10	TP 305 (CFC)	$[M+H]^+$ $[M+H-H_2O]^+$ $[M+H-NH_4]^+$ $[M+H-C_2H_5N]^+$	$C_{15}H_{17}FN_3O_3$ $C_{15}H_{15}FN_3O_2$ $C_{15}H_{13}FN_2O_3$ $C_{13}H_{12}FN_2O_3$	306.12485 288.11428 288.09047 263.08265	306.12619 288.11563 288.09177 263.08374	4.38 4.69 4.51 4.14	8.5 9.5 6.5 9.5	Direct	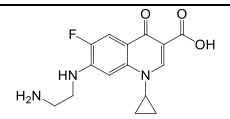	[10]
8.63	TP 287 (CFC)	$[M+H]^+$ $[M+H-H_2O]^+$ $[M+H-C_2H_5N]^+$	$C_{15}H_{18}N_3O_3$ $C_{15}H_{16}N_3O_2$ $C_{13}H_{13}N_2O_3$	288.13427 270.12370 245.09207	288.13483 270.12442 245.09248	1.94 2.67 1.67	8.5 9.5 8.5	Shifted	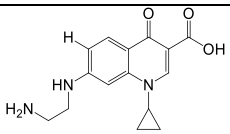	[10]
11.89	TP 262 (CFC)	$[M+H]^+$ $[M+H-H_2O]^+$ $[M+H-H_2O-C_3H_5]^+$ (HCD)	$C_{13}H_{12}FN_2O_3$ $C_{13}H_{10}FN_2O_2$ $C_{10}H_5FN_2O_2$	263.08265 245.07208 204.03296	263.08316 245.07254 204.03337	1.94 1.88 2.00	8.5 9.5 9.0	Direct	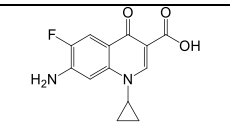	[10]
11.16	TP 244 (CFC)	$[M+H]^+$ $[M+H-H_2O]^+$ $[M+H-H_2O-C_3H_5]^+$ (HCD)	$C_{13}H_{13}N_2O_3$ $C_{13}H_{11}N_2O_2$ $C_{10}H_6N_2O_2$	245.09207 227.08150 186.04238	245.09250 227.08191 186.04303	1.75 1.81 3.49	8.5 9.5 9.0	Shifted	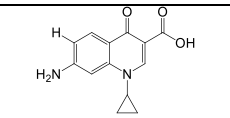	[11]
7.85	TP 189 (CFC)	$[M+H]^+$ $[M+H-H_2O]^+$ $[M+H-H_2O-CO_2]^+$	$C_{10}H_8NO_3$ $C_{10}H_6NO_2$ C_9H_6NO	190.04987 172.03931 144.04439	190.05061 172.03999 144.04500	3.89 3.95 4.23	7.5 8.5 7.5	Shifted	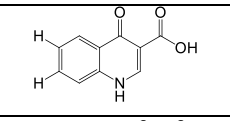	This article
9.38	**NFC**	$[M+H]^+$ $[M+H-H_2O]^+$ $[M+H-H_2O-C_2H_2]^+$	$C_{16}H_{19}FN_3O_3$ $C_{16}H_{17}FN_3O_2$ $C_{14}H_{15}FN_3O_2$	320.14050 302.12993 276.11428	320.14014 302.12961 276.11490	-1.12 -1.06 2.25	8.5 9.5 8.5	Direct	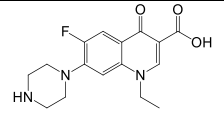	Reference standard
8.88	TP 293 (NFC)	$[M+H]^+$ $[M+H-NH_3]^+$ $[M+H-H_2O]^+$ $[M+H-C_2H_5N]^+$	$C_{14}H_{17}FN_3O_3$ $C_{14}H_{14}FN_2O_3$ $C_{14}H_{15}FN_3O_2$ $C_{12}H_{12}FN_2O_3$	294.12485 277.09830 276.11428 251.08265	294.12445 277.09784 276.11411 251.08232	-1.36 -1.66 -0.62 -1.31	7.5 8.5 8.5 7.5	Direct	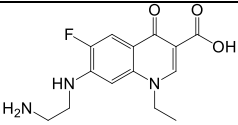	[10]
8.56	TP 275 (NFC)	$[M+H]^+$ $[M+H-NH_3]^+$ $[M+H-H_2O]^+$	$C_{14}H_{18}N_3O_3$ $C_{14}H_{15}N_2O_3$ $C_{14}H_{16}N_3O_2$	276.13427 259.10772 258.12370	276.13379 259.10718 258.12326	-1.74 -2.08 -1.70	7.5 8.5 8.5	Shifted	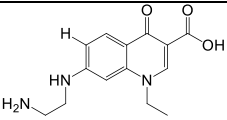	This article

11.61	TP 250 (NFC)	$[M+H]^+$ $[M+H-H_2O]^+$ $[M+H-NH_4]^+$ $[M+H-H_2O-C_2H_4]^+$ (HCD)	$C_{12}H_{12}FN_2O_3$ $C_{12}H_{10}FN_2O_2$ $C_{12}H_8FNO_3$ $C_{10}H_6FN_2O_2$	251.08265 233.07208 233.04827 205.04078	251.08211 233.07155 233.04715 205.04118	-2.15 -2.27 -4.81 1.95	7.5 8.5 9.0 8.5	Direct	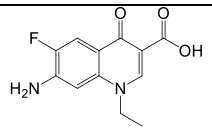	[12]
10.83	TP 232 (NFC)	$[M+H]^+$ $[M+H-H_2O]^+$ $[M+H-NH_4]^+$	$C_{12}H_{13}N_2O_3$ $C_{12}H_{11}N_2O_2$ $C_{12}H_9NO_3$	233.09207 215.08150 215.05769	233.09247 215.08192 215.05728	1.72 1.95 -1.91	7.5 8.5 9.0	Shifted	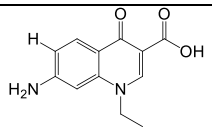	This article
7.85	TP 189 (NFC)	$[M+H]^+$ $[M+H-H_2O]^+$ $[M+H-H_2O-CO]^+$	$C_{10}H_8NO_3$ $C_{10}H_6NO_2$ C_9H_6NO	190.04987 172.03931 144.04439	190.05061 172.03999 144.04500	3.89 3.95 4.23	7.5 8.5 7.5	Shifted	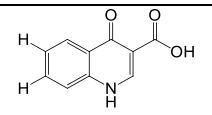	This article
8.82	**PMA**	$[M+H]^+$ $[M+H-H_2O]^+$ $[M+H-C_2H_5N]^+$	$C_{14}H_{18}N_5O_3$ $C_{14}H_{16}N_5O_2$ $C_{12}H_{13}N_4O_3$	304.14042 286.12985 261.09822	304.14093 286.13037 261.09875	1.68 1.82 2.03	8.5 9.5 8.5	Direct	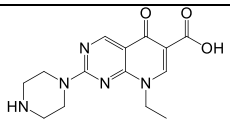	Reference standard
7.75	TP 277 (PMA)	$[M+H]^+$ $[M+H-H_2O]^+$	$C_{12}H_{16}N_5O_3$ $C_{12}H_{13}N_4O_3$	278.12477 261.09822	278.12493 261.09862	0.58 1.53	7.5 8.5	Shifted	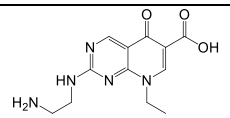	This article
8.77	TP 259 (PMA)	$[M+H]^+$ $[M+H-C_2H_5N]^+$	$C_{13}H_{18}N_5O$ $C_{11}H_{13}N_4O$	260.15059 217.10839	260.15140 217.10892	3.11 2.44	7.5 7.5	Shifted	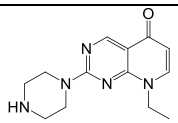	This article
8.19	TP 234 (PMA)	$[M+H]^+$ $[M+H-H_2O]^+$	$C_{10}H_{11}N_4O_3$ $C_{10}H_9N_4O_2$	235.08257 217.07200	235.08203 217.07185	-2.29 -0.69	7.5 8.5	Shifted	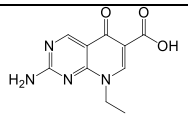	This article
9.34	**TMP**	$[M+H]^+$ $[M+H-C_2H_6]^+$ $[M+H-CH_5]^+$	$C_{14}H_{19}N_4O_3$ $C_{12}H_{13}N_4O_3$ $C_{13}H_{14}N_4O_2$ $C_{10}H_{13}O_3$	291.14517 261.09822 258.11113 181.08592	291.14593 261.09912 258.11194 181.08656	2.61 3.45 3.14 3.53	7.5 8.5 9.0 4.5	Direct	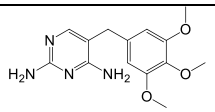	Reference standard
9.37	TP 274 (TMP)	$[M+H]^+$ $[M+H-H_2O]^+$ $[M+H-C_4H_6N_4]^+$	$C_{13}H_{15}N_4O_3$ $C_{13}H_{13}N_4O_2$ $C_9H_9O_3$	275.11387 257.10330 165.05462	275.11435 257.10406 165.05515	1.74 2.96 3.21	8.5 9.5 5.5	Shifted	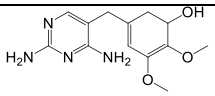	[13]
9.37	TP 260 (TMP)	$[M+H]^+$ $[M+H-NH_3]^+$ $[M+H-C_4H_6N_4]^+$	$C_{12}H_{13}N_4O_3$ $C_{12}H_{10}N_3O_3$ $C_8H_7O_3$	261.09822 244.07167 151.03897	261.09869 244.07278 151.03946	1.80 4.55 3.24	8.5 9.5 5.5	Shifted	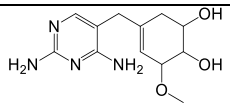	This article
10.04	**SPY**	$[M+H]^+$ $[M+H-H_2O]^+$ $[M+H-SO_2H_2]^+$	$C_{11}H_{12}N_3O_2S$ $C_{11}H_{10}N_3OS$ $C_{11}H_{10}N_3$	250.06447 232.05391 184.08692	250.06392 232.05351 184.08621	-2.19 -1.72 -3.85	7.5 8.5 8.5	Direct	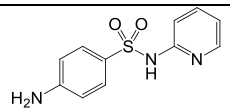	Reference standard
6.63	TP 185 (SPY)	$[M+H]^+$ $[M+H-NH_3]^+$	$C_{11}H_{12}N_3$ $C_{11}H_9N_2$	186.10257 169.07602	186.10216 169.07591	-2.20 -0.65	7.5 8.5	Shifted	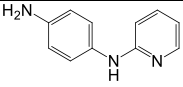	[14]

S4. References

[1] R.P. Hunter, D.E. Koch, R.L. Coke, M.A. Goatley, R. Isaza, Azithromycin metabolite identification in plasma, bile, and tissues of the ball python (Python regius), J. Vet. Pharmacol. Ther. 26 (2003) 117–121. doi:10.1046/j.1365-2885.2003.00464.x.

[2] D. Debremaeker, D. Visky, H.K. Chepkwony, A. Van Schepdael, E. Roets, J. Hoogmartens, Analysis of unknown compounds in azithromycin bulk samples with liquid chromatography coupled to ion trap mass spectrometry, Rapid Commun. Mass Spectrom. 17 (2003) 342–350. doi:10.1002/rcm.917.

[3] L. Tong, P. Eichhorn, S. Pérez, Y. Wang, D. Barceló, Photodegradation of azithromycin in various aqueous systems under simulated and natural solar radiation: Kinetics and identification of photoproducts, Chemosphere. 83 (2011) 340–348. doi:10.1016/j.chemosphere.2010.12.025.

[4] M. Llorca, S. Rodríguez-Mozaz, O. Couillerot, K. Panigoni, J. de Gunzburg, S. Bayer, R. Czaja, D. Barceló, Identification of new transformation products during enzymatic treatment of tetracycline and erythromycin antibiotics at laboratory scale by an on-line turbulent flow liquid-chromatography coupled to a high resolution mass spectrometer LTQ-Orbitrap, Chemosphere. 119 (2015) 90–98. doi:10.1016/j.chemosphere.2014.05.072.

[5] M. Morar, K. Pengelly, K. Koteva, G.D. Wright, Mechanism and diversity of the erythromycin esterase family of enzymes, Biochemistry. 51 (2012) 1740–1751. doi:10.1021/bi201790u.

[6] I. Gozlan, I. Koren, Identification, Mechanisms and Kinetics of Macrolide Degradation Product Formation under Controlled Environmental Conditions, J. Environ. Anal. Chem. 3 (2016) 1–9. doi:10.4172/2380-2391.1000171.

[7] S.R. Batchu, V.R. Panditi, K.E. O'Shea, P.R. Gardinali, Photodegradation of antibiotics under simulated solar radiation: Implications for their environmental fate, Sci. Total Environ. 470–471 (2014) 299–310. doi:10.1016/j.scitotenv.2013.09.057.

[8] F. Lange, S. Cornelissen, D. Kubac, M.M. Sein, J. von Sonntag, C.B. Hannich, A. Golloch, H.J. Heipieper, M. Möder, C. von Sonntag, Degradation of macrolide antibiotics by ozone: A mechanistic case study with clarithromycin, Chemosphere. 65 (2006) 17–23. doi:10.1016/j.chemosphere.2006.03.014.

[9] J. Jimenez-Villarin, A. Serra-Clusellas, C. Martínez, A. Conesa, J. Garcia-Montaño, E. Moyano, Liquid chromatography coupled to tandem and high resolution mass spectrometry for the characterisation of ofloxacin transformation products after titanium dioxide photocatalysis, J. Chromatogr. A. 1443 (2016) 201–210. doi:10.1016/j.chroma.2016.03.063.

[10] A.S. Maia, A.R. Ribeiro, C.L. Amorim, J.C. Barreiro, Q.B. Cass, P.M.L. Castro, M.E. Tiritan, Degradation of fluoroquinolone antibiotics and identification of metabolites/transformation products by liquid chromatography-tandem mass spectrometry, J. Chromatogr. A. 1333 (2014) 87–98. doi:10.1016/j.chroma.2014.01.069.

[11] E. Turiel, G. Bordin, A.R. Rodríguez, Study of the evolution and degradation products of ciprofloxacin and oxolinic acid in river water samples by HPLC-UV/MS/MS-MS, J. Environ. Monit. 7 (2005) 189–195. doi:10.1039/B413506G.

[12] A. Prieto, M. Möder, R. Rodil, L. Adrian, E. Marco-Urrea, Degradation of the antibiotics norfloxacin and ciprofloxacin by a white-rot fungus and identification of degradation products, Bioresour. Technol. 102 (2011) 10987–10995. doi:10.1016/j.biortech.2011.08.055.

[13] K.S. Jewell, S. Castronovo, A. Wick, P. Falås, A. Joss, T.A. Ternes, New insights into the transformation of trimethoprim during biological wastewater treatment, Water Res. 88 (2016) 550–557. doi:10.1016/j.watres.2015.10.026.

[14] C.E. Rodríguez-Rodríguez, M. Jesús García-Galán, P. Blánquez, M.S. Díaz-Cruz, D. Barceló, G. Caminal, T. Vicent, Continuous degradation of a mixture of sulfonamides by Trametes versicolor and identification of metabolites from sulfapyridine and sulfathiazole, J. Hazard. Mater. 213–214 (2012) 347–354. doi:10.1016/j.jhazmat.2012.02.008.

SUPPLEMENTARY MATERIAL

Metoprolol and metoprolol acid degradation in UV/H_2O_2 treated wastewaters: An integrated screening approach for the identification of hazardous transformation products

Adrián Jaén-Gil[a], Gianluigi Buttiglieri[a], Aleix Benito[b], Rafael Gonzalez-Olmos[b], Damià Barceló[a,c], Sara Rodríguez-Mozaz[a*]

[a] *Catalan Institute for Water Research (ICRA), H_2O Building, Scientific and Technological Park of the University of Girona, Emili Grahit 101, E-17003 Girona, Spain*

[b] *IQS School of Engineering, Universitat Ramon Llull, Via Augusta 390, 08017, Barcelona, Spain*

[c] *Water and Soil Quality Research Group, Department of Environmental Chemistry, (IDAEA-CSIC), Jordi Girona 18-26, E-08034 Barcelona, Spain*

S1. Sample preparation, instrumental analysis and Microtox bioassays

Hospital and industrial wastewater samples were treated following an SPE methodology previously described (Gros et al., 2012). Firstly, samples were filtered through 1 µm glass fiber filters followed by 0.45 µm PVDF membrane filters (Millipore; Billerica, MA, USA). Then, 50 mL of sample at initial and final time respectively were used adding the appropriate volume of Na_2EDTA. Samples were loaded into the SPE cartridges and conditioned with 5 mL of methanol followed by 5 mL of HPLC grade water. Cartridges were rinsed with 6 mL of HPLC grade water and further dried with air for 5 minutes to remove the remaining water. Finally, elution was carried out using 6 mL of pure methanol and extracts were reconstituted in 100 µL of methanol/water (10:90, v/v). In the case of pure water samples (a) pretreatment was not necessary before injection in LC-MS/MS system. Using this methodology, the recoveries obtained in wastewater effluents for the compounds with reference standards were: MTP 83.4 ± 5.2%, MTPA 49.0 ± 8.2%, α-HMTP 63.1 ± 3.9% and O-DMTP 45.9 ± 2.6% (Rubirola et al., 2014).

Chromatographic separation was carried out by using an Aria TLX-1 chromatographic system (Thermo Fisher Scientific) comprising a PAL auto sampler and two mixing quaternary pumps (eluting pump and loading pump). 20 µL of water sample were injected. The chromatographic separation was performed in a ZORBAX Eclipse XDB-C18 (150 mm × 4.6 mm, 5 µm; Agilent Technologies, Santa Clara, CA) applying the methodology described elsewhere (Jaén-Gil et al., 2019). The optimized chromatographic gradient was water with ammonium formate (10 mM, pH 3.0) (A) and acetonitrile (B). Solvent gradient was performed as follows: initial mobile phase composition (95% A) held for 1 min, followed by a decrease in composition A to 5% within 9 min, then to 0% in 3 min, held for 2 min, and finally up to 95% in 1 min and held for 1 min. The total run time was 17 min. The high-resolution mass spectrometer LTQ-OrbitrapVelos^{TM} (Thermo Fisher Scientific) was equipped with a heated electrospray ionization source (HESI-II). Analyses were carried out in positive and negative ionization mode. As no results were obtained for negative mode experiments, data processing was carried out in positive mode only. Samples were acquired through full scan from *m/z* 100 to 1000 range at a resolving power of 60,000 FWHM. MS/MS full scan fragmentation data was acquired in data dependent acquisition mode (DDA) at 30,000 FWHM from *m/z* 50 to 500 range. The MS/MS experiments were performed applying a dynamic mass exclusion mode to discriminate co-eluted compounds: ions fragmented more than 3 times during 25 seconds were further ignored for fragmentation during the following 30 seconds (corresponding to peak plus tailing). The conditions

for HESI-II were designed as follows: spray voltage at 3.5 kV, source heater temperature at 300 ˚C, capillary temperature at 350 ˚C, sheath gas flow at 40 and auxiliary gas flow at 20 (arbitrary units). Collision-induced dissociation (CID) was selected at a normalized collision energy of 30 eV (activation Q of 0.250 and an activation time of 30 ms) in an isolation width of 2 Da. The entire system was controlled via Aria software under Xcalibur 2.1.

The ISO 11348-3 protocol (ISO, 1998) for testing bacterial bioluminescence of wastewater matrices was used to assess toxicity throughout Microtox® Model 500 Toxicity Analyzer (Strategic Diagnostics Inc. Newark, DE, US). Briefly, solution for freeze-dried bacteria used was: 20,0 g Sodium chloride (NaCl), 2,035 g Magnesium chloride hexahydrate ($MgCl_2 \cdot 6H_2O$), 0,30 g Potassium chloride (KCl) and dissolved in water and make up to 1 L with water. The solution was stored in a freezer at —20 ˚C. Reference substances used were: Zinc sulfate heptahydrate ($ZnSO_4 \cdot 7H_2O$), 3,5-Dichlorophenol ($C_6H_4OCl_2$), Potassium dichromate ($K_2Cr_2O_7$). Sampling was conducted in chemically inert, clean containers in accordance with ISO 5667-16. pH adjustment and salt was added just before testing. Stain of luminescent bacteria *Vibrio fischeri* NRRL B-11177 were prepared from commercially available freeze-dried reagents stored at —20 ˚C. For sample preparation, if the pH was between 6 and 8.5 no adjustment was necessary. A quantity of 20 g of sodium chloride per liter to the water samples was added for to adjust the osmolality. When samples were strongly turbid, samples were centrifuged 10 min at 5,000 g. Then, the freeze-dried culture was removed from the —20 ˚C freezer immediately before reconstitution in water. The dilution series were prepared. For the reconstitution, 1 mL of distilled water was cooled in a glass tube to 3 ± 3 ˚C. The volume of cooled water was poured at once into the lyophilized bacteria in the vial, thereby minimizing cell damage during the rehydration process. This reconstituted luminescent bacteria suspension served as a stock suspension. The test suspensions were prepared directly in the test tubes. The presence of sodium thiosulfate in bioassay was tested and had no toxic effect on luminescent bacteria at the added concentration.

S2. Automatic software parameters

Table S1. Data processing parameters selected to perform and reproduce the integrated suspect screening methodology in Compound Discoverer 2.0.

<table>
<tr><th colspan="2">Peak filtering of candidates</th></tr>
<tr><td colspan="2"><u>Select Spectra</u>:
- Retention time range: 1 to 12 min
- Mass range: 50-400 Da
- S/N ratio: 3
<u>Align Retention Times</u>:
- Alignment Model: Adaptive curve
- Mass tolerance: 5 ppm
- Maximum retention time shift: 0.3 min
<u>Detect Unknown Compounds:</u>
- Mass tolerance: 5 ppm
- Intensity Tolerance: 30%
- S/N ratio: 10
- Min. Peak Intensity: 10^4
- Ions: $[M+H]^+$
- Max. Peak Width: 0.8 min
- Max. #Scan per peak: 5
- Min. #Isotopes: 2
<u>Group Unknown Compounds:</u>
- Mass tolerance: 5 ppm
- RT tolerance: 0.3 min</td></tr>
<tr><th colspan="2">Identification strategies</th></tr>
<tr><td><u>Analytical standard comparison (I)</u>

(MS, MS^2 and R_t comparison with spiked control files after data alignment)</td><td><u>In-house library comparison (II)</u>
<u>Search Mass Lists:</u>
- Mass tolerance: 5 ppm
- Retention time: Included
- Retention time tolerance: 0.3 min
- Input Files: “MTP/MTPA in-house library”</td></tr>
<tr><td><u>Software compound prediction (III)</u>
<u>Generate Expected Compounds:</u>
- Parent compound: MTP/MTPA
- Apply Dealkylation: True
- Apply Dearylation: False
- Max. # Dealkylation Steps: 2
- All reaction steps: 3
- Min. mass: 100 Da
- Ions considered: $[M+H]^+$
- Transformations: oxidation, reduction, desaturation, oxidative deamination to alcohol, oxidative deamination to ketone, dehydration, hydration.
- Phase II: (not specified)
- Max. # All Steps: 3
<u>Find Expected Compounds:</u>
- Mass tolerance: 5 ppm
- Intensity Tolerance: 30 %
- Intensity Threshold: 0.1 %
- Min. #Isotopes: 2
- Min. peak intensity: 1000
<u>FISh scoring:</u>
- Annotate Full Tree: True
- Match Transformations: True
- S/N threshold: 10
- Mass tolerance of fragments: 5 ppm
- Fragment prediction libraries: True
<u>Group Expected Compounds</u>
- RT tolerance: 0.3 min</td><td><u>Literature exact mass list comparison (IV)</u>
<u>Search Mass List:</u>
- Mass tolerance: 5 ppm
- Consider Retention time: Not included
- File loaded: “MTP/MTPA literature”</td></tr>
</table>

Table S2. List of the 39 suspect compounds included in the literature list.

Name	Molecular formula	Exact mass $[M+H]^+$	References
MTP	$C_{15}H_{25}NO_3$	268.19072	(Rubirola et al., 2014)
MTPA	$C_{14}H_{21}NO_4$	268.15433	(Rubirola et al., 2014)
TP74	$C_4H_{11}N$	74.09643	(Romero et al., 2016b)
TP102	$C_5H_{11}NO$	102.09134	(Wilde et al., 2014)
TP112	C_6H_9NO	112.07569	(Wilde et al., 2014)
TP114	$C_6H_{11}NO$	114.09134	(Wilde et al., 2014)
TP116	$C_6H_{13}NO$	116.10699	(Cavalcante et al., 2015; Romero et al., 2016a, 2016b)
TP118	$C_6H_{15}NO$	118.12264	(Romero et al., 2016b, 2015)
TP120	$C_5H_{13}NO_2$	120.10191	(Cavalcante et al., 2015)
TP121	C_8H_8O	121.06479	(Romero et al., 2016b)
TP134	$C_6H_{15}NO_2$	134.11756	(Cavalcante et al., 2015; Romero et al., 2016a, 2016b, 2015; Šojić et al., 2012)
TP150	$C_6H_{15}NO_3$	150.11247	(Cavalcante et al., 2015; Romero et al., 2016a, 2016b)
TP193	$C_{12}H_{16}O_2$	193.12231	(Romero et al., 2016a)
TP196	$C_{11}H_{17}NO_2$	196.13321	(Wilde et al., 2014)
TP208	$C_{12}H_{17}NO_2$	208.13321	(Romero et al., 2016a, 2016b, 2015)
TP216	$C_{10}H_{17}NO_4$	216.12303	(Wilde et al., 2014)
TP220	$C_{13}H_{17}NO_2$	220.13321	(Romero et al., 2016a)
TP226A	$C_{12}H_{19}NO_3$	226.14377	(Ma et al., 2007; Romero et al., 2016a; Slegers et al., 2006; Wilde et al., 2014)
TP226B	$C_{12}H_{19}NO_3$	226.14377	(Ma et al., 2007)
TP226C	$C_{11}H_{15}NO_4$	226.10738	(Jaén-Gil et al., 2019)
TP232	$C_{10}H_{17}NO_5$	232.11795	(Romero et al., 2016a, 2016b)
TP236	$C_{13}H_{17}NO_3$	236.12812	(Wilde et al., 2014)
TP238	$C_{13}H_{19}NO_3$	238.14377	(Cavalcante et al., 2015; Romero et al., 2016a, 2016b, 2015; Slegers et al., 2006; Šojić et al., 2012)
TP240	$C_{13}H_{21}NO_3$	240.15942	(Cavalcante et al., 2015; Romero et al., 2016a, 2016b; Šojić et al., 2012; Wilde et al., 2014)
TP241	$C_{12}H_{16}O_5$	241.10705	(Ma et al., 2007)
TP250	$C_{15}H_{23}NO_2$	250.18016	(Romero et al., 2016a)
TP252	$C_{14}H_{21}NO_3$	252.15942	(Cavalcante et al., 2015; Romero et al., 2016a, 2016b; Šojić et al., 2012)
TP254	$C_{13}H_{19}NO_4$	254.13868	(Šojić et al., 2012)
O-DMTP	$C_{14}H_{23}NO_3$	254.17507	(Cavalcante et al., 2015; Ma et al., 2007; Romero et al., 2016a, 2016b; Rubirola et al., 2014; Slegers et al., 2006; Šojić et al., 2012)
TP256	$C_{13}H_{21}NO_4$	256.15433	(Cavalcante et al., 2015)
TP270	$C_{14}H_{23}NO_4$	270.16998	(Cavalcante et al., 2015; Ma et al., 2007; Romero et al., 2016a, 2016b)
TP282	$C_{15}H_{23}NO_4$	282.16998	(Cavalcante et al., 2015; Romero et al., 2016a, 2016b, 2015; Rubirola et al., 2014; Šojić et al., 2012)
α-HMTP	$C_{15}H_{25}NO_4$	284.18563	(Cavalcante et al., 2015; Ma et al., 2007; Romero et al., 2016a, 2016b, 2015; Rubirola et al., 2014; Slegers et al., 2006; Šojić et al., 2012)
TP284	$C_{15}H_{25}NO_4$	284.18563	(Cavalcante et al., 2015; Romero et al., 2016a, 2016b, 2015; Slegers et al., 2006; Šojić et al., 2012)
TP298	$C_{15}H_{23}NO_5$	298.16490	(Cavalcante et al., 2015; Romero et al., 2016a, 2016b)
TP300	$C_{15}H_{25}NO_5$	300.18055	(Cavalcante et al., 2015; Romero et al., 2016a; Wilde et al., 2014)
TP316	$C_{15}H_{25}NO_6$	316.17546	(Cavalcante et al., 2015; Romero et al., 2016a)
TP318	$C_{15}H_{27}NO_6$	318.19111	(Cavalcante et al., 2015)
TP332	$C_{15}H_{25}NO_7$	332.17038	(Romero et al., 2016a)

Table S3. List of the 357 compounds present in the prediction list created automatically by Compound Discoverer 2.0.

Parent Compound	Molecular formula	Exact mass $[M+H]^+$	Dealkylated	Transformations
Metoprolol	C_6H_9N	96.0815	x	Dehydration, Dehydration
Metoprolol	C_8H_4	101.0393	x	Dehydration, Dehydration
Metoprolol	C_8H_6	103.05495	x	Dehydration, Dehydration
Metoprolol	C_6H_9NO	112.07641	x	Dehydration, Desaturation
Metoprolol	$C_6H_8O_2$	113.06043	x	Dehydration, Oxidative Deamination to Ketone
Metoprolol	$C_6H_{11}NO$	114.09206	x	Dehydration
Metoprolol	$C_6H_{10}O_2$	115.07608	x	Dehydration, Oxidative Deamination to Alcohol
Metoprolol	$C_6H_{13}NO$	116.10771	x	Dehydration, Reduction
Metoprolol Acid	C_8H_4O	117.03421	x	Dehydration, Dehydration
Metoprolol	C_8H_4O	117.03421	x	Dehydration, Desaturation
Metoprolol	C_9H_8	117.0706	x	Dehydration, Dehydration
Metoprolol	C_8H_6O	119.04986	x	Dehydration, Desaturation
Metoprolol	C_8H_6O	119.04986	x	Dehydration
Metoprolol	C_8H_8O	121.06551	x	Dehydration
Metoprolol	C_8H_8O	121.06551	x	Dehydration, Reduction
Metoprolol	$C_8H_{10}O$	123.08116	x	Dehydration, Reduction
Metoprolol	$C_6H_9NO_2$	128.07133	x	Desaturation, Desaturation
Metoprolol	$C_6H_8O_3$	129.05534	x	Desaturation, Oxidative Deamination to Ketone
Metoprolol	$C_6H_{11}NO_2$	130.08698	x	Desaturation
Metoprolol	$C_6H_{10}O_3$	131.07099	x	Oxidative Deamination to Ketone
Metoprolol	$C_6H_{13}NO_2$	132.10263	x	
Metoprolol	$C_8H_4O_2$	133.02913	x	Desaturation, Desaturation
Metoprolol Acid	$C_8H_4O_2$	133.02913	x	Dehydration, Desaturation
Metoprolol	C_9H_8O	133.06551	x	Dehydration, Desaturation
Metoprolol	$C_6H_{12}O_3$	133.08664	x	Oxidative Deamination to Alcohol
Metoprolol	$C_6H_{15}NO_2$	134.11828	x	Reduction
Metoprolol	$C_8H_6O_2$	135.04478	x	Desaturation, Desaturation
Metoprolol Acid	$C_8H_6O_2$	135.04478	x	Dehydration
Metoprolol	$C_8\ H_6\ O_2$	135.04478	x	Desaturation
Metoprolol	$C_9H_{10}O$	135.08116	x	Dehydration
Metoprolol	$C_6H_{14}O_3$	135.10229	x	Oxidative Deamination to Alcohol, Reduction
Metoprolol	$C_8H_8O_2$	137.06043	x	
Metoprolol_Acid	$C_8H_8O_2$	137.06043	x	Dehydration, Reduction
Metoprolol	$C_8H_8O_2$	137.06043	x	Desaturation
Metoprolol	$C_9H_{12}O$	137.09681	x	Dehydration, Reduction
Metoprolol	$C_8H_{10}O_2$	139.07608	x	Reduction
Metoprolol	$C_8H_{10}O_2$	139.07608	x	
Metoprolol	$C_8H_{12}O_2$	141.09173	x	Reduction
Metoprolol	$C_6H_{11}NO_3$	146.08189	x	Desaturation, Oxidation
Metoprolol	$C_6H_{10}O_4$	147.06591	x	Oxidation, Oxidative Deamination to Ketone
Metoprolol	$C_6H_{13}NO_3$	148.09754	x	Oxidation
Metoprolol Acid	$C_8H_4O_3$	149.02404	x	Desaturation, Desaturation
Metoprolol	$C_9H_8O_2$	149.06043	x	Desaturation, Desaturation
Metoprolol	$C_6H_{12}O_4$	149.08156	x	Hydration, Oxidative Deamination to Ketone
Metoprolol	$C_6H_{15}NO_3$	150.11319	x	Hydration
Metoprolol	$C_8H_6O_3$	151.03969	x	Desaturation, Oxidation
Metoprolol Acid	$C_8H_6O_3$	151.03969	x	Desaturation
Metoprolol	$C_9H_{10}O_2$	151.07608	x	Desaturation
Metoprolol	$C_6H_{14}O_4$	151.09721	x	Hydration, Oxidative Deamination to Alcohol
Metoprolol	$C_6H_{17}NO_3$	152.12884	x	Hydration, Reduction
Metoprolol	$C_8H_8O_3$	153.05534	x	Desaturation, Oxidation

Metoprolol Acid	$C_8H_8O_3$	153.05534	x	
Metoprolol	$C_8H_8O_3$	153.05534	x	Oxidation
Metoprolol	$C_9H_{12}O_2$	153.09173	x	
Metoprolol Acid	$C_8H_{10}O_3$	155.07099	x	Reduction
Metoprolol	$C_8H_{10}O_3$	155.07099	x	Oxidation
Metoprolol	$C_8H_{10}O_3$	155.07099	x	Hydration
Metoprolol	$C_9H_{14}O_2$	155.10738	x	Reduction
Metoprolol	$C_8H_{12}O_3$	157.08664	x	Hydration
Metoprolol	$C_8H_{12}O_3$	157.08664	x	Hydration, Reduction
Metoprolol	$C_8H_{14}O_3$	159.10229	x	Hydration, Reduction
Metoprolol	$C_6H_{13}NO_4$	164.09246	x	Oxidation, Oxidation
Metoprolol	$C_6H_{15}NO_4$	166.10811	x	Hydration, Oxidation
Metoprolol Acid	$C_8H_6O_4$	167.03461	x	Desaturation, Oxidation
Metoprolol	$C_9H_{10}O_3$	167.07099	x	Desaturation, Oxidation
Metoprolol Acid	$C_8H_8O_4$	169.05026	x	Oxidation
Metoprolol	$C_8H_8O_4$	169.05026	x	Oxidation, Oxidation
Metoprolol	$C_9H_{12}O_3$	169.08664	x	Oxidation
Metoprolol Acid	$C_8H_{10}O_4$	171.06591	x	Hydration
Metoprolol	$C_8H_{10}O_4$	171.06591	x	Hydration, Oxidation
Metoprolol	$C_8H_{10}O_4$	171.06591	x	Oxidation, Oxidation
Metoprolol	$C_9H_{14}O_3$	171.10229	x	Hydration
Metoprolol	$C_{11}H_8O_2$	173.06043	x	Dehydration, Dehydration
Metoprolol	$C_8H_{12}O_4$	173.08156	x	Hydration, Oxidation
Metoprolol Acid	$C_8H_{12}O_4$	173.08156	x	Hydration, Reduction
Metoprolol	$C_9H_{16}O_3$	173.11794	x	Hydration, Reduction
Metoprolol	$C_{11}H_{11}NO$	174.09206	x	Dehydration, Dehydration
Metoprolol	$C_{11}H_{10}O_2$	175.07608	x	Dehydration, Dehydration
Metoprolol	$C_{11}H_{13}NO$	176.10771	x	Dehydration, Dehydration
Metoprolol Acid	$C_8H_8O_5$	185.04517	x	Oxidation, Oxidation
Metoprolol	$C_9H_{12}O_4$	185.08156	x	Oxidation, Oxidation
Metoprolol Acid	$C_8H_{10}O_5$	187.06082	x	Hydration, Oxidation
Metoprolol	$C_9H_{14}O_4$	187.09721	x	Hydration, Oxidation
Metoprolol Acid	$C_{11}H_8O_3$	189.05534	x	Dehydration, Dehydration
Metoprolol	$C_{11}H_8O_3$	189.05534	x	Dehydration, Desaturation
Metoprolol	$C_{12}H_{12}O_2$	189.09173	x	Dehydration, Dehydration
Metoprolol Acid	$C_{11}H_{11}NO_2$	190.08698	x	Dehydration, Dehydration
Metoprolol	$C_{11}H_{11}NO_2$	190.08698	x	Dehydration, Desaturation
Metoprolol	$C_{12}H_{15}NO$	190.12336	x	Dehydration, Dehydration
Metoprolol	$C_{11}H_{10}O_3$	191.07099	x	Dehydration, Desaturation
Metoprolol	$C_{11}H_{10}O_3$	191.07099	x	Dehydration, Oxidative Deamination to Ketone
Metoprolol	$C_{11}H_{10}O_3$	191.07099	x	Dehydration
Metoprolol	$C_{11}H_{13}NO_2$	192.10263	x	Dehydration
Metoprolol	$C_{11}H_{13}NO_2$	192.10263	x	Dehydration, Desaturation
Metoprolol	$C_{11}H_{12}O_3$	193.08664	x	Dehydration, Oxidative Deamination to Alcohol
Metoprolol	$C_{11}H_{12}O_3$	193.08664	x	Dehydration
Metoprolol	$C_{11}H_{12}O_3$	193.08664	x	Dehydration, Reduction
Metoprolol	$C_{11}H_{12}O_3$	193.08664	x	Dehydration, Oxidative Deamination to Ketone
Metoprolol	$C_{11}H_{15}NO_2$	194.11828	x	Dehydration, Reduction
Metoprolol	$C_{11}H_{15}NO_2$	194.11828	x	Dehydration
Metoprolol	$C_{11}H_{14}O_3$	195.10229	x	Dehydration, Oxidative Deamination to Alcohol
Metoprolol	$C_{11}H_{14}O_3$	195.10229	x	Dehydration, Reduction
Metoprolol	$C_{11}H_{17}NO_2$	196.13393	x	Dehydration, Reduction
Metoprolol Acid	$C_{11}H_8O_4$	205.05026	x	Dehydration, Desaturation
Metoprolol	$C_{11}H_8O_4$	205.05026	x	Desaturation, Desaturation
Metoprolol	$C_{12}H_{12}O_3$	205.08664	x	Dehydration, Desaturation

Metoprolol Acid	$C_{11}H_{11}NO_3$	206.08189	x	Dehydration, Desaturation
Metoprolol	$C_{11}H_{11}NO_3$	206.08189	x	Desaturation, Desaturation
Metoprolol	$C_{12}H_{15}NO_2$	206.11828	x	Dehydration, Desaturation
Metoprolol	$C_{11}H_{10}O_4$	207.06591	x	Desaturation, Oxidative Deamination to Ketone
Metoprolol	$C_{11}H_{10}O_4$	207.06591	x	Desaturation, Desaturation
Metoprolol	$C_{11}H_{10}O_4$	207.06591	x	Desaturation
Metoprolol Acid	$C_{11}H_{10}O_4$	207.06591	x	Dehydration, Oxidative Deamination to Ketone
Metoprolol Acid	$C_{11}H_{10}O_4$	207.06591	x	Dehydration
Metoprolol	$C_{12}H_{14}O_3$	207.10229	x	Dehydration
Metoprolol	$C_{12}H_{14}O_3$	207.10229	x	Dehydration, Oxidative Deamination to Ketone
Metoprolol	$C_{11}H_{13}NO_3$	208.09754	x	Desaturation
Metoprolol	$C_{11}H_{13}NO_3$	208.09754	x	Desaturation, Desaturation
Metoprolol Acid	$C_{11}H_{13}NO_3$	208.09754	x	Dehydration
Metoprolol	$C_{12}H_{17}NO_2$	208.13393	x	Dehydration
Metoprolol	$C_{11}H_{12}O_4$	209.08156	x	
Metoprolol	$C_{11}H_{12}O_4$	209.08156	x	Desaturation
Metoprolol	$C_{11}H_{12}O_4$	209.08156	x	Desaturation, Oxidative Deamination to Ketone
Metoprolol	$C_{11}H_{12}O_4$	209.08156	x	Oxidative Deamination to Ketone
Metoprolol Acid	$C_{11}H_{12}O_4$	209.08156	x	Dehydration, Oxidative Deamination to Alcohol
Metoprolol Acid	$C_{11}H_{12}O_4$	209.08156	x	Dehydration, Reduction
Metoprolol	$C_{12}H_{16}O_3$	209.11794	x	Dehydration, Oxidative Deamination to Alcohol
Metoprolol	$C_{12}H_{16}O_3$	209.11794	x	Dehydration, Reduction
Metoprolol Acid	$C_{11}H_{15}NO_3$	210.11319	x	Dehydration, Reduction
Metoprolol	$C_{11}H_{15}NO_3$	210.11319	x	Desaturation
Metoprolol	$C_{11}H_{15}NO_3$	210.11319	x	
Metoprolol	$C_{12}H_{19}NO_2$	210.14958	x	Dehydration, Reduction
Metoprolol	$C_{11}H_{14}O_4$	211.09721	x	Oxidative Deamination to Alcohol
Metoprolol	$C_{11}H_{14}O_4$	211.09721	x	Reduction
Metoprolol	$C_{11}H_{14}O_4$	211.09721	x	
Metoprolol	$C_{11}H_{14}O_4$	211.09721	x	Oxidative Deamination to Ketone
Metoprolol	$C_{11}H_{17}NO_3$	212.12884	x	
Metoprolol	$C_{11}H_{17}NO_3$	212.12884	x	Reduction
Metoprolol	$C_{11}H_{16}O_4$	213.11286	x	Reduction
Metoprolol	$C_{11}H_{16}O_4$	213.11286	x	Oxidative Deamination to Alcohol
Metoprolol	$C_{11}H_{16}O_4$	213.11286	x	Oxidative Deamination to Alcohol, Reduction
Metoprolol	$C_{11}H_{19}NO_3$	214.14449	x	Reduction
Metoprolol	$C_{11}H_{18}O_4$	215.12851	x	Oxidative Deamination to Alcohol, Reduction
Metoprolol	$C_{14}H_{17}NO$	216.13901	x	Dehydration, Dehydration
Metoprolol	$C_{14}H_{19}NO$	218.15466	x	Dehydration, Dehydration
Metoprolol Acid	$C_{11}H_8O_5$	221.04517	x	Desaturation, Desaturation
Metoprolol	$C_{12}H_{12}O_4$	221.08156	x	Desaturation, Desaturation
Metoprolol Acid	$C_{11}H_{11}NO_4$	222.07681	x	Desaturation, Desaturation
Metoprolol	$C_{12}H_{15}NO_3$	222.11319	x	Desaturation, Desaturation
Metoprolol Acid	$C_{11}H_{10}O_5$	223.06082	x	Desaturation
Metoprolol	$C_{11}H_{10}O_5$	223.06082	x	Desaturation, Oxidation
Metoprolol Acid	$C_{11}H_{10}O_5$	223.06082	x	Desaturation, Oxidative Deamination to Ketone
Metoprolol	$C_{12}H_{14}O_4$	223.09721	x	Desaturation
Metoprolol	$C_{12}H_{14}O_4$	223.09721	x	Desaturation, Oxidative Deamination to Ketone
Metoprolol Acid	$C_{11}H_{13}NO_4$	224.09246	x	Desaturation
Metoprolol	$C_{11}H_{13}NO_4$	224.09246	x	Desaturation, Oxidation
Metoprolol	$C_{12}H_{17}NO_3$	224.12884	x	Desaturation
Metoprolol	$C_{11}H_{12}O_5$	225.07647	x	Oxidation
Metoprolol Acid	$C_{11}H_{12}O_5$	225.07647	x	Oxidative Deamination to Ketone
Metoprolol	$C_{11}H_{12}O_5$	225.07647	x	Desaturation, Oxidation
Metoprolol	$C_{11}H_{12}O_5$	225.07647	x	Oxidation, Oxidative Deamination to Ketone

Metoprolol Acid	$C_{11}H_{12}O_5$	225.07647	x	
Metoprolol	$C_{12}H_{16}O_4$	225.11286	x	Oxidative Deamination to Ketone
Metoprolol	$C_{12}H_{16}O_4$	225.11286	x	
Metoprolol Acid	$C_{11}H_{15}NO_4$	226.10811	x	
Metoprolol	$C_{11}H_{15}NO_4$	226.10811	x	Desaturation, Oxidation
Metoprolol	$C_{11}H_{15}NO_4$	226.10811	x	Oxidation
Metoprolol	$C_{12}H_{19}NO_3$	226.14449	x	
Metoprolol	$C_{11}H_{14}O_5$	227.09212	x	Hydration, Oxidative Deamination to Ketone
Metoprolol	$C_{11}H_{14}O_5$	227.09212	x	Oxidation, Oxidative Deamination to Ketone
Metoprolol	$C_{11}H_{14}O_5$	227.09212	x	Oxidation
Metoprolol Acid	$C_{11}H_{14}O_5$	227.09212	x	Reduction
Metoprolol	$C_{11}H_{14}O_5$	227.09212	x	Hydration
Metoprolol Acid	$C_{11}H_{14}O_5$	227.09212	x	Oxidative Deamination to Alcohol
Metoprolol	$C_{12}H_{18}O_4$	227.12851	x	Oxidative Deamination to Alcohol
Metoprolol	$C_{12}H_{18}O_4$	227.12851	x	Reduction
Metoprolol	$C_{11}H_{17}NO_4$	228.12376	x	Hydration
Metoprolol Acid	$C_{11}H_{17}NO_4$	228.12376	x	Reduction
Metoprolol	$C_{11}H_{17}NO_4$	228.12376	x	Oxidation
Metoprolol	$C_{12}H_{21}NO_3$	228.16014	x	Reduction
Metoprolol	$C_{11}H_{16}O_5$	229.10777	x	Hydration, Oxidative Deamination to Alcohol
Metoprolol	$C_{11}H_{16}O_5$	229.10777	x	Hydration, Reduction
Metoprolol	$C_{11}H_{16}O_5$	229.10777	x	Hydration
Metoprolol	$C_{11}H_{16}O_5$	229.10777	x	Hydration, Oxidative Deamination to Ketone
Metoprolol Acid	$C_{11}H_{16}O_5$	229.10777	x	Oxidative Deamination to Alcohol, Reduction
Metoprolol	$C_{12}H_{20}O_4$	229.14416	x	Oxidative Deamination to Alcohol, Reduction
Metoprolol Acid	$C_{14}H_{15}NO_2$	230.11828		Dehydration, Dehydration, Desaturation
Metoprolol	$C_{11}H_{19}NO_4$	230.13941	x	Hydration, Reduction
Metoprolol	$C_{11}H_{19}NO_4$	230.13941	x	Hydration
Metoprolol	$C_{15}H_{19}NO$	230.15466		Dehydration, Dehydration, Desaturation
Metoprolol Acid	$C_{14}H_{14}O_3$	231.10229		Dehydration, Dehydration, Oxidative Deamination to Ketone
Metoprolol	$C_{11}H_{18}O_5$	231.12342	x	Hydration, Oxidative Deamination to Alcohol
Metoprolol	$C_{11}H_{18}O_5$	231.12342	x	Hydration, Reduction
Metoprolol	$C_{15}H_{18}O_2$	231.13868		Dehydration, Dehydration, Oxidative Deamination to Ketone
Metoprolol	$C_{14}H_{17}NO_2$	232.13393	x	Dehydration, Desaturation
Metoprolol Acid	$C_{14}H_{17}NO_2$	232.13393		Dehydration, Dehydration
Metoprolol	$C_{11}H_{21}NO_4$	232.15506	x	Hydration, Reduction
Metoprolol	$C_{15}H_{21}NO$	232.17031		Dehydration, Dehydration
Metoprolol Acid	$C_{14}H_{16}O_3$	233.11794		Dehydration, Dehydration, Oxidative Deamination to Alcohol
Metoprolol	$C_{14}H_{16}O_3$	233.11794	x	Dehydration, Oxidative Deamination to Ketone
Metoprolol	$C_{15}H_{20}O_2$	233.15433		Dehydration, Dehydration, Oxidative Deamination to Alcohol
Metoprolol Acid	$C_{14}H_{19}NO_2$	234.14958		Dehydration, Dehydration, Reduction
Metoprolol	$C_{14}H_{19}NO_2$	234.14958	x	Dehydration
Metoprolol	$C_{14}H_{19}NO_2$	234.14958	x	Dehydration, Desaturation
Metoprolol	$C_{15}H_{23}NO$	234.18596		Dehydration, Dehydration, Reduction
Metoprolol	$C_{14}H_{18}O_3$	235.13359	x	Dehydration, Oxidative Deamination to Alcohol
Metoprolol	$C_{14}H_{18}O_3$	235.13359	x	Dehydration, Oxidative Deamination to Ketone
Metoprolol	$C_{14}H_{21}NO_2$	236.16523	x	Dehydration
Metoprolol	$C_{14}H_{21}NO_2$	236.16523	x	Dehydration, Reduction
Metoprolol	$C_{14}H_{20}O_3$	237.14924	x	Dehydration, Oxidative Deamination to Alcohol
Metoprolol	$C_{14}H_{23}NO_2$	238.18088	x	Dehydration, Reduction
Metoprolol Acid	$C_{11}H_{10}O_6$	239.05574	x	Desaturation, Oxidation
Metoprolol	$C_{12}H_{14}O_5$	239.09212	x	Desaturation, Oxidation
Metoprolol Acid	$C_{11}H_{13}NO_5$	240.08737	x	Desaturation, Oxidation
Metoprolol	$C_{12}H_{17}NO_4$	240.12376	x	Desaturation, Oxidation
Metoprolol Acid	$C_{11}H_{12}O_6$	241.07139	x	Oxidation, Oxidative Deamination to Ketone

Metoprolol	$C_{11}H_{12}O_6$	241.07139	x	Oxidation, Oxidation
Metoprolol Acid	$C_{11}H_{12}O_6$	241.07139	x	Oxidation
Metoprolol	$C_{12}H_{16}O_5$	241.10777	x	Oxidation, Oxidative Deamination to Ketone
Metoprolol	$C_{12}H_{16}O_5$	241.10777	x	Oxidation
Metoprolol	$C_{11}H_{15}NO_5$	242.10302	x	Oxidation, Oxidation
Metoprolol Acid	$C_{11}H_{15}NO_5$	242.10302	x	Oxidation
Metoprolol	$C_{12}H_{19}NO_4$	242.13941	x	Oxidation
Metoprolol	$C_{11}H_{14}O_6$	243.08704	x	Hydration, Oxidation
Metoprolol Acid	$C_{11}H_{14}O_6$	243.08704	x	Hydration, Oxidative Deamination to Ketone
Metoprolol Acid	$C_{11}H_{14}O_6$	243.08704	x	Hydration
Metoprolol	$C_{11}H_{14}O_6$	243.08704	x	Oxidation, Oxidation
Metoprolol	$C_{12}H_{18}O_5$	243.12342	x	Hydration
Metoprolol	$C_{12}H_{18}O_5$	243.12342	x	Hydration, Oxidative Deamination to Ketone
Metoprolol	$C_{11}H_{17}NO_5$	244.11867	x	Oxidation, Oxidation
Metoprolol	$C_{11}H_{17}NO_5$	244.11867	x	Hydration, Oxidation
Metoprolol Acid	$C_{11}H_{17}NO_5$	244.11867	x	Hydration
Metoprolol	$C_{12}H_{21}NO_4$	244.15506	x	Hydration
Metoprolol Acid	$C_{11}H_{16}O_6$	245.10269	x	Hydration, Reduction
Metoprolol Acid	$C_{11}H_{16}O_6$	245.10269	x	Hydration, Oxidative Deamination to Alcohol
Metoprolol	$C_{11}H_{16}O_6$	245.10269	x	Hydration, Oxidation
Metoprolol	$C_{12}H_{20}O_5$	245.13907	x	Hydration, Oxidative Deamination to Alcohol
Metoprolol	$C_{12}H_{20}O_5$	245.13907	x	Hydration, Reduction
Metoprolol Acid	$C_{14}H_{15}NO_3$	246.11319		Dehydration, Desaturation, Desaturation
Metoprolol	$C_{11}H_{19}NO_5$	246.13432	x	Hydration, Oxidation
Metoprolol Acid	$C_{11}H_{19}NO_5$	246.13432	x	Hydration, Reduction
Metoprolol	$C_{15}H_{19}NO_2$	246.14958		Dehydration, Desaturation, Desaturation
Metoprolol	$C_{12}H_{23}NO_4$	246.17071	x	Hydration, Reduction
Metoprolol Acid	$C_{14}H_{14}O_4$	247.09721		Dehydration, Desaturation, Oxidative Deamination to Ketone
Metoprolol	$C_{15}H_{18}O_3$	247.13359		Dehydration, Desaturation, Oxidative Deamination to Ketone
Metoprolol	$C_{14}H_{17}NO_3$	248.12884	x	Desaturation, Desaturation
Metoprolol Acid	$C_{14}H_{17}NO_3$	248.12884		Dehydration, Desaturation
Metoprolol	$C_{15}H_{21}NO_2$	248.16523		Dehydration, Desaturation
Metoprolol Acid	$C_{14}H_{16}O_4$	249.11286		Dehydration, Oxidative Deamination to Ketone
Metoprolol	$C_{14}H_{16}O_4$	249.11286	x	Desaturation, Oxidative Deamination to Ketone
Metoprolol	$C_{15}H_{20}O_3$	249.14924		Dehydration, Oxidative Deamination to Ketone
Metoprolol Acid	$C_{14}H_{19}NO_3$	250.14449		Dehydration
Metoprolol	$C_{14}H_{19}NO_3$	250.14449	x	Desaturation, Desaturation
Metoprolol	$C_{14}H_{19}NO_3$	250.14449	x	Desaturation
Metoprolol	$C_{15}H_{23}NO_2$	250.18088		Dehydration
Metoprolol	$C_{14}H_{18}O_4$	251.12851	x	Desaturation, Oxidative Deamination to Ketone
Metoprolol Acid	$C_{14}H_{18}O_4$	251.12851		Dehydration, Oxidative Deamination to Alcohol
Metoprolol	$C_{14}H_{18}O_4$	251.12851	x	Oxidative Deamination to Ketone
Metoprolol	$C_{15}H_{22}O_3$	251.16489		Dehydration, Oxidative Deamination to Alcohol
Metoprolol	$C_{14}H_{21}NO_3$	252.16014	x	Desaturation
Metoprolol	$C_{14}H_{21}NO_3$	252.16014	x	
Metoprolol Acid	$C_{14}H_{21}NO_3$	252.16014		Dehydration, Reduction
Metoprolol	$C_{15}H_{25}NO_2$	252.19653		Dehydration, Reduction
Metoprolol	$C_{14}H_{20}O_4$	253.14416	x	Oxidative Deamination to Ketone
Metoprolol Acid	$C_{14}H_{20}O_4$	253.14416		Dehydration, Oxidative Deamination to Alcohol, Reduction
Metoprolol	$C_{14}H_{20}O_4$	253.14416	x	Oxidative Deamination to Alcohol
Metoprolol	$C_{15}H_{24}O_3$	253.18054		Dehydration, Oxidative Deamination to Alcohol, Reduction
Metoprolol	$C_{14}H_{23}NO_3$	254.17579	x	Reduction
Metoprolol	$C_{14}H_{23}NO_3$	254.17579	x	
Metoprolol	$C_{14}H_{22}O_4$	255.15981	x	Oxidative Deamination to Alcohol, Reduction
Metoprolol	$C_{14}H_{22}O_4$	255.15981	x	Oxidative Deamination to Alcohol

Metoprolol	$C_{14}H_{25}NO_3$	256.19144	x	Reduction
Metoprolol Acid	$C_{11}H_{12}O_7$	257.0663	x	Oxidation, Oxidation
Metoprolol	$C_{12}H_{16}O_6$	257.10269	x	Oxidation, Oxidation
Metoprolol	$C_{14}H_{24}O_4$	257.17546	x	Oxidative Deamination to Alcohol, Reduction
Metoprolol Acid	$C_{11}H_{15}NO_6$	258.09794	x	Oxidation, Oxidation
Metoprolol	$C_{12}H_{19}NO_5$	258.13432	x	Oxidation, Oxidation
Metoprolol Acid	$C_{11}H_{14}O_7$	259.08195	x	Hydration, Oxidation
Metoprolol	$C_{12}H_{18}O_6$	259.11834	x	Hydration, Oxidation
Metoprolol Acid	$C_{11}H_{17}NO_6$	260.11359	x	Hydration, Oxidation
Metoprolol	$C_{12}H_{21}NO_5$	260.14997	x	Hydration, Oxidation
Metoprolol Acid	$C_{14}H_{15}NO_4$	262.10811		Desaturation, Desaturation, Desaturation
Metoprolol	$C_{15}H_{19}NO_3$	262.14449		Desaturation, Desaturation, Desaturation
Metoprolol Acid	$C_{14}H_{14}O_5$	263.09212		Desaturation, Desaturation, Oxidative Deamination to Ketone
Metoprolol	$C_{15}H_{18}O_4$	263.12851		Desaturation, Desaturation, Oxidative Deamination to Ketone
Metoprolol Acid	$C_{14}H_{17}NO_4$	264.12376		Desaturation, Desaturation
Metoprolol	$C_{15}H_{21}NO_3$	264.16014		Desaturation, Desaturation
Metoprolol Acid	$C_{14}H_{16}O_5$	265.10777		Desaturation, Oxidative Deamination to Ketone
Metoprolol	$C_{15}H_{20}O_4$	265.14416		Desaturation, Oxidative Deamination to Ketone
Metoprolol Acid	$C_{14}H_{19}NO_4$	266.13941		Desaturation
Metoprolol	$C_{14}H_{19}NO_4$	266.13941	x	Desaturation, Oxidation
Metoprolol	$C_{15}H_{23}NO_3$	266.17579		Desaturation
Metoprolol Acid	$C_{14}H_{18}O_5$	267.12342		Oxidative Deamination to Ketone
Metoprolol	$C_{14}H_{18}O_5$	267.12342	x	Oxidation, Oxidative Deamination to Ketone
Metoprolol	$C_{15}H_{22}O_4$	267.15981		Oxidative Deamination to Ketone
Metoprolol	$C_{14}H_{21}NO_4$	268.15506	x	Oxidation
Metoprolol Acid	$C_{14}H_{21}NO_4$	268.15506		
Metoprolol	$C_{14}H_{21}NO_4$	268.15506	x	Desaturation, Oxidation
Metoprolol	$C_{15}H_{25}NO_3$	268.19144		
Metoprolol	$C_{14}H_{20}O_5$	269.13907	x	Oxidation, Oxidative Deamination to Ketone
Metoprolol Acid	$C_{14}H_{20}O_5$	269.13907		Oxidative Deamination to Alcohol
Metoprolol	$C_{14}H_{20}O_5$	269.13907	x	Hydration, Oxidative Deamination to Ketone
Metoprolol	$C_{15}H_{24}O_4$	269.17546		Oxidative Deamination to Alcohol
Metoprolol Acid	$C_{14}H_{23}NO_4$	270.17071		Reduction
Metoprolol	$C_{14}H_{23}NO_4$	270.17071	x	Hydration
Metoprolol	$C_{14}H_{23}NO_4$	270.17071	x	Oxidation
Metoprolol	$C_{15}H_{27}NO_3$	270.20709		Reduction
Metoprolol	$C_{14}H_{22}O_5$	271.15472	x	Hydration, Oxidative Deamination to Alcohol
Metoprolol Acid	$C_{14}H_{22}O_5$	271.15472		Oxidative Deamination to Alcohol, Reduction
Metoprolol	$C_{14}H_{22}O_5$	271.15472	x	Hydration, Oxidative Deamination to Ketone
Metoprolol	$C_{15}H_{26}O_4$	271.19111		Oxidative Deamination to Alcohol, Reduction
Metoprolol	$C_{14}H_{25}NO_4$	272.18636	x	Hydration, Reduction
Metoprolol	$C_{14}H_{25}NO_4$	272.18636	x	Hydration
Metoprolol	$C_{14}H_{24}O_5$	273.17037	x	Hydration, Oxidative Deamination to Alcohol
Metoprolol	$C_{14}H_{27}NO_4$	274.20201	x	Hydration, Reduction
Metoprolol Acid	$C_{14}H_{17}NO_5$	280.11867		Desaturation, Desaturation, Oxidation
Metoprolol	$C_{15}H_{21}NO_4$	280.15506		Desaturation, Desaturation, Oxidation
Metoprolol Acid	$C_{14}H_{16}O_6$	281.10269		Desaturation, Oxidation, Oxidative Deamination to Ketone
Metoprolol	$C_{15}H_{20}O_5$	281.13907		Desaturation, Oxidation, Oxidative Deamination to Ketone
Metoprolol Acid	$C_{14}H_{19}NO_5$	282.13432		Desaturation, Oxidation
Metoprolol	$C_{15}H_{23}NO_4$	282.17071		Desaturation, Oxidation
Metoprolol Acid	$C_{14}H_{18}O_6$	283.11834		Oxidation, Oxidative Deamination to Ketone
Metoprolol	$C_{15}H_{22}O_5$	283.15472		Oxidation, Oxidative Deamination to Ketone
Metoprolol	$C_{14}H_{21}NO_5$	284.14997	x	Oxidation, Oxidation
Metoprolol Acid	$C_{14}H_{21}NO_5$	284.14997		Oxidation
Metoprolol	$C_{15}H_{25}NO_4$	284.18636		Oxidation

Metoprolol Acid	$C_{14}H_{20}O_6$	285.13399		Hydration, Oxidative Deamination to Ketone
Metoprolol	$C_{15}H_{24}O_5$	285.17037		Hydration, Oxidative Deamination to Ketone
Metoprolol	$C_{14}H_{23}NO_5$	286.16562	x	Oxidation, Oxidation
Metoprolol	$C_{14}H_{23}NO_5$	286.16562	x	Hydration, Oxidation
Metoprolol Acid	$C_{14}H_{23}NO_5$	286.16562		Hydration
Metoprolol	$C_{15}H_{27}NO_4$	286.20201		Hydration
Metoprolol Acid	$C_{14}H_{22}O_6$	287.14964		Hydration, Oxidative Deamination to Alcohol
Metoprolol	$C_{15}H_{26}O_5$	287.18602		Hydration, Oxidative Deamination to Alcohol
Metoprolol	$C_{14}H_{25}NO_5$	288.18127	x	Hydration, Oxidation
Metoprolol Acid	$C_{14}H_{25}NO_5$	288.18127		Hydration, Reduction
Metoprolol	$C_{15}H_{29}NO_4$	288.21766		Hydration, Reduction
Metoprolol Acid	$C_{14}H_{24}O_6$	289.16529		Hydration, Oxidative Deamination to Alcohol, Reduction
Metoprolol	$C_{15}H_{28}O_5$	289.20167		Hydration, Oxidative Deamination to Alcohol, Reduction
Metoprolol Acid	$C_{14}H_{19}NO_6$	298.12924		Desaturation, Oxidation, Oxidation
Metoprolol	$C_{15}H_{23}NO_5$	298.16562		Desaturation, Oxidation, Oxidation
Metoprolol Acid	$C_{14}H_{18}O_7$	299.11325		Oxidation, Oxidation, Oxidative Deamination to Ketone
Metoprolol	$C_{15}H_{22}O_6$	299.14964		Oxidation, Oxidation, Oxidative Deamination to Ketone
Metoprolol Acid	$C_{14}H_{21}NO_6$	300.14489		Oxidation, Oxidation
Metoprolol	$C_{15}H_{25}NO_5$	300.18127		Oxidation, Oxidation
Metoprolol Acid	$C_{14}H_{20}O_7$	301.1289		Hydration, Oxidation, Oxidative Deamination to Ketone
Metoprolol	$C_{15}H_{24}O_6$	301.16529		Hydration, Oxidation, Oxidative Deamination to Ketone
Metoprolol Acid	$C_{14}H_{23}NO_6$	302.16054		Hydration, Oxidation
Metoprolol	$C_{15}H_{27}NO_5$	302.19692		Hydration, Oxidation
Metoprolol Acid	$C_{14}H_{22}O_7$	303.14455		Hydration, Oxidation, Oxidative Deamination to Alcohol
Metoprolol	$C_{15}H_{26}O_6$	303.18094		Hydration, Oxidation, Oxidative Deamination to Alcohol
Metoprolol Acid	$C_{14}H_{25}NO_6$	304.17619		Hydration, Oxidation, Reduction
Metoprolol	$C_{15}H_{29}NO_5$	304.21257		Hydration, Oxidation, Reduction
Metoprolol Acid	$C_{14}H_{21}NO_7$	316.1398		Oxidation, Oxidation, Oxidation
Metoprolol	$C_{15}H_{25}NO_6$	316.17619		Oxidation, Oxidation, Oxidation
Metoprolol Acid	$C_{14}H_{23}NO_7$	318.15545		Hydration, Oxidation, Oxidation
Metoprolol	$C_{15}H_{27}NO_6$	318.19184		Hydration, Oxidation, Oxidation

Table S4. List of the 18 compounds present in the in-house library (Jaén-Gil et al., 2019).

R_t (min)	Compound	Ion	Molecular formula	Theoretical exact mass	RDBE	Suggested chemical structure
7.64	MTP	$[M+H]^+$	$C_{15}H_{26}NO_3$	268.19070	3.5	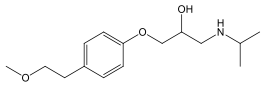
		$[M+H–(H_2O)]^+$	$C_{15}H_{24}NO_2$	250.18016	4.5	
		$[M+H–(C_3H_6)]^+$	$C_{12}H_{20}NO_3$	226.14377	3.5	
		$[M+H–(C_3H_{11}NO)]^+$	$C_{12}H_{15}O_2$	191.10666	5.5	
		$[M+H–(C_7H_{18}NO_2)]^+$	C_8H_9O	121.06479	4.5	
		$[M+H–(C_9H_{12}O_2)]^+$	$C_6H_{14}NO$	116.10699	0.5	
6.68	MTPA	$[M+H]^+$	$C_{14}H_{22}NO_4$	268.15432	4.5	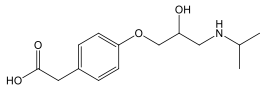
		$[M+H–(H_2O)]^+$	$C_{14}H_{20}NO_3$	250.14377	5.5	
		$[M+H–(C_3H_6)]^+$	$C_{11}H_{16}NO_4$	226.10738	4.5	
		$[M+H–(H_2O)–(C_3H_9N)]^+$	$C_{11}H_{11}O_3$	191.07027	6.5	
		$[M+H–(C_8H_{14}O_3)]^+$	$C_{10}H_9O$	145.06479	6.5	
		$[M+H–(C_8H_8O_3)]^+$	$C_6H_{14}NO$	116.10699	0.5	
2.87	TP134	$[M+H]^+$	$C_6H_{16}NO_2$	134.11754	-0.5	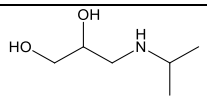
		$[M+H–(H_2O)]^+$	$C_6H_{14}NO$	116.10699	0.5	
		$[M+H–(C_3H_6)]^+$	$C_3H_{10}NO_2$	92.07061	-0.5	
6.21	TP226 A	$[M+H]^+$	$C_{12}H_{20}NO_3$	226.14376	3.5	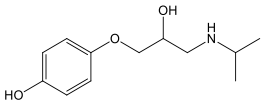
		$[M+H–(H_2O)]^+$	$C_{12}H_{18}NO_2$	208.13321	4.5	
		$[M+H–(C_3H_6)]^+$	$C_9H_{14}NO_3$	184.09682	3.5	
		$[M+H–(H_2O)–(C_3H_9N)]^+$	$C_9H_9O_2$	149.05971	5.5	
		$[M+H–(C_6H_6O_2)]^+$	$C_6H_{14}NO$	116.10699	0.5	
7.07	TP226 B	$[M+H]^+$	$C_{12}H_{20}NO_3$	226.14376	3.5	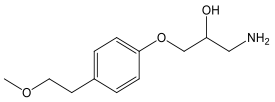
		$[M+H–(H_2O)]^+$	$C_{12}H_{18}NO_2$	208.13321	4.5	
		$[M+H–(H_2O)–(CH_2)]^+$	$C_{11}H_{16}NO_2$	194.11756	4.5	
		$[M+H–(H_2O)–(NH_3)]^+$	$C_{12}H_{15}O_2$	191.10666	5.5	
		$[M+H–(C_4H_{11}O_2)]^+$	C_8H_9O	121.06479	4.5	
		$[M+H–(C_9H_{12}O_2)]^+$	C_3H_8NO	74.06004	0.5	
6.66	TP226 C	$[M+H]^+$	$C_{11}H_{16}NO_4$	226.10738	4.5	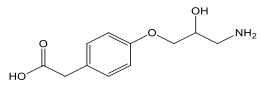
		$[M+H–(H_2O)]^+$	$C_{11}H_{14}NO_3$	208.09682	5.5	
		$[M+H–(H_2O)–(NH_3)]^+$	$C_{11}H_{11}O_3$	191.07027	6.5	
		$[M+H–(CH_7O_3)]^+$	$C_{10}H_9O$	145.06479	6.5	
		$[M+H–(C_8H_8O_3)]^+$	C_3H_8NO	74.06004	0.5	
6.83	TP238	$[M+H]^+$	$C_{13}H_{20}NO_3$	238.14376	4.5	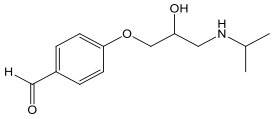
		$[M+H–(H_2O)]^+$	$C_{13}H_{18}NO_2$	220.13321	5.5	
		$[M+H–(C_3H_6)]^+$	$C_{10}H_{14}NO_3$	196.09682	4.5	
		$[M+H–(H_2O)–(C_3H_9N)]^+$	$C_{10}H_9O_2$	161.05971	6.5	
		$[M+H–(C_5H_{13}NO)]^+$ (HCD)	$C_8H_7O_2$	135.04405	5.5	
		$[M+H–(C_7H_6O_2)]^+$	$C_6H_{14}NO$	116.10699	0.5	
6.22	TP240	$[M+H]^+$	$C_{13}H_{22}NO_3$	240.15940	3.5	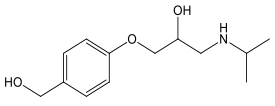
		$[M+H–(H_2O)]^+$	$C_{13}H_{20}NO_2$	222.14886	4.5	
		$[M+H–(C_3H_6)]^+$	$C_{10}H_{16}NO_3$	198.11247	3.5	
		$[M+H–(H_2O)–(C_3H_9N)]^+$	$C_{10}H_{11}O_2$	163.07536	5.5	
		$[M+H–(C_4H_{14}NO_2)]^+$	C_9H_9O	133.06479	5.5	
		$[M+H–(C_7H_8O_2)]^+$	$C_6H_{14}NO$	116.10699	0.5	
6.37	TP254	$[M+H]^+$	$C_{13}H_{20}NO_4$	254.13867	3.5	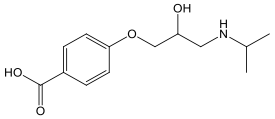
		$[M+H–(H_2O)]^+$	$C_{13}H_{18}NO_3$	236.12812	5.5	
		$[M+H–(C_3H_6)]^+$	$C_{10}H_{14}NO_4$	212.09173	4.5	
		$[M+H–(H_2O)–(C_3H_9N)]^+$	$C_{10}H_9O_3$	177.05462	6.5	
		$[M+H–(C_5H_{13}NO)]^+$ (HCD)	$C_8H_7O_3$	151.03897	5.5	
		$[M+H–(C_7H_6O_3)]^+$	$C_6H_{14}NO$	116.10699	0.5	

6.63	O-DMTP	$[M+H]^+$	$C_{14}H_{24}NO_3$	254.17505	4.5	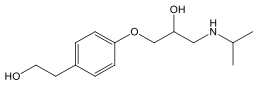
		$[M+H–(H_2O)]^+$	$C_{14}H_{22}NO_2$	236.16451	4.5	
		$[M+H–(C_3H_6)]^+$	$C_{11}H_{18}NO_3$	212.12812	3.5	
		$[M+H–(H_2O)–(C_3H_9N)]^+$	$C_{11}H_{13}O_2$	177.09101	5.5	
		$[M+H–(C_8H_{10}O_2)]^+$	$C_6H_{14}NO$	116.10699	0.5	
5.75	TP270	$[M+H]^+$	$C_{14}H_{24}NO_4$	270.16998	3.5	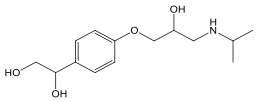
		$[M+H–(H_2O)]^+$	$C_{14}H_{22}NO_3$	252.15942	4.5	
		$[M+H–2(H_2O)]^+$	$C_{14}H_{20}NO_2$	234.14886	5.5	
		$[M+H–(C_3H_6)]^+$	$C_{11}H_{18}NO_4$	228.12303	3.5	
		$[M+H–(C_3H_{10}N)–(H_2O)]^+$	$C_{11}H_{13}O_3$	193.08592	5.5	
		$[M+H–(C_5H_{16}NO_3)]^+$	C_9H_9O	133.06479	5.5	
		$[M+H–(C_8H_{10}NO_3)]^+$	$C_6H_{14}NO$	116.10699	0.5	
6.69	TP282 A	$[M+H]^+$	$C_{15}H_{24}NO_4$	282.16997	4.5	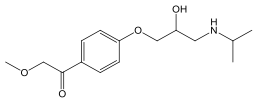
		$[M+H–(H_2O)]^+$	$C_{15}H_{22}NO_3$	264.15942	5.5	
		$[M+H–(C_3H_6)]^+$	$C_{12}H_{18}NO_4$	240.12303	4.5	
		$[M+H–(H_2O)–(C_3H_9N)]^+$	$C_{12}H_{13}O_3$	205.08592	6.5	
		$[M+H–(C_2H_5O)–(C_5H_{12}NO)]^+$ (HCD)	$C_8H_7O_2$	135.04405	5.5	
		$[M+H–(C_9H_{10}O_3)]^+$	$C_6H_{14}NO$	116.10699	0.5	
7.48	TP282 B	$[M+H]^+$	$C_{15}H_{24}NO_4$	282.16997	4.5	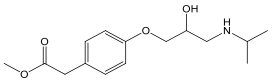
		$[M+H–(H_2O)]^+$	$C_{15}H_{22}NO_3$	264.15942	5.5	
		$[M+H–(C_3H_6)]^+$	$C_{12}H_{18}NO_4$	240.12303	4.5	
		$[M+H–(H_2O)–(C_3H_9N)]^+$	$C_{12}H_{13}O_3$	205.08592	6.5	
		$[M+H–(C_5H_{16}O_3)]^+$	$C_{10}H_9O$	145.06479	6.5	
		$[M+H–(C_9H_{10}O_3)]^+$	$C_6H_{14}NO$	116.10699	0.5	
6.40	α-HMTP	$[M+H]^+$	$C_{15}H_{26}NO_4$	284.18562	3.5	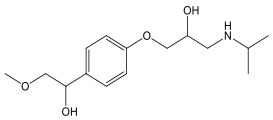
		$[M+H–(H_2O)]^+$	$C_{15}H_{24}NO_3$	266.17507	4.5	
		$[M+H–(H_2O)–(C_3H_5)]^+$	$C_{12}H_{18}NO_3$	224.12812	4.5	
		$[M+H–(H_2O)–(C_3H_9N)]^+$	$C_{12}H_{15}O_3$	207.10157	5.5	
		$[M+H–(CH_5O_2)–(C_5H_{12}NO)]^+$	C_9H_9O	133.06479	5.5	
		$[M+H–(C_9H_{12}O_3)]^+$	$C_6H_{14}NO$	116.10699	0.5	
7.31	TP284	$[M+H]^+$	$C_{15}H_{26}NO_4$	284.18562	3.5	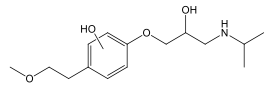
		$[M+H–(H_2O)]^+$	$C_{15}H_{24}NO_3$	266.17507	4.5	
		$[M+H–(CH_4O)]^+$	$C_{14}H_{22}NO_3$	252.15942	4.5	
		$[M+H–(H_2O)–(CH_4O)]^+$	$C_{14}H_{20}NO_2$	234.14886	5.5	
		$[M+H–(CH_5O)–(C_3H_3)]^+$	$C_{11}H_{14}NO_2$	192.10191	5.5	
		$[M+H–(H_2O)–(C_3H_9N)]^+$	$C_{11}H_{11}O_2$	175.07536	6.5	
		$[M+H–(CH_5O)–(C_5H_{12}NO)]^+$ (HCD)	$C_9H_9O_2$	149.05971	5.5	
		$[M+H–(C_9H_{12}O_3)]^+$	$C_6H_{14}NO$	116.10699	0.5	
6.86	TP298	$[M+H]^+$	$C_{15}H_{24}NO_5$	298.16488	4.5	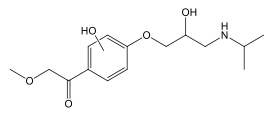
		$[M+H–(H_2O)]^+$	$C_{15}H_{22}NO_4$	280.15433	5.5	
		$[M+H–(CH_4O)]^+$	$C_{14}H_{20}NO_4$	266.13868	5.5	
		$[M+H–(C_3H_6)–(CH_3O)]^+$	$C_{11}H_{14}NO_4$	224.09173	5.5	
		$[M+H–(C_2H_5O)–(C_5H_{12}NO)]^+$ (HCD)	$C_8H_7O_3$	151.03897	5.5	
		$[M+H–(C_9H_{10}O_4)]^+$	$C_6H_{14}NO$	116.10699	0.5	
6.72	TP300	$[M+H]^+$	$C_{15}H_{26}NO_5$	300.18055	3.5	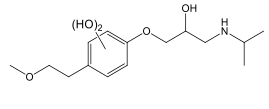
		$[M+H–(H_2O)]^+$	$C_{15}H_{24}NO_4$	282.16998	4.5	
		$[M+H–(CH_4O)]^+$	$C_{14}H_{22}NO_4$	268.15433	4.5	
		$[M+H–(H_2O)–(CH_4O)]^+$	$C_{14}H_{20}NO_3$	250.14377	5.5	
		$[M+H–(CH_5O)–(C_5H_{12}NO)]^+$	$C_9H_9O_3$	165.05462	5.5	
		$[M+H–(C_6H_{18}NO_3)]^+$	$C_9H_9O_2$	149.05971	5.5	
		$[M+H–(C_{13}H_{12}O_4)]^+$	$C_6H_{14}NO$	116.10699	0.5	
6.50	TP316	$[M+H]^+$	$C_{15}H_{26}NO_6$	316.17545	3.5	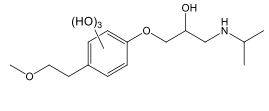
		$[M+H–(H_2O)]^+$	$C_{15}H_{24}NO_5$	298.16490	4.5	
		$[M+H–(C_3H_6)]^+$	$C_{12}H_{20}NO_6$	274.12851	3.5	
		$[M+H–(C_3H_8O)]^+$	$C_{12}H_{18}NO_5$	256.11795	4.5	
		$[M+H–(C_6H_{15}NO_2)]^+$	$C_9H_{11}O_4$	183.06519	4.5	
		$[M+H–(C_9H_{12}O_5)]^+$	$C_6H_{14}NO$	116.10699	0.5	

S3. MTP and MTPA degradation kinetics

UV, H_2O_2 and UV+H_2O_2 treatments at 25, 100, 250 and 1000 mg/L were performed in parallel to evaluate MTP removal (at initial concentration of 10 mg/L). MTP elimination was complete (>99%) after 10 minutes of reaction for all the tested experimental conditions, with the exception of the treatment with only H_2O_2 which was not effective (Fig. S1). On the contrary, the complete elimination of MTP was observed in this study using UV only. MTP is sometimes reported in the literature to be hardly degraded in photo-oxidation experiments with Xe lamps, emitting light in the 295-400 nm range (Filipe et al., 2017; Romero et al., 2015). However, in our study, a Hg lamp was emitting only UV-light (at 254 nm), closer to the typical absorption peaks described for MTP (221 and 273 nm). Therefore, the photolysis on MTP was more effective and a more complete elimination was observed. Actually, other authors have observed partial elimination of MTP, between 40-94%, using the same monochromatic UV-C light (254 nm), but with different conditions; namely different initial MTP concentration and exposure time (Rivas et al., 2010; Romero et al., 2015). For instance, Rivas et al. (2010) observed that increasing experiment initial concentration (from 20 to 150 mg/L) caused a decrease in MTP removal efficiency (from 70 to 40%). In another study a 60% of elimination was achieved after 256 min of irradiation of MTP at an initial concentration of 400 mg/L with a medium pressure lamp (254-579 nm emission light) (Toolaram et al., 2017). All these studies indicate that many parameters can influence in MTP removal under UV photolysis experiments.

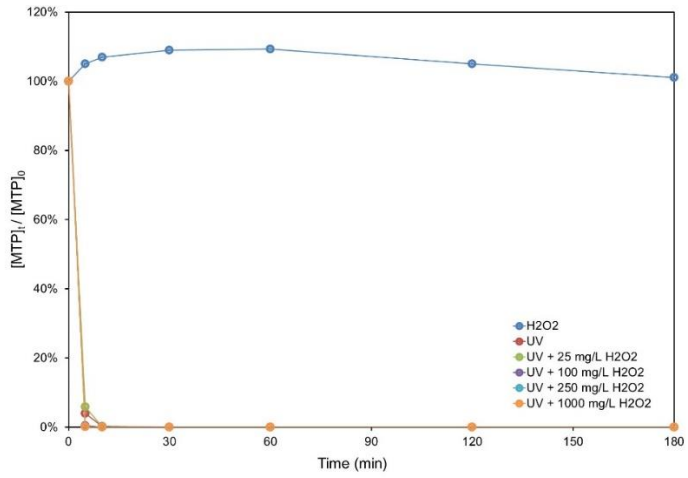

Figure S1. MTP removal with UV, H_2O_2 and UV+H_2O_2 at 25, 100, 250 and 1000 mg/L treatments (spiked MTP initial concentration of 10 mg/L).

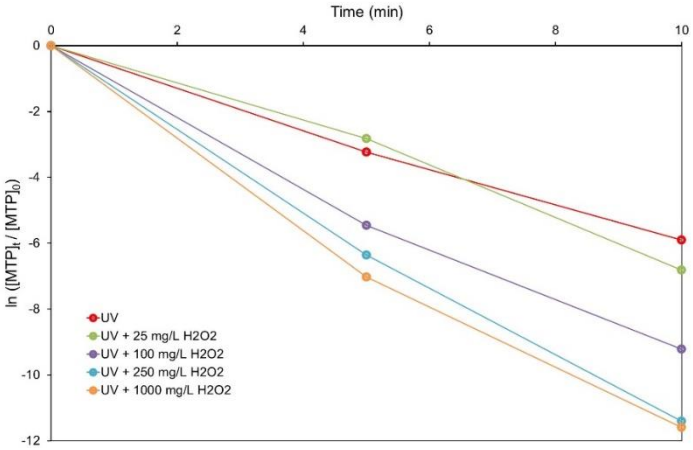

Figure S2. Plot of ln([MTP]/[MTP]$_0$) as a function of the reaction time with UV and UV+H_2O_2 at 25, 100, 250 and 1000 mg/L treatments (spiked MTP initial concentration of 10 mg/L).

Afterwards, individual degradation experiments at the optimized AOP conditions (25 mg/L H_2O_2 and 10 min of reaction) were also launched to describe degradation kinetics of MTP and MTPA (spiked at 2.5 mg/L each) in pure water. Finally, MTP and MTPA were monitored at an initial concentration of 2.5 mg/L each (in separated experiments) to describe their degradation kinetics (Fig. S3). In presence of a large excess of hydroxyl radicals (i.e. $[OH]_0 \geq 10\ [C]_0$), the reactions of MTP and MTPA with H_2O_2 exhibit a pseudo-first-order dependence on MTP and MTPA concentration (Fig. S4). The linear time-course plot between ln([C]/[C]$_0$) and the reaction can be described by equations (Eq. 1, 2 and 3), (Fig. S4):

$$\frac{d[C]}{dt} = -\ k\ \cdot [OH] \cdot [C] \qquad \text{(Eq. 1)}$$

$$\frac{d[C]}{dt} = -\ k_{obs} \cdot [C] \qquad \text{(Eq. 2)}$$

where k represent the second order rate constant for the overall reactions, *C* the concentration of MTP and MTPA and k_{obs} the pseudo-first-order kinetic constant, being $k_{obs} = k\ [OH]$, with $[OH] = [OH]_0$. Therefore, the equations can be written as follows (Eq. 3):

$$ln\frac{[C]_t}{[C]_0} = \ -k_{obs} \cdot t \qquad \text{(Eq. 3)}$$

Then, the kinetics of MTP and MTPA were confirmed as pseudo first-order with K_{obs} of 1.95 min^{-1} and 2.39 min^{-1} for MTP and MTPA, respectively.

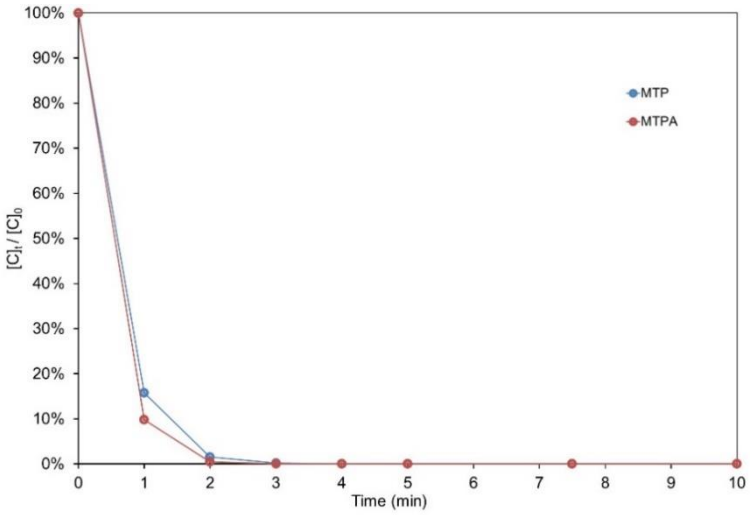

Figure S3. MTP and MTPA removal in pure water at the final selected conditions: initial MTP and MTPA concentrations of 2.5 mg/L each, 25 mg/L of H_2O_2 and 10 min of treatment.

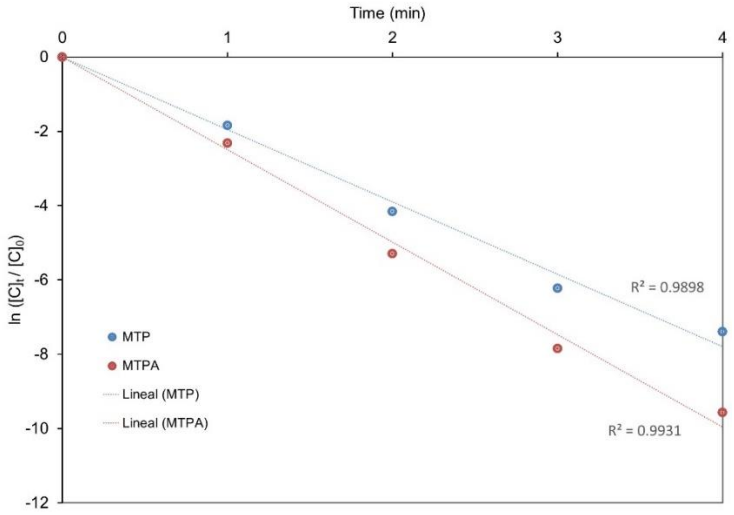

Figure S4. Plot of ln([C]/[C]$_0$) as a function of the reaction time: C is the concentration of MTP or MTPA at the selected conditions, initial MTP and MTPA concentrations of 2.5 mg/L each, 25 mg/L of H_2O_2, 10 min of treatment. After 4 minutes of reaction, almost total removal was observed and removal percentages could not be calculated anymore.

S4. Wastewaters' characterization

Table S5. Hospital and industrial wastewater characterization.

Sample	Hospital WW (mg/L)	Industrial WW (mg/L)
COD	210.4	535. 6
N-NO_2	1.6	<LOQ
N-NO_3	5.9	<LOQ
P-PO_4	2.0	<LOQ
N-NH_4	25.9	21.45
TOC	65.9	202.68
TN	46.8	68.68
TKN	31.9	65.95

S5. Detection of transformation products

Table S6. List of the total exact masses of the 85 compounds identified in the samples using the four identification strategies: literature list, compound prediction, in-house library and reference standards, (IF = identification factor).

Name	Literature	Compound prediction	In-house library	Reference standards	Maximum IF
MTP	X	X	X	X	4
MTPA	X	X	X	X	4
TP74	X				1
TP114	X[1]	X			2
TP116	X[1]	X			2
TP120	X				1
TP121	X[1]	X			2
TP134	X	X	X		3
TP150	X	X			2
TP176		X			2
TP192		X			2
TP194		X			2
TP196	X[1]				1
TP208	X[1]				1
TP212		X			2
TP218		X			2
TP220	X				1
TP226B	X	X	X		3
TP226C	X	X	X		3
TP232	X[1]				1
TP236	X				1
TP238	X		X		2
TP240	X[1]		X		2
TP250	X[1]	X			2
TP252	X[1]	X			2
TP254	X[1]		X		2
O-DMTP	X[1]	X	X	X	4
TP256	X[1]				1
TP270	X[1]	X	X		3
TP282A	X[1]	X	X		3
α-HMTP	X[1]	X	X	X	4
TP284	X	X	X		3
TP298	X[1]				1
TP300	X[1]	X	X		3
TP316	X[1]		X		2
TP318	X[1]				1
TP332	X[1]				1
Total % (85 candidates)	88%	26%	18%	5%	

([1]Exact mass detected in more than one retention time. Each retention time counts as a tentative feature).

S6. Identification of transformation products

Table S7. List of the 26 compounds identified (IF ≥ 2) in the three matrices (pure water, HWW and IWW) using compound prediction, in-house library and reference standards strategies, (IF = identification factor).

R_t (min)	Name	Ion	Molecular formula	Theor. *m/z*	Exp. *m/z*	Mass error (ppm)	RDBE	Suggested chemical structure	IF
7.50	MTP	$[M+H]^+$	$C_{15}H_{26}NO_3$	268.19070	268.19031	-1.45	3.5	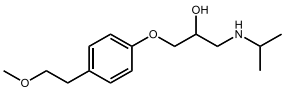	4
		$[M+H-(H_2O)]^+$	$C_{15}H_{24}NO_2$	250.18016	250.18059	1.71	4.5		
		$[M+H-(C_3H_6)]^+$	$C_{12}H_{20}NO_3$	226.14377	226.14406	1.28	3.5		
		$[M+H-(C_3H_{11}NO)]^+$	$C_{12}H_{15}O_2$	191.10666	191.10687	1.09	5.5		
		$[M+H-(C_9H_{12}O_2)]^+$	$C_6H_{14}NO$	116.10699	116.10731	2.75	0.5		
6.64	MTPA	$[M+H]^+$	$C_{14}H_{22}NO_4$	268.15432	268.15436	0.14	4.5	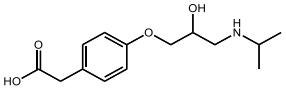	4
		$[M+H-(H_2O)]^+$	$C_{14}H_{20}NO_3$	250.14377	250.14455	3.11	5.5		
		$[M+H-(C_3H_6)]^+$	$C_{11}H_{16}NO_4$	226.10738	226.10796	2.56	4.5		
		$[M+H-(H_2O)-(C_3H_9N)]^+$	$C_{11}H_{11}O_3$	191.07027	191.07077	2.61	6.5		
		$[M+H-(C_8H_{14}O_3)]^+$	$C_{10}H_9O$	145.06479	145.06522	2.96	6.5		
1.86	TP114	$[M+H]^+$	$C_6H_{12}NO$	114.09134	114.09132	-0.17	1.5	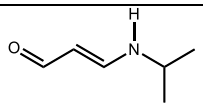	2
		$[M+H-(H_2O)]^+$	$C_6H_{10}N$	96.08078	96.08096	1.87	2.5		
		$[M+H-(C_3H_6)]^+$	C_3H_6NO	72.04439	72.04453	1.94	1.5		
2.96	TP116	$[M+H]^+$	$C_6H_{14}NO$	116.10699	116.10701	0.17	0.5	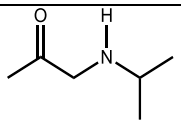	2
		$[M+H-(H_2O)]^+$	$C_6H_{12}N$	98.09643	98.09673	3.05	1.5		
		$[M+H-(C_3H_6)]^+$	C_3H_8NO	74.06004	74.06029	3.37	0.5		
		$[M+H-(C_2H_2O)]^+$	$C_4H_{10}N$	72.08078	72.08102	3.32	0.5		
7.76	TP121	$[M+H]^+$	C_8H_9O	121.06479	121.06483	0.33	4.5	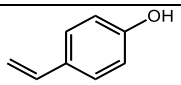	2
		$[M+H-(O)]^+$	C_8H_9	105.06988	105.07027	3.71	4.5		
		$[M+H-(C_2H_2)-(O)]^+$	C_6H_7	79.05423	79.05428	0.63	3.5		
2.88	TP134	$[M+H]^+$	$C_6H_{16}NO_2$	134.11754	134.11755	0.07	-0.5	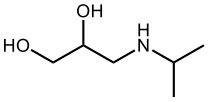	3
		$[M+H-(H_2O)]^+$	$C_6H_{14}NO$	116.10699	116.10740	3.53	0.5		
		$[M+H-(C_3H_6)]^+$	$C_3H_{10}NO_2$	92.07061	92.07104	4.67	-0.5		
2.72	TP150	$[M+H]^+$	$C_6H_{16}NO_3$	150.11247	150.11215	-2.13	-0.5	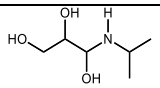	2
		$[M+H-(H_2O)]^+$	$C_6H_{14}NO_2$	132.10191	132.10194	0.22	0.5		
		$[M+H-(H_2O)-(H_2O)]^+$	$C_6H_{12}NO$	114.09134	114.09158	2.10	1.5		
7.22	TP176	$[M+H]^+$	$C_{11}H_{14}NO$	176.10699	176.10732	1.87	5.5	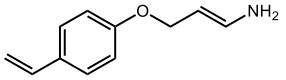	2
		$[M+H-(NH_3)]^+$	$C_{11}H_{11}O$	159.08044	159.08076	2.01	6.5		
		$[M+H-(NH_3)-(C_2H_2)]^+$	C_9H_9O	133.06479	133.06497	1.35	5.5		
		$[M+H-(NH_3)-(C_3H_2)]^+$	C_8H_9O	121.06479	121.06512	2.72	4.5		
7.04	TP192	$[M+H]^+$	$C_{11}H_{14}NO_2$	192.10191	192.10185	-0.31	5.5	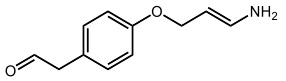	2
		$[M+H-(NH_3)]^+$	$C_{11}H_{11}O_2$	175.07536	175.07568	1.82	6.5		
		$[M+H-(NH_3)-(C_3H_2)]^+$	$C_8H_9O_2$	137.05971	137.05997	1.89	4.5		
		$[M+H-(NH_3)-(C_3H_2)-(O)]^+$	C_8H_9O	121.06479	121.06509	2.47	4.5		
5.86	TP194	$[M+H]^+$	$C_{11}H_{16}NO_2$	194.11756	194.11735	-1.08	4.5	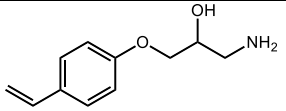	2
		$[M+H-(NH_3)]^+$	$C_{11}H_{13}O_2$	177.09101	177.09132	1.75	5.5		
		$[M+H-(NH_3)-(H_2O)]^+$	$C_{11}H_{11}O$	159.08044	159.08072	1.76	6.5		
		$[M+H-(NH_3)-(H_2O)-(C_3H_2)]^+$	C_8H_9O	121.06479	121.06508	2.39	4.5		
6.49	TP212	$[M+H]^+$	$C_{11}H_{18}NO_3$	212.12812	212.12770	-1.97	3.5	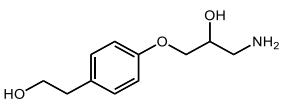	2
		$[M+H-(H_2O)]^+$	$C_{11}H_{16}NO_2$	194.11756	194.11806	2.57	4.5		
		$[M+H-(H_2O)-(NH_3)]^+$	$C_{11}H_{13}O_2$	177.09101	177.09149	2.71	5.5		
		$[M+H-(H_2O)-(NH_3)-(H_2O)]^+$	$C_{11}H_{11}O$	159.08044	159.08087	2.70	6.5		
7.35	TP218	$[M+H]^+$	$C_{14}H_{20}NO$	218.15394	218.15354	-1.83	5.5	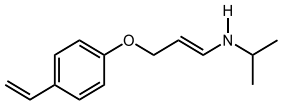	2
		$[M+H-(C_3H_6)]^+$	$C_{11}H_{14}NO$	176.10699	176.10730	1.76	5.5		
		$[M+H-(C_3H_6)-(NH_3)]^+$	$C_{11}H_{11}O$	159.08044	159.08070	1.63	6.5		
		$[M+H-(C_3H_6)-(NH_3)-(C_2H_2)]^+$	C_9H_9O	133.06479	133.06502	1.72	5.5		

7.08	TP226 B	$[M+H]^+$	$C_{12}H_{20}NO_3$	226.14376	226.14357	-0.84	3.5	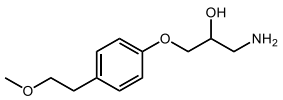	3
		$[M+H–(H_2O)–(CH_2)]^+$	$C_{11}H_{16}NO_2$	194.11756	194.11792	1.85	4.5		
		$[M+H–(H_2O)–(NH_3)]^+$	$C_{12}H_{15}O_2$	191.10666	191.10701	1.83	5.5		
		$[M+H–(C_4H_{11}O_2)]^+$	C_8H_9O	121.06479	121.06509	2.47	4.5		
6.64	TP226 C	$[M+H]^+$	$C_{11}H_{16}NO_4$	226.10738	226.10655	-3.67	4.5	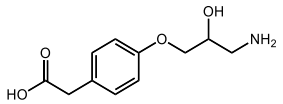	3
		$[M+H–(H_2O)]^+$	$C_{11}H_{14}NO_3$	208.09682	208.09671	-0.52	5.5		
		$[M+H–(H_2O)–(NH_3)]^+$	$C_{11}H_{11}O_3$	191.07027	191.07033	0.31	6.5		
		$[M+H–(CH_7O_3)]^+$	$C_{10}H_9O$	145.06479	145.06480	0.06	6.5		
6.70	TP238	$[M+H]^+$	$C_{13}H_{20}NO_3$	238.14376	238.14439	2.64	4.5	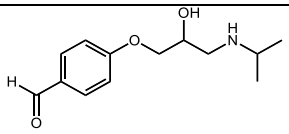	2
6.23	TP240	$[M+H]^+$	$C_{13}H_{22}NO_3$	240.15940	240.15898	-1.74	3.5	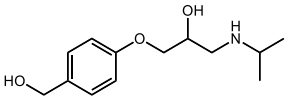	2
7.74	TP250	$[M+H]^+$	$C_{15}H_{24}NO_2$	250.18016	250.17982	-1.35	4.5	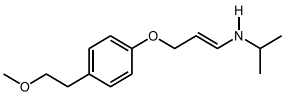	2
		$[M+H–(CH_4O)]^+$	$C_{14}H_{20}NO$	218.15394	218.15431	1.69	5.5		
		$[M+H–(C_3H_6)–(NH_3)]^+$	$C_{12}H_{15}O_2$	191.10666	191.10698	1.67	5.5		
		$[M+H–(CH_4O)–(C_3H_6)]^+$	$C_{11}H_{14}NO$	176.10699	176.10725	1.47	5.5		
		$[M+H–(C_9H_{12}O_2)]^+$	$C_6H_{12}N$	98.09643	98.09664	2.14	1.5		
6.85	TP252	$[M+H]^+$	$C_{14}H_{22}NO_3$	252.15942	252.16016	2.93	4.5	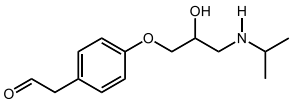	2
		$[M+H–(H_2O)]^+$	$C_{14}H_{20}NO_2$	234.14886	234.14830	-2.39	5.5		
		$[M+H–(C_3H_6)]^+$	$C_{11}H_{16}NO_3$	210.11247	210.11299	2.47	4.5		
		$[M+H–(H_2O)–(C_3H_6)–(NH_3)]^+$	$C_{11}H_{11}O_2$	175.07536	175.07582	2.62	6.5		
		$[M+H–(H_2O)–(C_3H_6)–(NH_3)–(C_3H_2)]^+$	$C_8H_9O_2$	137.05971	137.05994	1.67	4.5		
		$[M+H–(H_2O)\text{-}(C_3H_6)\text{-}(NH_3)\text{-}(C_2H_2)\text{-}(O)]^+$	C_9H_9O	133.06479	133.06512	2.47	5.5		
		$[M+H–(C_8H_{18}O_2)]^+$	$C_6H_{14}NO$	116.10699	116.10740	3.53	0.5		
6.37	TP254	$[M+H]^+$	$C_{13}H_{20}NO_4$	254.13867	254.13821	-1.81	3.5	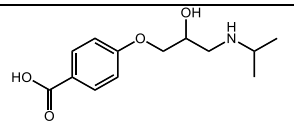	2
6.63	O-DMTP	$[M+H]^+$	$C_{14}H_{24}NO_3$	254.17505	254.17525	0.78	4.5	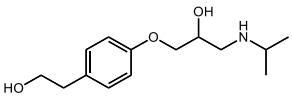	4
		$[M+H–(H_2O)]^+$	$C_{14}H_{22}NO_2$	236.16451	236.16518	2.83	4.5		
		$[M+H–(C_3H_6)]^+$	$C_{11}H_{18}NO_3$	212.12812	212.12875	2.96	3.5		
		$[M+H–(H_2O)–(C_3H_9N)]^+$	$C_{11}H_{13}O_2$	177.09101	177.09155	3.04	5.5		
		$[M+H–(C_8H_{10}O_2)]^+$	$C_6H_{14}NO$	116.10699	116.10747	4.13	0.5		
5.74	TP270	$[M+H]^+$	$C_{14}H_{24}NO_4$	270.16998	270.16995	-0.11	3.5	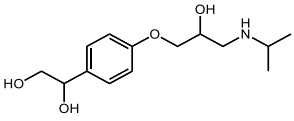	3
		$[M+H–(H_2O)]^+$	$C_{14}H_{22}NO_3$	252.15942	252.16023	3.21	4.5		
		$[M+H–2(H_2O)]^+$	$C_{14}H_{20}NO_2$	234.14886	234.14932	1.96	5.5		
		$[M+H–(C_3H_6)]^+$	$C_{11}H_{18}NO_4$	228.12303	228.12354	2.23	3.5		
		$[M+H–(C_3H_{10}N)–(H_2O)]^+$	$C_{11}H_{13}O_3$	193.08592	193.08635	2.22	5.5		
		$[M+H–(C_5H_{16}NO_3)]^+$	C_9H_9O	133.06479	133.06512	2.47	5.5		
6.70	TP282 A	$[M+H]^+$	$C_{15}H_{24}NO_4$	282.16997	282.16916	-2.87	4.5	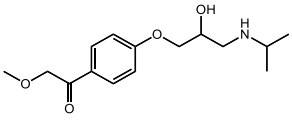	3
		$[M+H–(H_2O)]^+$	$C_{15}H_{22}NO_3$	264.15942	264.15924	-0.68	5.5		
		$[M+H–(C_3H_6)]^+$	$C_{12}H_{18}NO_4$	240.12303	240.12285	-0.74	4.5		
		$[M+H–(H_2O)–(C_3H_9N)]^+$	$C_{12}H_{13}O_3$	205.08592	205.08566	-1.26	6.5		
		$[M+H–(C_9H_{10}O_3)]^+$	$C_6H_{14}NO$	116.10699	116.10703	0.34	0.5		
6.41	α-HMTP	$[M+H]^+$	$C_{15}H_{26}NO_4$	284.18562	284.18509	-1.86	3.5	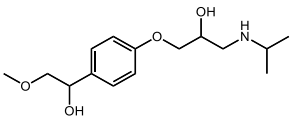	4
		$[M+H–(H_2O)]^+$	$C_{15}H_{24}NO_3$	266.17507	266.17592	3.19	4.5		
		$[M+H–(H_2O)–(C_3H_5)]^+$	$C_{12}H_{18}NO_3$	224.12812	224.12869	2.54	4.5		
		$[M+H–(H_2O)–(C_3H_9N)]^+$	$C_{12}H_{15}O_3$	207.10157	207.10213	2.70	5.5		
		$[M+H–(C_9H_{12}O_3)]^+$	$C_6H_{14}NO$	116.10699	116.10742	3.70	0.5		

7.31	TP284	$[M+H]^+$	$C_{15}H_{26}NO_4$	284.18562	284.18597	1.23	3.5	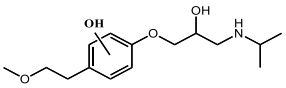	3
		$[M+H–(H_2O)]^+$	$C_{15}H_{24}NO_3$	266.17507	266.17578	2.66	4.5		
		$[M+H–(CH_4O)]^+$	$C_{14}H_{22}NO_3$	252.15942	252.16002	2.37	4.5		
		$[M+H–(H_2O)–(CH_4O)]^+$	$C_{14}H_{20}NO_2$	234.14886	234.14938	2.22	5.5		
		$[M+H–(CH_5O)–(C_3H_3)]^+$	$C_{11}H_{14}NO_2$	192.10191	192.10229	1.97	5.5		
		$[M+H–(H_2O)–(C_3H_9N)]^+$	$C_{11}H_{11}O_2$	175.07536	175.07578	2.39	6.5		
		$[M+H–(C_9H_{12}O_3)]^+$	$C_6H_{14}NO$	116.10699	116.10740	3.53	0.5		
6.85	TP300	$[M+H]^+$	$C_{15}H_{26}NO_5$	300.18055	300.18050	-0.16	3.5	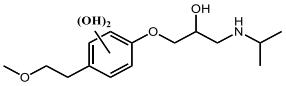	3
		$[M+H–(H_2O)]^+$	$C_{15}H_{24}NO_4$	282.16998	282.17068	2.48	4.5		
		$[M+H–(CH_4O)]^+$	$C_{14}H_{22}NO_4$	268.15433	268.15515	3.05	4.5		
		$[M+H–(H_2O)–(CH_4O)]^+$	$C_{14}H_{20}NO_3$	250.14377	250.14444	2.67	5.5		
6.50	TP316	$[M+H]^+$	$C_{15}H_{26}NO_6$	316.17545	316.17496	-1.54	3.5	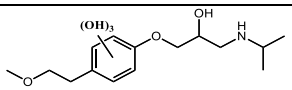	2

S7. Ecotoxicity of MTP and MTPA transformation products (*in silico*)

Table S8. Estimation of acute toxicity of the 26 compounds identified (IF ≥ 2) for the major groups of organisms (fish, *Daphnia* and green algae) using EPI Suite™ model (na stands for no possible to be estimated).

Name	Ecotoxicity (mg/L)-(ECOSAR)		
	Fish	*Daphnia*	Green algae
	LC_{50} (96-h)	LC_{50} (48-h)	EC_{50} (96-h)
MTP	81.6	9.4	8.3
MTPA	na	na	na
TP114	>100	41.5	54.1
TP116	>100	23.6	28.0
TP121	10.1	3.7	16.2
TP134	>100	>100	>100
TP150	>100	>100	>100
TP176	22.3	2.7	2.1
TP192	40.2	>100	>100
TP194	>100	19.2	20.2
TP212	>100	76.1	98.9
TP218	3.5	0.5	0.3
TP226B	na	>100	na
TP226C	>100	53.9	65.5
TP238	>100	18.1	18.2
TP240	>100	25.1	26.6
TP250	10.3	1.4	0.9
TP252	>100	24.2	25.3
TP254	>100	>100	>100
O-DMTP	>100	13.4	12.7
TP270	>100	>100	>100
TP282A	>100	65.8	79.6
α-HMTP	>100	48.3	55.5
TP284	>100	27.8	29.2
TP300	>100	57.4	67.3
TP316	>100	>100	>100

Table S9. Estimation for the 26 compounds identified in terms of bioaccumulation factor, mutagenicity and developmental using Toxicity Estimation Software Tool (T.E.S.T.) v. 4.2.1 program. Additionally, the Toxtree (Estimation of Toxic Hazard - A Decision Tree Approach) v. 3.1. was used to estimate chemical biodegradability, carcinogenesis and Cramer classification (Class III) according to Cramer rules (na stands for no possible to be estimated).

Name	Chemical biodegradability (Toxtree)	Bioaccumulation factor (T.E.S.T.)	Carcinogenicity (Toxtree)		Mutagenicity (T.E.S.T)	Developmental toxicity (T.E.S.T.)	Cramer classification (Toxtree)
			Genotoxic carcinogenicity	Non-genotoxic carcinogenicity			
MTP	Persistent	56.73	Negative	Negative	Negative	Positive	Class I
MTPA	Biodegradable	1.50	Negative	Negative	Negative	Positive	Class I
TP114	Biodegradable	na	Positive	Negative	Positive	Positive	Class III
TP116	Persistent	2.22	Negative	Negative	Negative	Negative	Class III
TP121	Biodegradable	12.52	Negative	Negative	Negative	Positive	Class I
TP134	Biodegradable	0.76	Negative	Negative	Negative	Positive	Class III
TP150	Biodegradable	0.46	Negative	Negative	Positive	Positive	Class III
TP176	Biodegradable	27.03	Negative	Negative	Negative	Positive	Class I
TP192	Biodegradable	na	Positive	Negative	Negative	Negative	Class I
TP194	Biodegradable	5.38	Negative	Negative	Negative	Positive	Class I
TP212	Biodegradable	2.52	Negative	Negative	Negative	Positive	Class I
TP218	na	34.88	Negative	Negative	Negative	Positive	Class I
TP226B	Biodegradable	0.55	Negative	Negative	Negative	Negative	Class I
TP226C	Persistent	6.71	Negative	Negative	Negative	Negative	Class I
TP238	Biodegradable	1.54	Positive	Negative	Negative	Negative	Class I
TP240	Biodegradable	13.52	Negative	Negative	Negative	Negative	Class I
TP250	Biodegradable	23.17	Negative	Negative	Negative	Positive	Class I
TP252	Biodegradable	2.32	Positive	Negative	Negative	Positive	Class I
TP254	Biodegradable	5.96	Negative	Negative	Negative	Positive	Class I
O-DMTP	Biodegradable	8.90	Negative	Negative	Negative	Negative	Class I
TP270	Biodegradable	2.28	Negative	Negative	Negative	Positive	Class I
TP282A	Persistent	10.20	Negative	Negative	Negative	Positive	Class I
α-HMTP	Persistent	7.82	Negative	Negative	Negative	Positive	Class I
TP284	Persistent	14.48	Negative	Negative	Negative	Negative	Class I
TP300	Persistent	11.39	Negative	Negative	Negative	Positive	Class I
TP316	Persistent	3.85	Negative	Negative	Negative	Negative	Class I

References

Cavalcante, R.P., Dantas, R.F., Wender, H., Bayarri, B., González, O., Giménez, J., Esplugas, S., Machulek, A., 2015. Photocatalytic treatment of metoprolol with B-doped TiO_2: Effect of water matrix, toxicological evaluation and identification of intermediates. Appl. Catal. B Environ. 176–177, 173–182. doi:10.1016/j.apcatb.2015.04.007

Filipe, O.M.S., Mota, N., Santos, S.A.O., Domingues, M.R.M., Silvestre, A.J.D., Grac, M., Neves, P.M.S., Simões, M.M.Q., Santos, E.B.H., 2017. Identification and characterization of photodegradation products of metoprolol in the presence of natural fulvic acid by HPLC-UV-MS^n 323, 250–263. doi:10.1016/j.jhazmat.2016.05.072

Gros, M., Rodríguez-Mozaz, S., Barceló, D., 2012. Fast and comprehensive multi-residue analysis of a broad range of human and veterinary pharmaceuticals and some of their metabolites in surface and treated waters by ultra-high-performance liquid chromatography coupled to quadrupole-linear ion trap tandem. J. Chromatogr. A 1248, 104–121. doi:10.1016/j.chroma.2012.05.084

IISO 11348-3:1998 - Water quality - Determination of the inhibitory effect of water samples on the light emission of *Vibrio fischeri* (Luminescent bacteria test). Int. Organ. Stand. (ISO).

Jaén-Gil, A., Castellet-Rovira, F., Llorca, M., Villagrasa, M., Sarrà, M., Rodríguez-Mozaz, S., Barceló, D., 2019. Fungal treatment of metoprolol and its recalcitrant metabolite metoprolol acid in hospital wastewater: Biotransformation, sorption and ecotoxicological impact. Water Res. 152, 171–180. doi:10.1016/j.watres.2018.12.054

Ma, B., Huang, H.H., Chen, X.Y., Sun, Y.M., Lin, L.H., Zhong, D.F., 2007. Biotransformation of metoprolol by the fungus *Cunninghamella blakesleeana*. Acta Pharmacol. Sin. 28, 1067–1074. doi:10.1111/j.1745-7254.2007.00567.x

Rivas, F.J., Gimeno, O., Borralho, T., Carbajo, M., 2010. UV-C radiation based methods for aqueous metoprolol elimination. J. Hazard. Mater. 179, 357–362. doi:10.1016/j.jhazmat.2010.03.013

Romero, V., Acevedo, S., Marco, P., Giménez, J., Esplugas, S., 2016a. Enhancement of Fenton and photo-Fenton processes at initial circumneutral pH for the degradation of the β-blocker metoprolol. Water Res. 88, 449–457. doi:10.1016/j.watres.2015.10.035

Romero, V., González, O., Bayarri, B., Marco, P., Giménez, J., Esplugas, S., 2016b. Degradation of Metoprolol by photo-Fenton: Comparison of different photoreactors performance. Chem. Eng. J. 283, 639–648. doi:10.1016/j.cej.2015.07.091

Romero, V., González, O., Bayarri, B., Marco, P., Giménez, J., Esplugas, S., 2015. Performance of different advanced oxidation technologies for the abatement of the beta-blocker metoprolol. Catal. Today 240, 86–92. doi:10.1016/j.cattod.2014.03.060

Rubirola, A., Llorca, M., Rodriguez-Mozaz, S., Casas, N., Rodriguez-Roda, I., Barceló, D., Buttiglieri, G., 2014. Characterization of metoprolol biodegradation and its transformation products generated in activated sludge batch experiments and in full scale WWTPs. Water Res. 63, 21–32. doi:10.1016/j.watres.2014.05.031

Slegers, C., Maquille, A., Deridder, V., Sonveaux, E., Habib Jiwan, J.L., Tilquin, B., 2006. LC-MS analysis in the e-beam and gamma radiolysis of metoprolol tartrate in aqueous solution: Structure elucidation and formation mechanism of radiolytic products. Radiat. Phys. Chem. 75, 977–989. doi:10.1016/j.radphyschem.2006.02.001

Šojić, D., Despotović, V., Orčić, D., Szabó, E., Arany, E., Armaković, S., Illés, E., Gajda-Schrantz, K., Dombi, A., Alapi, T., Sajben-Nagy, E., Palágyi, A., Vágvölgyi, C., Manczinger, L., Bjelica, L., Abramović, B., 2012. Degradation of thiamethoxam and metoprolol by UV, O_3 and UV/O_3 hybrid processes: Kinetics, degradation intermediates and toxicity. J. Hydrol. 472–473, 314–327. doi:10.1016/j.jhydrol.2012.09.038

Toolaram, A.P., Menz, J., Rastogi, T., Leder, C., Kümmerer, K., Schneider, M., 2017. Hazard screening of photo-transformation products from pharmaceuticals : Application to selective β1-blockers atenolol and metoprolol. Sci. Total Environ. 579, 1769–1780. doi:10.1016/j.scitotenv.2016.10.242

Wilde, M.L., Montipó, S., Martins, A.F., 2014. Degradation of β-blockers in hospital wastewater by means of ozonation and Fe^{2+}/ozonation. Water Res. 48, 280–295. doi:10.1016/j.watres.2013.09.039

Supporting information for

Effect-based identification of hazardous antibiotic transformation products after water chlorination

Adrián Jaén-Gil [a,b], María-José Farré [a,b], Alexandre Sànchez-Melsió [a,b], Albert Serra-Compte [a,b], Damià Barceló [a,b,c], Sara Rodríguez-Mozaz [a,b*]*

[a] Catalan Institute for Water Research (ICRA), Carrer Emili Grahit 101, 17003 Girona, Spain

[b] Universitat de Girona, Girona, Spain

[c] Water and Soil Quality Research Group, Department of Environmental Chemistry, (IDAEA-CSIC), Jordi Girona 18-26, E-08034 Barcelona, Spain

15 Pages, 8 Sections, 7 Tables, 3 Figures

Contents

S1. Mass list of transformation products for chemical analysis in LC-LTQ-Orbitrap

Table S1. Exact mass list of the most common azithromycin TPs found in literature.

Compound	Exact mass $[M+H]^+$	Chemical structure $[M+H]^+$	References
AZI	749.51580	$C_{38}H_{73}N_2O_{12}$	Reference standard
TP576	577.40590	$C_{29}H_{57}N_2O_9$	1
TP590	591.42150	$C_{30}H_{59}N_2O_9$	1,2
TP591	592.40550	$C_{30}H_{58}NO_{10}$	1,3,4
TP608	609.43210	$C_{30}H_{61}N_2O_{10}$	1
TP719	720.45280	$C_{36}H_{66}NO_{13}$	3
TP720	721.48450	$C_{36}H_{69}N_2O_{12}$	2,3
TP734	735.50020	$C_{37}H_{71}N_2O_{12}$	1,2,3,4
TP748	749.51580	$C_{38}H_{73}N_2O_{12}$	3
TP762	763.45910	$C_{38}H_{71}N_2O_{13}$	3
TP764	765.51070	$C_{38}H_{73}N_2O_{13}$	1
TP766	767.52640	$C_{38}H_{75}N_2O_{13}$	1
TP768	769.46110	$C_{37}H_{70}ClN_2O_{12}$	3
TP769	770.40880	$C_{36}H_{65}ClNO_{14}$	3
TP788	789.40650	$C_{36}H_{67}Cl_2N_2O_{12}$	3
TP803	804.36980	$C_{36}H_{64}Cl_2NO_{14}$	3

Table S2. Exact mass list of the most common ciprofloxacin TPs found in literature.

Compound	Exact mass $[M+H]^+$	Chemical structure $[M+H]^+$	References
CFC	332.14050	$C_{17}H_{19}FN_3O_3$	Reference standard
TP365	366.10152	$C_{17}H_{18}ClFN_3O_3$	5,6
TP365	366.14598	$C_{17}H_{21}FN_3O_5$	7
TP363	300.07790	$C_{15}H_{11}FN_3O_3$	8
TP361	362.11468	$C_{17}H_{17}FN_3O_5$	9–11
TP339	340.08587	$C_{15}H_{16}ClFN_3O_3$	5,6
TP333	334.11976	$C_{16}H_{17}FN_3O_4$	5,8,11
TP305	306.12485	$C_{15}H_{17}FN_3O_3$	1,5,7,10,12–15
TP296	297.04367	$C_{13}H_{11}ClFN_2O_3$	5,6,8
TP290	291.07709	$C_{14}H_{12}FN_2O_4$	11,15,16
TP287	288.13427	$C_{15}H_{18}N_3O_3$	1,5,12
TP262	263.08265	$C_{13}H_{12}FN_2O_3$	1,5,7,10,12,13,15
TP243	245.09207	$C_{13}H_{13}N_2O_3$	1,9,17–19

S2. Post-acquisition data processing workflow

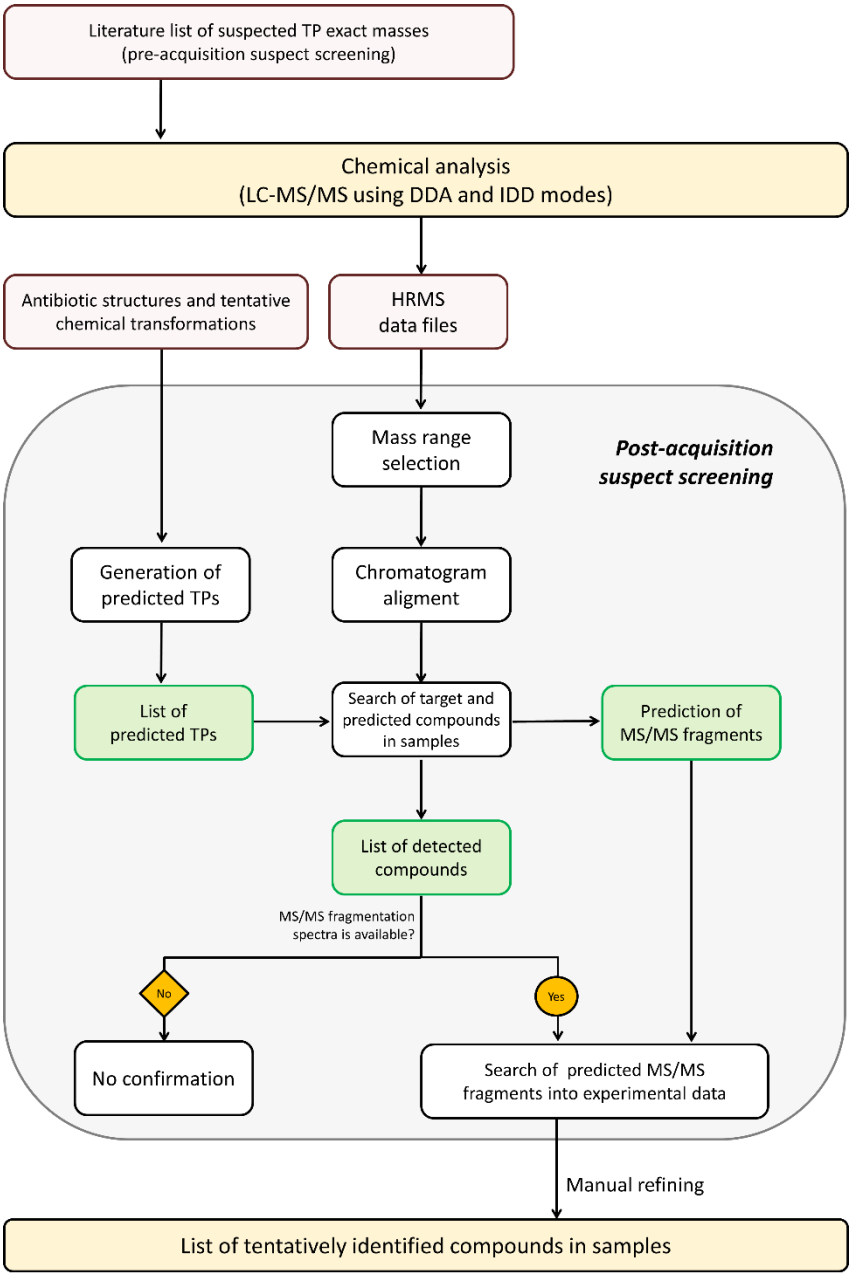

Figure S1. Automated suspect screening workflow adapted to Compound Discoverer 3.0 software.

Table S3. Data processing parameters selected to perform the integrated suspect screening methodology.

Peak filtering and identification of TP candidates

Select Spectra:

- Retention time range: 1 to 12 min
- Mass range: 100-1000 Da
- S/N ratio: 3
- Scan Polarity: +/-

Align Retention Times:

- Alignment Model: Adaptive curve
- Mass tolerance: ±5 ppm
- Maximum retention time shift: 0.3 min

Generate Expected Compounds:

- Parent compound: CFC/AZI
- Apply Dealkylation: True
- Apply Dearylation: True
- Max. # Dealkylation Steps: 2
- All reaction steps: 3
- Min. mass: 100 Da
- Ions considered: $[M+H]^+$ /$[M-H]^{-1}$
- Transformations: Dehydration (H_2 O ->), Hydration (-> H_2 O), Oxidation (-> O), Reduction (-> H_2), Desaturation (H_2 ->), Oxidative Deamination to Alcohol (H_2 N -> H O), Oxidative Deamination to Ketone (H_3 N -> O), Chlorination (H -> Cl), Reductive Defluorination (F -> H).
- Max. # All Steps: 3

Find Expected Compounds:

- Mass tolerance: ±5 ppm
- Intensity Tolerance: 30 %
- Intensity Threshold: 0.1 %
- Min. #Isotopes: 2
- Min. peak intensity: 1000

FISh scoring:

- Annotate Full Tree: True
- Match Transformations: True
- S/N threshold: 3
- Mass tolerance of fragments: ±5 ppm
- Fragment prediction libraries: True

Fragment Prediction Settings:

- Use General Rules: True
- Use Libraries: True
- Max. Depth: 5
- Aromatic Cleavage: True
- Min. Fragment m/z: 50

Group Expected Compounds:

- RT Tolerance [min]: 0.3
- Preferred Ions: $[M+H]^{+1}$/$[M-H]^{-1}$

Mark Background Compounds:

- Max. Sample/Blank: 3
- Hide Background: True

S3. Identified AZI TPs in chlorination experiments performed

Table S4. Azithromycin transformation products tentatively identified in the chlorinated samples.

R_t (min)	Compound	Ion	Molecular formula $[M+H]^+$	Theoretical exact mass $[M+H]^+$	Experiment exact mass $[M+H]^+$	Error mass (ppm)	RDBE	Suggested chemical structure
7.42	AZI	$[M+H]^+$ $[M+H-(L\text{-cladinose})]^+$ $[M+H-[O\text{-}(L\text{-cladinose})]]^+$ $[M+H-(d\text{-desosamine})\text{-}(L\text{-cladinose})]^+$	$C_{38}H_{73}N_2O_{12}$ $C_{30}H_{59}N_2O_9$ $C_{30}H_{57}N_2O_8$ $C_{22}H_{44}NO_7$	749.51580 591.42151 573.41094 434.31123	749.51294 591.42029 573.40997 434.31030	-3.81 -2.06 -1.69 -2.14	3.5 2.5 3.5 1.5	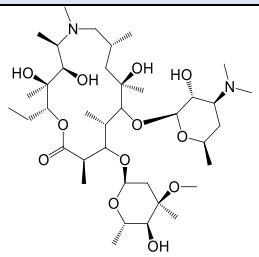
7.25	TP433	$[M+H]^+$ $[M+H-(H_2O)]^+$ $[M+H-(H_2O)-(C_6H_{10}O_2)]^+$	$C_{22}H_{44}NO_7$ $C_{22}H_{42}NO_6$ $C_{16}H_{30}NO_4$	434.31123 416.30066 300.21693	434.31010 416.29987 300.21640	-2.60 -1.89 -1.76	1.5 2.5 2.5	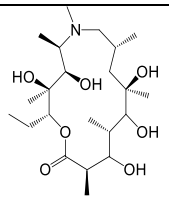
7.83	TP576	$[M+H]^+$ $[M+H-(H_2O)]^+$ $[M+H-(d\text{-desosamine-}CH_2)]^+$ $[M+H-(d\text{-desosamine-}CH_2)-(H_2O)]^+$	$C_{29}H_{57}N_2O_9$ $C_{29}H_{55}N_2O_8$ $C_{22}H_{44}NO_7$ $C_{22}H_{42}NO_6$	577.40586 559.39529 434.31123 416.30066	577.40448 559.39490 434.31110 416.30054	-2.39 -0.69 -0.29 -0.28	2.5 3.5 1.5 2.5	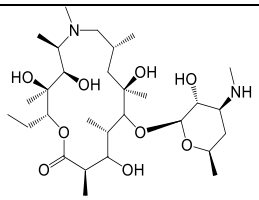
8.55	TP577 A	$[M+H]^+$ $[M+H-(C_6H_{10}O_2)]^+$ $[M+H-(L\text{-cladinose})]^+$ $[M+H-(L\text{-cladinose})-(H_2O)]^+$	$C_{29}H_{56}NO_{10}$ $C_{24}H_{46}NO_8$ $C_{21}H_{42}NO_7$ $C_{21}H_{40}NO_6$	578.38987 476.32179 420.29558 402.28501	578.38879 476.32092 420.29489 402.28427	-1.86 -1.82 -1.64 -1.83	2.5 2.5 1.5 2.5	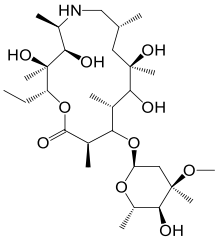
7.83	TP577 B	$[M+H]^+$ $[M+H-(C_5H_{10}O_2)]^+$ $[M+H-(L\text{-cladinose}-CH_2)]^+$ $[M+H-(L\text{-cladinose}-CH_2)-(H_2O)]^+$	$C_{29}H_{56}NO_{10}$ $C_{24}H_{46}NO_8$ $C_{22}H_{44}NO_7$ $C_{22}H_{42}NO_6$	578.38987 476.32179 434.31123 416.30066	578.38843 476.32056 434.31021 416.29965	-2.48 -2.58 -2.34 -2.42	2.5 2.5 1.5 2.5	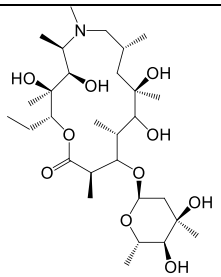
7.50	TP590	$[M+H]^+$ $[M+H-H_2O]^+$ $[M+H-(d\text{-desosamine})]^+$	$C_{30}H_{59}N_2O_9$ $C_{30}H_{57}N_2O_8$ $C_{22}H_{44}NO_7$	591.42151 573.41094 434.31123	591.41949 573.40930 434.30997	-3.41 -2.86 -2.90	2.5 3.5 1.5	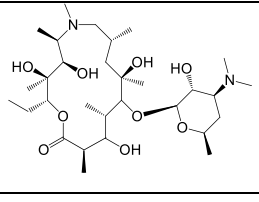

8.69	TP591	$[M+H]^+$ $[M+H–(L\text{-cladinose})]^+$	$C_{30}H_{58}NO_{10}$ $C_{22}H_{44}NO_7$	592.40552 434.31123	592.40369 434.31012	-3.08 -2.55	2.5 1.5	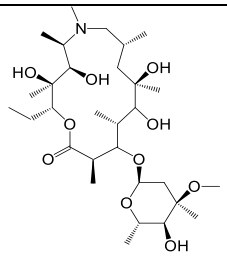
9.19	TP719	$[M+H]^+$ $[M+H–(L\text{-cladinose})]^+$ $[M+H–(L\text{-cladinose})–(H_2O)]^+$	$C_{36}H_{66}NO_{13}$ $C_{28}H_{52}NO_{10}$ $C_{28}H_{50}NO_9$	720.45287 562.35857 544.34801	720.45215 562.35822 544.34778	-0.99 -0.62 -0.42	4.5 3.5 4.5	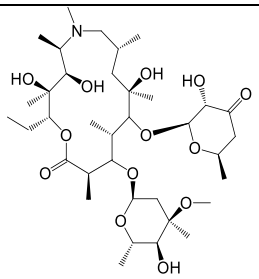
7.28	TP720 A	$[M+H]^+$ $[M+H–(d\text{-desosamine}–CH_2–CH_2)]^+$ $[M+H–(L\text{-cladinose})]^+$ $[M+H–(d\text{-desosamine}–CH_2–CH_2)–(L\text{-cladinose})]^+$	$C_{36}H_{69}N_2O_{12}$ $C_{30}H_{58}NO_{10}$ $C_{28}H_{55}N_2O_9$ $C_{22}H_{44}NO_7$	721.48450 592.40552 563.38947 434.31123	721.48285 592.40430 563.38940 434.31058	-2.28 -2.05 -0.12 -1.49	3.5 2.5 2.5 1.5	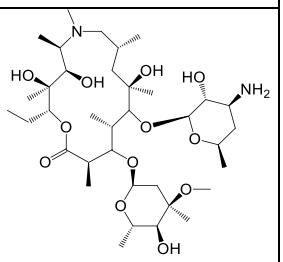
7.03	TP720 B	$[M+H]^+$ $[M+H–(L\text{-cladinose}–CH_2)]^+$ $[M+H–(L\text{-cladinose}–CH_2)–(H_2O)]^+$ $[M+H–(L\text{-cladinose}–CH_2)–(d\text{-desosamine}–CH_2)]^+$	$C_{36}H_{69}N_2O_{12}$ $C_{29}H_{57}N_2O_9$ $C_{29}H_{55}N_2O_8$ $C_{22}H_{44}NO_7$	721.48450 577.40586 559.39529 434.31123	721.48297 577.40503 559.39459 434.31064	-2.12 -1.46 -1.25 -1.35	3.5 2.5 3.5 1.5	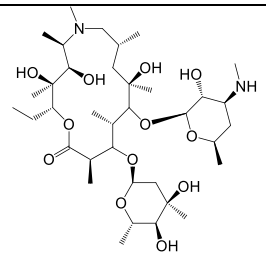
7.39	TP734 A	$[M+H]^+$ $[M+H–(L\text{-cladinose})]^+$ $[M+H–(L\text{-cladinose})–(H_2O)]^+$ $[M+H–(L\text{-cladinose})–(d\text{-desosamine}–CH_2)]^+$	$C_{37}H_{71}N_2O_{12}$ $C_{29}H_{57}N_2O_9$ $C_{29}H_{55}N_2O_8$ $C_{22}H_{44}NO_7$	735.50015 577.40586 559.39529 434.31123	735.49786 577.40601 559.39392 434.31146	-3.11 0.25 -2.44 0.52	3.5 2.5 3.5 1.5	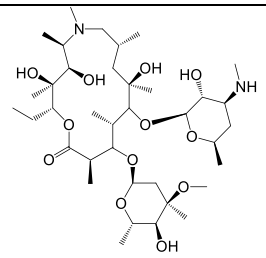
7.03	TP734 B	$[M+H]^+$ $[M+H–(L\text{-cladinose}–CH_2)]^+$ $[M+H–(L\text{-cladinose}–CH_2)–(H_2O)]^+$ $[M+H–(L\text{-cladinose}–CH_2)–(d\text{-desosamine})]^+$	$C_{37}H_{71}N_2O_{12}$ $C_{30}H_{59}N_2O_9$ $C_{30}H_{57}N_2O_8$ $C_{22}H_{44}NO_7$	735.50015 591.42151 573.41094 434.31123	735.50043 591.42181 573.41132 434.31146	0.38 0.50 0.66 0.52	3.5 2.5 3.5 1.5	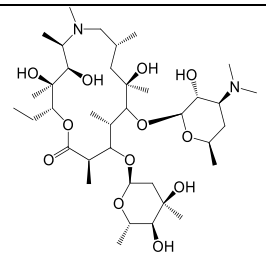

9.94	TP768	$[M+H]^+$ $[M+H–(L\text{-cladinose})]^+$ $[M+H–(L\text{-cladinose})–(H_2O)]^+$ $[M+H–(L\text{-cladinose+Cl-H})–(d\text{-desosamine})]^+$	$C_{37}H_{70}ClN_2O_{12}$ $C_{29}H_{56}ClN_2O_9$ $C_{29}H_{54}ClN_2O_8$ $C_{22}H_{44}NO_7$	769.46118 611.36689 593.35632 434.31123	769.45966 611.36572 593.35535 434.31030	-1.97 -1.91 -1.63 -2.14	3.5 2.5 3.5 1.5	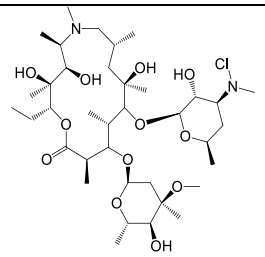
10.32	TP788	$[M+H]^+$ $[M+H–(L\text{-cladinose})]^+$ $[M+H–(L\text{-cladinose})–(H_2O)]^+$ $[M+H–(L\text{-cladinose+2Cl-2H})–(d\text{-desosamine})]^+$	$C_{36}H_{67}Cl_2N_2O_{12}$ $C_{28}H_{53}Cl_2N_2O_9$ $C_{28}H_{51}Cl_2N_2O_8$ $C_{22}H_{44}NO_7$	789.40656 631.31226 613.30170 434.31123	789.40497 631.31097 613.30078 434.31030	-2.01 -2.04 -1.50 -2.14	3.5 2.5 3.5 1.5	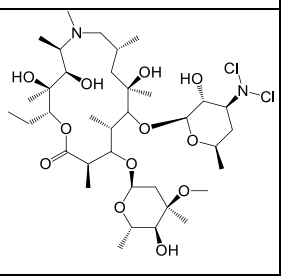

S4. Identified CFC TPs in chlorination experiments performed

Table S5. Ciprofloxacin transformation products tentatively identified in the chlorinated samples.

R_t (min)	Compound	Ion	Molecular formula $[M+H]^+$	Theoretical exact mass $[M+H]^+$	Experiment exact mass $[M+H]^+$	Error mass (ppm)	RDBE	Suggested chemical structure
6.95	CFC	$[M+H]^+$	$C_{17}H_{19}FN_3O_3$	332.14050	332.13959	-2.73	9.5	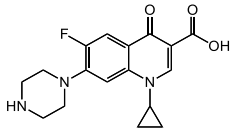
		$[M+H-(H_2O)]^+$	$C_{17}H_{17}FN_3O_2$	314.12993	314.12894	-3.15	10.5	
		$[M+H-(CO_2)]^+$	$C_{16}H_{19}FN_3O$	288.15067	288.14984	-2.88	8.5	
		$[M+H-(H_2O)-(CO)-(C_2H_3N)]^+$	$C_{14}H_{14}FN_2O$	245.10847	245.10771	-3.10	8.5	
8.56	TP262	$[M+H]^+$	$C_{13}H_{12}FN_2O_3$	263.08265	263.08173	-3.49	8.5	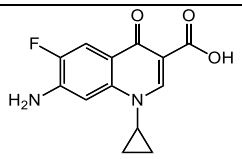
		$[M+H-(H_2O)]^+$	$C_{13}H_{10}FN_2O_2$	245.07208	245.07124	-3.42	9.5	
		$[M+H-(C_3H_5)]^+$ (HCD)	$C_{10}H_7FN_2O_3$	222.04352	222.04411	2.65	8.0	
		$[M+H-(H_2O)-(CO)]^+$ (HCD)	$C_{12}H_{10}FN_2O$	217.07717	217.07776	2.71	8.5	
		$[M+H-(C_3H_5)-(H_2O)]^+$ (HCD)	$C_{10}H_5FN_2O_2$	204.03296	204.03357	2.98	9.0	
8.36	TP290	$[M+H]^+$	$C_{14}H_{12}FN_2O_4$	291.07756	291.07709	-1.61	9.5	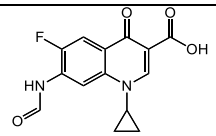
		$[M+H-(H_2O)]^+$	$C_{14}H_{10}FN_2O_3$	273.06700	273.06656	-1.61	10.5	
		$[M+H-(H_2O)-(CO)]^+$ (HCD)	$C_{13}H_{10}FN_2O_2$	245.07208	245.07155	-2.16	9.5	
7.93	TP292	$[M+H]^+$	$C_{14}H_{14}FN_2O_4$	293.09321	293.09308	-0.44	8.5	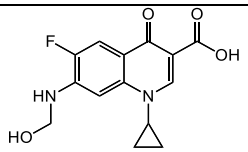
		$[M+H-(H_2O)]^+$	$C_{14}H_{12}FN_2O_3$	275.08265	275.08246	-0.69	9.5	
		$[M+H-(H_2O)-(C)]^+$ (HCD)	$C_{13}H_{12}FN_2O_3$	263.08265	263.08337	2.73	8.5	
		$[M+H-(H_2O)-(C)-(H_2O)]^+$ (HCD)	$C_{14}H_{10}FN_2O_2$	257.07208	257.07272	2.48	10.5	
9.44	TP296	$[M+H]^+$	$C_{13}H_{11}ClFN_2O_3$	297.04367	297.04324	-1.44	8.5	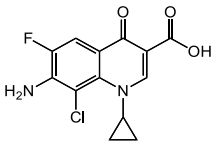
		$[M+H-(H_2O)]^+$	$C_{13}H_9ClFN_2O_2$	279.03311	279.03275	-1.29	9.5	
		$[M+H-(C_3H_5)]^+$ (HCD)	$C_{10}H_6ClFN_2O_3$	256.00455	256.00513	2.26	8.0	
		$[M+H-(H_2O)-(CO)]^+$ (HCD)	$C_{12}H_9ClFN_2O$	251.03820	251.03871	2.03	8.5	
		$[M+H-(C_3H_5)-(H_2O)]^+$ (HCD)	$C_{10}H_4ClFN_2O_2$	237.99398	237.99454	2.35	9.0	
		$[M+H-(H_2O)-(CO)-(Cl)]^+$ (HCD)	$C_{12}H_9FN_2O$	216.06934	216.06984	2.31	9.0	
6.73	TP305	$[M+H]^+$	$C_{15}H_{17}FN_3O_3$	306.12485	306.12418	-2.18	8.5	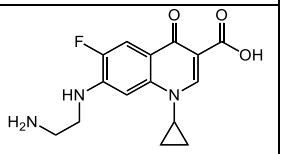
		$[M+H-(NH_3)]^+$	$C_{15}H_{14}FN_2O_3$	289.09830	289.09760	-2.42	9.5	
		$[M+H-(H_2O)]^+$	$C_{15}H_{15}FN_3O_2$	288.11428	288.11371	-1.97	9.5	
		$[M+H-(NH_3)-(C_2H_2)]^+$	$C_{13}H_{12}FN_2O_3$	263.08265	263.08206	-2.24	8.5	
7.88	TP333	$[M+H]^+$	$C_{16}H_{17}FN_3O_4$	334.11976	334.11938	-1.13	9.5	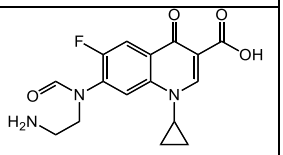
		$[M+H-(H_2O)]^+$	$C_{16}H_{15}FN_3O_3$	316.10920	316.10892	-0.88	10.5	
		$[M+H-(H_2O)-(CO)]^+$ (HCD)	$C_{15}H_{15}FN_3O_2$	288.11428	288.11376	-1.80	9.5	
7.03	TP339	$[M+H]^+$	$C_{15}H_{16}ClFN_3O_3$	340.08587	340.08578	-0.26	8.5	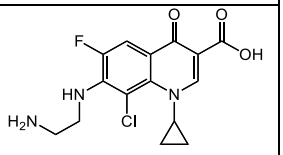
		$[M+H-(H_2O)]^+$	$C_{15}H_{14}ClFN_3O_2$	322.07531	322.07520	-0.34	9.5	
		$[M+H-(C_2H_5N)]^+$	$C_{13}H_{11}ClFN_2O_3$	297.04367	297.04350	-0.57	8.5	
		$[M+H-(CH_2NH_2)-(Cl)]^+$	$C_{14}H_{12}FN_2O_3$	275.08265	275.08255	-0.36	9.5	

S5. UV spectra of CFC and the intermediates identified in HPLC-DAD

A) *Ciprofloxacin*

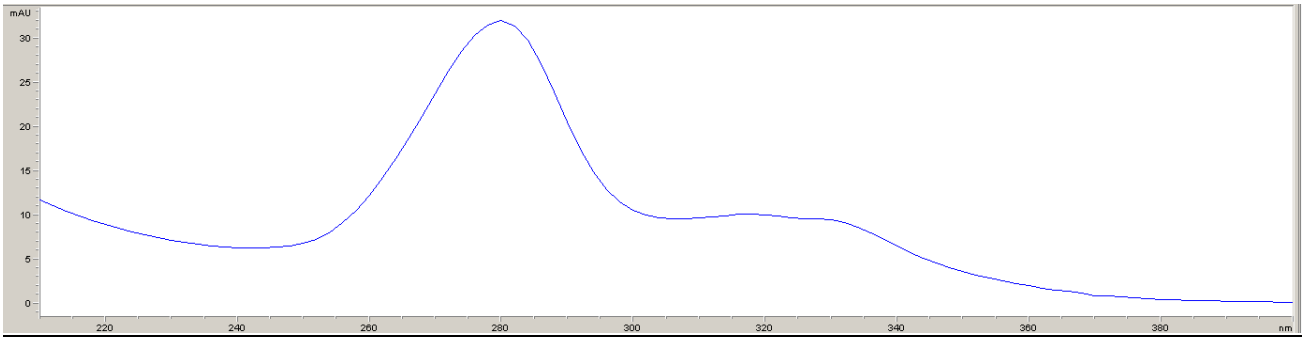

B) *TP262*

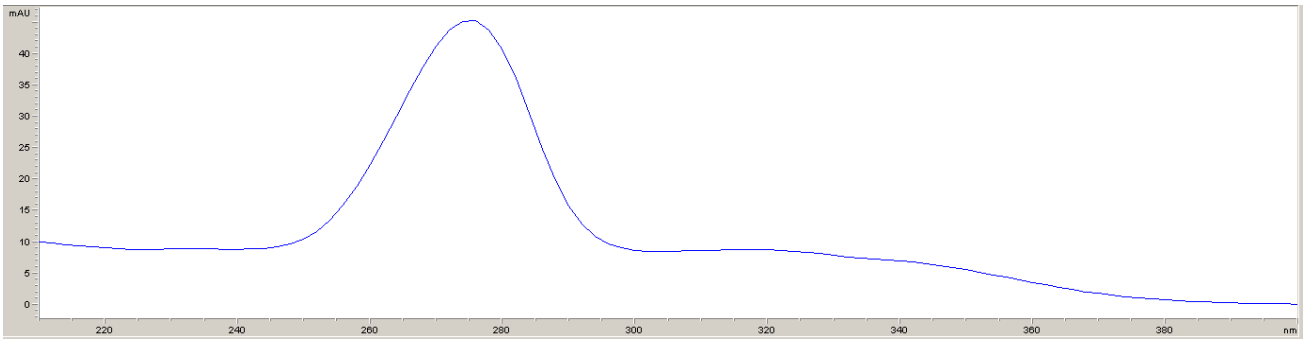

C) *TP296*

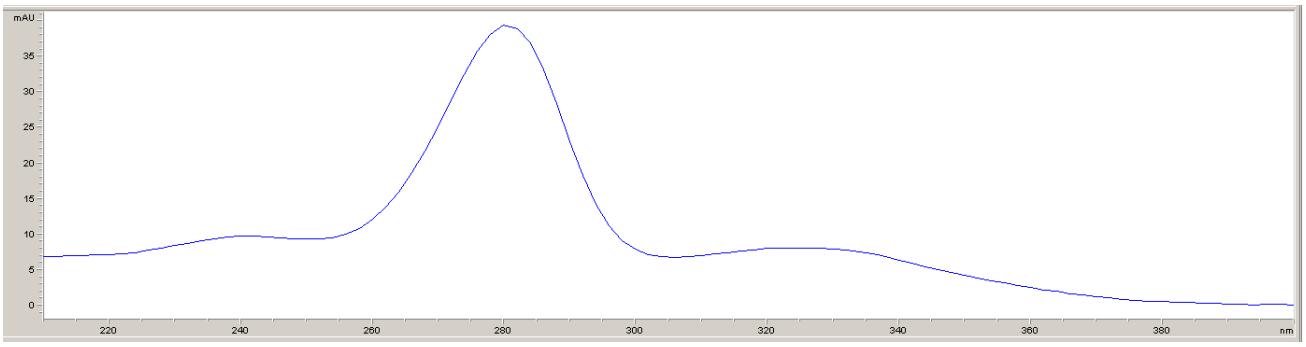

D) *TP333*

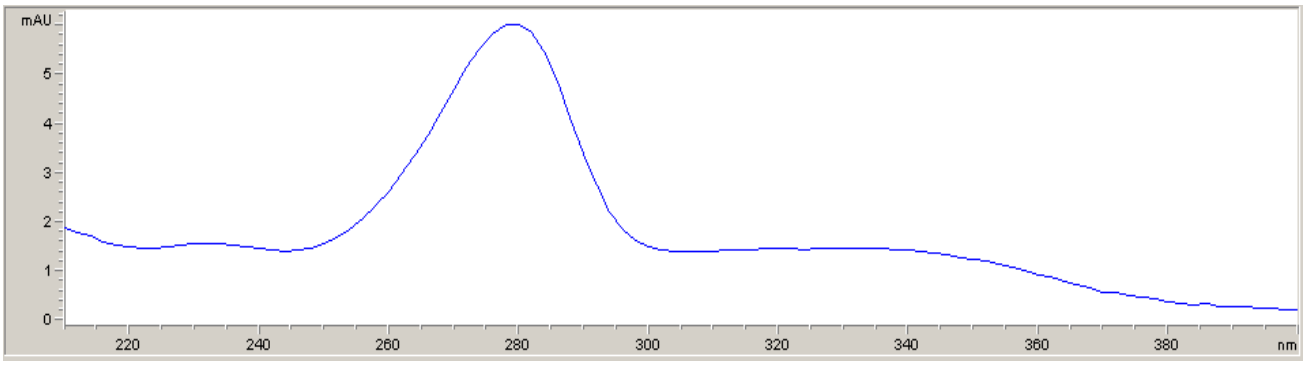

Figure S2. Diode array spectra (271 nm) of ciprofloxacin and the structurally related intermediates TP262, TP296 and TP333 after fractionation and isolation.

S6. R-Scripts for PCA estimation

Data Set antibiotic activity

Table S6. Data set for antibiotic activity and R-script.

Concentration	TP262	TP290	TP292	TP296	TP305	TP333	TP339	Antibiotic activity
1	61.77867288	0.15610719	0.20672387	3.953537225	21.40380872	9.91661171	0.04465318	6.62
2	94.67011208	0.35636040	0.37708936	29.63124793	4.153874119	9.33776629	0.02255637	40.68
3	28.92713318	0.06593322	0.08164407	44.20554488	1.481034155	4.17793122	0.01976572	44.23
4	5.492257606	0.00763349	0.00767229	38.58086892	0.418623492	1.38043811	0.03073293	30.10

R-Script of antibiotic activity using FactoMineR (RcmdrPlugin.FactoMineR interface)

```
Antibiotic.Activity <- readXL("C:/…. PCA datos AA.xlsx",
   rownames = FALSE, header = TRUE, na = "", sheet = "Hoja2", stringsAsFactors = TRUE)
editDataset(Antibiotic.Activity)
Antibiotic.Activity.PCA <- Antibiotic.Activity[, c("TP262", "TP290", "TP292", "TP296",
   "TP305", "TP333", "TP339", "Antibiotic.activity")]
res <- PCA(Antibiotic.Activity.PCA, scale.unit = TRUE, ncp = 5, graph = FALSE)
print(plot.PCA(res, axes = c(1, 2), choix = "ind", habillage = "none", col.ind = "black",
   col.ind.sup = "blue", col.quali = "magenta", label = c("ind", "ind.sup", "quali"),
   new.plot = TRUE))
print(plot.PCA(res, axes = c(1, 2), choix = "var", new.plot = TRUE, col.var = "black",
   col.quanti.sup = "blue", label = c("var", "quanti.sup"), lim.cos2.var = 0))
summary(res, nb.dec = 3, nbelements = 10, nbind = 10, ncp = 3, file = "")
remove(Antibiotic.Activity.PCA)
```

Data Set acute toxicity

Table S7. Data set for acute toxicity and R-script.

Concentration	TP262	TP290	TP292	TP296	TP305	TP333	TP339	Acute toxicity
1	61.77867288	0.15610719	0.20672387	3.953537225	21.40380872	9.91661171	0.04465318	2.46730816
2	94.67011208	0.35636040	0.37708936	29.63124793	4.153874119	9.33776629	0.02255637	4.08830744
3	28.92713318	0.06593322	0.08164407	44.20554488	1.481034155	4.17793122	0.01976572	2.44100895
4	5.492257606	0.00763349	0.00767229	38.58086892	0.418623492	1.38043811	0.03073293	2.24534091

R-Script acute toxicity using FactoMineR (RcmdrPlugin.FactoMineR interface)

```
Acute.Toxicity <- readXL("C:/….. PCA datos Tox.xlsx",
   rownames = FALSE, header = TRUE, na = "", sheet = "Hoja2", stringsAsFactors = TRUE)
editDataset(Acute.Toxicity)
Acute.Toxicity.PCA <- Acute.Toxicity[, c("TP262", "TP290", "TP292", "TP296", "TP305",
   "TP333", "TP339", "Acute.toxicity")]
res <- PCA(Acute.Toxicity.PCA, scale.unit = TRUE, ncp = 5, graph = FALSE)
print(plot.PCA(res, axes = c(1, 2), choix = "ind", habillage = "none", col.ind = "black",
   col.ind.sup = "blue", col.quali = "magenta", label = c("ind", "ind.sup", "quali"),
   new.plot = TRUE))
print(plot.PCA(res, axes = c(1, 2), choix = "var", new.plot = TRUE, col.var = "black",
   col.quanti.sup = "blue", label = c("var", "quanti.sup"), lim.cos2.var = 0))
summary(res, nb.dec = 3, nbelements = 10, nbind = 10, ncp = 3, file = "")
remove(Acute.Toxicity.PCA)
```

S7. Microtox evaluation of chlorinated sample and fractions

Chlorinated mixture sample

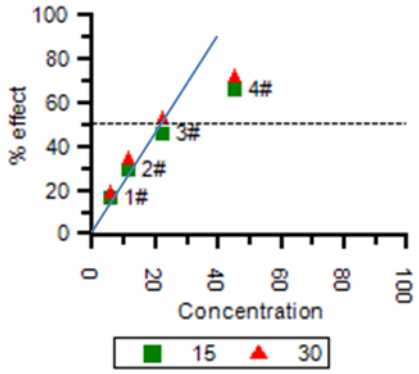

$(\%\ effect)_y = 1.99 \times EC_y$; EC10 = 5.02 mg/L

Control sample

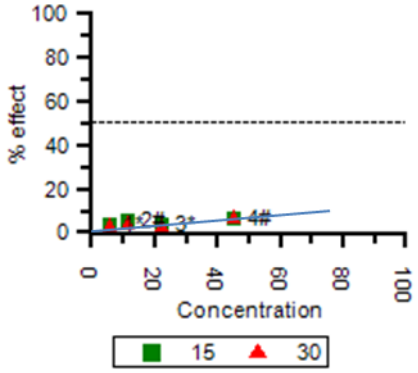

$(\%\ effect)_y = 0.15 \times EC_y$; EC_{10} = 66.66 mg/L

Fraction 2

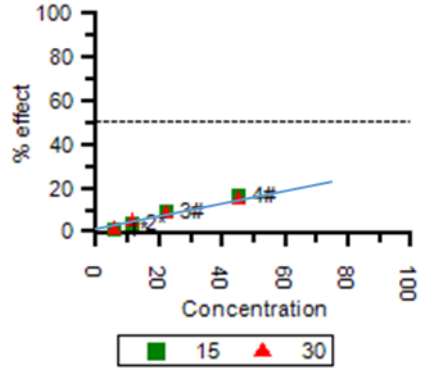

$(\%\ effect)_y = 0.37 \times EC_y$; EC_{10} = 27.02 mg/L

Fraction 3

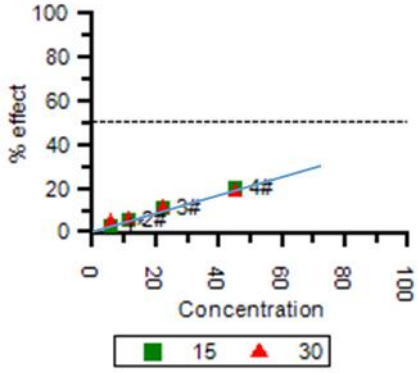

$(\%\ effect)_y = 0.46 \times EC_y$; EC_{10} = 21.73 mg/L

Fraction 4

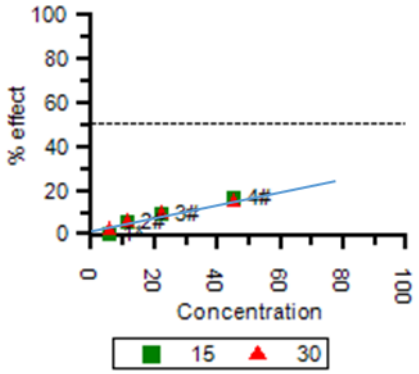

$(\%\ effect)_y = 0.39 \times EC_y$; EC_{10} = 25.64 mg/L

Fraction 5

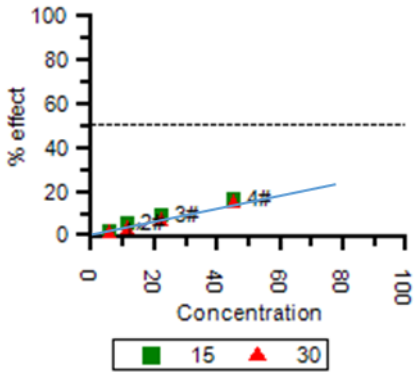

$(\%\ effect)_y = 0.35 \times EC_y$; EC_{10} = 28.57 mg/L

Figure S3. Microtox evaluation of chlorinated sample and fractions collected.

S8. References

(1) Jaén-Gil, A.; Hom-Diaz, A.; Llorca, M.; Vicent, T.; Blánquez, P.; Barceló, D.; Rodríguez-Mozaz, S. An automated on-line turbulent flow liquid-chromatography technology coupled to a high resolution mass spectrometer LTQ-Orbitrap for suspect screening of antibiotic transformation products during microalgae wastewater treatment. *J. Chromatogr. A* **2018**, *1568*, 57–68.

(2) Tong, L.; Eichhorn, P.; Pérez, S.; Wang, Y.; Barceló, D. Photodegradation of azithromycin in various aqueous systems under simulated and natural solar radiation: Kinetics and identification of photoproducts. *Chemosphere* **2011**, *83* (3), 340–348.

(3) Guo, Q.; Du, Z.; Shao, B. Simulation and experimental study on the mechanism of the chlorination of azithromycin. *J. Hazard. Mater.* **2018**, *359* (July), 31–39.

(4) Terzic, S.; Udikovic-Kolic, N.; Jurina, T.; Krizman-Matasic, I.; Senta, I.; Mihaljevic, I.; Loncar, J.; Smital, T.; Ahel, M. Biotransformation of macrolide antibiotics using enriched activated sludge culture: Kinetics, transformation routes and ecotoxicological evaluation. *J. Hazard. Mater.* **2018**, *349* (August 2017), 143–152.

(5) Wang, H.; Hu, C.; Liu, L.; Xing, X. Interaction of ciprofloxacin chlorination products with bacteria in drinking water distribution systems. *J. Hazard. Mater.* **2017**, *339*, 174–181.

(6) Dodd, M. C.; Shah, A. D.; Von Gunten, U.; Huang, C. H. Interactions of fluoroquinolone antibacterial agents with aqueous chlorine: Reaction kinetics, mechanisms, and transformation pathways. *Environ. Sci. Technol.* **2005**, *39* (18), 7065–7076.

(7) Gomes Júnior, O.; Silva, V. M.; Machado, A. E. H.; Sirtori, C.; Lemos, C. R.; Freitas, A. M.; Trovó, A. G. Correlation between pH and molar iron/ligand ratio during ciprofloxacin degradation by photo-Fenton process: Identification of the main transformation products. *J. Environ. Manage.* **2018**, *213*, 20–26.

(8) Wang, P.; He, Y. L.; Huang, C. H. Oxidation of fluoroquinolone antibiotics and structurally related amines by chlorine dioxide: Reaction kinetics, product and pathway evaluation. *Water Res.* **2010**, *44* (20), 5989–5998.

(9) Li, S.; Hu, J. Transformation products formation of ciprofloxacin in UVA/LED and UVA/LED/TiO2 systems: Impact of natural organic matter characteristics. *Water Res.* **2018**, *132*, 320–330.

(10) Wachter, N.; Aquino, J. M.; Denadai, M.; Barreiro, J. C.; Silva, A. J.; Cass, Q. B.; Rocha-Filho, R. C.; Bocchi, N. Optimization of the electrochemical degradation process of the antibiotic ciprofloxacin

using a double-sided β-PbO 2 anode in a flow reactor: kinetics, identification of oxidation intermediates and toxicity evaluation. *Environ. Sci. Pollut. Res.* **2019**, *26* (5), 4438–4449.

(11) Feng, M.; Wang, Z.; Dionysiou, D. D.; Sharma, V. K. Metal-mediated oxidation of fluoroquinolone antibiotics in water: A review on kinetics, transformation products, and toxicity assessment. *J. Hazard. Mater.* **2018**, *344*, 1136–1154.

(12) Maia, A. S.; Ribeiro, A. R.; Amorim, C. L.; Barreiro, J. C.; Cass, Q. B.; Castro, P. M. L.; Tiritan, M. E. Degradation of fluoroquinolone antibiotics and identification of metabolites/transformation products by liquid chromatography-tandem mass spectrometry. *J. Chromatogr. A* **2014**, *1333*, 87–98.

(13) Deng, J.; Wu, G.; Yuan, S.; Zhan, X.; Wang, W.; Hu, Z. H. Ciprofloxacin degradation in UV/chlorine advanced oxidation process: Influencing factors, mechanisms and degradation pathways. *J. Photochem. Photobiol. A Chem.* **2019**, *371* (November 2018), 151–158.

(14) Rusch, M.; Spielmeyer, A.; Zorn, H.; Hamscher, G. Biotransformation of ciprofloxacin by Xylaria longipes: structure elucidation and residual antibacterial activity of metabolites. *Appl. Microbiol. Biotechnol.* **2018**, *102* (19), 8573–8584.

(15) Feng, X.; Wang, P.; Hou, J.; Qian, J.; Ao, Y.; Wang, C. Significantly enhanced visible light photocatalytic efficiency of phosphorus doped TiO2with surface oxygen vacancies for ciprofloxacin degradation: Synergistic effect and intermediates analysis. *J. Hazard. Mater.* **2018**, *351* (October 2017), 196–205.

(16) Lin, Y. C.; Hsiao, K. W.; Lin, A. Y. C. Photolytic degradation of ciprofloxacin in solid and aqueous environments: kinetics, phototransformation pathways, and byproducts. *Environ. Sci. Pollut. Res.* **2018**, *25* (3), 2303–2312.

(17) Turiel, E.; Bordin, G.; Rodríguez, A. R. Study of the evolution and degradation products of ciprofloxacin and oxolinic acid in river water samples by HPLC-UV/MS/MS-MS. *J. Environ. Monit.* **2005**, *7* (3), 189–195.

(18) Gupta, A.; Garg, A. Degradation of ciprofloxacin using Fenton's oxidation: Effect of operating parameters, identification of oxidized by-products and toxicity assessment. *Chemosphere* **2018**, *193*, 1181–1188.

(19) Deng, J.; Ge, Y.; Tan, C.; Wang, H.; Li, Q.; Zhou, S.; Zhang, K. Degradation of ciprofloxacin using A-MnO2 activated peroxymonosulfate process: Effect of water constituents, degradation intermediates and toxicity evaluation. *Chem. Eng. J.* **2017**, *330* (May), 1390–1400.

SUPPLEMENTARY MATERIAL

Combining biological processes with UV/H_2O_2 for metoprolol and metoprolol acid removal in hospital wastewater

Adrián Jaén-Gil[a,b], Gianluigi Buttiglieri[a,b], Aleix Benito[c], Josep Anton Mir-Tutusaus[d], Rafael Gonzalez-Olmos[c], Glòria Caminal[e], Damià Barceló[a,b,f], Montserrat Sarrà[d], Sara Rodriguez-Mozaz[a,b]*

[a]*Catalan Institute for Water Research (ICRA), Carrer Emili Grahit 101, 17003 Girona, Spain*

[b]*Universitat de Girona, Girona, Spain*

[c]*IQS School of Engineering, Universitat Ramon Llull, Via Augusta 390, 08017, Barcelona, Spain*

[d]*Departament d'Enginyeria Química Biològica i Ambiental, Escola d'Enginyeria, Universitat Autònoma de Barcelona, 08193 Bellaterra, Barcelona, Spain*

[e]*Institut de Química Avançada de Catalunya (IQAC-CSIC). C. Jordi Girona 18-26, 08034 Barcelona, Spain*

[f]*Department of Environmental Chemistry, Institute of Environmental Assessment and Water Research (IDAEA-CSIC), C. Jordi Girona 18-26, 08034 Barcelona, Spain*

S1. Identification of transformation products

Data treatment was adapted and it is presented in Fig. S1 [1]. Automatic data processing starts with MS data filtering between 100 and 1000 Da and from 1 to 12 min with a S/N ratio of 3. To compensate small differences in retention times, chromatographic alignment was performed by using a mass tolerance error of ± 5 ppm and a maximum retention time shift of 0.3 min. Immediately after, data processing was performed in two different steps: a) by detection of unknown compounds (where features above a S/N of 10 with a minimum peak intensity of 10^4 counts were selected) and b) by detection of expected compounds from compound prediction (where more complete MS full scan data was required without being filter out). Then, an in-house library (Table S2), a predicted list automatically created by the software applying chemical modifications (dealkylation, oxidation, reduction, desaturation, oxidative deamination to alcohol, oxidative deamination to ketone, dehydration, hydration) to MTP and MTPA chemical structures (Table S3), and a literature list (Table S4) were used to identify the TPs generated. C*onfirmed structures* were identified with reference standards through comparison with MS exact masses, retention time and MS/MS ion fragmentation pattern from control spiked samples. The in-house library (Table S2) was used to identify *probable structures* by comparison of reported TP exact masses, experimental retention times and MS/MS ion spectra. The list of predicted TPs (Table S3) was used to identify *tentative structures* by comparison of compound exact masses and predicted MS/MS scans of potential TPs. The list from literature (Table S4) was used to identify *unequivocal molecular formulas* by comparison of compound exact masses.

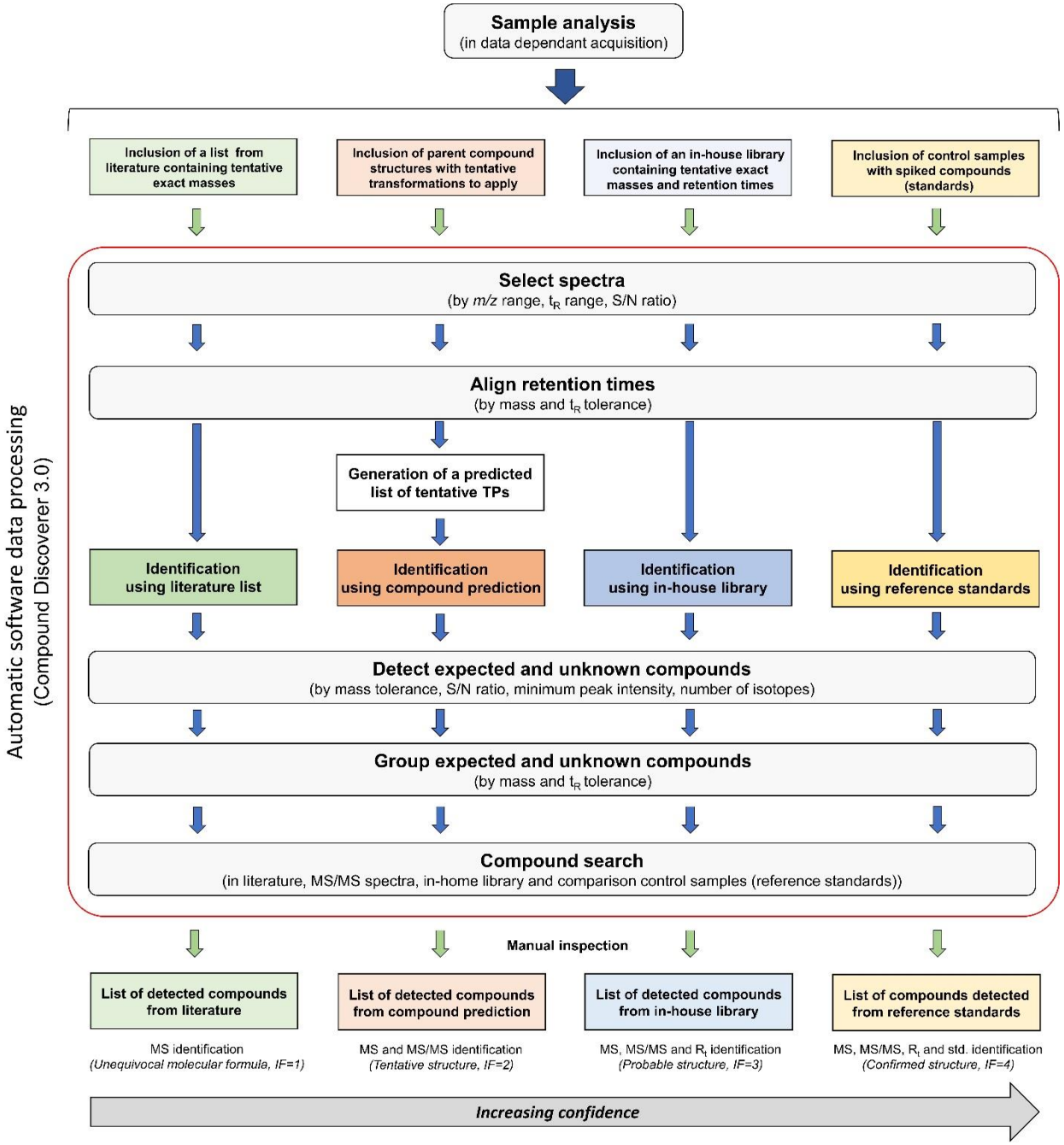

Fig. S1. Screening workflow for the identification of the transformation products generated. This methodology was adapted to Compound Discoverer 3.0 [1].

Table S1. Data processing parameters selected to perform and reproduce the integrated suspect screening methodology in Compound Discoverer 3.0 [1].

Peak filtering of candidates

Select Spectra:
- Retention time range: 1 to 12 min
- Mass range: 100-1000 Da
- S/N ratio: 3

Align Retention Times:
- Alignment Model: Adaptive curve
- Mass tolerance: ± 5 ppm
- Maximum retention time shift: 0.3 min

Detect Unknown Compounds:
- Mass tolerance: ± 5 ppm
- Intensity Tolerance: 30%
- S/N ratio: 10
- Min. Peak Intensity: 10^4
- Ions: $[M+H]^+/[M+H]^-$
- Max. Peak Width: 0.8 min
- Max. #Scan per peak: 5
- Min. #Isotopes: 2

Group Unknown Compounds:
- Mass tolerance: ± 5 ppm
- RT tolerance: 0.3 min

Mark Background Compounds:
- Max. Sample/Blank: 3
- Hide Background: True

Identification strategies

Analytical standard comparison (I)

(MS, MS^2 and R_t comparison with spiked control files after data alignment)

In-house library comparison (II)

Search Mass Lists:
- Mass tolerance: ± 5 ppm
- Retention time: Included
- Retention time tolerance: 0.3 min
- Input Files: "MTP/MTPA in-house library"

Software compound prediction (III)

Generate Expected Compounds:
- Parent compound: MTP/MTPA
- Apply Dealkylation: True
- Max. # Dealkylation Steps: 2
- All reaction steps: 3
- Min. mass: 100 Da
- Ions considered: $[M+H]^+/[M+H]^-$
- Transformations: oxidation, reduction, desaturation, oxidative deamination to alcohol, oxidative deamination to ketone, dehydration, hydration.
- Max. # All Steps: 3

Find Expected Compounds:
- Mass tolerance: ± 5 ppm
- Intensity Tolerance: 30 %
- Intensity Threshold: 0.1 %
- Min. #Isotopes: 2
- Min. peak intensity: 10^4

FISh scoring:
- Annotate Full Tree: True
- Match Transformations: True
- S/N threshold: 10
- Mass tolerance of fragments: ± 5 ppm
- Fragment prediction libraries: True

Group Expected Compounds
- RT tolerance: 0.3 min

Literature exact mass list comparison (IV)

Search Mass List:
- Mass tolerance: ± 5 ppm
- Consider Retention time: Not included
- File loaded: "MTP/MTPA literature"

Table S2. List of the 29 compounds present in the in-house library (from information reported in previous scientific manuscripts [1,2]).

Retention time (min)	Compound	Ion	Elemental composition	Theoretical m/z	RDB	Suggested chemical structure
7.64	MTP	$[M+H]^+$	$C_{15}H_{26}NO_3$	268.19070	3.5	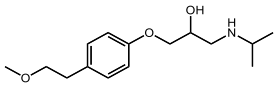
		$[M+H-(H_2O)]^+$	$C_{15}H_{24}NO_2$	250.18016	4.5	
		$[M+H-(C_3H_6)]^+$	$C_{12}H_{20}NO_3$	226.14377	3.5	
		$[M+H-(C_3H_{11}NO)]^+$	$C_{12}H_{15}O_2$	191.10666	5.5	
		$[M+H-(C_7H_{18}NO_2)]^+$	C_8H_9O	121.06479	4.5	
		$[M+H-(C_9H_{12}O_2)]^+$	$C_6H_{14}NO$	116.10699	0.5	
6.68	MTPA	$[M+H]^+$	$C_{14}H_{22}NO_4$	268.15432	4.5	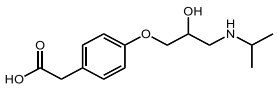
		$[M+H-(H_2O)]^+$	$C_{14}H_{20}NO_3$	250.14377	5.5	
		$[M+H-(C_3H_6)]^+$	$C_{11}H_{16}NO_4$	226.10738	4.5	
		$[M+H-(H_2O)-(C_3H_9N)]^+$	$C_{11}H_{11}O_3$	191.07027	6.5	
		$[M+H-(C_8H_{14}O_3)]^+$	$C_{10}H_9O$	145.06479	6.5	
		$[M+H-(C_8H_8O_3)]^+$	$C_6H_{14}NO$	116.10699	0.5	
1.86	TP114	$[M+H]^+$	$C_6H_{12}NO$	114.09134	1.5	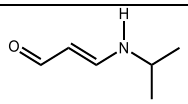
		$[M+H-(H_2O)]^+$	$C_6H_{10}N$	96.08078	2.5	
		$[M+H-(C_3H_6)]^+$	C_3H_6NO	72.04439	1.5	
2.96	TP116	$[M+H]^+$	$C_6H_{14}NO$	116.10699	0.5	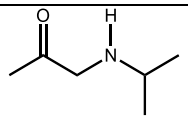
		$[M+H-(H_2O)]^+$	$C_6H_{12}N$	98.09643	1.5	
		$[M+H-(C_3H_6)]^+$	C_3H_8NO	74.06004	0.5	
		$[M+H-(C_2H_2O)]^+$	$C_4H_{10}N$	72.08078	0.5	
7.76	TP121	$[M+H]^+$	C_8H_9O	121.06479	4.5	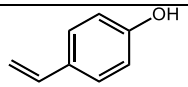
		$[M+H-(O)]^+$	C_8H_9	105.06988	4.5	
		$[M+H-(C_2H_2)-(O)]^+$	C_6H_7	79.05423	3.5	
2.87	TP134	$[M+H]^+$	$C_6H_{16}NO_2$	134.11754	-0.5	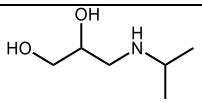
		$[M+H-(H_2O)]^+$	$C_6H_{14}NO$	116.10699	0.5	
		$[M+H-(C_3H_6)]^+$	$C_3H_{10}NO_2$	92.07061	-0.5	
2.72	TP150	$[M+H]^+$	$C_6H_{16}NO_3$	150.11247	-0.5	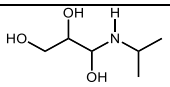
		$[M+H-(H_2O)]^+$	$C_6H_{14}NO_2$	132.10191	0.5	
		$[M+H-(H_2O)-(H_2O)]^+$	$C_6H_{12}NO$	114.09134	1.5	
7.22	TP176	$[M+H]^+$	$C_{11}H_{14}NO$	176.10699	5.5	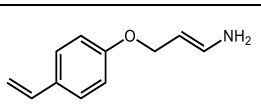
		$[M+H-(NH_3)]^+$	$C_{11}H_{11}O$	159.08044	6.5	
		$[M+H-(NH_3)-(C_2H_2)]^+$	C_9H_9O	133.06479	5.5	
		$[M+H-(NH_3)-(C_3H_2)]^+$	C_8H_9O	121.06479	4.5	
7.04	TP192	$[M+H]^+$	$C_{11}H_{14}NO_2$	192.10191	5.5	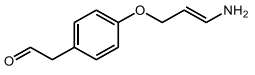
		$[M+H-(NH_3)]^+$	$C_{11}H_{11}O_2$	175.07536	6.5	
		$[M+H-(NH_3)-(C_3H_2)]^+$	$C_8H_9O_2$	137.05971	4.5	
		$[M+H-(NH_3)-(C_3H_2)-(O)]^+$	C_8H_9O	121.06479	4.5	
5.86	TP194	$[M+H]^+$	$C_{11}H_{16}NO_2$	194.11756	4.5	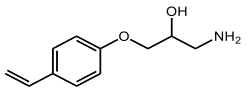
		$[M+H-(NH_3)]^+$	$C_{11}H_{13}O_2$	177.09101	5.5	
		$[M+H-(NH_3)-(H_2O)]^+$	$C_{11}H_{11}O$	159.08044	6.5	
		$[M+H-(NH_3)-(H_2O)-(C_3H_2)]^+$	C_8H_9O	121.06479	4.5	
6.49	TP212	$[M+H]^+$	$C_{11}H_{18}NO_3$	212.12812	3.5	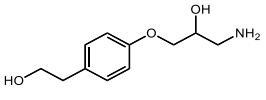
		$[M+H-(H_2O)]^+$	$C_{11}H_{16}NO_2$	194.11756	4.5	
		$[M+H-(H_2O)-(NH_3)]^+$	$C_{11}H_{13}O_2$	177.09101	5.5	
		$[M+H-(H_2O)-(NH_3)-(H_2O)]^+$	$C_{11}H_{11}O$	159.08044	6.5	
7.35	TP218	$[M+H]^+$	$C_{14}H_{20}NO$	218.15394	5.5	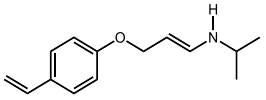
		$[M+H-(C_3H_6)]^+$	$C_{11}H_{14}NO$	176.10699	5.5	
		$[M+H-(C_3H_6)-(NH_3)]^+$	$C_{11}H_{11}O$	159.08044	6.5	
		$[M+H-(C_3H_6)-(NH_3)-(C_2H_2)]^+$	C_9H_9O	133.06479	5.5	

6.21	TP226 A	$[M+H]^+$	$C_{12}H_{20}NO_3$	226.14376	3.5	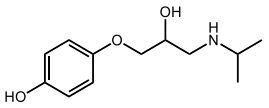
		$[M+H–(H_2O)]^+$	$C_{12}H_{18}NO_2$	208.13321	4.5	
		$[M+H–(C_3H_6)]^+$	$C_9H_{14}NO_3$	184.09682	3.5	
		$[M+H–(H_2O)–(C_3H_9N)]^+$	$C_9H_9O_2$	149.05971	5.5	
		$[M+H–(C_6H_6O_2)]^+$	$C_6H_{14}NO$	116.10699	0.5	
6.66	TP226B	$[M+H]^+$	$C_{11}H_{16}NO_4$	226.10738	4.5	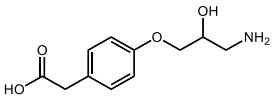
		$[M+H–(H_2O)]^+$	$C_{11}H_{14}NO_3$	208.09682	5.5	
		$[M+H–(H_2O)–(NH_3)]^+$	$C_{11}H_{11}O_3$	191.07027	6.5	
		$[M+H–(CH_7O_3)]^+$	$C_{10}H_9O$	145.06479	6.5	
		$[M+H–(C_8H_8O_3)]^+$	C_3H_8NO	74.06004	0.5	
7.07	TP226C	$[M+H]^+$	$C_{12}H_{20}NO_3$	226.14376	3.5	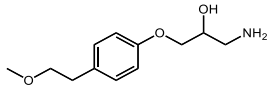
		$[M+H–(H_2O)]^+$	$C_{12}H_{18}NO_2$	208.13321	4.5	
		$[M+H–(H_2O)–(CH_2)]^+$	$C_{11}H_{16}NO_2$	194.11756	4.5	
		$[M+H–(H_2O)–(NH_3)]^+$	$C_{12}H_{15}O_2$	191.10666	5.5	
		$[M+H–(C_4H_{11}O_2)]^+$	C_8H_9O	121.06479	4.5	
		$[M+H–(C_9H_{12}O_2)]^+$	C_3H_8NO	74.06004	0.5	
6.83	TP238	$[M+H]^+$	$C_{13}H_{20}NO_3$	238.14376	4.5	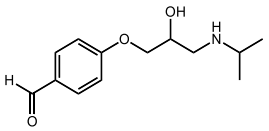
		$[M+H–(H_2O)]^+$	$C_{13}H_{18}NO_2$	220.13321	5.5	
		$[M+H–(C_3H_6)]^+$	$C_{10}H_{14}NO_3$	196.09682	4.5	
		$[M+H–(H_2O)–(C_3H_9N)]^+$	$C_{10}H_9O_2$	161.05971	6.5	
		$[M+H–(C_5H_{13}NO)]^+$ (HCD)	$C_8H_7O_2$	135.04405	5.5	
		$[M+H–(C_7H_6O_2)]^+$	$C_6H_{14}NO$	116.10699	0.5	
6.22	TP240	$[M+H]^+$	$C_{13}H_{22}NO_3$	240.15940	3.5	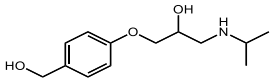
		$[M+H–(H_2O)]^+$	$C_{13}H_{20}NO_2$	222.14886	4.5	
		$[M+H–(C_3H_6)]^+$	$C_{10}H_{16}NO_3$	198.11247	3.5	
		$[M+H–(H_2O)–(C_3H_9N)]^+$	$C_{10}H_{11}O_2$	163.07536	5.5	
		$[M+H–(C_4H_{14}NO_2)]^+$	C_9H_9O	133.06479	5.5	
		$[M+H–(C_7H_8O_2)]^+$	$C_6H_{14}NO$	116.10699	0.5	
7.74	TP250	$[M+H]^+$	$C_{15}H_{24}NO_2$	250.18016	4.5	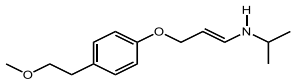
		$[M+H–(CH_4O)]^+$	$C_{14}H_{20}NO$	218.15394	5.5	
		$[M+H–(C_3H_6)–(NH_3)]^+$	$C_{12}H_{15}O_2$	191.10666	5.5	
		$[M+H–(CH_4O)–(C_3H_6)]^+$	$C_{11}H_{14}NO$	176.10699	5.5	
		$[M+H–(C_9H_{12}O_2)]^+$	$C_6H_{12}N$	98.09643	1.5	
6.85	TP252	$[M+H]^+$	$C_{14}H_{22}NO_3$	252.15942	4.5	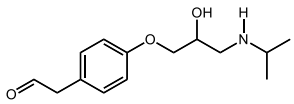
		$[M+H–(H_2O)]^+$	$C_{14}H_{20}NO_2$	234.14886	5.5	
		$[M+H–(C_3H_6)]^+$	$C_{11}H_{16}NO_3$	210.11247	4.5	
		$[M+H–(H_2O)–(C_3H_6)–(NH_3)]^+$	$C_{11}H_{11}O_2$	175.07536	6.5	
		$[M+H–(H_2O)–(C_3H_6)–(NH_3)–(C_3H_2)]^+$	$C_8H_9O_2$	137.05971	4.5	
		$[M+H–(H_2O)-(C_3H_6)-(NH_3)-(C_2H_2)-(O)]^+$	C_9H_9O	133.06479	5.5	
		$[M+H–(C_8H_{18}O_2)]^+$	$C_6H_{14}NO$	116.10699	0.5	
6.37	TP254	$[M+H]^+$	$C_{13}H_{20}NO_4$	254.13867	3.5	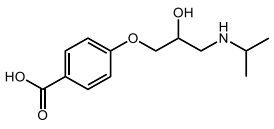
		$[M+H–(H_2O)]^+$	$C_{13}H_{18}NO_3$	236.12812	5.5	
		$[M+H–(C_3H_6)]^+$	$C_{10}H_{14}NO_4$	212.09173	4.5	
		$[M+H–(H_2O)–(C_3H_9N)]^+$	$C_{10}H_9O_3$	177.05462	6.5	
		$[M+H–(C_5H_{13}NO)]^+$ (HCD)	$C_8H_7O_3$	151.03897	5.5	
		$[M+H–(C_7H_6O_3)]^+$	$C_6H_{14}NO$	116.10699	0.5	
6.63	O-DMTP	$[M+H]^+$	$C_{14}H_{24}NO_3$	254.17505	4.5	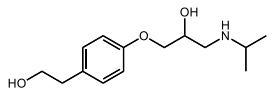
		$[M+H–(H_2O)]^+$	$C_{14}H_{22}NO_2$	236.16451	4.5	
		$[M+H–(C_3H_6)]^+$	$C_{11}H_{18}NO_3$	212.12812	3.5	
		$[M+H–(H_2O)–(C_3H_9N)]^+$	$C_{11}H_{13}O_2$	177.09101	5.5	
		$[M+H–(C_8H_{10}O_2)]^+$	$C_6H_{14}NO$	116.10699	0.5	
5.75	TP270	$[M+H]^+$	$C_{14}H_{24}NO_4$	270.16998	3.5	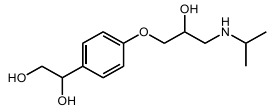
		$[M+H–(H_2O)]^+$	$C_{14}H_{22}NO_3$	252.15942	4.5	
		$[M+H–2(H_2O)]^+$	$C_{14}H_{20}NO_2$	234.14886	5.5	
		$[M+H–(C_3H_6)]^+$	$C_{11}H_{18}NO_4$	228.12303	3.5	
		$[M+H–(C_3H_{10}N)–(H_2O)]^+$	$C_{11}H_{13}O_3$	193.08592	5.5	

		$[M+H–(C_5H_{16}NO_3)]^+$	C_9H_9O	133.06479	5.5	
		$[M+H–(C_8H_{10}NO_3)]^+$	$C_6H_{14}NO$	116.10699	0.5	
6.69	TP282A	$[M+H]^+$	$C_{15}H_{24}NO_4$	282.16997	4.5	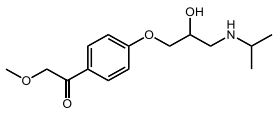
		$[M+H–(H_2O)]^+$	$C_{15}H_{22}NO_3$	264.15942	5.5	
		$[M+H–(C_3H_6)]^+$	$C_{12}H_{18}NO_4$	240.12303	4.5	
		$[M+H–(H_2O)–(C_3H_9N)]^+$	$C_{12}H_{13}O_3$	205.08592	6.5	
		$[M+H–(C_2H_5O)–(C_5H_{12}NO)]^+$ (HCD)	$C_8H_7O_2$	135.04405	5.5	
		$[M+H–(C_9H_{10}O_3)]^+$	$C_6H_{14}NO$	116.10699	0.5	
7.48	TP282B	$[M+H]^+$	$C_{15}H_{24}NO_4$	282.16997	4.5	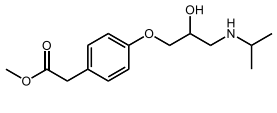
		$[M+H–(H_2O)]^+$	$C_{15}H_{22}NO_3$	264.15942	5.5	
		$[M+H–(C_3H_6)]^+$	$C_{12}H_{18}NO_4$	240.12303	4.5	
		$[M+H–(H_2O)–(C_3H_9N)]^+$	$C_{12}H_{13}O_3$	205.08592	6.5	
		$[M+H–(C_5H_{16}O_3)]^+$	$C_{10}H_9O$	145.06479	6.5	
		$[M+H–(C_9H_{10}O_3)]^+$	$C_6H_{14}NO$	116.10699	0.5	
6.40	α-HMTP	$[M+H]^+$	$C_{15}H_{26}NO_4$	284.18562	3.5	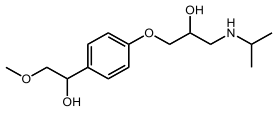
		$[M+H–(H_2O)]^+$	$C_{15}H_{24}NO_3$	266.17507	4.5	
		$[M+H–(H_2O)–(C_3H_5)]^+$	$C_{12}H_{18}NO_3$	224.12812	4.5	
		$[M+H–(H_2O)–(C_3H_9N)]^+$	$C_{12}H_{15}O_3$	207.10157	5.5	
		$[M+H–(CH_5O_2)–(C_5H_{12}NO)]^+$	C_9H_9O	133.06479	5.5	
		$[M+H–(C_9H_{12}O_3)]^+$	$C_6H_{14}NO$	116.10699	0.5	
7.31	TP284	$[M+H]^+$	$C_{15}H_{26}NO_4$	284.18562	3.5	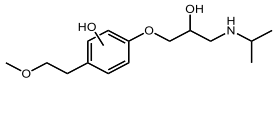
		$[M+H–(H_2O)]^+$	$C_{15}H_{24}NO_3$	266.17507	4.5	
		$[M+H–(CH_4O)]^+$	$C_{14}H_{22}NO_3$	252.15942	4.5	
		$[M+H–(H_2O)–(CH_4O)]^+$	$C_{14}H_{20}NO_2$	234.14886	5.5	
		$[M+H–(CH_5O)–(C_3H_3)]^+$	$C_{11}H_{14}NO_2$	192.10191	5.5	
		$[M+H–(H_2O)–(C_3H_9N)]^+$	$C_{11}H_{11}O_2$	175.07536	6.5	
		$[M+H–(CH_5O)–(C_5H_{12}NO)]^+$ (HCD)	$C_9H_9O_2$	149.05971	5.5	
		$[M+H–(C_9H_{12}O_3)]^+$	$C_6H_{14}NO$	116.10699	0.5	
6.86	TP298	$[M+H]^+$	$C_{15}H_{24}NO_5$	298.16488	4.5	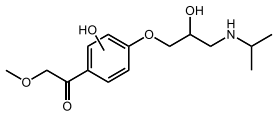
		$[M+H–(H_2O)]^+$	$C_{15}H_{22}NO_4$	280.15433	5.5	
		$[M+H–(CH_4O)]^+$	$C_{14}H_{20}NO_4$	266.13868	5.5	
		$[M+H–(C_3H_6)–(CH_3O)]^+$	$C_{11}H_{14}NO_4$	224.09173	5.5	
		$[M+H–(C_2H_5O)–(C_5H_{12}NO)]^+$ (HCD)	$C_8H_7O_3$	151.03897	5.5	
		$[M+H–(C_9H_{10}O_4)]^+$	$C_6H_{14}NO$	116.10699	0.5	
6.72	TP300	$[M+H]^+$	$C_{15}H_{26}NO_5$	300.18055	3.5	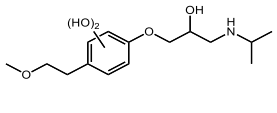
		$[M+H–(H_2O)]^+$	$C_{15}H_{24}NO_4$	282.16998	4.5	
		$[M+H–(CH_4O)]^+$	$C_{14}H_{22}NO_4$	268.15433	4.5	
		$[M+H–(H_2O)–(CH_4O)]^+$	$C_{14}H_{20}NO_3$	250.14377	5.5	
		$[M+H–(CH_5O)–(C_5H_{12}NO)]^+$	$C_9H_9O_3$	165.05462	5.5	
		$[M+H–(C_6H_{18}NO_3)]^+$	$C_9H_9O_2$	149.05971	5.5	
		$[M+H–(C_{13}H_{12}O_4)]^+$	$C_6H_{14}NO$	116.10699	0.5	
6.50	TP316	$[M+H]^+$	$C_{15}H_{26}NO_6$	316.17545	3.5	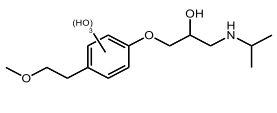
		$[M+H–(H_2O)]^+$	$C_{15}H_{24}NO_5$	298.16490	4.5	
		$[M+H–(C_3H_6)]^+$	$C_{12}H_{20}NO_6$	274.12851	3.5	
		$[M+H–(C_3H_8O)]^+$	$C_{12}H_{18}NO_5$	256.11795	4.5	
		$[M+H–(C_6H_{15}NO_2)]^+$	$C_9H_{11}O_4$	183.06519	4.5	
		$[M+H–(C_9H_{12}O_5)]^+$	$C_6H_{14}NO$	116.10699	0.5	

Table S3. List of the 356 compounds present in the prediction list created automatically by Compound Discoverer 3.0.

Parent Compound	Formula	Exact mass $[M+H]^+$	Dealkylated	Transformations
Metoprolol	C8 H4	101.0393	x	Dehydration, Dehydration
Metoprolol	C8 H6	103.05495	x	Dehydration, Dehydration
Metoprolol	C6 H9 N O	112.07641	x	Dehydration, Desaturation
Metoprolol	C6 H8 O2	113.06043	x	Dehydration, Oxidative Deamination to Ketone
Metoprolol	C6 H11 N O	114.09206	x	Dehydration
Metoprolol	C6 H10 O2	115.07608	x	Dehydration, Oxidative Deamination to Alcohol
Metoprolol	C6 H13 N O	116.10771	x	Dehydration, Reduction
Metoprolol_Acid	C8 H4 O	117.03421	x	Dehydration, Dehydration
Metoprolol	C8 H4 O	117.03421	x	Dehydration, Desaturation
Metoprolol	C9 H8	117.0706	x	Dehydration, Dehydration
Metoprolol	C8 H6 O	119.04986	x	Dehydration, Desaturation
Metoprolol	C8 H6 O	119.04986	x	Dehydration
Metoprolol	C8 H8 O	121.06551	x	Dehydration
Metoprolol	C8 H8 O	121.06551	x	Dehydration, Reduction
Metoprolol	C8 H10 O	123.08116	x	Dehydration, Reduction
Metoprolol	C6 H9 N O2	128.07133	x	Desaturation, Desaturation
Metoprolol	C6 H8 O3	129.05534	x	Desaturation, Oxidative Deamination to Ketone
Metoprolol	C6 H11 N O2	130.08698	x	Desaturation
Metoprolol	C6 H10 O3	131.07099	x	Oxidative Deamination to Ketone
Metoprolol	C6 H13 N O2	132.10263	x	
Metoprolol	C8 H4 O2	133.02913	x	Desaturation, Desaturation
Metoprolol_Acid	C8 H4 O2	133.02913	x	Dehydration, Desaturation
Metoprolol	C9 H8 O	133.06551	x	Dehydration, Desaturation
Metoprolol	C6 H12 O3	133.08664	x	Oxidative Deamination to Alcohol
Metoprolol	C6 H15 N O2	134.11828	x	Reduction
Metoprolol	C8 H6 O2	135.04478	x	Desaturation, Desaturation
Metoprolol_Acid	C8 H6 O2	135.04478	x	Dehydration
Metoprolol	C8 H6 O2	135.04478	x	Desaturation
Metoprolol	C9 H10 O	135.08116	x	Dehydration
Metoprolol	C6 H14 O3	135.10229	x	Oxidative Deamination to Alcohol, Reduction
Metoprolol	C8 H8 O2	137.06043	x	
Metoprolol_Acid	C8 H8 O2	137.06043	x	Dehydration, Reduction
Metoprolol	C8 H8 O2	137.06043	x	Desaturation
Metoprolol	C9 H12 O	137.09681	x	Dehydration, Reduction
Metoprolol	C8 H10 O2	139.07608	x	Reduction
Metoprolol	C8 H10 O2	139.07608	x	
Metoprolol	C8 H12 O2	141.09173	x	Reduction
Metoprolol	C6 H11 N O3	146.08189	x	Desaturation, Oxidation
Metoprolol	C6 H10 O4	147.06591	x	Oxidation, Oxidative Deamination to Ketone
Metoprolol	C6 H13 N O3	148.09754	x	Oxidation
Metoprolol_Acid	C8 H4 O3	149.02404	x	Desaturation, Desaturation
Metoprolol	C9 H8 O2	149.06043	x	Desaturation, Desaturation
Metoprolol	C6 H12 O4	149.08156	x	Hydration, Oxidative Deamination to Ketone
Metoprolol	C6 H15 N O3	150.11319	x	Hydration
Metoprolol	C8 H6 O3	151.03969	x	Desaturation, Oxidation
Metoprolol_Acid	C8 H6 O3	151.03969	x	Desaturation
Metoprolol	C9 H10 O2	151.07608	x	Desaturation
Metoprolol	C6 H14 O4	151.09721	x	Hydration, Oxidative Deamination to Alcohol
Metoprolol	C6 H17 N O3	152.12884	x	Hydration, Reduction
Metoprolol	C8 H8 O3	153.05534	x	Desaturation, Oxidation
Metoprolol_Acid	C8 H8 O3	153.05534	x	
Metoprolol	C8 H8 O3	153.05534	x	Oxidation
Metoprolol	C9 H12 O2	153.09173	x	
Metoprolol_Acid	C8 H10 O3	155.07099	x	Reduction
Metoprolol	C8 H10 O3	155.07099	x	Oxidation
Metoprolol	C8 H10 O3	155.07099	x	Hydration
Metoprolol	C9 H14 O2	155.10738	x	Reduction
Metoprolol	C8 H12 O3	157.08664	x	Hydration
Metoprolol	C8 H12 O3	157.08664	x	Hydration, Reduction
Metoprolol	C8 H14 O3	159.10229	x	Hydration, Reduction
Metoprolol	C6 H13 N O4	164.09246	x	Oxidation, Oxidation
Metoprolol	C6 H15 N O4	166.10811	x	Hydration, Oxidation
Metoprolol_Acid	C8 H6 O4	167.03461	x	Desaturation, Oxidation
Metoprolol	C9 H10 O3	167.07099	x	Desaturation, Oxidation
Metoprolol_Acid	C8 H8 O4	169.05026	x	Oxidation
Metoprolol	C8 H8 O4	169.05026	x	Oxidation, Oxidation
Metoprolol	C9 H12 O3	169.08664	x	Oxidation

Metoprolol_Acid	C8 H10 O4	171.06591	x	Hydration
Metoprolol	C8 H10 O4	171.06591	x	Hydration, Oxidation
Metoprolol	C8 H10 O4	171.06591	x	Oxidation, Oxidation
Metoprolol	C9 H14 O3	171.10229	x	Hydration
Metoprolol	C11 H8 O2	173.06043	x	Dehydration, Dehydration
Metoprolol	C8 H12 O4	173.08156	x	Hydration, Oxidation
Metoprolol_Acid	C8 H12 O4	173.08156	x	Hydration, Reduction
Metoprolol	C9 H16 O3	173.11794	x	Hydration, Reduction
Metoprolol	C11 H11 N O	174.09206	x	Dehydration, Dehydration
Metoprolol	C11 H10 O2	175.07608	x	Dehydration, Dehydration
Metoprolol	C11 H13 N O	176.10771	x	Dehydration, Dehydration
Metoprolol_Acid	C8 H8 O5	185.04517	x	Oxidation, Oxidation
Metoprolol	C9 H12 O4	185.08156	x	Oxidation, Oxidation
Metoprolol Acid	C8 H10 O5	187.06082	x	Hydration, Oxidation
Metoprolol	C9 H14 O4	187.09721	x	Hydration, Oxidation
Metoprolol_Acid	C11 H8 O3	189.05534	x	Dehydration, Dehydration
Metoprolol	C11 H8 O3	189.05534	x	Dehydration, Desaturation
Metoprolol	C12 H12 O2	189.09173	x	Dehydration, Dehydration
Metoprolol_Acid	C11 H11 N O2	190.08698	x	Dehydration, Dehydration
Metoprolol	C11 H11 N O2	190.08698	x	Dehydration, Desaturation
Metoprolol	C12 H15 N O	190.12336	x	Dehydration, Dehydration
Metoprolol	C11 H10 O3	191.07099	x	Dehydration, Desaturation
Metoprolol	C11 H10 O3	191.07099	x	Dehydration, Oxidative Deamination to Ketone
Metoprolol	C11 H10 O3	191.07099	x	Dehydration
Metoprolol	C11 H13 N O2	192.10263	x	Dehydration
Metoprolol	C11 H13 N O2	192.10263	x	Dehydration, Desaturation
Metoprolol	C11 H12 O3	193.08664	x	Dehydration, Oxidative Deamination to Alcohol
Metoprolol	C11 H12 O3	193.08664	x	Dehydration
Metoprolol	C11 H12 O3	193.08664	x	Dehydration, Reduction
Metoprolol	C11 H12 O3	193.08664	x	Dehydration, Oxidative Deamination to Ketone
Metoprolol	C11 H15 N O2	194.11828	x	Dehydration, Reduction
Metoprolol	C11 H15 N O2	194.11828	x	Dehydration
Metoprolol	C11 H14 O3	195.10229	x	Dehydration, Oxidative Deamination to Alcohol
Metoprolol	C11 H14 O3	195.10229	x	Dehydration, Reduction
Metoprolol	C11 H17 N O2	196.13393	x	Dehydration, Reduction
Metoprolol_Acid	C11 H8 O4	205.05026	x	Dehydration, Desaturation
Metoprolol	C11 H8 O4	205.05026	x	Desaturation, Desaturation
Metoprolol	C12 H12 O3	205.08664	x	Dehydration, Desaturation
Metoprolol_Acid	C11 H11 N O3	206.08189	x	Dehydration, Desaturation
Metoprolol	C11 H11 N O3	206.08189	x	Desaturation, Desaturation
Metoprolol	C12 H15 N O2	206.11828	x	Dehydration, Desaturation
Metoprolol	C11 H10 O4	207.06591	x	Desaturation, Oxidative Deamination to Ketone
Metoprolol	C11 H10 O4	207.06591	x	Desaturation, Desaturation
Metoprolol	C11 H10 O4	207.06591	x	Desaturation
Metoprolol_Acid	C11 H10 O4	207.06591	x	Dehydration, Oxidative Deamination to Ketone
Metoprolol_Acid	C11 H10 O4	207.06591	x	Dehydration
Metoprolol	C12 H14 O3	207.10229	x	Dehydration
Metoprolol	C12 H14 O3	207.10229	x	Dehydration, Oxidative Deamination to Ketone
Metoprolol	C11 H13 N O3	208.09754	x	Desaturation
Metoprolol	C11 H13 N O3	208.09754	x	Desaturation, Desaturation
Metoprolol_Acid	C11 H13 N O3	208.09754	x	Dehydration
Metoprolol	C12 H17 N O2	208.13393	x	Dehydration
Metoprolol	C11 H12 O4	209.08156	x	
Metoprolol	C11 H12 O4	209.08156	x	Desaturation
Metoprolol	C11 H12 O4	209.08156	x	Desaturation, Oxidative Deamination to Ketone
Metoprolol	C11 H12 O4	209.08156	x	Oxidative Deamination to Ketone
Metoprolol_Acid	C11 H12 O4	209.08156	x	Dehydration, Oxidative Deamination to Alcohol
Metoprolol_Acid	C11 H12 O4	209.08156	x	Dehydration, Reduction
Metoprolol	C12 H16 O3	209.11794	x	Dehydration, Oxidative Deamination to Alcohol
Metoprolol	C12 H16 O3	209.11794	x	Dehydration, Reduction
Metoprolol_Acid	C11 H15 N O3	210.11319	x	Dehydration, Reduction
Metoprolol	C11 H15 N O3	210.11319	x	Desaturation
Metoprolol	C11 H15 N O3	210.11319	x	
Metoprolol	C12 H19 N O2	210.14958	x	Dehydration, Reduction
Metoprolol	C11 H14 O4	211.09721	x	Oxidative Deamination to Alcohol
Metoprolol	C11 H14 O4	211.09721	x	Reduction
Metoprolol	C11 H14 O4	211.09721	x	
Metoprolol	C11 H14 O4	211.09721	x	Oxidative Deamination to Ketone
Metoprolol	C11 H17 N O3	212.12884	x	
Metoprolol	C11 H17 N O3	212.12884	x	Reduction
Metoprolol	C11 H16 O4	213.11286	x	Reduction

Metoprolol	C11 H16 O4	213.11286	x	Oxidative Deamination to Alcohol
Metoprolol	C11 H16 O4	213.11286	x	Oxidative Deamination to Alcohol, Reduction
Metoprolol	C11 H19 N O3	214.14449	x	Reduction
Metoprolol	C11 H18 O4	215.12851	x	Oxidative Deamination to Alcohol, Reduction
Metoprolol	C14 H17 N O	216.13901	x	Dehydration, Dehydration
Metoprolol	C14 H19 N O	218.15466	x	Dehydration, Dehydration
Metoprolol_Acid	C11 H8 O5	221.04517	x	Desaturation, Desaturation
Metoprolol	C12 H12 O4	221.08156	x	Desaturation, Desaturation
Metoprolol_Acid	C11 H11 N O4	222.07681	x	Desaturation, Desaturation
Metoprolol	C12 H15 N O3	222.11319	x	Desaturation, Desaturation
Metoprolol_Acid	C11 H10 O5	223.06082	x	Desaturation
Metoprolol	C11 H10 O5	223.06082	x	Desaturation, Oxidation
Metoprolol_Acid	C11 H10 O5	223.06082	x	Desaturation, Oxidative Deamination to Ketone
Metoprolol	C12 H14 O4	223.09721	x	Desaturation
Metoprolol	C12 H14 O4	223.09721	x	Desaturation, Oxidative Deamination to Ketone
Metoprolol_Acid	C11 H13 N O4	224.09246	x	Desaturation
Metoprolol	C11 H13 N O4	224.09246	x	Desaturation, Oxidation
Metoprolol	C12 H17 N O3	224.12884	x	Desaturation
Metoprolol	C11 H12 O5	225.07647	x	Oxidation
Metoprolol_Acid	C11 H12 O5	225.07647	x	Oxidative Deamination to Ketone
Metoprolol	C11 H12 O5	225.07647	x	Desaturation, Oxidation
Metoprolol	C11 H12 O5	225.07647	x	Oxidation, Oxidative Deamination to Ketone
Metoprolol_Acid	C11 H12 O5	225.07647	x	
Metoprolol	C12 H16 O4	225.11286	x	Oxidative Deamination to Ketone
Metoprolol	C12 H16 O4	225.11286	x	
Metoprolol_Acid	C11 H15 N O4	226.10811	x	
Metoprolol	C11 H15 N O4	226.10811	x	Desaturation, Oxidation
Metoprolol	C11 H15 N O4	226.10811	x	Oxidation
Metoprolol	C12 H19 N O3	226.14449	x	
Metoprolol	C11 H14 O5	227.09212	x	Hydration, Oxidative Deamination to Ketone
Metoprolol	C11 H14 O5	227.09212	x	Oxidation, Oxidative Deamination to Ketone
Metoprolol	C11 H14 O5	227.09212	x	Oxidation
Metoprolol_Acid	C11 H14 O5	227.09212	x	Reduction
Metoprolol	C11 H14 O5	227.09212	x	Hydration
Metoprolol_Acid	C11 H14 O5	227.09212	x	Oxidative Deamination to Alcohol
Metoprolol	C12 H18 O4	227.12851	x	Oxidative Deamination to Alcohol
Metoprolol	C12 H18 O4	227.12851	x	Reduction
Metoprolol	C11 H17 N O4	228.12376	x	Hydration
Metoprolol_Acid	C11 H17 N O4	228.12376	x	Reduction
Metoprolol	C11 H17 N O4	228.12376	x	Oxidation
Metoprolol	C12 H21 N O3	228.16014	x	Reduction
Metoprolol	C11 H16 O5	229.10777	x	Hydration, Oxidative Deamination to Alcohol
Metoprolol	C11 H16 O5	229.10777	x	Hydration, Reduction
Metoprolol	C11 H16 O5	229.10777	x	Hydration
Metoprolol	C11 H16 O5	229.10777	x	Hydration, Oxidative Deamination to Ketone
Metoprolol_Acid	C11 H16 O5	229.10777	x	Oxidative Deamination to Alcohol, Reduction
Metoprolol	C12 H20 O4	229.14416	x	Oxidative Deamination to Alcohol, Reduction
Metoprolol_Acid	C14 H15 N O2	230.11828		Dehydration, Dehydration, Desaturation
Metoprolol	C11 H19 N O4	230.13941	x	Hydration, Reduction
Metoprolol	C11 H19 N O4	230.13941	x	Hydration
Metoprolol	C15 H19 N O	230.15466		Dehydration, Dehydration, Desaturation
Metoprolol_Acid	C14 H14 O3	231.10229		Dehydration, Dehydration, Oxidative Deamination to Ketone
Metoprolol	C11 H18 O5	231.12342	x	Hydration, Oxidative Deamination to Alcohol
Metoprolol	C11 H18 O5	231.12342	x	Hydration, Reduction
Metoprolol	C15 H18 O2	231.13868		Dehydration, Dehydration, Oxidative Deamination to Ketone
Metoprolol	C14 H17 N O2	232.13393	x	Dehydration, Desaturation
Metoprolol_Acid	C14 H17 N O2	232.13393		Dehydration, Dehydration
Metoprolol	C11 H21 N O4	232.15506	x	Hydration, Reduction
Metoprolol	C15 H21 N O	232.17031		Dehydration, Dehydration
Metoprolol_Acid	C14 H16 O3	233.11794		Dehydration, Dehydration, Oxidative Deamination to Alcohol
Metoprolol	C14 H16 O3	233.11794	x	Dehydration, Oxidative Deamination to Ketone
Metoprolol	C15 H20 O2	233.15433		Dehydration, Dehydration, Oxidative Deamination to Alcohol
Metoprolol_Acid	C14 H19 N O2	234.14958		Dehydration, Dehydration, Reduction
Metoprolol	C14 H19 N O2	234.14958	x	Dehydration
Metoprolol	C14 H19 N O2	234.14958	x	Dehydration, Desaturation
Metoprolol	C15 H23 N O	234.18596		Dehydration, Dehydration, Reduction
Metoprolol	C14 H18 O3	235.13359	x	Dehydration, Oxidative Deamination to Alcohol
Metoprolol	C14 H18 O3	235.13359	x	Dehydration, Oxidative Deamination to Ketone
Metoprolol	C14 H21 N O2	236.16523	x	Dehydration
Metoprolol	C14 H21 N O2	236.16523	x	Dehydration, Reduction
Metoprolol	C14 H20 O3	237.14924	x	Dehydration, Oxidative Deamination to Alcohol

Metoprolol	C14 H23 N O2	238.18088	x	Dehydration, Reduction
Metoprolol_Acid	C11 H10 O6	239.05574	x	Desaturation, Oxidation
Metoprolol	C12 H14 O5	239.09212	x	Desaturation, Oxidation
Metoprolol_Acid	C11 H13 N O5	240.08737	x	Desaturation, Oxidation
Metoprolol	C12 H17 N O4	240.12376	x	Desaturation, Oxidation
Metoprolol_Acid	C11 H12 O6	241.07139	x	Oxidation, Oxidative Deamination to Ketone
Metoprolol	C11 H12 O6	241.07139	x	Oxidation, Oxidation
Metoprolol_Acid	C11 H12 O6	241.07139	x	Oxidation
Metoprolol	C12 H16 O5	241.10777	x	Oxidation, Oxidative Deamination to Ketone
Metoprolol	C12 H16 O5	241.10777	x	Oxidation
Metoprolol	C11 H15 N O5	242.10302	x	Oxidation, Oxidation
Metoprolol_Acid	C11 H15 N O5	242.10302	x	Oxidation
Metoprolol	C12 H19 N O4	242.13941	x	Oxidation
Metoprolol	C11 H14 O6	243.08704	x	Hydration, Oxidation
Metoprolol_Acid	C11 H14 O6	243.08704	x	Hydration, Oxidative Deamination to Ketone
Metoprolol_Acid	C11 H14 O6	243.08704	x	Hydration
Metoprolol	C11 H14 O6	243.08704	x	Oxidation, Oxidation
Metoprolol	C12 H18 O5	243.12342	x	Hydration
Metoprolol	C12 H18 O5	243.12342	x	Hydration, Oxidative Deamination to Ketone
Metoprolol	C11 H17 N O5	244.11867	x	Oxidation, Oxidation
Metoprolol	C11 H17 N O5	244.11867	x	Hydration, Oxidation
Metoprolol_Acid	C11 H17 N O5	244.11867	x	Hydration
Metoprolol	C12 H21 N O4	244.15506	x	Hydration
Metoprolol_Acid	C11 H16 O6	245.10269	x	Hydration, Reduction
Metoprolol_Acid	C11 H16 O6	245.10269	x	Hydration, Oxidative Deamination to Alcohol
Metoprolol	C11 H16 O6	245.10269	x	Hydration, Oxidation
Metoprolol	C12 H20 O5	245.13907	x	Hydration, Oxidative Deamination to Alcohol
Metoprolol	C12 H20 O5	245.13907	x	Hydration, Reduction
Metoprolol_Acid	C14 H15 N O3	246.11319		Dehydration, Desaturation, Desaturation
Metoprolol	C11 H19 N O5	246.13432	x	Hydration, Oxidation
Metoprolol_Acid	C11 H19 N O5	246.13432	x	Hydration, Reduction
Metoprolol	C15 H19 N O2	246.14958		Dehydration, Desaturation, Desaturation
Metoprolol	C12 H23 N O4	246.17071	x	Hydration, Reduction
Metoprolol_Acid	C14 H14 O4	247.09721		Dehydration, Desaturation, Oxidative Deamination to Ketone
Metoprolol	C15 H18 O3	247.13359		Dehydration, Desaturation, Oxidative Deamination to Ketone
Metoprolol	C14 H17 N O3	248.12884	x	Desaturation, Desaturation
Metoprolol_Acid	C14 H17 N O3	248.12884		Dehydration, Desaturation
Metoprolol	C15 H21 N O2	248.16523		Dehydration, Desaturation
Metoprolol_Acid	C14 H16 O4	249.11286		Dehydration, Oxidative Deamination to Ketone
Metoprolol	C14 H16 O4	249.11286	x	Desaturation, Oxidative Deamination to Ketone
Metoprolol	C15 H20 O3	249.14924		Dehydration, Oxidative Deamination to Ketone
Metoprolol_Acid	C14 H19 N O3	250.14449		Dehydration
Metoprolol	C14 H19 N O3	250.14449	x	Desaturation, Desaturation
Metoprolol	C14 H19 N O3	250.14449	x	Desaturation
Metoprolol	C15 H23 N O2	250.18088		Dehydration
Metoprolol	C14 H18 O4	251.12851	x	Desaturation, Oxidative Deamination to Ketone
Metoprolol_Acid	C14 H18 O4	251.12851		Dehydration, Oxidative Deamination to Alcohol
Metoprolol	C14 H18 O4	251.12851	x	Oxidative Deamination to Ketone
Metoprolol	C15 H22 O3	251.16489		Dehydration, Oxidative Deamination to Alcohol
Metoprolol	C14 H21 N O3	252.16014	x	Desaturation
Metoprolol	C14 H21 N O3	252.16014	x	
Metoprolol_Acid	C14 H21 N O3	252.16014		Dehydration, Reduction
Metoprolol	C15 H25 N O2	252.19653		Dehydration, Reduction
Metoprolol	C14 H20 O4	253.14416	x	Oxidative Deamination to Ketone
Metoprolol_Acid	C14 H20 O4	253.14416		Dehydration, Oxidative Deamination to Alcohol, Reduction
Metoprolol	C14 H20 O4	253.14416	x	Oxidative Deamination to Alcohol
Metoprolol	C15 H24 O3	253.18054		Dehydration, Oxidative Deamination to Alcohol, Reduction
Metoprolol	C14 H23 N O3	254.17579	x	Reduction
Metoprolol	C14 H23 N O3	254.17579	x	
Metoprolol	C14 H22 O4	255.15981	x	Oxidative Deamination to Alcohol, Reduction
Metoprolol	C14 H22 O4	255.15981	x	Oxidative Deamination to Alcohol
Metoprolol	C14 H25 N O3	256.19144	x	Reduction
Metoprolol_Acid	C11 H12 O7	257.0663	x	Oxidation, Oxidation
Metoprolol	C12 H16 O6	257.10269	x	Oxidation, Oxidation
Metoprolol	C14 H24 O4	257.17546	x	Oxidative Deamination to Alcohol, Reduction
Metoprolol_Acid	C11 H15 N O6	258.09794	x	Oxidation, Oxidation
Metoprolol	C12 H19 N O5	258.13432	x	Oxidation, Oxidation
Metoprolol_Acid	C11 H14 O7	259.08195	x	Hydration, Oxidation
Metoprolol	C12 H18 O6	259.11834	x	Hydration, Oxidation
Metoprolol_Acid	C11 H17 N O6	260.11359	x	Hydration, Oxidation
Metoprolol	C12 H21 N O5	260.14997	x	Hydration, Oxidation

Metoprolol_Acid	C14 H15 N O4	262.10811		Desaturation, Desaturation, Desaturation
Metoprolol	C15 H19 N O3	262.14449		Desaturation, Desaturation, Desaturation
Metoprolol_Acid	C14 H14 O5	263.09212		Desaturation, Desaturation, Oxidative Deamination to Ketone
Metoprolol	C15 H18 O4	263.12851		Desaturation, Desaturation, Oxidative Deamination to Ketone
Metoprolol_Acid	C14 H17 N O4	264.12376		Desaturation, Desaturation
Metoprolol	C15 H21 N O3	264.16014		Desaturation, Desaturation
Metoprolol_Acid	C14 H16 O5	265.10777		Desaturation, Oxidative Deamination to Ketone
Metoprolol	C15 H20 O4	265.14416		Desaturation, Oxidative Deamination to Ketone
Metoprolol_Acid	C14 H19 N O4	266.13941		Desaturation
Metoprolol	C14 H19 N O4	266.13941	x	Desaturation, Oxidation
Metoprolol	C15 H23 N O3	266.17579		Desaturation
Metoprolol_Acid	C14 H18 O5	267.12342		Oxidative Deamination to Ketone
Metoprolol	C14 H18 O5	267.12342	x	Oxidation, Oxidative Deamination to Ketone
Metoprolol	C15 H22 O4	267.15981		Oxidative Deamination to Ketone
Metoprolol	C14 H21 N O4	268.15506	x	Oxidation
Metoprolol_Acid	C14 H21 N O4	268.15506		
Metoprolol	C14 H21 N O4	268.15506	x	Desaturation, Oxidation
Metoprolol	C15 H25 N O3	268.19144		
Metoprolol	C14 H20 O5	269.13907	x	Oxidation, Oxidative Deamination to Ketone
Metoprolol_Acid	C14 H20 O5	269.13907		Oxidative Deamination to Alcohol
Metoprolol	C14 H20 O5	269.13907	x	Hydration, Oxidative Deamination to Ketone
Metoprolol	C15 H24 O4	269.17546		Oxidative Deamination to Alcohol
Metoprolol_Acid	C14 H23 N O4	270.17071		Reduction
Metoprolol	C14 H23 N O4	270.17071	x	Hydration
Metoprolol	C14 H23 N O4	270.17071	x	Oxidation
Metoprolol	C15 H27 N O3	270.20709		Reduction
Metoprolol	C14 H22 O5	271.15472	x	Hydration, Oxidative Deamination to Alcohol
Metoprolol_Acid	C14 H22 O5	271.15472		Oxidative Deamination to Alcohol, Reduction
Metoprolol	C14 H22 O5	271.15472	x	Hydration, Oxidative Deamination to Ketone
Metoprolol	C15 H26 O4	271.19111		Oxidative Deamination to Alcohol, Reduction
Metoprolol	C14 H25 N O4	272.18636	x	Hydration, Reduction
Metoprolol	C14 H25 N O4	272.18636	x	Hydration
Metoprolol	C14 H24 O5	273.17037	x	Hydration, Oxidative Deamination to Alcohol
Metoprolol	C14 H27 N O4	274.20201	x	Hydration, Reduction
Metoprolol_Acid	C14 H17 N O5	280.11867		Desaturation, Desaturation, Oxidation
Metoprolol	C15 H21 N O4	280.15506		Desaturation, Desaturation, Oxidation
Metoprolol_Acid	C14 H16 O6	281.10269		Desaturation, Oxidation, Oxidative Deamination to Ketone
Metoprolol	C15 H20 O5	281.13907		Desaturation, Oxidation, Oxidative Deamination to Ketone
Metoprolol_Acid	C14 H19 N O5	282.13432		Desaturation, Oxidation
Metoprolol	C15 H23 N O4	282.17071		Desaturation, Oxidation
Metoprolol_Acid	C14 H18 O6	283.11834		Oxidation, Oxidative Deamination to Ketone
Metoprolol	C15 H22 O5	283.15472		Oxidation, Oxidative Deamination to Ketone
Metoprolol	C14 H21 N O5	284.14997	x	Oxidation, Oxidation
Metoprolol_Acid	C14 H21 N O5	284.14997		Oxidation
Metoprolol	C15 H25 N O4	284.18636		Oxidation
Metoprolol_Acid	C14 H20 O6	285.13399		Hydration, Oxidative Deamination to Ketone
Metoprolol	C15 H24 O5	285.17037		Hydration, Oxidative Deamination to Ketone
Metoprolol	C14 H23 N O5	286.16562	x	Oxidation, Oxidation
Metoprolol	C14 H23 N O5	286.16562	x	Hydration, Oxidation
Metoprolol_Acid	C14 H23 N O5	286.16562		Hydration
Metoprolol	C15 H27 N O4	286.20201		Hydration
Metoprolol_Acid	C14 H22 O6	287.14964		Hydration, Oxidative Deamination to Alcohol
Metoprolol	C15 H26 O5	287.18602		Hydration, Oxidative Deamination to Alcohol
Metoprolol	C14 H25 N O5	288.18127	x	Hydration, Oxidation
Metoprolol_Acid	C14 H25 N O5	288.18127		Hydration, Reduction
Metoprolol	C15 H29 N O4	288.21766		Hydration, Reduction
Metoprolol_Acid	C14 H24 O6	289.16529		Hydration, Oxidative Deamination to Alcohol, Reduction
Metoprolol	C15 H28 O5	289.20167		Hydration, Oxidative Deamination to Alcohol, Reduction
Metoprolol_Acid	C14 H19 N O6	298.12924		Desaturation, Oxidation, Oxidation
Metoprolol	C15 H23 N O5	298.16562		Desaturation, Oxidation, Oxidation
Metoprolol_Acid	C14 H18 O7	299.11325		Oxidation, Oxidation, Oxidative Deamination to Ketone
Metoprolol	C15 H22 O6	299.14964		Oxidation, Oxidation, Oxidative Deamination to Ketone
Metoprolol_Acid	C14 H21 N O6	300.14489		Oxidation, Oxidation
Metoprolol	C15 H25 N O5	300.18127		Oxidation, Oxidation
Metoprolol_Acid	C14 H20 O7	301.1289		Hydration, Oxidation, Oxidative Deamination to Ketone
Metoprolol	C15 H24 O6	301.16529		Hydration, Oxidation, Oxidative Deamination to Ketone
Metoprolol_Acid	C14 H23 N O6	302.16054		Hydration, Oxidation
Metoprolol	C15 H27 N O5	302.19692		Hydration, Oxidation
Metoprolol_Acid	C14 H22 O7	303.14455		Hydration, Oxidation, Oxidative Deamination to Alcohol
Metoprolol	C15 H26 O6	303.18094		Hydration, Oxidation, Oxidative Deamination to Alcohol
Metoprolol_Acid	C14 H25 N O6	304.17619		Hydration, Oxidation, Reduction

Metoprolol	C15 H29 N O5	304.21257		Hydration, Oxidation, Reduction
Metoprolol_Acid	C14 H21 N O7	316.1398		Oxidation, Oxidation, Oxidation
Metoprolol	C15 H25 N O6	316.17619		Oxidation, Oxidation, Oxidation
Metoprolol_Acid	C14 H23 N O7	318.15545		Hydration, Oxidation, Oxidation
Metoprolol	C15 H27 N O6	318.19184		Hydration, Oxidation, Oxidation

Table S4. List of the 39 suspect compounds included in the literature list.

Name	Molecular formula	Exact mass $[M+H]^+$	References
MTP	$C_{15}H_{25}NO_3$	268.19072	[3]
MTPA	$C_{14}H_{21}NO_4$	268.15433	[3]
TP74	$C_4H_{11}N$	74.09643	[4]
TP102	$C_5H_{11}NO$	102.09134	[5]
TP112	C_6H_9NO	112.07569	[5]
TP114	$C_6H_{11}NO$	114.09134	[5]
TP116	$C_6H_{13}NO$	116.10699	[4,6,7]
TP118	$C_6H_{15}NO$	118.12264	[4,8]
TP120	$C_5H_{13}NO_2$	120.10191	[7]
TP121	C_8H_8O	121.06479	[4]
TP134	$C_6H_{15}NO_2$	134.11756	[4,6–9]
TP150	$C_6H_{15}NO_3$	150.11247	[4,6,7]
TP193	$C_{12}H_{16}O_2$	193.12231	[6]
TP196	$C_{11}H_{17}NO_2$	196.13321	[5]
TP208	$C_{12}H_{17}NO_2$	208.13321	[4,6,8]
TP216	$C_{10}H_{17}NO_4$	216.12303	[5]
TP220	$C_{13}H_{17}NO_2$	220.13321	[6]
TP226A	$C_{12}H_{19}NO_3$	226.14377	[5,6,10,11]
TP226B	$C_{12}H_{19}NO_3$	226.14377	[11]
TP226C	$C_{11}H_{15}NO_4$	226.10738	[2]
TP232	$C_{10}H_{17}NO_5$	232.11795	[4,6]
TP236	$C_{13}H_{17}NO_3$	236.12812	[5]
TP238	$C_{13}H_{19}NO_3$	238.14377	[4,6–10]
TP240	$C_{13}H_{21}NO_3$	240.15942	[4–7,9]
TP241	$C_{12}H_{16}O_5$	241.10705	[11]
TP250	$C_{15}H_{23}NO_2$	250.18016	[6]
TP252	$C_{14}H_{21}NO_3$	252.15942	[4,6,7,9]
TP254	$C_{13}H_{19}NO_4$	254.13868	[9]
O-DMTP	$C_{14}H_{23}NO_3$	254.17507	[3,4,6,7,9–11]
TP256	$C_{13}H_{21}NO_4$	256.15433	[7]
TP270	$C_{14}H_{23}NO_4$	270.16998	[4,6,7,11]
TP282	$C_{15}H_{23}NO_4$	282.16998	[3,4,6–9]
α-HMTP	$C_{15}H_{25}NO_4$	284.18563	[3,4,6–11]
TP284	$C_{15}H_{25}NO_4$	284.18563	[4,6–10]
TP298	$C_{15}H_{23}NO_5$	298.16490	[4,6,7]
TP300	$C_{15}H_{25}NO_5$	300.18055	[5–7]
TP316	$C_{15}H_{25}NO_6$	316.17546	[6,7]
TP318	$C_{15}H_{27}NO_6$	318.19111	[7]
TP332	$C_{15}H_{25}NO_7$	332.17038	[6]

S3. TP distribution in UV/H_2O_2 combined processes treating pure water

AOP+FG

Table S5. Individual TPs distribution (Eq.3) and sum of TP individual distributions in AOP and AOP+FG treating pure water.

TP generation	Compound	Individual TPs distribution in AOP (%)	Sum of TPs individual distribution in AOP (%)	Individual TP distribution in AOP+FG (%)	Sum of TPs individual distribution in AOP+FG (%)
1st	α-HMTP	3.2 ± 1.8%	3.6%	1.8 ± 0.7%	3.2%
	TP284	n.d.		n.d.	
	O-DMTP	< 1%		< 1%	
	TP226C	n.d.		1.3 ± 0.1%	
2nd	TP300	n.d.	19.0%	1.9 ± 0.1%	15.9%
	TP282A	n.d.		< 1%	
	TP270	n.d.		n.d.	
	MTPA	8.5 ± 2.4%		2.2 ± 0.1%	
	TP240	10.0 ± 3.2%		8.8 ± 0.5%	
	TP238	< 1%		2.2 ± 0.1%	
≥3rd	TP316	n.d.	77.4%	n.d.	80.8%
	TP282B	< 1%		n.d.	
	TP254	n.d.		< 1%	
	TP252	< 1%		n.d.	
	TP226A	n.d.		n.d.	
	TP150	26.7 ± 6.7%		5.3 ± 1.1%	
	TP134	42.7 ± 10.6%		52.6 ±5.2%	
	TP116	6.3 ± 0.1%		21.1 ±6.2%	
	TP114	1.2 ± 1.3%		1.2 ± 1.2%	

FG+AOP

Table S6. Individual TPs distribution (Eq.3) and sum of TP individual distributions in FG and FG+AOP treating pure water.

TP generation	Compound	Individual TPs distribution in FG (%)	Sum of TPs individual distribution in FG (%)	Individual TP distribution in FG+AOP (%)	Sum of TPs individual distribution in FG+AOP (%)
1st	α-HMTP	13.3 ± 0.5%	16.3%	11.1 ± 0.1%	21.9%
	TP284	< 1%		7.2 ± 1.4%	
	O-DMTP	2.8 ± 0.1%		3.5 ± 0.3%	
	TP226C	n.d.		< 1%	
2nd	TP300	n.d.	46.6%	n.d.	41.4%
	TP282A	2.8 ± 0.1%		< 1%	
	TP270	< 1%		< 1%	
	MTPA	n.d.		n.d.	
	TP240	41.6 ± 1.5%		29.0 ± 0.2%	
	TP238	2.0 ± 0.4%		11.7 ± 1.0%	
≥3rd	TP316	< 1%	37.1%	< 1%	36.7%
	TP282B	1.6 ± 0.1%		2.2 ± 0.5%	
	TP254	23.0 ± 1.2%		2.5 ± 0.5%	
	TP252	n.d.		1.2 ± 0.1%	
	TP226A	n.d.		2.5 ± 0.1%	
	TP150	1.0 ± 0.3%		1.5 ± 0.1%	
	TP134	7.3 ± 0.2%		22.7 ± 1.3%	
	TP116	4.0 ± 0.1%		3.6 ± 0.1%	
	TP114	< 1%		< 1%	

AOP+CAS

Table S7. Individual TPs distribution (Eq.3) and sum of TP individual distributions AOP and AOP+CAS treating pure water.

TP generation	Compound	Individual TPs distribution in AOP (%)	Sum of TPs individual distribution in AOP (%)	Individual TP distribution in AOP+CAS (%)	Sum of TPs individual distribution in AOP+CAS (%)
1st	α-HMTP	3.2 ± 1.8%	3.6%	2.5 ± 0.2%	3.6%
	TP284	n.d.		< 1%	
	O-DMTP	< 1%		< 1%	
	TP226C	n.d.		n.d.	
2nd	TP300	n.d.	19.0%	n.d.	31.6%
	TP282A	n.d.		5.4 ± 0.3%	
	TP270	n.d.		1.2 ± 0.6%	
	MTPA	8.5 ± 2.4%		15.6 ± 7.9%	
	TP240	10.0 ± 3.2%		8.5 ± 1.5%	
	TP238	< 1%		< 1%	
≥3rd	TP316	n.d.	77.4%	n.d.	64.8%
	TP282B	< 1%		< 1%	
	TP254	n.d.		< 1%	
	TP252	< 1%		< 1%	
	TP226A	n.d.		n.d.	
	TP150	26.7 ± 6.7%		n.d.	
	TP134	42.7 ± 10.6%		41.4 ± 0.7%	
	TP116	6.3 ± 0.1%		17.9 ± 0.8%	
	TP114	1.2 ± 1.3%		4.0 ± 1.1%	

CAS+AOP

Table S8. Individual TPs distribution (Eq.3) and sum of TP individual distributions in CAS and CAS+AOP treating pure water.

TP generation	Compound	Individual TPs distribution in CAS (%)	Sum of TPs individual distribution in CAS (%)	Individual TP distribution in CAS+AOP (%)	Sum of TPs individual distribution in CAS+AOP (%)
1st	α-HMTP	< 1%	2.0%	< 1%	3.6%
	TP284	< 1%		< 1%	
	O-DMTP	< 1%		2.2 ± 0.1%	
	TP226C	< 1%		< 1%	
2nd	TP300	n.d.	91.2%	n.d.	17.2%
	TP282A	1.1 ± 0.1%		n.d.	
	TP270	< 1%		< 1%	
	MTPA	89.3 ± 9.6%		7.6 ± 0.5%	
	TP240	< 1%		4.2 ± 0.1%	
	TP238	< 1%		5.2 ± 0.1%	
≥3rd	TP316	n.d.	6.8%	n.d.	79.2%
	TP282B	< 1%		1.5 ± 0.1%	
	TP254	2.0 ± 0.1%		< 1%	
	TP252	n.d.		< 1%	
	TP226A	< 1%		< 1%	
	TP150	n.d.		6.1 ± 0.1%	
	TP134	1.0 ± 0.1%		67.1 ± 1.2%	
	TP116	3.2 ± 0.1%		4.0 ± 0.1%	
	TP114	< 1%		< 1%	

S4. TP distribution in UV/H_2O_2 combined processes treating HWW

AOP+FG

Table S9. Individual TPs distribution (Eq.3) and sum of TP individual distributions in AOP and AOP+FG treating HWW.

TP generation	Compound	Individual TPs distribution in AOP (%)	Sum of TPs individual distribution in AOP (%)	Individual TP distribution in AOP+FG (%)	Sum of TPs individual distribution in AOP+FG (%)
1st	α-HMTP	38.8 ± 6.3%	41.3%	44.1 ± 7.2%	45.2%
	TP284	2.1 ± 0.3%		< 1%	
	O-DMTP	< 1%		< 1%	
	TP226C	n.d.		< 1%	
2nd	TP300	n.d.	56.3%	< 1%	44.8%
	TP282A	3.0 ± 0.1%		< 1%	
	TP270	< 1%		< 1%	
	MTPA	2.6 ± 0.5%		1.5 ± 0.5%	
	TP240	49.4 ± 9.4%		42.5 ± 8.1%	
	TP238	1.0 ± 0.2%		< 1%	
≥3rd	TP316	< 1%	2.4%	< 1%	10.0%
	TP282B	< 1%		< 1%	
	TP254	< 1%		< 1%	
	TP252	< 1%		6.1 ± 1.0%	
	TP226A	n.d.		n.d.	
	TP150	< 1%		2.3 ± 0.6%	
	TP134	< 1%		< 1%	
	TP116	< 1%		< 1%	
	TP114	n.d.		n.d.	

FG+AOP

Table S10. Individual TPs distribution (Eq.3) and sum of TP individual distributions in FG and FG+AOP treating HWW.

TP generation	Compound	Individual TPs distribution in FG (%)	Sum of TPs individual distribution in FG (%)	Individual TP distribution in FG+AOP (%)	Sum of TPs individual distribution in FG+AOP (%)
1st	α-HMTP	37.4 ± 4.1%	41.8%	34.8 ± 0.9%	41.0%
	TP284	< 1%		< 1%	
	O-DMTP	< 1%		< 1%	
	TP226C	4.1 ± 0.1%		5.6 ± 0.5%	
2nd	TP300	n.d.	50.2%	< 1%	51.4%
	TP282A	< 1%		1.2 ± 0.5%	
	TP270	n.d.		< 1%	
	MTPA	14.2 ± 0.2%		8.0 ± 0.2%	
	TP240	34.5 ± 1.9%		40.3 ± 0.1%	
	TP238	1.4 ± 0.3%		1.8 ± 0.2%	
≥3rd	TP316	1.7 ± 0.1%	7.9%	1.7 ± 0.1%	7.6%
	TP282B	< 1%		< 1%	
	TP254	< 1%		< 1%	
	TP252	1.4 ± 0.2%		< 1%	
	TP226A	< 1%		< 1%	
	TP150	3.2 ± 0.2%		4.0 ± 0.3%	
	TP134	< 1%		< 1%	
	TP116	< 1%		< 1%	
	TP114	n.d.		n.d.	

AOP+CAS

Table S11. Individual TPs distribution (Eq.3) and sum of TP individual distributions in AOP and AOP+CAS treating HWW.

TP generation	Compound	Individual TPs distribution in AOP (%)	Sum of TPs individual distribution in AOP (%)	Individual TP distribution in AOP+CAS (%)	Sum of TPs individual distribution in AOP+CAS (%)
1st	α-HMTP	38.8 ± 6.3%	41.3%	4.4 ± 0.1%	12.0%
	TP284	2.1 ± 0.3%		6.0 ± 0.6%	
	O-DMTP	< 1%		< 1%	
	TP226C	n.d.		1.3 ± 0.1%	
2nd	TP300	n.d.	56.3%	< 1%	22.8%
	TP282A	3.0 ± 0.1%		3.3 ± 0.4%	
	TP270	< 1%		7.9 ± 1.2%	
	MTPA	2.6 ± 0.5%		5.1 ± 1.5%	
	TP240	49.4 ± 9.4%		4.9 ± 1.1%	
	TP238	1.0 ± 0.2%		1.1 ± 0.7%	
≥3rd	TP316	< 1%	2.4%	< 1%	65.2%
	TP282B	< 1%		1.3 ± 1.5%	
	TP254	< 1%		56.3 ± 3.5%	
	TP252	< 1%		1.7 ± 0.2%	
	TP226A	n.d.		1.5 ± 0.4%	
	TP150	< 1%		3.1 ± 0.1%	
	TP134	< 1%		< 1%	
	TP116	< 1%		< 1%	
	TP114	n.d.		n.d.	

CAS+AOP

Table S12. Individual TPs distribution (Eq.3) and sum of TP individual distributions in CAS and CAS+AOP treating HWW.

TP generation	Compound	Individual TPs distribution in CAS (%)	Sum of TPs individual distribution in CAS (%)	Individual TP distribution in CAS+AOP (%)	Sum of TPs individual distribution in CAS+AOP (%)
1st	α-HMTP	5.7 ± 0.8%	10.9%	19.3 ± 0.4%	27.8%
	TP284	3.4 ± 0.1%		3.2 ± 0.2%	
	O-DMTP	< 1%		3.0 ± 0.8%	
	TP226C	1.2 ± 0.7%		2.3 ± 0.2%	
2nd	TP300	< 1%	23.8%	< 1%	51.3%
	TP282A	2.2 ± 0.5%		4.2 ± 0.7%	
	TP270	4.2 ± 3.6%		5.7 ± 0.1%	
	MTPA	5.4 ± 0.7%		4.4 ± 0.4%	
	TP240	10.5 ± 1.5%		35.0 ± 2.0%	
	TP238	1.3 ± 0.5%		1.8 ± 0.2%	
≥3rd	TP316	< 1%	65.2%	< 1%	21.0%
	TP282B	1.7 ± 0.9%		2.0 ± 0.2%	
	TP254	33.5 ± 10.8%		n.d.	
	TP252	21.7 ± 7.5%		1% ± 0.1%	
	TP226A	< 1%		< 1%	
	TP150	6.7 ± 2.3%		13.9 ± 1.8%	
	TP134	< 1%		2.7 ± 0.9%	
	TP116	< 1%		< 1%	
	TP114	n.d.		n.d.	

S4. Spearman correlation

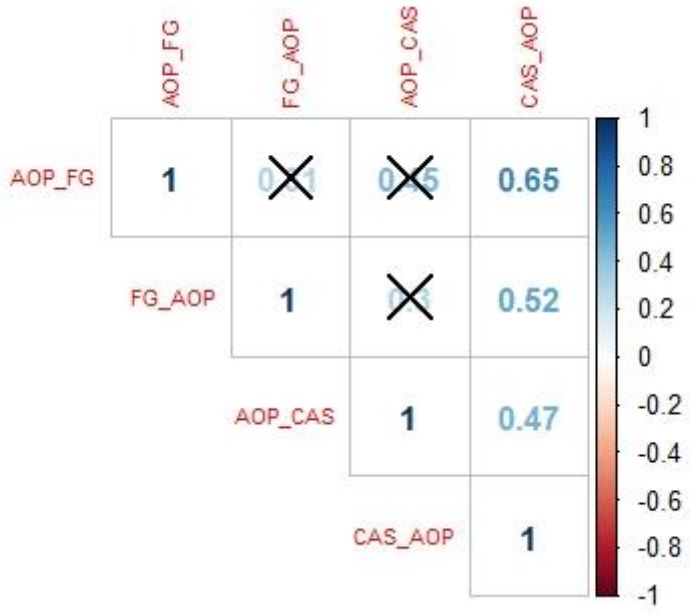

Fig. S2. Spearman correlations (r_s) calculated between the pairs of treatments tested in spiked pure water: 0.00-0.19 “very weak”, 0.20-0.39 “weak”, 0.40-0.59 “moderate”, 0.60-0.79 “strong”, 0.80-1.0 “very strong”. Non significate values ($p > 0.05$) are represented as (X).

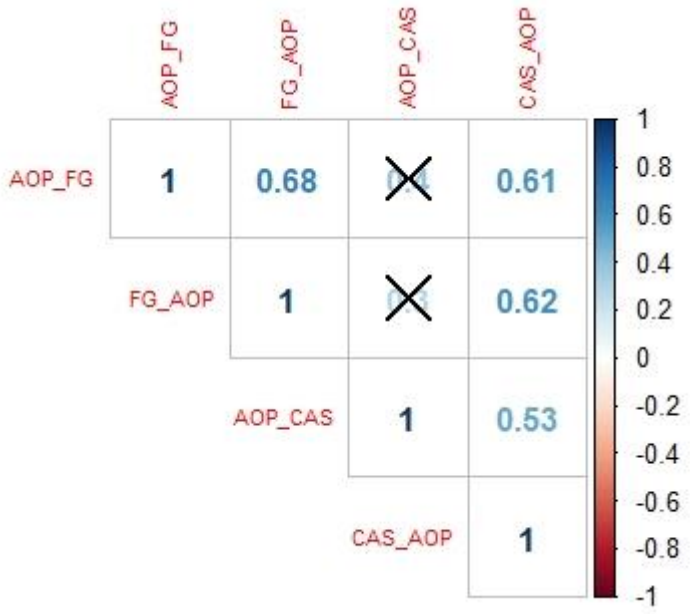

Fig. S3. Spearman correlations (r_s) calculated between the pairs of treatments tested in spiked HWW: 0.00-0.19 “very weak”, 0.20-0.39 “weak”, 0.40-0.59 “moderate”, 0.60-0.79 “strong”, 0.80-1.0 “very strong”. Non significate values ($p > 0.05$) are represented as (X).

References

[1] A. Jaén-Gil, G. Buttiglieri, A. Benito, R. Gonzalez-Olmos, D. Barceló, S. Rodríguez-Mozaz, Metoprolol and metoprolol acid degradation in UV/H2O2 treated wastewaters: An integrated screening approach for the identification of hazardous transformation products, J. Hazard. Mater. (2019) 120851. doi:10.1016/j.jhazmat.2019.120851.

[2] A. Jaén-Gil, F. Castellet-Rovira, M. Llorca, M. Villagrasa, M. Sarrà, S. Rodríguez-Mozaz, D. Barceló, Fungal treatment of metoprolol and its recalcitrant metabolite metoprolol acid in hospital wastewater: Biotransformation, sorption and ecotoxicological impact, Water Res. 152 (2019) 171–180. doi:10.1016/j.watres.2018.12.054.

[3] A. Rubirola, M. Llorca, S. Rodriguez-Mozaz, N. Casas, I. Rodriguez-Roda, D. Barceló, G. Buttiglieri, Characterization of metoprolol biodegradation and its transformation products generated in activated sludge batch experiments and in full scale WWTPs, Water Res. 63 (2014) 21–32. doi:10.1016/j.watres.2014.05.031.

[4] V. Romero, O. González, B. Bayarri, P. Marco, J. Giménez, S. Esplugas, Degradation of Metoprolol by photo-Fenton: Comparison of different photoreactors performance, Chem. Eng. J. 283 (2016) 639–648. doi:10.1016/j.cej.2015.07.091.

[5] M.L. Wilde, S. Montipó, A.F. Martins, Degradation of β-blockers in hospital wastewater by means of ozonation and Fe^{2+}/ozonation, Water Res. 48 (2014) 280–295. doi:10.1016/j.watres.2013.09.039.

[6] V. Romero, S. Acevedo, P. Marco, J. Giménez, S. Esplugas, Enhancement of Fenton and photo-Fenton processes at initial circumneutral pH for the degradation of the β-blocker metoprolol, Water Res. 88 (2016) 449–457. doi:10.1016/j.watres.2015.10.035.

[7] R.P. Cavalcante, R.F. Dantas, H. Wender, B. Bayarri, O. González, J. Giménez, S. Esplugas, A. Machulek, Photocatalytic treatment of metoprolol with B-doped TiO_2: Effect of water matrix, toxicological evaluation and identification of intermediates, Appl. Catal. B Environ. 176–177 (2015) 173–182. doi:10.1016/j.apcatb.2015.04.007.

[8] V. Romero, O. González, B. Bayarri, P. Marco, J. Giménez, S. Esplugas, Performance of different advanced oxidation technologies for the abatement of the beta-blocker metoprolol, Catal. Today. 240 (2015) 86–92. doi:10.1016/j.cattod.2014.03.060.

[9] D. Šojić, V. Despotović, D. Orčić, E. Szabó, E. Arany, S. Armaković, E. Illés, K. Gajda-Schrantz, A. Dombi, T. Alapi, E. Sajben-Nagy, A. Palágyi, C. Vágvölgyi, L. Manczinger, L. Bjelica, B. Abramović, Degradation of thiamethoxam and metoprolol by UV, O_3 and UV/O_3 hybrid processes: Kinetics, degradation intermediates and toxicity, J. Hydrol. 472–473 (2012) 314–327. doi:10.1016/j.jhydrol.2012.09.038.

[10] C. Slegers, A. Maquille, V. Deridder, E. Sonveaux, J.L. Habib Jiwan, B. Tilquin, LC-MS analysis in the e-beam and gamma radiolysis of metoprolol tartrate in aqueous solution: Structure elucidation and formation mechanism of radiolytic products, Radiat. Phys. Chem. 75 (2006) 977–989. doi:10.1016/j.radphyschem.2006.02.001.

[11] B. Ma, H.H. Huang, X.Y. Chen, Y.M. Sun, L.H. Lin, D.F. Zhong, Biotransformation of metoprolol by the fungus Cunninghamella blakesleeana, Acta Pharmacol. Sin. 28 (2007) 1067–1074. doi:10.1111/j.1745-7254.2007.00567.x.